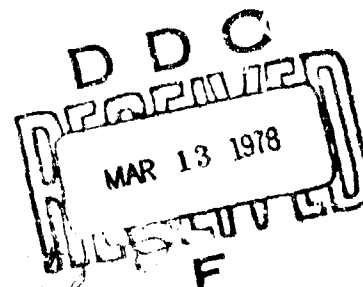USAAMRDL-TR-77-40C

AD A050059

# HEAVY LIFT HELICOPTER FLIGHT CONTROL SYSTEM

VOLUME III - Automatic Flight Control System Development and Feasibility Demonstration

Boeing Vertol Company
P.O. Box 16858
Philadelphia, Pa. 19142

D D C

MAR 13 1978

F

September 1977

Final Report for Period July 1971 - JULY 1975

Approved for public release;
distribution unlimited.

Prepared for

U. S. ARMY AVIATION RESEARCH AND DEVELOPMENT COMMAND
P.O. Box 209
St. Louis, Mo. 63166

APPLIED TECHNOLOGY LABORATORY
U. S. ARMY RESEARCH AND TECHNOLOGY LABORATORIES (AVRADCOM)
Fort Eustis, Va. 23604

## APPLIED TECHNOLOGY LABORATORY POSITION STATEMENT

Due to the termination of the HLH program, reports summarizing the strides made in many of the supporting technology programs were never published. In an effort to make as much of this information available as possible, selected draft reports prepared under contract prior to termination have been edited and converted to the DOD format by the Applied Technology Laboratory. The reader will find many instances of poor legibility in drawings and charts which could not, due to the funding and manpower constraints, be redone. It is felt, however, that some benefit will be derived from their inclusion and that where essential details are missing, sufficient information exists to allow the direction of specific questions to the contractor and/or the U.S. Army.

| REPORT DOCUMENTATION PAGE | | READ INSTRUCTIONS BEFORE COMPLETING FORM |
|---|---|---|
| 1. REPORT NUMBER  USAAMRDL-TR-77-40C | 2. GOVT ACCESSION NO. | 3. RECIPIENT'S CATALOG NUMBER |
| 4. TITLE (and Subtitle)  HEAVY LIFT HELICOPTER FLIGHT CONTROL SYSTEM, Volume III, Automatic Flight Control System Development and Feasibility Demonstration. | | 5. TYPE OF REPORT & PERIOD COVERED  Final Report, Jul 71 - Jul 75 |
| | | 6. PERFORMING ORG. REPORT NUMBER |
| 7. AUTHOR(s)  J. Davis, T. Garnett J. Gaul | | 8. CONTRACT OR GRANT NUMBER(s)  DAAJ01-71-C-0840 (P6A) |
| 9. PERFORMING ORGANIZATION NAME AND ADDRESS  Boeing Vertol Company  P. O. Box 16858  Philadelphia, PA  19142 | | 10. PROGRAM ELEMENT, PROJECT, TASK AREA & WORK UNIT NUMBERS |
| 11. CONTROLLING OFFICE NAME AND ADDRESS  U. S. Army Aviation R&D Command  P. O. Box 209  St. Louis, MO  63166 | | 12. REPORT DATE  Sep 77 |
| | | 13. NUMBER OF PAGES  703 |
| 14. MONITORING AGENCY NAME & ADDRESS(if different from Controlling Office)  Applied Technology Laboratory, Research and Technology Laboratories (AVRADCOM), Fort Eustis, VA  23604 | | 15. SECURITY CLASS. (of this report)  Unclassified |
| | | 15a. DECLASSIFICATION/DOWNGRADING SCHEDULE |

16. DISTRIBUTION STATEMENT (of this Report)

Approved for public release; distribution unlimited.

17. DISTRIBUTION STATEMENT (of the abstract entered in Block 20, if different from Report)

18. SUPPLEMENTARY NOTES

Volume III of a three-volume report.

19. KEY WORDS (Continue on reverse side if necessary and identify by block number)

| | | |
|---|---|---|
| Helicopters | Interfaces | Stabilization |
| Flight Control System | Test Equipment | Systems |
| Automatic Pilots | Servomechanisms | Load Control |
| Cockpit Controller Subsystem | Transducers | |
| Electrical Equipment | Hovering | |

20. ABSTRACT (Continue on reverse side if necessary and identify by block number)

The U. S. Army Heavy Lift Helicopter Advanced Technology Component program required the design, development, and feasibility demonstration of an electrohydraulic flight control system. This volume details the evolution of an automatic flight control system (AFCS), operating by means of a direct electrical linkage. AFCS software and hardware development and testing are discussed. The results of flight clearance testing and in-flight evaluations of

DD FORM 1473  EDITION OF 1 NOV 65 IS OBSOLETE

Block 20 (Cont):

cont. AFCS control laws are examined.

Associated documents are: Volume I - Production Recommendations, and Volume III - Primary Flight Control System Development and Feasibility Demonstration.

DISTRIBUTION/AVAILABILITY CODES

SUMMARY

A fail-operational Automatic Flight Control System (AFCS) was
developed for the U.S. Army Heavy Lift Helicopter to enable
that aircraft to perform rapid and precise external load oper-
ations in all weather conditions.  The AFCS provides both full-
time stability and control augmentation (SCAS), as well as
pilot-selectable modes for altitude hold, hover hold, load-
controlling crewman precision hover control, external load
stabilization and navigation/guidance coupling.  The heart of
the system consists of triplex digital computers which process
redundant sensor inputs to generate differential and parallel
command outputs.

A developmental version of the AFCS has been designed, built,
and tested under the HLH Advanced Technology Components Pro-
gram.  This developmental system utilizes serial incremental
digital computers with cross channel bit-by-bit synchroniza-
tion; median signal select for sensor inputs; failure monitor-
ing with auto shutdown at the system, axis, and control mode
levels and off-line Built-In Test Equipment (BITE).

The flight test of the SCAS concept on the Boeing Vertol Model
347 helicopter indicated good-to-excellent performance.  The
most significant results were:

   ● Control response was crisp and maneuverability was good
      in all axes.  Good trim coordination was demonstrated in
      rapid roll reversals up to +45 degrees of bank.

   ● Ground referenced velocity feedback below 40 knots IAS
      significantly improved both stability and trimmability
      in hover maneuvering.

   ● Airspeed hold was excellent in cruise flight with max-
      imum deviations of + 2 to 4 knots in moderate to heavy
      turbulence and in turns up to 30/35 degrees.

   ● A positive lateral control gradient "security blanket"
      concept provided good recovery to wings-level trim from
      forward flight banked turns.  This feature significantly
      reduces pilot workload in making heading changes,
      especially under IMC.

Selectable mode response characteristics were very satisfact-
ory and adequately demonstrated the practicality of the
respective concepts.  In those few instances where deficien-
cies were found, these were accountable to the developmental
state of several of the sensing devices.

3

Altitude hold accuracy was +20 feet in cruise flight. Radar
altitude hold in hover flight was accurate to +6 inches
following the tailoring of a complementary filter to remove
the effects of radar spikes over grass.

The high-gain stability loops of the hover hold mode provided
excellent gust rejection and maintained the selected hover
condition with minimum drift using inertial velocity feedbacks.
Hover hold accuracy using position feedbacks from a precision
hover sensor (PHS), with all controls fixed, demonstrated a
circular error probability of 4.0 inches and 6.8 inches with
winds gusting up to 13 knots and 24 knots, respectively,for a
2-minute run.    PHS performance over a high contrast ground
was satisfactory; however, it did not lock on over grass or
other low contrast scenes. Although this deficiency could not
be corrected in the ATC equipment, it did not negate the
evaluation of the control laws and their signal processing.

The load-controlling crewman, operating through the hover hold
mode, demonstrated an impressive capability to provide vernier
response to move the aircraft or external load into precise
positions. Also, load handling experience revealed that load
shuttle over short distances under control of the LCC was a
very practical capability.

Rapid suspension cable/load hookup was easily performed by a
ground crewman as a result of the LCC's ability to precisely
position the helicopter. MILVAN acquisition in less than one
minute without ground crewman assistance was demonstrated by
positioning a top-lift adapter on the MILVAN. Precise place-
ment of a MILVAN onto the transporter lockpins was demonstra-
ted but required a fair amount of hover maneuvering time on
the part of the LCC. With flared guide vanes installed on
the transporter, it became possible to deposit the MILVAN on
the locking pins - within the +1.0 inch-accuracy required -
in one minute or less.

Flight training requirements for a load controlling crewman
would be minimal. Load operations were performed by two
Army pilots after 30 minutes of no-load flight familiariza-
tion. Following the completion of developmental testing, 54
hours of demonstrations were conducted in which 163 pilots
and non-pilots flew from the LCC station. Control of the
aircraft without a load was quickly acquired with less than
5 minutes of familiarization.

The load stabilization system (LSS) provided a significant
increase in load damping, both in hover and forward flight.
The greatest need for damping augmentation is during an attempt
to precisely position a load on long cables (load natural
damping decreases with increasing cable length). The concept

4

utilized cable feedbacks into the AFCS and although effective, was judged to be inferior to the active pendant concepts.

The automatic approach to hover mode was configured to demonstrate the feasibility to manually (following flight director commands) or automatically fly the aircraft down an approach path terminating in a stabilized hover. Both manual and automatic approaches were performed very satisfactorily.

## INTRODUCTION

HLH ATC (Advanced Technology Component) program elements
associated with development of the flight control system are
divided into four separate tasks in the SOW, with Task I
having two parts. The initial work performed under the first
task (Task I, Part 1) was accomplished during the second half
of 1971. Objectives were to select candidate FCS concepts
for the HLH to determine the necessity for developing a side-
arm controller, and to identify high risk areas and critical
components requiring further development. Results of Task I,
Part 1, were documented completely in Reference 1, and will
be summarized later in this section.

## PURPOSE

The purpose of this report is to review ATC flight control
work performed subsequent to Task I, Part 1, and directed
toward definition of the AFCS for the 347 Flight Research
Vehicle. Summarized in this document are results of the
following phases of the program:

- Task I, Part 2 — Analytical design of the AFCS and veri-
fication through large moving base
simulation.

- Task II — Development and test of AFCS computer
and sensor hardware.

- Task III — Precision hover and load stabilization
demonstration (including integration
testing and flight demonstration of
the basic AFCS and selectable control
modes).

- Task IV — Controller development

Task IV controller development is confined to the Load Con-
trolling Crewman's Controller (LCCC), and its interrelationship
with the low speed AFCS selectable control modes. Other
Task IV activities, including design and test of the HLH
cockpit Primary Electrical Control System (PECS), Programmable
Force-Feel Unit (PFFU), and Cockpit Control Driver Actuators are
discussed in Volume II of this report.

Volume II covers all work associated with the Primary Flight Con-
trol System (PFCS) for the 347 Flight Vehicle. A major portion
of the report deals with the Direct Electrical Linkage System
(DELS), which couples cockpit control inputs and AFCS commands
to the swashplate electromechanical actuators. DELS work was
accomplished under FCS ATC Task II.

6

A third FCS document, Volume I, defines the recommended flight control system for the HLH aircraft, based upon results of the ATC program as substantiated in Volumes II and III.

## AFCS DEVELOPMENT

A significant number of FCS analytical design, fabrication, and test activities were in progress at the same time during the ATC program. AFCS work was oriented generally into two areas of activity:

- Software development, including analysis to define control laws and logic, simulation, and flight test evaluation, and

- Hardware development, encompassing design, fabrication (or procurement), and test of system components.

To provide a clear understanding of how the AFCS ATC Program was structured, activity phasing charts were prepared identifying what was done and when. Tables 1 and 2 annotate all major tasks accomplished within the ATC after completion of the Task I, Part 1 phase. Work associated with software development is shown on Table 1, and in Table 2, hardware oriented tasks are listed.

7

TABLE I

TASK II, TASK III, AND TASK IV
HELICOPTER AFCS SOFTWARE DEVELOPMENT PROGRAM ANALYSIS
SIMULATION SCHEDULE

TABLE 2

[illegible title] TASK III AND TASK IV

[illegible] AND HARDWARE DEVELOPMENT PROGRAM

[illegible DATE] APR [illegible]

## TASK I, PART 1 SUMMARY

1971 HLH FCS concept selection trade studies proceeded simultaneously along two major paths. The first was a small pertu bation moving base flight simulation in which math modeling techniques permitted variation of aircraft control response characteristics. Accountability for winds, gusts, and external sling-load dynamics was included in the simulator evaluation.

The second major path dealt with mechanization of the HLH flight control system from cockpit controllers to the swash-plate actuators. This effort proceeded by first defining two basic fly-by-wire schemes at the functional block diagram level. Subcontractors were then selected on a competitive basis to study the hardware impact of the two basic schemes at various redundancy levels.

### Simulation Studies

Three types of maneuvers were performed in the simulator to evaluate eight candidate control augmentation concepts. The maneuvers included final approach to hover from a point several hundred feet behind, to the side of, and above a target; manual hover over a spot; and steep approach from cruising flight. Results of the simulation indicated that precision hover and low-speed maneuvers were accomplished best while using a low sensitivity linear velocity system. This type of control mode was recommended for use by both the pilot and load controlling crew member for all hover hold and low-speed maneuvering.

For steep angle approach applications, the linear ground velocity system was again found to be the best choice, followed by rate - attitude response. Based upon related flight experience for full envelope operation, linear velocity responses were once again found to be desirable in both the longitudinal and lateral axes. A viable alternative for the lateral AFCS was a rate-attitude system.

Recommended implementation of the velocity control concept included use of linear ground-speed reference in low-speed flight, blending to an air mass reference in forward flight.

### Mechanization Studies

The two control system mechanizations evaluated in the Task I, Part 1 study are shown schematically in Figure 1.

Scheme A contains a direct link which is an electrical signalling path equivalent to the usual mechanical flight control system. The stability and control augmentation
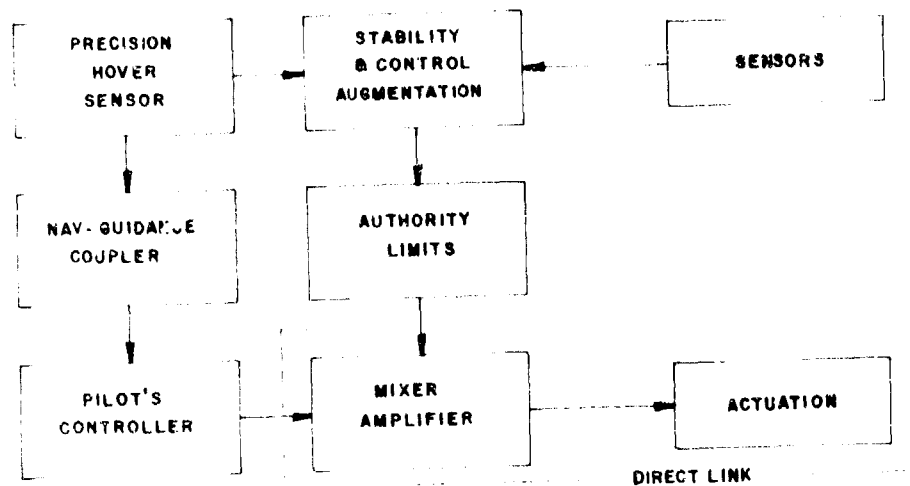
MECHANIZATION SCHEME A



MECHANIZATION SCHEME B

FIGURE 1.   CANDIDATE HLH FLIGHT CONTROL SYSTEM
CONCEPTS

11

system (SCAS) signals are fed to the direct link differen-
tially through authority limits. A navigation/guidance
coupler drives the cockpit controls in parallel with the
pilot's inputs. Typical HLH inputs to the coupler include:
precision hover sensor signals, and ILS or navigation infor-
mation. An important distinguishing feature of Scheme A is
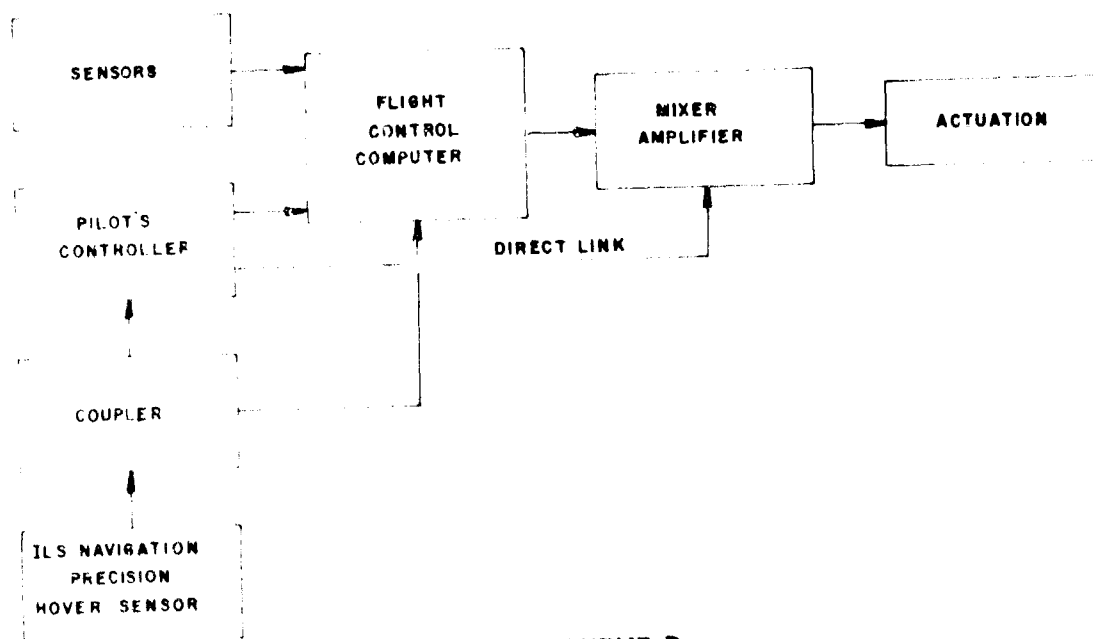that while the pilot's control commands full swashplate
authority, the SCAS, on the other hand, is authority limited
to that necessary to achieve the desired handling qualities.
Authority limiting allows flexibility in redundancy levels
everywhere except in the direct link.

In Scheme B, a direct link is also provided. However, in
Scheme B, it is a backup. A distinguishing feature of B is
that, by concept, the pilot controls the swashplate (100-percent
authority) through the flight control computer. Therefore,
hardover protection must be achieved by the redundancy level,
fault isolation, voting, and switching capability of the
computer.

On the basis of relative cost and flight safety reliability,
the differences between Schemes A and B were not found to be
significant. A subjective evaluation of the two mechaniza-
tions dealing with operation, performance, flexibility and
growth, technical risk, environmental factors, and maintaina-
bility, significantly favored Scheme A, however.

The preferred Scheme A mechanization includes a 2-Fail
Operative (2FO) direct link, and single Fail Operative (SFO)
SCAS or navigation/guidance coupled modes. The reasoning for
the single fail operative preference is as follows:

a.  Flight safety reliability is provided by the direct
    electrical link and is not a function of AFCS
    redundancy level.

b.  The mission reliability for the defined baseline
    mission is essentially equivalent for a dual or SFO
    AFCS.

c.  Mission safety was examined for more realistic and
    demanding HLH mission requirements where precision
    cargo operation is required and natural or induced IFR
    (blowing snow, sand or dust) could be present. Load
    and aircraft motions induced by transients associated
    with dual system failures were judged too severe for
    these missions.

## Sub-Level Trade Studies

Mechanization studies included sub-level trades which
lead to the configuration recommendations summarized
below.

### Actuators

It was concluded that the HLH actuators should be inte-
grated, with combined servo control and power actuation.

### Computers

For the SCAS functions, analog, special purpose digital,
general purpose digital, and combinations of these were
studied. It was concluded that general purpose digital
was the better choice.

### Inertial Reference Unit

It was concluded that strap-down inertial references are
the best choice. A skewed pentad configuration was
recommended.

### Direct Link

It was the choice of the study that the direct link be
an active on-line, in-line monitored system. Dual fail-
operate redundancy level is provided by triple channels,
each with a model.

### Sidearm Controller Study

Conventional and unconventional controllers for the
cockpit were studied. The configurations evaluated
ranged from 4-axis sidearm to the common mechanically
synchronized helicopter control sticks.

Final study recommendations included use of an improved
cyclic stick, thrust lever, and pedal combination for
the HLH vehicle.

# TABLE OF CONTENTS

15

## TABLE OF CONTENTS (CONTINUED)

17

TABLE OF CONTENTS (CONTINUED)

TABLE OF CONTENTS (CONTINUED)

## TABLE OF CONTENTS (CONTINUED)

20

TABLE OF CONTENTS (CONTINUED)

21

## TABLE OF CONTENTS (CONCLUDED)

## LIST OF ILLUSTRATIONS

23

24

25

26

27

29

31

32

33

## LIST OF ILLUSTRATIONS (CONTINUED)

35

## LIST OF ILLUSTRATIONS (CONCLUDED)

LIST OF TABLES

37

## LIST OF TABLES (CONCLUDED)

# 1.0 PROGRAM OVERVIEW AND RESULTS

## 1.1 BACKGROUND

### 1.1.1 ATC Program

The HLH (Heavy Lift Helicopter) was a new aircraft being developed by the U.S. Army under contract to the Boeing Vertol Company. Preliminary design activities culminated in June 1971 when the Army selected the tandem rotor design for the HLH, and awarded Boeing an Advanced Technology Components (ATC) contract for development and integration testing of items critical to HLH success. This contract was modified in January 1973 to include development of a prototype HLH flight article (the XCH-62), which was scheduled to fly in 1976. The program was terminated in 1975.

The ATC program, conducted between June 1971 and October 1974, was comprised of five separate projects, including a four-task flight control effort to design the FCS (Flight Control System) for the HLH. The design consists of analysis and hardware development required to demonstrate critical FCS elements, using a modified CH-47 test aircraft designated the 347 Flight Research Vehicle. Critical control system elements demonstrated in the ATC flight program include: the Primary Flight Control System (PFCS), Automatic Flight Control System (AFCS) control laws, and associated redundancy management techniques.

The purpose of this report is to present a final summary of ATC flight control activities directed toward development and demonstration of the HLH Automatic Flight Control System on the 347 Flight Research Vehicle. Information presented in this document serves as technical substantiation for the recommended HLH AFCS described in Volume I.

### 1.1.2 HLH Mission

The principal mission of the Heavy Lift Helicopter involves airborne transfer of external payloads (up to 35 tons in weight), between various sites in VFR and IFR weather, day or night. Dictates of the mission require precision load handling capability for efficient acquisition and deposit of containerized cargo within confined areas, including moving ships. To facilitate this type of operation, the HLH aircraft is configured with a rear-facing crew station occupied by a Load

Controlling Crewman (LCC). The LCC has an unobstructed view
of the load, and separate aircraft controls optimized for pre-
cise maneuvering and trim hold functions required for cargo
transfer.

### 1.1.3  Flight Control System Concept and Requirements

The real key to HLH success lies in high efficiency load
acquisition and placement. Existing transport helicopters
handle relatively large external loads, but not within con-
fined areas in instrument weather. Rapid load acquisition
requires that ground-referenced linear velocity control
responses be provided to the load crewman. The necessity for
controlling the aircraft relative to ground velocity at low
speed arises because the primary task is to transfer the load
with respect to ground coordinates, and not air mass references.
Forward flight, on the other hand, requires the use of air-
mass velocity reference to match the vehicle control task.

An integrated "fly-by-wire" flight control system was con-
tractually specified by the Army for the HLH. To meet this
requirement, a control system concept was defined (during the
FCS ATC Task 1, Part 1), which incorporates a 100% authority
primary flight control path interfaced with a limited author-
ity automatic flight control system. Figure 2 illustrates
how the FCS concept is implemented in the HLH vehicle.

The primary flight control system, as shown at the top of the
diagram, is composed of cockpit controls and a direct electri-
cal linkage system (DELS). The DELS is a multi-redundant
electrical analogy of the pushrods, bellcranks, boosts, and
stability augmentation actuator interfacing found in conven-
tional mechanical control systems. It forms a direct path
between the cockpit controls and the rotors, and is character-
ized by functional simplicity resulting in very high relia-
bility. A complete description of this system is presented
in FCS Volume II.

The AFCS is a limited-authority system providing stability
and control augmentation and autopilot-type capability. It
has both differential and parallel outputs in each control
axis, as shown in the lower part of the chart, and incorporates
sophisticated control law technology to effect the high level
of handling qualities required for the HLH mission. Variations
in required handling qualities for different types of missions

40
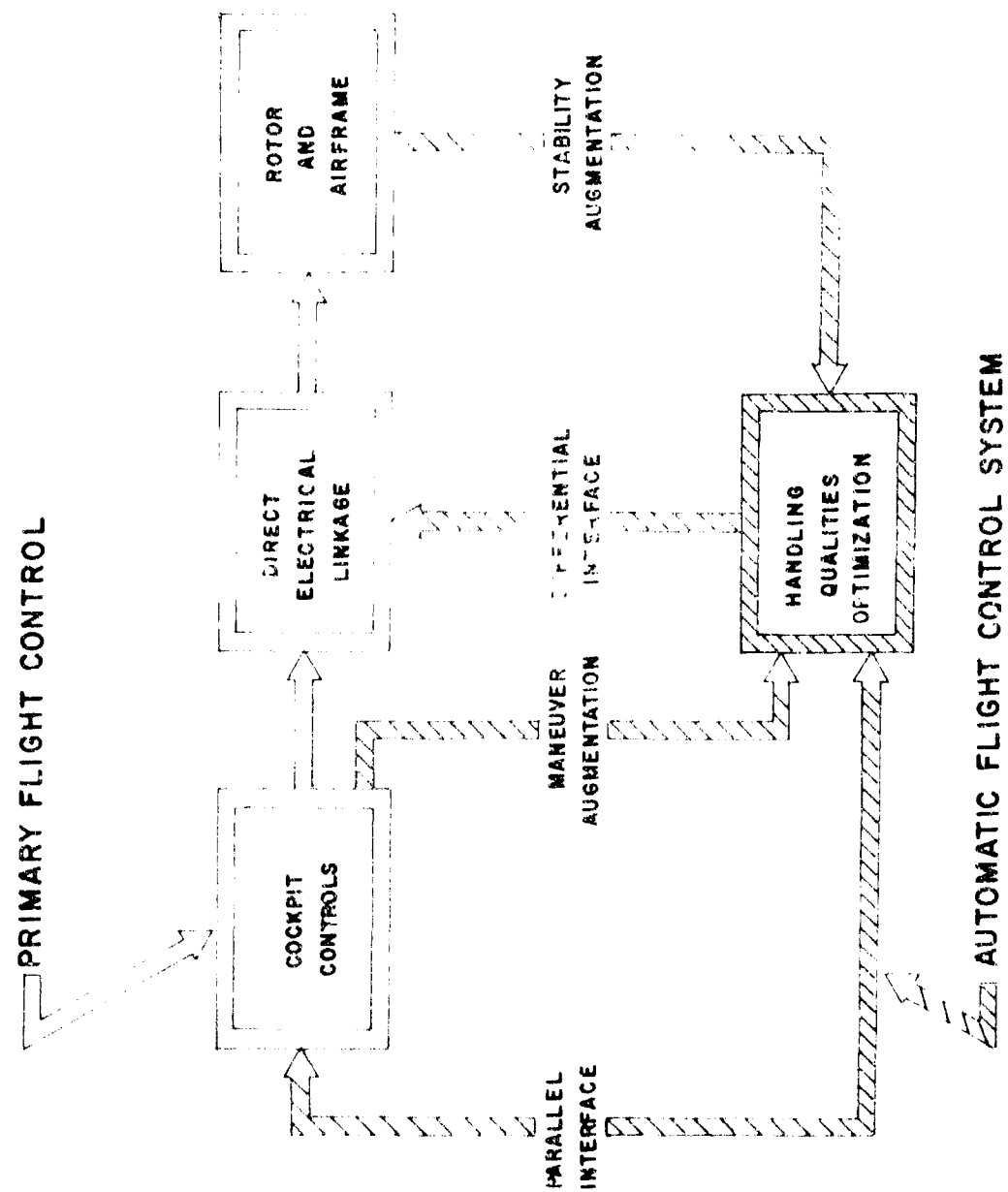
FIGURE 2. HLH FLIGHT CONTROL SYSTEM CONFIGURATION

41

are met through the use of selectable AFCS modes. This approach to control system implementation permits design options which encompass different redundancy levels, software mechanizations, and mission discharge prerequisites.

The selected control system concept was chosen in lieu of a full-authority AFCS (with no primary control path) because:

- Ultimate flight safety is dependent on the primary flight control system. Since the direct path has the minimum number of components, the highest flight safety is achieved at the lowest cost.

- Missions not requiring an AFCS can be accomplished with the AFCS inoperative since the airframe has been provided with neutral stability through use of careful aerodynamic design of the fuselage and delta three hinging on the forward rotor.

- AFCS optimization can be carried out independent of the primary control system. This will be a particularly useful feature for both the initial aircraft and growth models, when new or improved AFCS modes are identified by flight experience

- The primary flight control system and AFCS can utilize different redundancy levels and management techniques.

- The AFCS can always be easily overridden by the pilot, enabling maximum vehicle usage to or beyond established envelope extremes. For example, if it is necessary to perform evasive maneuvers, the AFCS does not impose any envelope constraint (as may happen with a 100-percent authority system).

## 1.2  AFCS DESIGN OBJECTIVES

Specific AFCS handling qualities design objectives for th HLH were established in the original ATC Statement of Work (Reference 2), and were then amplified in the Reference 3

Prime Item Description Document. Objectives oriented toward handling qualities were to:

- Simplify the piloting task

- Optimize vehicle handling qualities

- Minimize pilot switching modes of operation between flight regimes and eliminate transients introduced as a result of mode switching or control transfer between pilots.

Performance goals for the augmented aircraft included:

- Providing the pilot with a precision control capability to position the helicopter (or load) within ± 4 inches vertically and horizontally and ±2 degrees in azimuth with respect to a selected reference within two minutes, starting from a point several hundred feet away from the target, under gusty conditions, with steady wind velocities of up to 45 knots applied from any azimuth.

- Providing automatic positioning of the helicopter over a load after cable attachment, and automatic load stabilization, thus permitting IFR operations without requiring pilot inputs for stabilizing the aircraft.

In addition to meeting the handling qualities and performance objectives stated above, Reference 3 stipulates that the requirements of MIL-H-8501A (Reference 4), and its approved Army deviations, should also be adhered to in design of the HLH flight control system.

Objectives related to AFCS redundancy management were set to meet mission reliability goals, and comprised the following tasks:

- To provide single-fail-operational computational AFCS capability.

- To interface the AFCS with the two-fail operative DELS, without degrading the DELS.

43

- To couple simplex, duplex, and triplex sensors to the triple AFCS computer complex.

- To eliminate time-critical switching to avoid false turnoff problems.

## 1.3 DESIGN APPROACH

To achieve the objectives just outlined, the following technical approach was adopted:

1. Implementation of a basic stability and control augmentation mode for IFR flight operation, supplemented by additional pilot selectable modes for special mission tasks, including altitude hold, automatic approach to hover, hover hold and load stabilization and positioning, and hover trim.

2. Application of the concept of separate stability and maneuverability optimization, through the use of carefully designed feedback and feedforward networks and logic. This approach avoids the usual compromise in AFCS design where high levels of stability result in poor maneuverability and vice versa.

3. Incorporation of a true transient-free switching capability into the AFCS software and hardware to eliminate the effect of transitioning from groundspeed to airspeed reference or from one flight mode to another.

Use of this design approach in the development of AFCS software and hardware packages for the 347 Flight Research Aircraft is discussed next.

## 1.4 AFCS SOFTWARE IMPLEMENTATION - CONTROL LAWS AND LOGIC

The path followed in developing control laws and logic for the 347 Research Vehicle AFCS started with extensive theoretical analysis aimed at defining preliminary block diagrams for each control axis. Initial control law mechanizations have been updated and modified over the past three years, through use of linear and full envelope flight simulation techniques which provided both unpiloted and piloted evaluation data. These

44

developmental simulations were carried out at Boeing Vertol,
and in the Northrop large amplitude and low speed rotational
simulators located in Hawthorne, California.  Final AFCS
refinement was accomplished on the 347 aircraft during the
spring and summer of 1974, where changes in control laws and
logic were incorporated to produce the desired handling quali-
ties for the flight evaluation.

The AFCS developed through this evolutionary process provides
augmentation in all four control axes.  Functionally, there
are six differential AFCS output signals associated with air-
craft control.  They include:  longitudinal control
(generated through differential collective pitch, and longi-
tudinal cyclic pitch on both rotors at low speed); lateral
and directional control (provided by lateral cyclic pitch);
and vertical control introduced through changes in collective
pitch on both rotors simultaneously.  Each control axis also
incorporates an output parallel command signal to backdrive
the cockpit controls for trim compensation, or guidance.

The AFCS control laws provide for a basic Stability and Control
Augmentation (SCAS) mode of operation, and other selectable
modes engaged only for execution of special tasks.  The
Stability and Control Augmentation mode is summarized first.

### 1.4.1   Basic Stability and Control Augmentation Mode (SCAS)

Table 3   presents a summary of stability and maneuverability
characteristics with the SCAS mode engaged.  Three axes of
augmentation are provided; longitudinal, lateral and direc-
tional.  A linear velocity demand response referenced to
ground speed was selected for the longitudinal and lateral
axes at low speed.  In forward flight, (with airspeed > 45
knots) velocity control is maintained in the longitudinal
axis through airspeed, while lateral control becomes bank angle
or turn command.  In the directional axis, turn rate response
is commanded at low speed and sideslip at high speed.  Rate of
climb is maintained for vertical response at all speeds, and
this is obtained entirely through basic aircraft damping.

The software associated with each AFCS axis is comprised of
separate feedback and feedforward networks for effecting the
desired levels of stability and manueverability.  All axes
utilize angular rate damping and attitude hold for stability

45

TABLE 3.   HLH AFCS BASIC HANDLING QUALITIES

| AXIS | STABILITY | | MANEUVERABILITY | |
|---|---|---|---|---|
| | HOVER & LOW SPEED | FORWARD FLIGHT** | HOVER & LOW SPEED | FORWARD FLIGHT** |
| LONGITUDINAL* | GROUND SPEED HOLD | AIRSPEED HOLD | GROUND SPEED DEMAND | AIRSPEED DEMAND |
| LATERAL* | GROUND SPEED HOLD | BANK ANGLE HOLD (ANY BANK ANGLE) | GROUND SPEED DEMAND | BANK ANGLE FOR BANK ANGLES < ±5° / ROLL RATE FOR ANGLES > ±5° / AUTOMATIC TURN COORDINATION |
| VERTICAL | | | ALTITUDE RATE | ALTITUDE RATE |
| DIRECTIONAL* | HEADING HOLD | HEADING HOLD | HEADING RATE | SIDESLIP |

* VERNIER CONTROL (BEEP) PROVIDED     ** GREATER THAN 45 KN

46

along with the velocity loops already mentioned. Feedforward "quickening" functions are provided in the lateral and directional axes along with feedback paths for turn compensation. The lateral axis also features a limited bank attitude stick gradient for IFR handling qualities enhancement. As indicated in Table 3, all axes except vertical are provided with vernier "beep" control capability.

Two significant concepts resulting from the handling qualities requirements are embodied in the detail control laws: stability criteria are undictated by maneuverability considerations and switching from hover to forward flight response characteristics is instantaneous, automatic, and transient free.

1.4.4.1 Stability and Maneuverability

Feedback-feedforward summing networks and logic switching techniques are used to avoid the usual compromises that must be made in establishing stability and maneuverability levels; i.e., when stability is high, maneuverability is too low or vice versa. Summing methods are applied where a control gradient requirement exists. The summing approach used in the longitudinal AFCS axis is illustrated in Figure 3, wherein pitch attitude and velocity feedbacks are summed with filtered stick position. A 65-knot-per-inch stable longitudinal stick gradient results. Speed stability, controlled exclusively by the feedback signals, is characterized by a 10-knot-per-inch equivalent stick gradient.

For a longitudinal step input, the system response will initially be pitch rate blending into attitude, which causes aircraft acceleration. As the velocity approaches that commanded by the stick, helicopter attitude adjusts to the trim value (see Figure 4). The vehicle thus exhibits extremely strong velocity hold characteristics. Feedback signals are used to optimize stability, and feedforward inputs are then determined solely on the basis of desired maneuverability or control gradient.

47
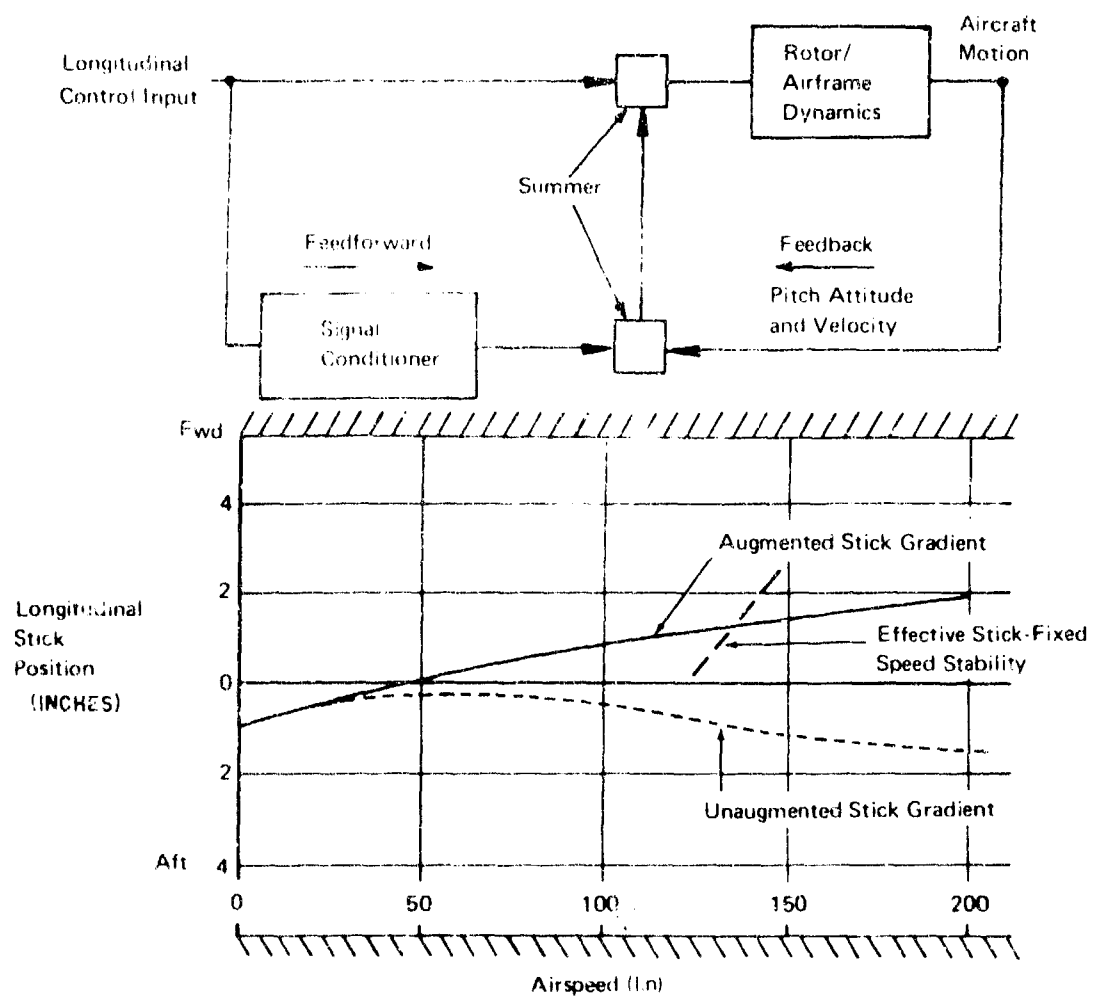
**FIGURE 3. LONGITUDINAL STABILITY/MANEUVERABILITY (SUMMING TECHNIQUE)**

48
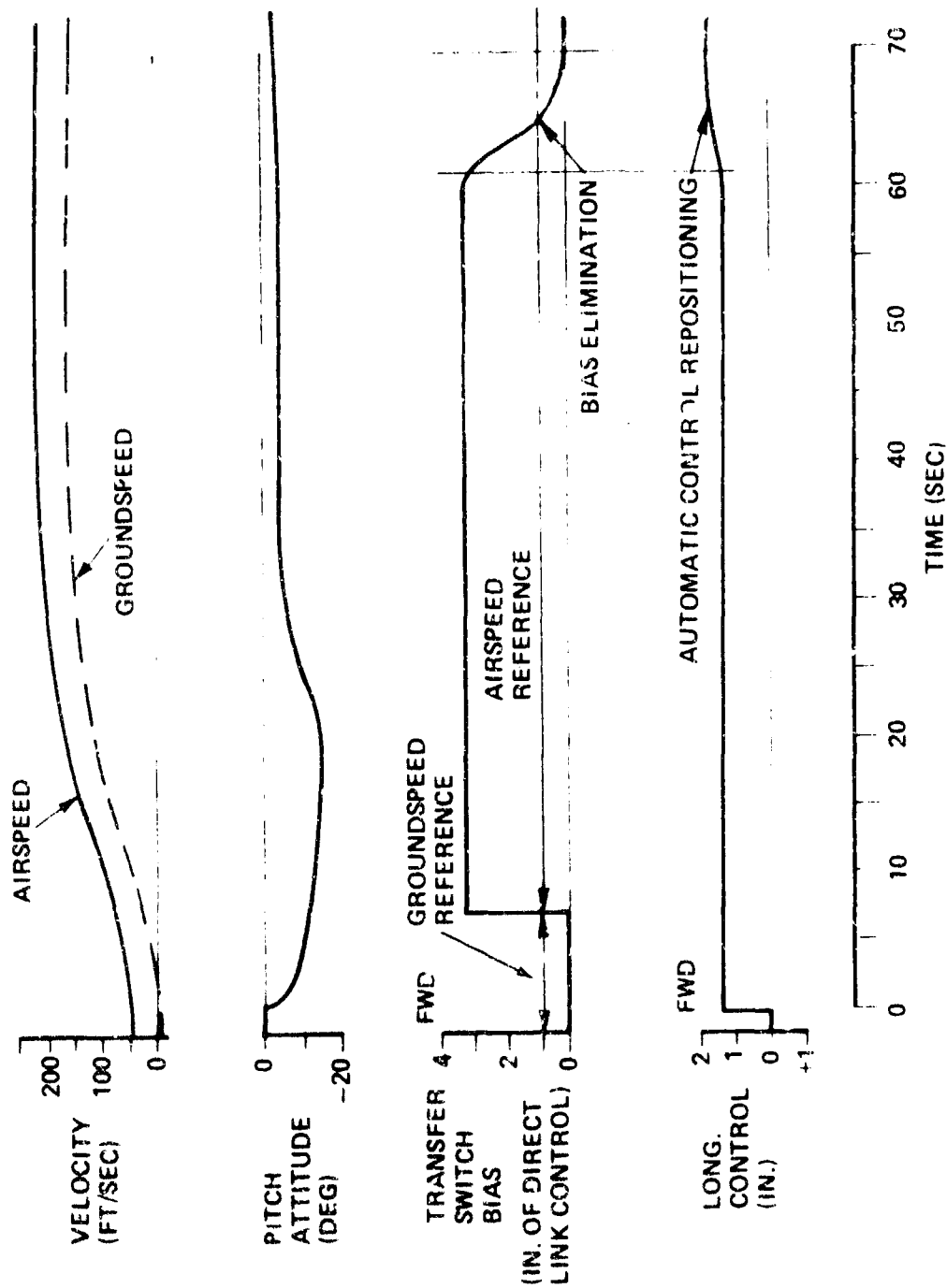
FIGURE 4. INSTANTANEOUS GROUNDSPEED TO AIRSPEED REFERENCE TRANSFER BIAS ELIMINATION, 30 KNOT HEAD WIND

49

The low speed heading hold and yaw rate command control laws,
(shown in Figure 5), are an example of use of logic techniques
to effect separate functional optimization within the AFCS.
Directional stability is provided by yaw rate and heading
signals. The heading signal is also processed through a
synchronizer. Pilot maneuver initiation causes instantaneous
heading synchronization (with the heading feedback going to
zero), and the result is a yaw rate response. At maneuver
completion, synchronization ceases and a smooth return to the
heading hold condition follows.

1.4.1.2  Low Speed to Forward Flight Velocity Reference Change

The desired velocity reference is groundspeed for low speed
operations, and airspeed in forward flight (as shown in
Table 3). Winds create a difference in the reference feed-
back signal which would tend to introduce transients on
switching if provisions were not made in the AFCS to correct
for the problem. To illustrate the point, an aircraft hovering
in a 40-knot wind would see an airspeed of 40 knots, and the
groundspeed would be zero.

Transients resulting from switching between these two ref-
erences are avoided with a velocity reference transfer switch,
which provides a bias signal to reposition the cockpit stick
and cancel the disparity between the references. The bias
signal is proportional to the amount the cockpit control is
offset from its true groundspeed or airspeed position. Bias
is removed after force trimming the stick, by slowly parallel
backdriving the controls to their correct position without
disturbing the aircraft (see Figure 4).

As pointed out earlier in Table 3, changes occur in lateral
and directional control functions between low and high speed
flight. In hover, heading is controlled by the directional
pedals and in forward flight by lateral stick motion. This
crossover is accomplished by using the same transfer logic
described for the longitudinal axis, with the bias signal
representing the difference between lateral velocity feedback
at low speed, and bank angle in forward flight.

50
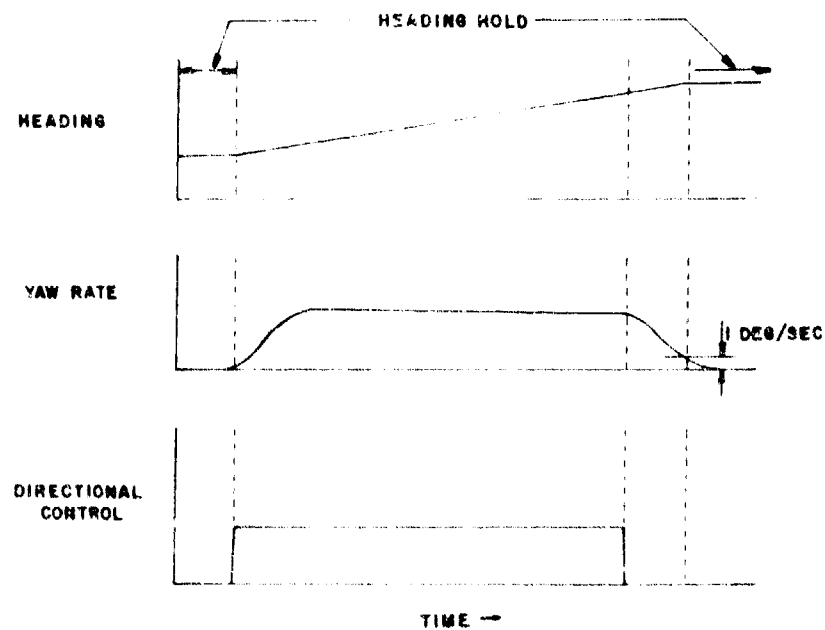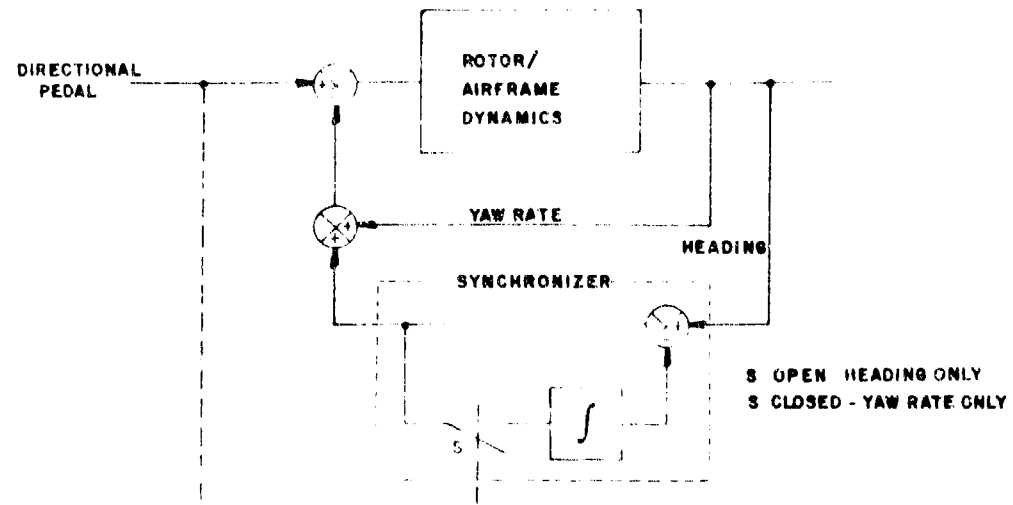
FIGURE 5
DIRECTIONAL STABILITY/MANEUVERABILITY
(LOGIC TECHNIQUE)

51

### 1.4.2  Additional Selectable AFCS Control Modes

#### 1.4.2.1  Altitude Hold Mode

Altitude hold engagement results in automatic altitude main-
tenance over the full flight envelope.  When the aircraft is
less than 200 feet above the ground, the system uses radar
reference.  Above 200 feet, barometric reference is utilized.
Inertial damping is provided at all altitudes, using a fil-
tered vertical acceleration signal on barometric reference,
and radar altitude rate complemented with vertical accelera-
tion on radar reference.

#### 1.4.2.2  Hover Hold Mode

The precision hover accuracies specified for helicopter and/
or load control necessitate an automatic hover positioning
and hold system.  With the helicopter hovering 50 feet above
the surface, human perception and reaction times are inadequate
for manual performance of the task without assistance.

To provide automatic precision hold capability, high gain
feedback loop closures using extremely accurate ground velocity
and position information are incorporated into the AFCS con-
trol laws.  A self-contained gyro-stabilized Precision Hover
Sensor (PHS) developed specifically for the HLH, generates
the required position and velocity feedbacks relative to the
scene observed beneath the helicopter.  The sensor uses an
optical position tracking scheme for perceiving movement in
the horizontal plane, and a laser ranging device to establish
vertical motion.  Design accuracies for the sensor reflect a
$\pm$ 1 inch or better position capability for all axes, and a
velocity tolerance of $\pm 1$ inch per second.  Maximum velocities
are limited to three feet per second.  Horizontal range is
$\pm$ 4 feet and the altitude operating band lies between 25 and
125 feet.

Estimated aircraft position hold capability as a function of turbulence level is shown in Figure 6. Note that the lateral axis is most sensitive, with the $\pm4$-inch position hold objective achieved in turbulence having peak gusts up to 5 feet per second. Flight test results with the 347 Research Vehicle show these estimates to be reasonable.

If the signals from the PHS sensor are unavailable due to poor scene contrast or excessive aircraft translational speed, the hover hold system reverts to a tight velocity maintenance system using groundspeed references from inertial and radar sources.

The load-controlling crewman (LCC) operates through the Hover Hold system to precisely control the aircraft, using a four-axis sidearm finger/ball controller to accomplish the task (see Figure 7). The controller stick is manipulated with the fingers and thumb of the right hand, while the forearm and wrist are supported by an armrest. The left hand is free for winch control operation.

Fore-and-aft stick motion produces up to $\pm15$ feet per second longitudinal groundspeed and right or left movement commands up to $\pm15$ feet per second lateral velocity. Twisting the ball results in up to $\pm8$ degrees per second yaw rate; while vertical motion commands as much as $\pm360$ feet per minute rate of climb. By visualizing the ball as the aircraft center of gravity, the LCC can easily relate his control input to movement of the aircraft.

Velocity commands are non-linear in all axes. As illustrated in Figure 7, low magnitude inputs around trim result in very small (creep) velocity changes. Larger inputs afford substantially greater (leap) velocity responses. With the precision hover sensor operating, LCC controller (beep) pulses are used to produce aircraft displacements of $\pm2$ inches about the precision sensor fix. This allows individual axis position tuning without the loss of position hold, which is particularly important in turbulent conditions. Command authorities are referenced to relative groundspeed, as noted in the figure and are applicable with winds up to 45 knots from any direction. Zero relative ground speed may be referenced to either a fixed or moving target (such as a ship steaming at sea).

53
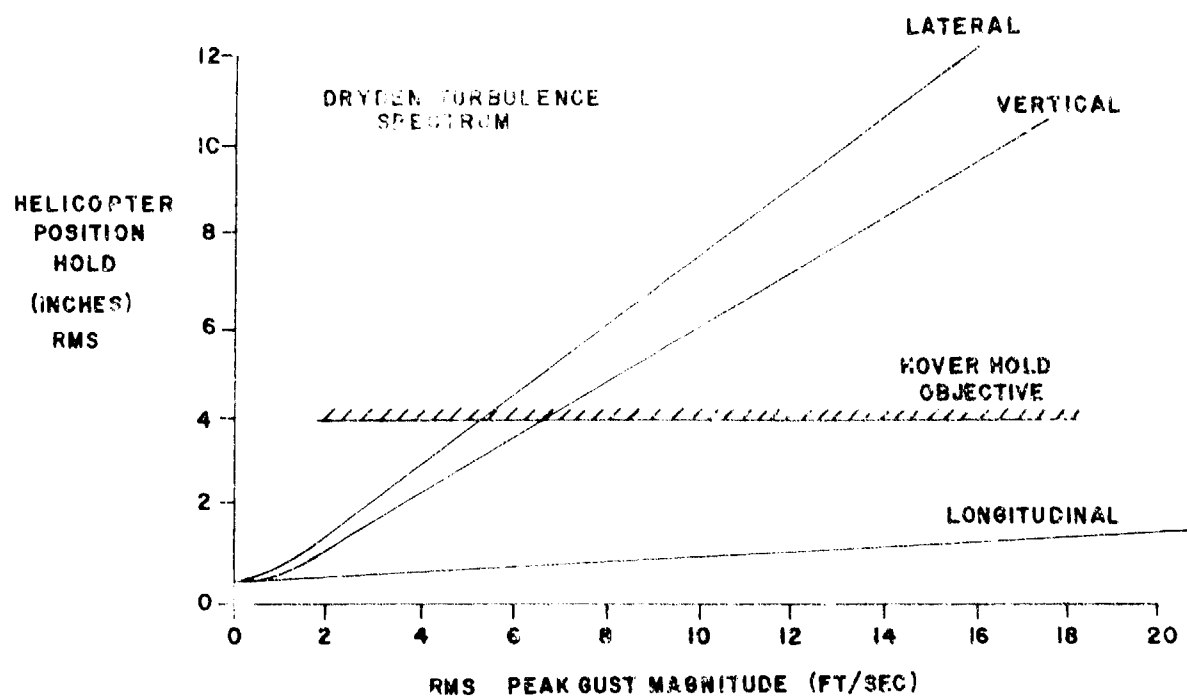
FIGURE 6.   HELICOPTER HOLD CAPABILITY IN TURBULENCE

54
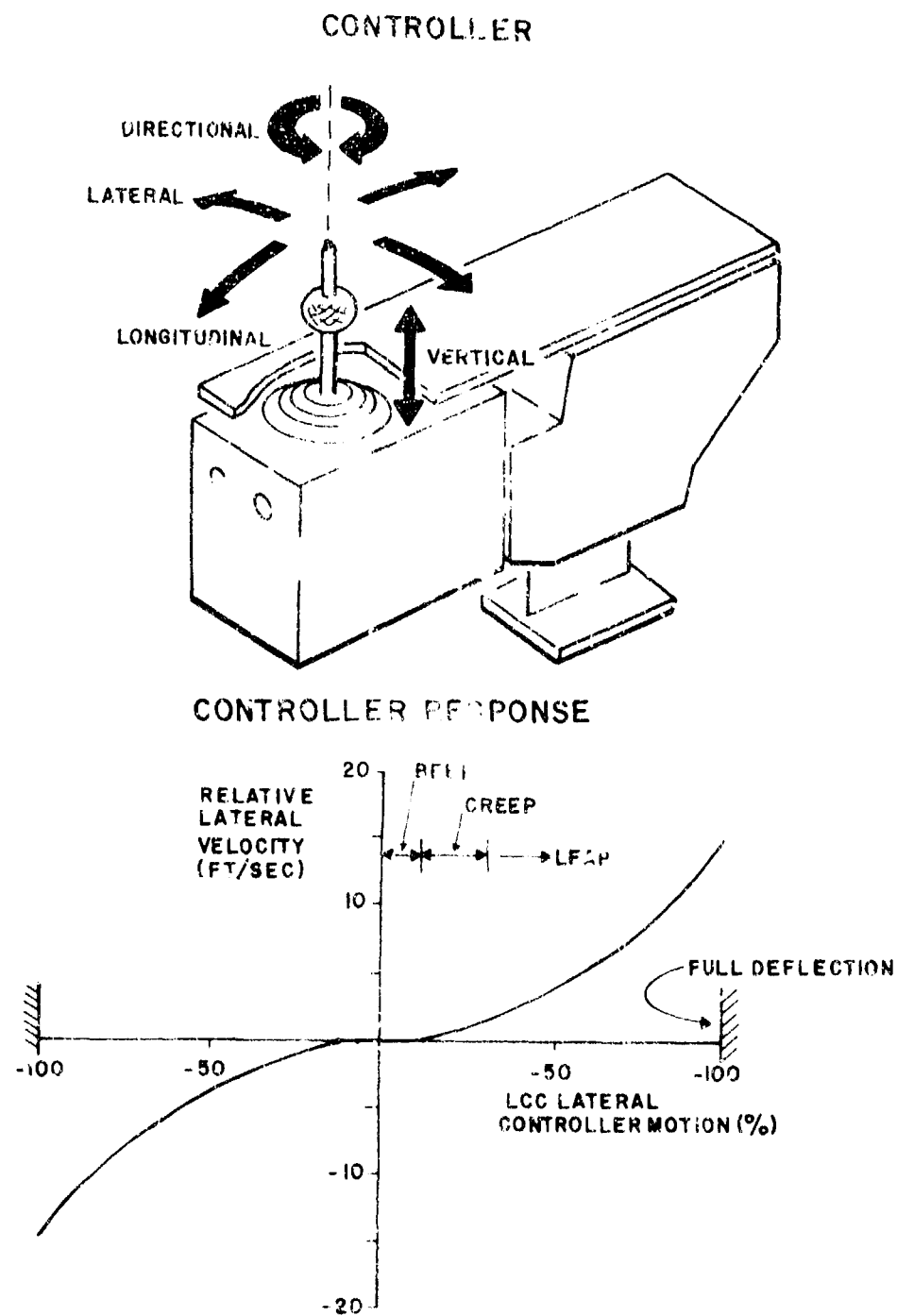
FIGURE 7.
LCC CONTROLLER CONFIGURATION & RESPONSE SCHEDULING

The tandem rotor helicopter design affords a unique translational velocity response characteristic for LCC longitudinal maneuvers, through use of longitudinal cyclic pitch or thrust vector tilt. Longitudinal translation is effected with minimal fuselage pitch rotation, thereby eliminating the usual lags in position response associated with this type of maneuver.

1.4.2.3    Load Stabilization Mode

The load stabilization system (LSS) provides three control functions, all of which are illustrated in Figure 8. These include:

Load Centering - where the aircraft is automatically centered and held over a load until liftoff to prevent load dragging.

Load Stabilization - providing pendular mode damping enhancement.

Load Position Hold - which maintains aircraft position over the load during liftoff, and holds load position relative to the ground when airborne.

Lightly damped low-frequency load pendulum modes cause two significant problems relative to the HLH mission. First, the task of placing the load accurately is difficult and time consuming, since load oscillations created by aircraft maneuvering or turbulence require an exceptionally long time to decay. Second, sustained low-frequency longitudinal helicopter accelerations due to load motion are disorienting and fatiguing to the pilot, and can lead to pilot-in-the-loop oscillations during instrument flight.

1.4.2.4    Hover Trim Mode

To overcome the problem of establishing zero groundspeed in low visibility IFR conditions, a hover trim system was developed and evaluated. When the mode is selected, aircraft controls are automatically driven to a force trim reference corresponding to zero groundspeed.

56
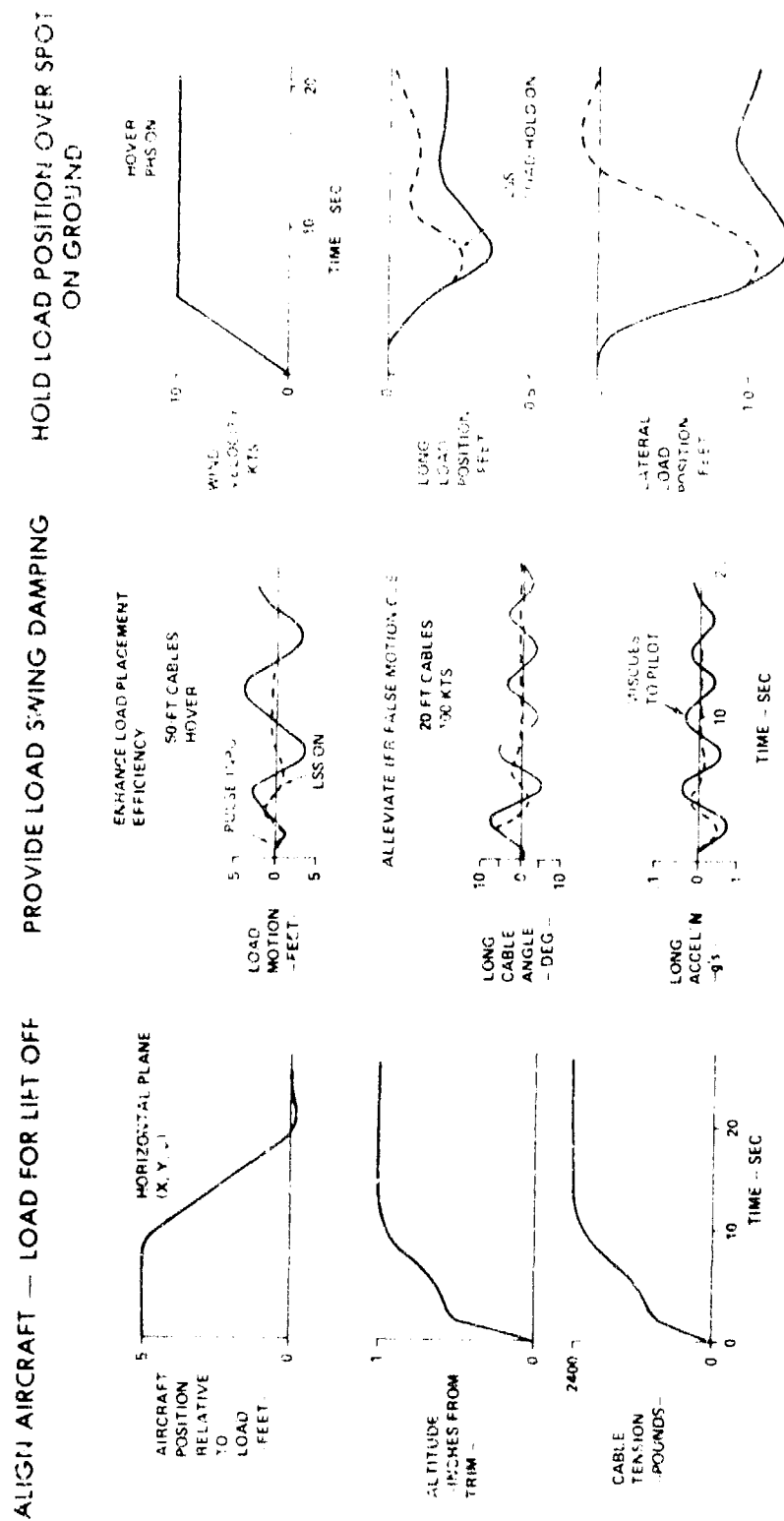
FIGURE 8.
LOAD STABILIZATION

### 1.4.2.5 Automatic Approach to Hover Mode

The automatic approach to hover mode requires navigation and guidance processing. The navigation information is required for present position and destination coordinate references. Guidance processing consists of programming the vehicle to follow a predetermined transition to hover. Only the guidance control laws required to perform the actual transition, with the pilot either in or out of the loop, were covered in the ATC program. The system can then be coupled to various types of navigation systems which provide the proper coordinate references.

### 1.4.3 Control Law Applicability to HLH

Due to aerodynamic similarity, the set of control laws developed for demonstration on the 347 Flight Research Vehicle will be directly applicable to the HLH AFCS. Unpiloted hybrid simulation results indicate that the HLH will have handling qualities similar to those exhibited by the 347, with only minor changes in control system gains, time constants, etc., required to achieve this capability.

### 1.5 AFCS HARDWARE IMPLEMENTATION

Hardware developed for feasibility demonstration of the HLH AFCS on the 347 Flight Research Vehicle includes a set of triplex incremental digital flight control computers and input/output processors (IOPs), various sensors (including the Precision Hover Sensor already discussed), and associated control and display panels.

AFCS computers, IOPs, and special panels were developed and built by the Aircraft Equipment Division of the General Electric Company. The AFCS mechanization concept relating AFCS hardware components and the primary flight control system is illustrated in Figure 9. On the left are shown the different control input signals and mode selections passing into the computers through analog to digital (A/D) converters and the discrete interface. Analog sensor signals for stability augmentation are shown on the right.
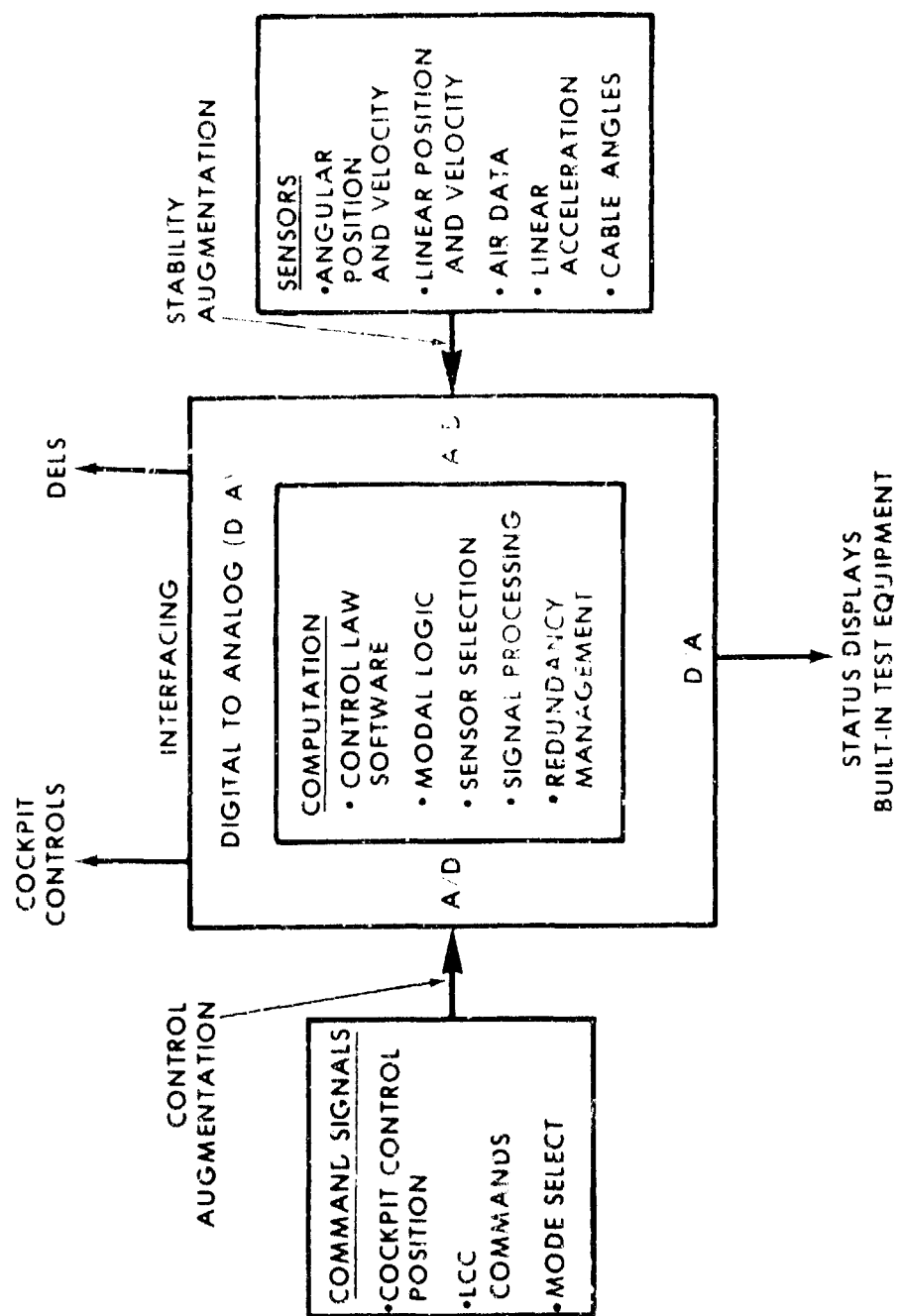
**FIGURE 9.**

**AFCS MECHANIZATION CONCEPT**

Control law computations, sensor selections, signal processing, and redundancy management tasks are carried out within the computer/IOP network, along with required modal logic switching. Processed output commands pass through D/A converters to the cockpit driver actuators or into the DELS.

A description of the major AFCS hardware elements and the functional relationships existing between components follows.

## 1.5.1  Flight Control Computers and IOP Processors

Digital techniques were selected to perform the AFCS computations because of requirements for:

* Maximum transfer function flexibility

* Precision in axis transformation and integration of functions while maintaining adequate stability margins in the presence of high-gain loops

* Close tracking of redundant signals to minimize failure transients

* Built-in test capabilities which generally involve software rather than hardware.

### 1.5.1.1  Computers

The three computers utilized for processing AFCS control laws (see Figure 10) are identically programmed serial-incremental machines. A time-shared incremental arithmetic unit (in each computer) is a mechanization of a special algorithm which is specifically designed for efficient solution of algebraic and differential equations. Processing operations performed by the arithmetic unit are specified by software program instructions for each algorithm function. Individual computers have processing capability for 256 algorithms with branching available for an additional 256. Computations utilize 16-bit effective word/lengths corresponding to $\pm 32,767$ machine units.

The basic computer system bandwidth is established by the slew rate limit, input filters, and sampling rate. Slew rate limits define the peak rate at which internal variables can change in incremental type computers. The largest variable increment

60

INPUT/OUTPUT PROCESSORS

INCREMENTAL DIGITAL COMPUTERS
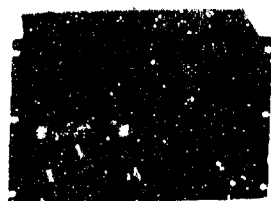
PARAMETER CONTROL & DISPLAY UNIT     MODE SELECT PANEL     TEST FUNCTION PANEL     FAILURE STATUS DISPLAY
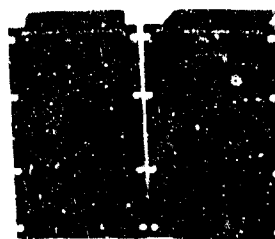
DISCRETE SIGNAL STATUS DISPLAY     BITE

FIGURE 10.

FLIGHT RESEARCH VEHICLE AUTOMATIC FLIGHT CONTROL
SYSTEM COMPONENTS

61

used is 64 machine units (iterated approximately 101 times per second) to produce a slew rate maximum of 6510 machine units per second.

Each computer contains extensive on-line internal monitoring. Parity checks and timing monitors are used to provide a comprehensive failure detection capability. Functions such as integration have software limiters programmed for overflow protection. Hardware monitoring is available to shut down an affected computer in the event of computational overflow. Program control and address instructions, along with fixed parameter data are stored in four read-only-memory (ROM) circuit boards. Shift registers and random access memory devices provide storage for whole word and incremental variables. Memory protection is incorporated into the ROM design so that power loss or electrical transients will not alter stored data.

The HLH prototype vehicle will use the AFCS computing hardware demonstrated on the Flight Research Vehicle with minor reprogramming for HLH parameters.

1.5.1.2  IOP Processing

Each of the three IOPs (shown in Figure 11) performs the following operations in support of its associated computer:

● Sensor and discrete input signal conditioning; i.e., demodulation, filtering, and level changing

● Input signal multiplexing and analog-to-digital conversion

● Cross-channel serial digital data communication

● Input signal failure monitoring and signal selection

● System and axis level fail shutdown logic

● Hardware processing of flight control law modal logic

● Digital-to-analog conversion and sample/hold for command and display outputs

● Off-line BITE, i.e., control, sequencing, and monitoring

62
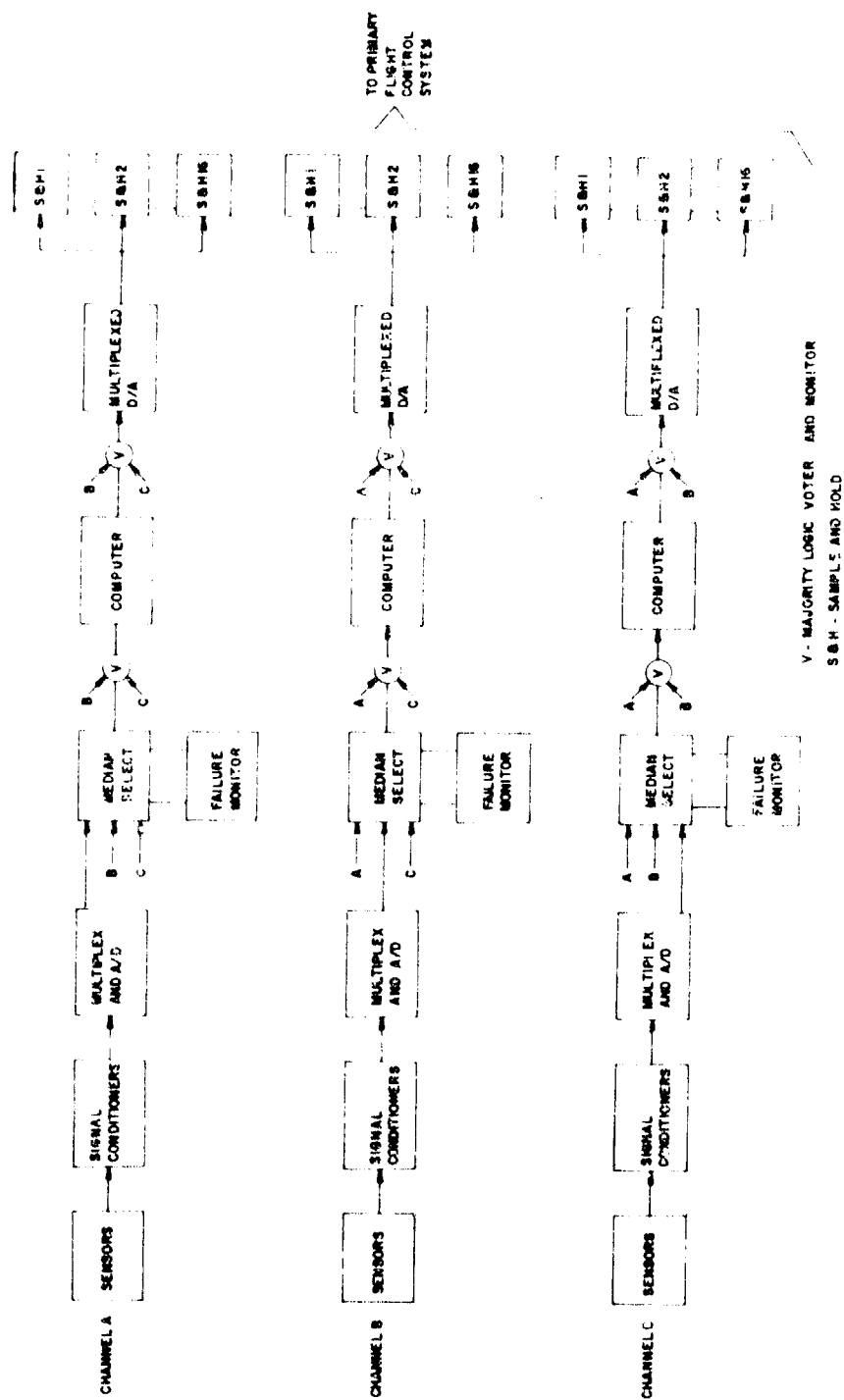
FIGURE II. SIGNAL INTERFACE FLOW FOR TRIPLEX SENSORS AND COMPUTERS

V - MAJORITY LOGIC VOTER AND MONITOR

S & H - SAMPLE AND HOLD

63

Individual IOP processors accept 32 channels of differential analog AC and DC data, four channels of 400 Hz, AC synchro, and 2 channels of serial-digital whole-word data, and 64 discrete logic inputs. Outputs include 16 channels of DC analog sample-hold data and 110 discrete signals.

As depicted in Figure 11, sensor signals input to each IOP are passed through signal-conditioning circuitry. The signals are then crossfed among the three IOPs followed by a median selection in the input processor. This insures that each processor transmits the same data signal to its computer. Concurrent with median selection is a failure monitoring function to determine which signal, if any, exceeds allowable tolerances. Correct identification of sensor failure constitutes the most difficult part of redundancy management.

Subsequent to a first failure, the remaining two signals are averaged which minimizes any transient in the event of a second identical sensor or signal-conditioning failure. The AFCS, being single-fail operational, will continue to function normally after first failure, but will shut down after an identical second failure. The averaging will generally reduce any transient associated with the signal zeroing after second failure. The signals are majority voted within the computers. This precludes a transmission line failure between the IOP and computer which would cause a computer shutdown.

The majority voting insures that the three computers all receive the same input signals so that each computer processes data identical to the least significant bit. The three signals are again voted in the output stage of the input/output processor, then converted to analog for transfer to the primary flight control system, or to the various status and control panels, as appropriate.

Built-in Test Equipment (BITE) functions are an important part of the IOP design. The BITE system is semi-automatic and is used to check system failure detection circuits. The concept employed can determine during preflight test that all failure monitors are working properly, greatly reducing the probability of an undetected in-flight failure. The BITE system can only be armed when the engine throttle levers are in the OFF position; otherwise BITE is inhibited to preclude inadvertent operation during flight which would cause AFCS failures.

64

## 1.5.2  Sensors and Control/Display Panels

The continuous sensors utilized in the AFCS include triple-,
dual-, and single-redundant sensors.

- Triple-redundant sensors include pitch and roll attitude;
  heading; pitch, roll, and yaw rate gyros; load-control-
  ling crewman controller individual axis positions; side-
  slip, and airspeed.

- Dual-redundant sensors include longitudinal and lateral
  ground speed, reference barometric altitude, and vertical
  acceleration.

- Single sensors include a precision hover sensor to sense
  three-axis incremental position and three-axis ground
  reference velocity, a radar altimeter to sense altitude
  and altitude rate, forward and aft external load cable
  angles, and forward and aft external load cable tensions.

The AFCS also utilizes various discrete sensors such as cock-
pit control detents and ground contact switches.

Control and display panels used in the AFCS flight demonstra-
tion are divided into two groups.  The first covers those
panels required for the production HLH configuration, including
mode select, two failure status depiction panels, and BITE.
A second group required to support flight testing of the
developmental system has a parameter change/display unit, a
system test function panel, and two discrete status panels.

The mode select panel (shown in Figure 10) provides normal
control of pilot selectable modes as well as BITE arm and
fault reset functions.  The AFCS failure status panel provides
a display of failures within the computers and IOP units, and
a "second fail" display is also available.  The BITE panel
utilizes a rotary detent switch to select a channel for testing,
and incorporates a series of six lights to identify the test
number in progress.

65

### 1.5.3   Redundancy Management Scheme

The combined sensor, IOP, and computer system depicted at the bottom of Figure 10 provides fail-operational/fail-safe performance for triplex sensors, failsafe performance for dual sensors, and fail-limited performance for single sensors. Fail operational is used for a system first failure. Fail operational performance is defined as that condition where no system performance degradation is experienced with a system first failure. Fail-safe is used when a system second failure occurs. Fail-safe performance is defined as that condition where any transient control signal transmitted to the primary flight control system upon a failure can be safely compensated for by pilot action. Fail limited is defined as that condition where failure of a nonredundant sensor associated with a selectable mode is limited to a magnitude which permits the pilot to override and/or switch off the affected mode.

The AFCS, although not considered essential to safety of flight, is categorized into three regimes regarding criticality and consequent functional capability following loss or degradation of equipment capability:

- System level failures are deemed most critical, requiring total AFCS shutdown and reversion to unaugmented flight.

- AFCS axis failures require the shutdown of individual or multiple combinations of axes.

- Selectable mode failures, deemed least critical, require manual disengagement or pilot override of the selected mode.

Majority Logic Voting/Failure Monitoring - As shown in Figure 11, the processed sensor signal is sent from each IOP to all three computers, whereupon separate input voters compare the three inputs, (bit-by-bit), two at a time. The voter outputs a signal corresponding to two of its three inputs. If one input differs from the other two, a first failure output is generated. Subsequent to the first failure, a second failure output is generated when the remaining (and previously non-failed) signals differ. Voter and failure monitoring circuits are placed at strategic points throughout the computer and IOP network to assist in rapid fault detection.

### 1.5.4 DELS Interfacing for the AFCS

AFCS interfacing with the DELS consists of splitting the
differential signal into trim and dynamic compensation paths
as illustrated in Figure 12. The trim path provides long-term
trim correction of a low-frequency nature, as typified by
the directional pedal offset with airspeed. High-frequency
compensation requirements like yaw rate damping are provided
by the dynamic path. Separate amplitude limits are included
for each path. Cross signaling from the static path contin-
ually recenters the dynamic path.

The network reduces smoothly to zero after AFCS disengagement-
switch closure. This means that cockpit control sensitivity,
power, and margins are unaffected by AFCS hardover conditions.
Authorities and signal conditioning were selected to keep
short-term impulse-type disturbances after hardover, as well
as long-term trim changes, within safe levels. Thus, the
AFCS can experience a hardover without impairing flight
safety.

### 1.6 FLIGHT EVALUATIONS

### 1.6.1 347 HLH/ATC Demonstrator Aircraft

The Boeing 347 Flight Research Aircraft was used to demon-
strate HLH fly-by-wire feasibility and handling quality con-
cepts. Inherent stability and control characteristics of the
347 are similar to the HLH.

A retractable capsule was installed to simulate the HLH load-
controlling crewman station. The station was equipped with
the prototype finger/ball controller and necessary mode select
panels. A two-point load suspension system is incorporated,
and a top lift adapter with remote LCC locking mechanism con-
trol was available for acquisition of an 8x8x20-foot MILVAN
container.

The mechanical control runs between the cockpit controls and
swashplate power actuators were disconnected and replaced by
a DELS fly-by-wire linkage (Volume II). The automatic control
system used triplex incremental digital computers with sep-
arate input/output processors containing modal logic.

67
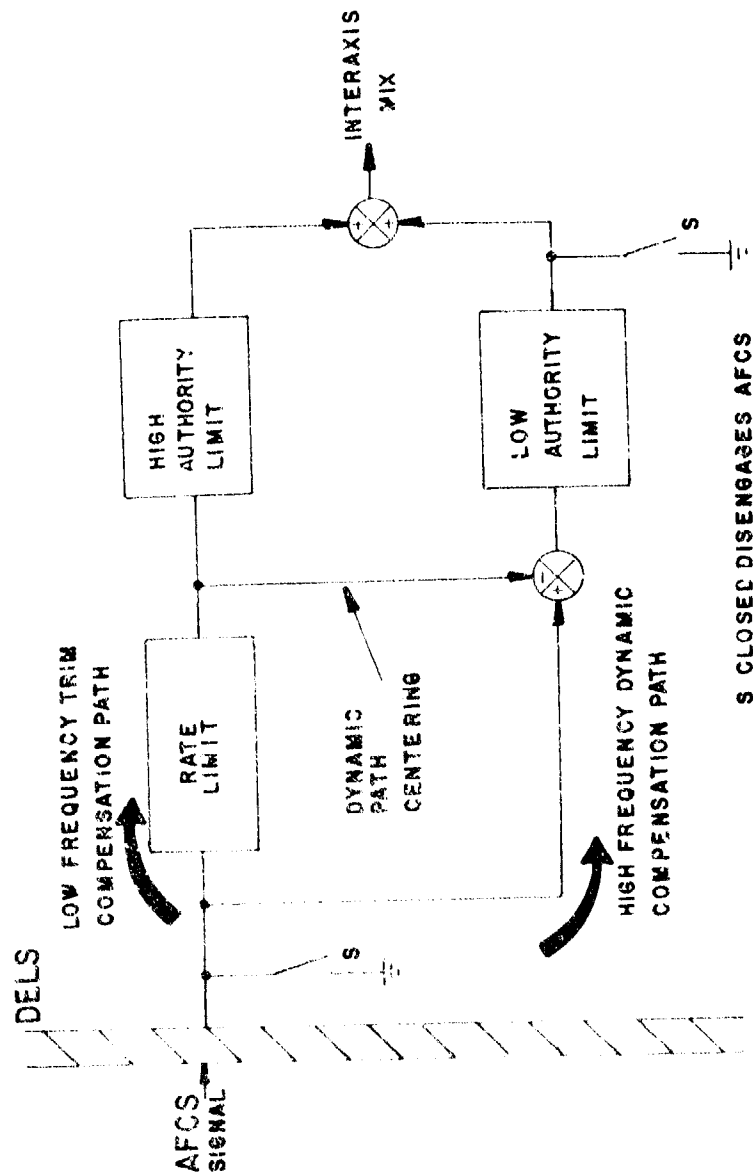
FIGURE 12. HLH FLIGHT CONTROL SYSTEM DELS AFCS INTERFACE

## 1.6.2  Testing

Flight development testing was conducted between April and October of 1974 with approximately 36 hours devoted to basic SCAS, 46 hours to hover hold and LCC operation without a load, and 64 hours with a load including load stabilization. Two U.S. Army preliminary evaluations were conducted.

AFCS flight testing was accomplished in a sequential manner using four software program phases- (1) Basic SCAS, (2) Basic SCAS and Hover Hold, (3) Basic SCAS, Hover Hold, and Load Stabilization, and (4) Basic SCAS and Automatic Approach to Hover.

## 1.7  RESULTS AND CONCLUSIONS

The principal conclusions of the ATC program reviewed in this section reflect results of the AFCS flight evaluations.

Recommendations are based on test results and address the feasibility of HLH handling qualities concepts.  Basic SCAS is covered first, followed by selectable modes.

### 1.7.1  Basic SCAS

The basic SCAS operation was evaluated throughout the flight envelope and included assessments of dynamic and static stability, controllability, and velocity reference mode switching.

#### 1.7.1.1  Dynamic Stability

Dynamic stability evaluations were performed by injecting pulses and steps into the flight controls by means of the AFCS test function panel controls (differential pulses and parallel steps), and also by manual inputs by the pilot.  Dynamic stability in all axes was very good with a pilot qualitative rating (PQRS) of 1.5.  Damping augmentation in the vertical axis was found to be unnecessary because of high inherent damping of the basic airframe.

## 1.7.1.2  Static Stability

Static longitudinal and lateral/directional tests were con-
ducted in level flight, turns, climbs, partial power descents
and autorotation.  Control trim gradients and groundspeed,
airspeed, bank angle and heading hold characteristics were
assessed.  Longitudinal, lateral and directional control
gradient augmentation performed very satisfactorily.  Large
changes could be made in either airspeed or vertical speed
with no need for pilot trimming in any other axis.

Airspeed hold above 100 knots was excellent (PQRS A-1) in
both stabilized and maneuvering flight.  In turn maneuvers at
slow to moderate speeds (50-80 knots), airspeed hold was poor.
Airspeed increased 5 to 10 knots in right turns and decreased
slightly in left turns (A-4).

Groundspeed Hold below 45 knots was acceptable for normal
hover and low speed maneuvering (A-3).  The velocity gains
were too low, however, to enable the pilot to precisely
acquire and maintain a zero velocity trim for holding posi-
tion during cargo operations (A-4).  The higher hover hold
gains (6X SCAS levels) were near optimum for meeting these
requirements.

Bank angle and heading hold stability was satisfactory over
the complete envelope (A1.5).

## 1.7.1.3  Controllability

Aircraft response to primary control and beep trim inputs was
evaluated during hover, transition, and forward flight. Approach
and departure maneuvers, including roll-on landings and run-
ning takeoffs, were conducted.

Beep trim was acceptable in longitudinal and lateral control
(A1 to 1.5), however, the desirability of a variable rate beep
trim control in lieu of fixed rate control was indicated. The
present compromised gain is too high for vernier beep inputs
in hover, and too low for "beep and hold" inputs used to change
speed or conduct turn maneuver in cruise.  Directional beep
trim control operated acceptably.  It was judged to be
unnecessary in the Model 347 aircraft, due to good pedal
control characteristics of the augmented aircraft.

Maneuverability characteristics demonstrated in longitudinal
accelerations and decelerations, pedal fixed coordinated
turns, and sideslips, etc., were excellent (A1 to 1.5).
During "hands off" level flight rapid deceleration maneuvers,
using high nose up attitudes, AFCS/DELS interface authority
was bottomed at approximately 20 knots and required pilot
stability inputs to complete the maneuver. The limited bank
angle lateral stick gradient (security blanket) offered
improved trimmability about zero bank angle, as well as a
control free return to "wing level" trim.

The 347 helicopter was equipped with a "fixed" control force
feel system, consisting of breakout forces, linear gradients
and viscous damping. In ATC flight tests covering all areas
of HLH flight operations, there was no indication of any
shortcoming in the fixed force feel system; nor did there
appear to be much potential for significant improvement in
handling qualities with a programmable force feel system.

1.7.1.4  Velocity Mode Transfer Switching

The automatic transfer between ground referenced IMU veloci-
ties below 45 knots, and airspeed reference (or visa versa)
was thoroughly checked by performing straight and turning
acceleration and deceleration maneuvers in different effec-
tive wind conditions.

For most maneuvers, velocity reference transfer was transient
free and bias elimination through control backdrive generally
went undetected by the pilot (A2 to 2.5). During accelerations
wherein steep turns were initiated just prior to velocity
reference switchover, the lateral bias magnitude was suffi-
ciently large to exceed available AFCS/DELS authority limits
making retrim difficult (U-7).

1.7.1.5  Basic SCAS Recommendations

All basic SCAS functions are desirable for incorporation in the
HLH AFCS except for vertical damping augmentation. The
following improvements should be incorporated to overcome the
deficiencies noted above.

72

Airspeed Hold in Turns (60 to 80 knots) - Incorporate a bank angle crossfeed into the longitudinal axis, scheduled with airspeed to compensate for airspeed deviations.

Pilot Control in Hover Hold Mode - Provide the pilot a vernier velocity control capability through stick beep trim when the hover hold mode is engaged. In addition, incorporate a pilot override capability of any individual axis when on hover hold. This permits larger position change maneuvers on basic SCAS without disengaging all hover hold axes.

Hands-Off Steep Flare Controllability - Incorporate a parallel stick backdrive command to provide additional attitude stabilization when the AFCS/DELS interface is approaching saturation.

Force Feel System - Eliminate programmable force feel from the HLH requirements.

Velocity Mode Transfer Switch - Incorporate a limit on the output of the lateral velocity transfer switch to provide AFCS control margin for damping. Revise logic to inhibit lateral velocity mode transfer until bias magnitude is below a preselected value.

1.7.2   Altitude Hold

1.7.2.1   Barometric Reference

Reasonable altitude hold characteristics were realized on barometric reference (A-2). Small continuously changing collective and power corrections to maintain altitude during cruise in turbulent air were very undesirable. Excessive altitude deviations ($\pm$60-80 feet) occurred in steep banked turns at slow airspeeds.

Transmission overtorque by automatic collective pitch drive occurred when operating near torque limits (A-5). Test pilot monitor and collective override maintained acceptable limits in the ATC test program.

1.7.2.2  Radar Reference

Altitude hold in the hover region on radar reference was
acceptable when the sensor was performing satifactorily
(A1), but was substantially degraded during flight over grass
due to frequent sensor noise spikes.  In addition, load
interference with the radar beam for 50-foot cables caused
heavy aircraft vertical deviations (U-8).  In forward flight
below 200 feet altitude, sharp movements of the collective
were created in an attempt to follow the terrain contour.

1.7.2.3  Automatic Baro/Radar Reference Switching

Transitions through the 200-foot switch point were accomplished
with no apparent transients (A-2).  Aircraft transients due
to hardover failures of the single radar altitude reference
are unsafe and unacceptable during precision cargo operations
(U-8).

1.7.2.4  Altitude Hold Recommendations

Both radar and baro hold functions are desirable for use in
the HLH with the following modifications.

Altitude Hold Control Laws

Provide barometric altitude hold in cruise through the longi-
tudinal AFCS by programming small attitude and airspeed cor-
rections, and retain collective pitch programming for long
term trimming only.

Provide torque limiting to prevent dynamic system overtorque
in turn maneuvers and heavy load acquisition with altitude
hold on.

Provide an airspeed interlock for the automatic altitude hold
sensor logic to inhibit automatic selection of radar altitude
above 50 knots.

73

Radar Altimeter Signal Quality

Noise Spikes - incorporate software modifications to compensate for signal deficiencies or improve existing sensor or replace with new sensor.

External Load Interference - incorporate baro signal selection capability on hover hold or reconfigure hardware.

Radar Altimeter Failure - incorporate vertical axis frequency splitter and provide redundant sensor.

1.7.3   Hover Hold Mode and LCC   Operation

1.7.3.1   Hover Hold/IMU - Radar

Hover hold stability and controllability characteristics (both with and without external loads) were evaluated by means of pilot and LCC step and pulse inputs, differential pulse inputs, aircraft maneuvers in and out of ground effect, and precision positioning of loads.  Gains set for this mode were judged near optimum to enable the LCC to control and stabilize the helicopter to zero relative velocity; however, pilot control was limited to the override only capability described earlier.

Heading and velocity hold performance on IMU reference was rated as good to excellent (A-1.5).  Vertical hover hold operations were also satisfactory when the radar altimeter was functioning properly, but problems with this altitude sensor caused deterioration in altitude hold capability as mentioned in 1.7.2.2.

Roll axis stability was degraded with external loads attached to the aircraft, causing a tendancy for roll oscillations to develop.

1.7.3.2 LCC Control

Longitudinal, directional, and vertical LCCC control response
and sensitivity were very good (A-1.5), but further development
is required in the lateral axis (A-4) to achieve precision load
positioning. Good acceleration and velocity hold
characteristics were demonstrated for shuttle maneuvers (A-2).
Additional LCC control authority was found to be desirable to
increase maximum translational velocity in the longitudinal
and lateral axes for further load shuttle optimization.

The "drift clear" function for removing IMU drift operated
acceptably (A-4), but requires improvement to reduce LCC
effort and eliminate transients and velocity errors. Trim
establishment following large wind shifts or commanded heading
changes at zero groundspeed was not quick enough, and apprec-
iable drifting of the aircraft occurred. The problem was
associated primarily with lateral cockpit control backdriving
rate, which was too slow.

Flight training requirements for the load controlling crewman
were minimal. Following development testing, 54 hours of
demonstrations at U.S. Army facilities were conducted in which
163 pilots and non-pilots flew from the capsule. Control of
the aircraft without a load was quickly mastered in 5 to 10
minutes, enabling precise positioning. Load operations were
performed by two Army pilots after 30 minutes of "no load"
familiarization.

1.7.3.3 Hover Hold/PHS

Excellent precision hold performance was demonstrated for the
Hover Hold/PHS mode over a high contrast checkerboard target
grid (A-1). The PHS would not lock on to grass or
other low contrast targets, however, and consistently exhibited
poor reliability during testing. For these reasons, the
sensor was not considered operationally acceptable in its
current state of development.

When the PHS did operate as designed, it was very useful for automatic drift clearing of the IMU. If the aircraft was was maneuvered over the target and the LCC released to detent, the PHS drove the aircraft to zero velocity and cleared any existing IMU drift.

Low velocity hover hold maneuvering while using the PHS reference was hampered by frequent undesirable control transients, and was therefore downgraded in performance because of this fact (A-5). The "beep" position control, on the other hand, performed well and was considered an excellent solution for achieving best accuracy.

1.7.3.4  Cargo Handling Characteristics

Cargo handling tasks including load hookup, shuttle, and placement with 10-and 30-foot cables were performed. Execution of these maneuvers was evaluated without benefit of the PHS due to the operational problems mentioned above.

Rapid load cable hookup by a ground crewman was performed easily since the LCC could precisely position the helicopter. MILVAN acquisition without ground crewman assistance was accomplished by positioning a toplift adapter on the MILVAN. Load maneuvering to maximum shuttle groundspeeds could be performed routinely.

With the final hover hold configuration, the MILVAN on 10-foot cables was placed consistently within a 1-foot accuracy, and on the load transporter pins ($\pm$ 1 in. accuracy required) occasionally. The MILVAN can be lowered onto the transporter pins with relative ease, using 18-inch guide vanes which funnel the load onto the transporter.

1.7.3.5  Hover Hold/LCCC Recommendations

Both hover hold modes were determined to be feasible for
application in the HLH AFCS.  The LCC control concept was also
validated.  Although the PHS requires additional
development before being used operationally, hover hold/PHS
control laws were sufficiently refined to meet precision
hold and positioning goals of the HLH mission.

The improvements listed below should be incorporated to
eliminate deficiencies delineated earlier.

Hover Hold/IMU-Radar:  Improved schemes for pilot override
and vernier control to position and trim the aircraft with
the hover hold mode engaged are necessary, as spelled out
in 1.7.1.5.

Recommendations for providing better radar altitude hold
performance, along with suggested improvements in sensor
signal quality and failure protection, are listed in
Section 1.7.2.4.

LCC Control

LCC Lateral Control Response:  Improve lateral response,
evaluate feasibility of increasing LCCC travel, and modify
controller command scheduling.

Aircraft Roll Excitation with Load:  Incorporate programmable
gain variation as a function of load weight.

LCC Control Authority for Shuttle Operation:  Adjust longi-
tudinal and lateral authority to permit an increase in
shuttle velocity to a maximum of 12 knots.  Reduce maximum
vertical velocity from 360 feet per minute to 240 feet per
minute.

Drift Clear Transients and Selection:  Latch the drift clear
operation until groundspeed errors decay to zero and/or
maintain groundspeed feedback throughout the drift clear
maneuver.  Evaluate relocation of the drift clear switch for
the load crewman.

Trim Re-establishment after Wind Shift or Turn Maneuver:
Increase CCDA backdrive gains when directional LCC is out of
detent, and evaluate feeding lateral LCCC commands into the
CCDA as a proportional drive.

Hover Hold/PHS: Use of the hover hold/PHS mode is desirable
whenever HLH mission requirements dictate precise hold and
position maneuvering with large external loads. Successful
application of the mode is heavily dependent upon reliable
signals being generated by the PHS. To provide these
signals, sensor development should be continued to:

- Ensure lock-on and accurate noise-free tracking over
  any type of surface, regardless of contrast.

- Substantially improve operational reliability.

- Package sensor components to minimize size and
  weight for production implementation.

### 1.7.4  Load Stabilization System (LSS) Mode

LSS pendular damping was evaluated in hover and forward flight
to speeds where the aircraft became power limited. Long and
short two-point inverted "Y" and "V" cable suspension config-
urations were tested, and the primary load utilized was an
8X8X20-foot MILVAN container. A high-density load and single-
point trolley combination was also tested. LSS damping was
assessed in hover from both the pilot's and load-controlling
crewman's stations.

The capability for automatic aircraft centering over the load
prior to liftoff was evaluated by starting out with the
helicopter displaced from the stationary load on the ground.
Aircraft/load offset was varied during the testing, and an
effort was made to maintain positive tension on both cargo
hooks throughout the maneuver to achieve satisfactory
performance.

The third LSS feature assessed was load position hold, which
required both the pendular damping mode and PHS to be active
for its operation. Test results for each of the three LSS
modes are reviewed below.

78

### 1.7.4.1   Pendular Damping

Load pendular damping provided by the LSS was very effective in attenuating load oscillations for all cable lengths, with the longer configurations being helped most. Using the 30-foot inverted "Y" suspension (which has low inherent damping because of the long cables), LSS damping contributions were judged to be good (A-3) for hover and load placement maneuvers, and particularly beneficial in stopping large amplitude directional limit cycling. A longer 50-foot sling load (of the type required to lower a load into confined areas) could not be manually stabilized by the pilot (or LCC) until the LSS damping loops were engaged.

Short cable testing (with an 11-foot forward and 9-foot aft inverted "V" arrangement) also showed improved damping provided by the LSS. Ride qualities in cruise were degraded slightly, however, as the aircraft was displaced to damp load motion (A-4), making light loads feel like heavier ones to the pilot. In hover and load placement maneuvering, lateral LSS damping inputs tended to work in opposition to lateral axis LCCC commands. Since the short sling lateral pendulum mode exhibits some inherent damping, LSS gains in the lateral axis were set to zero to correct the LSS/LCC conflict.

High density load testing showed significantly improved longitudinal/lateral damping characteristics with the LSS damping loops engaged. Increased control sensitivity associated with the higher load weight required the use of reduced roll attitude and rate gains in the SCAS with LSS on.

### 1.7.4.2   Aircraft Centering Over Load

Automatic aircraft centering over the load before liftoff was found to be feasible and the concept worked well for small ( 4-foot) aircraft/load offsets. Undesirable transients were produced if either cable became slack during the centering process, and this occurred frequently with larger lateral load offsets (rated U-7). Without the LSS centering feature engaged, the LCC found the manual centering task to be relatively easy. Because of this, requirements for a centering mode are relegated to a low priority for application on the HLH.

### 1.7.4.3 Automatic Load Position Hold

Use of additional LSS control laws, operating with the LSS damping and hover hold/PHS loops to stabilize load position was successful for the directional and vertical axes only. Essentially no improvement over basic LSS damping could be achieved because the position feedbacks tended to degrade damping levels. Due to the frequency response of the load modes, little improvement could be expected with the position loops engaged, since the load with LSS damping only is almost as tight as the aircraft without a load.

The most satisfactory configuration for load position hold utilized only the LSS damping loops and the hover hold/PHS networks.

### 1.7.4.4 LSS Recommendations

LSS Pendular Damping - Use of the LSS pendular damping mode is recommended for heavy lift applications. The feasibility of modifying lateral LSS control laws for the short cable configuration should be evaluated to ensure transient-free lateral maneuvering with the LCCC for the hover/load placement task. Also, an active pendant system should be considered (AAELSS).

Aircraft/Load Centering - An automatic load-centering capability is not necessary unless requirements for very low visibility centering with long sling load cables are instituted at some time in the future. Successful application of this LSS feature will require some type of automatic winch control to maintain cable tension throughout the centering operation.

Automatic Load Position Hold - Incorporation of additional LSS control laws for load position hold is not recommended for HLH implementation. The best hold performance is achieved with only the LSS damping and PHS position hold loops engaged.

### 1.7.5 Automatic Approach to Hover.

### 1.7.5.1 Description and Test Results

The automatic approach to hover mode was configured for demonstrating the feasibility to manually (following flight director commands) or automatically fly the aircraft down an approach path terminating in a stabilized hover. A "present"

approach profile was used, starting at 1,000 feet above the terrain and about 2-1/2 miles from the intended hover point and descending to a 100 foot hover following a flaring maneuver initiated 1/2 mile out at 295 feet.

Because of the fixed profile used, the point of termination depended upon where the pilot engaged the approach. Precise maneuvering was required to reach an initial approach gate which ensured terminal hover over the desired area. The concept mechanized for the test program was intended for demonstration of control processing and requires additional functional capability for operational implementation.

Manually controlled approaches using the flight director reference were easily accomplished under simulated IFR conditions (under the hood) both with and without external loads. The approach profile flown by the aircraft was very close to the planned path (A-3).

Automatic coupled approaches were also performed very satisfactorily (A-2.5), with and without load. No pitch attitude limits were incorporated in the approach control laws. Occasionally during developmental testing, excessive pitch attitudes resulted due to exceeding AFCS authority limits requiring pilot recovery.

1.7.5.2 Automatic Approach to Hover Recommendations

Automatic approach to hover would enhance HLH operational capability provided the approach gate and/or desired terminal hover position could be dialed into the INS. Control laws to permit this type of referencing should be developed, along with limits to correct for the occasional pitch attitude excursion problem described above.

A flight director is required for pilot monitor of automatic approaches. In addition, a selectable missed approach profile is also required on the flight director to assist the pilot in safe approach abort maneuvering in adverse weather.

### 1.7.6  Hover Trim

#### 1.7.6.1  System Performance

The hover trim mode was conceived to trim the aircraft to
hover (zero IMU velocity in the longitudinal and lateral
axes) from any flight configuration.  This capability offered
no significant mission enhancement, and as experience was
gained, the feature was judged useful only at slow speeds
(less than 40 knots) for automatically trimming the aircraft to
a hover.  System gains produced a very slow trim rate and
any IMU drift was reflected in the final trim condition
(A-5).  This mode was not optimized.

#### 1.7.6.2  Hover Trim Recommendations

Further development of the hover trim mode for HLH imple-
mentation is not recommended.

## 2.0 ATC SOFTWARE DEVELOPMENT – ANALYSIS AND FLIGHT SIMULATION

This report section summarizes the various analytical and piloted flight simulation tasks accomplished over two and one-half years in support of HLH AFCS software development. The work has been performed as part of the HLH Advanced Technology Component (ATC) program, with the principle effort directed toward flight demonstration of the HLH control laws and logic on the 347 Flight Research Vehicle, during the spring and summer of 1974.

Outlined below are the major areas of analysis and simulation reviewed in this report section:

- Design Analysis – Design criteria and approach are presented, followed by discussion of SCAS development and synthesis of each selectable AFCS Mode. Also given is a synopsis of the development of the redundancy management techniques applied in design of the AFCS.

- Piloted Flight Simulation – Both the full envelope AFCS evaluation flown on the Northrop Large Amplitude Simulator (LAS/WAVS) and the load crewman/LCC testing conducted on the Northrop Rotational Simulator are described.

- HLH AFCS Synthesis – Applicability of the Flight Research Vehicle control laws and logic to the larger HLH aircraft is established through analysis and unpiloted hybrid simulation.

- Computer Software – The programming approach, features of software control, and computing capacity, are treated.

## 2.1 DESIGN ANALYSIS

### 2.1.1 Criteria and Requirements

Comprehensive criteria were established for design of the HLH Automatic Flight Control System early in the ATC Program. The original ATC Statement of Work (Reference 2) contained a set of "design objectives" for the AFCS, and the Prime Item Description Document (PIDD) (Reference 3), delineated both objectives and requirements. The SOW design objectives are divided roughly into two groups with about half pertaining to handling qualities improvement and the remainder to specific "performance" type goals for the augmented aircraft. Handling qualities objectives include:

- Simplification of the piloting task.

- Optimization of vehicle handling qualities.

- Minimization of pilot switching modes of operation between flight regimes, and elimination of transients introduced as a result of mode switching or transfer of control between pilots.

Performance-oriented goals for the augmented aircraft are somewhat more specific in nature as indicated by requirements to provide:

- Capability for the pilot to position the helicopter and/or load (without visual ground reference) to a prescribed heading, at any height above the terrain up to 100 feet, and within 4 inches of a ground reference point. The design should permit accomplishment of the positioning task within 2 minutes, starting from a point 200 feet above ground level and 300 feet horizontally from the reference point, under gusty wind conditions, with steady winds of up to 45 knots from any azimuth.

- Capability for hands-off hovering (with or without suspended load) within $\pm$ 4 inches vertically, $\pm$ 4 inches horizontally, and within 2 degrees of a given heading, under the wind conditions prescribed above.

- Capability for automatic positioning of the helicopter vertically over a load once cables are attached and under tension.

- Capability for automatic load stabilization to eliminate dangerously unstable moments, thereby permitting the helicopter to be flown in IFR conditions without stabilization inputs by the pilot.

Other SOW objectives dealing with hardware performance are reviewed later in the AFCS hardware writeup (Section 5.0), or in the Flight Control System Volume II document which covers the PFCS.

Requirements defined in the PIDD, Volume I, relate handling qualities to mission accomplishment. This document states that the HLH flying and ground handling maneuverability and stability, with or without external payload, at all usable weights, CGs, airspeeds, and altitudes within the normal flight envelope, "shall be adequate to perform the design mission(s) in both IFR or VFR flight conditions". Included in the normal flight envelope are airspeeds to 45 knots in any direction starting from hover in still air.

The PIDD also stipulates that the MIL-H-8501A specification (Reference 4), with approved Army deviations for autorotational descent and landing, should be adhered to in determining aircraft handling qualities for both augmented and unaugmented flight or ground operation.

In addition to the PIDD Volume I requirements mentioned above, PIDD Volume II lists additional "stability and control" objectives for use as guidelines in design and verification of the AFCS. These relate to subjective pilot evaluations of handling qualities through use of the Cooper-Harper rating system (Reference 5). For the augmented vehicle (with AFCS operating normally) ratings of 2.0 or better are desired. With the neutrally stable unaugmented aircraft, ratings of no worse than 5.0 are desired. Cooper-Harper rating techniques were utilized extensively throughout the various piloted AFCS simulations and flight demonstrations to gauge progress in developing the superior handling qualities required for the HLH mission.

## 2.1.2 AFCS Development and Design Approach

Development - The development of AFCS control laws and logic for the HLH helicopter was influenced from its inception by two related helicopter handling qualities improvement programs in progress at the time ATC work was started. These were the joint U.S. Army-Canadian government-Boeing Vertol Tactical Aircraft Guidance System (TAGS) program and the Vertol-sponsored Model 347 effort monitored by the Army.

TAGS features considered attractive as candidates for the HLH AFCS included linear velocity control, referenced to groundspeed at low aircraft velocity and to airspeed in the cruise region of the flight envelope, and digital techniques for AFCS control law computation. Elements of the 347 stability augmentation system with potential HLH application were an improved longitudinal control gradient with strong velocity hold capability, and utilization of separate stability and maneuverability optimization techniques to achieve desired handling quality improvements, such as command bank angle and heading hold.

With background of the TAGS and 347 programs available during the HLH concept selection phase, preliminary analytical investigations and "nudge base" piloted simulations were conducted at Boeing Vertol to provide data for an initial definition of baseline AFCS control law mechanizations for later development in the ATC program. These mechanizations were documented in the form of functional block diagrams for each of the four control axes. The AFCS definition effort carried out since concept selection has consisted primarily of refining and updating the original control law software in order to meet requirements and objectives previously adopted.

85

Extensive piloted and unpiloted full-flight envelope simulations were performed at Boeing Vertol and at Northrop to supplement and confirm analytical control system development. Final control law optimization and validation was accomplished with the 347 Flight Research Vehicle. Changes in mechanization of control laws were minimized on the flight vehicle because of the comprehensive simulation efforts preceding the flight demonstration program.

In the refinement of AFCS control and stability loops since Task I, Part 1, the principal analytical and simulation tasks have been associated with:

- Determination of transient-free groundspeed/airspeed phasing and lateral/directional control crossover techniques.

- Development of low-speed/hover-control laws for precision maneuver or position holding with required load crewman controller and Precision Hover Sensor interfacing.

- Development of load stabilization and positioning capability.

- Synthesis of an automatic approach to hover system.

- Definition of requirements for control features, such as the limited lateral bank angle stick gradient, and the altitude hold AFCS mode.

Design Approach - As a result of the concept selection studies, it was decided that the HLH FCS would be made up of a 100-percent-authority direct electrical linkage (DELS) primary control path, interfaced with a limited-authority Automatic Flight Control System (shown schematically in Figure 13). The DELS is an electrical analogy of components usually found in the mechanical control runs of current production helicopters. Its functions include transmitting pilot control inputs to the rotor system (after appropriate mixing or blending), and introducing feed-forward control commands into the AFCS. Differential AFCS/DELS interfacing is accomplished through a frequency selective network which splits the signal into trim and dynamic compensation components, and serves to minimize the effects of potential AFCS system-level hardover failures.

The operational success of the HLH vehicle for cargo operations in all types of weather will depend upon the helicopter having superior IFR flight characteristics, and very good low-speed control and position-hold capabilities. To achieve the required level of handling qualities, two important design concepts were incorporated into the AFCS early in its development cycle. They include:

86

PRIMARY FLIGHT CONTROL

POTOR AND AIRFRAME

DIRECT ELECTRICAL LINKAGE

COCKPIT CONTROLS

HANDLING QUALITIES OPTIMIZATION

STABILITY AUGMENTATION

DIFFERENTIAL INTERFACE

MANUEVER AUGMENTATION

PARALLEL INTERFACE

AUTOMATIC FLIGHT CONTROL SYSTEM
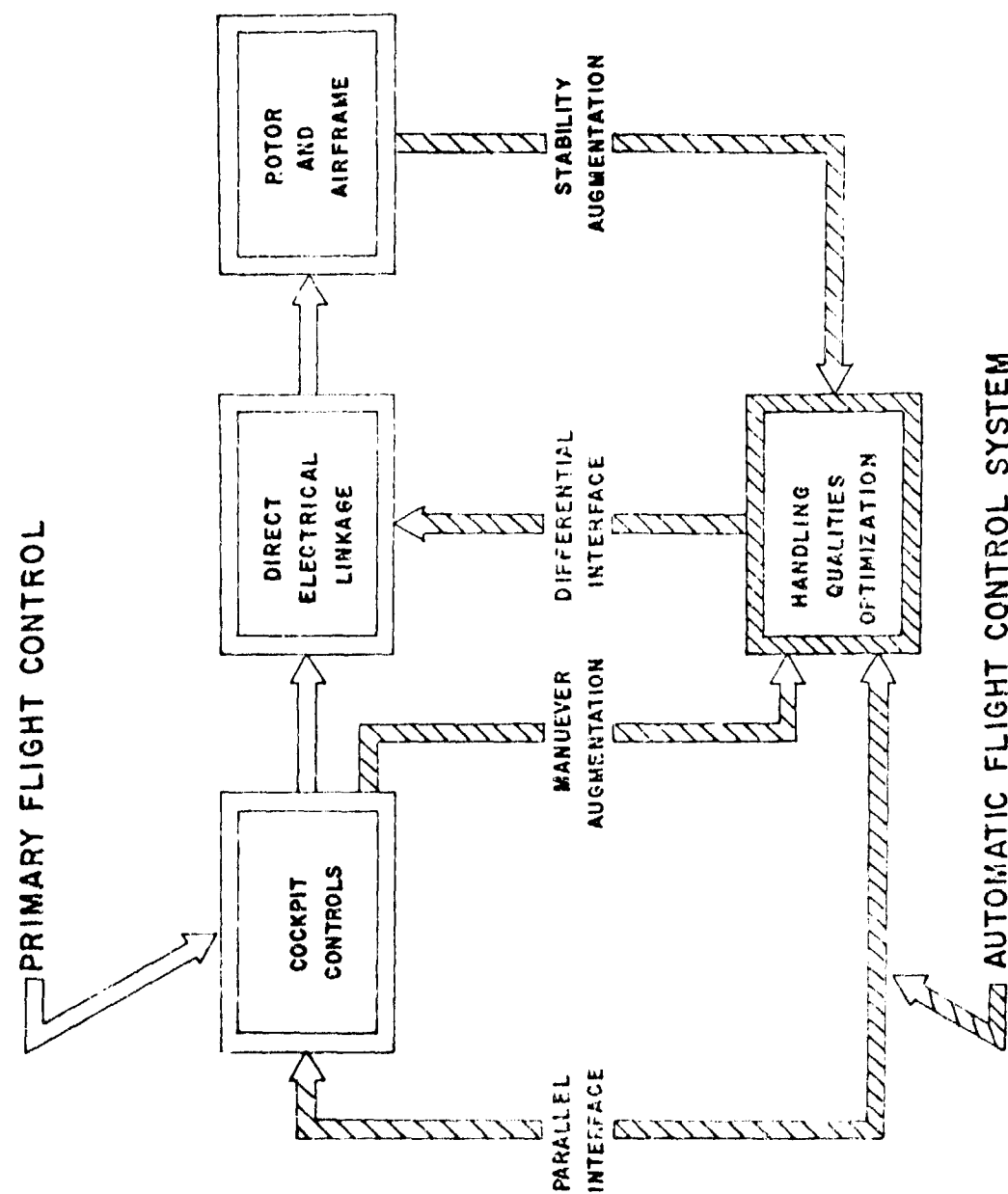
FIGURE 13. HLH FLIGHT CONTROL SYSTEM CONFIGURATION

87

- Velocity control, and

- Pilot-selectable AFCS mode capability, ranging from basic
  stability and control augmentation (SCAS) for IFR flight,
  to special functional mode selection for altitude hold,
  automatic approach to hover, hover hold, load stabiliza-
  tion and positioning, and hover trim.

The basic SCAS augmentation system features relatively high
levels of stability and maneuverability. The conventional
compromises usually existing between the two (i.e., too much
stability resulting in poor maneuverability or vice versa)
have been avoided in design of the AFCS through application
of either feedback-feedforward summing or logic techniques.
These methods are also utilized in the AFCS software to pro-
vide transient-free switching between flight modes.

An overall summary of vehicle stability and controllability
is presented in Table 4. Shown in the Table are stability
characteristics of the aircraft with full-time SCAS augmenta-
tion engaged, and with various selectable AFCS modes in opera-
tion. The Table also illustrates helicopter controllability
by showing the steady state response of the aircraft to step
control inputs in each axis.

In the discussion which follows, all axes of the basic SCAS
are described individually, and significant analytical devel-
opment are summarized. Selectable mode capabilities are
covered later in the section.

TABLE 4. AFCS- STABILITY AND CONTROL FEATURES

| AXIS | BASIC SCAS MODE | | | | SELECTABLE MODES | | | | |
|---|---|---|---|---|---|---|---|---|---|
| | HOVER & LOW SPEED | | FORWARD FLIGHT (>45KTS) | | HOVER HOLD | | LCC CONTROL | LOAD STABILIZATION | ALTITUDE HOLD |
| | STABILITY | PILOT CONTROL | STABILITY | PILOT CONTROL | STABILITY VELOCITY | POSITION | | | |
| LONGITUDINAL | GROUNDSPEED HOLD | GROUNDSPEED 80 FT/SEC/IN | AIRSPEED HOLD | AIRSPEED 90 TO 130 FT/SEC/IN. | GROUNDSPEED HOLD (IMU) | GROUND POSITION HOLD | GROUNDSPEED 1 TO 18 FT/SEC/IN | LONGITUDINAL PENDULUM MODE DAMPING | |
| LATERAL | GROUNDSPEED HOLD | GROUNDSPEED 90 FT/SEC/IN | BANK ANGLE HOLD (ANY BANK ANGLE) | BANK ANGLE (φ) FOR φ <5° 10 DEG/IN. ROLL RATE FOR φ >5° 16 DEG/SEC/IN | GROUNDSPEED HOLD (IMU) | GROUND POSITION HOLD | GROUNDSPEED 1 TO 23 FT/SEC/IN | LATERAL PENDULUM MODE DAMPING | |
| VERTICAL | | ALTITUDE RATE 26 FT/SEC/IN (BASIC AIRCRAFT) | | ALTITUDE RATE 20 FT/SEC/IN (BASIC AIRCRAFT) | ALTITUDE HOLD (RADAR) | ALTITUDE HOLD (PRECISION HOVER SENSOR) | ALTITUDE RATE 3 TO 6 FT/SEC/IN | | ALTITUDE HOLD (BAROMETRIC OR RADAR) |
| DIRECTIONAL | HEADING HOLD | HEADING RATE 20 DEG/SEC/IN | HEADING HOLD (FOR ZERO TURN COMMAND) SIDESLIP STABILITY | SIDESLIP 15 TO 35 DEG/IN | HEADING HOLD (IMU) | HEADING HOLD (IMU) | HEADING RATE 0.3 TO 12 DEG/SEC/DEG | BIFILAR PENDULUM MODE DAMPING | |

### 2.1.3 AFCS Basic Stability and Control Augmentation System (SCAS)

The HLH airframe and rotor system combination is designed to produce approximately neutral static stability without AFCS augmentation. Similar characteristics are found on the 347 Flight Research Vehicle which was used to demonstrate the validity of HLH control law mechanization. In both aircraft, neutral stability is achieved through careful aerodynamic shaping of the fuselage and rotor pylons, and by installing delta-three hinging on the forward rotor to reduce lift slope and gust sensitivity.

Although handling characteristics of the unaugmented aircraft are adequate for VFR flight, HLH IFR mission accomplishment requires engagement of the basic AFCS stability and control system (SCAS). The SCAS provides three-axis control and stability augmentation and is designed to meet the criteria stated earlier in this section. Other interesting design features include:

- Elimination of control axis coupling and trim control offsets with airspeed

- Coordinated turn capability with single-axis control inputs, and

- Provisions for vernier "beep" trim

Control Method - The basic helicopter control system (without augmentation) is capable of changing rotor thrust either collectively or differentially to produce vertical or angular pitching motion. In addition, the rotor thrust vectors may be tilted laterally or longitudinally in the same direction to generate rolling motion or longitudinal translation. Differential lateral thrust tilt provides yawing motion. Step control inputs in pitch, roll, and yaw result initially in angular acceleration (and later blend into constant angular rates) when no augmentation feedback loops are engaged. Vertical control inputs create vertical acceleration and then vertical rate.

90

Augmentation - By feeding back (or forward) the desired para-
meters in an automatic servo control system, basic airframe
response may be modified to reflect the stability (and
controllability) levels of the outermost loops engaged. In
the case of the SCAS, full-time angular rate damping and atti-
tude feedback loops are provided in all (but the vertical)
axes. Feedforward networks are included for response shaping,
and for generating the desired control gradients with speed
or bank angle.

Continuous development of HLH control laws has been in progress
for several years. Each significant developmental step has
had its own set of functional block diagrams (and substantia-
ting analysis or test results) to describe the improved con-
trol function. Rather than discuss these efforts chronologi-
cally in the order in which they occurred, the final control
laws synthesized from the flight demonstration are presented
first, along with descriptions of how they operate.

Significant analysis and simulation work is then detailed as
necessary to shed light on why the final control law mechani-
zations and associated logic were adopted.

SCAS Objectives - In addition to meeting the quantitative
requirements of MIL-H-8501A while developing the SCAS, other
performance goals were also adopted to guide the design and
evaluation process. Among these were objectives delineated
for the flight test demonstration which are tabulated below.

In "light-to-moderate turbulence", target accuracies for
operation with SCAS are:

Airspeed      - $\pm 2$ knots of trimmed speed in steady level
                flight. $\pm 4K$ of entry trim speed in 30°
                banked turns with recovery to $\pm 2K$ of
                entry speed

Groundspeed - $\pm 2$ knots of trimmed longitudinal or lateral
                speed

Bank Angle   - $\pm 2°$ of established bank angle while in
                steady turn

Heading      - $\pm 2°$ of established heading in level flight

91

2.1.3.1 Longitudinal SCAS Synthesis

Figure 14 presents a functional block diagram representation
of the complete longitudinal AFCS control law package (except
for the Automatic Approach to Hover loops which will be
covered later, and the logic switching network schematics
detailed in Appendix A). At this time, only the basic SCAS
functions will be described and most of these are found in
the top half of the diagram.

Inputs and Outputs - For the purposes of orientation, para-
meters illustrated on the right hand side of the cross
hatched AFCS "box" are feedback variables associated with
stability augmentatio... They are generated by sensors located
outside of the AFCS triplex computer matrix on the aircraft.
Control paths shown within the hatched enclosure represent
software control law mechanization and logic switching
computations performed by the AFCS computers. Most logic
gating is physically performed within the computer IOPs, and
as indicated above, is detailed in the report appendix.
Discreet logic signals pass from the IOP units into the AFCS
to set switches as will be described later. A limited amount
of logic is performed in software.

Shown at the top center of the diagram, (on the outside of the
AFCS box) is the "differential" AFCS output path. It is
interfaced with the DELS through the frequency selective net-
work ("frequency splitter") described earlier. This differ-
ential signal goes directly to the rotor system (after passing
through various control mixing stages in the DELS) without
moving the cockpit controls.

Depicted to the left of the DELS/AFCS interface box on the
diagram is a feedforward signal going from the pilot's cockpit
stick (through the DELS) and into the AFCS. This path per-
mits the velocity and low speed longitudinal cyclic pitch
commands to enter the AFCS. It also provides a path for
feedforward signals used in removing trim bias associated with
groundspeed/airspeed switching by the velocity mode transfer
switch (described later).

**FIGURE 14.**

Longitudinal AFCS Functional Block Diagram
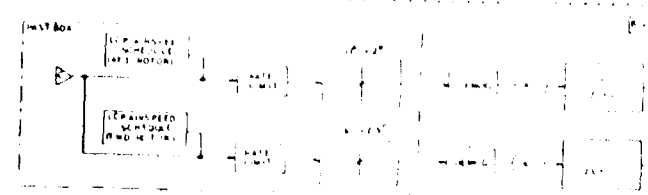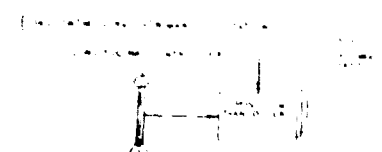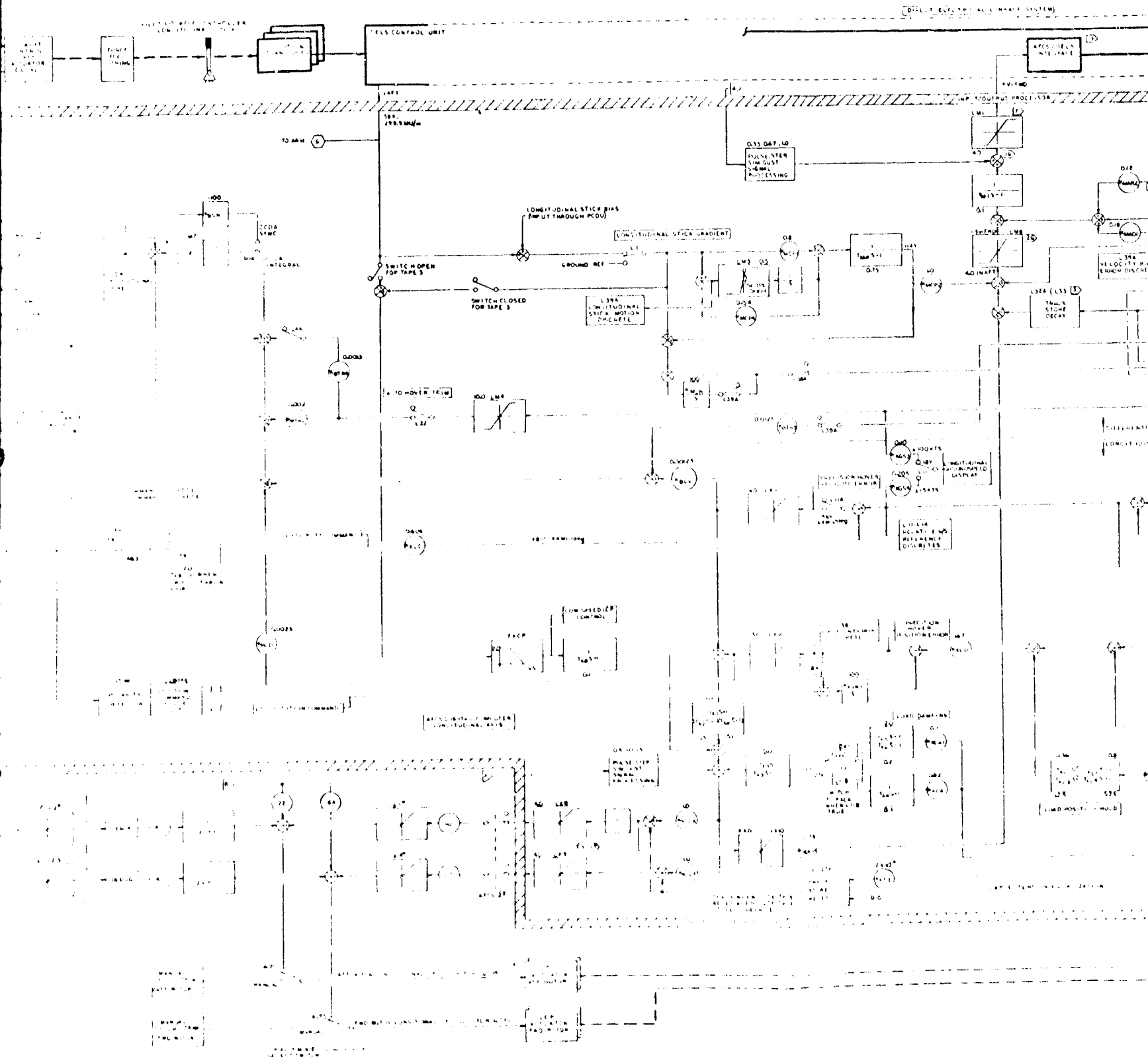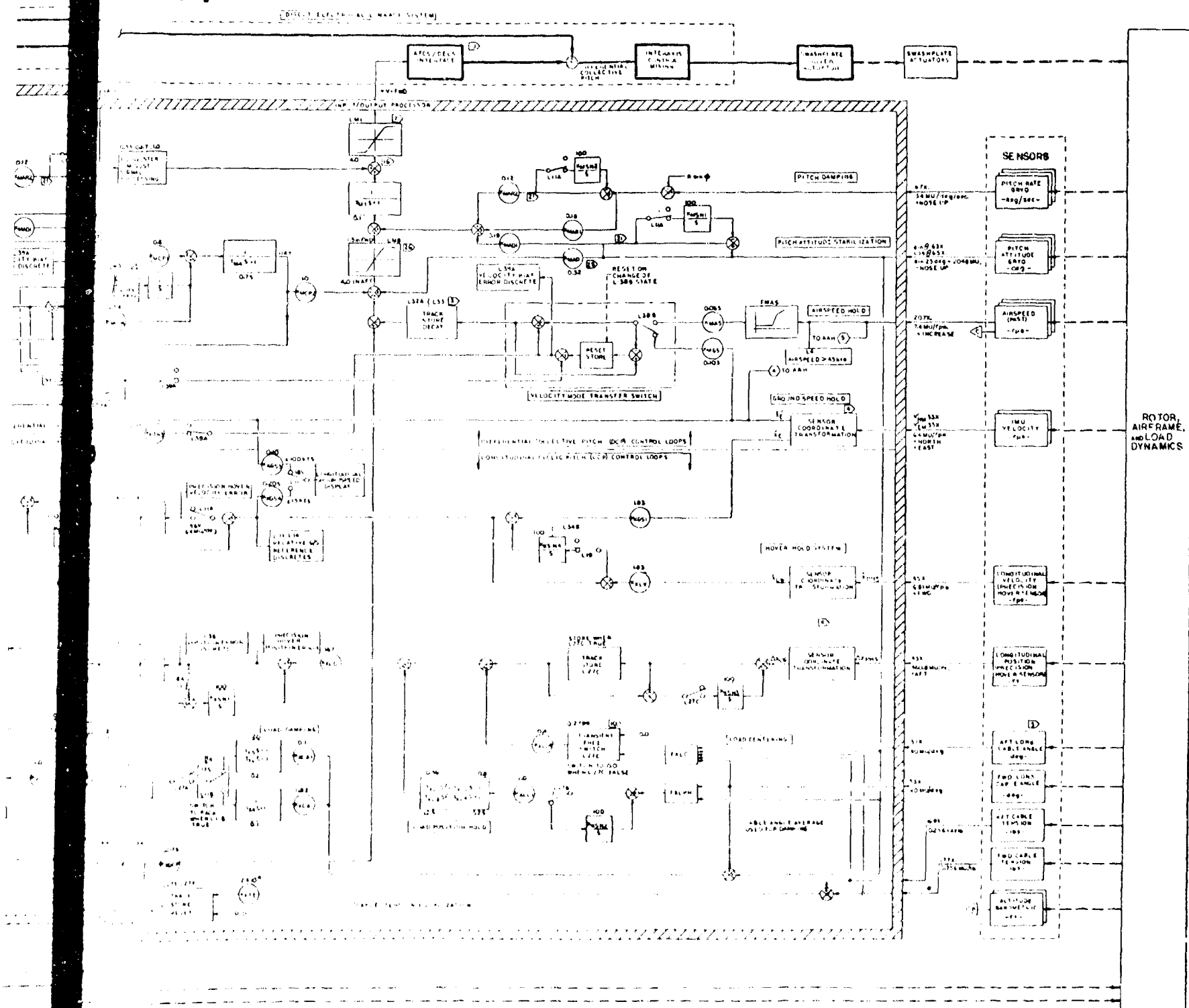
93

On the top left hand side of the AFCS box is a cockpit stick
backdrive command path which causes a Cockpit Control Driver
Actuator  (CCDA) to move the stick through a magnetic brake/
force-feel spring arrangement.  The spring forces may be
released and rezeroed by pressing a "mag" brake button on the
pilot's longitudinal stick.  Beneath the backdrive network
is a pilot "beep" trim control path utilized to parallel drive
the cockpit stick for vernier velocity adjustments.  The trim
signal is generated when the pilot depresses a "coolie hat"
trim button also found on the longitudinal stick grip.

Other functions shown on the left side of the AFCS box con-
cern load crewman control inputs through the LCCC which are
discussed later under "hover hold" mode operation.  Additional
signals are related to navigational guidance information and
special test functions.

LCP Trim - On the lower left hand corner of the box are shown
the "q"-sensed cyclic trim (LCP) signals.  These longitudinal
cyclic inputs are identical to those used on present tandem
aircraft, and vary according to a present schedule with air-
speed on each rotor.  As helicopter speed increases, forward
cyclic is introduced into the rotors to reduce shaft aero
flapping (and bending loads), and to trim the aircraft pitch
attitude for drag reduction and pilot comfort.

Summed with the "q"-sensed cyclic signals are AFCS outputs
from the hover hold system, and pilot's LCP stick commands.
The summed LCP signals then pass directly into the longi-
tudinal cyclic pitch actuators through existing 347 system
hardware without entering the DELS as other AFCS outputs do.
The LCP paths complete the longitudinal AFCS input-output
interfacing.

2.1.3.1.1   Inner Loop Longitudinal SCAS Stabilization and
Control

Pitch Damping - The top right hand stabilization feedback
loop shown in Figure 14 represents the primary pitch damping
path in the SCAS.  Through it passes an airframe body axis
pitch rate signal which has been summed with a correction
term (R sin $\phi$) representing the product of body axis yaw
rate and the sine of aircraft roll angle.  The correction
term removes the steady pitch rate component picked up by
the body axis gyro in turns to preclude signal saturation.

95

The K sinφ correction takes the place of an earlier high pass
filter (washout) network, which was installed in the pitch
rate damping loops of previous tandem aircraft with simpler
stability augmentation systems. The need for an improved
approach to steady pitch rate correction was identified during
the HLH Flight Research Vehicle demonstration program, wherein
A/S loss or gain during turn entries was unsatisfactory.
Some improvement was achieved as detailed in the flight test
section.

As shown on the diagram, the damping signal first passes
through a system "gain" factor, where pitch rate is converted
to inches of equivalent stick. (Most control law computations
are performed within the computers using inches of stick or
equivalent control throw in degrees of pitch change). After
being "gained", the signal is filtered through a first order
low-pass shaping network. It is then passed through an
authority limiter, and thence into the AFCS/DELS interface.

The low-pass filter effectively prevents airframe vibration
(and other unwanted high frequency signals) from entering the
damping path. Prior to the flight program, only the pitch
damping signal was modulated at high frequency with this type
of shaping. The presence of undesirable sensor or computer
noise spikes necessitated moving the filter to the output
path of the entire axis where attitude, velocity, and feed-
forward signals were also included. Similar low-pass filters
have been inserted in the differential outputs of all of the
remaining AFCS axes.

Low-Speed LCP Control Augmentation - A feedforward path from
the pilot's stick to the longitudinal cyclic pitch actuators
on both rotors is incorporated for translation control
"quickening" at low speed. As shown in the diagram, the
"cyclic on the stick" command signal passes through a variable
gain box (FXCP), which begins LCP effectivity below 40 knots
groundspeed. Full system gain is achieved at all speeds less
than 27 knots, as shown in the Appendix A schedule.

Incremental LCP commands associated with cockpit stick move-
ment are the same for both rotors. These cyclic inputs pro-
duce direct longitudinal airframe accelerations, without
requiring pitch rotation of the fuselage. They act in concert
with the DCP longitudinal controls, which provide a lagged
response because the aircraft must change attitude before
any translational acceleration can start.

96

As initially envisioned in early analyses and simulation work, the low-speed LCP command signal was summed with a high pass filtered groundspeed feedback; but this velocity path was eliminated during the flight program due to undesirable pitch attitude changes created by the washout. When the velocity feedback loop was deleted, a low-speed control shaping feed-forward path (which acted along with the LCP/velocity combination) was also removed as being unnecessary.

2.1.3.1.2  Outer Loop Longitudinal SCAS Stabilization and Control

Outer loop paths include pitch attitude and velocity hold functions for stabilization. In addition, SCAS control augmentation loops are provided for generating a stable stick gradient and velocity command capability throughout the flight envelope. The methodology for transferring from low-speed ground referenced velocity to airspeed in cruise, and for generating an acceptable longitudinal stick gradient (while at the same time maintaining strong velocity hold capability) is perhaps the most important part of the SCAS description. Development of these two longitudinal SCAS features is covered in some depth, since similar control law manipulations are also utilized in the lateral axis.

Pitch Attitude Stabilization - The pitch attitude signal is processed through a simple sensitivity (gain) constant, and is then summed with the velocity hold and command signals. Attitude hold stability is maintained throughout the flight envelope with a constant gain of about 1/3 of an inch of corrective control applied for every degree of pitch attitude deviation from zero. Static hover fuselage attitude is slightly nose up, and becomes progressively more nose down as speed increases. The result is a differential static aft "equivalent stick" requirement going into the rotors as air-craft speed builds, and "corrective" type inputs when the attitude changes due to an external disturbance.

The attitude gradient increment is a relatively small component of the total longitudinal DCP rotor control input requirement processed by the AFCS. Stick gradient and velocity inputs dominate the outer loop mechanization and are discussed next.

97

VELOCITY STABILIZATION, COMMAND, AND STICK GRADIENT

Stability - As shown in Figure 14, feedback velocity hold
signals consisting of pitot-static airspeed and inertially
referenced groundspeed (from the IMU) are introduced into the
Velocity Mode Transfer switch (after passing through
appropriate gains). The switch selects the proper velocity
through application of logic techniques, and passes either
the low-speed groundspeed or airspeed-referenced signal into
the differential AFCS path. Switching between the two ref-
erences is transient free, and occurs at 45 knots airspeed
when velocity is increasing, and at 40 knots airspeed when the
aircraft is slowing down.

Because of the importance of the velocity mode switch to over-
all AFCS success, a separate discussion of its development and
detail operation is included later in this section. For now,
all that need be understood is that the switch passes a single
velocity-referenced signal for low- or high-speed flight, and
causes the pilot's cockpit stick trim position to reflect the
type of velocity reference in use at any point in time.

The groundspeed hold at low velocity, and airspeed hold above
40/45 knots is achieved by utilizing fairly high gain factors
(KMAS and KMGS) equivalent to approximately 1 inch of equiv-
alent stick for every 9 knots of airspeed. The airspeed
signal is processed through a FMAS function which was orig-
inally incorporated into the velocity loop to keep the air-
speed signal constant and equal to 40 knots beneath this
speed so as not to interfere with the groundspeed path.
Below 40 knots, groundspeed is the velocity reference.

In the flight program, additional velocity hold gain was
found to be desirable while operating on airspeed reference
between 60 and 120 knots. This increase was incorporated in
a non-linear fashion by "bowing" the FMAS schedule gradient
above 40 knots to meet the desired requirement. The original
schedule, synthesized from analysis and simulation, had incor-
porated a 45-degree slope (i.e. 100 knots in gave 100 knots
out) above 40 KIAS. The modified airspeed schedule and gain
tabulations are presented in Appendix A, along with all other
gains, functions, limiter values, and logic diagrams for the
AFCS package.

Groundspeed velocity signals generated by the aircraft IMU
(Internal Measuring Unit) sensors are referenced to the plane
of the earth's surface and are oriented into "V North" and
"V East" vector components. A sensor coordinate transforma-
tion within the computer AFCS complex resolves the IMU veloci-
ties into a system aligned with the aircraft longitudinal
and lateral axes (still in the earth surface plane). A
further transform references the velocity signals to the air-
craft center of gravity instead of the IMU location.

As seen in the sensor coordinate transformation box, two
longitudinal groundspeed signals are available as outputs;
$\dot{X}_E$ and $X_E'$. These are identical except for the fact that the
$X_E$ term may be "drift cleared" to eliminate small IMU drifting
errors which would otherwise degrade performance of the AFCS
while operating in the hover hold mode. The $\dot{X}_E'$ term, on the
other hand, is a continuous output and is utilized in velocity
holding through the KMGS path, or for the automatic hover
trim feature described later.

Operation Without Velocity Reference - The velocity-referenced
stability described so far implies that either airspeed- or
groundspeed-oriented signals are utilized for all normal
flight modes. This is true unless the pilot wishes to perform
maneuvers which do not require velocity feedback (such as
stationary, or nearly stationary towing operations). In such
a case, the pilot might desire to use an "attitude-referenced"
system. The HLH control laws have been set up so that an
attitude system of this type can be achieved by disabling
the velocity feedbacks.

99

A track-store-decay box that has several important functions
is shown on the output of the velocity mode transfer switch
(Figure 13). These functions are controlled by two
switches on the pilot's mode select panel, illustrated in
Figure 10A. The pilot may elect to use as a velocity reference
any of the following:

- o  Auto - automatic switching from G/S to A/S

- o  A/S  - airspeed reference at all speeds

- o  G/S  - groundspeed reference at all speeds

The pilot has another switch which controls the manner in
which the previously selected velocity reference is used.
The velocity switch also has three modes of operation: n:

- ●  NORMAL - where either of the three previously selected
              velocity reference options may be utilized,
              and the "track" function shown in the diagram
              is in operation.

- ●  OFF or - where no variable velocity signal passes, but
   DISABLE    the final value of velocity at shutdown is
              "stored" to permit transient-free disengage-
              ment of the velocity mode.

- ●  DECAY  - which permits the velocity feedback to slowly
              decay to zero at a rate of .5 inches of
              equivalent stick per second.

Information presented in Table 5 summarizes the overall air-
craft stability response for each control axis with any of
the above velocity references selected. Comparable control
responses with similar velocity references are given in
Table 6.

Longitudinal Stick Gradient - The HLH airframe and rotor
system combination has been designed to produce close to
neutral static stability without augmentation. This built-
in neutral stability results in a longitudinal stick gradient
that flattens rather than increases linearly with speed as
desired.

100

TABLE 5. MANUAL VELOCITY REFERENCE SELECT – STABILITY FEATURES

| AXIS & FLIGHT CONDITION | VELOCITY REFERENCE | | | |
|---|---|---|---|---|
| | NORMAL (AUTO) | GROUND SPEED | AIRSPEED | DISABLE |
| HOVER / LOW SPEED LONGITUDINAL | LONG. GROUNDSPEED HOLD | LONG. GROUNDSPEED HOLD | PITCH ATTITUDE HOLD | PITCH ATTITUDE HOLD |
| LATERAL | LAT. GROUND SPEED HOLD | LAT. GROUND SPEED HOLD | BANK ANGLE HOLD | BANK ANGLE HOLD |
| FWD FLIGHT (>45 KM) LONGITUDINAL | LONG. AIRSPEED HOLD | LONG. GROUNDSPEED HOLD | LONG. AIRSPEED HOLD | PITCH ATTITUDE HOLD |
| LATERAL | BANK ANGLE HOLD | LAT. GROUND SPEED HOLD | BANK ANGLE HOLD | BANK ANGLE HOLD |

101

TABLE 6. MANUAL VELOCITY REFERENCE SELECT - CONTROL RESPONSES

| AXIS & FLIGHT CONDITION | VELOCITY REFERENCE | | | |
|---|---|---|---|---|
| | NORMAL (AUTO) | GROUND SPEED | AIRSPEED | DISABLE |
| **HOVER/LOW SPEED** | | | | |
| LONGITUDINAL | LONG. GROUNDSPEED | LONG. GROUNDSPEED | PITCH ATTITUDE | PITCH ATTITUDE |
| LATERAL | LAT. GROUNDSPEED | LAT. GROUNDSPEED | BANK ANGLE FOR BANK ANGLES $\leq \pm 5°$ <br> ROLL RATE FOR ANGLES $> \pm 5°$ | BANK ANGLE FOR BANK ANGLES $\leq \pm 5°$ <br> ROLL RATE FOR ANGLES $> \pm 5°$ |
| **FWD FLIGHT(>45..N)** | | | | |
| LONGITUDINAL | LONG. AIRSPEED | LONG. GROUNDSPEED | LONG. AIRSPEED | PITCH ATTITUDE |
| LATERAL | BANK ANGLE FOR BANK ANGLES $< \pm 5°$ <br> ROLL RATE FOR ANGLES $> \pm 5°$ <br> AUTOMATIC PEDAL FIXED TURN COORDINATION FOR ALL BANK ANGLE COMMANDS | LAT. GROUNDSPEED | BANK ANGLE FOR BANK ANGLES $\leq \pm 5°$ <br> ROLL RATE FOR ANGLES $> \pm 5°$ <br> AUTOMATIC PEDAL FIXED TURN COORDINATION FOR ALL BANK ANGLE COMMANDS | BANK ANGLE FOR BANK ANGLES $\leq \pm 5°$ <br> ROLL RATE FOR ANGLES $> \pm 5°$ <br> AUTOMATIC PEDAL FIXED TURN COORDINATION FOR ALL BANK ANGLE COMMANDS |

102

"Basic" aircraft stick gradient requirements are illustrated schematically by the heavy dashed line annotated with a ① in Figure 15. This dashed curve represents the DCP control in inches of equivalent cockpit stick which must be put in at the rotor heads (and in the cockpit with SCAS off) to trim the helicopter in level flight.

Changes in aircraft gross weight or cg move the basic curve some slight amount, but this movement (and the absolute magnitude of the basic stick requirement itself) is quite small when compared with other DCP inputs available from the AFCS at the rotor head. These additional inputs constitute the velocity hold ③ and feedforward stick "pickoff" ⑤ gradients described below.

To understand how the final cockpit stick gradient is generated by the AFCS for the pilot, assume that a total travel of 3 inches of forward stick motion is desired, and will be put in between hover and 200 knots in the cockpit. The resultant travel reflects a positive stable gradient, producing about 65 knots of speed for every inch of cockpit stick input. This desired cockpit gradient is illustrated by the heavy dark line ② on the schematic. Although the 65 knot per inch gradient was found to be adequate in developmental simulation work, the flight demonstration program indicated need for a tighter gradient to optimize handling qualities. This revised gradient reflected a slope increase of about 40 percent out to 100 knots, and 25 percent above that speed.

As seen on the schematic, the desired cockpit gradient is further forward than the basic aircraft rotor head requirement to trim. Accordingly, aft equivalent stick must be put in between the cockpit and rotor head (in an amount equal to the difference between curves ① and ②), so that the pilot will move the stick in a forward direction to achieve the positive gradient he wants. For the purpose of this explanation, it may be assumed that the basic aircraft gradient is sufficiently small to be neglected in further discussion.

103
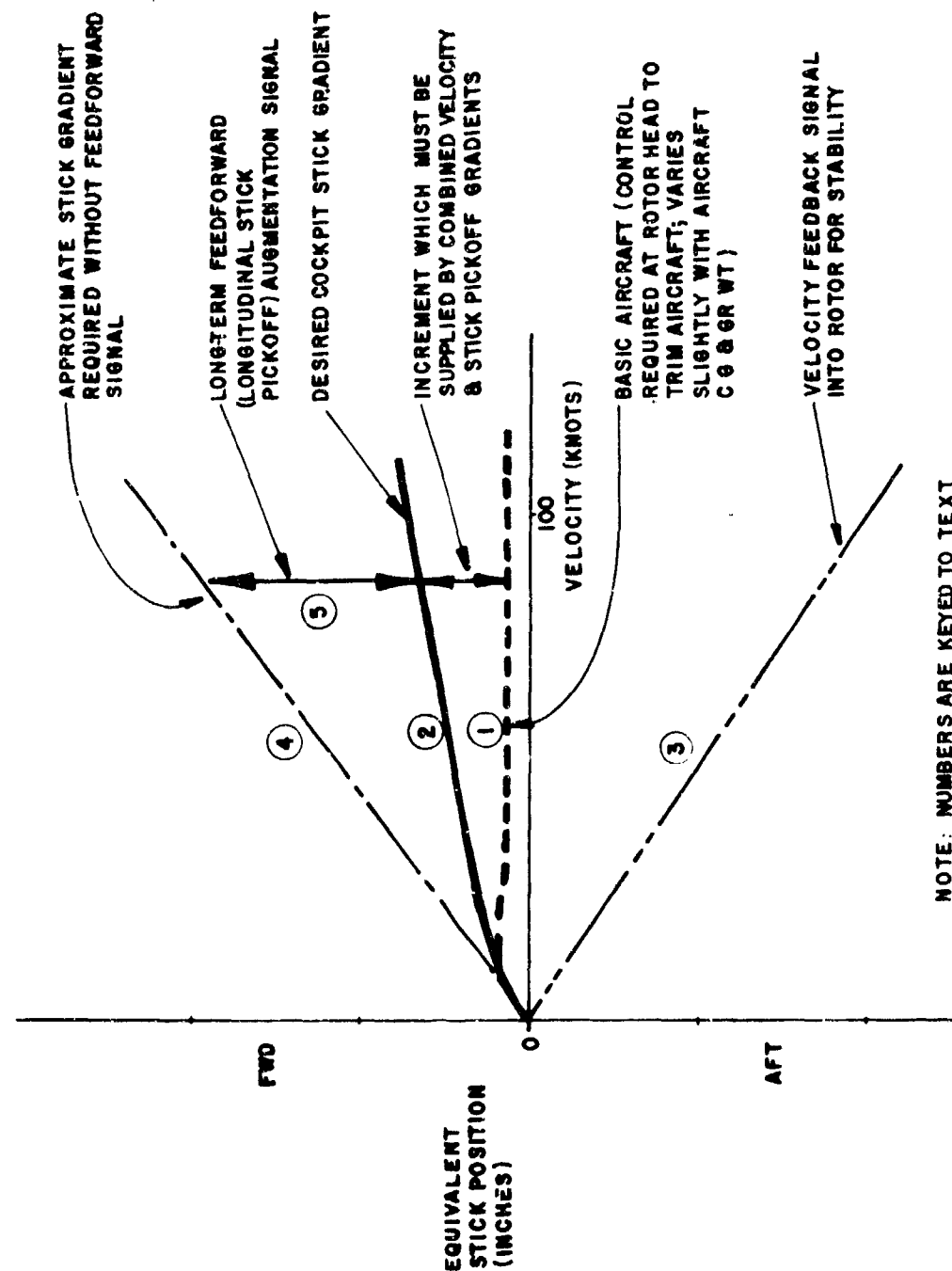
FIGURE 15. LONGITUDINAL STICK GRADIENT SYNTHESIS

NOTE: NUMBERS ARE KEYED TO TEXT

104

The aft stick that must be put in beneath the rotor to pro-
duce the desired increment between ① and ② is made up of
two very steep SCAS gradients.  One of these is the strong
velocity hold feedback detailed earlier, which would put in
about 20 inches of aft stick (curve ③) at the head at 200
knots, if it could (giving a 10-knot-per-inch equivalent
stick gradient).  Obviously, 20 inches of forward stick
(as illustrated by curve ④ ) cannot be made available in the
cockpit to "buck out" the velocity requirement.

If, however, the 3 inches of cockpit desired forward
stick are used against the 20 inches of aft velocity
requirement, 17 additional inches of forward input need be
provided at the rotor to achieve equilibrium.  This additional
forward "stick" requirement ⑤ is generated by using a
feedforward pickoff on the pilot's stick which puts in several
inches of equivalent rotor control for every inch put in by
the pilot.  A stick pickoff multiplying circuit was devel-
oped along with a rate-limiting feature to accomplish the
feedforward task.  It is annotated on the Figure 14 diagram
beneath the longitudinal stick gradient box.

Because of its inertia, the aircraft will not produce airspeed
changes as fast as the pilot can move the stick.  A rate-
limiting function must therefore be incorporated into the
longitudinal control gradient which will allow the pilot's
amplified stick signal to enter the rotor system at about
the same rate that the counterbalancing velocity hold signal
can be generated by aircraft speed changes.

This rate limiting is achieved by passing the feedforward
stick signal through a very high gain limiter (LM3), and then
integrating its output.  The result is a ramped stick response
with time, which is virtually independent of stick amplitude
because of the sharp initial slope.  A feedback path around
the limiter through the KMCP4 gain provides the steady state
multiplication or amplification necessary to stand off the
strong velocity gradient.

The two loops described above address only the static gradient
and do not produce an optimum short period helicopter attitude
response.  A third "straight through" path with no rate limit
is provided to augment the direct linkage input for attitude
control.  This path serves to stand off the pitch attitude

105

associated input already discussed. On a steady state basis, the network just discussed will produce slightly more than 7 inches of equivalent AFCS input (per inch of cockpit stick), to sum with the velocity hold signal. The output of this network is low-pass filtered for smoothing to avoid any stick jerk tendencies.

For a 1-inch forward control displacement in the cockpit, the aircraft will speed up about 65 knots (or slightly less due to the flight test optimized gradient), causing the velocity feedback to generate a requirement for about (-) 7 inches of equivalent stick to sum with the (+) 7 inches from the feedforward path. No further AFCS input goes in through these paths unless the stick is again moved, or the aircraft encounters an external disturbance such as a gust.

## Stability and Maneuverability

A fundamental SCAS design factor reiterated throughout the report so far has been the deliberate separation of stability and maneuverability functions for individual optimization. Most of the loops are interdependent in some way, but have been separately optimized to give the highest possible levels of both stability and controllability without incurring major compromises in either.

An illustrative example of the strong longitudinal stability and high controllability exhibited by the augmented aircraft is presented in the Figure 16 sketch. Maneuverability is demonstrated by the cockpit longitudinal stick push and hold step response (shown by the solid line). This 1/2-inch stick step produces an 8-degree maximum pitch attitude transient and a smooth airspeed buildup to 35 knots, typical of a pilot speed change demand.

An external gust disturbance which upsets the rotors by an equivalent amount (of control step), results in a mild 3-degree pitch attitude variation and a 3-4-knot velocity change. The difference in the two responses clearly shows that stability can be maintained without compromising desired levels of maneuverability.

106

OBJECTIVE: STABILITY – MANEUVERABILITY DESIGNED FOR IFR



FIGURE 16. LONGITUDINAL SCAS

## VELOCITY MODE TRANSFER SWITCH

Groundspeed-to-Airspeed Blending - Velocity feedbacks for
stability are referenced to groundspeed for low speed opera-
tions, and to airspeed during forward flight. The presence
of headwinds or tailwinds creates a difference in the ref-
erence feedback signal, which could create transients on
switching. Options for velocity reference transfer are shown
in Figure 17 wherein airspeed-referenced control positions
are presented as a function of groundspeed for zero wind,
and for headwinds and tailwinds of 40 knots. Note that a con-
stant control position exists for all wind states at the same
airspeed.

The no wind curve on the figure also represents the ground-
speed referenced control for all wind states. When operating
with a 40 knot headwind, the control position follows the no-
wind or groundspeed reference to 5 knots (45 knots of
airspeed), and must then transition to the 40-knot headwind
curve. Two options shown in Figure 17 are available to effect
switchover: (1) continuous transfer, and (2) instantaneous
switching. Both methods were extensively explored during
piloted nudge base flight simulation work conducted in late
1972.

Switching Options - The first velocity reference transfer
option, known as the continuous blending scheme, (and
proposed in the original block diagram schematics), phased
from one reference to another over a discreet airspeed
range. The continuous blending approach was found to be
unsatisfactory for the following reasons:

- The width of the phasing zone, wherein the velocity
  feedback is a mixture of groundspeed and airspeed,
  varies with wind strength and encompasses most of the
  useful flight envelope. This results in longitudinal
  trim control positions that vary with winds at constant
  airspeed.

- Performance is compromised, particularly at low speeds
  where airspeed is not held constant while turning in
  winds, resulting in power and/or altitude fluctuations.
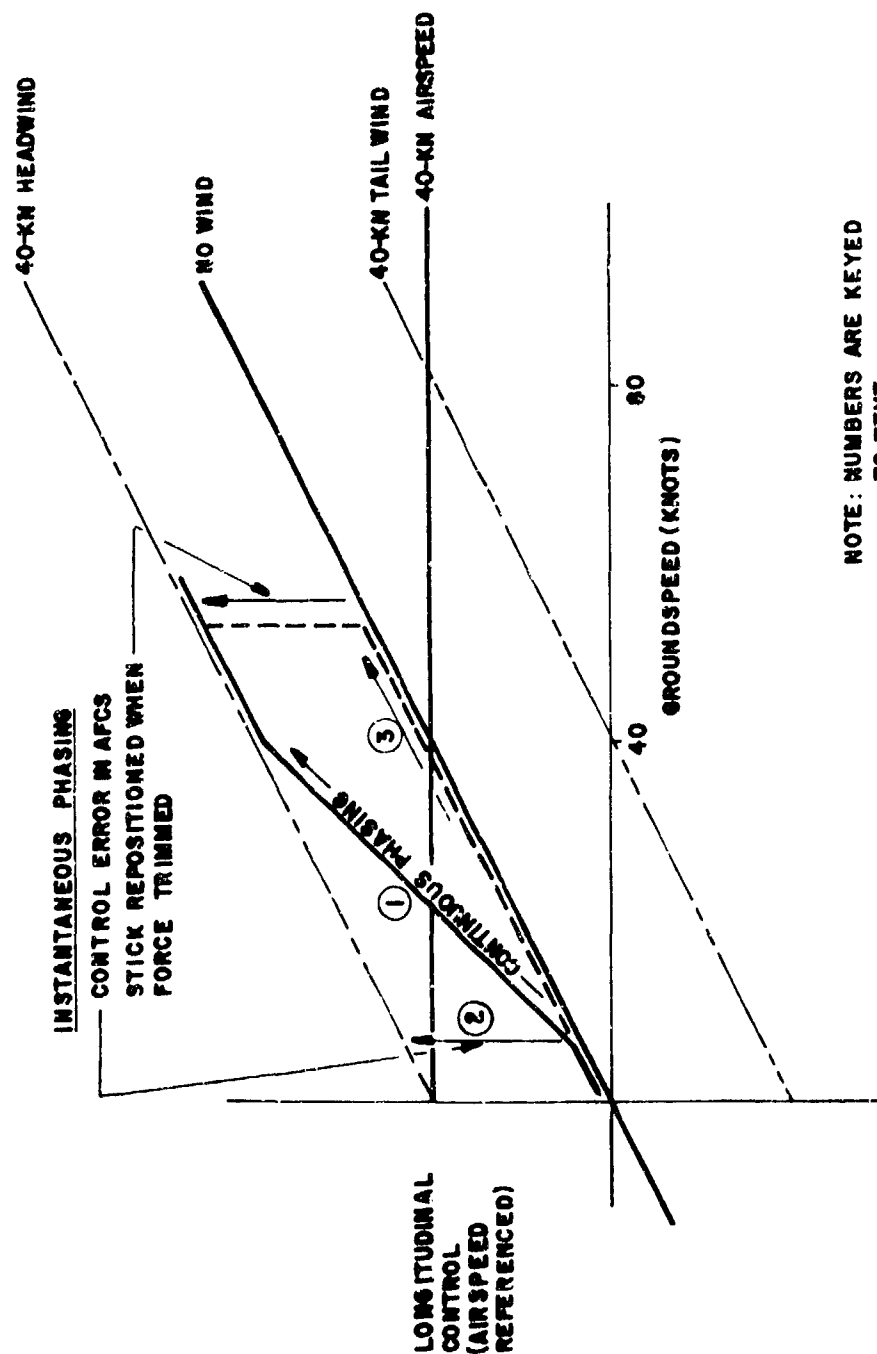
FIGURE 17. GROUNDSPEED TO AIRSPEED PHASING OPTIONS

NOTE: NUMBERS ARE KEYED TO TEXT

● Pilot workload increased because of not having direct control over the flight variables normally monitored, such as torque, altitude, airspeed, and turn rate.

A revised instantaneous switching concept was developed in which the difference between the two velocity feedback signals is provided through the AFCS on switchover to eliminate transients. This difference or bias signal (generated by the velocity mode transfer switch) is proportional to the amount the cockpit control is offset from its true airspeed or groundspeed position. The bias is removed as shown in Figure 17 upon force trimming, by slowly parallel-driving the controls to their correct position (without disturbing the aircraft by moving the rotor head controls).

Detailed operation of the velocity mode transfer switch is shown schematically in Figure 18 and is described in the following summary. It should be noted that Figure 18 is a blowup of the transfer switch detailed on the Figure 14 Functional Block Diagram. The switch is identical to one used for similar switching in the lateral axis. Numbers and letters shown on the blowup refer to signal paths or various positions within the transfer switch.

Transfer Switch Operation - Suppose, for example, that the groundspeed signal (1) is 10 knots and airspeed signal (2) is 50 knots (i.e., a 40-knot headwind). Initially, the system is a groundspeed reference as shown, and the velocity feedback (5) is also 10 knots. To switch to an airspeed system, the following takes place in the order shown:

(A) Switch to airspeed

(B) Sum airspeed with previous velocity signal: -50 + 10 = -40 knots

(C) Reset the bias to the value at (B) = -40 knots

(D) Sum airspeed with (C) = 50 -40 = 10 knots

110

FIGURE 18. OPERATION OF VELOCITY-TRANSFER SWITCH
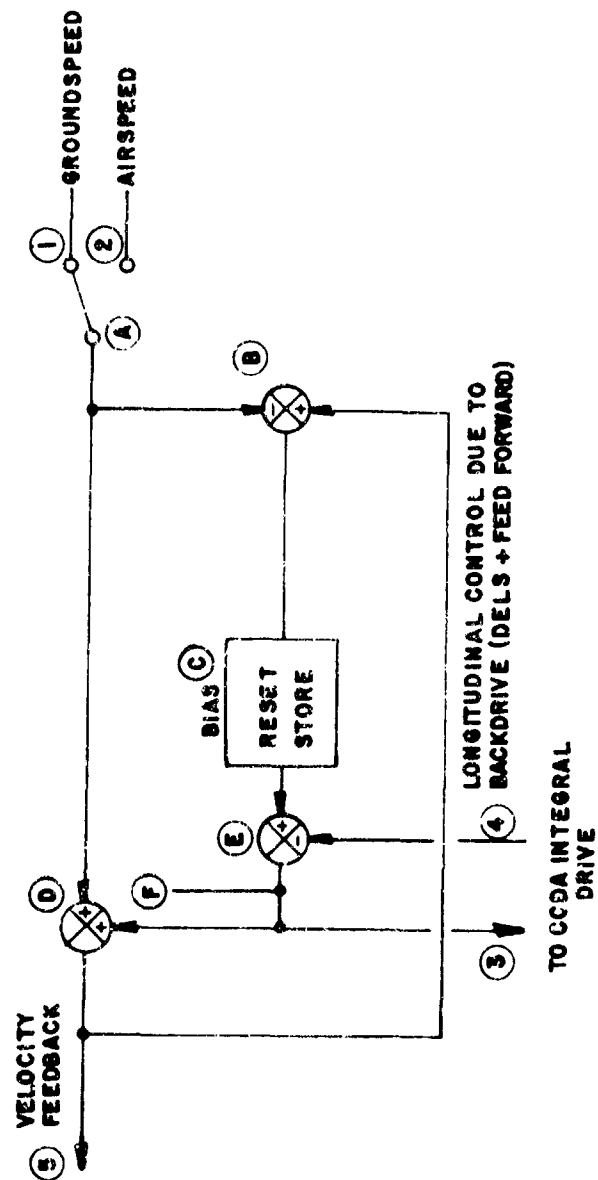
NOTE: LETTERS AND NUMBERS ARE KEYED TO THE TEXT

Hence, the velocity feedback has remained at 10 knots creating no transient. The feedback signal is now airspeed, and the bias stored in the Reset/Store. (C) provides a signal to make up the difference.

To eliminate this signal, the bias is fed into the CCDA integral drive (3) which begins to reposition the primary controls. The control motion, in turn, is fed back (4) and subtracted from the bias at (E) until point (F) is approximately zero, indicating the bias has been removed. The Reset/Store is then reset to zero and the velocity feedback is now 50 knots. Since the bias eliminator signal reduces the bias to zero at the same rate that the back-driven control is going into the DELS mix, no transient occurs.

Two options on the switching points were considered:

(A) Switch to an airspeed mode when airspeed was greater than 40 knots and groundspeed greater than 10 knots. Switch back to a groundspeed mode when groundspeed was less than 10 knots.

(B) Switch to an airspeed mode when airspeed was greater than 45 knots. Switch back to groundspeed mode when airspeed was less than 40 knots. (This was the option chosen).

No airspeed reference is available for either option below 40 knots. Figure 19 shows the acceleration and deceleration characteristics for these two options in a 15-knot tailwind. During the deceleration phase, the lack of a velocity reference signal for Option A created an undesirable pitch attitude increase. In addition, the stabilized rearward trim speed was greater than the initial speed.

These undesirable characteristics were not obtained with Option B logic, and it was selected for piloted flight evaluations. Note that the acceleration characteristics are not identical in these records due to system gain modifications that occurred between run days.
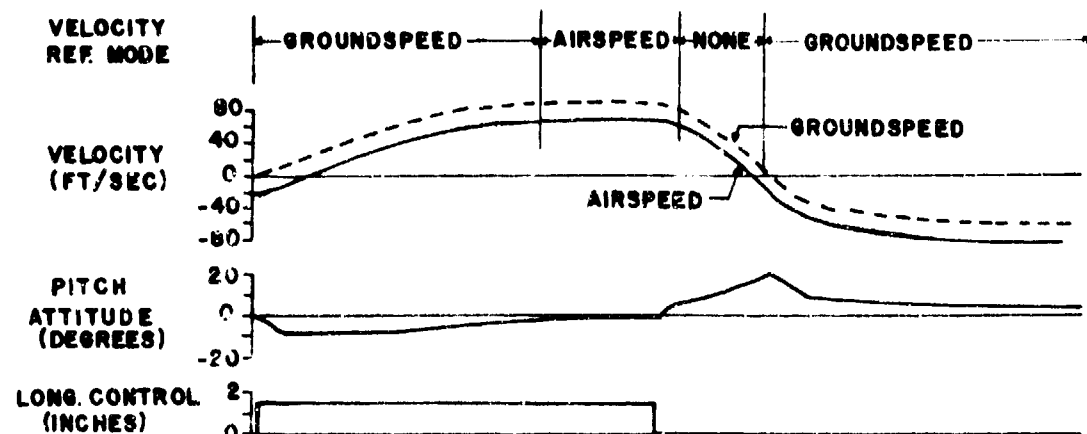
112
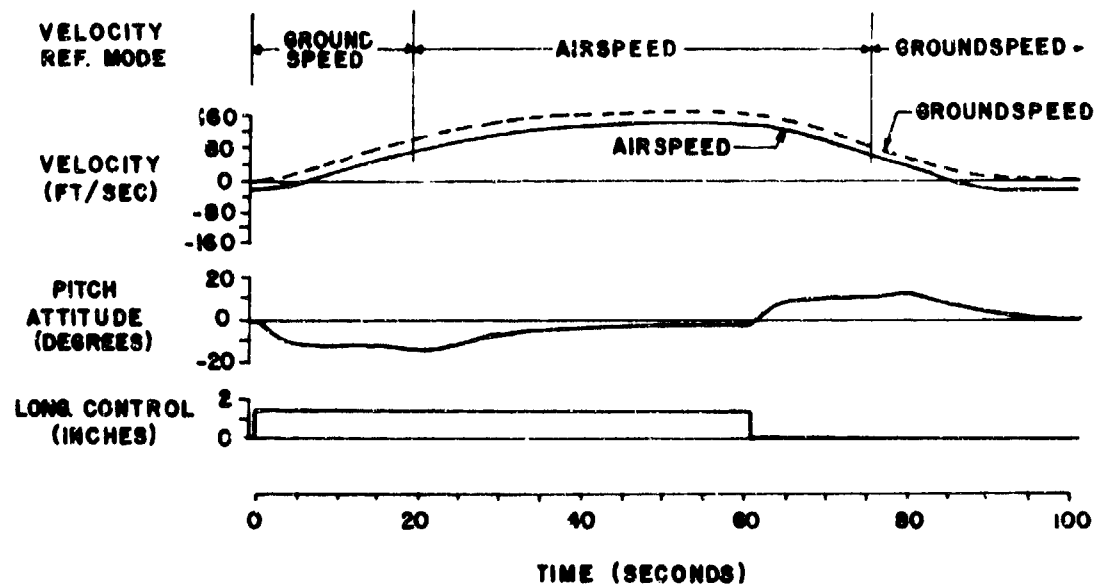
FIGURE 19. OPTIONS FOR INSTANTANEOUS GROUNDSPEED TO AIRSPEED REFERENCE TRANSFER

113

Figure 20 shows the bias elimination feature via parallel
drive of the cockpit control. An acceleration to a stabilized
speed above the switch point in a 30-knot headwind is followed
by a simulated force trim, which activates the bias elimination
feature.

Integral Backdrive Command - In understanding the parallel
backdriving of the cockpit stick for bias elimination, several
features should be mentioned. The first of these relates to
the fact that bias is removed only when the cockpit control is
in a trimmed condition with the stick in detent and may brake
not depressed (see Logic L-39A in Appendix A). Any longi-
tudinal stick motion not associated with the backdriving
function will open the backdrive path and prevent further
parallel stick movement.

The backdrive bias elimination command passes through an
integral drive mechanization which smoothes the signal going
to the stick driver actuators, and continues to output a
driving signal until the input to the integrator is zero.
The integral drive path shown in the upper left corner of
Figure 14 also has a synchronizing loop (controlled by
L-30A logic) wrapped around the integrator to stop the
backdrive command when the cyclic magnetic brake is depressed.
Similar integral parallel stick drives are used in all axes.

2.1.3.1.3  Low-Versus-High-Sensitivity Stick Gradient

One of the recommendations of the Task 1, Part 1, concept
selection simulation studies was incorporation of low
sensitivity LCP control into the AFCS for the precision hover
and low speed maneuvering task. Sensitivities on the order
of about 5 fps per inch of stick were suggested. However,
for arm reach considerations in the cruise flight region,
much higher sensitivity DCP controls are required, with
typical gains varying up to 20 times the hover requirement.
The methodology for phasing from low sensitivity LCP to
high sensitivity DCP control was not addressed in the Task 1,
Part 1 results.
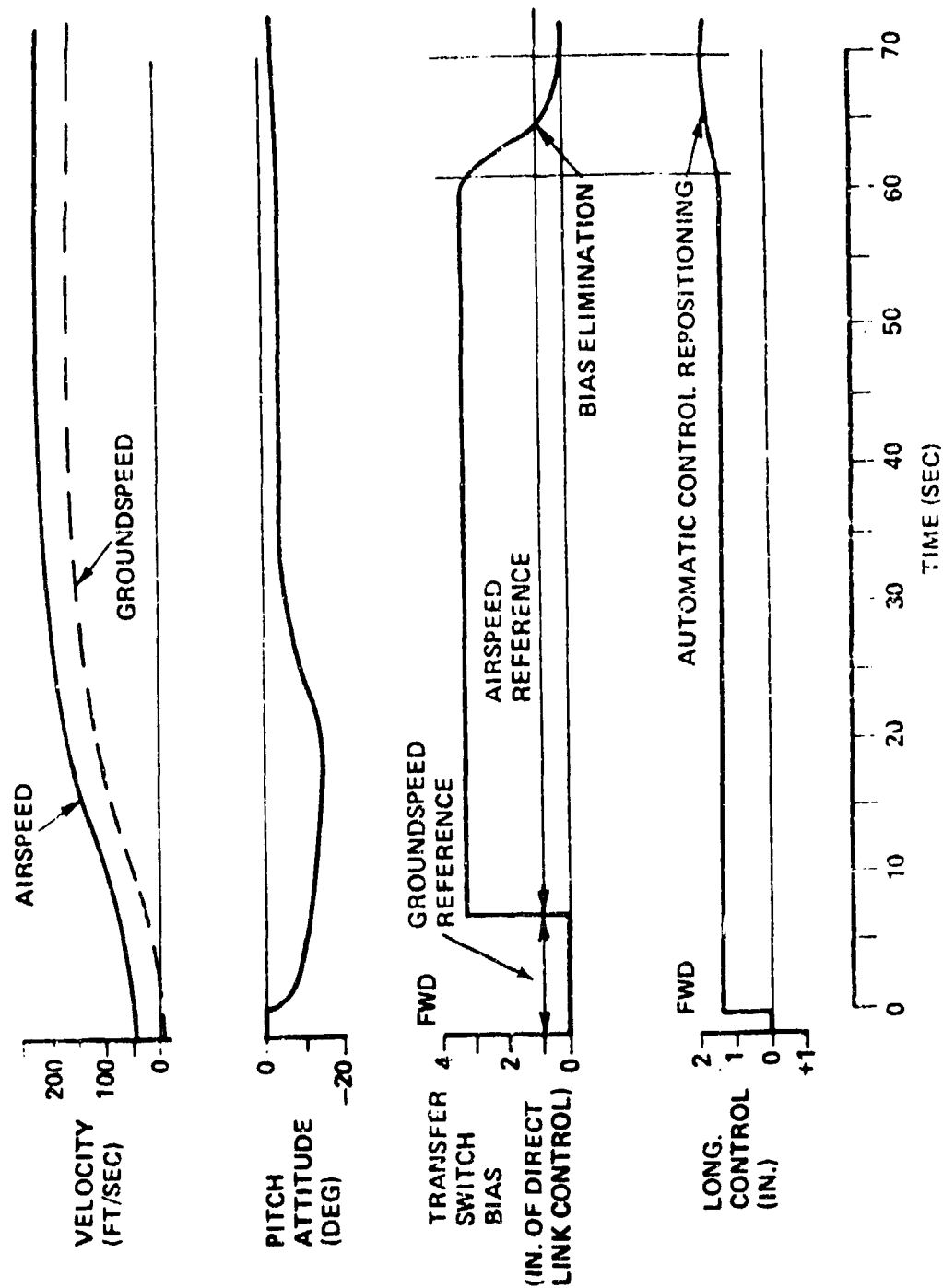
FIGURE 20. INSTANTANEOUS GROUNDSPEED TO AIRSPEED REFERENCE TRANSFER BIAS ELIMINATION, 50-KNOT HEAD WIND

115

Studies were performed to develop a longitudinal stick gradient with a dual sensitivity range, which used either LCP/DCP or DCP only at low speed to maintain compatibility with the high speed control configuration. Figure 21 shows a sketch of the proposed approach.

Piloted nudge base simulations were conducted wherein the low speed sensitivity was varied from 5-20 fps per inch of stick within a stick range about a hover reference varying in width from 1/4 to 1 inch. Lagged DCP inputs were tested, along with additions of up to ±4 degrees of longitudinal cyclic pitch. Satisfactory pilot ratings of the dual-range DCP gradient were achieved (using the 5 fps/inch stick sensitivity at low speed with ±2 degrees of LCP).

Follow-on analysis showed that potential problems arose with the mechanization when winds were present. Since basic aircraft characteristics are airspeed dependent, trim controls were required to maintain zero groundspeed in windy conditions. This trim control requirement created a skewing effect on the hover gradient, producing a variable sensitivity slope with wind. Variation of aircraft cg had essentially the same effect. Time constraints prohibited development of a control law mechanization to overcome the deficiency.

The desired reduced hover sensitivity and LCP control is provided to the load-controlling crewman by using a separate controller for the precision hover/maneuver task. This LCCC incorporates a non-linear optimal low sensitivity stick gradient which will be detailed in the hover hold section. The load crewman performs the precision hover task, and the pilot controls the aircraft longitudinally through the DCP/LCP gradients discussed in Section 4.1.3.1.2, for normal low-speed maneuvers not requiring extreme precision.

In the flight demonstration program, Cooper-Harper rating results indicate that the selected stick sensitivity solution was satisfactory. Zero groundspeed trimming, however, was not optimum from the pilot's station.

116
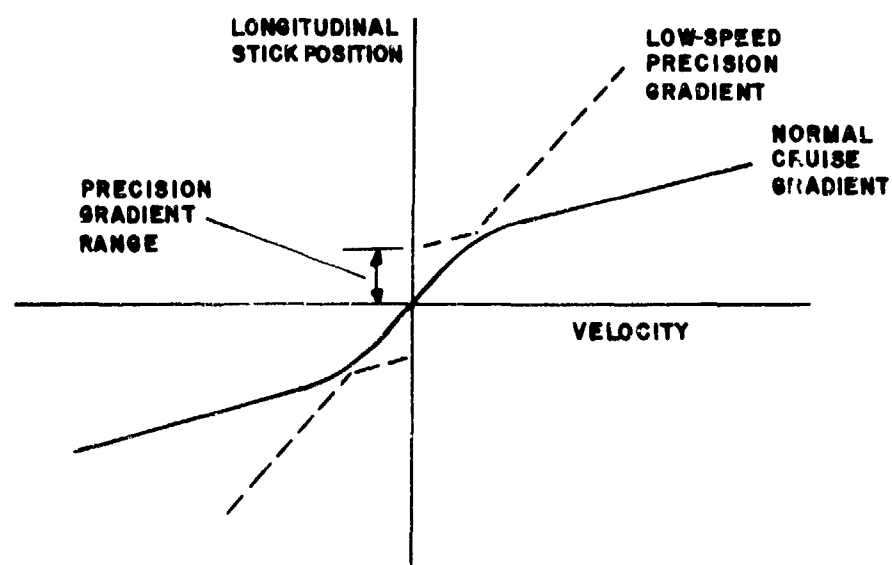
FIGURE 21. LOW SPEED STICK SENSITIVITY BLENDING APPROACH

2.1.3.1.4  Ground Operation of the AFCS

Microswitch circuitry is incorporated on the landing gear
oleo struts of the HLH (and Flight Research) aircraft to
change the operating status of the AFCS/SCAS for ground
operation.  Ground contact logic implemented on the 347/ATC
test aircraft provided transient suppression switching to
disengage the vertical, lateral, and directional axes by
ramping the AFCS differential commands to zero upon ground
contact.  The longitudinal axis maintained pitch attitude
and pitch rate stability on the ground, but the stick pickoff
command was switched to a ground reference value of zero and
the velocity command signal ramped to zero to provide a net
zero velocity command on the ground.

Aircraft control by the pilot on the ground is maintained in
each axis by only the direct path through DELS, with parallel
beep trim commands being processed through the AFCS.  No other
backdrive commands are generated on the ground by the AFCS,
since synchronization of bank angle, heading, and altitude
signal paths is continuous.

Selectable modes such as automatic hover trim, hover hold,
and altitude hold are also disabled on the ground.  The
velocity mode transfer switch bias error is set to zero when
ground contact is made to insure proper initialization of
the switch in the fly mode, and the backdrive path from the
switch is disconnected.  A summary of ground contact logic
operations performed by the AFCS follows.

GROUND CONTACT - 347/ATC Program

   LONGITUDINAL AXIS - Retain stability augmentation for pitch
   attitude and pitch rate.

   (1)  Set stick pickoff command to ground reference value
        of zero.

   (2)  Set decay velocity command path to zero.

   (3)  Reset velocity mode transfer switch bias error value
        to zero and eliminate velocity mode transfer switch.

   (4)  Disable automatic hover trim mode.

118

VERTICAL AXIS

(1)  Switch off differential command.

( )  Disable altitude hold mode and synchronize altitude
     reference (L-6).

LATERAL AXIS

(1)  Ramp lateral differential command signal to zero.

(2)  Reset velocity mode transfer switch bias error value
     to zero and eliminate velocity mode transfer switch
     backdrive path.

(3)  Synchronize bank angle reference (L-3).

(4)  Disable automatic hover trim mode.

DIRECTIONAL AXIS

(1)  Ramp directional differential command signal to zero.

(2)  Synchronize heading reference (L-5).

The hover hold mode and LCC control paths are disabled in
all axes through L-11 and L-20 logic.

2.1.3.1.5  DELS Interfacing for the AFCS ("Frequency Splitter")

All differential SCAS (and AFCS) outputs pass through frequency
selective networks in the DELS interface which split the signal
into trim and dynamic compensation paths as shown in Figure
22.  Each control axis has its own frequency splitter.

The trim path includes a high-authority, rate-limited
signal which provides long-term correction of a low-frequency
nature, such as directional pedal offset with airspeed.  High-
frequency  compensation requirements such as pitch rate damping
are provided by passing the signal through both authority
limiters (with the lower authority dominating)
prior to sending it on to the rotors.  Cross signaling from
the static path continually recenters the dynamic path.

119
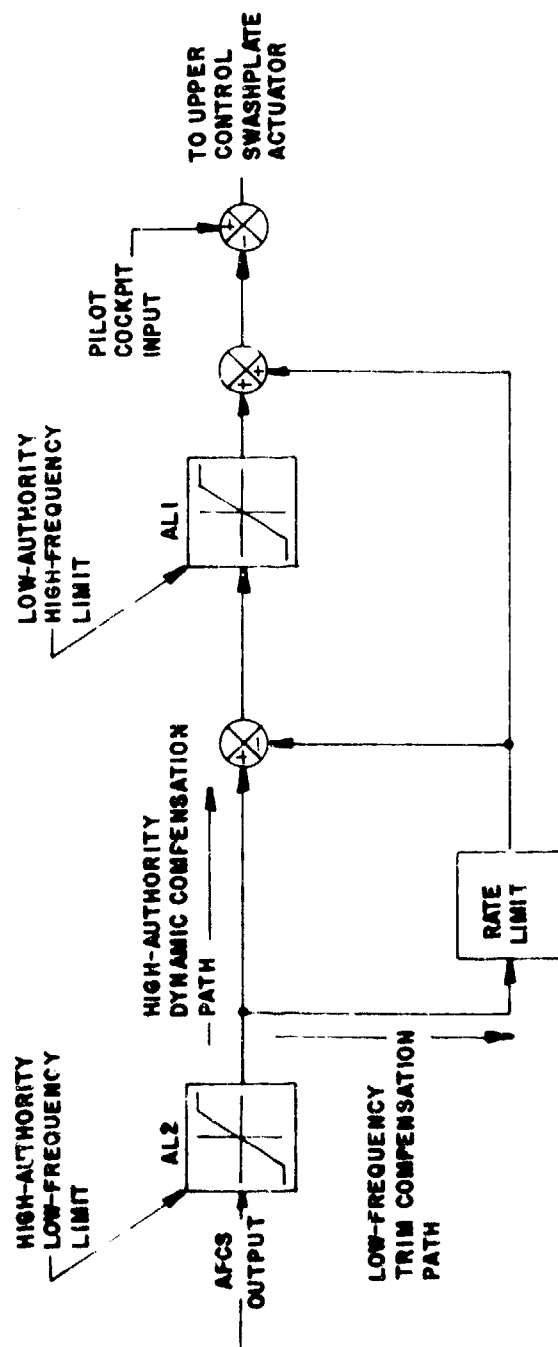
FIGURE 22. DELS/AFCS INTERFACE — 347 AFCS FREQUENCY
SPLITTER MECHANIZATION

120

The frequency splitter network reduces smoothly to zero after
AFCS disengagement-switch closure. This means that cockpit
control sensitivity, power, and margins are unaffected by
AFCS hardover conditions. Authorities and signal conditioning
were selected to keep short-term-impulse type disturbances
after hardover, as well as long-term trim changes, within
safe levels. Thus, the AFCS can experience a hardover without
impairing flight safety.

The table below summarizes all limiter settings for the
interface frequency splitters in each of the four AFCS axes.

| AXIS | AL1 HIGH FREQUENCY LIMIT | AL2 LOW FREQUENCY LIMIT | RATE LIMIT |
|------|--------------------------|-------------------------|------------|
| Longitudinal | $\pm 1.0$ inch | +4.0, -2.5 inch | .5 in/sec |
| Lateral | $\pm 0.75$ inch | $\pm 1.5$ inch | .4 in/sec |
| Directional | $\pm 0.6$ inch | $\pm 1.5$ inch | .2 in/sec |
| Vertical | $\pm 1.0$ inch | ----- | ----- |

## 4.1.3.2 LATERAL SCAS SYNTHESIS

The lateral SCAS axis is depicted in the top half of the
Figure 23 functional block diagram. The layout of this diagram
is similar to the one described earlier for the longitudinal
axis, wherein the SCAS loops are detailed along with all
selectable mode features except for automatic approach to
hover.

Stability feedback parameters are shown on the right side
of the diagram, with DELS interfacing including differential
AFCS outputs and feedforward inputs annotated along the top.
CCDA drives, "beep" trim, and LCCC inputs are arrayed down
the left side of the figure. All control law network paths
shown within the sectioned box enclosure represent calcula-
tions or switching performed within the triplex computer/
IOP complex on the aircraft.

**FIGURE 23.** Lateral AFCS Functional Block Diagram

123

2.

3
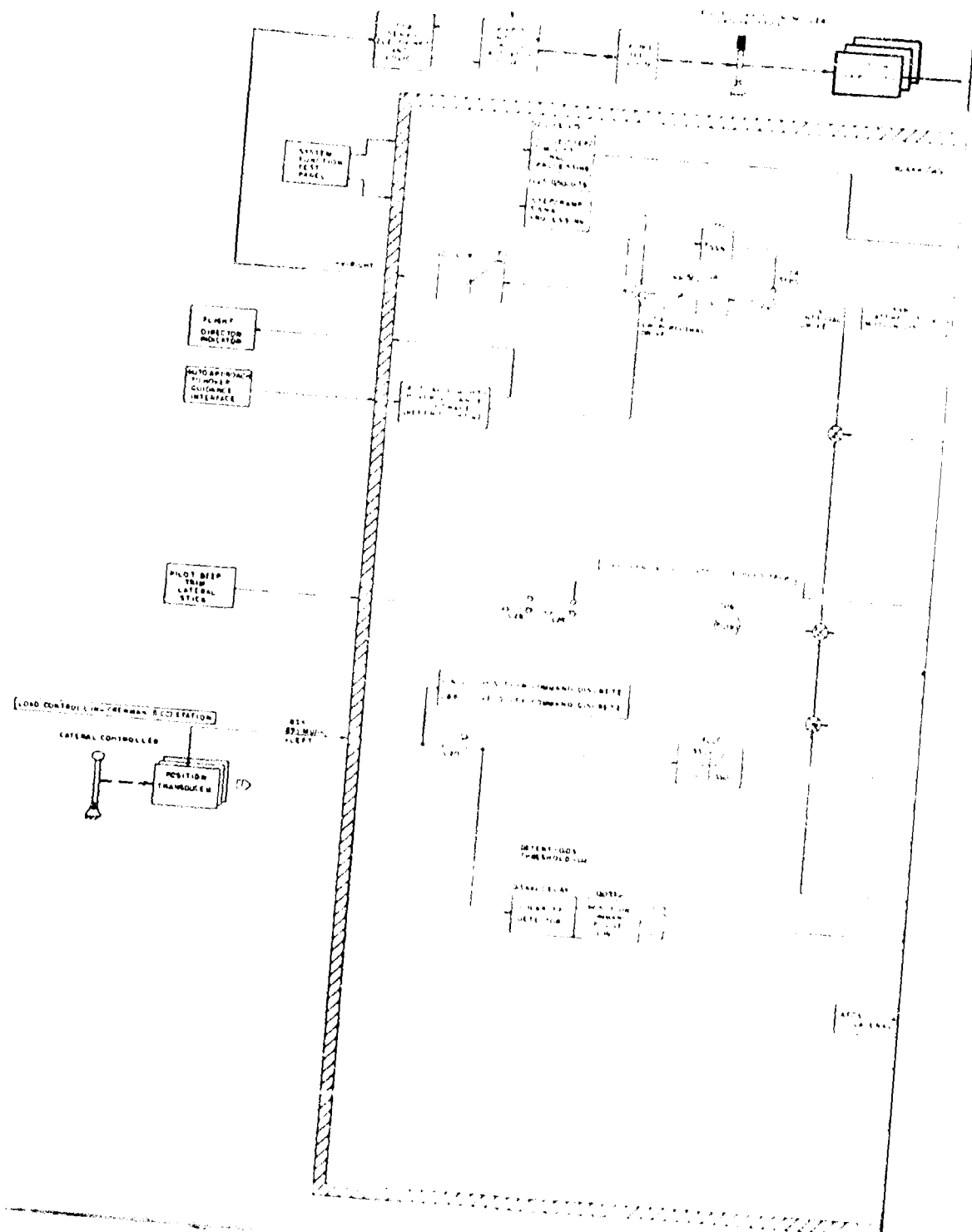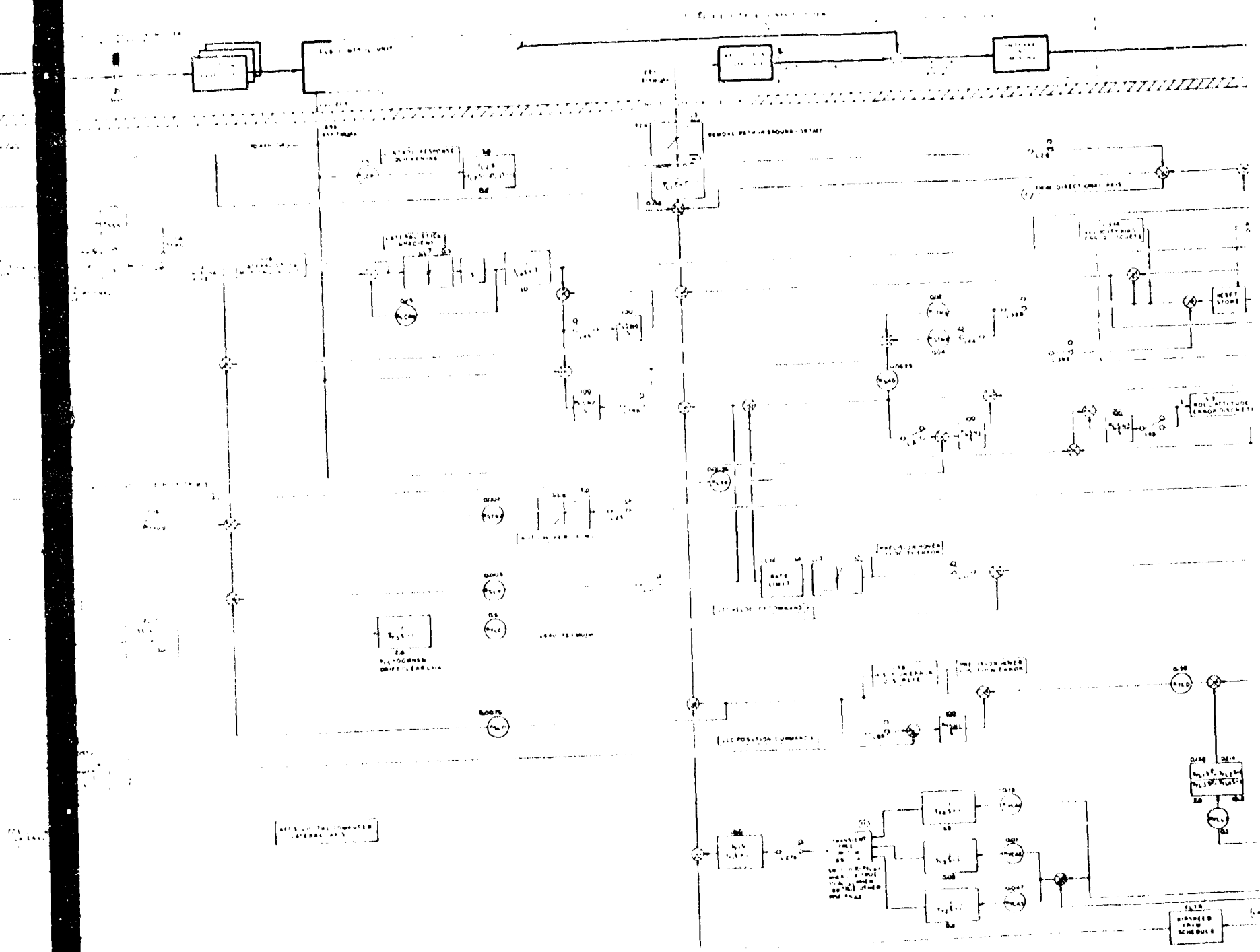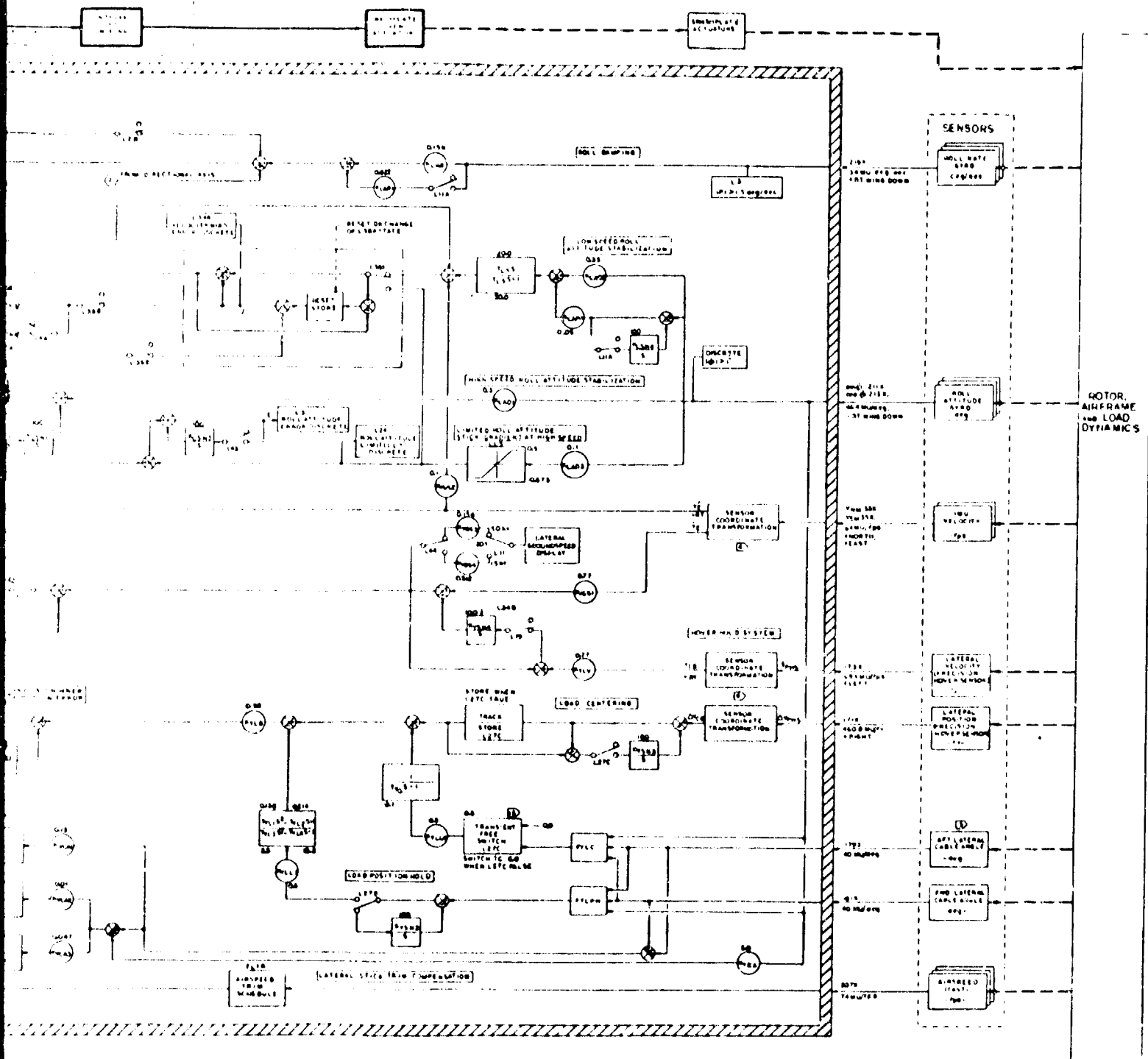
As indicated previously in Table 4, stability and control functions of the lateral SCAS change as the aircraft transitions from low- to high-speed flight. In hover and at low speed, the basic SCAS provides "hands off" lateral groundspeed hold capability. Angular rate damping and attitude loops are included along with a lateral ground speed path to achieve the desired stability levels.

To maneuver the aircraft, the pilot commands sideward translation (i.e., lateral groundspeed) through the cyclic stick, with the resultant velocity being directly proportional to stick deflection. Velocity commands are processed through a high gain rate limited-feed forward stick pickoff path, which acts in conjunction with a "quickening" function to shape the response.

Above 45 knots airspeed, bank angle is the stability parameter being held. Lateral stick deflections command bank angle up to 5 degrees of roll attitude, and govern roll rate above that point. The region of bank angle commanded around wings level permits fine adjustment of the flight path through a limited roll attitude stick gradient called the "security blanket". This control feature will automatically roll the aircraft out when the pilot releases the stick (providing that a stick force retrim has not been executed through application of the "mag" brake).

In normal turn entries where bank angles exceed 5 degrees, roll rate is stopped by moving the stick toward neutral as the desired bank angle is approached. When the roll rate is zeroed, force retrimming of the stick will cause the aircraft to stabilize at the new roll attitude. Signals crossfed between the roll and yaw SCAS axes ensure coordinated turn maneuvers.

Small incremental changes in low-speed velocity and high-speed bank angle can be made by the pilot through use of beep trim. Actuation of the trim button on top of the stick causes a parallel stick driving motion when the aircraft is flown at low speed. Parallel drive is also utilized in the cruise flight regime when bank angles are 5 degrees or less. Trim command signals are applied differentially above the 5-degree "limited" gradient.

125

Described below are the inner and outer loop stability and
control mechanizations utilized in the lateral SCAS axis.

### 2.1.3.2.1  Inner Loop Lateral SCAS Stabilization and Control

ROLL DAMPING - The stabilization loop depicted at the top of
Figure 23 constitutes the primary roll-damping path within
the lateral SCAS.  This network transmits airframe roll rate
through a gain factor and low-pass filter which eliminates
unwanted high frequency signal components generated by air-
frame vibration.  After filter passage, the damping signal is
summed with a shaped lateral feedforward "quickener" input, and
with a pedal pickoff compensation term from the SCAS yaw axis.

Yaw axis compensation corrects for airframe roll rates genera-
ted by directional control inputs in low-speed flight.
The forward and aft rotor pylons are not the same          are
height; therefore, a rolling moment is produced when dif-
ferential lateral thrust vector tilt is applied to yaw the
aircraft.  Rolling moments are in the opposite direction to
the pedal input (i.e., right directional control rolls the
aircraft to the left).  The sign of the compensation signal
is adjusted accordingly.

The output of the damping loop summer is low-pass filtered,
as described earlier, to remove the effects of sensor and
computer noise spikes.  The entire differential path output
is then authority limited prior to DELS interfacing to mini-
mize transients in the event of hardover failures.

CONTROL QUICKENING - Inner loop control augmentation is pro-
vided by the control response "quickening" loop shown in
the top center of Figure 23.  This feedforward signal is
taken from the cockpit stick and augments the direct DELS
path control input to the rotors.  The signal passes through
a frequency selective network which provides both a low-pass
filter for control smoothing, and a high-pass transfer
function (washout) to preclude signal saturation due to
stick offset.

Through the L-2 logic switching network, control response
quickening is removed when flying with coupled flightpath
control modes such as automatic approach to hover.

126

2.1.3.2.2  Outer Loop Lateral SCAS Stabilization and Control

ROLL ATTITUDE STABILIZATION - In high-speed flight, lateral
stability is maintained by the roll attitude stabilization
loop.  The high-speed path goes directly across the drawing
to the left through the LL3 authority limiter.  After being
converted to inches of equivalent stick (KLAD gain), the
attitude signal passes through a roll synchronizer, which
permits the pilot to stabilize roll angle at any desired bank
attitude.  The synchronizer loop is represented on the diagram
with an open L-3 switch and by an integrator annotated with gain
KLSN1.

Synchronizer Operation - The operating principles of a typical
AFCS synchronizer are shown in the Figure 24 sketch.  In this
illustration, an "analog" analogy is used to aid in visualiz-
ing signal flow and integrator function within the synchroni-
zation network.  The digital computer mechanization of this
device on the aircraft differs slightly from the analogy
shown, but the net operating principles are the same.

In its simplest form, the synchronizer either passes the
incoming signal along the lower path while stabilizing, or
feeds back this signal to eliminate output while operating
in the synchronizing (sync) mode.  When switching from an a
synchronize to a stabilize mode, the last value of the input
signal into the integrator IC is held so that roll attitude
stabilization is resumed about the new angle.  The integrator
initial condition (IC) path is used to either hold or pass
directly (without integration) signals presented the
integrator.

During stabilized operation, an additional signal (such as a
beep trim command) can be passed through the integrator.
This signal is rapidly "integrated up" to sum with the incom-
ing attitude input, thereby rereferencing the output of the
synchronizer.

In high-speed level flight, the roll synchronizer passes
attitude stabilization signals which are usually very small
unless the aircraft is disturbed by a gust.  When the pilot
initiates a turn maneuver, the stick is moved laterally out
of detent, and the L-3 switch closes to rapidly reduce
roll attitude feedback to zero (so as not to "fight" the
turn entry).

127

(A) FEEDBACK SIGNAL GOES INTO INTEGRATOR IC AND IS PASSED DIRECTLY (TRACKED) WHEN L3 SWITCH IS CLOSED

(B) WITH L3 OPEN, LAST VALUE INTO IC IS HELD (STORED)

L3 LOGIC SWITCHING

IC

INTEGRATOR

INPUT ATTITUDE REFERENCE SIGNAL

DIFFERENTIAL ROLL ATTITUDE BEEP TRIM SIGNALS ARE "INTEGRATED UP" TO PRODUCE NEW TRIM REFERENCE WHEN SYNCHRONIZER IS STABILIZING

OUTPUT INTO DIFFERENTIAL PATH

NOTE: SYNCHRONIZER SHOWN IN "STABILIZE" MODE WITH ATTITUDE SIGNAL BEING PASSED DIRECTLY

FIGURE 24. SCHEMATIC OF TYPICAL SYNCHRONIZER OPERATION (ANALOG ANALOGY) — ROLL ATTITUDE

The detent is characterized by a small increment of stick ;
motion established on either side of the zero force position
of the stick. This zero force stick position is set by the
pilot through use of the magnetic brake button which unlocks
the magnetic brake force-feel capsule from its reference
position. When the button is released, a new force reference
is established.

In addition to passing through the LL3 limiter, roll attitude
synchronizer outputs also are processed through the integral
stick drive CCDA path shown on Figure 23. Sync outputs are
transmitted through this loop (which starts with the KSAD gain
factor) primarily to keep the synchronizer output as close to
zero as possible while maintaining the steady state roll
attitude reference. A characteristic of the integral path
is to remove inherent lateral stick offset with speed which
ensures the correct lateral stick to swashplate trim
relationship.

Low-Speed Attitude Stabilization - Above the high-speed roll
attitude loop on Figure 23 is a similar path for low-speed
operation. This attitude feedback network adds low-speed
velocity damping for the inertial velocity path described
below.

The roll attitude signal is processed through a high-pass
filter which provides short-term stabilization while accommo-
dating steady roll attitude requirements associated with wind
changes.

LOW-SPEED VELOCITY STABILIZATION - As introduced earlier,
ground speeds generated by the Inertial Measuring Unit (and
transformed within the computers to the proper reference
axis) are used for velocity stabilization in the low-speed
range of the flight envelope. The $Y_E$ and $Y_E'$ lateral ground-
speed feedback signals lie in the plane of the earth's surface,
and serve the same function as similar velocities already
described for the longitudinal axis.

Switching between velocity stabilization at low speed, and
bank angle hold (including coordinated turn capability) at
high speed, is accomplished with a velocity mode transfer
switch which operates very much like the one already described
for the longitudinal axis. A discussion of this crossover
switching operation follows.

Lateral/Directional Control Crossover - The instantaneous
reference blending scheme adopted for the longitudinal SCAS
axis was applied to the lateral/directional SCAS using the
same switchover logic methodology. When airspeed is greater
than 45 knots, an airspeed mode (coordinated turn/bank angle
hold) is utilized. On decreasing airspeed to below 40 knots,
the system reverts to a groundspeed/lateral velocity type of
operation.

The bias signal generated on switchover represents the dif-
ference between the lateral velocity feedback and roll
attitude signals. Aircraft maneuvers created on going
through transition are mild, and very similar to those that
would be experienced in present helicopters without lateral
groundspeed systems. Typical transition time histories
taken during hybrid simulation studies are presented in
Figures 25 and 26.

Both of these figures represent longitudinal accelerations
and decelerations initiated with the aircraft in sideward
flight of 40- to 50-fps lateral velocity. In Figure 25, the
lateral stick is force trimmed (or in detent) during transi-
tion, while in Figure 26 it is left out of detent. Bias
elimination through parallel drive is observed in Figure 26.

In Figure 26, on the left side of the velocity mode transfer
switch module, are shown the backdrive integral command, and
feedforward paths associated with lateral axis bias elimina-
tion. The integral backdrive path has a multiple gain network
which increases the input to the CCDA integrator at airspeeds
above 45 knots. As in the case of the longitudinal feed-
forward signal into the transfer switch, a lateral synchronizer
is installed (KLSN2/S) to keep the path zeroed except during
actual backdriving operations.

LATERAL/DIRECTIONAL - CONTROL CROSSOVER, RIGHT LATERAL STICK IN DETENT

MODEL 347 HYBRID COMPUTER DATA
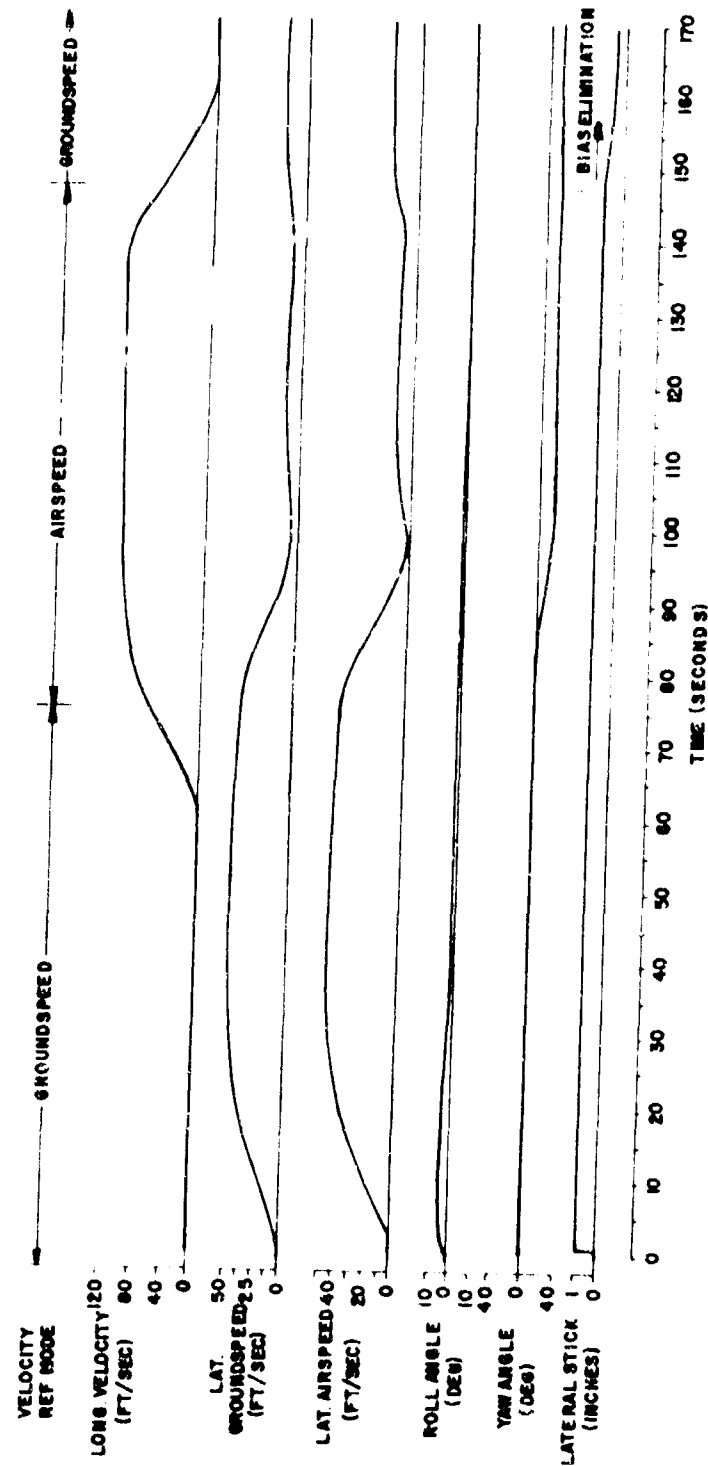
FIGURE 25 INSTANTANEOUS GROUNDSPEED-TO-AIRSPEED REFERENCE TRANSFER

131

LATERAL/DIRECTIONAL- CONTROL CROSSOVER, RIGHT LATERAL STICK OUT OF DETENT

MODEL 347 HYBRID COMPUTER DATA
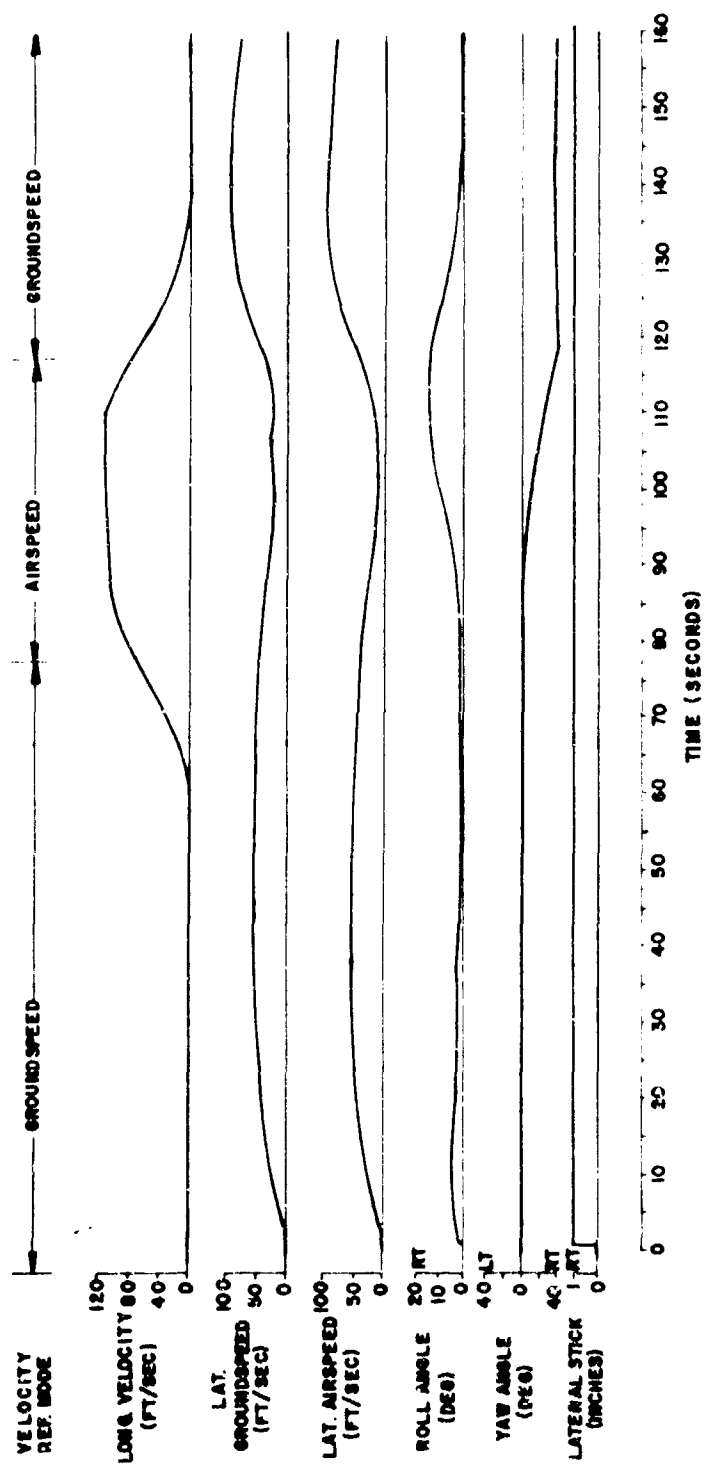
FIGURE 26. INSTANTANEOUS GROUNDSPEED-TO AIRSPEED REFERENCE TRANSFER

132

During nudge base flight simulations conducted at Vertol to optimize lateral/directional crossover control law mechanizations, accelerating and decelerating transitions in headwinds and sidewinds were evaluated. Numerous maneuvers in the transition area of 40 knots $\pm 10$ were accomplished with the following results:

- The switching concept from groundspeed to airspeed produced no objectionable transients.

- Stick retrim for bias elimination was satisfactory.

CONTROL AUGMENTATION - Two paths are provided within the lateral SCAS for outer loop control augmentation. These include a lateral stick gradient circuit used in low-speed flight, and a limited roll attitute stick gradient feature for high-speed precision maneuvering. The low-speed stick gradient is shown in the right center of Figure 23, and the limited roll attitude gradient is directly below the high-speed roll attitude loop on the same diagram. Both augmentation networks are discussed briefly below.

Low-Speed Lateral Stick Gradient - The feedforward stick gradient loops included for low speed flight are mechanized in a manner similar to those already described for the longitudinal SCAS. A rate limit and multiplying circuit are included followed by a low-pass filter. This network operates against the strong low-speed velocity hold feedbacks to provide command lateral groundspeed. As shown on the diagram, the feedforward stick gradient input is summed with the stabilizing velocity signal just prior to entry into the velocity mode switch. The sensitivity is approximately 35 knots per inch of lateral control.

Beneath the first order low-pass filter in the gradient network is a cross-feed path passing through a synchronizer controlled by an L-45 switch. This path is a component element of the feedforward portion of the bias elimination feature of the lateral velocity mode switch. The synchronizer prevents transients associated with groundspeed/ airspeed transfer, and permits the augmented feedforward stick signal to pass at low speed only.

133

High-Speed Limited Roll Attitude Stick Gradient - To facili-
tate fine adjustment of the flight path in the cruise envelope
region, a limited stick gradient is provided out to 5° of roll
angle with up to +.5 inches of lateral stick. This control
feature also provides a backup for IFR disorientation recovery
in that if the stick is released, the aircraft rolls out of
the maneuver to a wings-level attitude.

The gradient is generated by passing roll attitude feedback
through a gain and limiter (LL5 on Figure 23) which restricts
feedback corrective control inputs in excess of 5 degrees.
The limiter output forms a bias signal which must be "stood
off" with opposite control in the cockpit, thereby generating
a bank angle gradient with stick deflection. Note that the
limiter is slightly assymmetrical (i.e., (-).5 inches and
(+).675 inches) to account for trim requirements associated
with forward rotor delta-three hinging.

The limiter output passes through the velocity mode switch
(and into the differential AFCS path). The output also goes
to a summer where the attitude signal is compared with the
cockpit stick commands to provide an error signal for input
to the L-3 logic switching network. When the error is small,
the stick is near its position for trimmed flight. An L-43
controlled synchronizer prevents calculation of the error
signal unless the pilot deliberately maneuvers the aircraft.
The intent of the synchronizer is to prevent gust-generated
attitude errors from inadvertently unlatching roll stabiliza-
tion. Use of the limited gradient is illustrated on the
following examples.

Control Inputs   0.5 inches - When the pilot introduces a
lateral stick step of .5 inches, the aircraft will begin to
roll due to the direct path DELS input at the swashplate, and
the response quickner input. At the summer described above,
the .5 inches of stick fed into the AFCS will appear as an
error of .5 inches (before roll angle starts to build up).

As roll angle increases from its initial value, the output of the LL5 limiter passing through the velocity mode switch will start to put in corrective control through the differential path, which builds until an equivalent of 5 degrees of bank is reached. At this time the control mix sees no net control input at the rotor (i.e., cockpit control = differential AFCS output), and further rolling motion stops. The summer error is also zero.

All conditions for (L-3) stabilization at the new commanded bank angle are met, except for the fact that the stick is out of detent. Stabilization is achieved by "mag" braking, which places the stick within the detent again.

During early control system synthesis work, including piloted simulations, the limited lateral gradient was extended out to 10 degrees of bank angle. Flight test results, however, indicated need for a tighter return to trim characteristic, and this improvement was achieved by doubling the attitude gain into the LL5 limiter (which halved the maximum bank angle within the limited gradient).

Larger Control Inputs - Figure 27 illustrates a typical rolling maneuver response where the aircraft is either returned to wings level by releasing the stick, or is stabilized at a fixed bank angle to reduce pilot workload while turning. Data shown in the plot was generated from developmental simulation results.

A stick step of several seconds duration is put in by the pilot to initiate the maneuver. If the pilot wishes to roll out of the turn without stabilizing bank angle, he releases the stick and it returns to the neutral force point. Return of the stick to the limited roll attitude gradient range causes a corrective control to be put in by the AFCS which rolls the aircraft to wings level (security blanket effect). Should the pilot desire to stabilize bank angle during the turn entry, he merely returns the stick toward neutral and force trims (with the mag brake) when roll rate falls to zero. (Note that roll rate will be zero when the stick is at the edge of the roll attitude limiter).

135
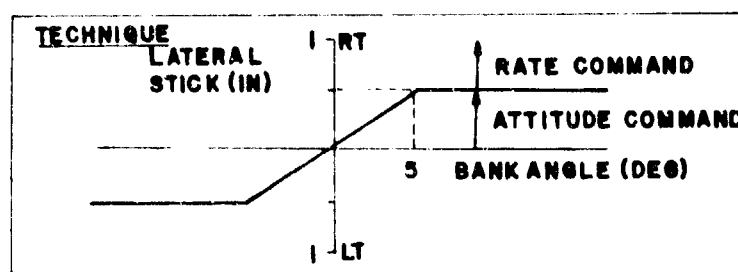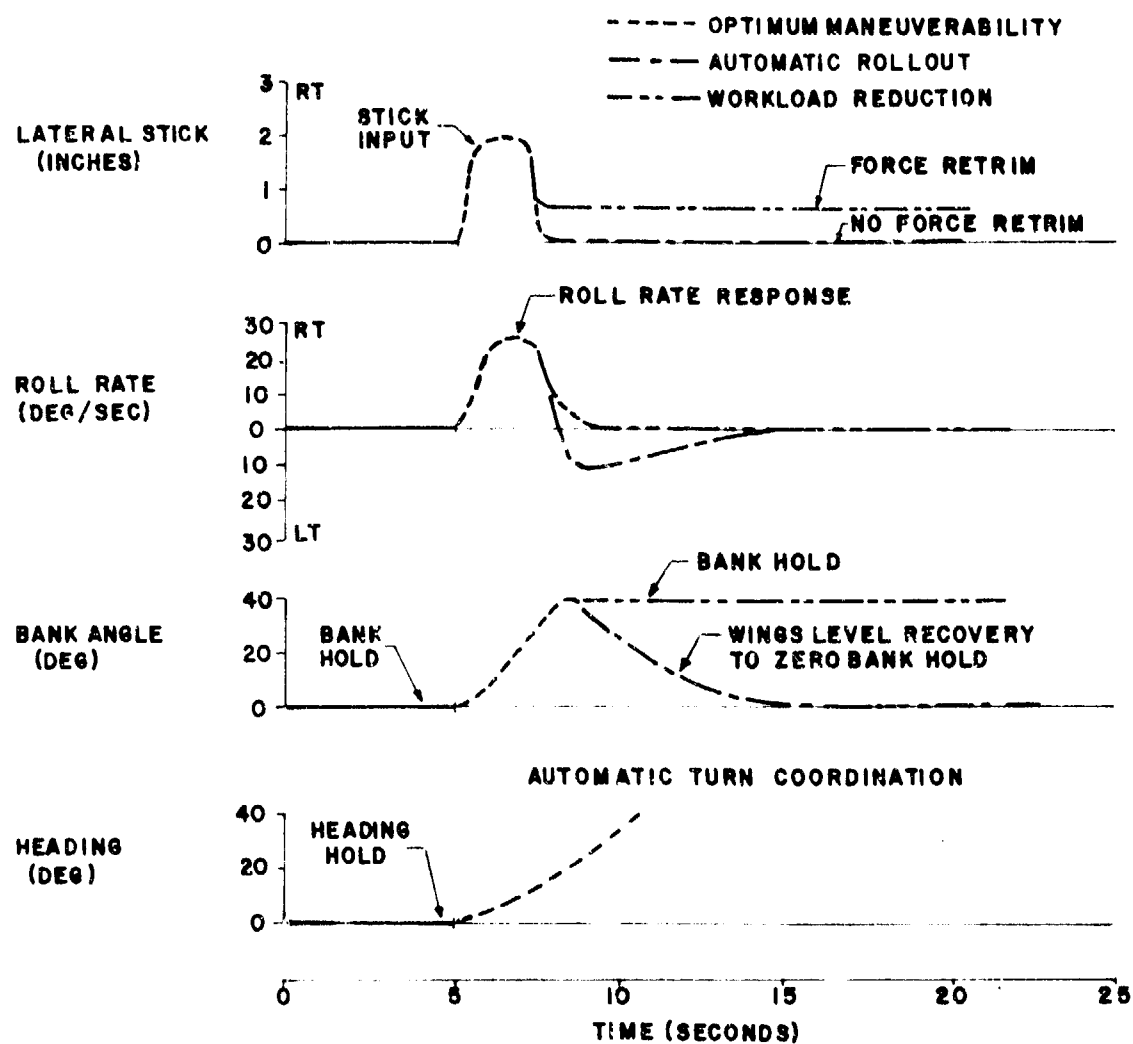
FIGURE 27. FORWARD FLIGHT-LATERAL DIRECTIONAL SCAS

136

Lateral Stick Trim Compensation - Shown at the bottom of
Figure 23 is a feedback path which produces a differential
signal to correct for inherent lateral stick trim offset with
airspeed. This loop helps keep the stick position in the
cockpit zeroed when the aircraft is trimmed in level flight.
The proper signs for the airspeed trim gain schedule (FLTR)
correction used in the 347 Flight Research Vehicle are shown
in Figure 23. The HLH aircraft will use a similar correction
path but with opposite sign because of the different rotor
rotational direction.

VELOCITY REFERENCE SELECTION - As described earlier for the
longitudinal SCAS, the lateral axis can be manually programmed
through the mode select panel to provide either groundspeed
or airspeed reference at any flight velocity. By selecting
"airspeed" reference in the low-speed region, the lateral
stability parameter becomes bank angle hold as shown in
Table 6. Response to step control inputs in this area of
the envelope is bank angle up to 5 degrees of roll attitude,
and roll rate above this point. Table 7 summarizes control
response information for manual velocity selection.

Use of groundspeed reference for high-speed flight causes
the aircraft to hold lateral groundspeed for stability.
Step control inputs also produce groundspeed responses.

2.1.3.3  Directional SCAS Synthesis

Directional SCAS control law mechanizations are summarized
in the Figure .8 functional block diagram. Layout of the
chart is similar to that of the two SCAS axes already described,
with stability feedbacks on the right, DELS interfacing at
the top, and LCC, beep trim, and CCDA backdrive command paths
on the left.

Tables 4 and 5 in Section 2.1.2 describe both the low- and high-
speed functional characteristics of the helicopter with the
directional SCAS engaged. In low-speed flight, aircraft
heading is the stability parameter held, while heading rate
is commanded by step control inputs. Above 45 knots airspeed,
heading is held (for zero turn command) and sideslip stability
is provided. Sideslip is also the parameter commanded when
step inputs are introduced with the pedals.

137
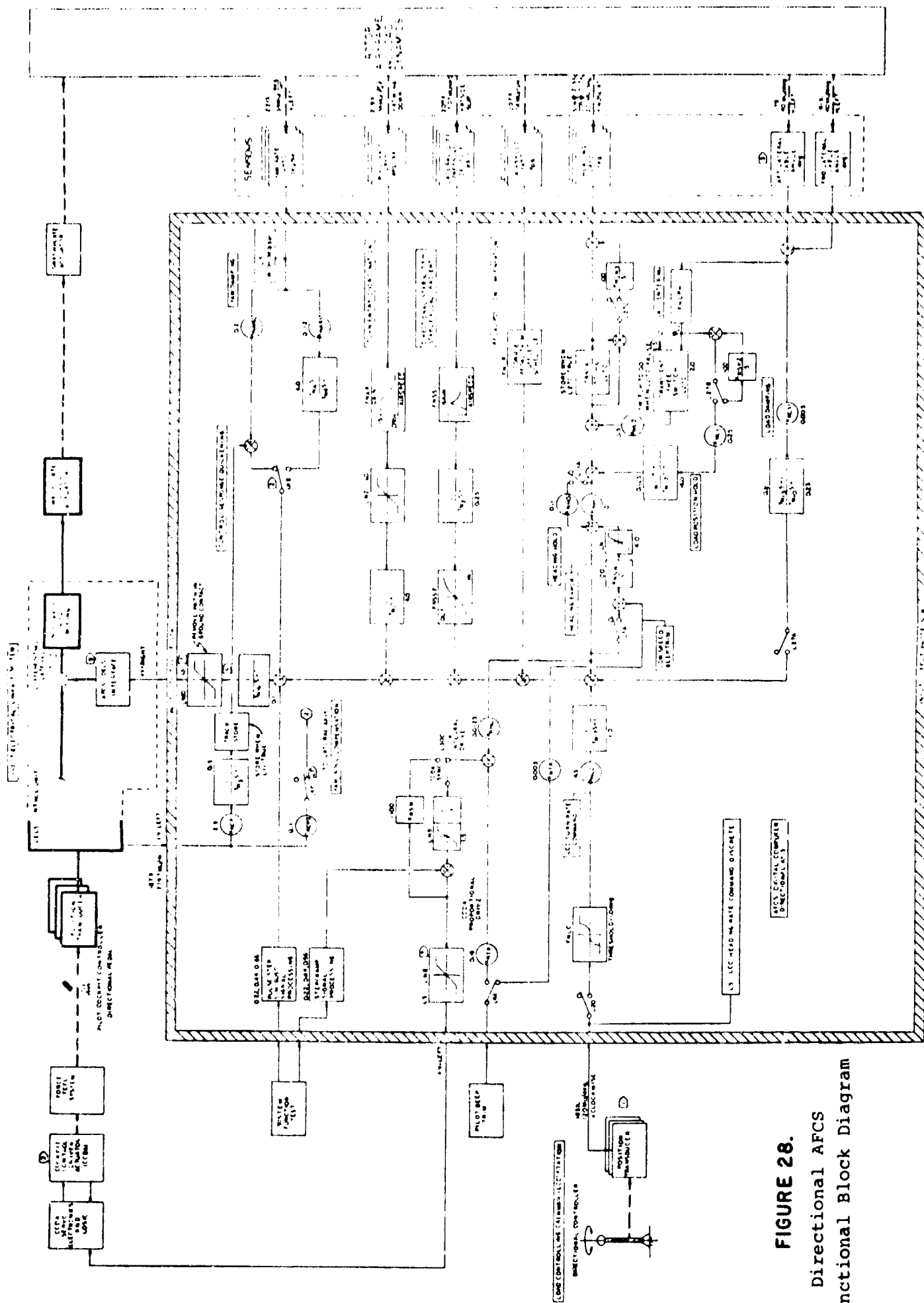
**FIGURE 28.**

Directional AFCS
Functional Block Diagram

139

Several of the stability loops utilized in the directional
SCAS are similar to those incorporated on current (or
developmental derivatives of) production tandem helicopters
such as the CH-47C. These stability networks include yaw
rate damping, turn coordination through roll rate crossfeed,
stable sideslip gradient, and heading hold features. A
low-speed pedal pickoff "quickener" of the type used on the
347 is also included in the HLH Flight Research Vehicle AFCS
mechanization.

As in the case of the longitudinal and lateral axes, the
directional SCAS also provides fine tuning control capability
through use of beep trim.n.

A trim button (coolie hat) located on the collective stick
in the cockpit activates this control system feature. Below
45 knots airspeed, beeping is accomplished through the dif-
ferential path to modify aircraft heading. Trim control
commands pass directly into the heading synchronizer to
rereference its output (in a manner similar to that used in
the lat al axis). At high speed, parallel pedal beep trim
is utilized, and the parameter varied is sideslip angle.

Details of inner and outer loop control law mechanization
for the directional SCAS are presented next.

2.1.3.3.1  Inner Loop Directional SCAS Stabilization and
Control

YAW DAMPING -- Illustrated in the top right hand corner of
Figure 28 are the high- and low-speed damping paths utilized
in the directional SCAS. The low-speed loop is shown nearest
the diagram top, with L-4 switching incorporated to transfer
airframe yaw rate feedback (in a transient-free manner) from
one path to another at 45 knots. Switching between loops is
accomplished at a single airspeed, and does not depend upon
whether the aircraft is speeding up or slowing down as in the
case of the SCAS axes already covered.

141

The single output of the damping network goes through a low-pass filter prior to authority limiting and DELS frequency splitter interfacing. The first order filter removes the effects of airframe vibration from the damping signal, and also compensates for the small computer/sensor noise spikes described earlier. In analytical and simulation modeling of the damping loops, the filter was originally placed adjacent to the input gain, but was later moved to accommodate all of the differential outputs for improved AFCS performance.

The frequency selective directional SCAS/DELS interface is similar to the one described earlier for the longitudinal axis, and a description of its operation (and authority limitations) appears at the end of Section 4.1.3.1.5.

As shown in the block diagram, a washout filter is incorporated in the high-speed damping path to preclude yaw rate signal saturation in steady coordinated turns. This high pass filter is eliminated at low speed to ensure a linear yaw rate pedal gradient. Leaving in the washout at low speed would cause the filter to act as a differentiator, which would produce acceleration like feedbacks, and unwanted aircraft responses.

CONTROL RESPONSE QUICKENING - Summed with the low-speed damping signal is a feedforward pedal pickoff "quickener" input. The quickening consists of processing directional pedal position through a low-pass filter to augment the steady yaw rate, rise time, and amplitude produced by the direct path control input. When used in conjunction with the damping loop described above, the quickener produces linear fi st order yaw rate responses (to pedal step inputs). The feedforward signal, by standing off the feedback yaw rate, allows higher steady rates to be developed without increasing authority.

2.1.3.3.2 Outer Loop Directional SCAS Stabilization and Control

DIRECTIONAL STABILITY, STABLE PEDAL GRADIENT - Static directional stability incorporated into the basic 347 Flight Research Vehicle and HLH prototype airframes is very close to neutral without AFCS augmentation. The 347 exhibits low levels of positive stability, and the HLH is slightly negative at angles of attack in the cruise region of the flight envelope. As a result of low inherent stability, which is

142

a useful feature for gust rejection, very flat cockpit pedal gradients with sideslip angle are generated by the basic aircraft.

To improve this situation for the pilot, augmentation is provided in the form of a pedal gradient network that utilizes measured airframe sideslip information. The sideslip feedback is generated by a set of pressure ports located in the nose of the helicopter, which produce a differential pressure proportional to sideslip angle. The sideslip signal is passed through a variable gain network and low-pass filter to produce the required stability feedback.

Variable sideslip gain is developed in two sections. As shown in Figure 28, the first of these (FNSS1) modulates sideslip sensitivity as a function of airspeed, resulting in constant gain as a function of sideward velocity. Gain is reduced to zero in the low-speed region to preclude introduction of any rotor-induced downwash components into the static ports which become pronounced as the aircraft slows down.

The second section of the sideslip network programs gain as a function of sideslip angle, with a higher gain (and stability) in the region close to zero sideslip. This feature allows sideslip feedback over a wide range of angles wwithout requiring excessive control authority.

In addition to the low-speed induced velocity effects just mentioned, the rotor also produces a series of periodic pressure pulses which enter the sideslip ports each time a blade passes in front of the aircraft. These high frequency pressure pulses are removed from the sideslip signal by the low-pass filter shown on the diagram.

When the aircraft is trimmed at any sideslip angle (other than zero) the SCAS augmentation feedback puts a corrective pedal movement directly into the rotor through the differential path. If the pilot did nothing, the resulting control moment would return the helicopter to straight flight. Instead, the pilot applies pedal in the direction he wishes to hold the aircraft nose for trim, which is equal and opposite to the differential SCAS increment. The resulting relationship between cockpit pedal and sideslip is the desired stable gradient, requiring progressively more pedal to hold the aircraft in trim as sideslip angle builds up.

143

COURSE PEDAL TRIM COMPENSATION - As airspeed is increased
from hover, right pedal is required to trim the basic
unaugmented aircraft at zero sideslip. This offset results
from induced swirl effects imparted into the slipstream by
rotor rotation. The twisting downwash applies side force to
both rotor pylons and to the fuselage which must be compensated
for by application of differential lateral thrust tilt
(pedal input).

An airspeed scheduled feedback path is incorporated into the
directional SCAS to compensate for the zero sideslip pedal
requirement. By putting in a rough approximation of the
differential lateral cyclic required to trim the aircraft
(through the differential path), the pedal position in the
cockpit is maintained at close to zero throughout the trim-
speed range of the helicopter. When this feature is mechani-
zed in the HLH AFCS, opposite signs must be used for the
feedback to account for the change in direction of rotor
rotation.

HEADING HOLD - Heading hold capabilities are incorporated into
the directional SCAS through the path shown in the lower right
hand side of Figure 28. The network includes only the
straight-through loops utilizing the KNHD gain, and KNSN1/S
synchronizer discussed earlier. The remainder of the heading
hold mechanization is associated with load stabilization
features which will be discussed later.

At low speed, heading is held whenever the aircraft is being
maneuvered sideward with the lateral stick. To make a pedal
turn, heading hold is unlocked through the L-5 logic and is
synchronized until the pedals are returned to the detent
indicating the pilot's desire to stop the turn.

In forward flight, heading is unlocked for turns commanded
with the lateral stick, or when sideslipped trim flight
conditions are being set up. At other times, the heading
synchronizer is maintained in a stabilized mode and aircraft
heading is held unless the pilot applies beep trim to
adjust the flight condition slightly. A typical turn entry
is shown in Figure 29, where heading synchronizer operation
is illustrated in the responses shown at the bottom of
the sketch.

144
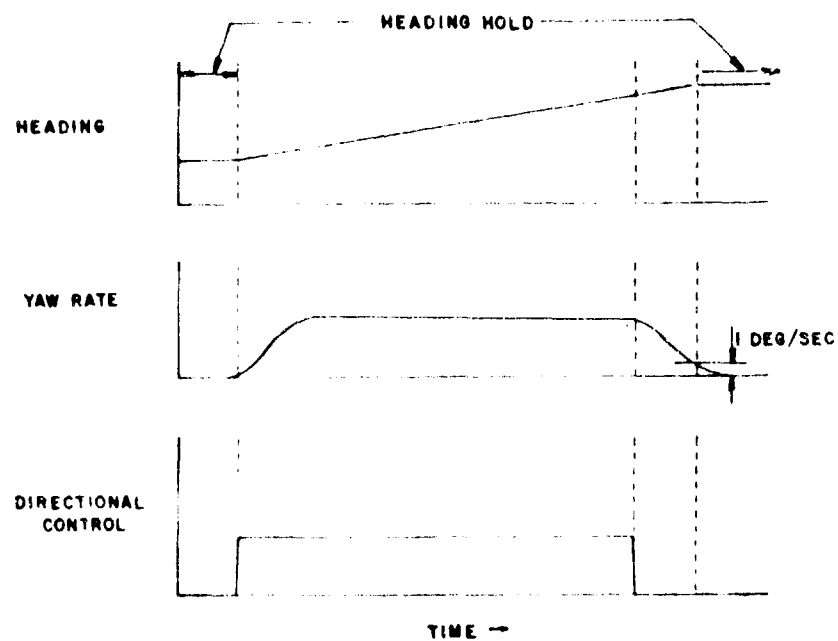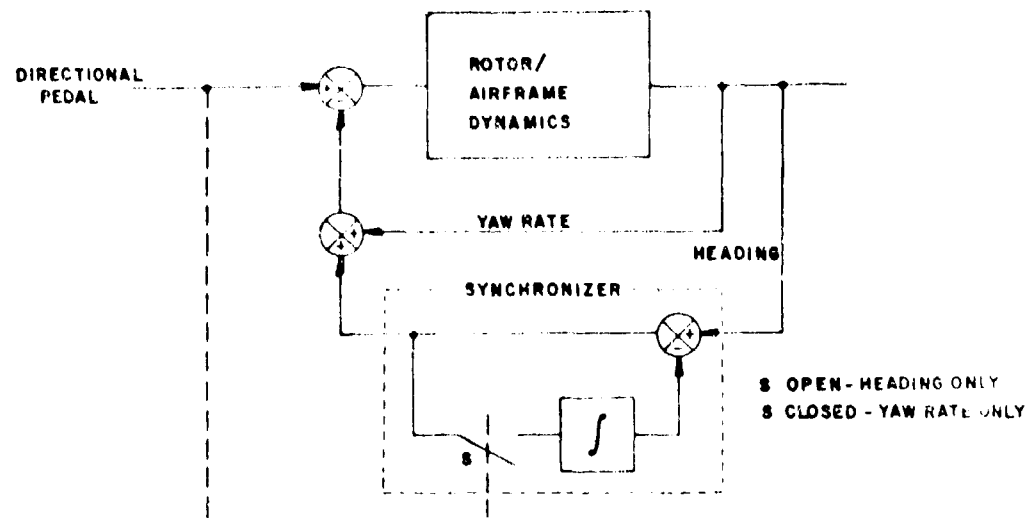
FIGURE 29.
DIRECTIONAL STABILITY/MANEUVERABILITY
(LOGIC TECHNIQUE)

145

TURN ENTRY COORDINATION - Entry into stabilized turns in for-
ward flight is facilitated by a directional SCAS loop which
utilizes aircraft roll rate feedback to provide coordination.
This loop effectively prevents the yaw rate damping path from
"fighting" the desired heading change at the start of a turn.
The coordination path passes roll rate through an airspeed
modulated gain and low-pass filter as shown in Figure 28.

The filter has been adjusted to minimize the effects of lat-
eral acceleration during turn entry, permitting lateral stick-
only turns to be accomplished with a centered turn and slip
ball indication.

### 2.1.3.4 Altitude Hold Synthesis

Although the altitude hold function in the vertical SCAS may
be considered as a selectable mode, it is discussed in the
accompanying SCAS writeup because in the final AFCS config-
uration vertical SCAS operation is possible only when
altitude hold (or hover hold) is selected. With either
barometric or radar reference enabled, the altitude hold mode
should provide altitude hold capabilities within the following
tolerances:

- Barometric Mode - $\pm 10$ feet of established altitude
  level flight

  $\pm 30$ feet of entry altitude in turns to 30-degree bank

- Radar Mode - $\pm 10$ percent or $\pm 5$ feet of established
  altitude, whichever is greater, in the hover regime.

The functional block diagram presented in Figure 30 summarizes
the control law package developed for the vertical AFCS.
Illustrated along with the basic SCAS are altitude hold, load
stabilization, and hover hold selectable mode features. As
shown in the figure, the vertical AFCS provides feedback
stability augmentation through a differential path interfaced
with the DELS, and both integral and proportional CCDA
commands for backdriving the cockpit collective stick. The
AFCS accepts LCCC inputs in conjunction with hover hold
operations which will be covered in the next report section.

146
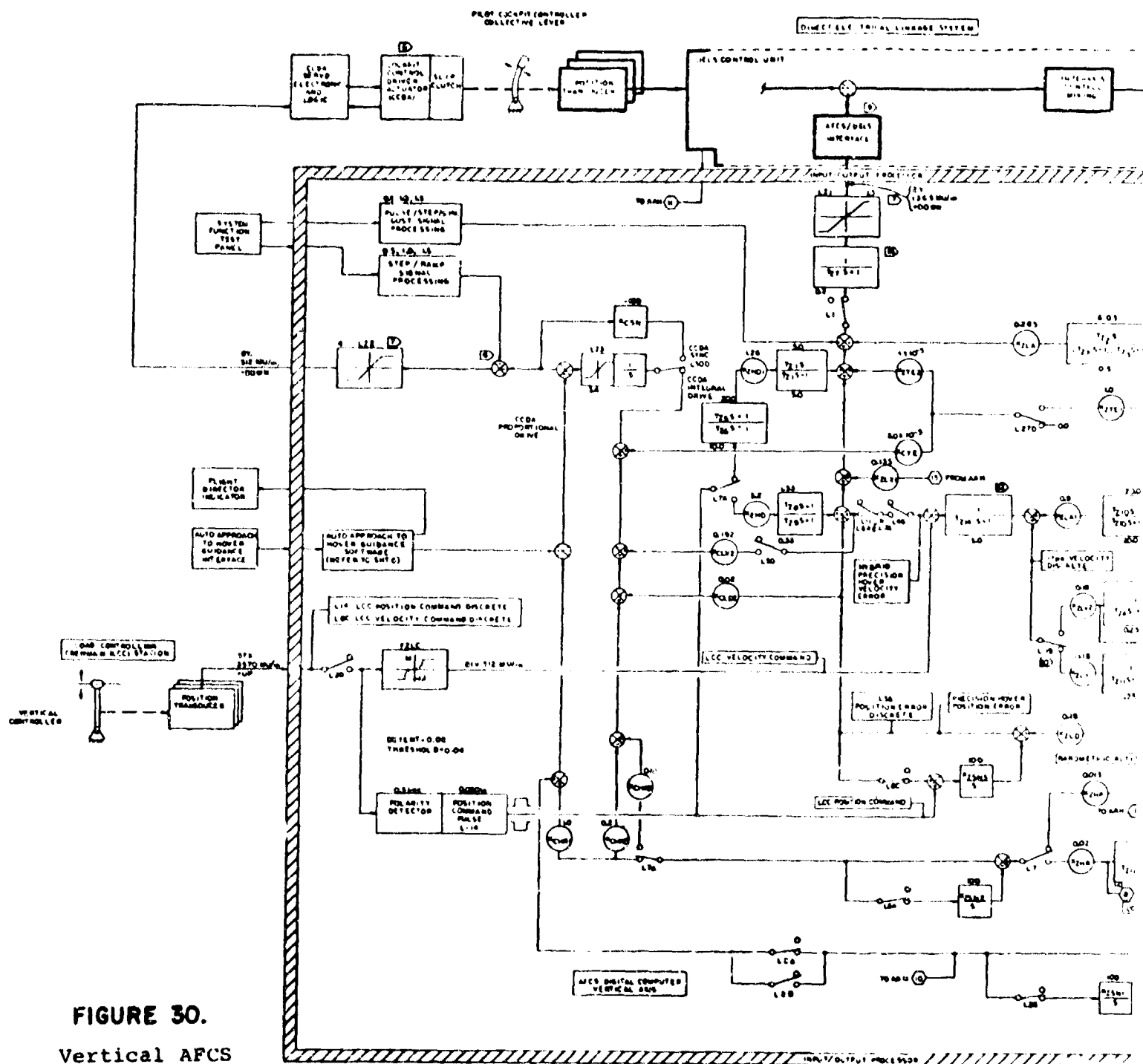
**FIGURE 30.**

Vertical AFCS

Functional Block Diagram

147
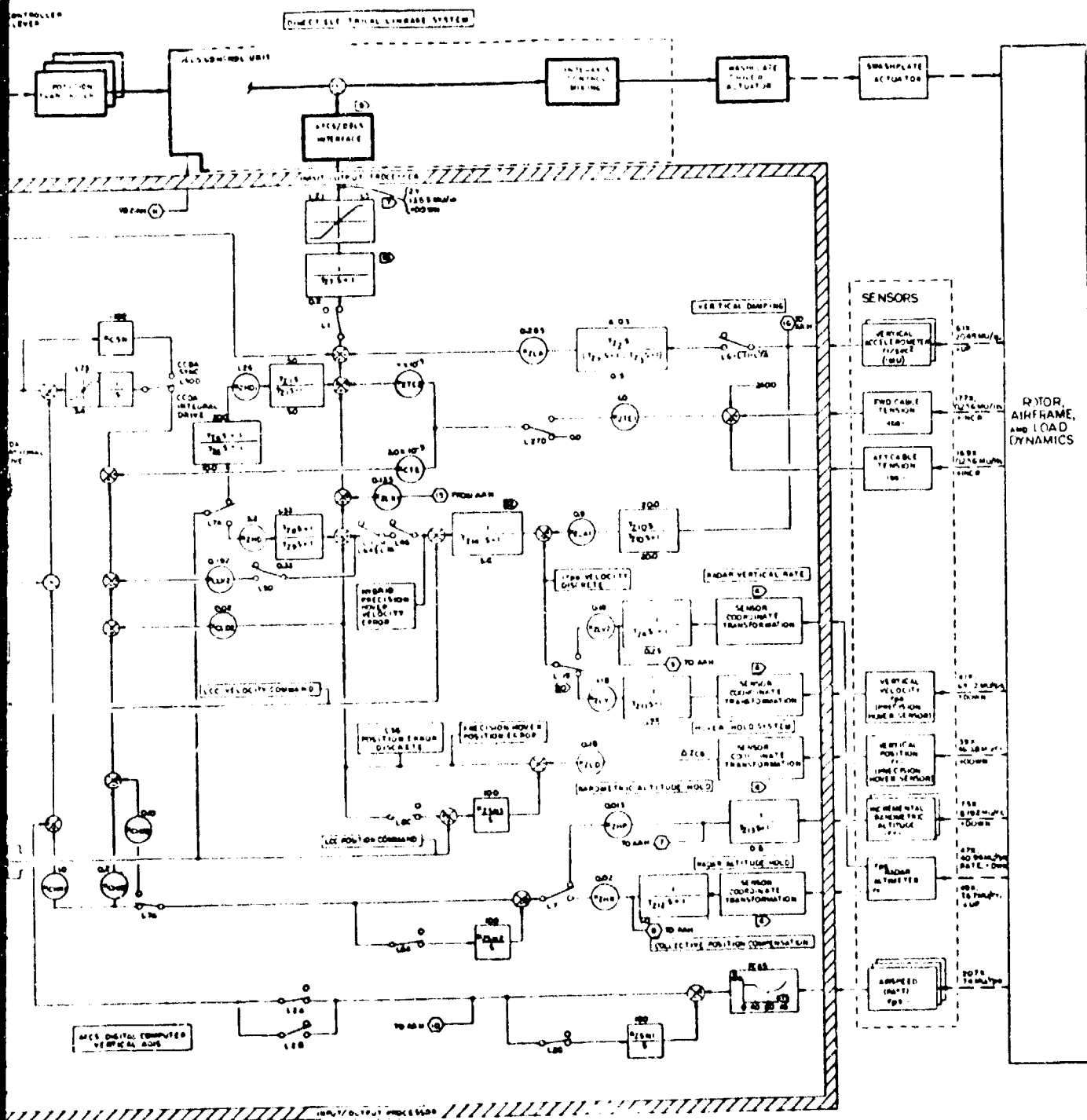
The original vertical SCAS mechanization is relatively simple when compared with other axes. Only one feedback parameter was utilized (airframe vertical acceleration); and no feed-forward augmentation or beep trim features were incorporated. Acceleration feedbacks provide short term vertical velocity damping. Flight test results indicate that this type of damping was desirable only when either the altitude hold or hover hold mode was engaged, i.e., continuous use of airframe acceleration feedback was not required; hence, there is no vertical SCAS per se.

This section of the report describes combined operation of the vertical SCAS and altitude hold mode. When altitude hold is selected, the aircraft is automatically maintained at a constant height above a selected datum through use of radar or barometric altitude feedback information. With this dual altitude reference system, barometric pressure altitude is used primarily in the cruise region of the flight envelope, and radar data when the helicopter is maneuvering near the ground (generally below 200 feet). Switching between radar and "baro" altitude reference is normally accomplished automatically, but the pilot also has a manual selection capability.

The vertical velocity damping network is utilized with both types of altitude reference. An additional feedback (vertical rate of climb generated by sensor differentiation of the radar altitude signal) is employed for stability augmentation when the radar mode is engaged. Backdriving of the collective stick maintains the correct cockpit-to-swashplate control relationship, with both integral and proportional drives employed while operating on baro reference. In the radar mode, only integral drive signals are passed to the CCDA actuators.

Of the four axes, the vertical AFCS underwent perhaps the greatest developmental change from its initial Task 1, Part 1, conceptual mechanization, to the final flight validated system. Significant modifications of the original control laws were necessitated by unanticipated CCDA collective actuator and radar altitude sensor performance characteristics. In the writeup which follows, the improved control laws are reviewed, along with detailed discussion of each inner and outer stability and control loop.

149

2.1.5.4.1 Inner and Outer Loop Vertical Stabilization and Control with Altitude Hold Engaged

VERTICAL VELOCITY DAMPING – The vertical damping loop shown at the top of Figure 30 passes airframe vertical acceleration signals through a frequency selective (lag/washout) network into the differential AFCS/DELS interface. This path is active only when altitude hold using barometric reference information is selected.

The low-pass filter (TZ3) annotated on the diagram attenuates unwanted accelerometer signal components caused by aircraft vibration. It acts essentially as a short term "integrator" of the acceleration signal (as shown in the frequency response sketch at the top of Figure 31), approximately a velocity-type feedback for stability enhancement at high frequency. The accompanying high-pass filter (TZ2) is incorporated to eliminate static signal drift and zero frequency acceleration components of the type generated in steady turning maneuvers, etc. A second low-pass filter (TZ7) is inserted in the differential output path of the vertical axis to remove computer/sensor noise spikes, as described earlier.

Radar rate information is used to complement the acceleration-derived vertical damping feedback when radar altitude hold is engaged. In this mode of operation, acceleration signals follow a different path than the one described above for the baro reference. As seen in Figure 30, accelerometer feedbacks pass through a 20-second-high pass filter (TZ10) and 5-second first order lag (TZ14).

This washout/low pass filter network is similar to the shaping used in the baro mode, with different time constants and gains selected to facilitate blending the acceleration signal with the radar vertical rate feedback. Combining the two signals is achieved with a complementary filter mechanization which produces single, smoothed, constant gain output of the type shown at the bottom of Figure 32. The advantage of using complementary filtering lies in the fact that the best frequency range of both constituent signals ( A and B ) can be utilized to produce the desired output ( C ).

150
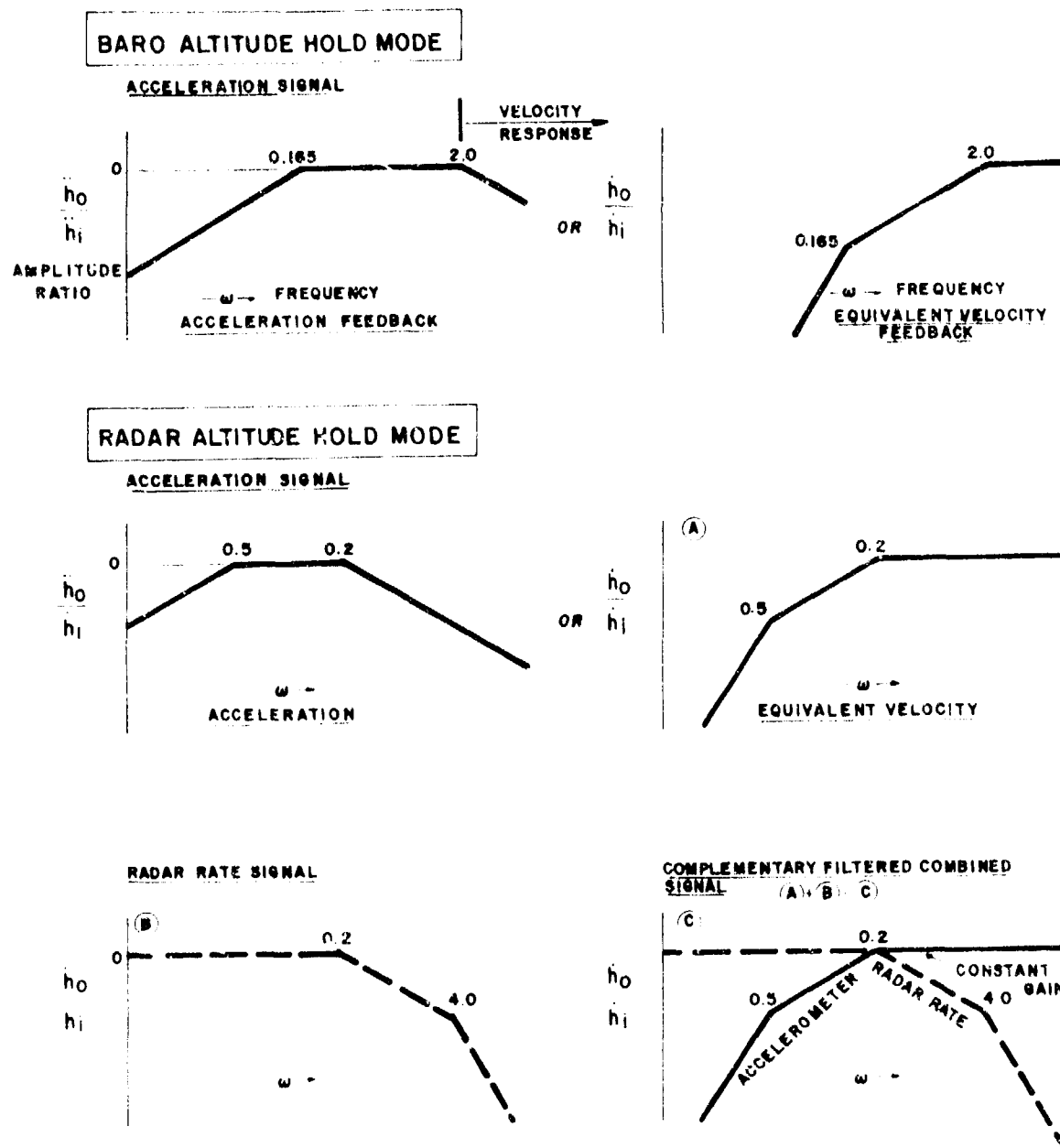
FIGURE 31.
AFCS VERTICAL AXIS
FREQUENCY RESPONSE CHARACTERISTICS OF PURE ACCELERATION &
ACCELERATION / VELOCITY VERTICAL DAMPING FEEDBACKS

151

When the control laws were first formulated for the vertical axis, it was anticipated that vertical damping (through acceleration feedback) would be a full-time SCAS function. This mechanization was retained as a viable augmentation candidate through piloted simulation evaluations at Jorthrop.

With the start of SCAS testing on the flight research vehicle, however, problems were identified. The resultant response characteristics reflected a miscoordination between the differential feedback path and the pilot's collective input while maneuvering, due to the acceleration washout characteristics. The problem was solved by eliminating acceleration as a continuous feedback, except when altitude hold or hover hold was engaged along with the stick backdriving loops. Basic aircraft vertical velocity damping levels were judged high enough to provide good vertical control.

ALTITUDE HOLD - As indicated earlier, either radar or barometric altitude information is used as a stability feedback with altitude hold engaged. The two altitude loops are shown entering the AFCS in the bottom right hand corner of Figure 30. L-7 logic switching determines which type of altitude data is processed through the differential and parallel output control paths of the vertical axis. Mechanization of the L-7 logic matrix is illustrated in Figure 32.

This logic diagram indicates that when the pilot selects automatic altitude hold operation, radar altitude is the reference below 200 feet. Once engaged, the radar mode stays latched until the aircraft exceeds 220 feet above the ground. At this point, the altitude hold reference automatically reverts to the barometric feedback. Manual selection of radar reference is possible up to a maximum altitude of 250 feet, but baro reference can be utilized at any altitude.

When the pilot selects altitude hold, L-6 logic engages the vertical damping and altitude loops as shown in Figure 30. (Details of the L-6 logic switching network are presented in Appendix A). If the pilot wishes to re-reference altitude for any reason, he first unlocks the magnetic brake to permit collective stick motion. A "mag" brake discreet signal is generated which changes the state of all L-6 logic controlled switches, thereby disengaging altitude hold until such time as the brake button is released to relock the collective stick. Collective stick movement produces an aircraft

152
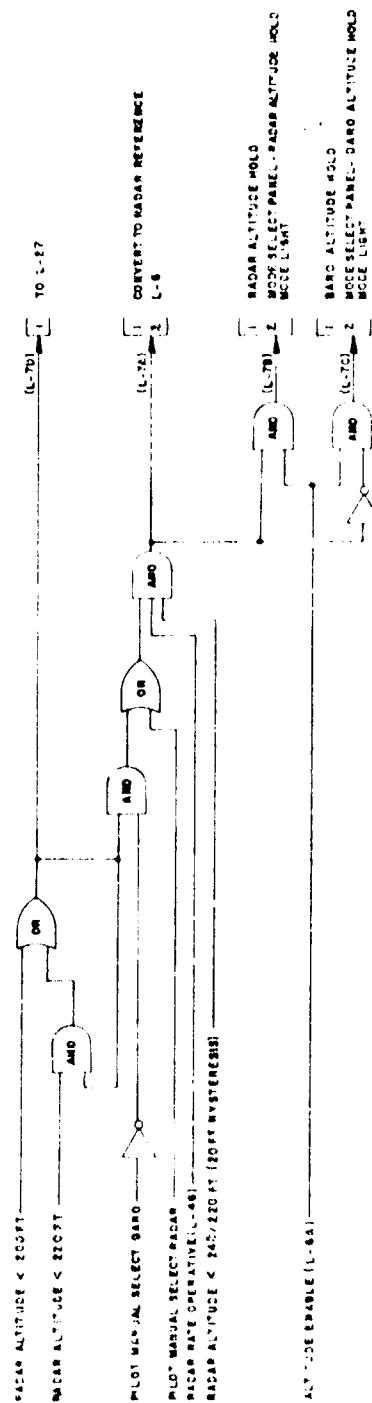
FIGURE 32. L-7 ALTITUDE HOLD REFERENCE

153

vertical rate which the pilot stops as he approaches the
desired altitude by readjusting stick position.

Both altitude signals are low-pass filtered initially to
eliminate sensor noise. The radar signal must also undergo
a coordinate transformation to achieve the proper axis orien-
tation (perpendicular to the earth surface plane), and
reference with respect to the aircraft cg location. After
passing through the L-7 switch, the selected altitude refer-
ence signal enters a synchronizer, which is incorporated to
eliminate altitude hold mode engagement transients. The
altitude signal continues on into both the high frequency
differential output path, and the lower frequency collective
backdrive network.

The L-7A switch shown in the differential path directs the
radar reference signal through a lead-lag filter ($T_Z8/T_Z9$),
and the baro reference feedback through a similar lead-lag
($T_Z5/T_Z6$) and washout ($T_Z1$). The lead-lag filters provide
phase advancement for the radar signal, and high frequency
gain increase on barometric reference. The washout was
incorporated to prevent standoffs between the differential
and parallel output paths (in the barometric mode) due to
a drifting reference condition noted with the baro sensor.
The radar signal is not washed out since it provides velocity
feedback for LCC control.

Configuration of the differential output path for the altitude
loop was modified extensively during the first Northrop
piloted simulation to compensate for collective CCDA actuator
performance. The actuator produced a lagged rate limited
response with 0.1 to 0.2 inches of equivalent collective
stick backlash in the gearing mechanism. To get around the
problem in the simulator, the differential lead-lag path
($T_Z5/T_Z6$) shown on the Figure 30 diagram was inserted, with
both radar and baro signals passing through the washout.

154

In addition to the differential paths just described, altitude
feedbacks are also utilized to generate backdrive commands for
the stick. Based on earlier 347 flight program results, both
proportional and integral stick drive mechanisms were
incorporated into the original candidate Task 1, Part 1, vertical
axis. Proportional drives had been found to require a companion
integral drive capability, since the proportional signals did
not eliminate bias offsets which developed.

In the final flight-validated backdrive mechanism, a
combination of proportional and integral CCDA command paths
was found to work best when baro reference was being used.
With the radar mode, only the integral path was required. As
in other axes, this integral drive loop is configured with a
synchronizer to zero output of the path while the aircraft
is being maneuvered vertically with the collective stick.
The synchronizer prevents engagement transients from occurring
when altitude hold is resumed.

COLLECTIVE POSITION COMPENSATION - With the altitude hold
or automatic approach to hover modes selected, a collective
stick position compensation loop is engaged as shown at the
bottom of Figure 30. This control path causes the proportional
CCDA backdrives to move the collective stick in the cockpit.
It provides an approximation of the collective pitch require-
ments in level flight (i.e. power) as a function of airspeed.
Since the loop does not operate continuously, it has a
synchronizer incorporated to eliminate engagement transients.

The position compensation path is basically an "anticipator"
network which is intended to alleviate some of the altitude
hold integral control drive workload. Use of the loop results
in less aircraft altitude transients during accelerating or
decelerating flight with altitude hold engaged. It is noted
that collective compensation also facilitates a smaller glide
slope error during automatic approach to hover maneuvers.

Downstream of the synchronizer, the compensation path includes
a switching network (L2A/L2B) which allows the pilot to fly
either an automatic coupled, or manual approach to hover.
During manual approach maneuvers, the loop is disengaged.

155

## 2.1.5.4.2  Vertical AFCS/DELS Interface

Differential outputs of the vertical AFCS are interfaced with
the DELS through a single authority limiter, as described
earlier in Section 2.1.3.1.5.  The vertical interface is dif-
ferent from other axes, in that a frequency splitter was
not employed.  This is because of the relatively low vertical
axis equivalent control authority, which is only $\pm 1.5$ inches
out of a total 9.0-inch travel in the cockpit.

## 2.1.4  Hover Hold/LCCC Operation

A pilot selectable Hover Hold mode was developed for the AFCS
to meet the stringent ± 4-inch and ± 2° HLH hover acquisition
and hold performance goals detailed earlier in Section 4.1.1.
This mode is intended to be used primarily by the load con-
trolling crewman while he maneuvers the aircraft at low speed
with the LCC controller, or automatically holds position
after acquiring the hover target.  The pilot can also utilize
the stability features of the Hover Hold mode to maintain
velocity or position.  Depressing the cyclic stick "mag"
brake disengages these loops and permits normal low-speed
maneuvering on the basic SCAS as described earlier.

Hover Hold has two major sub-modes of operation.  They are the:

- Hover Hold/Precision Hover Sensor (PHS) that provides a
  precise automatic hold and maneuver capability through
  high-gain loop closures and low-sensitivity controller
  commands, based upon very accurate ground velocity and po-
  sition information generated by the PHS.  The downward-
  looking PHS incorporates an optical position tracking
  scheme to determine horizontal aircraft movement, and
  laser ranging to establish vertical motion.

- Hover Hold/IMU-Radar - where velocity information
  only from IMU and radar altimeter sources is utilized
  (along with LCCC inputs) to maintain a tight velocity
  control, when signals from the PHS are unusable due
  to excessive aircraft speed or poor scene correlation
  beneath the aircraft.

The rearward facing load-controlling crewman (LCC)
maneuvers the helicopter with a four-axis, single-stick,
"finger-ball" controller of the type shown in Figure 33.
This controller employs an optimized non-linear control sen-
sitivity (generated through use of an input function in the
AFCS computer) to provide "beep" position, and "creep" or
"leap" velocity changes.

When the helicopter is operated in the PHS position hold mode,
small beep pulse commands can be introduced through the
controller to re-reference the horizontal or vertical location
of the aircraft.  Each pulse input moves the helicopter
approximately 2 inches.  Larger control deflections produce
"creep" and "leap" velocity responses, as shown in Figure 33,
which reflect increasing control sensitivity with stick mo-
tion.  Maximum longitudinal and lateral stick inputs produce
translational velocities of up to ± 15 feet per second.  Max
vertical speed capability is on the order of ± 360 feet per
minute with full control, and the yaw rate maximum is approxi-
mately ± 9 degrees per second.

157

CONTROLLER

DIRECTIONAL

LATERAL

LONGITUDINAL

VERTICAL

CONTROLLER RESPONSE

RELATIVE LATERAL VELOCITY (FT/SEC)

BEEP

CREEP

LEAP

FULL DEFLECTION

LCC LATERAL CONTROLLER MOTION (%)
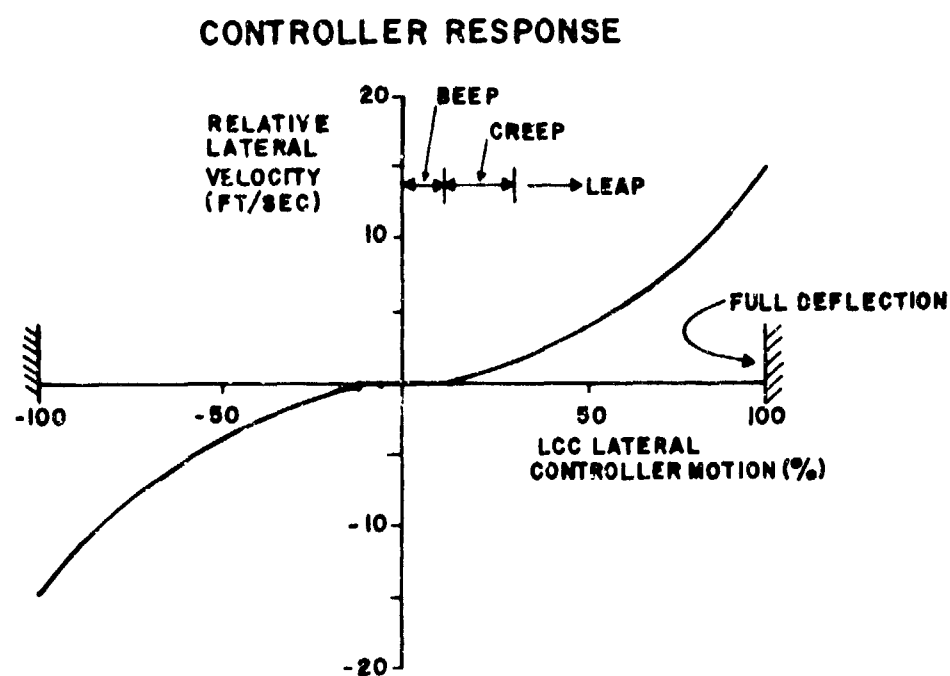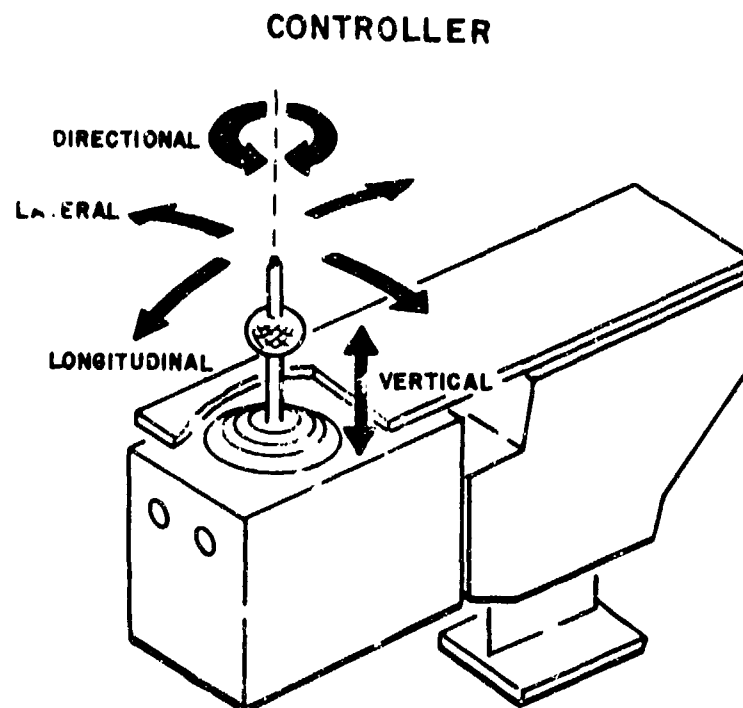
FIGURE 33.
LCC CONTROLLER CONFIGURATION & RESPONSE SCHEDULING

158

HOVER HOLD ENGAGEMENT - The Hover Hold mode can be engaged at any speed where the Velocity Mode Transfer switch is utilizing groundspeed reference (i.e., below 40-45 knots). This capability is very useful when the aircraft is required to track a moving target, such as a ship, after acquiring or depositing external cargo.

A "drift-clearing" feature is incorporated into the velocity feedback loops to facilitate velocity lockon at other than zero speed as determined by the Inertial Measuring Unit. This feature automatically synchronizes the groundspeed feedback output to zero prior to Hover Hold engagement, and then increments velocity changes from that point on for stability. Manual drift clearing by the pilot is also possible so that he can eliminate the effects of any IMU drift, etc., which would require a controller input to maintain desired trim speed.

DEMONSTRATION RESULTS - During the flight evaluation of Hover Hold and LCC operation, photo optical tracking of the aircraft (over a painted target on the ground) was accomplished to establish the accuracy of automatic and manual position hold capability with Hover Hold engaged. A sample of the tracking results is presented in Figure 34. Test data shown on the plot typify automatic position hold performance with PHS engaged in gusty and non-gusty flight conditions. The data indicate a circular error probability (CEP) of maintaining desired position that is very close to the +4-inch performance goal established for Hover Hold. As shown in the figure, the effects of wind gusts are relatively small with the PHS operating.

This section of the report describes development of the Hover Hold mode, precision hover with the PHS, and LCC controller operation. Synthesis of Hover Hold control laws and logic is covered first in Section 2.1.4.1, where each AFCS axis is treated individually. Section 2.2.4.2 follows with a synopsis of the key developments in the design analysis of the Hover Hold mode and controller interfacing.

347/ATC DEMONSTRATOR
VARIABLE WIND CONDITIONS AS NOTED
POSITION DATA SAMPLE 3 SECONDS
2-MINUTE RUN

WIND 10 TO 12 KN, GUSTING TO 24 KN

WIND 10 KT, MILD GUST

CEP(50%)

6.8 IN.

4.0 IN.

LONG(FT)

LAT(FT)

VERTICAL EXCURSION   2.5-IN.RMS
HEADING EXCURSION 0.30 DEG
FLIGHT 795 RECORD 6

VERTICAL EXCURSION   4.3-IN.RMS
HEADING EXCURSION   0.36 DEG
FLIGHT 812 RECORD 11
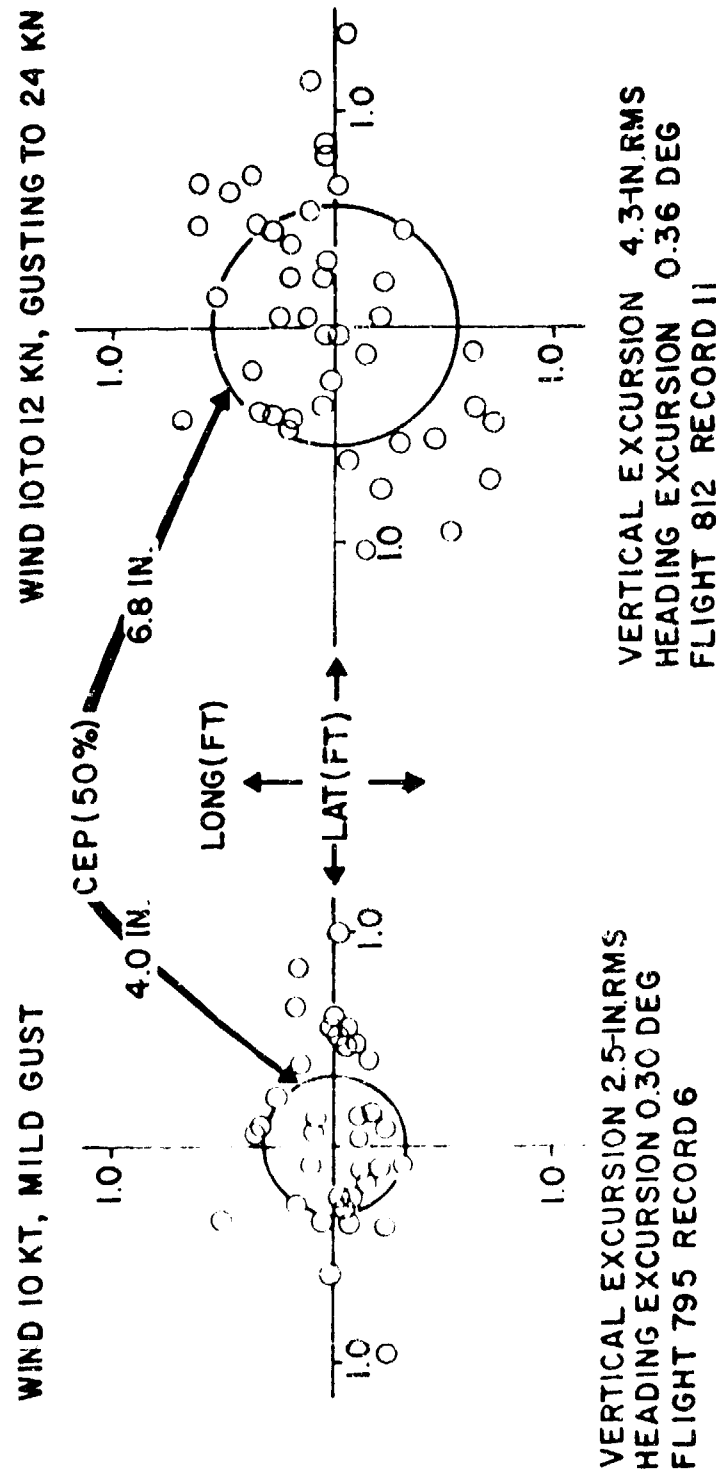
FIGURE 34.

HELICOPTER POSITION HOLD DATA WITH PRECISION HOVER SENSOR

### 2.1.4.1 Synthesis of Hover Hold Control Laws and Logic

Hover Hold control law mechanizations are similar for the longitudinal, lateral, and vertical axes. With the PHS locked on and producing valid signals, the AFCS processes sensor-derived precision velocity and position feedback information for stability, and LCCC commands for control. Angular rate and attitude feedback loops are retained from the basic longitudinal and lateral SCAS, along with the lateral groundspeed path described earlier. CCDA cockpit control backdrives are also maintained to ensure proper trim positioning of the stick and pedals.

The directional axis incorporates all of the low-speed SCAS loops described earlier (except for the pedal pickoff "quickener") and an LCC controller velocity path for commanding aircraft yaw rate. No position beep capability is required in this axis.

When the PHS is unable to provide valid signals, Hover Hold reverts to a velocity maintenance system using transformed IMU groundspeed feedbacks (or vertical radar rate), and the angular rate, attitude, and CCDA loops just described. LCCC inputs command velocity only. The directional axis functions are identical to those mentioned above.

Control laws associated with both modes of Hover Hold operation are illustrated in the bottom half of the AFCS functional block diagrams previously discussed in connection with SCAS performance. A description of the operation of each axis is presented next.

### 2.1.4.1.1 Longitudinal Hover Hold and LCCC Operation

Figure 14 in Section 2.1.3.1 summarizes the complete longitudinal Hover Hold control law package as it existed at completion of the ATC flight demonstration program. Stability feedbacks (in the form of IMU velocity, PHS velocity, and PHS position signals) are shown on the right side of the diagram, along with LCC controller inputs on the lower left. Differential DELS interfacing is depicted at the top of the chart and Hover Hold-associated LCP outputs at the bottom. Parallel backdrive CCDA command loops are illustrated in the top left hand corner of the diagram.

Since the Hover Hold/IMU mode encompasses the simplest control law mechanization, it is described first.

161

2.1.4.1.1.1  Hover Hold/IMU Velocity Mode - Stability feed-
backs include pitch rate, pitch attitude, and longitudinal
groundspeed signals generated by the IMU.

Rate and attitude gains are increased over the basic SCAS
through use of the L-11A switching in order to minimize pitch
response and to ensure compatibility with the higher gain veloci-
ty feedback path added for Hover Hold.  Operation of Hover
Hold engagement logic (including L-11 and L-11A switching) is
summarized at the top of Figure 35.

To select Hover Hold/IMU, the pilot depresses the "Hold"
button on the Mode Select Panel in the cockpit which lights
up when the mode engages.  A similar "LCC" button is used to
activate the controller.  As shown in Figure 35, Hover Hold
remains engaged until the pilot (or load crewman) "drift
clears" the IMU velocity path.  Disengagement also occurs
when the pilot depresses the cyclic "mag" brake to retrim
stick forces, or maneuvers the aircraft in such a manner as
to vary groundspeed by more than 15 knots from the velocity
existing at the time of engagement.  When the aircraft ex-
ceeds 45 knots airspeed, the mode will also automatically
disengage.

The $X_E$ IMU groundspeed feedback employed during the hover hold
operation is processed through the longitudinal cyclic pitch
(LCP) path, rather than through the differential DELS inter-
face previously described in the SCAS writeup.  With Hover
Hold engaged, the SCAS associated $X_E'$ velocity feedback is
not used.  Instead, it is stored in the Track-Store-Decay
element shown on Figure 14 when L-11 logic is true.

After being transformed to the proper axis system and cg
reference, the $X_E$ feedback passes through a transfer/switching
network which selects the proper IMU or PHS velocity (depend-
ing upon PHS sensor validity), and then sums this signal with
the LCC controller commands.  The transfer/switching loops
provide smooth transition between velocity references as
described next.

IMU/PHS Velocity Reference Transfer and "Drift Clear"
Operation - An explanatory sketch showing how the PHS/IMU
velocity transfer network operates is presented in Figure 36.
This diagram represents an approximate analog analogy of the
various operations performed within the AFCS digital com-
puters when transferring from one Hover Hold velocity source
to another.

Prior to engaging Hover Hold, the IMU (or upper velocity path
shown in the figure) is continuously "drift cleared" to zero
output.  Zeroing of this path is accomplished with a synchro-
nizer of the type described earlier.  When Hover Hold is
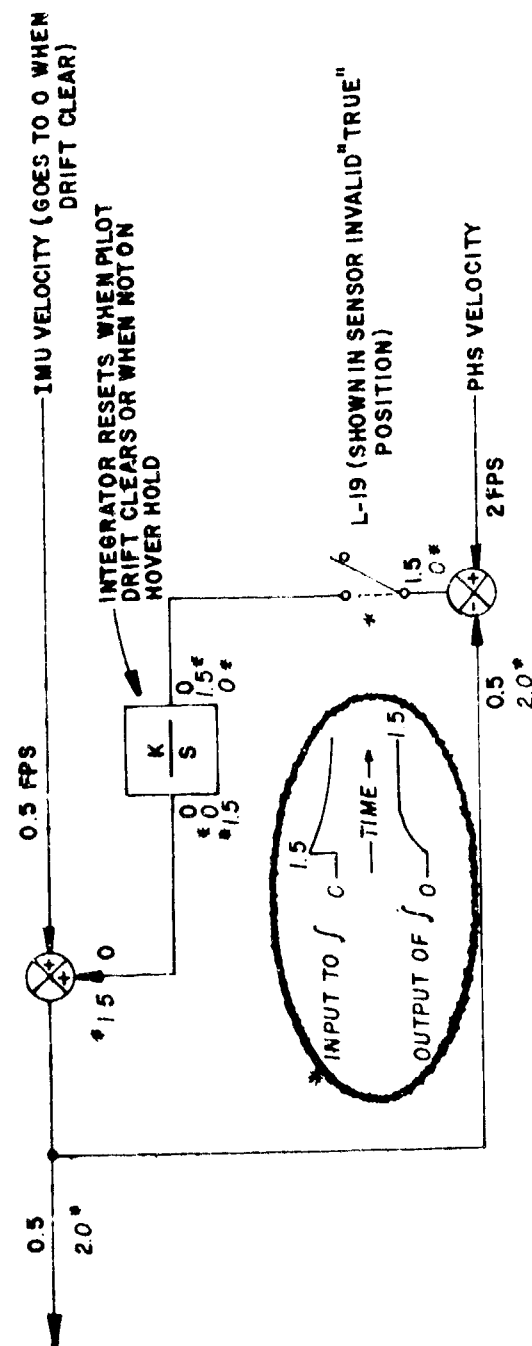
162

**FIGURE 35.**

**TYPICAL HOVER HOLD-ASSOCIATED LOGIC NETWORKS**

FIGURE 36. APPROXIMATE ANALOG ANALOGY OF IMU TO PHS VELOCITY TRANSFER SWITCHING

1. START WITH IMU VELOCITY = 0.5 FPS. ASSUME HOVER HOLD SELECTED AND SENSOR INVALID.

2. WHEN PHS BECOMES VALID, L-19 GOES FALSE (SWITCH CLOSES). INTEGRATOR IMMEDIATELY INTEGRATES UP 1.5 FPS ERROR ON LOWER SUMMER AND OUTPUT OF UPPER SUMMER BECOMES 2.0 OR PHS VELOCITY – NEW REFERENCE VELOCITY IS PHS.

3. WITH VALID PHS, ONLY PHS VELOCITY PASSES ON INTO FEEDBACK PATH BECAUSE OF WAY SWITCHING TRANSFER FUNCTION IS MECHANIZED.

4. SWITCHING BACK TO IMU REFERENCE WHEN SENSOR GOES INVALID OPENS L-19 SWITCH, INTEGRATOR HOLDS LAST VALUE, AND FEEDBACK VELOCITY FOLLOWS IMU CHANGES FROM THIS POINT ON.

selected (and L-11 logic permits mode engagement), synchronization of the IMU ground speed stops. From this point on, incremental changes in IMU velocity are passed on into the feedback path for stability. The L-19 switch (detailed in Figure 35) is open at first due to the assumed invalid sensor state, and only the IMU velocity signal is allowed to pass. The groundspeed signal was initialized to zero at the time of mode engagement, but has grown to .5 feet per second in the example because of some external disturbance, such as a wind gust or velocity command by the LCC.

Small differences between PHS and IMU reference velocities occur because of the relative accuracy of the two-signal sources. In the example, the more precise PHS velocity assumes a value of 2.0 feet per second as the sensor becomes valid. When this occurs, the L-19 switch closes, permitting the integrator to pass the error (between the two velocity signals) into the upper summing junction. The output of this summer changes rapidly to reflect the PHS signal level, and tracks the sensor signal as long as it remains valid. On reversion back to IMU reference, the integrator holds its final value and the feedback velocity follows IMU variations from then on.

After Hover Hold/IMU engagement, the aircraft may drift slightly unless the pilot or load crewman puts in a corrective control. This "hands off" drifting is most likely caused by very small inherent IMU velocity migrations, or it may be the result of not having the helicopter perfectly stabilized at zero velocity when the mode is engaged. The problem is easily overcome by first stopping aircraft motion with the stick or LCCC, and then manually "drift clearing" the IMU path to rese. X and Y velocity to zero.

A final step in the manual drift clear operation consists of releasing the LCCC stick to return to its zero force position before releasing the "drift clear" button. L-34 logic outlined in Figure 35 defines the manual and automatic "drift clear" switching networks.

LCCC Command Control - The LCCC path is activated by L-20 logic switching as shown in Figure 14. This switching network permits controller engagement after the pilot has depressed the "LCC" button on the Mode Select Panel, providing Hover Hold L-11 logic is true. Force-trimming the cyclic or collective stick in the cockpit automatically disengages the LCCC and returns control to the pilot. Disengagement also occurs when L-11 logic changes state, or when the pilot depresses the "LCC" button for the second time.

The optimized non-linear control gradient referred to earlier in connection with LCCC operation is achieved through the

165

FXLC command function and KXLC gain illustrated in Figures 37 and 14. The same command scheduling is utilized for both Hover Hold modes.

In the IMU mode, velocity commands of ever increasing magnitude are developed once the load crewman deflects the stick beyond its velocity threshold. PHS operation is similar with an additional "position pulse" logic discrete command being generated when the controller exceeds a very small preset detent about the null stick position.

As shown in Figure 37, stick sensitivity is very low around the null position, picking up gradually as the controller is deflected toward its limits. This type of gradient is characteristic of all Hover Hold axes, and is incorporated to desensitize the mode for optimum aircraft response. Substantial effort was expended during the simulation and flight test programs to define the best control shaping for each axis. Higher initial sensitivity slopes (and wider velocity threshold bands) were evaluated but were rejected because of their tendency to cause pilot over-control problems.

It is noted that a significant amount of LCP is commanded with full control throw. These large control gains are required in order to "buck out" the strong stability hold velocity gradient already described.

After the velocity command passes through the non-linear control function module, it is low-pass filtered to remove high frequency LCCC input signal components. The filter is automatically converted to a unity gain (with no lag) during drift clearing operations. This change prevents any controller dynamics associated with stick return from occurring subsequent to release of the drift clear button. Without this feature, transients could be introduced into both the LCP and CCDA loops each time the IMU velocity is drift cleared.

The processed controller commands and velocity hold feedbacks are summed to produce a velocity error signal which is limited and transmitted through the LCP and cockpit backdrive control paths. The 1X1 limiter prevents the helicopter from generating large accelerations due to the high control gains, and at the same time inhibits excessive backdrive signal commands from reaching the CCDA actuators. This backdrive signal forces the cockpit stick to the proper trim position for the velocity commanded. Without the back-driven cockpit controls, transients can occur each time the pilot resumes control of the aircraft at the end of LCC operations.

Velocity error-signal processing in the LCP path includes a lead/lag shaping network combined with a low-pass filter. Time constants of this processor are tailored primarily to

166
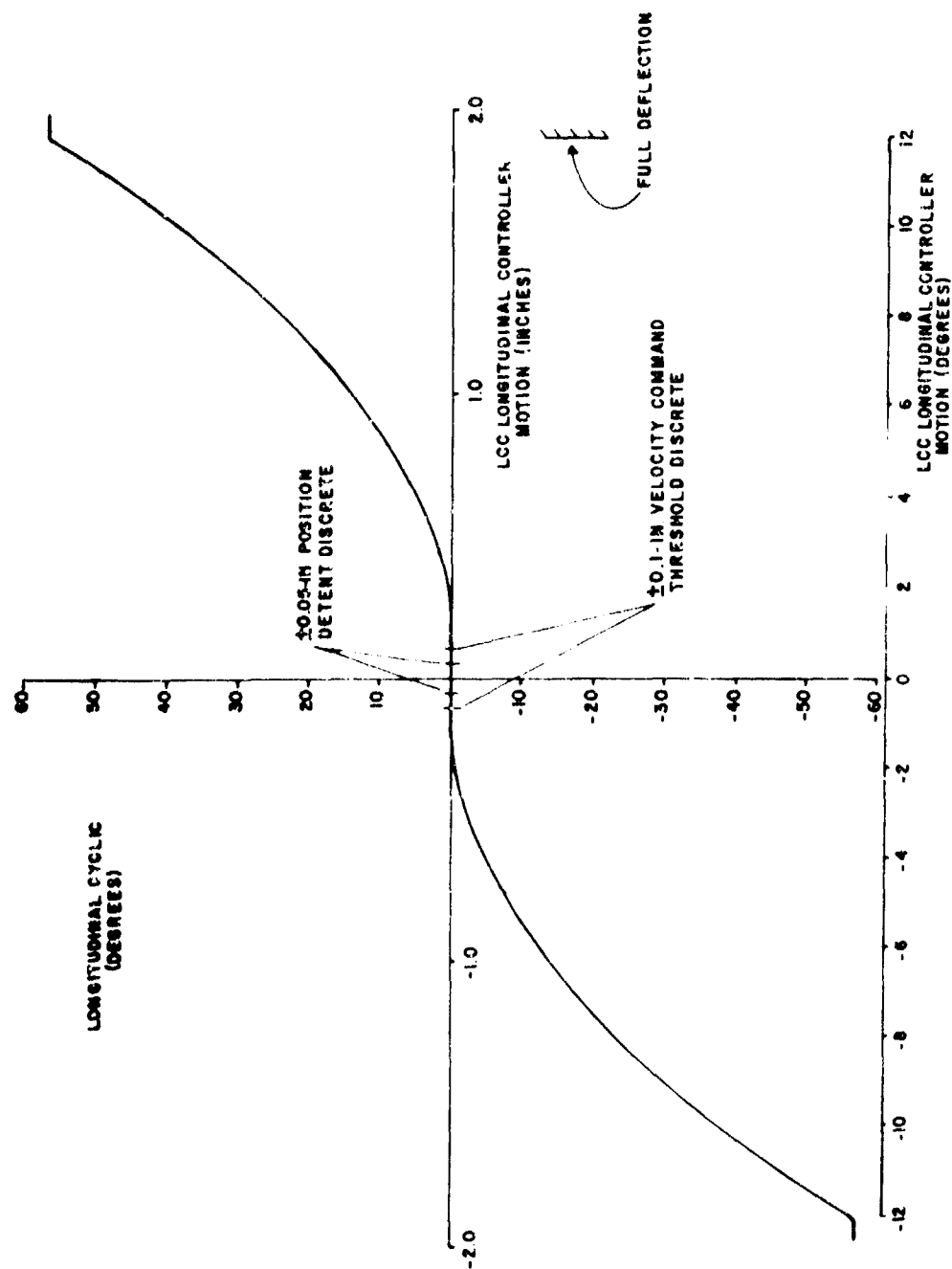
FIGURE 37.

LCC LONGITUDINAL VELOCITY COMMAND FUNCTION

167

achieve phase and gain improvement in the PHS mode, and to
prevent high frequency longitudinal cyclic pitch commands
from reaching the rotor system.

2.1.4.1.1.2  Longitudinal Hover Hold/PHS Mode - Automatic
stability and control functions associated with the PHS Hover
Hold mode are similar to those just described for IMU opera-
tion, with the following exceptions:

1.  Velocity (and position) information is generated by
    the PHS sensor instead of the IMU.

2.  Very accurate automatic position holding is possible
    because of the addition of position stability feed-
    back loops, and because the PHS signals are
    somewhat more precise than those of the IMU.

3.  Small incremental "beep" command pulses can be intro-
    duced with the controller to fine tune the stabilized
    position of the aircraft during hover.

Since the PHS represents an essential part of
Hover Hold/PHS selectable mode, its operation is described
next before dealing with details of the AFCS control laws.

PHS Operation -

The Precision Hover Sensor is a self-contained gyro-stabilized
optical device capable of tracking low-speed aircraft position
and velocity with great accuracy.  It is mounted in the tail
of the helicopter where it observes the scene beneath the
vehicle to generate required feedback signals.  An optical
position correlation and tracking scheme is utilized for
determining movement in the horizontal plane, and a laser
ranging device establishes vertical motion.  Velocity infor-
mation produced by the PHS is derived by differentiation of
the measured sensor position data.

Design accuracy requirements for the RCA built sensor reflect
a $\pm$ 1-inch or better position measurement capability, and a
velocity tolerance of $\pm$ 1-inch per second.  Horizontal range
extends to $\pm$ 4 feet in both the X and Y directions (before
the sensor unlocks to re-reference itself), and the altitude
operating band lies between 25 and 125 feet above the surface.
Maximum design velocity was initially established at close to
8 feet per second, but was later reduced to 3 feet per second
during the flight program in order to improve operation.

In early Hover Hold/PHS flight testing, a sensor deficiency
was identified which resulted in poor tracking performance
over certain low contrast surface features, such as airport
runways, ramp areas, etc.

In order to verify the validity of the Hover Hold/PHS control law mechanizations, a black and white checkerboard target was painted on the runway to assist the sensor with its correlation/tracking task. PHS operation over this painted target area was marginally satisfactory. Details of the flight test results are reviewed in Section 7.

A simplified Precision Hover Sensor block diagram and its functions is given in Figure 38. This chart depicts the sensor model used during AFCS flight simulation work at Northrop. The model was somewhat less complex than the actual hardware, but its mechanization is sufficiently close to the flight article to warrant its presentation for explanatory purposes. Significant differences between the simulation and flight test configurations are delineated in the lower right hand corner of the diagram.

The essential fundamentals of sensor operation are outlined below:

1. To energize the PHS, the pilot first moves the PHS ENABLE switch to the on position. The sensor immediately goes to a locked-on condition, providing scene contrast is adequate for correlation purposes, and the maximum PHS translational velocity limit is not exceeded. When locked onto a target, the sensor generates a "LOCK" discrete signal which goes to the L-19 logic switching network.

   The PHS initial reference or "target" position is defined as a location on the ground directly beneath the sensor centerline at the time lock-on occurs.

2. The sensor stays locked on the initial target until one of the following events takes place:

   a. Helicopter movement over the target exceeds $\pm$ 4 feet in either the X or Y direction, or

   b. Helicopter movement exceeds $\pm$ 2 feet and the difference between commanded position and actual position (i.e. position error) relative to the target is less than .2 feet (due to position "beep" commands), or

   c. Sensor velocity across the target area exceeds the maximum limitation of 3 feet per second. Logic switching networks associated with unlocking the sensor under conditions (A), (B), or (C) are illustrated on the left hand side of Figure 38.

169

FIGURE 38. PRECISION HOVER SENSOR MATH MODEL USED DURING PILOTED SIMULATION

3. When either (A) or (B) are true, the sensor executes an internal "relock" maneuver. The PHS unlocks and remains unlocked (with L-19 logic false) for a period of approximately .7 second during which time it is establishing another target reference directly beneath its new position. While unlocked, the sensor position and velocity signals are set to zero as illustrated in the top right hand corner of the block diagram.

4. At the termination of the "relock" cycle, position measurement starts again, (but referenced to the new target). Velocity information is also generated.

5. When the PHS velocity limit is exceeded as in (C), the sensor unlocks permanently and cannot relock until the velocity decreases to a value below the limit, and conditions for scene relock are satisfied.

During the period of time that the PHS is unlocked (i.e., is invalid), velocity reference for Hover Hold reverts to the IMU, and position signals are no longer available. Sensor transformation terms used for re-referencing lateral position (and based on aircraft heading changes) are also synchronized to zero in the AFCS computers when the PHS is unlocked. This synchronization and transformation process is shown schematically in the bottom right hand corner of Figure 38. A more comprehensive sensor transformation description is given in Appendix A.

## Longitudinal Hover Hold/PHS Control Law Mechanization

As shown in the Figure 14 block diagram, longitudinal Hover Hold/PHS control laws retain the LCCC velocity command and stability feedback mechanizations described earlier for IMU operation. Additional paths may be engaged when the PHS is locked, providing the aircraft is moving slow enough and L-8/L-8A logic is satisfied, as indicated in Figure 35. These loops facilitate automatic position holding, and at the same time, permit small incremental positional changes to be "beeped" in with the LCCC. Position feedbacks and LCCC beep commands are summed to form an error signal which is passed to the longitudinal cyclic and CCDA back-drive actuators like the velocity error.

When small "creep"-type velocities are commanded with the controller, position loops automatically disengage. As indicated earlier, the PHS stays locked on its original target during initial aircraft movement if the commanded speed is not too great. PHS velocity feedback information is utilized by the AFCS until the 4-foot sensor envelope boundary (described earlier) is reached.

171

When the boundary is crossed, the PHS relocks internally, velocity reverts momentarily to the IMU, and finally the sensor locks on again with velocity switching back to PHS reference. If the control deflection is held in, the locking and unlocking process repeats itself as the helicopter slowly translates across the ground.

STABILITY - The $X_{PHS}$ velocity feedback used in the PHS mode (and shown in Figure 14) is transformed to the proper coordinate system, and represents aircraft cg movement just as in the case of the IMU signal. Switching between the IMU and PHS velocity paths was described earlier. With the sensor locked, PHS signals pass directly through the velocity switching network and on for summation with the LCCC commands. Further processing of the velocity error is handled in exactly the same manner as described for the IMU signal.

Incremental longitudinal position ( $X_{PHS}$) signals for position stability are first transformed to the proper coordinate system, and are then processed through the various L-27C controlled automatic load stabilization loops. Operation of the LSS selectable mode is covered fully in Section 4.1.5.

When the LSS is not engaged, the transformed position feedback passes directly into the KXLD high-gain module and through a synchronizer where LCCC beep commands are summed in. The resulting error is limited, and then passed to the LCP and CCDA rotor and cockpit controls.

The synchronizer in the position loop operates exactly like the roll attitude sync, described earlier. With the PHS sensor locked, position feedback signals will pass through the synchronizer to stabilize the helicopter, providing L-8A logic is true (i.e., switch open). The L-8A logic network stabilizes whenever L-8 is true, aircraft speed is below .5 feet per second, and velocity commands are not being made with the controller, as shown in Figure 35. Both velocity and position feedback loops are engaged while holding position.

Should the sensor become invalid for some reason, L-8 and L-8A logic discretes go false, and the position loop is immediately synchronized to zero output. Velocity feedback is switched to the IMU, and automatic position holding is no longer possible. Once the sensor signals become valid again (and conditions for stabilizing L-8A are met), the synchronizer will restabilize. In this mode, the load crewman can introduce beep command pulses into the sync integrator to re-reference the stabilized location of the aircraft, as described next.

LCCC CONTROL - "Leap" and "creep" velocity commands, as
defined earlier, are produced by continuous controller deflec-
tions beyond the stick velocity threshold (i.e., 0.1 inches
for the longitudinal and lateral axes as indicated in Figure
37). Beep position commands, on the other hand, are gen-
erated each time the controller is moved out of detent.
The position detent represents a small segment of controller
motion defined about the null stick position, and is half the
size of the velocity threshold.

Whenever controller deflections exceed the detent, a discrete
logic signal is generated which activates L-15 logic causing
a single longitudinal position command pulse to be introduced
into the LCCC position path. Pulse duration and amplitude
are tailored to produce an error command bias (on the ouput
of the sync integrator) which is not satisfied until the heli-
copter has moved approximately 2 inches. Every time the stick
is returned to the detent and then moved out again, a new
pulse is generated. By continuously pulsing the controller in
one direction, the helicopter can be translated slowly across
the ground to re-reference its location.

As indicated in Figure 35, L-8A logic does not automatically
disengage (with subsequent reversion to velocity control)
every time the stick exceeds the velocity threshold. Instead,
the controller must be held beyond this point for at least
0.5 seconds to change from the position beep mode to a ve-
locity response. The time delay feature was incorporated to
simplify the beep control task by eliminating maximum ampli-
tude requirements that the load crewman would otherwise have
to observe while beeping aircraft position.

Response to Controller Inputs - Figure 39 shows a typical air-
craft response to longitudinal (and lateral) position beep
commands put in with the LCCC. Information presented in this
figure was generated during hybrid simulation testing con-
ducted at Vertol.

Longitudinal aircraft position shown near the top of the
figure varies in a "stair-step" fashion after each controller
pulse input. When several beep inputs follow one another in
rapid succession, position changes become continuous. Note
that opposite polarity inputs cause the aircraft to return to
its initial trim position in the example shown. Since none
of the beep pulses exceeded 0.5 seconds duration, and velocity
never went above 0.5 feet per second, the position loop
remained in the stabilize mode throughout the entire maneuver.

Figure 40 illustrates a series of typical responses to random
LCCC velocity commands executed with the Hover Hold mode
engaged. Controller inputs are annotated at the bottom of
the chart with variations in ground speed and position shown
at the top. LCP input commands to the rotor system are also
given as a function of time. 173

LONGITUDINAL & LATERAL POSITION RESPONSE TO LCC CONTROLLER COMMANDS
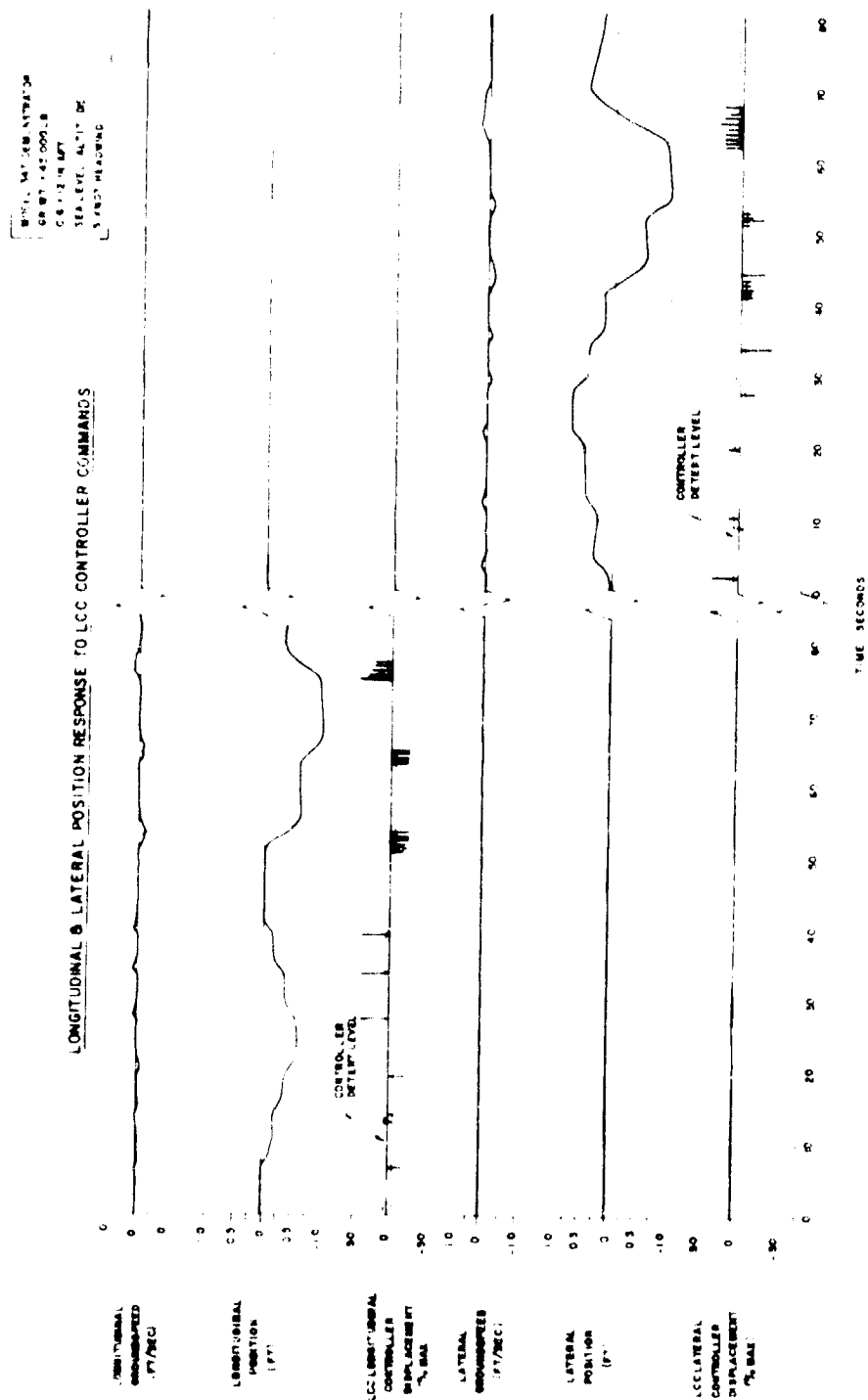
FIGURE 39

HLH/ATC PRECISION HOVER & LCC CONTROL SIMULATION

174

FIGURE 40.

HLH/ATC PRECISION HOVER & LCC CONTROL SIMULATION

175

Full controller steps produce a gradual increase in velocity which peaks out at approximately 15 feet per second. The velocity maintains a maximum value until the control input is removed, whereupon ground speed returns to zero and position stabilization is resumed. The output of the position synchronizer indicates a need for only small control inputs to maintain the new aircraft location once the position loop is re-engaged.

2.1.4.1.2  Lateral Hover Hold and LCCC Operation

Lateral-axis Hover Hold/IMU and Hover Hold/PHS control laws
are summarized in the Figure 23 block diagram introduced
earlier.  Detailed mechanization and functional operation of
these laws is essentially the same as described for the
longitudinal axis, except for obvious differences in the area
of parameter gains, time constants, etc., and retention of
the low-speed SCAS lateral velocity feedback path.  Because
of the strong similarities between the lateral and longitu-
dinal Hover Hold modes, only a limited discussion of the
lateral axis is required.

As shown in the diagram, roll rate and attitude stability
feedbacks are processed through the low-speed SCAS networks
with increased gain level applied for Hover Hold.  Dual lat-
eral IMU ground speed paths are also utilized in the lateral
mode.  One of these (designated $Y_E$) may be drift cleared as
in the longitudinal axis, but the other $Y_E'$ signal is not
cleared and remains engaged throughout all Hover Hold opera-
tions.  With an invalid PHS, the $Y_E$ IMU signal is used
as the velocity reference.  When the PHS is locked, its output
becomes the feedback.

Position signal processing, including both the stability and
control functions, is handled like the longitudinal axis.
Lateral beep commands entering the position synchronizer
are controlled with beep logic signals, and operation of the
sync itself is controlled by the L-8B discrete.  Details of the
various lateral axis Hover Hold logic networks are given in
Appendix A.

Velocity and position error signals are formed by summing the
LCCC command with the appropriate feedback.  The net error is
then passed to the rotor system via the differential lateral
AFCS output path and DEEC interface described previously.
The error signals also provide parallel backdrive commands
for the cockpit controls which compensate for variations in
stick trim requirements associated with wind.

Lateral LCC controller sensitivity was modified extensively
during the developmental simulation and flight programs.
Figure 41 compares the final lateral and longitudinal con-
troller schedules expressed in terms of steady velocity
response per unit of control deflection.  Note the reduction
in lateral sensitivity (for small controller displacements)
required for satisfactory handling qualities.  This sensi-
tivity flattening was introduced during the flight testing
to eliminate undesirable external load excitation created at
the start of lateral maneuvers.

LATERAL LCCC FUNCTION

LONGITUDINAL LCCC FUNCTION
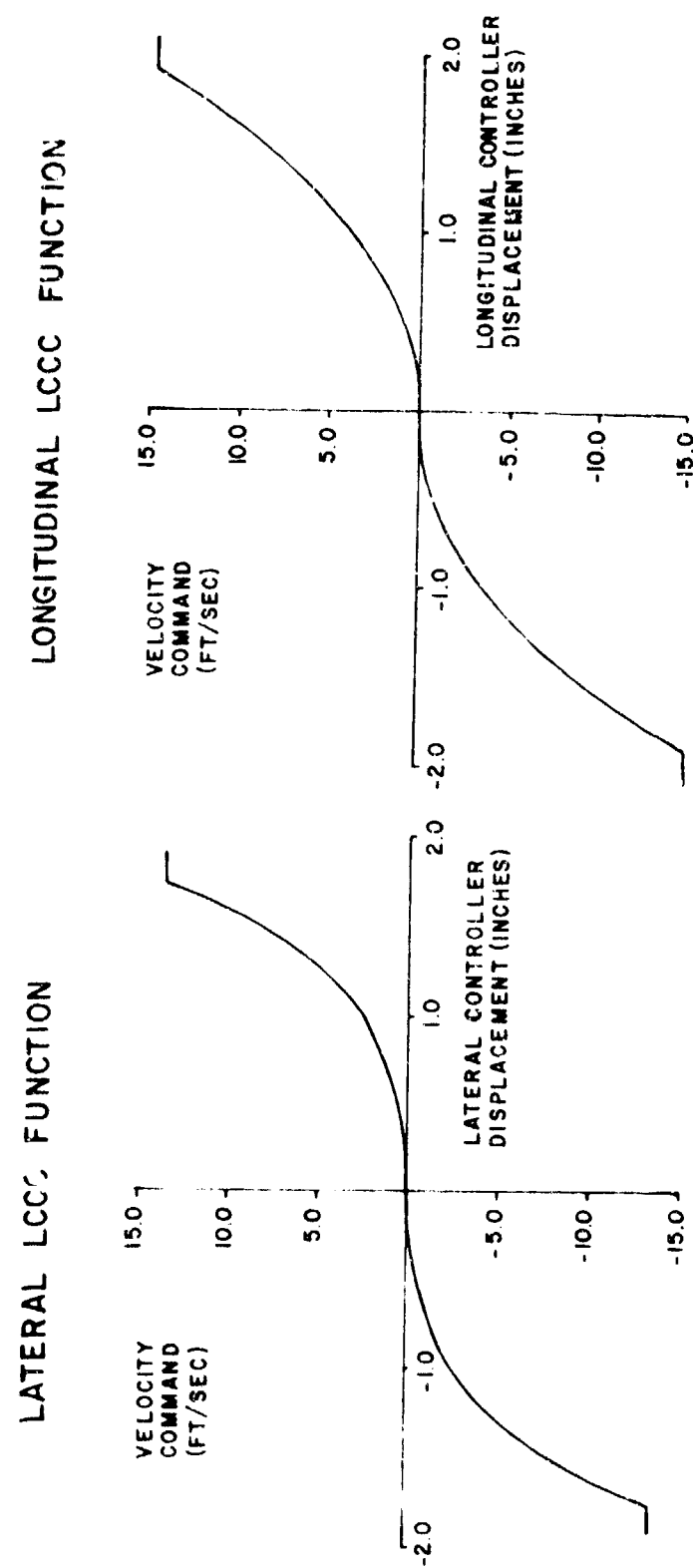


FIGURE 41.

COMPARISON OF LATERAL & LONGITUDINAL CONTROL
RESPONSE WITH 4-AXIS FINGER/BALL CONTROLLER

Figure 42 presents simulation data for typical lateral velocity response and position hold maneuvering. Controller input steps in both directions are shown to produce almost constant velocity response characteristics with the control held in. When the LCCC deflection is removed, lateral velocity smoothly returns to zero and the position loops relock.

To assist the load crewman in executing the shuttle-type translational maneuvers depicted in Figure 42, the LCCC is configured with a magnetic brake which "locks in" any desired lateral or longitudinal control displacement. The brake is locked and unlocked by successively depressing a button located on top of the controller stick. With the brake engaged, the load crewman is relieved of the requirement to maintain continuous push or pull forces against the built-in controller force gradient.

2.1.4.1.3  Directional Hover Hold and LCCC Operation

Directional Hover Hold control laws retain all of the low-speed SCAS loops described earlier except for the pedal pickoff. A yaw rate command path is added for LCCC inputs. No PHS signals are involved and no heading beep capability is required. Figure 28 illustrates the Hover Hold control law package defined at the end of the flight program.

Stability - On the right side of the figure, yaw rate, pedal compensation, and aircraft heading feedbacks are shown to be engaged for Hover Hold operations. Only the heading signal processing must be modified in the Hover Hold mode. This is accomplished by doubling the attitude feedback gain, and by halving the heading synchronizer limit value as shown in the diagram.

Control - Load crewman inputs are introduced into the command loop by twisting the ball on the controller stick in a clockwise or counterclockwise direction with the thumb and forefinger of the right hand. The resultant angular rate responses have the same sense as the controller input, and are proportional to angular rotation of the ball. Maximum yaw rate with full controller displacement is on the order of 9 degrees per second.

Non-linear directional LCCC heading rate commands are processed similarly to the longitudinal and lateral inputs. Since the yaw rate signal does not require drift clearing, controller signal low-pass filtering need not be removed during this operation as it is in the lateral and longitudinal axes. Controller schedules are detailed in Appendix A.

FIGURE 42.

HLH/ATC PRECISION HOVER & LCC CONTROL SIMULATION

180

When either Hover Hold/IMU or Hover Hold/PHS are engaged, the
directional control laws maintain constant aircraft heading
as long as no controller inputs are made.  If a heading change
is required to reorient the aircraft, the load crewman applies
a control deflection (similar to the type shown in the simula-
tion time history, Figure 43) and a constant yaw rate results.

Since the helicopter yaws about its own cg, repeated lock-
ing and unlocking of the PHS will accompany heading  ading
changes (because of the displaced sensor location in the tail
of the aircraft).  The back and forth reversion between PHS
and IMU references results in a tendency toward slight longi-
tudinal and lateral cg drift during pure yaw maneuvers.

The impact of the drifting was hard to assess through the limited
yaw maneuvering possible in the flight evaluation of the
Hover Hold/PHS mode, because the aircraft rapidly moved off
the painted target grid shortly after initiation of each yaw
run .  Yaw maneuvering on IMU reference; while attempting to
hold horizontal position manually, appeared to be satisfac-
tory.  Details of the flight evaluation results, and proposed
solutions to problems not resolved during the program are
presented in Section 5.0.

### 2.1.4.1.4  Vertical Hover Hold and LCCC Operation

Vertical AFCS Hover Hold control laws are summarized in
Figure 30.  As shown in the block diagram, the Hover Hold
associated control law mechanization processes either PHS or
radar altimeter derived velocity and position feedback infor-
mation for stability (along with the normal acceleration
signals discussed earlier), and LCCC commands for control.
When Hover Hold operations are predicated upon PHS-
generated feedback signals, the mode is referred to as Hover
Hold/PHS.  At times when the sensor is not enabled or produc-
ing valid signals, the Hover Hold stability reference changes
to the radar altimeter.  This type of operation is called
Hover Hold/Radar in the discussion that follows and is analo-
gous to the longitudinal and lateral Hover Hold/IMU mode.

Stability - Unlike the longitudinal and lateral Hover Hold
axes which provide only one position stability mode, i.e.,
PHS; the vertical axis has two.  That is, altitude can be
maintained automatically (hands off) with either the PHS or
less accurate radar reference in use.

When Hover Hold/Radar is selected, the same stability loops
are engaged as those used for the Radar Altitude Hold mode
described in Section 2.1.3.4.  Radar rate is combined with
the acceleration feedback, through use of a complementary
filter network, to ensure smooth vertical damping characteris-
tics over a wide range of response frequencies.  The same

DIRECTIONAL RESPONSE TO LCC CONTROLLER COMMAND

MODEL 347 DEMONSTRATOR    SEA LEVEL 4 °   .DF
GR WT = 45,000 LB         5 KNOT HEADWIN
CG = 12 IN AFT

LCC
DIRECTIONAL
CONTROLLER
~ % TRAVEL

YAW RATE
~ DEG/SEC

HEADING (WITH
RESPECT TO
WIND) — DEG

FACING INTO WIND

PRECISION HOVER
SENSOR
LONG ERROR
SIGNAL
~ FT

CG LONG
POSITION CHANGE
~ FT

INITIAL POSITION REFERENCE

PRECISION HOVER
SENSOR
LATERAL ERROR
SIGNAL
~ FT

CG LATERAL
POSITION CHANGE
~ FT

INITIAL POSITION REFERENCE

TIME - SECONDS

FIGURE 43    HLH/ATC PRECISION HOVER & LCC CONTROL SIMULATION

182

approach toward vertical damping enhancement was adopted in the Hover Hold/PHS mechanization as shown in the figure.

Controls - While operating on PHS reference, the load crewman can introduce "beep", "creep", or "leap" type LCCC inputs to move the aircraft vertically. Beep inputs are made by pulsing the controller stick vertically so as to reference stabilized aircraft altitude. When the controller is displaced beyond its .04-inch velocity threshold for more than half a second, velocity responses are commanded. These are initially referenced to the PHS velocity signal, but revert to radar rate when the PHS unlocks.nlocks.

If the PHS has not been enabled, only velocity responses can be commanded with the controller. Radar rate (and normal acceleration) data provide the feedbacks for this type of maneuver. Vertical aircraft movement can be stopped at any time by removing the controller displacement. As velocity falls below one foot per second, the radar altitude loops re-engage and automatic altitude hold resumes.

In addition to the Hover Hold control and stability functions mentioned above, there are also integral backdrive command paths incorporated in the vertical AFCS to position the cockpit collective stick. The parallel drive commands are processed for all modes of Hover Hold operation providing trim compensation as required.

Details of the Vertical Hover Hold control laws are covered next, starting with an explanation of the PHS mode.

2.1.4.1.4.1 Hover Hold/PHS - When the Hover Hold/PHS mode is engaged, the normal acceleration signal enters the AFCS box, and passes down and to the left through a 20-second washout and gain module. The upper horizontal acceleration path is eliminated during Hover Hold operations by the (1-6 and NOT L-11 and NOT L-7A) logic switch positioned as shown in the diagram.

Subsequent to the KZLA1 gain operation, the acceleration signal is summed with the low-pass-filtered and coordinate-transformed PHS vertical velocity feedback, and the result passed through a 5-second lag. The combined "complementary" filtered velocity damping signal provides a smoothed, constant gain feedback which minimizes the differences in signal quality exhibited by the vertical accelerometer and PHS outputs. Details of the complementary filter mechanization and operation are covered in depth in Section 2.1.3.4, and in the Figure 31, frequency response Bode plots.

Prior to summation with the acceleration signal, the PHS velocity feedback must pass through an L-19 logic-controlled switch. As in the longitudinal and lateral axes, the vertical

PHS velocity signal can only be utilized when the sensor is
enabled, and in a locked condition (see the Figure 38 explana-
tion of sensor operation). When the sensor unlocks due to air-
craft motion or some other cause, the L-19 switch throws and
velocity feedback reverts to radar rate as described earlier.

Assuming that the PHS velocity signal is valid, and has been
complemented with the high-pass filtered accelerometer signals,
the combined hybrid feedback is then summed with the LCCC
velocity command path output to form an error signal. LCCC
velocity commands are generated through use of a non-linear
gain function (FZLC).

Exceeding the velocity threshold with the controller produces
a continuous velocity demand which is satisfied when the air-
craft reaches the commanded speed. At the time the command
speed is achieved, the error summer output is zero.

Following generation of the "hybrid precision hover velocity
error", the damping signal next passes on into the differen-
tial output path, providing the L-46 and L-11 switches are
closed. L-46 logic is true, and the switch is closed, whenever
the radar altimeter is capable of providing valid vertical rate
information. This switch is inserted in the velocity damping
path to ensure availability of reliable radar rate information
whenever the Hover Hold mode is engaged. Without its presence,
Hover Hold/PHS operation would not be possible since there
might not be a radar rate signal available to transfer to each
time the PHS unlocked.

Branched off the velocity error path after the L-11 switch is
an integral collective stick backdrive loop controlled by L-50
logic. This path is engaged each time vertical velocity com-
mands are introduced with the LCC controller, and it remains
operational as long as the velocity exceeds 1 foot per sec-
ond. The purpose of the loop is to provide the additional trim
collective stick required, any time that the aircraft descends
into ground effect or picks up an external load.

As initially configured at the start of flight testing, the
Hover Hold velocity backdrive path was engaged full time to
compensate for the anticipated effects of steady vertical wind
gusts, etc. This mechanization was similar to the one used in
both the longitudinal and lateral axes. With the progress of
testing, however, it was determined that backdrive (KCLV2) gain
levels set for adequate LCC controllability were, in fact, too
high for good hands-off stability. Accordingly, the L-50
switching was incorporated to energize the backdrive loop only
during periods when LCCC velocity commands were being made.

The precision vertical position stability and control network
operates in concert with the acceleration and velocity loops

184

just described, and has a functional mechanization quite similar to the one found in the longitudinal and lateral axes. The constituent parts of the position network include:

- A position feedback path for the incremental PHS signal which is engaged through an L-8C logic-controlled synchronizer

- A pulsed beep command control path interfaced with the position feedback loop (at the synchronizer) to form a position error signal

- A position error backdrive command loop for trim compensation, and

- A differential output path for the processed position signal

As shown in the diagram, the PHS position signal is transformed first to the proper coordinate system, and is then converted to inches of equivalent corrective stick by the KZLD gain. The feedback is synchronized to zero output until such time as the L-8C "Vertical PHS Position Stabilize" logic becomes true. This occurs when the vertical velocity is less than 1 foot per second; no velocity commands are being made with the LCCC; and the L-8, L-46, and L-20 logic states are true. (Appendix A presents a complete summary of all logic network functions).

After L-8C changes to a true state, the synchronizer reverts to its stabilizing mode of operation. In this mode, position feedbacks are passed on directly. Also permitted are pulsed LCCC inputs to the synchronizer which are "integrated up" to form a net error signal, and this in turn is passed to the integral parallel and differential output paths mentioned above. The pulse magnitude and duration are selected to produce approximately 2 inches of vertical motion for each individual beep input.

During the flight test evaluation of the vertical Hover Hold/ PHS function, tight automatic altitude hold characteristics were observed. In mildly gusty conditions with 10-knot steady winds, the measured RMS variation in vertical position was on the order of 2.5 inches. With winds gusting to 20 knots, the vertical excursion was only slightly greater (approximately 4.3 inches RMS) for a typical 2-minute test point. Additional test results have been analyzed, and a summary of these is presented in Section 5.0.

2.1.4.1.4.2 Vertical Hover Hold/Radar - As indicated in the introduction to this section of the report, Hover Hold/Radar stability functions are identical to those employed with the Altitude Hold mode, and therefore need not be discussed again. The controllability aspects of the two modes, however, are different in a number of respects, and these differences are reviewed below.

When the pilot depresses the magnetic brake to move the collective stick while flying with Altitude Hold selected, control augmentation reverts to the basic aircraft with the radar rate (and acceleration) stability feedbacks disengaged. Hover Hold/ Radar operation differs, of course, since the hybrid acceleration/rate feedbacks remain engaged when vertical velocity commands are introduced by the load crewman. Note that the acceleration, rate, and radar altitude loops all remain operational during LCCC beeping maneuvers. A final difference between the two modes is the use of the L-50 controlled back-drive path to provide additional collective control for Hover Hold maneuvering. This loop is not utilized in the Altitude Hold AFCS mechanization.

2.1.4.2 Hover Hold Design Analysis - Key Developments

Parametric studies accomplished in Task 1, Part 1, established low sensitivity linear velocity control as the best approach for accomplishing the hover mission. A control system was synthesized by adding linear velocity and position feedback paths (and control loops) to the basic SCAS mechanization whenever precision hover operations were required.

Early in 1972, an analytical study was conducted confirming the feasibility of meeting design goals with this type of AFCS mode. The analysis generated estimates of vehicle performance while operating under the influence of atmospheric turbulence, or over the deck of a moving ship.

In November and December 1972, a nudge base flight simulation was conducted at Vertol to assess "pilot in the loop" handling characteristics with the Hover Hold mode engaged. The aircraft was flown with several different LCC candidates installed in the cockpit for evaluation. Both Vertol and customer pilots (and engineering representatives) participated in the program. The best controller ( a four-axis fi  ier-ball configuration) was selected for continued development and later application in the 347 flight research vehicle test program.

Further  analytical refinement of precision Hover Hold control laws and logic were pursued during the summer months of 1973 to prepare for the Northrop load crewman flight simulation in December of that year. The Vertol full envelope hybrid simulation math model was used for this effort. The principal

emphasis in the program was placed upon modeling the dynamic characteristics of the Precision Hover Sensor (PHS), and determining the effect of the sensor on Hover Hold performance.

A synopsis of key Hover Hold developments from the three analytical programs just described, and subsequent to Task 1, Part 1, is presented next.

2.1.4.2.1  Feasibility of a Precision Hover System for the Heavy Lift Helicopter

A comprehensive theoretical design analysis was conducted during the latter part of Task 1, Part 1, and throughout the first three months of 1972 to develop a workable Hover Hold concept for the HLH.  Data from this analysis confirmed the feasibility of using high-gain loop closures in the AFCS to satisfy the tight position-hold requirements of the HLH hover mission.

Study results were utilized in a number of areas, and were summarized in Vertol Document D301-10128-1, titled "A Theoretical Discussion of the Precision Hover System for the Heavy Lift Helicopter" (see Reference 6).

An early application of this analysis involved the generation of preliminary performance requirement specifications for the Precision Hover Sensor.  Results were also used, as indicated earlier, in subsequent Hover Hold control law optimization work.

Small perturbation decoupled dynamic equations were utilized in the feasibility analysis, and perfect sensor performance was assumed.  The aircraft considered was a 67,000-pound HLH with no external load.  An early approach toward establishing loop gains, time constants, etc., (in which the feedback paths were closed one at a time), was found to be unsatisfactory due to the low damping levels of the basic roots.  Alternative solutions were developed in which techniques similar to optimal control analysis were employed to close all stability paths in each control axis simultaneously.

The stability root analysis performed with the final gains included in the velocity and position loops typically reflected critical damping ratios (of the least stable mode) which were no lower than $\zeta = .50$.  An example of the relatively high-gain levels required to meet the $\pm 4.0$-inch hover hold goals, and at the same time provide adequate damping, is given in the table below:

| HOVER HOLD AXIS | LINEAR VELOCITY GAIN | POSITION GAIN |
|---|---|---|
| Longitudinal | 7.0 Deg LCP/Ft/Sec | 13.8 Deg LCP/Ft |
| Lateral | 2.2 In. Stick/Ft/Sec | 1.7 In. Stick/Ft |

With the gain levels and shaping time constants defined, further analysis was done to determine aircraft position hold characteristics in turbulent wind conditions. A Dryden turbulence spectrum approach was assumed for modeling the gust. Figure 44 summarizes the major turbulence study results, and demonstrates the feasibility of meeting the hover objectives in moderate turbulences.

As shown in the figure, estimated longitudinal hold capability was significantly better than lateral or vertical performance. This characteristic is due to a combination of low-gust sensitivity in the longitudinal axis, and application of direct force control via longitudinal cyclic pitch. It is interesting to note that flight testing conducted at the end of the ATC program verified the predicted performance superiority of the longitudinal Hover Hold axis (even though the feedback gains had been reduced substantially from the preliminary ones used in this study).

By replacing the linear velocity and displacement feedback signals with ones representing position and velocity error relative to a target on a moving ship deck, the information shown in Figure 45 was generated. This chart addresses the containership loading and unloading mission requirement spelled out earlier in Section 2.1.1.

Ship motions assumed for the study were considered to be sinusoidal in nature and at the representative frequency stated. Sea-state modeling was predicted upon information supplied by the Naval Oceanographic Office and a C3-5-37A containership was used to define the combined ship/sea motion trends applied in the analysis.
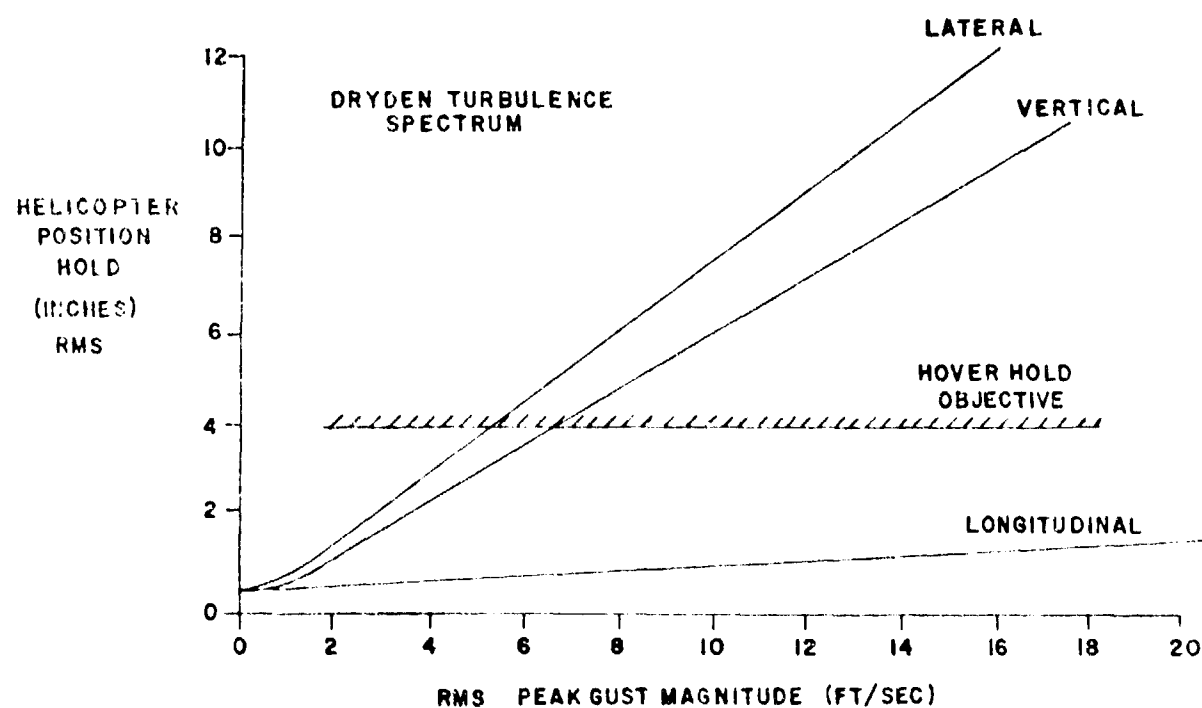
FIGURE 44. HELICOPTER HOLD CAPABILITY IN TURBULENCE

189
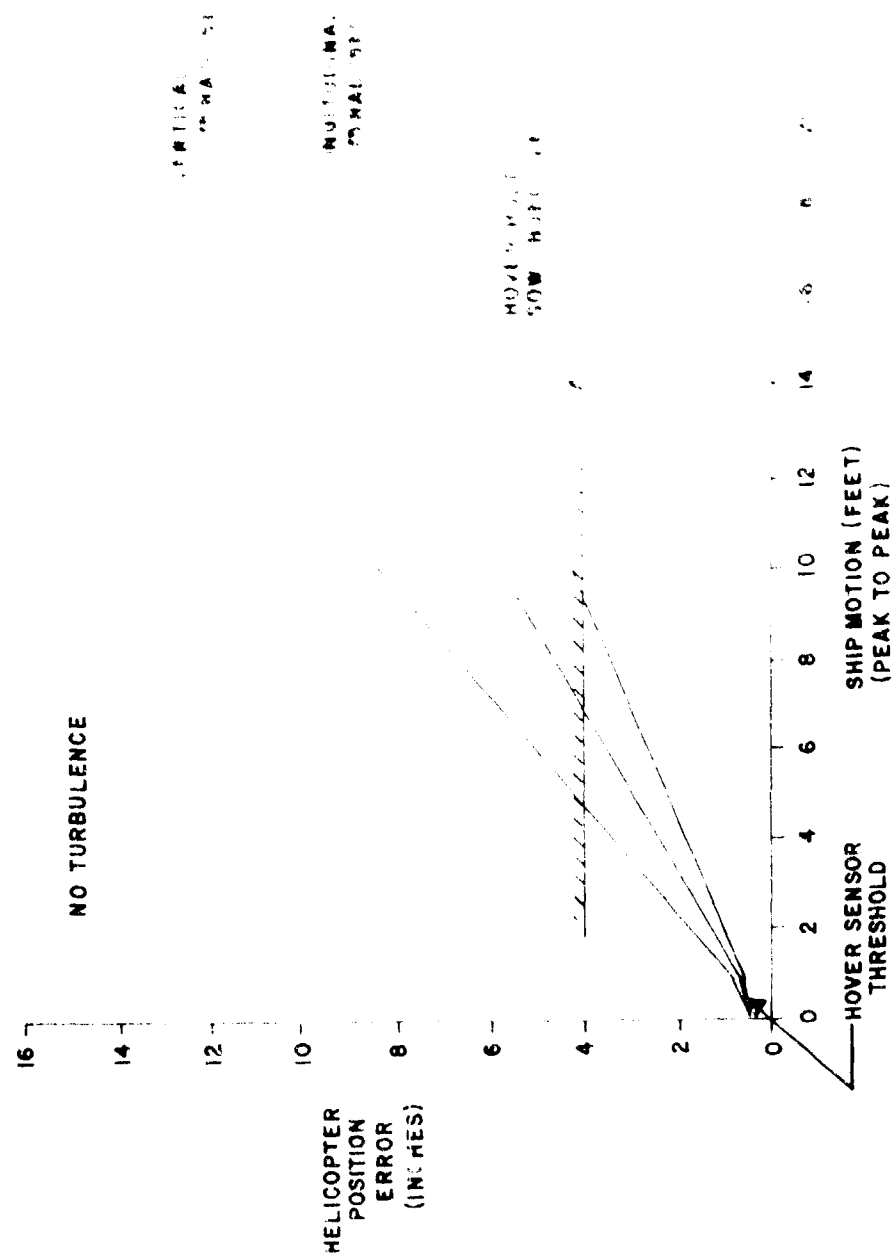
FIGURE 45.

HELICOPTER-TO-SHIP TRACKING CAPABILITY

2.1.4.2.2   Precision Hover Hold Nudge Simulation

The December 1972 simulation program conducted on the Vertol
6-degree-of-freedom Nudge Simulator utilized a small per-
turbation 347 helicopter airframe model, and a digital
mechanization of the AFCS.   Program objectives were to:

- Demonstrate acceptability of the Precision Hover Hold
  control laws proposed by the AFCS block diagrams in the
  design data package, and

- Support development and selection of an optimized LCC
  Controller configuration.

Both piloted and unpiloted simulation studies were accom-
plished to meet these objectives.   The scope of this activity
included minor modification of control laws and logic to
improve Hover Hold handling qualities with a "load crewman"
pilot in the loop.   Additional effort went into defining a
satisfactory set of nonlinear velocity command stick sensi-
tivity schedules for the various controller candidates.

As a part of the mockup LCC design review then
in progress at Vertol, customer representatives participated
in a Precision Hover Hold concept familiarization and an LCC
evaluation.

SIMULATION PROGRAM - Pilot and engineering evaluators "flew"
a series of assigned tracking and maneuvering tasks with each
of four controller candidates.   The defined tasks were
designed to provide qualitative trend data and associated
pilot comment concerning both the Precision Hover Hold mode
and controller being evaluated.

Simulation visual cues for large-scale maneuvers were provided
by TV projections of a computer-generated horizon and moun-
tain scene, and by a landing pad on the fantail of a simulated
ship at sea.   Since the TV scene was inadequate for precise
hover maneuvering over a target on the ground, an oscillo-
scope with a tracking grid attached was employed to present
the ground tracking problem to the pilot.

Tasks flown with reference to the scope presentation typically
consisted of straight flight,accompanied by diagonal and turn-
ing maneuvers commanded by the controller.   Both the veloci-
ty and beep modes of controller operation were used for
maneuvering the aircraft.

LCC CONTROL - Four self-contained LCCC units used in the
evaluation were built by Simulator Laboratory personnel.

Configurations tested included:

- A four-axis, right-hand finger/ball controller (Fig. 101)

- A four-axis, right-hand grip controller with a thumb-operated vertical command switch (shown at the bottom of Figure 101)

- A three-axis, right-hand grip controller with single-axis left-hand vertical controller

- A three-axis, right-hand finger controller with separate left-hand control of vertical commands.

The total motion permissible with each test controller configuration (or type of control switch installed) is listed in the table below:

| MOTION | FINGER | GRIP | SINGLE-AXIS VERTICAL LEVER |
|---|---|---|---|
| LONGITUDINAL | ±2.75 in. (±25 Deg) | ±2.75 in. (±25 Deg) | — |
| LATERAL | ±1.5 in. (±15 Deg) | ±2.95 in. (±27 Deg) | -- |
| DIRECTIONAL | ± 27 Deg. | Detent Switch | — |
| VERTICAL | ± 1.05 in. | Thumb Switch | 1.5 in. |

Non-linear ICC control sensitivity schedules, similar to those illustrated in Figures 38 and 42, had been developed for the design data package prior to the Nudge Simulation. These schedules were revised both before and during the simulation to provide satisfactory aircraft response with each controller.

Longitudinal sensitivity variation for both the finger/ball and grip controllers was found to be about the same for best performance with approximately 2 to 2-¼ inches of stick required for maximum velocity commands (± 15 ft per second). Lateral sensitivity on the other hand was higher for the finger controller than for the grip configuration (1¾-in. vs. 2¼-in. maximum deflection) because of total travel limitations in the test installation. No significant performance degradation was observed to have resulted from these controller

differences. Directional control scheduling with the finger LCCC utilized the full range of the test controller ( $\pm$ 27°) to command yaw rates of up to 4.5 degrees per second. This schedule reflected a control sensitivity one-third lower than had been proposed previously in the design data package.

A substantial difference between design data and the actual system demonstrated on the simulator occurred with the vertical axis. Pilots determined that vertical LCCC sensitivity should be increased by a factor of about two for both the finger and single-axis controllers, decreasing vertical travel to .5 and .75 inches, respectively. It was also recommended that maximum vertical velocity should be set at approximately 400 feet per minute with symmetrical velocity command capability in both the up and down directions.

On the basis of simulator evaluation of all four LCCC candidates (used in conjunction with mockup controller design review results), the four-axis finger/ball configuration was chosen for continued development. Further comparative testing of the finger/ball and grip-type controllers was performed during the December 1973 Northrop simulation under BOA #12. Results of this program are presented later in the report.

PRECISION HOVER HOLD CONTROL LAWS –

The Precision Hover Hold control laws demonstrated during the LCCC evaluations reflected only minor modifications to the pre-simulation design data package information. Feedback gains, etc., utilized in the simulation were selected primarily on the basis of qualitative pilot assessments of vehicle handling qualities, rather than on any exhaustive optimization study results. Pre-test gain levels were found to produce satisfactory levels of hands-off vehicle stability as expected, but were adjusted downward in some cases to provide good control response characteristics for maneuvering. A summary of system modifications is given below:

- Longitudinal IMU ground speed feedback gain in the basic SCAS (KMGS) had to be set to zero with the Precision Hover velocity and position feedbacks engaged. Without this feature, consistent velocity responses were not possible and the PHS limiter bottomed.

- Longitudinal and lateral position feedback gains were reduced by 2/3 and 1/2, respectively (to 3.95 degrees/foot and 0.85 inches/foot). The use of higher gains resulted in more overshoot in the position response of the helicopter.

- Lateral velocity error limiting (LL3) was increased to $\pm$ 1.5 inches to improve lateral acceleration response to LCCC inputs.

193

- Logic element L-8 was revised to include latching of the position hold loop in a synchronization mode (with no position feedback), when velocity was above 2 feet per second. Test results also indicated desirability of synchronizing <u>individual</u> position loops (rather than all at the same time), when the controller was deflected beyond the velocity threshold in any axis. Pilots found that simultaneous synchronization of all position loops, while the controller was commanding velocity response in only one axis, created an unnecessary increase in work load.

2.1.4.2.3   Effect of the Precision Hover Sensor on Hover
            Hold Control Laws

Throughout the summer and fall of 1973, both analytical and unpiloted hybrid simulation studies were carried out at Vertol to prepare for the upcoming load crewman simulation in California. The major emphasis of this pre-Northrop work was focused on the Precision Hover Sensor, and its relationship to Hover Hold control law requirements. A stability root analysis was also performed to refine feedback gains, etc., for the Hover Hold/IMU and PHS modes.

STABILITY ANALYSIS - Examples of the stability analysis results from the Hover Hold studies are presented in Figures 46, 47, and 48. Illustrated on these plots are the stability roots of the basic combined airframe/AFCS response modes, as affected by variations in Hover Hold velocity and position feedback gain level.

Figure 46 shows the complex root migration of the dominant longitudinal/vertical response modes resulting from changes in only the longitudinal position feedback gain (KXLD). Decreasing this gain improves damping and reduces response frequency for the short period mode (illustrated in the uppermost right-hand set of roots). The effect of gain variation on other modes is shown to have only a small influence on damping but does change the damped frequency somewhat. These theoretical roots are based upon analysis work which utilized the nominal AFCS parameters listed at the top of the plot. Most of the gains and time constants were revised later during the Northrop simulation and final flight test evaluation.

In order to relate the final flight configuration and the one used in the analysis, rough estimates of stability root placement were made with the final flight test gain settings applied. These roots are annotated on the plot with the star symbol.

Figure 47 illustrates the effect of varying lateral velocity gain on the lateral/directional modes. Again, as in the previous figure, only one Hover Hold feedback parameter (lateral velocity) is changed to move the stability roots. When ground-

194

FIGURE 59.
LONGITUDINAL/VERTICAL PNS STABILITY ROOT ANALYSIS SUMMARY

FIGURE 4:
LATERAL/DIRECTIONAL PHS STABILITY ROOT ANALYSIS SUMMARY

speed gain is increased, damping of both the short and long period lateral modes improves for a while, but then begins to decrease sharply (for the long period mode) with further gain elevation.

The plot clearly illustrates the complexity involved in attempting to select a final system gain level, based on an analytical approach which varies only one parameter at a time. This problem was also identified in early phases of the 1972 Hover Hold feasibility study discussed earlier. Note that although only single parameter gain variations are depicted in Figures 46 and 47, additional analysis was accomplished for all Hover Hold axes to determine trends resulting from changing both velocity and position gains simultaneously.

Figure 48 presents a typical set of Hover Hold-associated roots wherein both velocity and position gain levels are varied together. The plot depicts the longitudinal/vertical mode again, but in this case, the roots are responding to vertical-axis climb rate and altitude feedback gain changes. As shown in the figure, the short period vertical mode reflects an increase in both damping and frequency when velocity gain is increased. Raising the position gain, on the other hand, reduces vertical damping appreciably, especially when lower velocity gains are being used.

PHS AND DRIFT CLEAR MODELING - In preparing for the Hover Hold flight simulation at Northrop, substantial effort went into modeling the PHS for analysis. Sensor lock-ing, unlocking, and relock characteristics were considered, along with the drift clear and IMU/PHS velocity switchover features covered earlier in Section 2.1.4.3.1.1.

Using the gains determined in the Root Analysis described above as a starting point, helicopter response to LCCC inputs (with sensor effects included) were explored on the hybrid full envelope simulation model. One of the LCCC units used on the earlier Hover Hold Nudge simulation was hooked up in the hybrid lab to introduce load crewman controller pulses and steps into the model. Complete cockpit control back drives were also simulated for the first time.

Data from the hybrid analysis confirmed that PHS sensor lock-ing and unlocking characteristics would not degrade Hover Hold performance appreciably when compared with continuous sensor results. Several changes were required, however, in other aspects of the Hover Hold mechanization to achieve the desired performance potential of this selectable AFCS mode. These included:

FIGURE 48.
LONGITUDINAL / VERTICAL PHS STABILITY ROOT ANALYSIS SUMMARY

- The need for backdriving the primary controls in the longitudinal and lateral axes with a _position error signal_ in addition to the velocity error. This change tends to continuously drive the long-term position error toward zero.

- The necessity to add _0.5-second time delays_ to the LCC velocity control threshold discretes input to L-8 logic. These delays were incorporated in order to clearly differentiate between position beep and velocity commands, and to make aircraft response to precision position commands predictable.

- The requirement to modify _IMU to PHS velocity switching_ networks to eliminate undesirable transients as described in Figure 36.

2.1.5   LOAD STABILIZATION SYSTEM

2.1.5.1   Requirements and Objectives

The Load Stabilization System (LSS) is a selectable mode of
the AFCS which is designed to aid the pilot and LCC in hand-
ling an external load.  The LSS, in conjunction with the
hover hold and PHS modes, should allow rapid and much easier
load attachment, pickup, shuttling, and positioning.  Lightly
damped load pendulum modes would cause two significant prob-
lems relative to the HLH mission.  First, the task of placing
the load accurately would be difficult and time consuming,
as load oscillations created by aircraft maneuvering or turb-
ulence require an exceptionally long time to decay.  Second,
sustained low-frequency longitudinal accelerations in the
lifting helicopter due to load motion, particularly with a
heavy load, are disorienting and fatiguing to the pilot and
can lead to pilot-in-the-loop oscillations during instrument
flight.

The LSS has three sub-modes to accomplish its function;
aircraft/load centering, load damping, and load position
hold.  The system switches between these modes automatically
when the appropriate conditions are present with the LSS
selected.

2.1.5.1.1   Aircraft/Load Centering

The requirement of the aircraft/load centering mode is to
center the aircraft over the load automatically prior to load
pickup to prevent load swing as it is lifted off.  Although
the cable tensions produce an inherent centering force on the
aircraft, the PHS would prohibit the aircraft from moving.
The LSS is designed to command the PHS to provide a well-
controlled and precise centering.  After the cables are
attached and the LSS is selected, the system makes and keeps
the cables taut while automatically centering the aircraft
over the load longitudinally, laterally, and directionally.
The tension must be kept large enough to keep the cables
straight for accurate cable angle measurement, but small
enough to avoid dragging the load before the aircraft is
centered over it.  The system continues to maintain the air-
craft position over the load as the LCC increases tension to
lift the load off.

200

The specific objective of this mode is to limit any load
swing during liftoff to less than ±4 inches horizontally
and ±2 degrees directionally.

## 2.1.5.1.2   Load Damping

The requirement of the load damping mode is to provide a high
degree of load pendular mode damping to allow the precise
load position hold and placement that is required.  The load
damping mode switches on automatically when the load leaves
the ground (or ship).  The specific objective is to maintain
the following levels of pendular mode damping.

- 20 percent or greater for longitudinal and lateral
  modes with hover hold or PHS on.

- 15 percent or greater for longitudinal and lateral
  modes with basic SCAS in hover and forward flight.

- 15 percent or greater directionally.

These damping levels are well above the MIL-H-8501A IFR min-
imum requirements of 5.5 percent for a period greater than
5 seconds and 11 percent for a period less than 5 seconds.

## 2.1.5.1.3   Load Position Hold

The requirement of the position hold mode is to automatically
maintain a constant load position relative to the ground
(or ship) when the load is airborne and the PHS is on.  This
mode switches on automatically when the load becomes airborne,
and off when the aircraft leaves hover, i.e., when the PHS
switches off.  When the LCC or pilot repositions the load,
the LSS will maintain the new load position.  The LCC can
switch the load position hold mode off if it is desirable to
hold the aircraft position, rather than load position.

The specific objective is to maintain the load center-of-
gravity such that placement accuracy is within ±4 inches
horizontally and vertically, and ±2 degrees directionally
relative to the ground.

## 2.1.5.2  System Synthesis

The LSS is designed to have a minimum impact on the structure
of the other AFCS loops.  Simplex signals are supplied to the
LSS loops from each cargo hook.  These signals are measurements
of longitudinal and lateral cable angles relative to the air-
craft and cable tensions.  Several simplifications were made
for the ATC demonstration system since some aspects of the
system were considered unnecessary for the demonstration
program.  The control loop synthesis, including simplifica-
tions, is discussed in the following sections.

### 2.1.5.2.1  Aircraft/Load Centering

The aircraft position change required to center it over the
load is calculated from the cable tensions, cable angles
relative to the aircraft, and the aircraft pitch and roll
attitudes.  These signals then command the aircraft, via
the PHS and heading stabilization loops, to move the approp-
riate distance.  The structure of these loops and their
interface with the AFCS are shown in Figures 14, 23, 28, and 30.

The equations used to describe the aircraft's position relative
to the vertical over the load are:

$$X_{LC} = \frac{L}{57.3} \left( \frac{\theta + T_F \rho_F + T_R \rho_R}{T_F + T_R} \right) \tag{1}$$

$$Y_{LC} = \frac{L}{57.3} \left( \frac{\phi + X_F + X_R}{2} \right) \tag{2}$$

$$\psi_{LC} = \frac{L}{L_{LX}} \left( X_F - X_R \right) \tag{3}$$

202

Refer to Figure 49 for a definition of the cable angles relative to the aircraft. When $X_{LC}$, $Y_{LC}$, and $\psi_{LC}$ are driven to zero, the total tension force on the load is approximately aligned with the gravity vector with zero directional moment. These terms replace the normal PHS position and heading terms to accomplish the centering function. A transient-free switch is used to switch the load-centering terms in and out. The switch provides a centering rate equal to its decay rate, i.e., a decay rate of 1 fps produces a steady-state aircraft velocity of 1 fps as it moves over the load. The PHS position and heading terms are removed with a track-store-synchronizer element so there is no transient when the centering mode switches in and out.

The design includes a velocity term in the longitudinal and lateral axes to cancel the PHS velocity term. While no frequency shaping is required in the longitudinal and directional axes, a 1.67-second time-constant lag is required on the lateral position term. The velocity term gains are 0.5 that of the PHS velocity loops and the centering rates are set at 1 fps and 2 degrees/second. (The centering velocity terms were removed during the system flight test development as discussed in the flight test section of this report.)

The load centering loops assume that the cable angles read zero when the cables are parallel to the aircraft vertical axis. With 50-foot cables, a 0.1 degree null error would cause the aircraft to be centered incorrectly by 1.1 inch. Bias terms may be required in the software to accomplish the required null.

The centering mode has loops in the vertical and longitudinal axes to make and keep the tension in both cables constant at a value approximately equal to one-fourth of the load weight. Since the anticipated ATC demonstration load weight is in the order of 5000 pounds, the vertical axis is set to drive the sum of the tensions to 2400 pounds. This is accomplished with proportional-plus-integral control into the collective pitch control, as shown in Figure 14  The equation for this loop is

$$\delta_c = -\left(5 \times 10^{-5} + \frac{2.5 \times 10^{-5}}{s}\right)\left(T_F + T_R - 2400\right) \qquad (4)$$
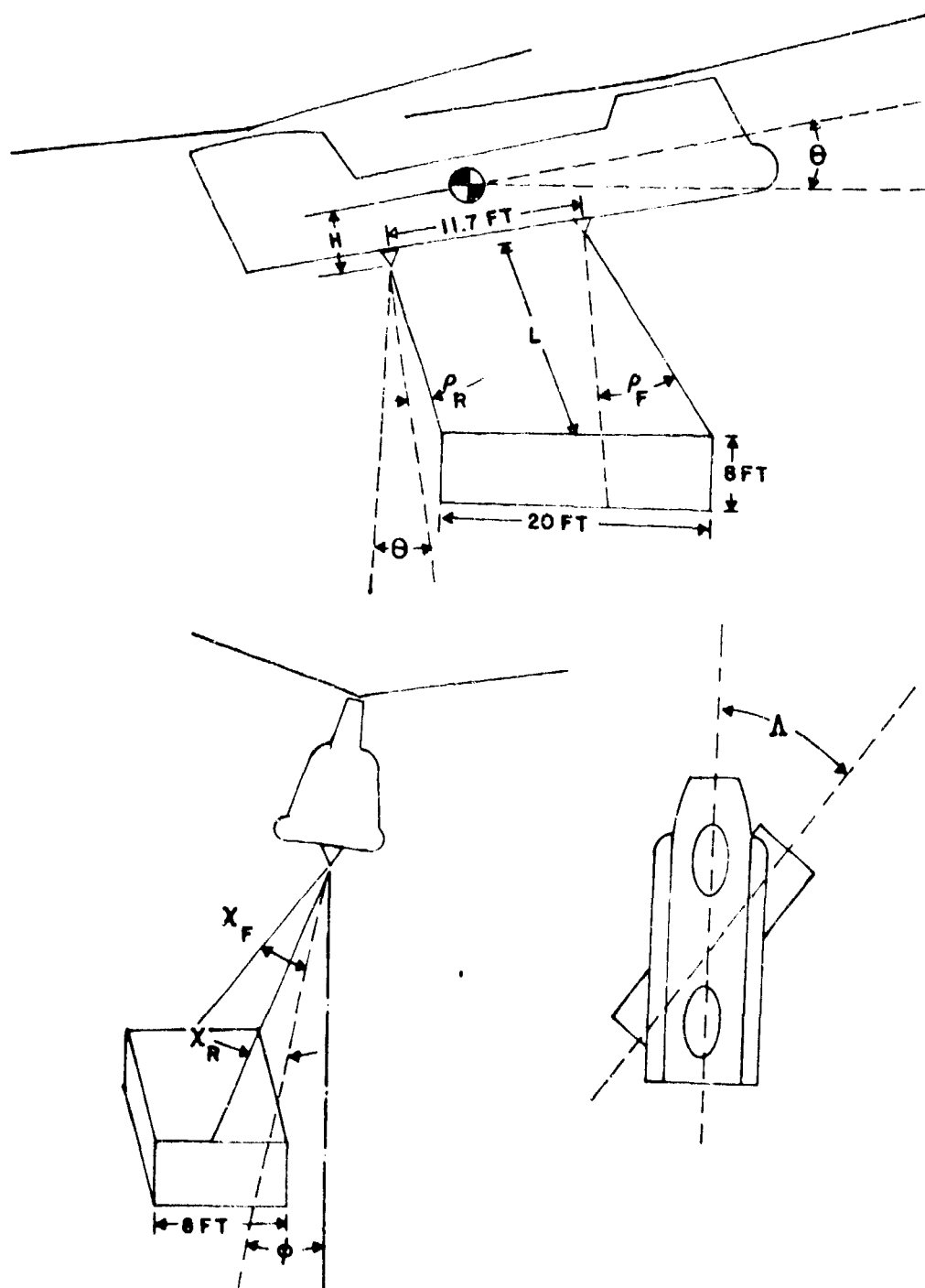
FIGURE 49.
LOAD GEOMETRY AND CABLE ANGLE DEFINITION

A tension equalization loop is incorporated which drives the longitudinal cyclic to maintain the forward and aft tensions equal.

The cyclic variations change the aircraft trim pitch attitude to equalize the tensions. The equation for this loop is

$$B_{ICF} = B_{ICR} = 5 \times 10^{-4} (T_F - T_R) \tag{5}$$

The loop is introduced by a track-store-reset element which is controlled as follows:

- Track when load-centering mode is on.
- Reset to zero when load becomes airborne.
- Store otherwise.

On the HLH the winch mechanism could be used to equalize tensions. Some approximations and limitations associated with the aircraft/load-centering mode, as demonstrated in the ATC program, should be mentioned.

- Small angle approximations are used in the centering equations. This is a valid approximation since the cable angles will be reasonably small when the aircraft is centered.

- The system is not designed for LCC augmenting override during the centering maneuver.

- Small switching transients can occur since transient-free switches are not used in the tension control loops.

2.1.5.2.2 **Load Damping**

The load damping loops use the cable angle and aircraft pitch and roll attitude signals to modulate the longitudinal cyclic, lateral cyclic, and differential lateral cyclic AFCS control outputs. The aircraft is maneuvered by these loops to keep the load hooks over the load, i.e., keep the cables aligned with the gravity vector. Block diagrams of these loops are shown in Figures 14, 23, and 28. A vertical load damping loop is not required since the load has no significant vertical mode.

The following relationships are used to form cable angles relative to the gravity vector from the cable angles relative to the aircraft.

$$\rho_G = \frac{\rho_F + \rho_R}{2} + \theta \tag{6}$$

$$\chi_G = \frac{\chi_F + \chi_R}{2} + \phi \tag{7}$$

$$\Lambda = \frac{L}{L_{LX}} (\chi_R - \chi_F) \tag{8}$$

These cable angles are used in the damping loops. The $\phi$ term is removed for the lateral axis when the hover hold mode is off to reduce switching transients which are discussed later. The cable angles provide good load damping eliminating the need for cable angular rate feedback. The gain and frequency shaping required to give the desired load and aircraft damping are applied to these signals. A 10-second washout is incorporated to remove cable angle trim values associated with forward flight, lateral flight, and steady winds. A washout is not required in the directional axis since the trim bifilar angle will remain reasonably small.

The load damping loops are very dependent upon the AFCS mode that is being used. No single load damping configuration could be found which would provide good damping regardless of whether the hover hold and PHS modes are on or off. Consequently, the system is designed to switch automatically between appropriate damping loops when these modes switch on and off. The $K_{XCA1}$ and $K_{YCA1}$ loops are used with the basic SCAS, while the $K_{XCA}$ and $K_{YCA3}$ loops are used when the PHS is on. For the lateral axis, an additional loop, $K_{YCA2}$, is required when the hover hold velocity loop is applied without the PHS position term. Transient-free switches are required to prevent excessive aircraft/load excitation when switching between these damping loops in a transient state. The loops that apply for the SCAS in hover are also used to damp the load in forward flight.

The current HLH cargo handling design uses an inverted-V suspension for forward flight which greatly reduces direct-ional load motion and eliminates unsteady aerodynamic stability problems. If pendant cables are used instead for forward flight, another directional load damping loop may be required.

### 2.1.5.2.3 Load Position Hold

The load position and heading change relative to the ground is calculated from the cable angles relative to the aircraft, aircraft attitudes and heading, and aircraft position relative to the ground. These signals command the aircraft, via the PHS and heading stabilization loops, to maintain the load center-of-gravity and heading constant over the ground. Refer to Figures 14, 23, and 28 for the detailed block diagrams of the load position hold loops. No vertical loop, beyond the PHS loops, is required since the load's vertical position relative to the aircraft will remain essentially constant. The load damping mode remains on to provide good load damping while the load position hold mode is on.

The following equations determine the load position relative to the ground.

$$X_{LOAD} = \frac{(H+L)\Theta + L \rho_F}{57.3} + X_{PHS} = X_{LPH} + X_{PHS} \tag{9}$$

$$Y_{LOAD} = \frac{-(H+L)\phi + L(\chi_F + \chi_R)/2}{57.3} + Y_{PHS} = -Y_{LPH} + Y_{PHS} \tag{10}$$

$$\Psi_{LOAD} = \frac{-L(\chi_F - \chi_R)}{L_{LX}} + \psi = -\Psi_{LPH} + \psi \tag{11}$$

Lag-lead frequency shaping is applied to $X_{LPH}$, $Y_{LPH}$ and $\psi$ LPH to maintain a high level of load damping. Then these signals are summed with the PHS position and aircraft heading signals to form $X_{LOAD}$, $Y_{LOAD}$, and $\psi$ LOAD. Pseudo velocity terms are formed by applying a washout to the position terms to cancel the PHS velocity feedback and provide phase advance. The final load position hold configuration is simplified by combining the position and velocity terms using an equivalent second-order filter as seen in Figures 14 and 23. This is

easily done since the PHS position and velocity loops have the same transfer function apart from gain. The continuous system frequency response of the longitudinal and lateral filters is shown in Figure 50. The steady-state gain is unity to provide the correct load position signal.

A synchronizing element is used to switch the load position hold loop into the system. The loop is synchronized to a zero output value while it is not required. The synchronization stops when the loop is switched in so that subsequent changes in load position are seen by the system. Thus, the system attempts to hold the load at its position when the mode is switched on.

The load position hold loops move the aircraft in the opposite direction from which the load swings in order to bring the load back to its initial position. Since the aircraft needs to move in the direction of the load swing to damp it, there is a conflict between load damping and position hold. Consequently, the position hold loops are frequency shaped, as described above, to reduce the gain substantially at the load frequency while maintaining the gain as near unity as possible at lower frequencies. This is seen in Figure 50, knowing the longitudinal and lateral load frequencies are in the order of 1 rad/sec. It can also be seen that a substantial phase advance is obtained at the load frequency. The system should be effective in holding load position in wind shifts and gusts whose frequencies are less than the load frequency.

There are several approximations and limitations associated with the load position hold loops as configured for the ATC demonstration.

- Small angle approximations are used in determining the load position relative to the aircraft. This is valid since the angle changes should be small while the load position hold mode is on.

- The load position equations are incorrect for spot turns in a steady wind.

$$\text{LONGITUDINAL} - \frac{2.5S^2 + 2.1S + 1}{1.67S^2 + 3.81S + 1}$$

$$\text{LATERAL} - \frac{1.58S^2 + 0.48S + 1}{1.76S^2 + 7.27S + 1}$$
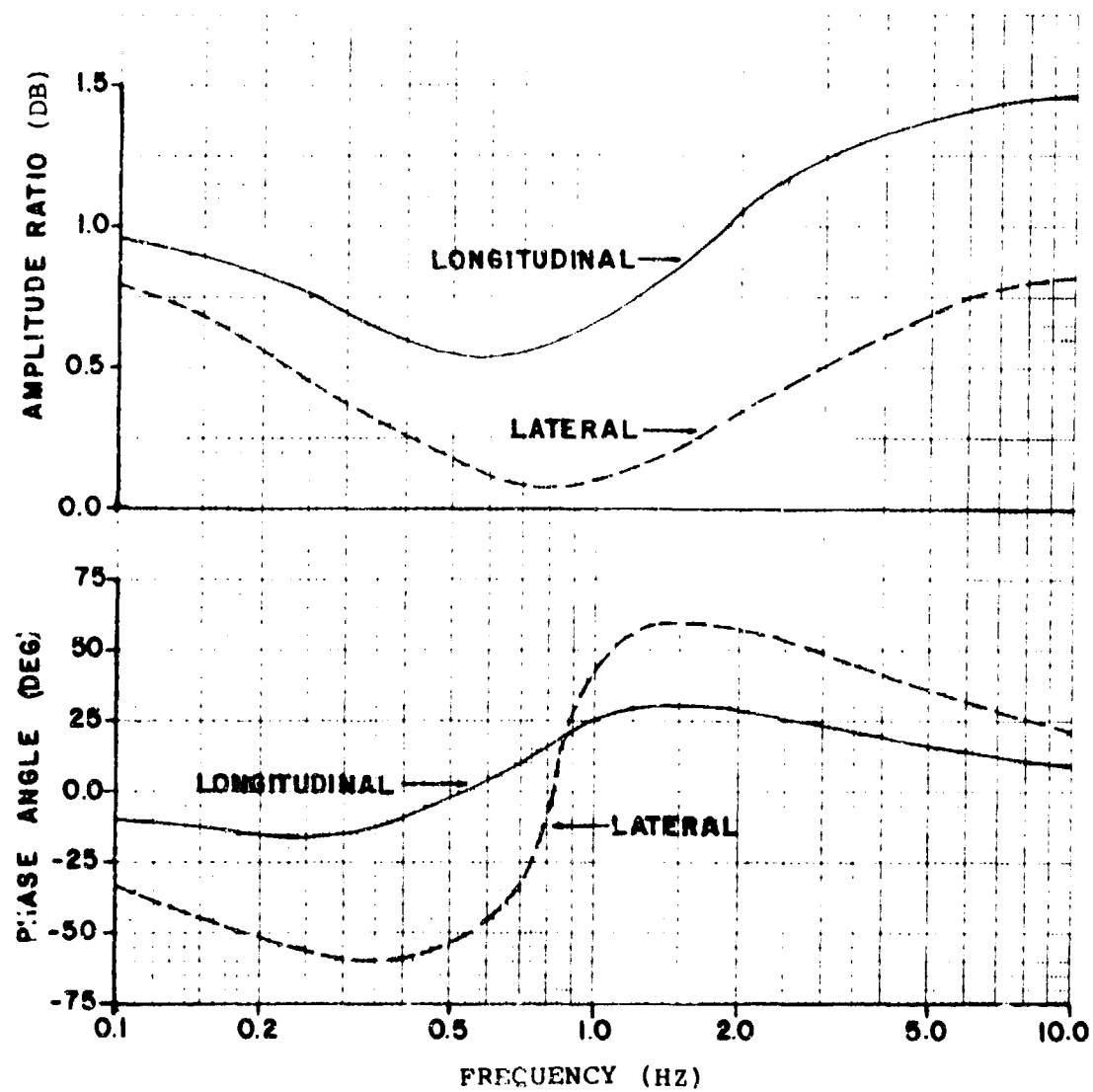


FIGURE 50.
FREQUENCY RESPONSE OF LOAD POSITION HOLD
LOOP SHAPING

209

- The load position hold switchoff is not transient-free when the PHS loops remain on.

- There is no automatic load position hold mode inhibit if the load is swinging with a large amplitude when the PHS switches on.

2.1.5.2.4  Logic

The LSS logic (L27) is designed to switch the LSS submodes in and out of the AFCS when the proper conditions are present. This logic (Figure 51) is implemented in the IOPs and receives/ sends discretes to the computers.

The cable tension control discrete (L27D) becomes true when the LSS is selected if the load is sitting on the ground and the hover hold mode is engaged. The load is determined to be on the ground if the total tension is less than 75 percent of the load weight. This discrete switches the tension control loop into the AFCS vertical axis. In addition, the altitude hold loop is synchronized allowing the aircraft to climb to make the cables taut. The tension control stops when the pilot depresses the collective magnetic brake to start lift-ing the load off the ground. The tension control will not switch on if the aircraft is centered over the load, and remains centered, when the load is set down.

The tension equalization discrete (L27E) becomes true when the tension control loop is operating and one of the cables becomes taut, i.e., when the largest tension becomes greater than 800 pounds. This switches the tension equalization loop into the AFCS longitudinal axis. When the load is leaving the ground, L27F becomes true, resetting the loop to avoid interference with hover hold.

The load-centering discrete (L27C) becomes true when all of the following conditions are present.

- LSS is selected.
- Load is on the ground.
- Longitudinal and lateral PHS position loops are engaged.

210

FIGURE 51. LOAD STABILIZATION SYSTEM LOGIC

- Heading is being stabilized.
- Both cables have become taut, i.e., the least tension is 800 pounds.

Both cables must be straight in order to provide correct cable angle measurements for the centering loops. The load-centering loops are switched into the AFCS longitudinal, lateral, and directional axes when L27C becomes true. The aircraft is centered within tolerance; E2 becomes true when all of the following are true.

- Both cables are taut.

- $|X_{LC}| < 2$ in.

- $|Y_{LC}| < 2$ in.

- $|\psi_{LC}| < 1$ deg

The LCC or pilot can lift the load off before E2 becomes true. The load centering mode is switched off, L27C becomes false, as the load is leaving the ground. As the aircraft moves over the load, a small pitch attitude change occurs which can cause the smallest tension to drop below 800 pounds for a short period of time. Consequently, a lag and hysteresis are incorporated in the smallest tension discrete as illustrated in Figure 52.

The load damping discrete (L27A) becomes true when the AFCS is engaged with the LSS selected and the load is airborne. Actually, the discrete becomes true before the load is airborne when the total tension becomes greater than 75 percent of load weight. The load damping loops are switched into the system when L27A is true. Additional logic is included to allow rapid descent entries without switching the load damping mode off. This logic keeps the load damping operating during descent entries if the aircraft is greater than 200 feet above the ground and the largest tension remains greater than 800 pounds. This still allows the damping mode to switch off if the load is set down or if the load is released while it is airborne.

212
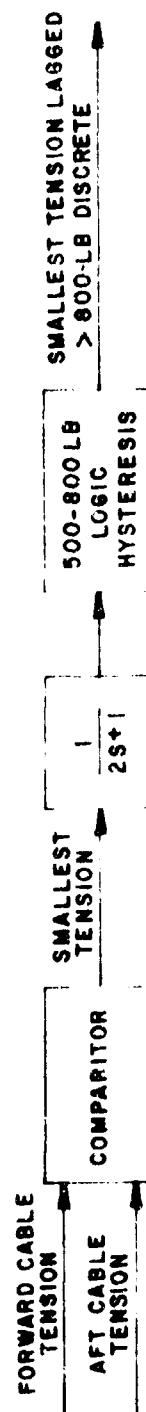
FIGURE 52. SMALLEST CABLE TENSION DISCRETE

The load position hold discrete (L27B) becomes true when the following conditions exist.

- LSS and hold position hold are selected.
- PHS position loops are engaged.
- Heading is being stabilized.
- Load is airborne (or nearly airborne).

The load position hold loops are switched into the system when L27B is true. It should be noted that the load damping loops will always be operating when the load position hold mode is engaged.

In addition to the IOP logic described above, there is software logic which switches to the proper load damping loop as the hover hold/PHS loops switch in and out.

There are several limitations in the logic as synthesized for the ATC demonstration program.

- There is no automatic method of detecting when the load has become airborne. Consequently, the tensions are compared to the approximate load weight to form this discrete. LCC override of this logic would be desirable for an operational system.

- The 800-pound tension threshold levels do not change automatically with load weight.

- There is no automatic switchoff and inhibit of the cable tension control loop if the cables are released.

- There are no lights to tell the pilot or LCC which LSS submode is operating or when the aircraft has been centered over the load within tolerance.

2.1.5.3   System Design Analysis

2.1.5.3.1   Analytical Models

Three analytical models were used to set the LSS parameter
values and analyze the LSS performance; root locus, Continu-
ous System Modeling Program (CSMP), and total force simulation.
The load pendulum motion equations, LSS loops, and LSS logic
were incorporated in each model, as appropriate.   The root
locus model uses a derivative representation of the aircraft
to provide the system eigenvalues.   The CSMP model, which also
has a derivative aircraft representation, produces transient
responses.   Logic and switching can be analyzed to some extent
using this model.   The total force simulation is used to
evaluate system performance during large perturbation maneuvers
and disturbances.   It also allows a more thorough check of
system logic, interfacing with the other AFCS modes, and
switching performance.   Most physical aspects of the load,
cables, and sensors are included in the models.   The effect
of cable stiffness on tension control, cable angle sensor
hysteresis, and aerodynamic forces are included.

Each model was checked out and good agreement was found between
the three models.

The following configuration and parameter variations were
evaluated in the system analysis.

- Load:   8- x 8- x 20-ft MILVAN with weights of 5000, 8000,
  and 10,000 pounds.

- Cable configurations:   long pendants and inverted VEE.

- Cable lengths:   20 and 50 feet.

- Vertical distance between aircraft center of gravity
  and load hook:   4, 6, 8, and 10 feet.

- Cable stiffness:   10,000, 20,000, and 50,000 lb/in.

- Hover with Hover Hold on and off, PHS on and off, and
  heading stabilized and synchronized.

215

- 60- and 90-knot forward flight.

- All LSS modes.

- Variations in key LSS/AFCS parameters.

The following nominal configuration was used for the major part of the analysis.

- Load Weight:  5000 pounds

- Cable Configuration:  50-foot pendants.

- Vertical distance between aircraft center of gravity and load hook:  8 feet

- Cable Stiffness:  10,000 pounds/inch

Several characteristics are not contained in the analytical models.  Cable angle bow due to wind drag is not included, i.e., the cables are assumed to be perfectly straight, regardless of wind and rotor downwash conditions.  Since the LSS has to determine the load's position using the load hook angle, cable bow will produce an incorrect measurement of load position.  Figure 53 shows this load position error as a function of wind strength and load weight.  This indicates that the effect of cable bow can be significant, but should not exceed the position hold and centering objective level for the nominal load weight and cable length.  With the exception of hysteresis, perfect signal quality is assumed in the analytical models.  Signal quality is not anticipated to present a problem.  The second-order analog filters at 60 rps, in combination with the short computer frame time (0.01 seconds), should provide good signal quality.  Gusts, rotor downwash, and ground effect are not included in the models.  However, the responses to wind ramps and sine waves at various frequencies and magnitudes were evaluated.

216

- 50-FT. CABLES WITH 0.5-INCH DIAMETER
- DRAG COEFFICENT = 1.2

ERROR (INCHES)

STEADY WIND (KNOTS)
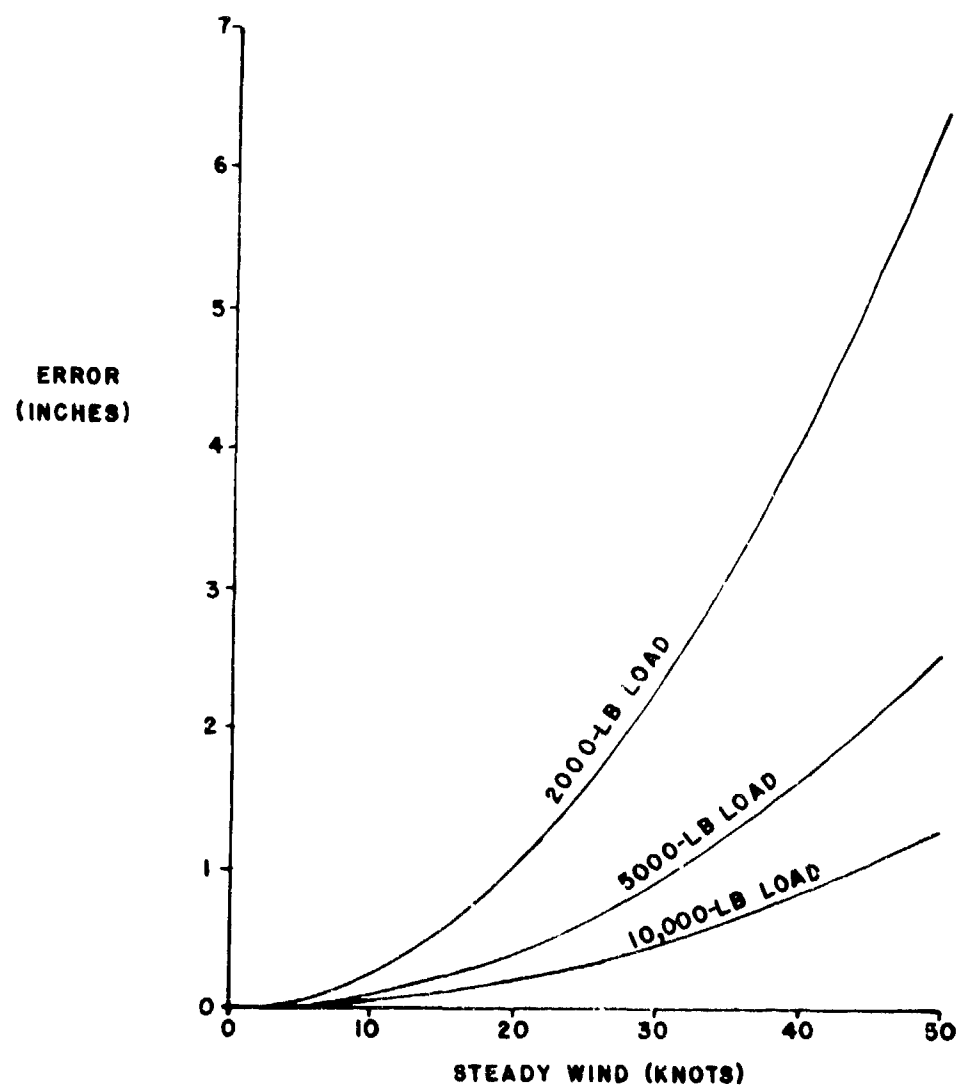
FIGURE 53.
LOAD POSITION ERROR DUE TO CABLE BOW

217

### 2.1.5.3.2   Root Locus Studies

The root locus model was used to study the load and aircraft stability as a function of load configuration and control system parameters.  All LSS/AFCS modes and their inter-relationship were studied.  The basic LSS configuration design and parameter values were determined using this model.  The significant results for each LSS sub-mode are discussed in the following paragraphs.

### Load Damping Mode

Basic root locus plots for each axis in hover with the PHS on are presented in Figures 54-56.  These plots show how the load damping varies as a function of the load damping loop gain and time constant.  The root location for the nominal gain and time constant value is indicated on each plot.  The load frequencies and damping ratios obtained with the nominal configuration are summarized in Table 7.  The load is well damped, particularly with 50-foot cables and with the PHS on. With the LSS off and PHS on, the load roots in hover are as follows:

- Longitudinal:  $\omega = 0.8$ **rps**, $\zeta = 0.01$

- Lateral:  $\omega = 0.8$ **rps**, $\zeta = 0.02$

- Directional:  $\omega = 1.3$ **rps**, $\zeta = 0.01$

Thus the load is only very lightly damped in each axis without the LSS.

The analysis determined that the load damping loop configuration is very dependent upon the AFCS configuration.  The configuration that provides good load damping with the hover hold/PHS mode on is unstable with the basic SCAS.  Consequently, separate loops are used when the PHS is on and off as discussed previously.  The required phase shift in the lateral axis changes drastically as a function of the hover hold/PHS loops as shown in Figure 57.

218
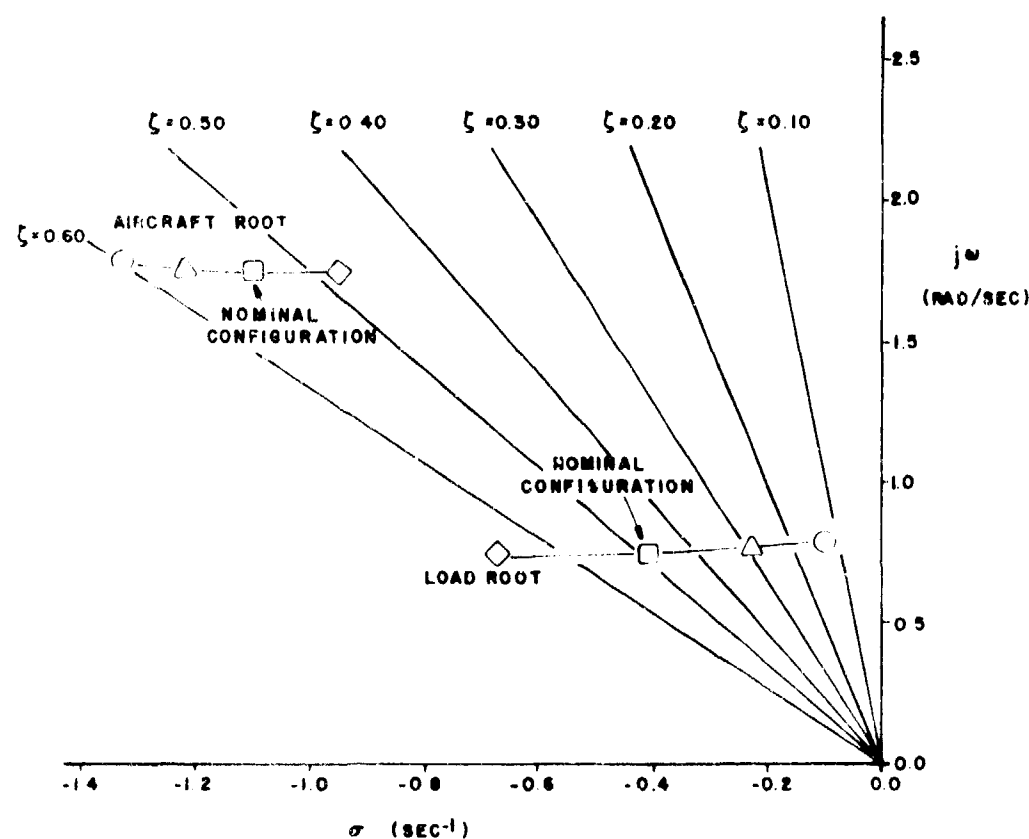
FIGURE 54.
AIRCRAFT AND LOAD LONGITUDINAL DAMPING AS A
FUNCTION OF DAMPING LOOP GAIN

| SYM | KYCA3 | TY2 |
|-----|-------|-----|
| ◯ | 0 09 | 0.4 |
| △ | 0 09 | 0 75 |
| ▢ | 0.09 | 1.5 |
| ◑ | 0.13 | 0.4 |
| ◭ | 0 13 | 0.75 |
| ◧ | 0.13 | 1.5 |
| ● | 0 17 | 0 4 |
| ▲ | 0.17 | 0 75 |
| ■ | 0.17 | 1.5 |

• 5000-LB LOAD
• 50 FT CABLES
• HOVER WITH PHS ON
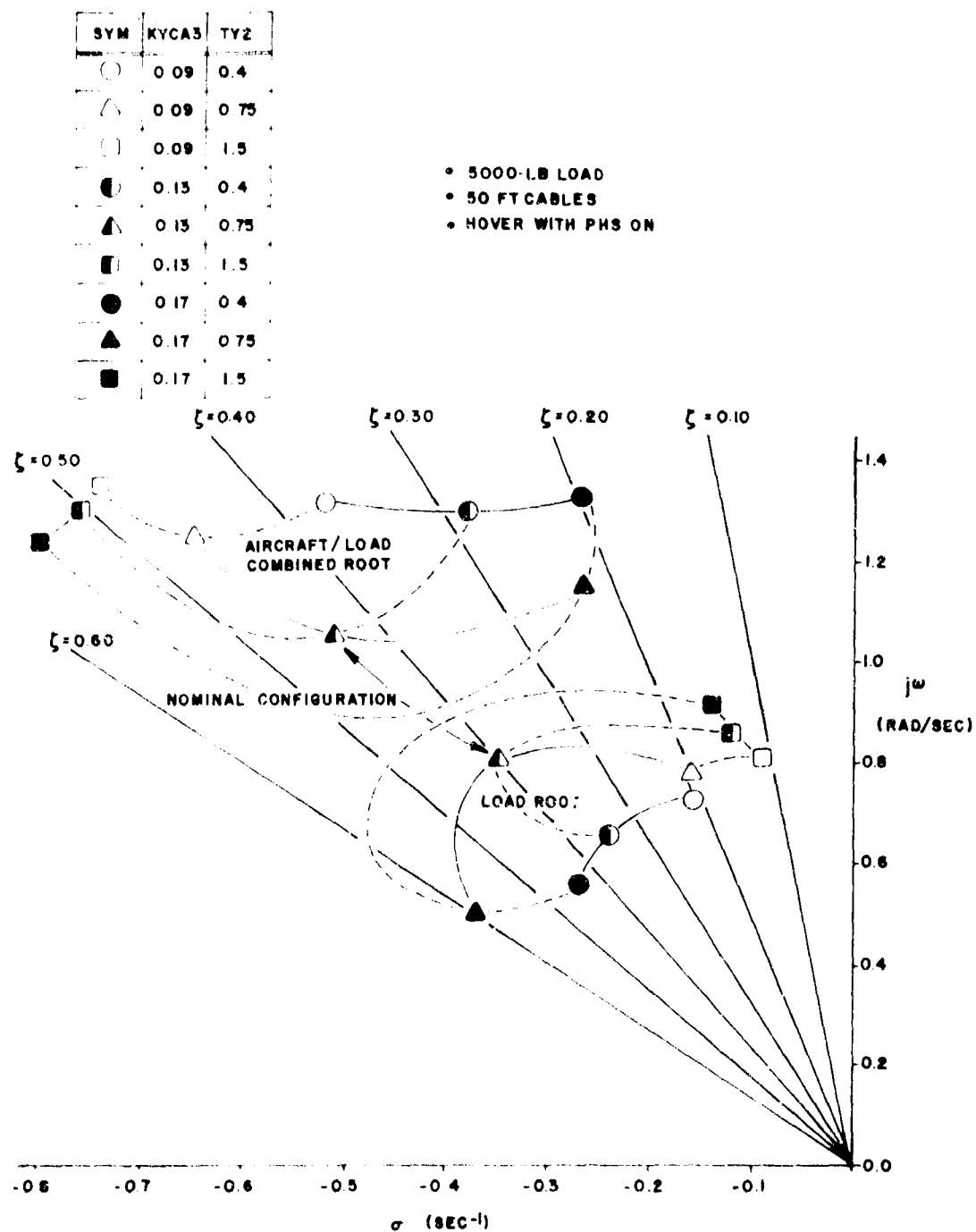
FIGURE 55.
LOAD LATERAL DAMPING AS A FUNCTION OF
DAMPING LOOP GAIN AND TIME CONSTANT

220

| SYM | KNCAI | TNIO |
|-----|-------|------|
| ◜ | 0.175 | 0 025 |
| ◿ | 0.175 | 0 1 |
| ▯ | 0.175 | 0.4 |
| ◐ | 0.262 | 0.025 |
| △ | 0.262 | 0.1 |
| ◧ | 0.262 | 0.4 |
| ◐ | 0 349 | 0.025 |
| ▲ | 0 349 | 0.1 |
| ◧ | 0 349 | 0.4 |
| ● | 0 436 | 0.025 |
| ▲ | 0.436 | 0 1 |
| ■ | 0.436 | 0.4 |

- 5000-LB LOAD
- 50-FT CABLES
- HOVER WITH PHS ON
- HEADING STABILIZED
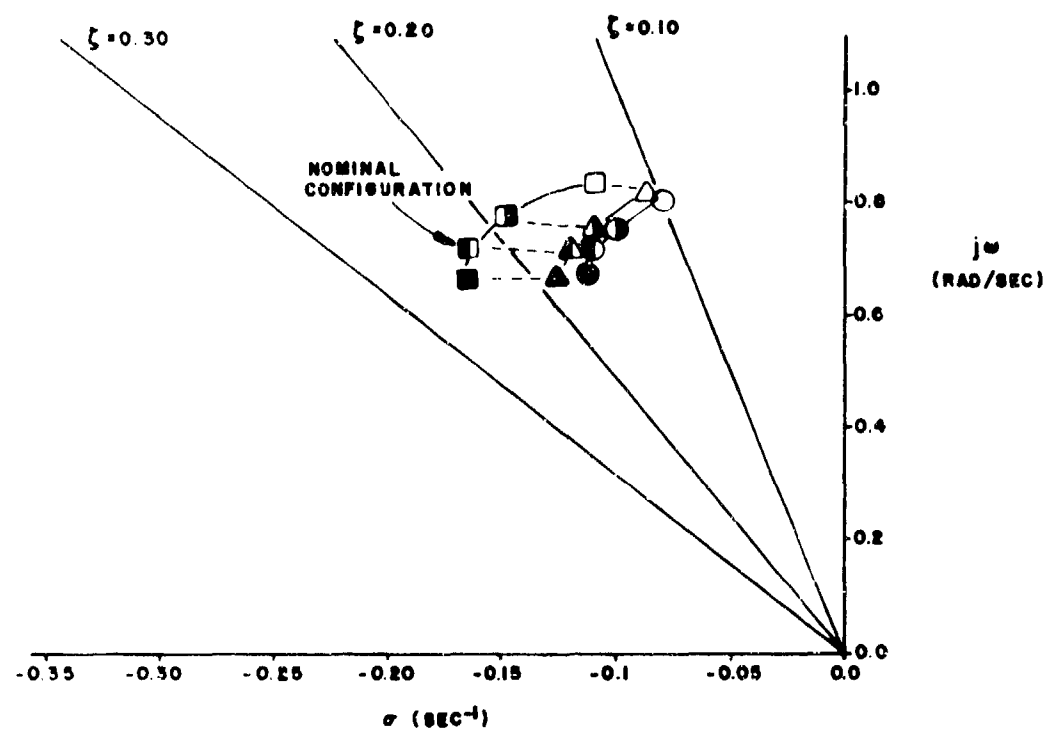
FIGURE 56.
LOAD DIRECTIONAL DAMPING AS A FUNCTION
OF DAMPING LOOP GAIN AND TIME CONSTANT

221

## TABLE 7.
## LOAD FREQUENCY & DAMPING WITH LOAD POSITION
## HOLD MODE ON

|  | LONGITUDINAL | | LATERAL | | DIRECTIONAL | |
|---|---|---|---|---|---|---|
|  | FREQUENCY RAD/SEC | DAMPING RATIO | FREQUENCY RAD/SEC | DAMPING RATIO | FREQUENCY RAD/SEC | DAMPING RATIO |
| **SCAS** | | | | | | |
| 50-FT CABLES | 1.2 | 0.21 | 0.8 | 0.17 | 0.7 | 0.23 |
| 20-FT CABLES | 2.0 | 0.12 | 1.1 | 0.18 | — | — |
| **HOVER HOLD ON** | | | | | | |
| 50-FT CABLES | 1.0 | 0.32 | 0.9 | 0.33 | 0.7 | 0.22 |
| 20-FT CABLES | 1.7 | 0.22 | 1.3 | 0.17 | — | — |
| **PHS ON** | | | | | | |
| 50-FT CABLES | 0.8 | 0.49 | 0.9 | 0.40 | 0.7 | 0.22 |
| 20-FT CABLES | 1.9 | 0.28 | 1.2 | 0.26 | — | — |

222
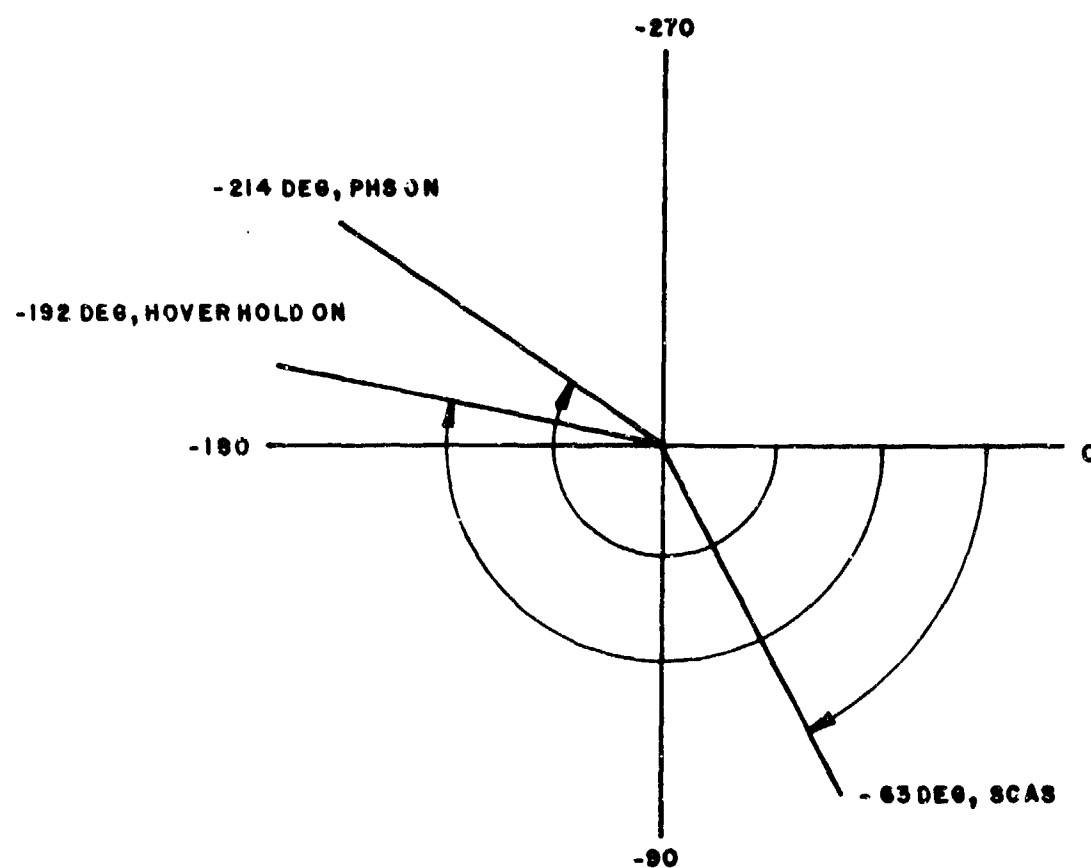
FIGURE 57.
LATERAL LOAD DAMPING LOOP PHASE ANGLE

The load damping configuration requirement varies substantially with cable length, particularly in the lateral axis. The following parameters have to vary with cable length to obtain good load damping.

| PARAMETER | 20-FT CABLES | 50-FT CABLES |
|---|---|---|
| KXCA | 1.0 DEG/DEG | 1.5 DEG/DEG |
| TY4 | 1.5 SEC | 2.5 SEC |
| KYCA2 | 0.07 IN./DEG | 0.175 IN./DEG |
| TY3 | 0.1 SEC | 0.25 SEC |
| KYCA3 | 0.031 IN./DEG | 0.13 IN./DEG |
| TY2 | 0.25 SEC | 0.75 SEC |

These changes were made to obtain the results summarized in Table 7. Without these changes, the load becomes very lightly damped, if not unstable, with 20-foot cables. The directional load damping with 20-foot inverted-V cables was analyzed using the CSMP and total force simulation models and will be discussed later.

The load damping was evaluated in 60-knot forward flight and was found to be adequately damped with the basic SCAS load damping loops. The results indicate that the longitudinal damping can be further increased by increasing the phase advance.

In general, the load damping is very sensitive to gain and phase changes. However, with a few exceptions, the aircraft roots are not significantly affected by the LSS. The most significant effects of LSS/AFCS parameter variations are as follows:

● With the hover hold/PHS mode off, the longitudinal load damping increases when the phase advance is increased.

224

- With the Hover Hold/PHS mode on, the longitudinal load damping increases when the gain is increased. However, the aircraft damping decreases with increased gain, as seen in Figure 54.

- The longitudinal load damping gain has to decrease as the hover hold/PHS gains decrease.

- In forward flight, the longitudinal load damping has a knee when the gain is 0.25 deg/deg., i.e., the damping decreases if the gain is either increased or decreased.

- With the Hover Hold/PHS mode off, the lateral load damping increases as the gain magnitude increases. However, increasing the gain further aggravates a switching problem which is discussed later.

- The lateral load damping decreases sharply if either the gain, time constant, or hover hold/PHS gains are increased or decreased from their nominal values.

- The lateral load damping phase lag has to decrease if the hover hold/PHS gains are decreased.

- The directional load damping can be increased with increased phase lag as seen in Figure 56. However, this decreases the aircraft stability.

- The directional load damping decreases by approximately 50 percent with aircraft heading feedback synchronized.

There is negligible coupling between the axes as the load, cable, and LSS parameters are varied. The load damping remains good as the following parameters vary over the range described previously.

- Load weight

- Vertical distance between the aircraft center of gravity and load hook.

## Load Position Hold Mode

Basic root locus plots for each axis with the load position hold mode on are shown in Figures 58-60. The root location for the nominal parameter values is indicated on each plot. The load frequencies and damping ratios obtained with the nominal configuration are summarized in Table 8. While the load damping with 50-foot cables is reduced by the load position hold mode, the load is still well damped. In the position hold mode, the load damping configuration requirement varies substantially with cable length, as it does with the position hold mode off. The following parameters have to change with cable length to obtain the results shown in Table 8.

| PARAMETER | 20-FT CABLES | 50-FT CABLES |
|-----------|--------------|--------------|
| TXL1 | 1.50 | 2.50 |
| TXL2 | 1.80 | 2.10 |
| TYL1 | 0.52 | 2.10 |
| TYL2 | 0.25 | 0.41 |

Directional load position hold with the 20-foot inverted-V cables will be discussed later.

The most significant result from the stability analysis of the load position hold mode is that the load damping increases as the load position hold gain decreases at the load frequency. Further, the gain has to decrease when the hover hold/PHS or load damping loop gains decrease.

## Load-Centering Mode

During the load-centering mode operation, the load stability is not of concern since the load is sitting on the ground. The aircraft longitudinal and directional stability is good; it is similar to that without the cables attached. No frequency shaping is required except in the lateral axis which has a lag in the position term. The root locus in Figure 61 shows how the aircraft lateral roots vary in the load centering mode as a function of gain and lag time constant. It can be

| SYM | TXL1 | TXL2 |
|-----|------|------|
| ○ | 1.5 | 1.8 |
| △ | 2.5 | 2.1 |
| □ | 3.5 | 2.4 |
| ◇ | 4.5 | 2.7 |

- 5000-LB LOAD
- 50-FT CABLES
- LOAD POSITION HOLD ON
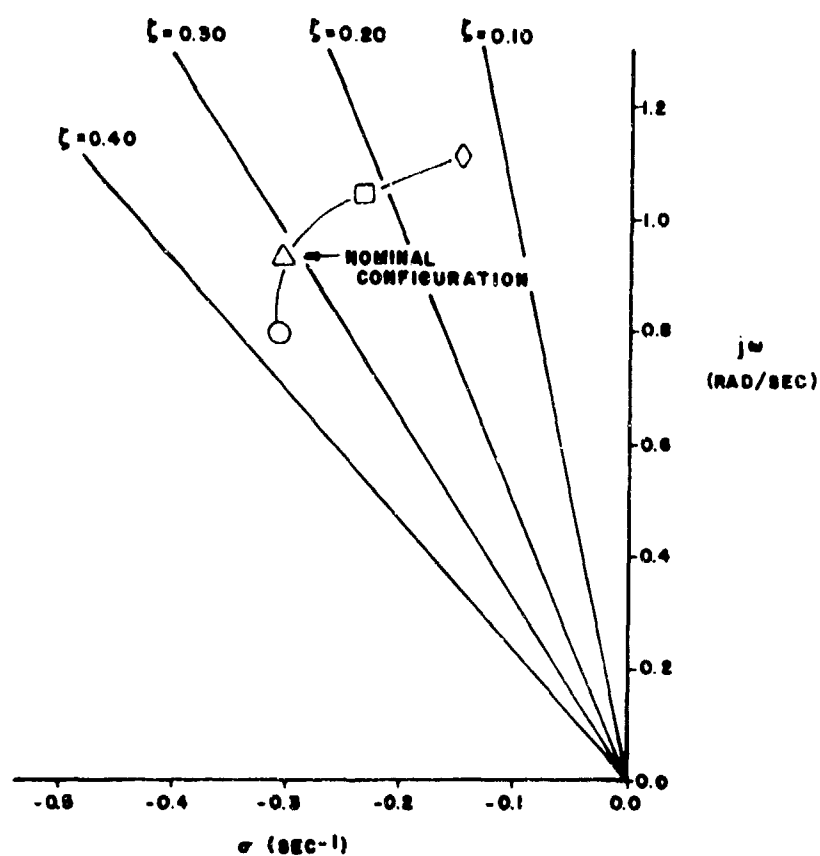
FIGURE 58.

LOAD LONGITUDINAL DAMPING WITH LOAD
POSITION HOLD MODE ON

227
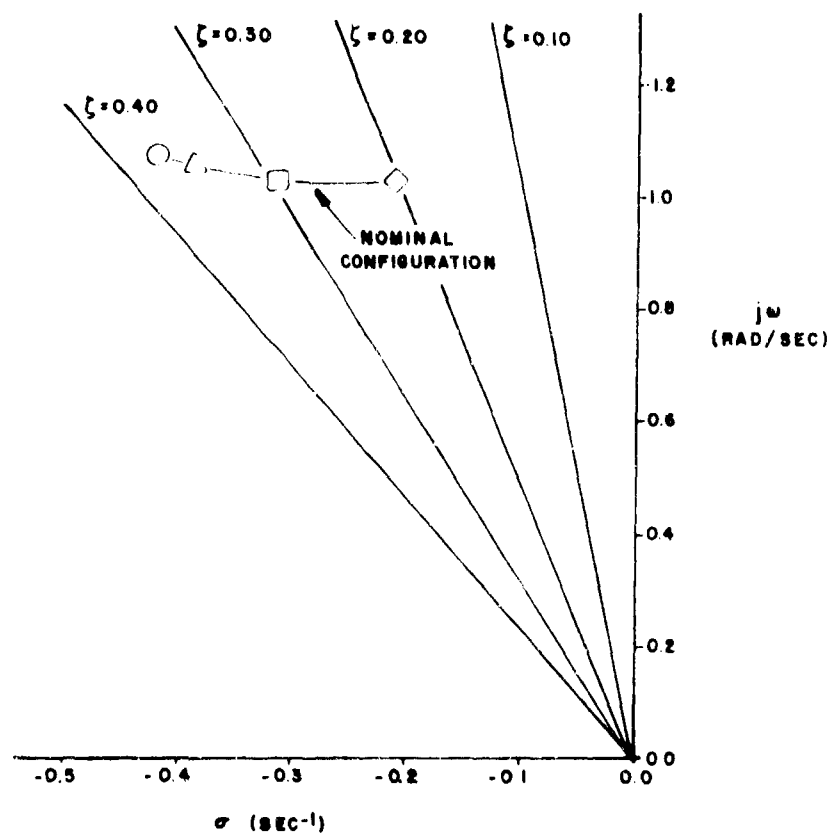
FIGURE 59.
LOAD LATERAL DAMPING WITH LOAD
POSITION HOLD MODE ON

228
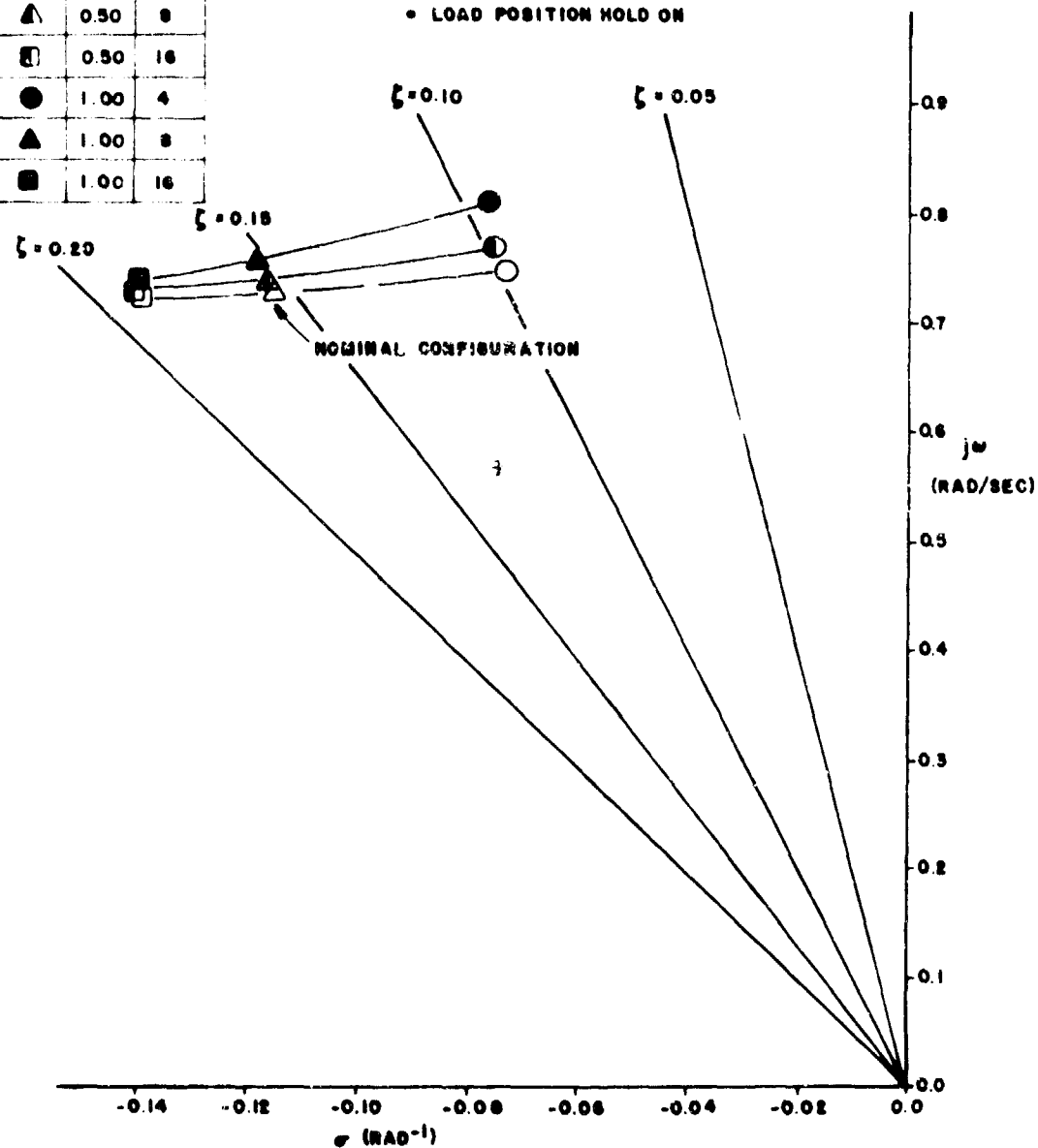
FIGURE 60.
LOAD DIRECTIONAL DAMPING WITH POSITION
HOLD MODE ON

229

## TABLE 8.
## LOAD FREQUENCY & DAMPING WITH LOAD POSITION HOLD MODE ON

| | LONGITUDINAL | | LATERAL | | DIRECTIONAL | |
|---|---|---|---|---|---|---|
| | FREQUENCY RAD/SEC | DAMPING RATIO | FREQUENCY RAD/SEC | DAMPING RATIO | FREQUENCY RAD/SEC | DAMPING RATIO |
| 50-FT CABLES | 1.0 | 0.31 | 1.1 | 0.25 | 0.7 | 0.16 |
| 20-FT CABLES | 17 | 0.21 | 1.2 | 0.28 | — | — |
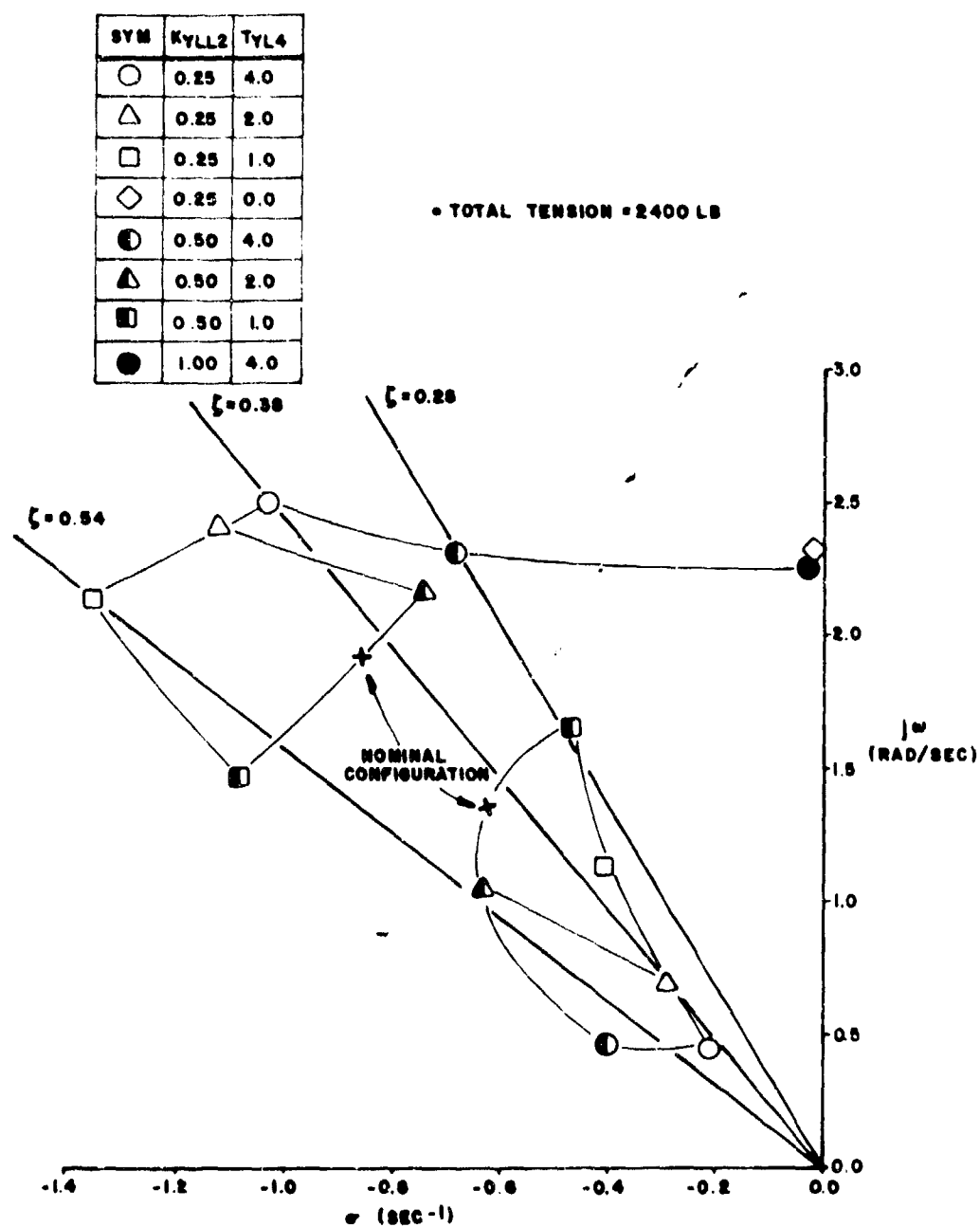
FIGURE 61.
AIRCRAFT LATERAL STABILITY WITH
LOAD CENTERING MODE ON

231

seen that the aircraft is somewhat underdamped laterally with
the nominal configuration. However, the transient responses
that will be discussed in the following sections show good
lateral centering performance.

The aircraft is well damped vertically in the centering mode
with the cables taut and the tension control loop operating.
The tension control performance will be discussed further in
the following sections.

### 2.1.5.3.3 CSMP Studies

The CSMP model was used to study system transient responses
and performance in meeting the LSS objectives. Although
it is a small perturbation model, it is valid for most LSS
considerations since the aircraft and load excursions are
small for practically all aspects of LSS operation. All modes
of LSS/AFCS operation were studied for the nominal 50-foot
cables, 5000-pound load configuration.

The high degree of load damping obtained in each axis can be
seen in Figures 62-64. These transient responses were
obtained by applying pulses at the pilot's controls with
the PHS and LSS on. These results, along with the CSMP
results for the other modes of LSS/AFCS operation, closely
match the root locus analysis predictions.

Load damping in the directional axis with 20-foot inverted-V
cables was evaluated using the CSMP model. The pendulum
equation of motion was modified to include a large restoring
moment for small directional load angles. The normal pendulum
restoring moment is still present when the load angle becomes
large enough to make opposite cable legs become slack. The
total restoring moment used in the model is shown in Figure
65. The results show that the load should be well-behaved
directionally with the inverted-V suspension system. The
peak directional excursion relative to the aircraft is only
0.2 degree when a 1-inch pedal pulse is applied in hover
or forward flight. A very small directional load limit cycle
of ±0.04 degrees at 2 hertz persists with the inverted-V
suspension.

232
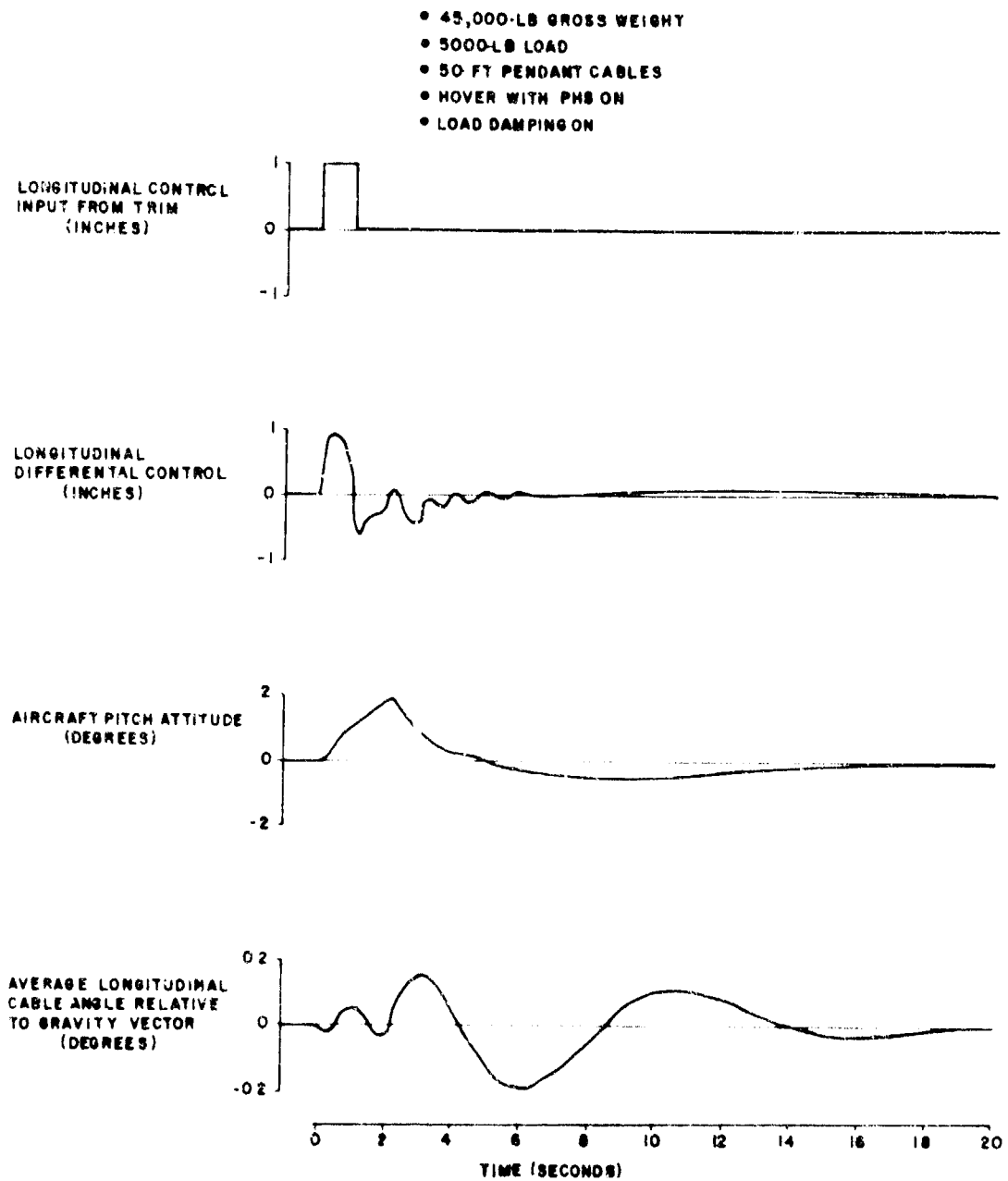
FIGURE 62.
LOAD LONGITUDINAL DAMPING-CSMP MODEL

233

- 45,000-LB GROSS WEIGHT
- 5000 LB LOAD
- 50-FT PENDANT CABLES
- HOVER WITH PHS ON
- LOAD DAMPING ON

LATERAL COCKPIT CONTROL (INCHES)

LATERAL DIFFERENTIAL CONTROL (INCHES)

AIRCRAFT ROLL ATTITUDE (DEGREES)

AVERAGE LATERAL CABLE ANGLE RELATIVE TO GRAVITY VECTOR (DEGREES)

TIME (SECONDS)
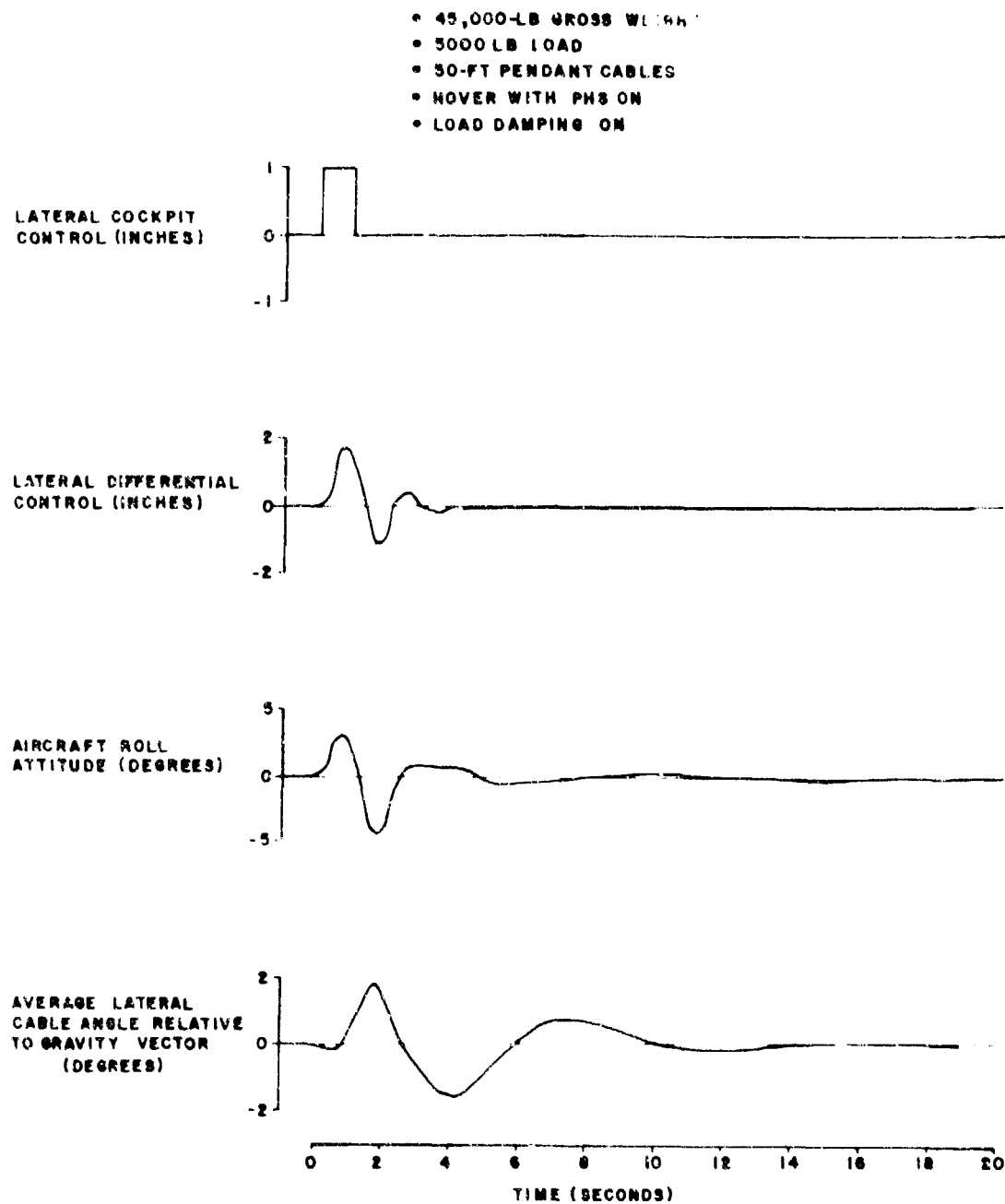
FIGURE 63.
LOAD LATERAL DAMPING - CSMP MODEL

234

- 45,000-LB GROSS WEIGHT
- 5000-LB LOAD
- 50-FT PENDANT CABLES
- HOVER WITH PHS ON
- LOAD DAMPING ON
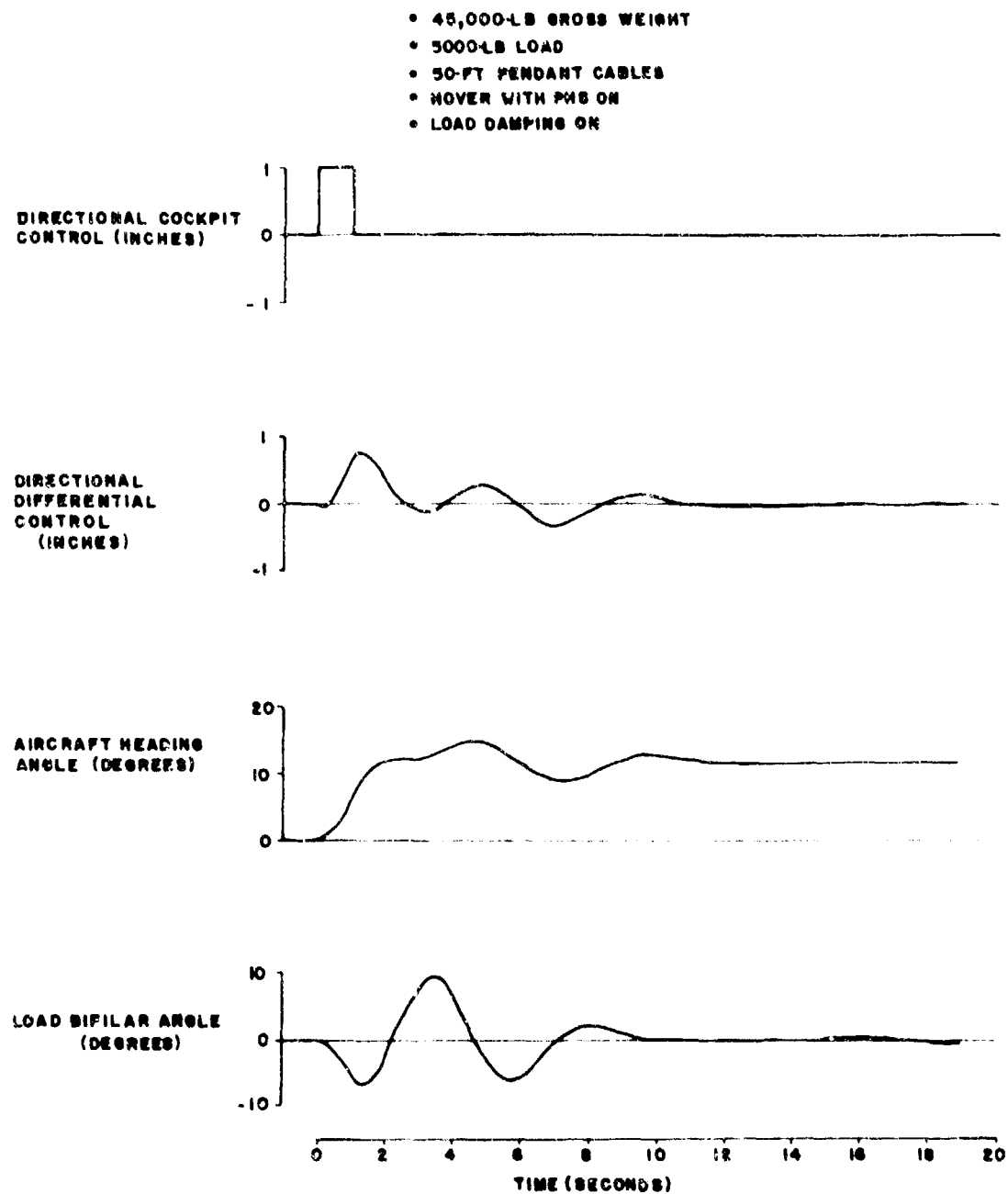
FIGURE 64.
LOAD DIRECTIONAL DAMPING - CSMP MODEL

235
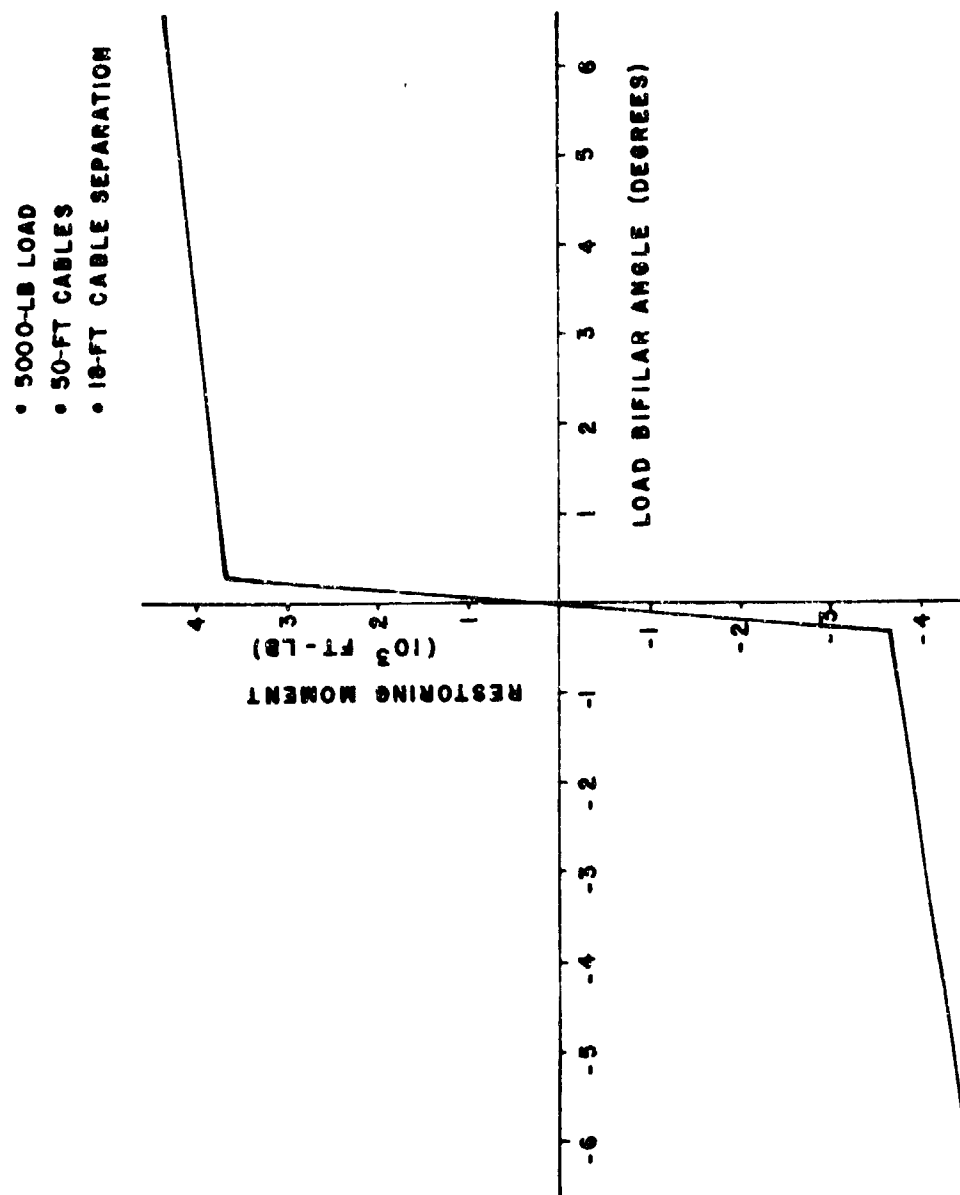
FIGURE 65.
LOAD DIRECTIONAL RESTORING MOMENT –
INVERTED VEE SUSPENSION

236

Wind gusts, rotor downwash, and ground effect were not modeled for the LSS analysis or simulation. However, the aircraft and load response to wind ramps and sinusoidals was evaluated. In Figure 66, the load longitudinal excursion relative to the ground due to a 10 fps headwind ramp is shown. Four cases are included to illustrate the effect of the load damping and position hold loops. The load motion is well damped with the load damping mode on. With the load position hold loop on, the load peak excursion is 0.27 foot and the load returns to its initial position. The effect of load weight and cable length on load longitudinal motion is shown in Figure 67. In Figure 68, the load and aircraft are subjected to a 20 fps peak-to-peak longitudinal sinusoidal wind with a frequency of 0.5 rps. The peak-to-peak load excursion is 0.44 foot. The load lateral response to a 10 fps cross-wind ramp is shown in Figure 69 where the peak load excursion is 0.96 foot.

The effect of cable angle sensing hysteresis on LSS performance was investigated using the CSMP model and found to be significant for hysteresis angles in the order of $\pm 0.1$ degree or greater. The transient responses in Figures 70-71 illustrate this effect for various magnitudes of hysteresis angle.

In Figure 70, a 10 fps headwind ramp is applied to the aircraft and load. The resulting load longitudinal excursion and damping with perfect sensing is compared to that with different magnitudes of sensing hysteresis. With perfect sensing, the load returns quickly to its initial position in a very well-damped manner. If the hysteresis band is as large as $\pm 0.46$ degree, the load stability deteriorates to neutral damping and the load position cannot be held within a band of $\pm 0.4$ foot. The lateral sensing hysteresis creates an aircraft roll attitude limit cycle as seen in Figure 71. With a hysteresis angle of $\pm 0.11$ degree, the roll attitude limit cycle level is approximately doubled. The degradation in lateral load damping is insignificant compared to the roll attitude limit cycle that results. The Teflon/steel load hook bearing used in the 347 demonstrator is theoretically estimated to have a longitudinal hysteresis angle between $\pm 0.04$ and $\pm 0.09$ degree and a lateral hysteresis angle between $\pm 0.03$ and $\pm 0.07$ degree. Originally, a bronze/steel bearing which would have produced a hysteresis band approximately three times as large was planned to be used.
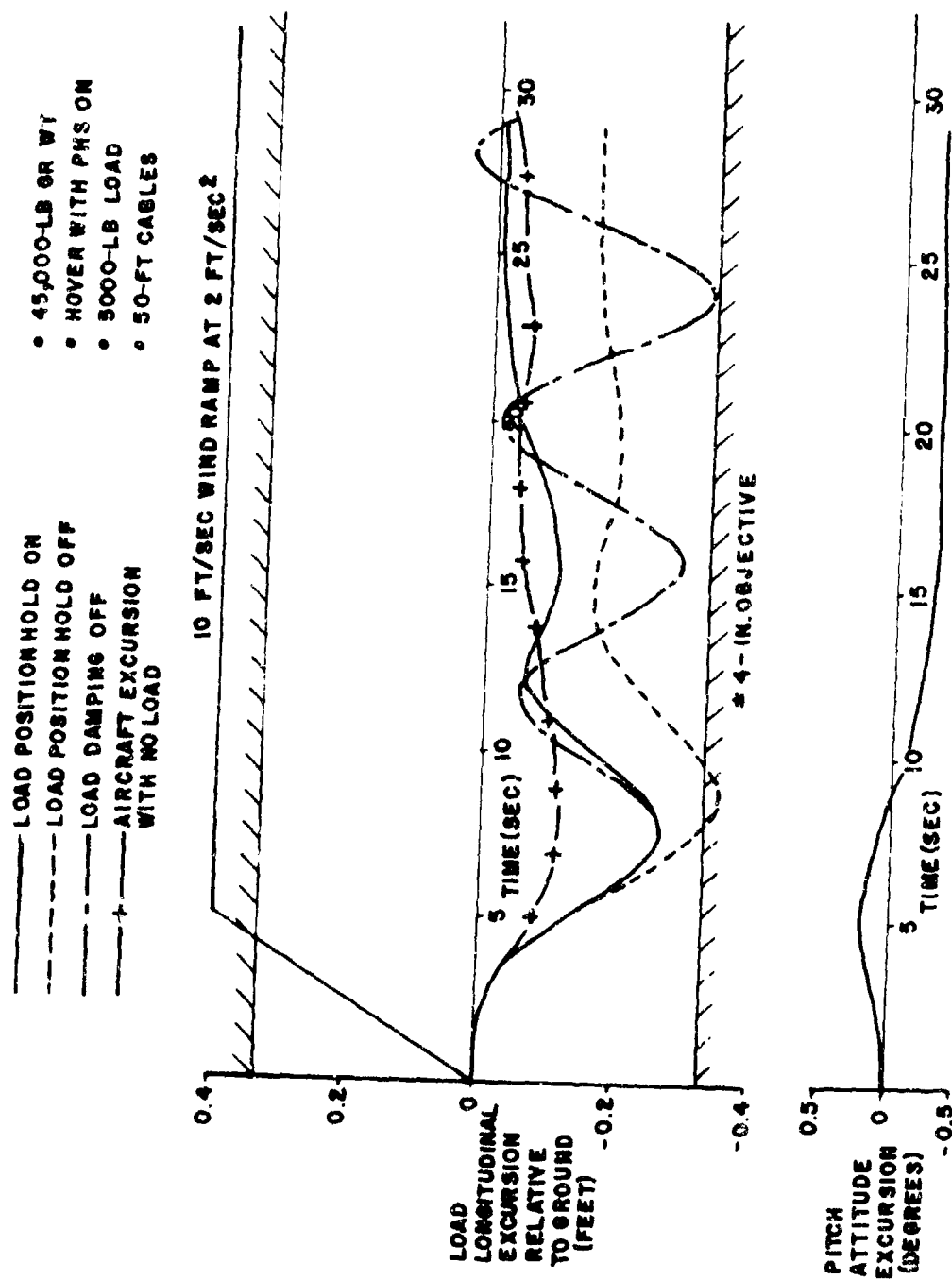
FIGURE 66.

AIRCRAFT PITCH ATTITUDE & LOAD LONGITUDINAL EXCURSION IN WIND RAMP

238
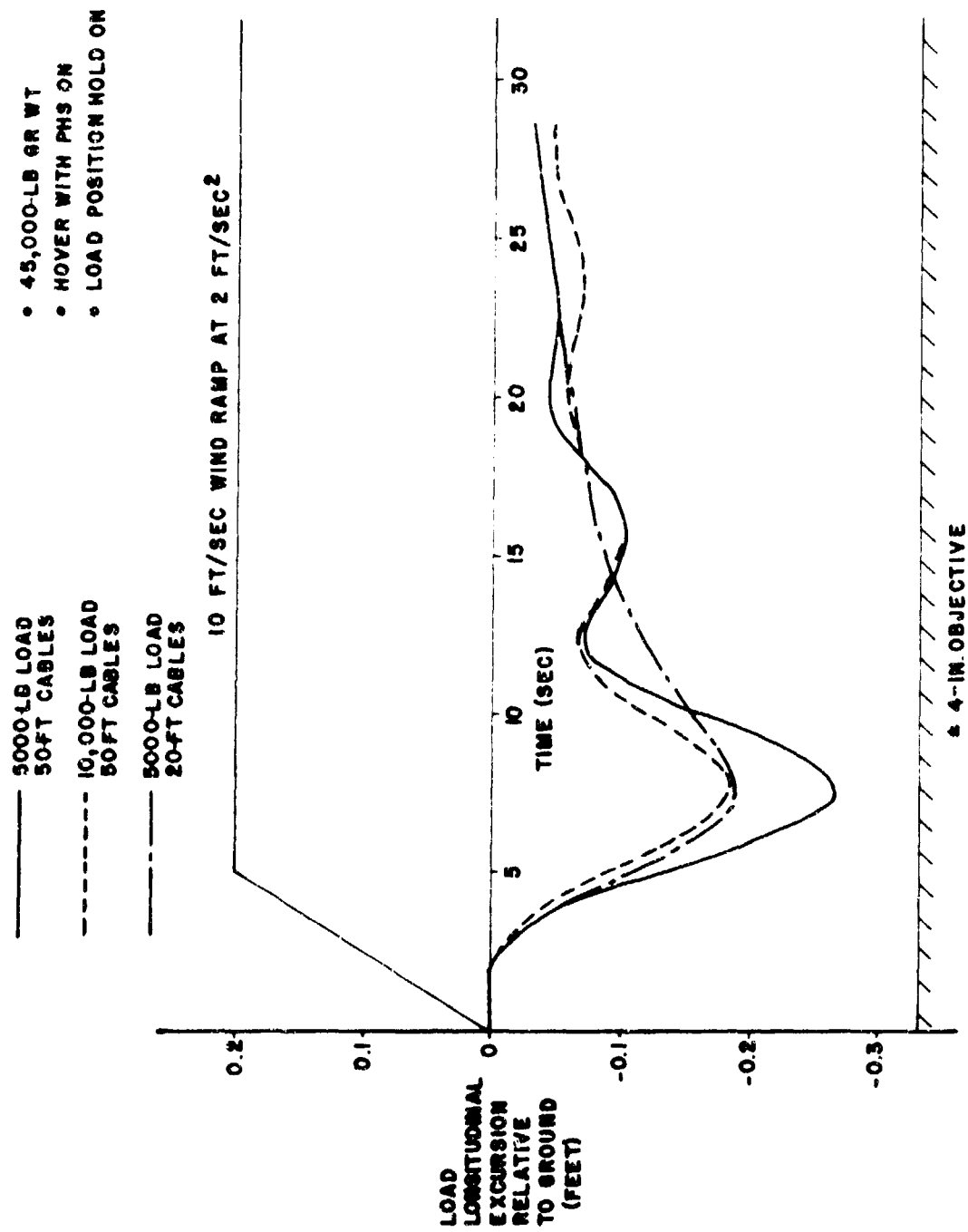
FIGURE 67.

EFFECT OF LOAD WEIGHT AND CABLE LENGTH ON LONGITUDINAL LOAD MOTION
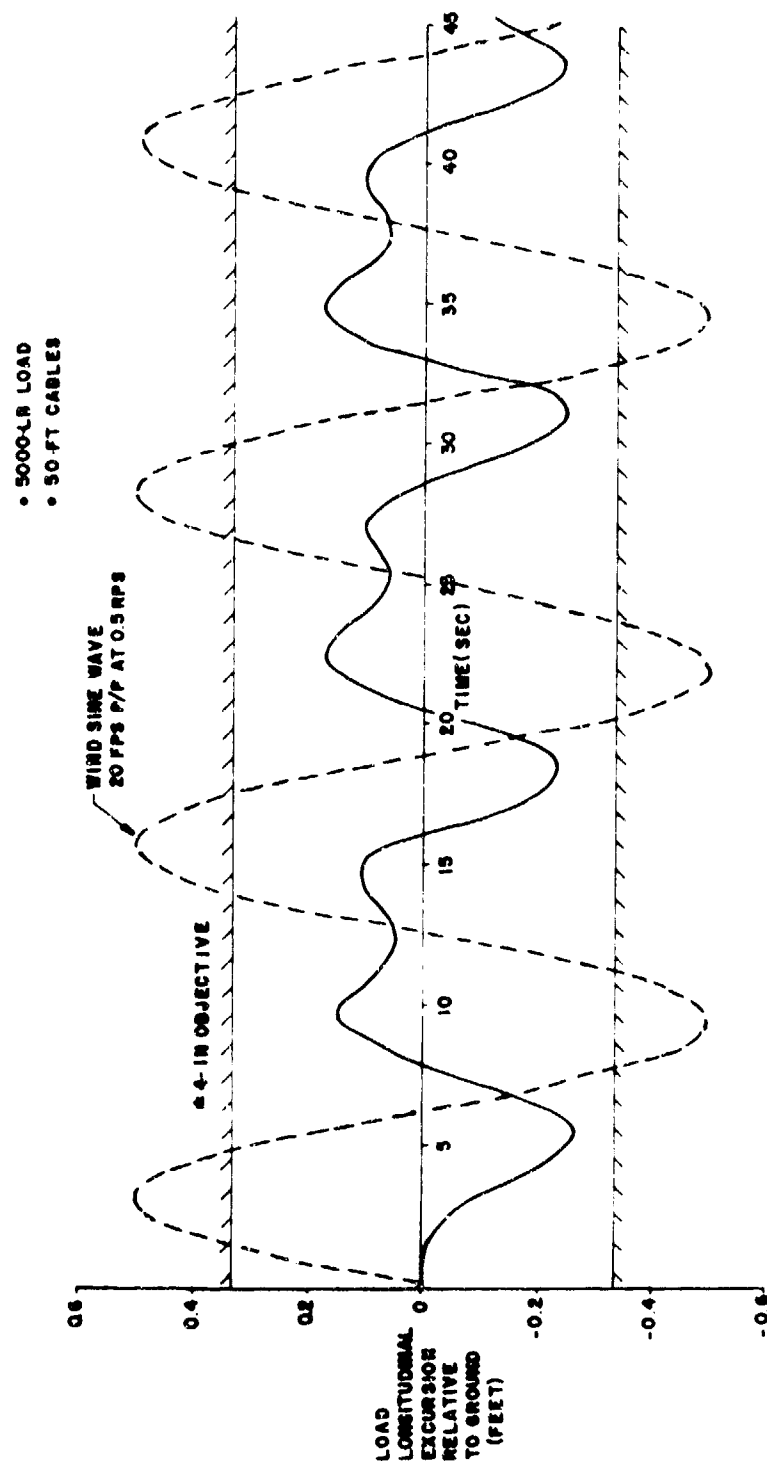
FIGURE 68
LOAD LONGITUDINAL EXCURSION IN SINUSOIDAL WIND

240

- 5000-LB LOAD
- 30-FT CABLES
- HOVER WITH PHS ON
- LOAD POSITION HOLD ON
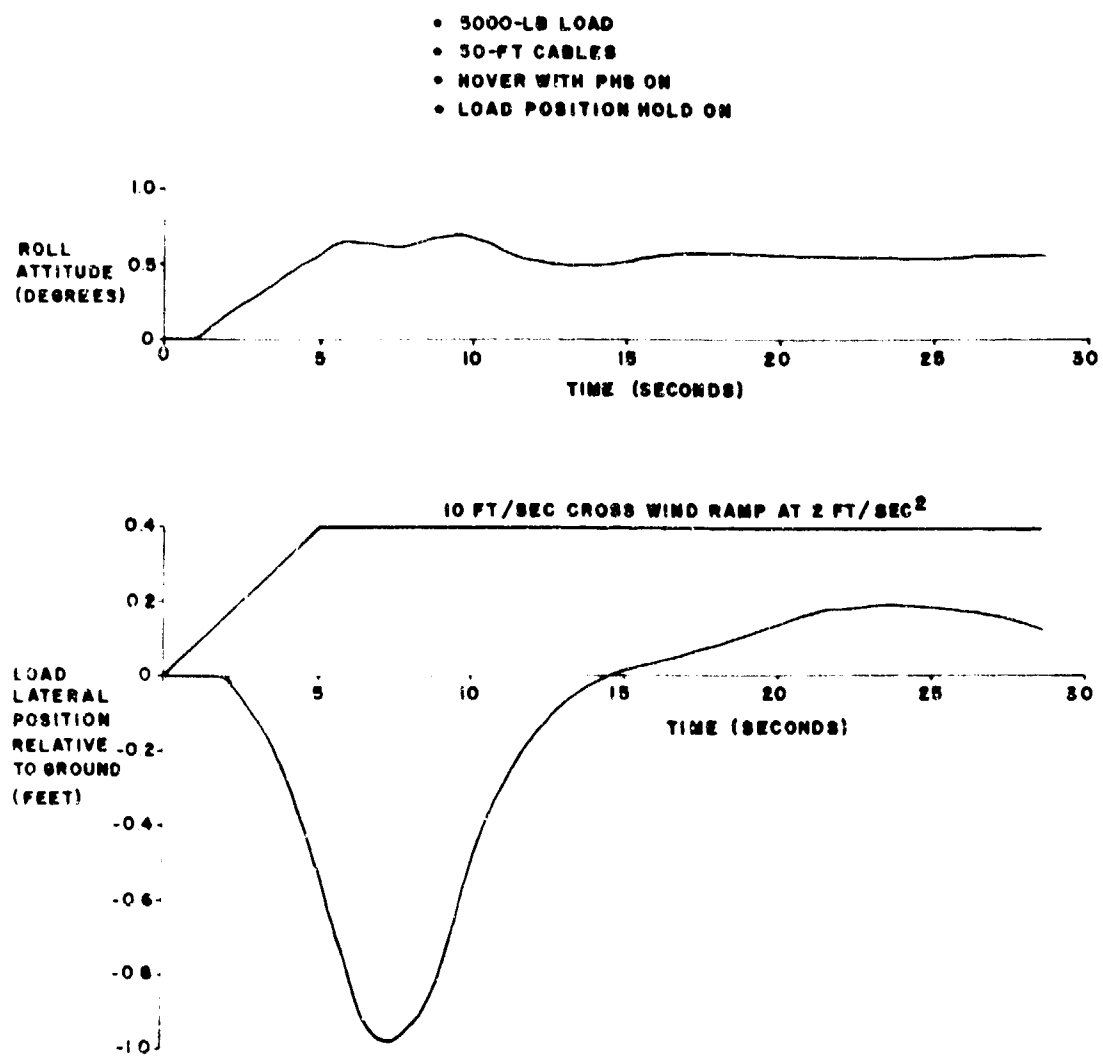
FIGURE 69.
AIRCRAFT ROLL ATTITUDE & LOAD LATERAL
EXCURSION IN WIND RAMP
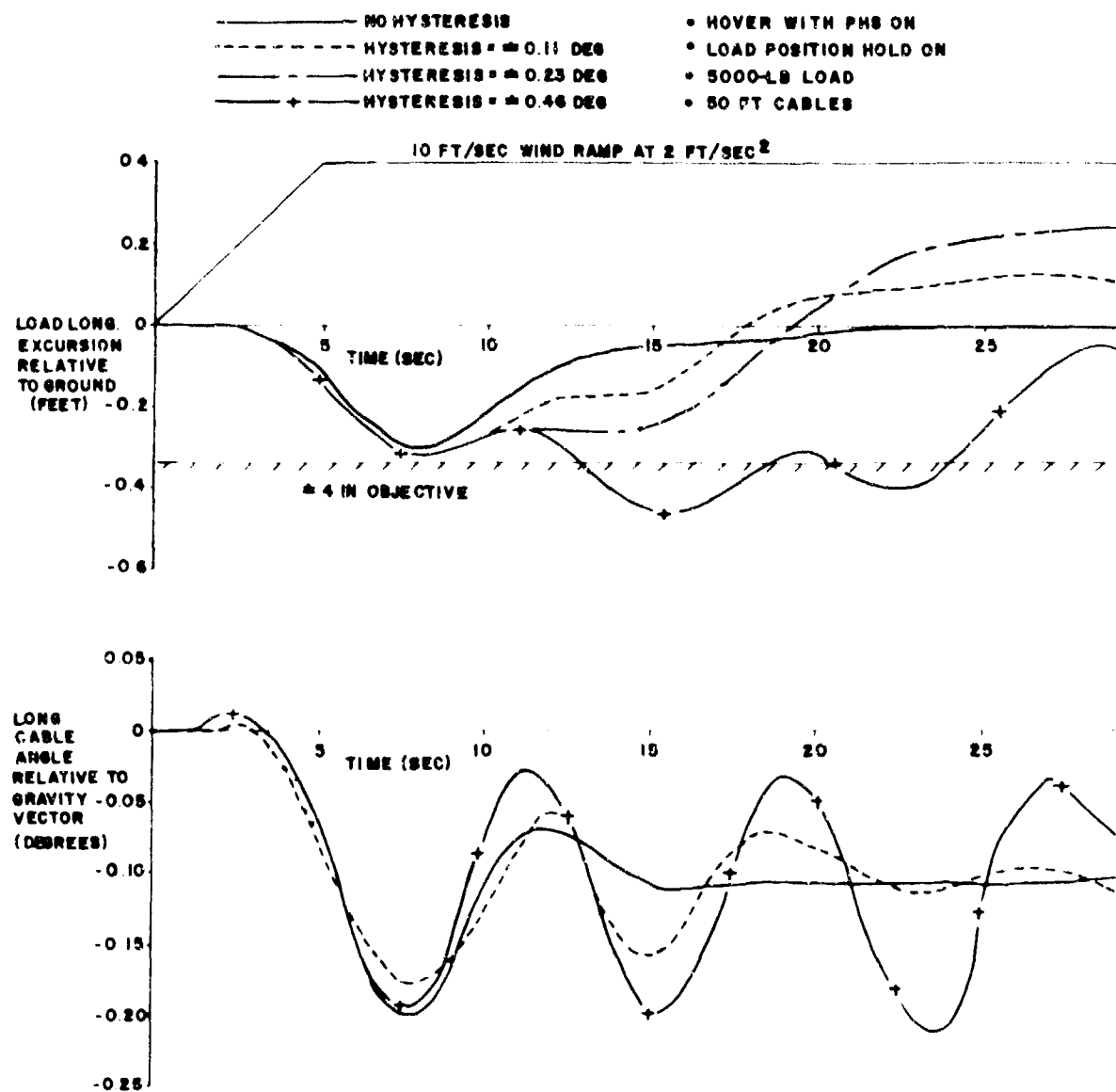
FIGURE 70.
LOAD LONGITUDINAL EXCURSION AND DAMPING AS A
FUNCTION OF SENSING HYSTERESIS
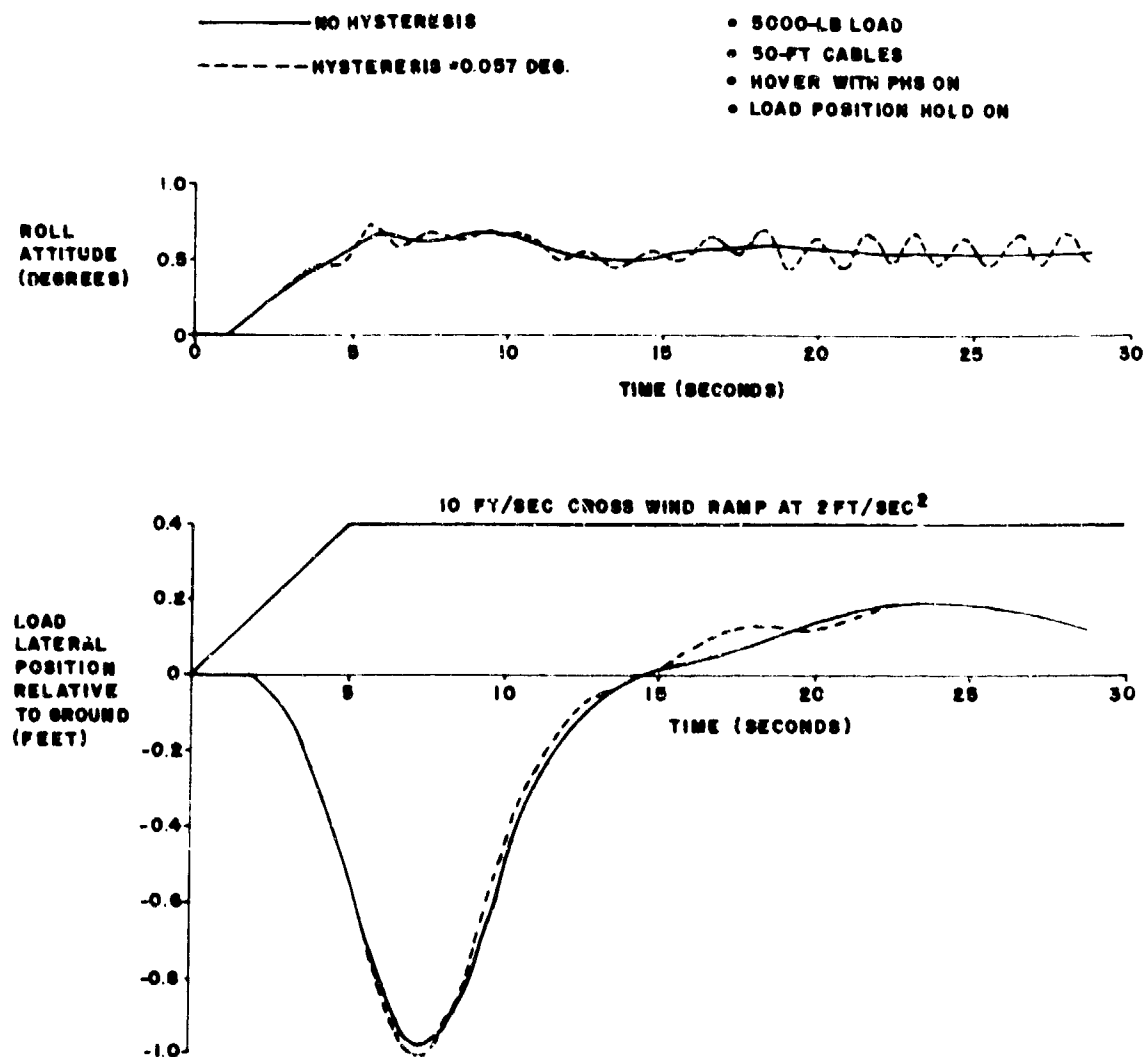
FIGURE 71.
AIRCRAFT ROLL ATTITUDE & LOAD LATERAL EXCURSION
AS A FUNCTION OF SENSING HYSTERESIS

243

The load-centering mode operation was tested with the CSMP model. In Figure 72, the forward and aft cable tensions are initially zero and 600 pounds, respectively. The LSS is switched on and both tensions are automatically increased to approximately 1200 pounds and held at that value. When the smallest tension exceeds 800 pounds, the LSS automatically centers the aircraft over the load longitudinally, laterally, and directionally, as shown in Figure 73. In this case, the aircraft was initially misaligned 5 feet longitudinally, 3 feet laterally, and 8 degrees directionally. The aircraft is centered (under ideal conditions) within a 2-inch and 1-degree tolerance within 7 seconds in a smooth, well-damped manner.

2.1.5.3.4 Hybrid Simulation

The hybrid total force simulation was used to study overall system performance, including logic, and to verify the root locus/CSMP results. All modes of LSS/AFCS operation were evaluated,using pulse, wind ramp, and LCC controller inputs.

While the simulation study concentrated on the nominal load/cable configuration, the responses for a 10,000-pound load and for 20-foot cables were verified.

The responses to pilot pulses are shown in Figures 74-82 for hover and 60 knot flight. The load damping improvement afforded by the LSS can be readily seen for each axis. The aircraft attitude excursions required to damp the load are very small. Basic SCAS, hover hold, and PHS cases are shown for the longitudinal and lateral axes in hover. In Figures 83-84, 10 fps headwind and crosswind ramps are applied to the aircraft and load. The load position hold mode returns the load to its original position within 15 seconds. Notice that the aircraft is displaced from its initial position in order to restore the load's position. Maximum longitudinal and lateral LCC step inputs are applied in Figures 85-86. The load excursions caused by these inputs are damped out quickly by the LSS, whereas the damping would be less than 5% critical if the LSS were off. The value of the load damping can be seen in Figure 87 where the load is repositioned through a distance of 20 feet using the LCC controller and a scope display of the load's position. With the LSS on, the load

- 5000-LB LOAD SITTING ON GROUND
- CABLE STIFFNESS= 10,000 LB/FT
- PHS ON
- LSS SWITCHED ON AT ZERO TIME
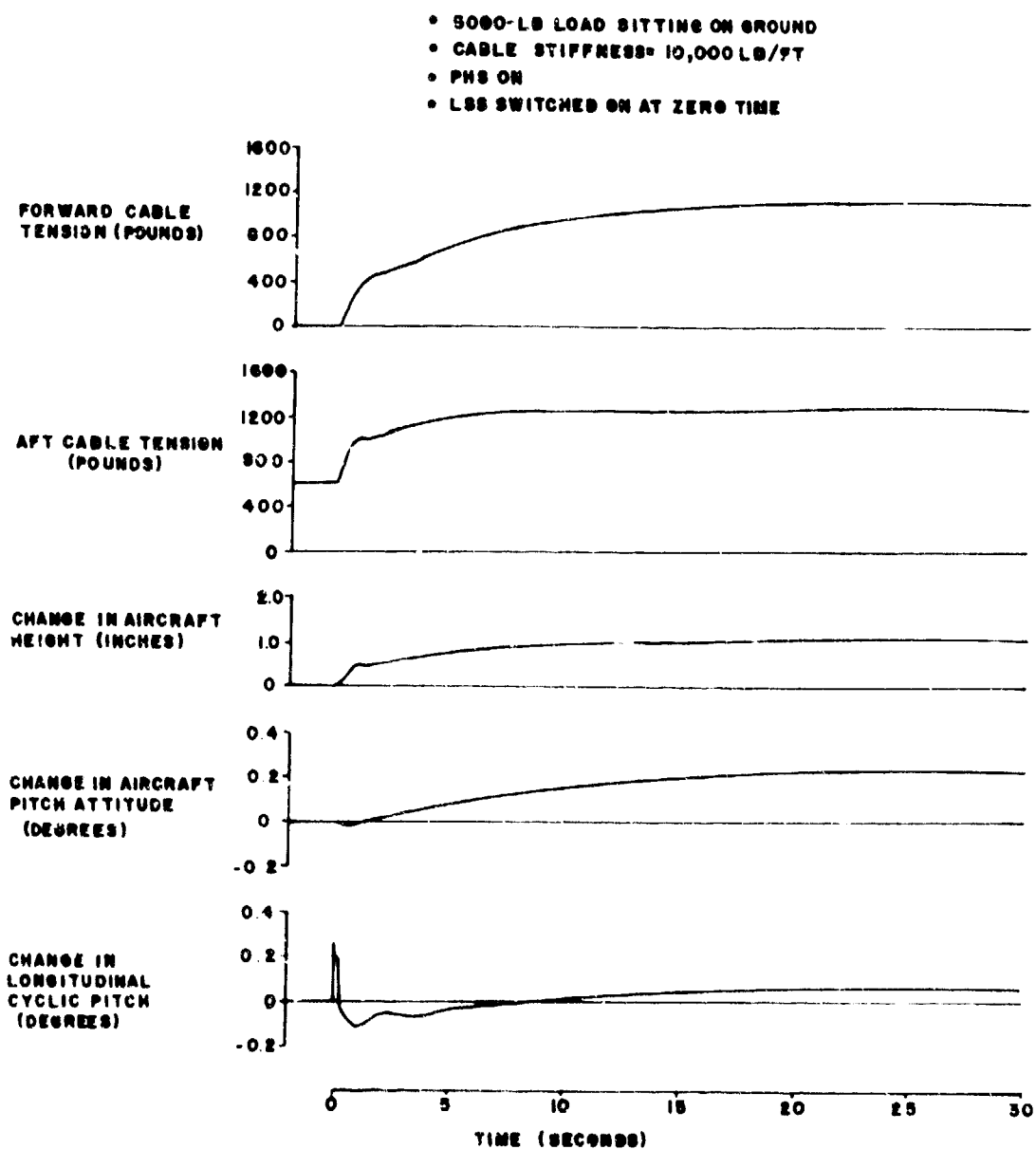
FIGURE 72.
CABLE TENSION CONTROL

245
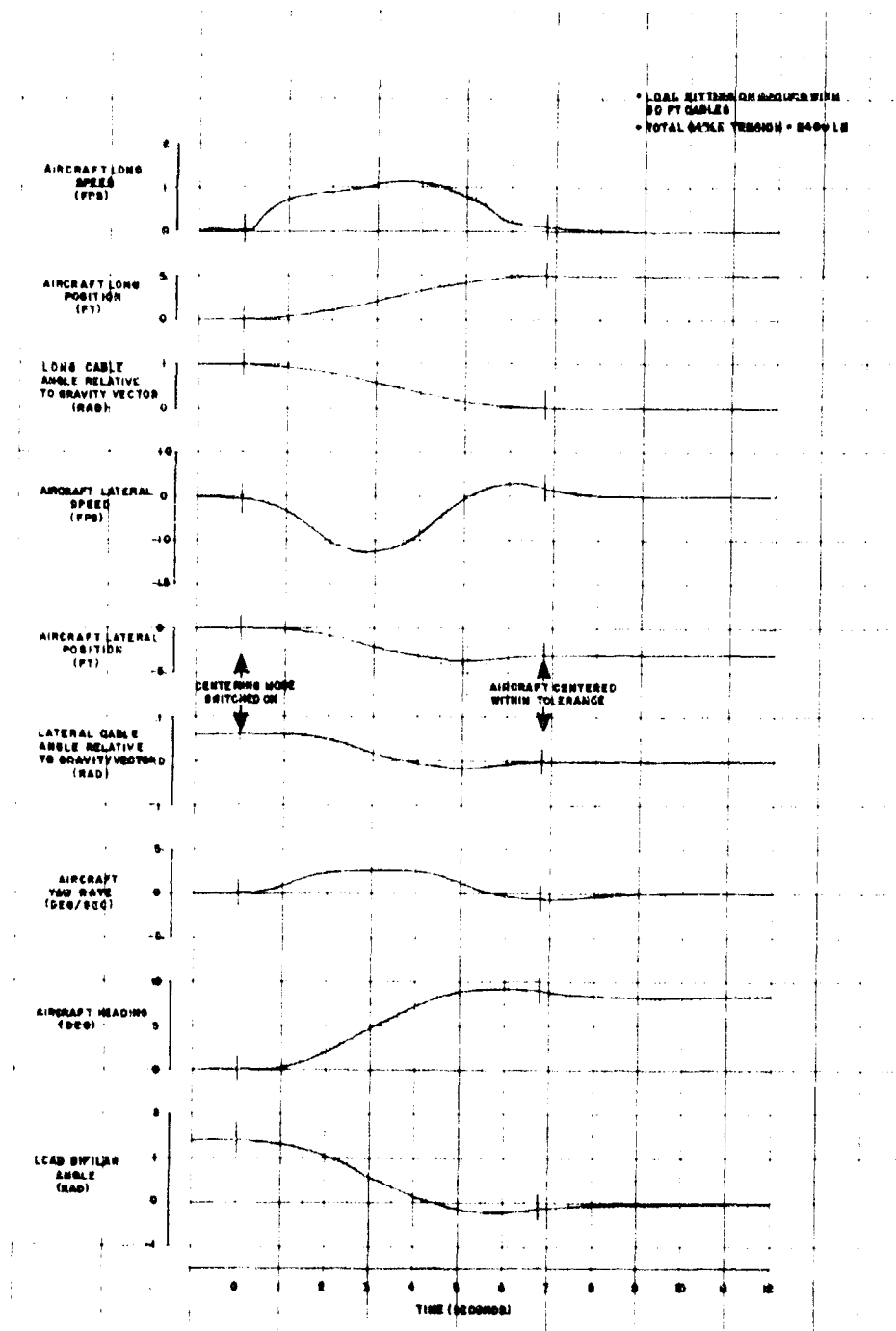
FIGURE 73  AIRCRAFT/LOAD CENTERING

246
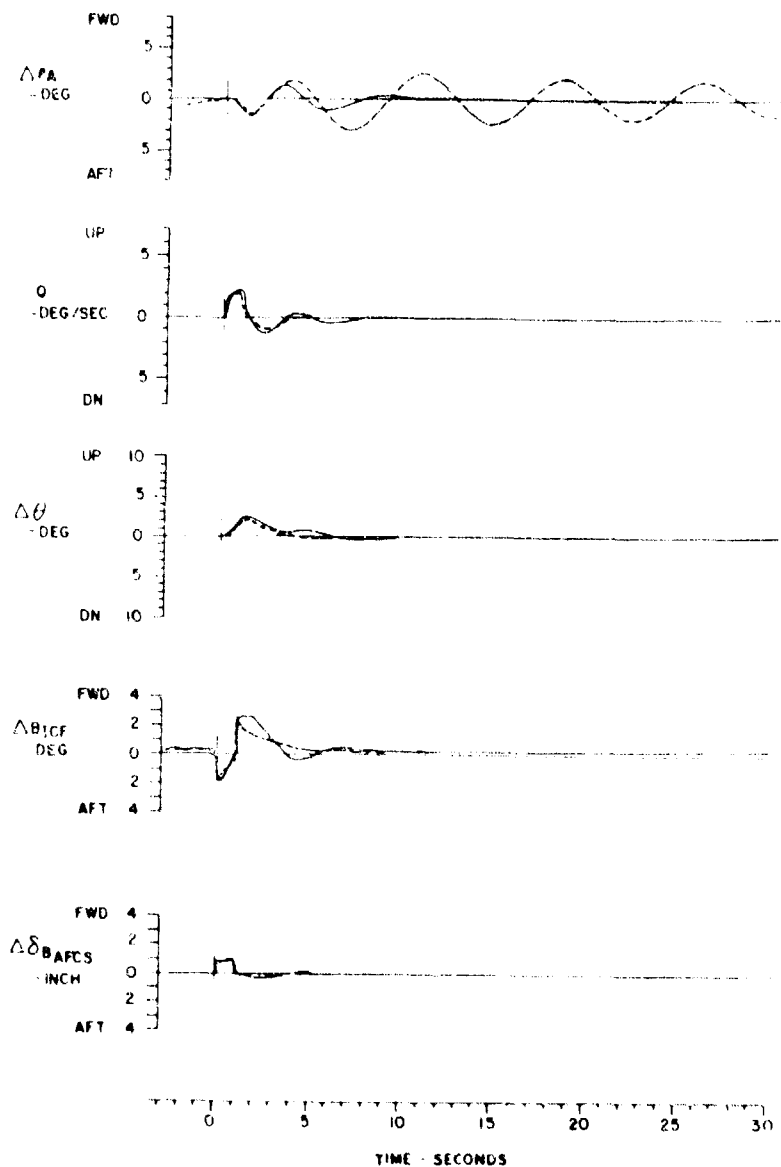
FIGURE 74.
SIMULATION DATA   LOAD  LONGITUDINAL LOAD DAMPING IN HOVER-SCAS

247

GROSS WEIGHT = 45,000 LB
LOAD WEIGHT = 5000 LB
50-FT CABLES
1 IN, 1 SEC δB PULSE
LSS DAMPING ON
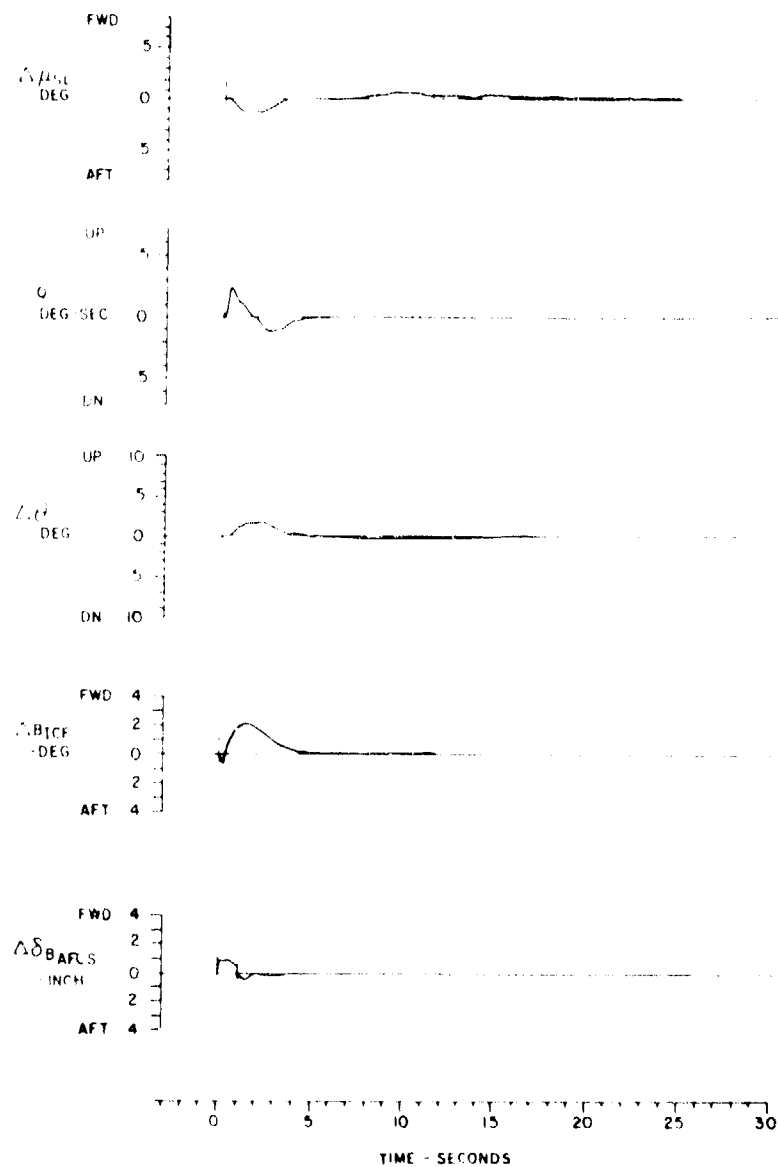
FIGURE 75
SIMULATION DATA  LOAD LONGITUDINAL DAMPING IN HOVER - HOVER HOLD
(VELOCITY ONLY)

248

GR WT = 43,000 LB
LOAD WT = 5000 LB
50-FT CABLES
1 IN, 1 SEC $B_B$ PULSE
PHS ON

————— LSS DAMPING ON
—— LSS OFF
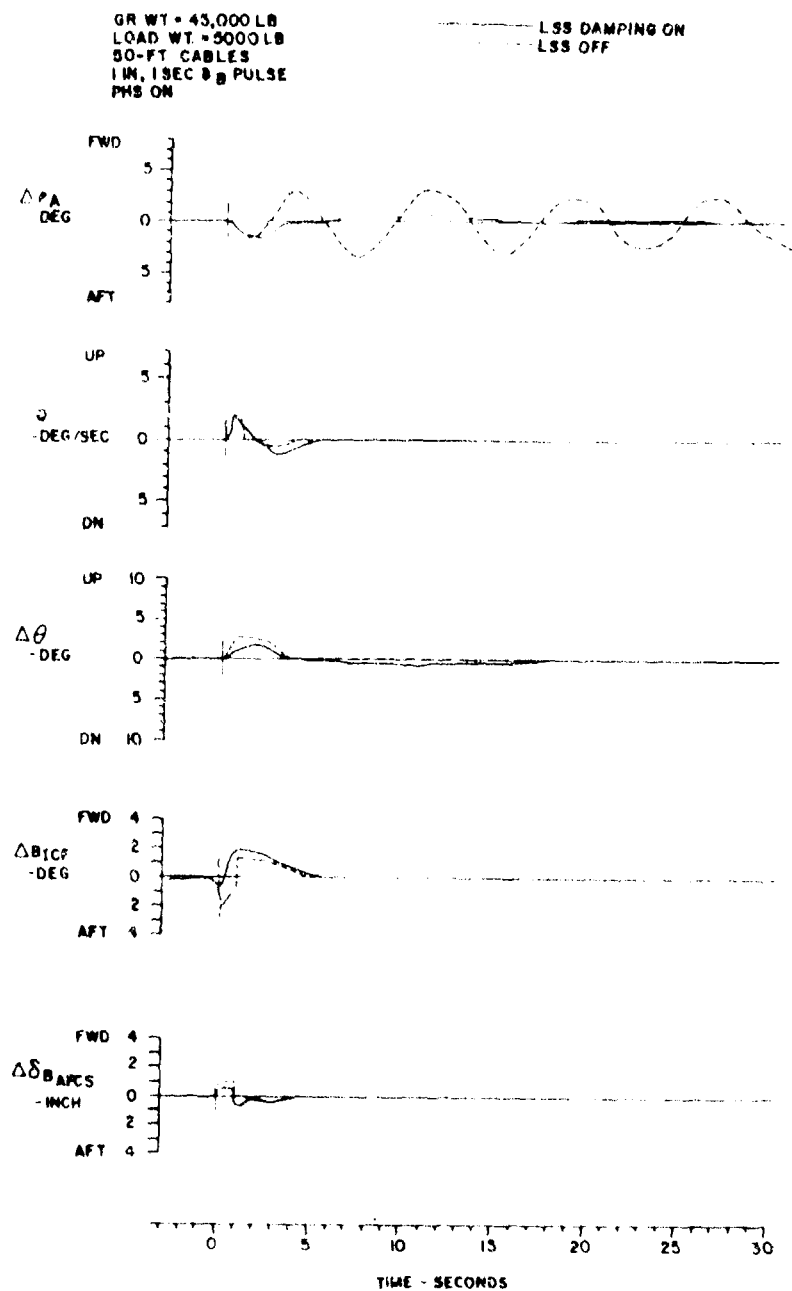
FIGURE 76
SIMULATION DATA    LOAD LONGITUDINAL DAMPING IN HOVER - PHS

249

GR WT = 45,000 LB          LSS DAMPING ON
LOAD WT = 5000 LB          LSS OFF
50 FT CABLES
1 IN, 1 SEC θ$_S$ PULSE
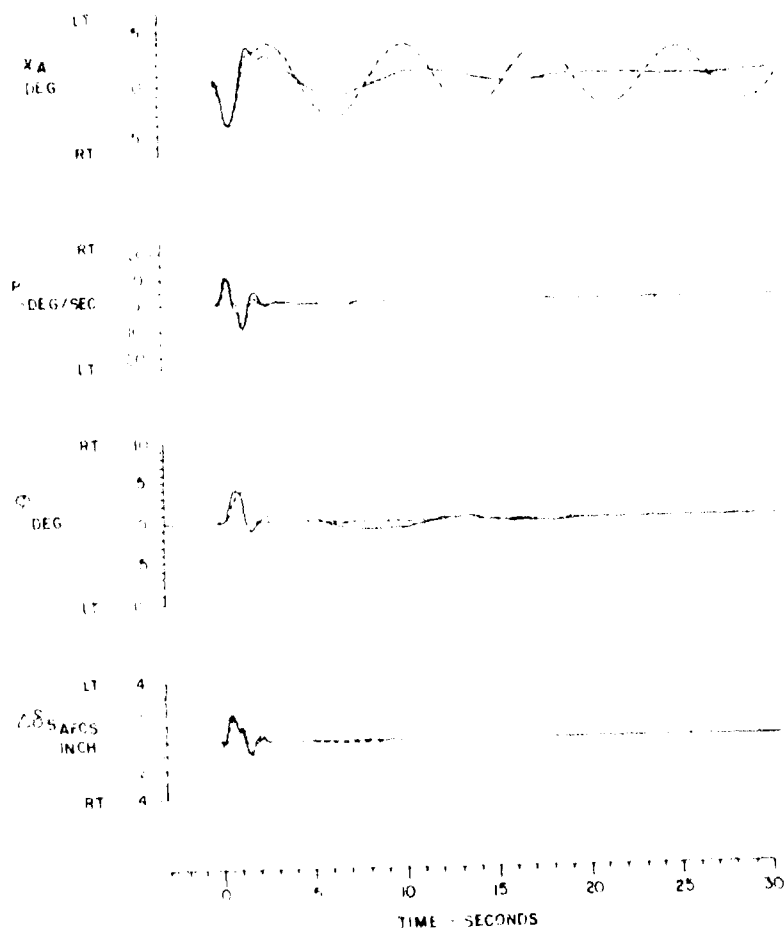
FIGURE 77.
SIMULATION DATA    LOAD LATERAL DAMPING IN HOVER-SCAS

250

GR WT = 45,000 LB
LOAD WT = 5000 LB
50 FT CABLES

I IN, I SEC 8 s PULSE
LSS DAMPING ON
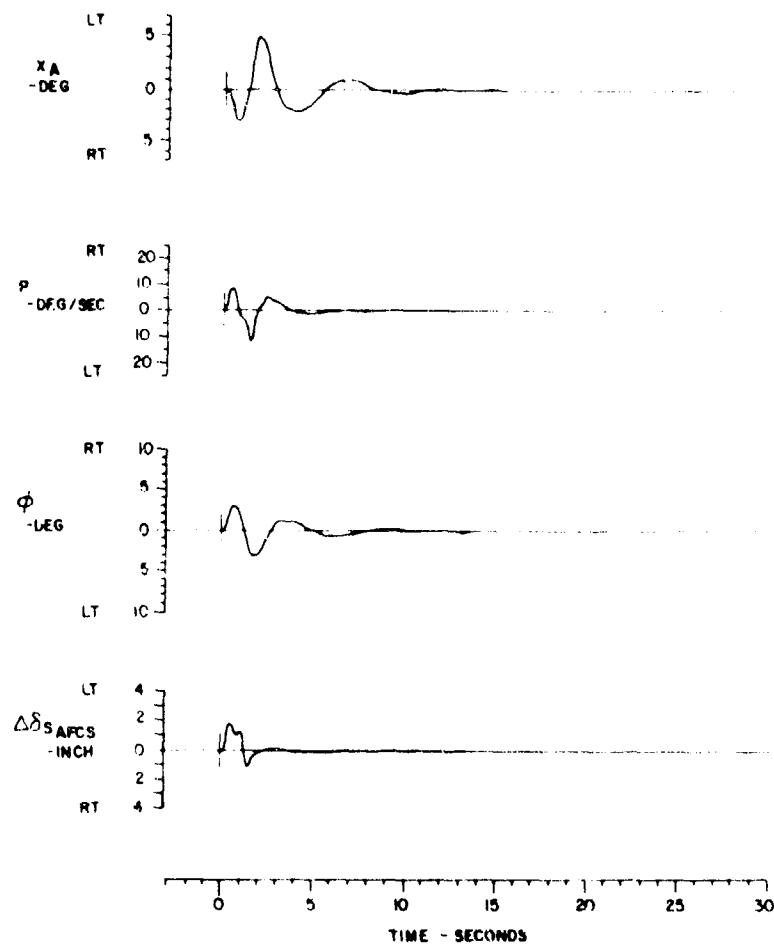
FIGURE 78.
SIMULATION DATA  LOAD LATERAL DAMPING IN HOVER - HOVER HOLD (VELOCITY ONLY)

251

GR WT = 45,000 LB
LOAD WT = 5000 LB
50-FT CABLES
1 IN, 1 SEC $B_s$ PULSE
PHS ON

LSS DAMPING ON
LSS OFF
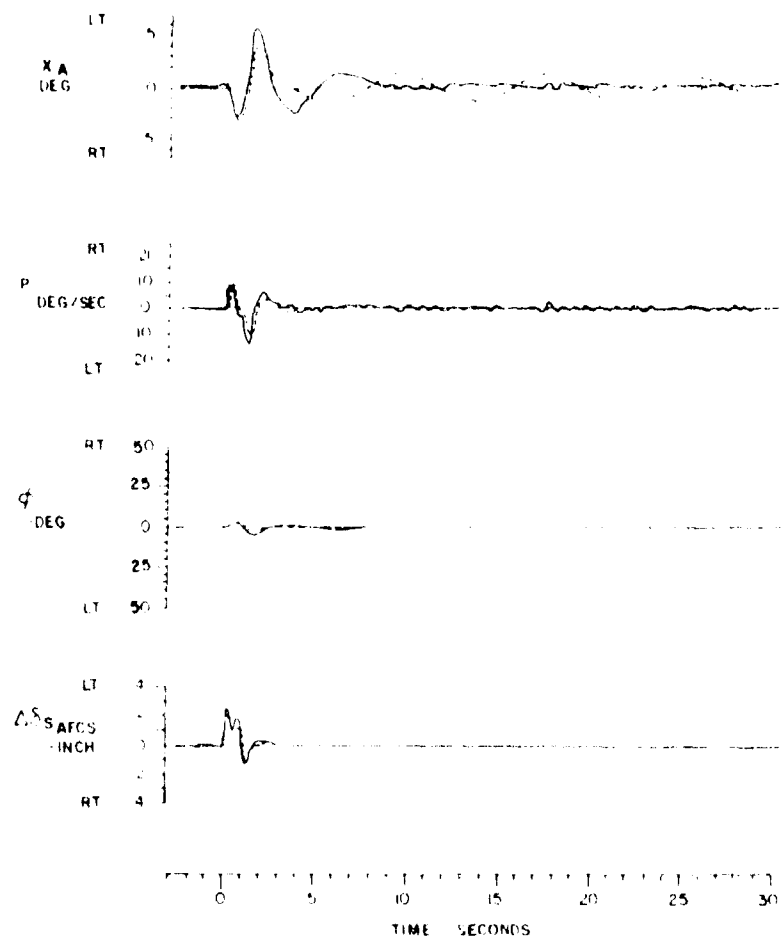
FIGURE 79
SIMULATION DATA    LOAD LATERAL DAMPING IN HOVER - PHS

252

GROSS WT = 45,000 LB
LOAD WT = 5000 LB
50 FT PENDANT CABLES
1 IN, 1SEC $\delta_R$ PULSE

----- LSS DAMPING ON
---- LSS OFF
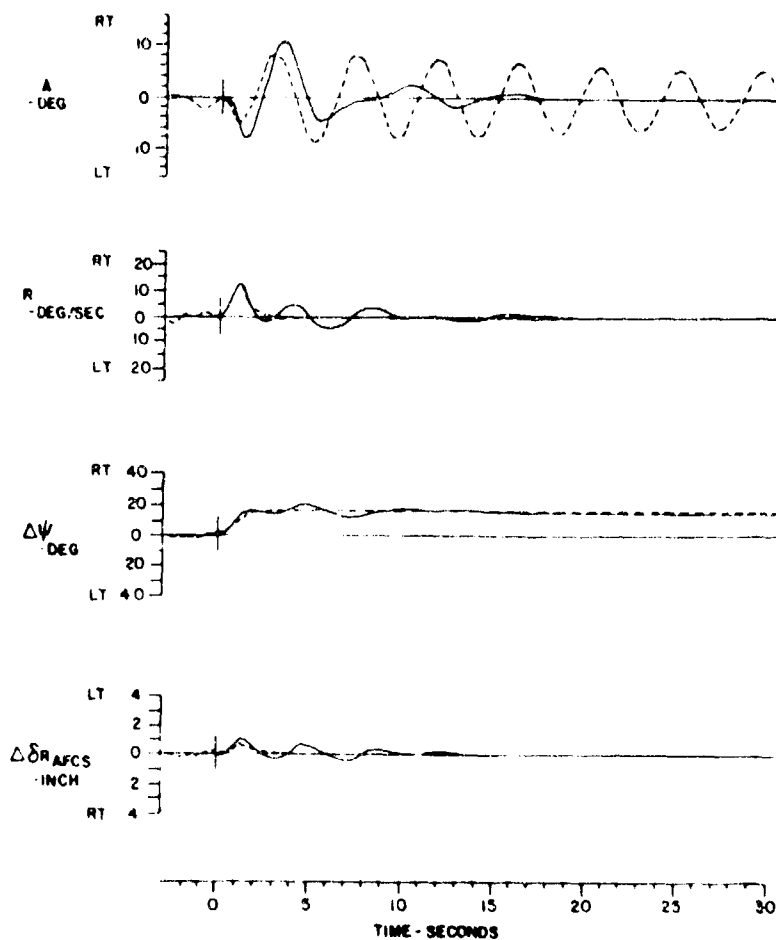
FIGURE 80.
SIMULATION DATA: LOAD DIRECTIONAL DAMPING IN HOVER - SCAS

253

GR WT = 45,000 LB                          LSS DAMPING ON
LOAD WT = 5000 LB                          LSS OFF
AIRSPEED = 60 KN
20 FT INVERTED VEE CABLES
1 IN, 1 SEC $\delta_B$ PULSE
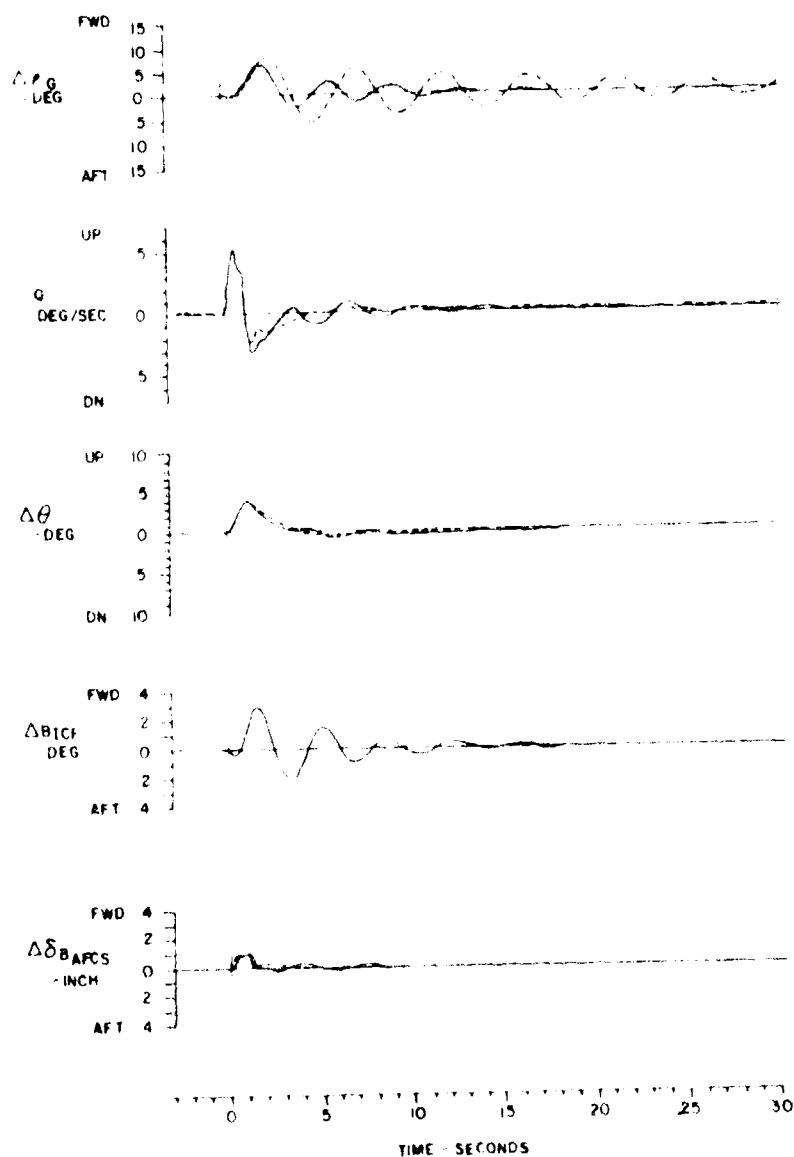


FIGURE 81.
SIMULATION DATA   LOAD LONGITUDINAL DAMPING AT 60 KN

254
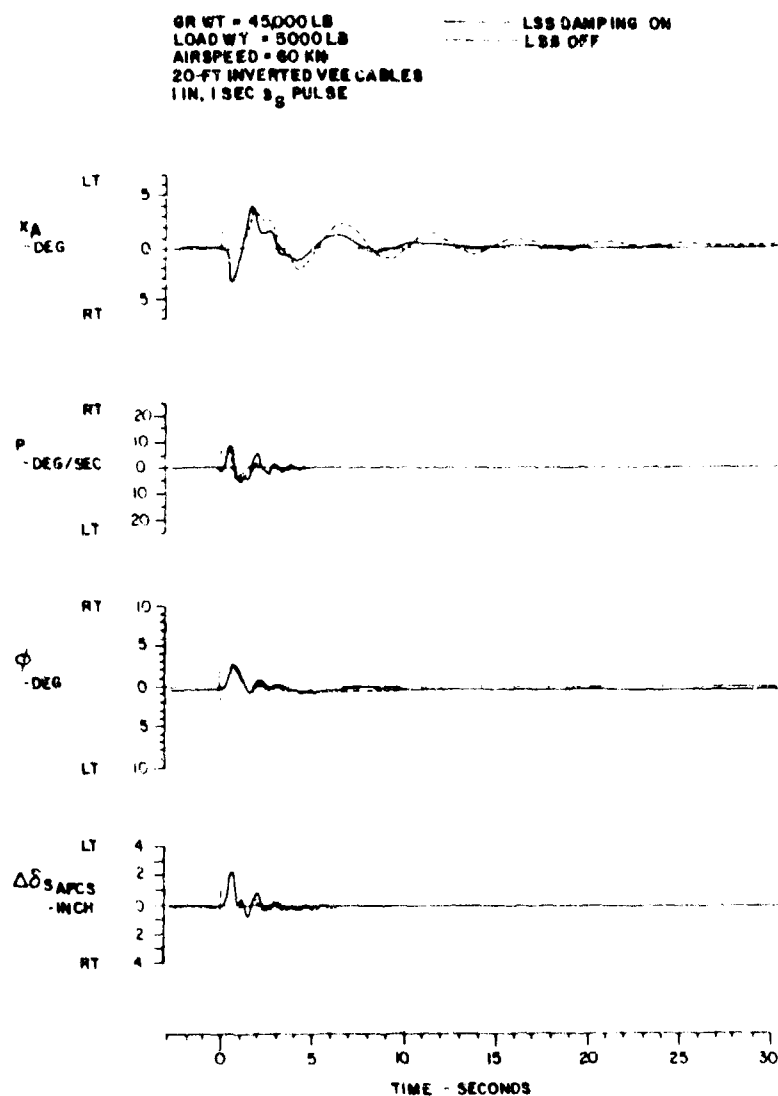
FIGURE 82.
SIMULATION DATA: LOAD LATERAL DAMPING AT 60 KNOTS

255

GR WT = 45,000 LB
LOAD WT = 5000 LB
50-FT CABLES
10 FPS HEADWIND RAMP AT 2 FT/SEC$^2$
LSS LOAD POSITION HOLD ON
PHS ON
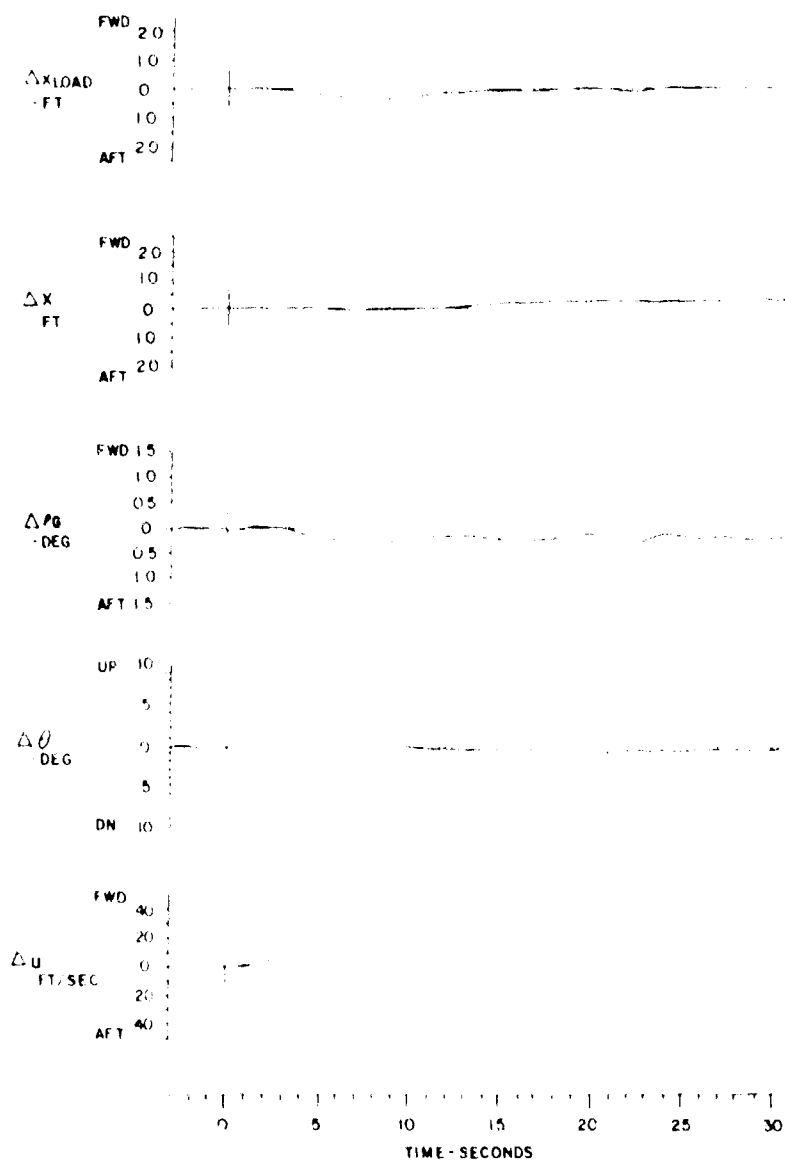
FIGURE 83.

SIMULATION DATA LOAD LONGITUDINAL POSITION HOLD DURING HEADWIND RAMP

256

GR WT = 45,000 LB
LOAD WT = 5000 LB
50 FT CABLES
10 FPS SIDEWIND RAMP AT 2FT/SEC$^2$
LSS LOAD POSITION HOLD ON
PHS ON
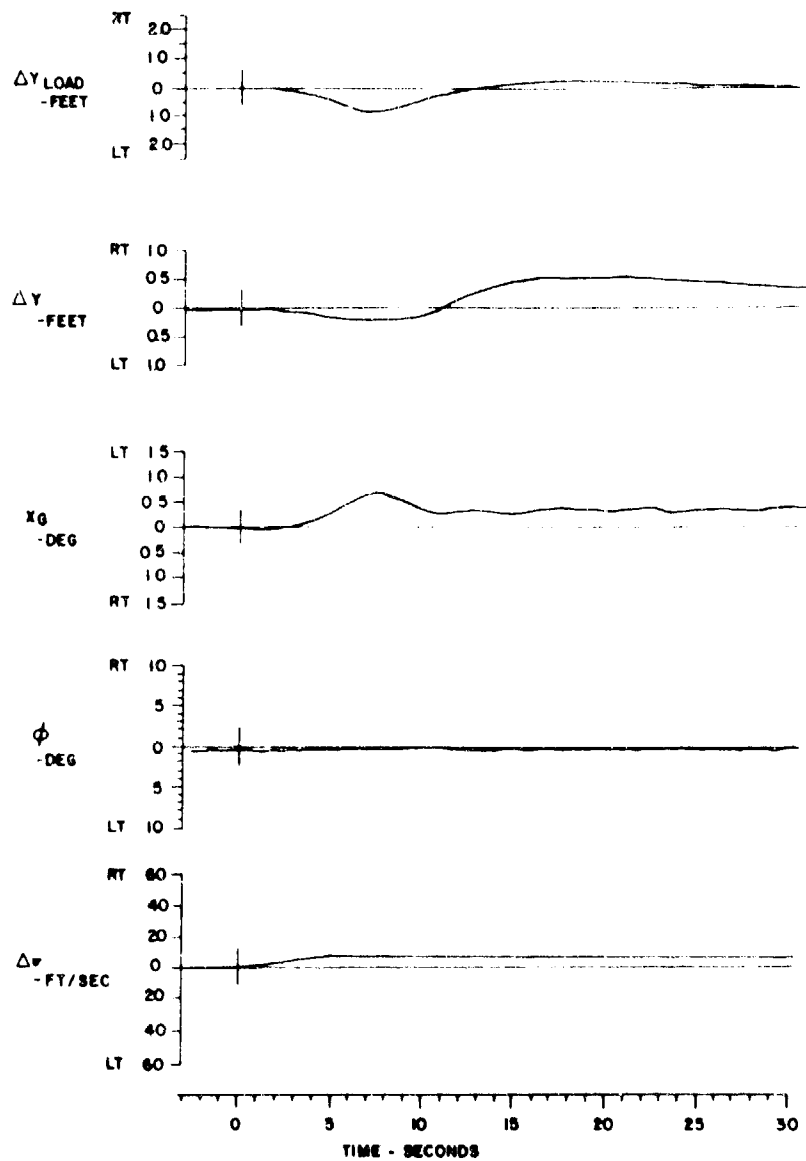
FIGURE 84.
SIMULATION DATA. LOAD LATERAL POSITION HOLD DURING SIDEWIND RAMP

257
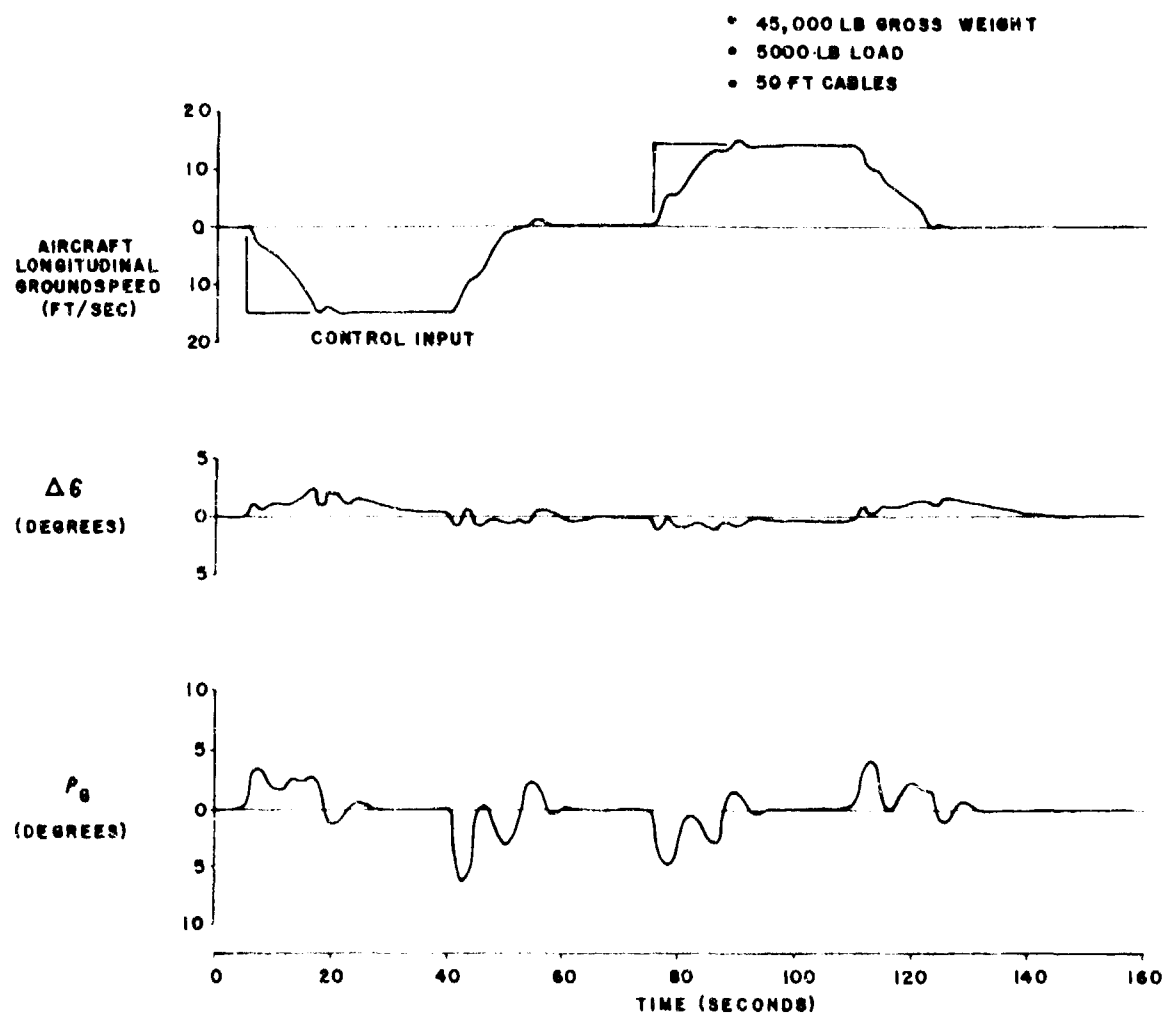
FIGURE 85 SIMULATION DATA: AIRCRAFT AND LOAD RESPONSE TO MAXIMUM LONGITUDINAL LCC INPUTS

258
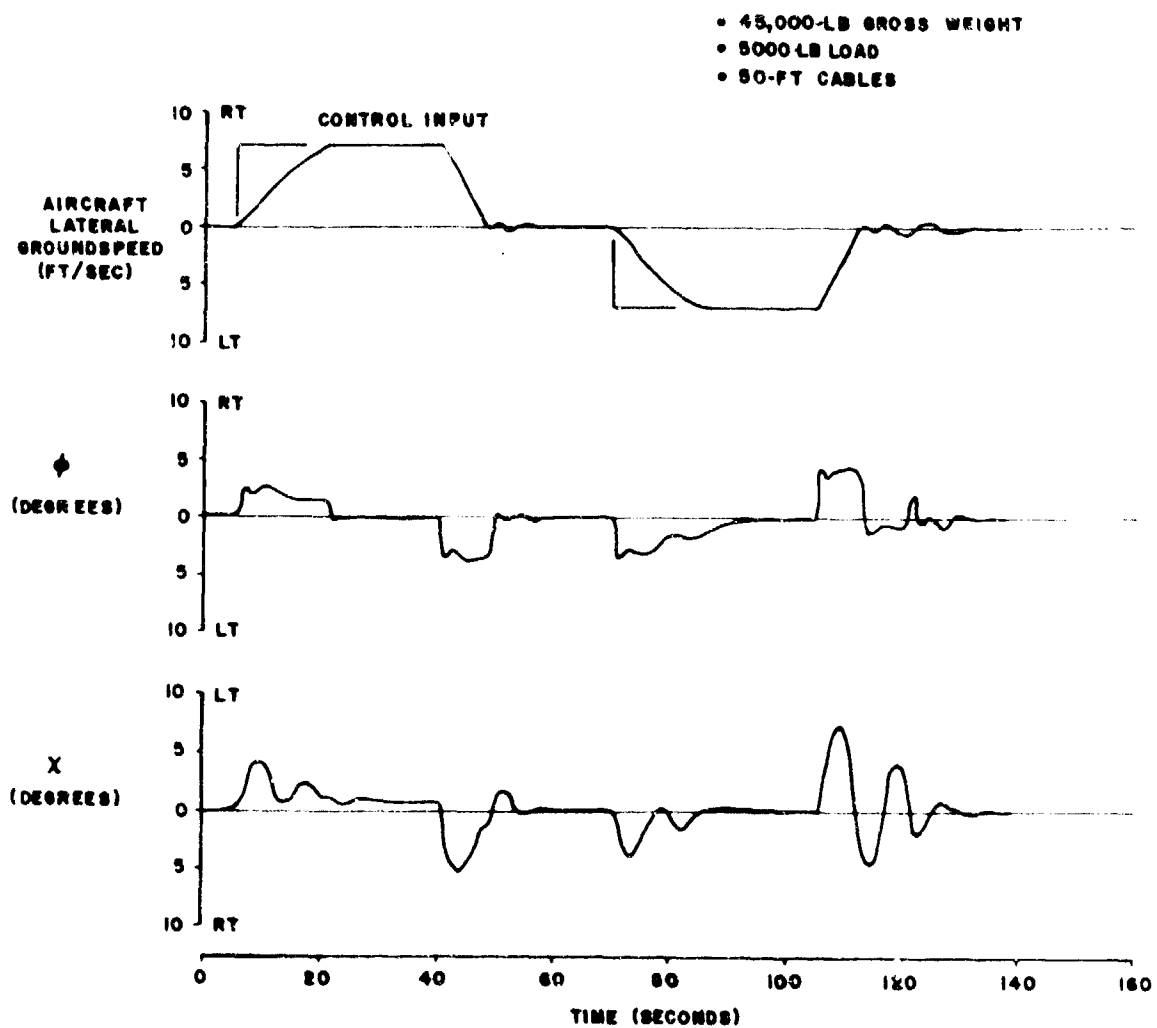
FIGURE 86. SIMULATION DATA: AIRCRAFT AND LOAD RESPONSE TO MAXIMUM LATERAL LCC INPUTS

259

MODEL 347
AIRCRAFT WEIGHT - 38,000 LB
LOAD WEIGHT - 5000 LB
CABLE LENGTH - 50 FEET
HOVER HOLD (PHS) ON
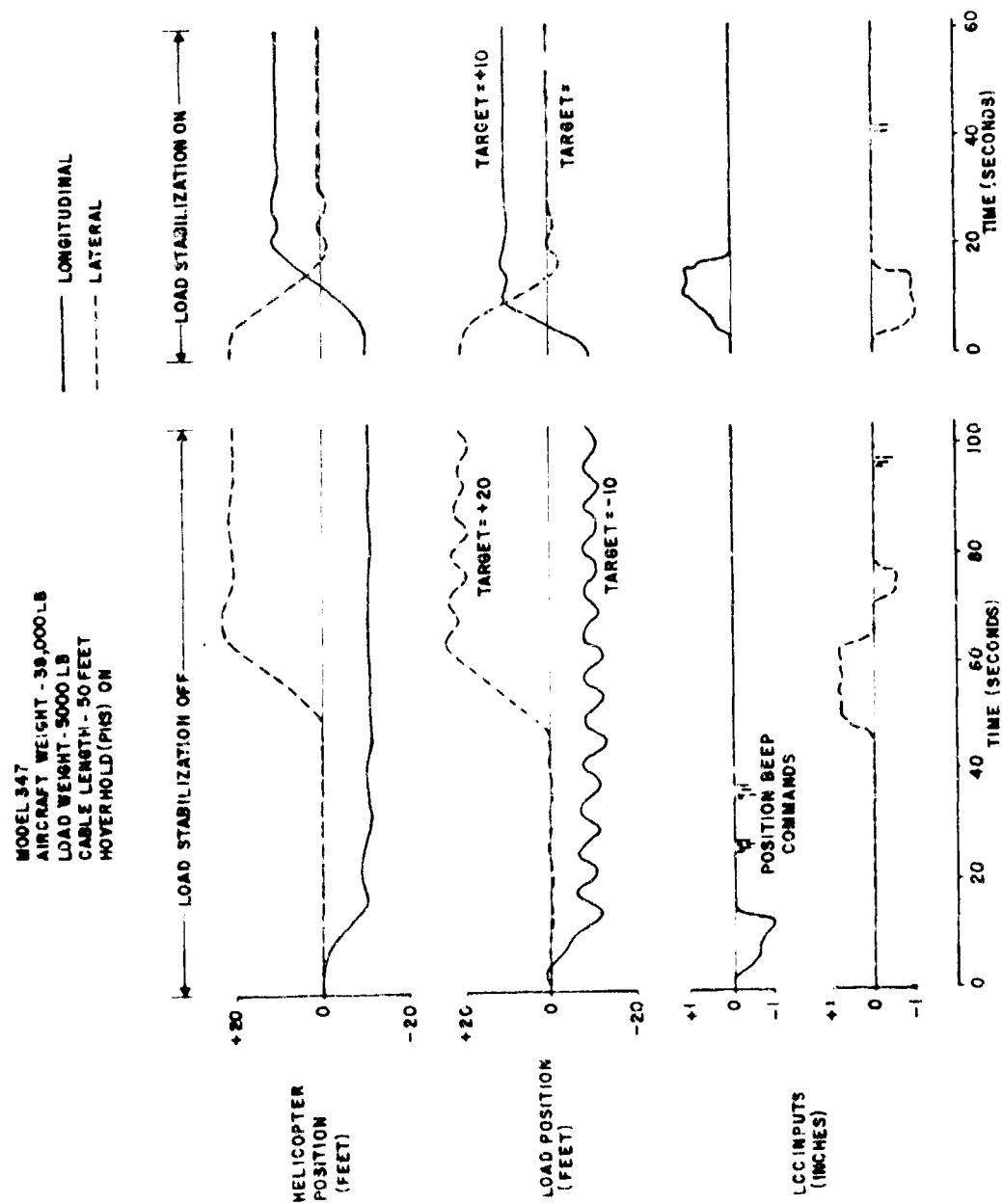
FIGURE 87. LOAD POSITIONING – SIMULATION DATA

can be positioned easily and precisely, whereas without the
LSS, lightly damped load oscillations build up making precise
load positioning difficult and time consuming.

The LSS logic performed well during the simulation verification
with two exceptions: (1) hysteresis had to be added to the
load centering tension discrete as discussed previously, and
(2) an LCC/LSS interface problem was found which is described
below.

The simulation and CSMP results are in very close agreement
as can be seen by comparing corresponding simulation results
with the CSMP results presented previously. The only signi-
ficant disagreement is in the directional damping loop where
the simulation requires a considerably smaller gain and time
constant than the root locus model recommends.

### 2.1.5.4 Major Problems

### 2.1.5.4.1 Sensitivity to Cable Length and AFCS Modes

As discussed previously, the required LSS configuration is
dependent on the cable length and AFCS mode that is being
used. The current system design automatically changes the
LSS configuration as a function of AFCS mode changes. For
an operational system, several LSS parameters, as noted
previously, would have to change automatically as the cable
length changes.

### 2.1.5.4.2 LCC/LSS Interface

A problem was encountered when LCC inputs were attempted on
the total force simulation with the LSS on. The hover hold
mode limits the longitudinal and lateral velocity error
signals to approximately 1 fps to provide the desired aircraft
acceleration. This limit masks the velocity term until the
velocity has reached the commanded value. Since the LSS
configuration is dependent on whether velocity feedback is
applied to the aircraft, the load became unstable when the
velocity term was masked by the limit. Logic was added to

switch the LSS to the proper damping loop when this limit is reached. This provides good load damping continuously during LCC and pilot maneuvering with the hover hold and precision hover modes on.

2.1.5.4.3 Conflict Between Load Damping and Position Hold

The aircraft responses required for load damping and load position hold are in opposite directions as described previously. Consequently, the position hold loops have to operate at a low frequency to avoid a self-defeating reduction in load damping.

## 2.1.6  Automatic Approach to Hover

### 2.1.6.1  Objectives and Concepts

The primary objective of the HLH/ATC automatic approach to hover system was to demonstrate the feasibility of an automatic approach system.

Since the objective is to demonstrate feasibility and not operational capability, the following ground rules were established to permit system simplification.

- Pilot establishes desired track; initial longitudinal groundspeed at 70 kn ± 5 kn, initial descent rate of 0 fpm to 400 fpm, and initial altitude at approximately 1000 feet above hover point.

- Fixed approach profile, and hover altitude.

- Track at time of approach initiation will be held constant during approach by stabilizing heading and maintaining zero cross-track velocity and position error.

- Desired track velocity will be maintained through longitudinal velocity commands.

- Altitude will be phased from baro to radar during final portion of approach.

- Velocity commands will be input to the flight director and, when performing an automatic approach, to the CCDA's.

- A coupled or manual approach may be selected anytime during the approach.

The auto approach handling qualities objectives are:

- To reduce pilot workload during approach.

- No excessive control inputs.

- No excessive or lightly damped aircraft responses.

263

Performance goals for the auto approach are:

## Initial and Descent Phases

Glidepath error

40-foot vertical error
80-foot lateral error

Groundspeed error ± 6 knots

## Deceleration Phase

Glidepath error

10-foot vertical error
40-foot lateral error

Groundspeed error ± 4 knots.


## 2.1.6.2  Auto Approach Profile Description

The pilot initiates the automatic approach by first manually
flying the helicopter to the following trim conditions.

- Groundspeed = 70 kn ± 5 kn

- Rate of descent – 0 fpm to 400 fpm

- Altitude – 1000 ft. (above hover point)

- Helicopter stabilized along desired track

- Groundspeed velocity mode selected

Initiation of the approach occurs with engagement of the
"auto approach initiate" switch, see Figure 88.

The approach profile is described by three separate phases,
see Figure 89.  In the initial approach phase, the helicopter
will maintain 70 knots ground speed and 1000 feet altitude
for a distance of 1930 feet.  During the phase, the FDI
velocity commands are based upon errors from the desired
level-flight condition.  The vertical error displayed corres-
ponds to the displacement from the projected glide slope.

At 1930 feet from the initiate point, the helicopter enters
the descent phase of the approach profile.  During this phase,
the track velocity is maintained at 70 knots and rate of
descent at 10.33 fps.  This corresponds to a 5° glide slope.
The desired altitude profile is determined from the rate of
descent.
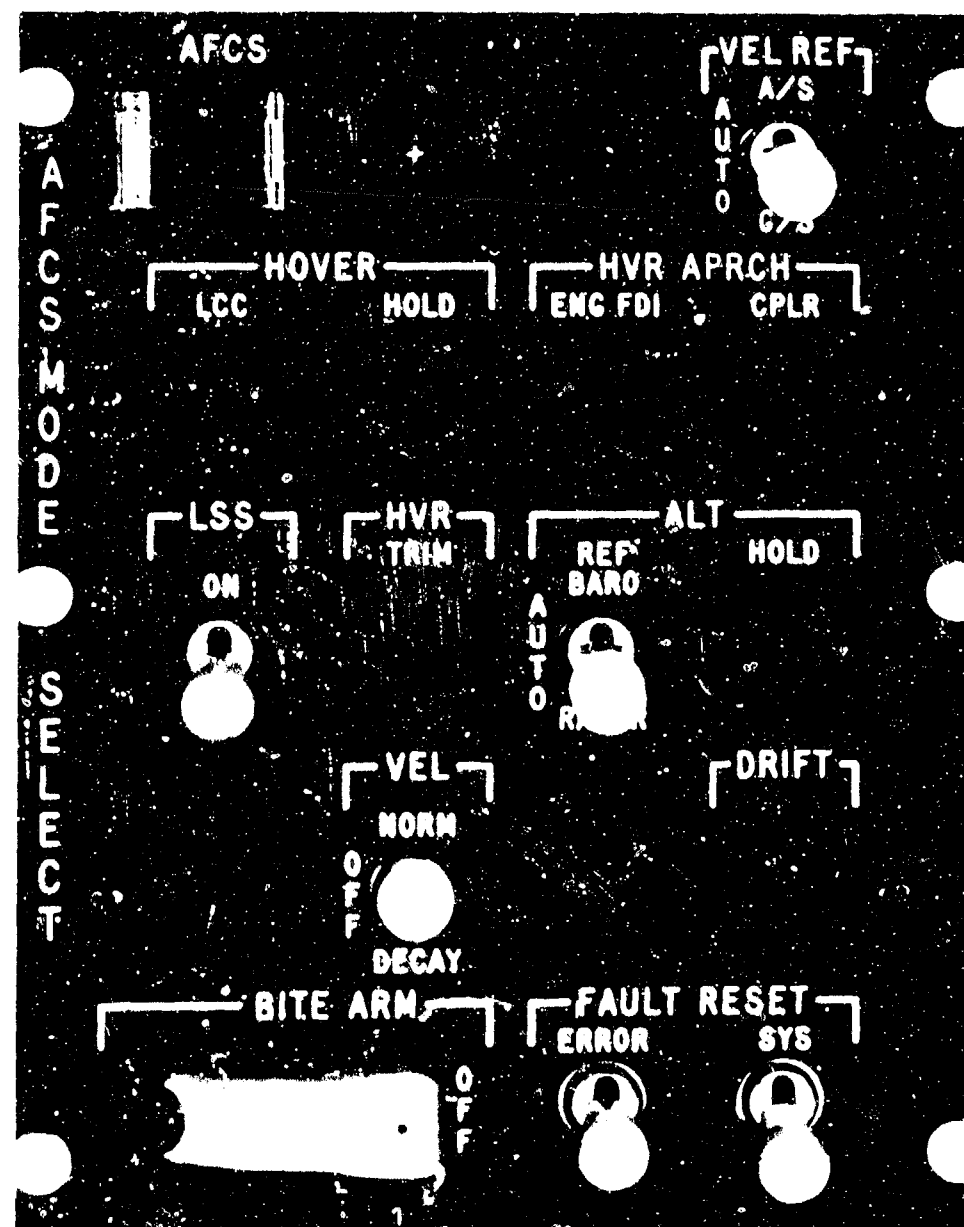
FIGURE 88. AFCS MODE SELECT PANEL
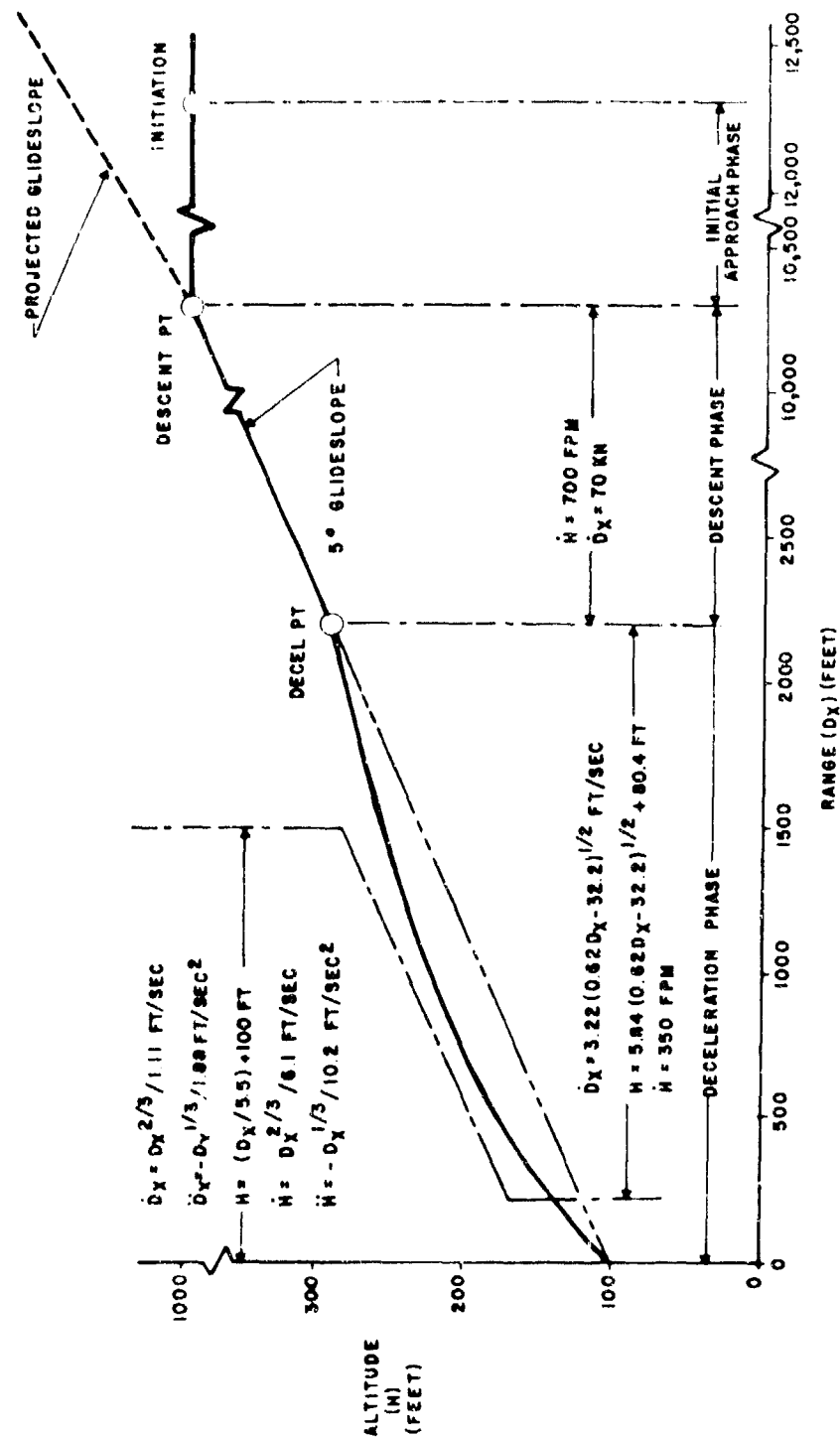
FIGURE 89.
AUTO APPROACH DEMONSTRATION PROFILE

At 10,010 feet from the initiate point (2290 feet from the hover point), the helicopter enters the initial deceleration phase. During this phase, the aircraft flares to decelerate and reduces its rate of descent to 5.83 fps. At 214 feet from the hover point, the deceleration and rate of descent are slowly reduced to achieve hover at 12,300 feet from the initiate point at an altitude of 100 feet.

2.1.6.3  Automatic Approach to Hover Control System

The initial auto approach control laws and logic for the
347/ATC were developed utilizing unpiloted simulation, first
with a linear, small perturbation digital simulation, and
then with the full-flight envelope simulation.  Final adjust-
ment of the control laws was accomplished on the 347/ATC air-
craft.  These adjustments consisted primarily of changes in
gains, time constants, and feedback signal generation.

The final automatic approach to hover system, which is the
result of the above development, is shown on Figure 90.

The control system performs open loop determination of the
distance from the hover point, $D_X$.  This is used to generate
the desired approach profiles (rate of descent, altitude, and
track velocity), and stick commands which approximate these
profiles.  Proportional and integral feedback of profile
errors is used to maintain zero error between actual and
desired responses.  The summation of the open loop stick
command and the proportional and integral feedback signals
represents the required stick command.

For a manual approach, the difference between the required
stick commands and cockpit stick motion is fed to the flight
director velocity command bars (see Figure 91).  The pilot
performs a manual approach by inputting control motions to
maintain the command bars in the null position.

For an automatic approach, the pilot activates both the FDI
and coupler switches and the required stick commands are
then fed directly to the cockpit controls through the CCDA
actuators.  The pilot can monitor the approach by observing
the control motions and the flight director velocity command
bars.  The approach can be aborted by either mag braking or
with the coupler switch on the mode select panel.

2.1.6.3.1  Longitudinal Control Loops

The longitudinal control loops are shown on Figure 90.  The
functions FBXV, and FBDB, Appendix Data Package, describe
the desired track velocity profile and the open-loop stick
function, respectively; FVXTRK performs the track velocity
coordinate transformation from north-south coordinates to
track coordinates.  The difference between FBXV and FVXTRK
represents the track velocity error which is fed to the con-
trol system through proportional and integral paths with
gain $K_{BXV}$ and $K_{BXD}$, respectively.  Limiters $L_{M9}$ and $L_{M10}$
are placed on the integral and total feedback paths to pre-
vent excessive control inputs.
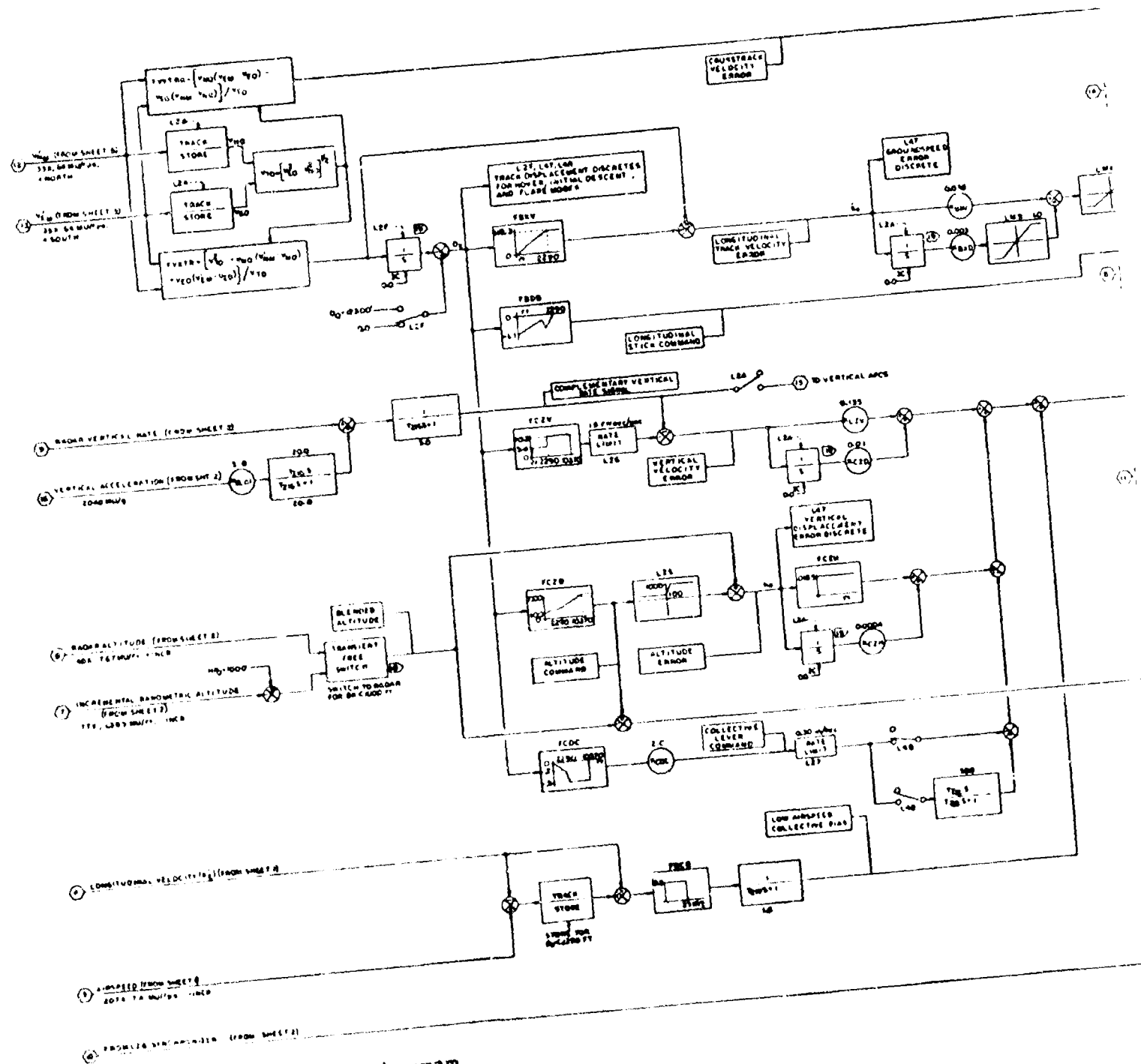
FIGURE 90. AAH Block Diagram

269

OUT-OF-TOLERANCE FLAG

VERTICAL VELOCITY COMMAND BAR

VERTICAL DISPLACEMENT ERROR

LATERAL VELOCITY COMMAND BAR

LONGITUDINAL VELOCITY COMMAND BAR

OUT-OF-TOLERANCE FLAG

LATERAL DISPLACEMENT ERROR
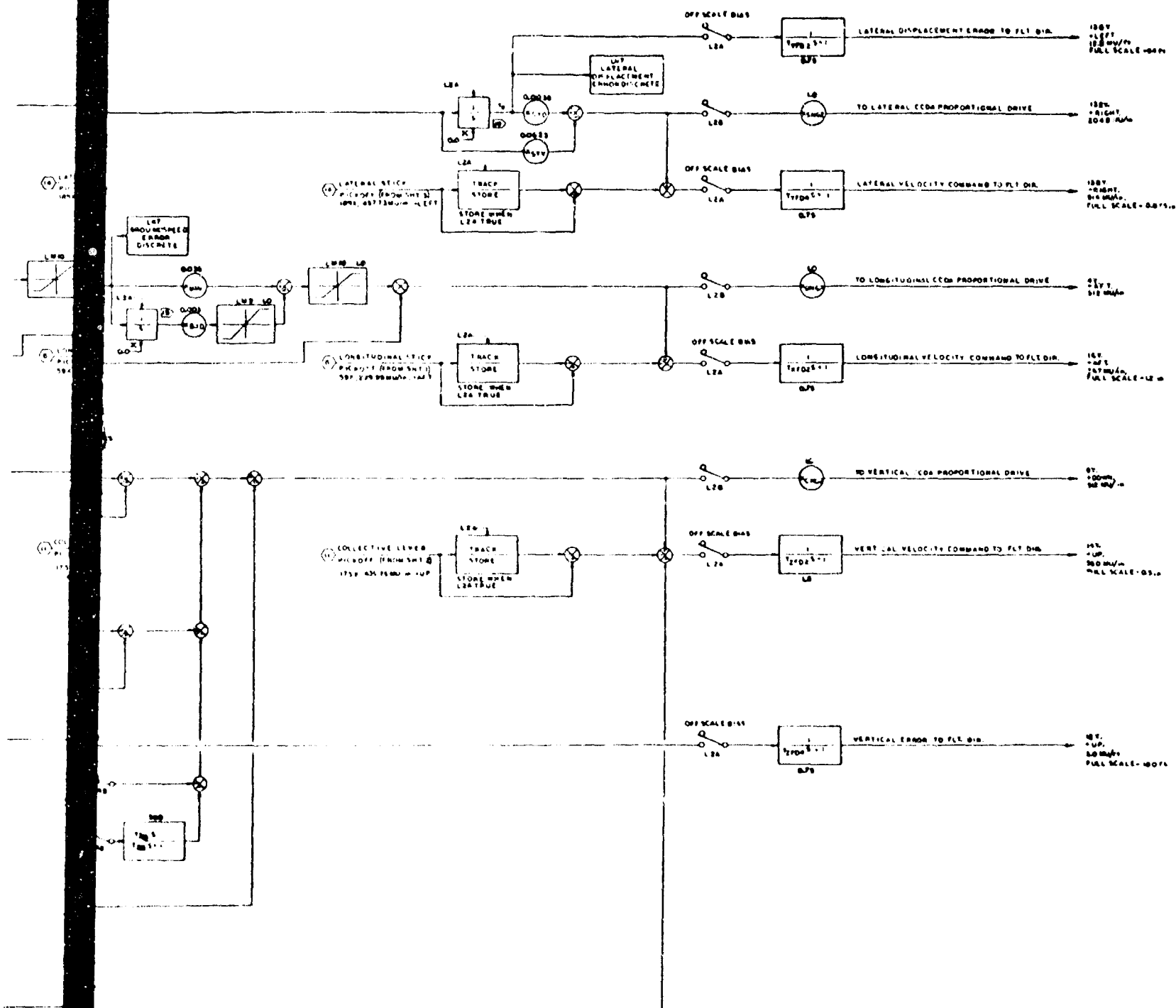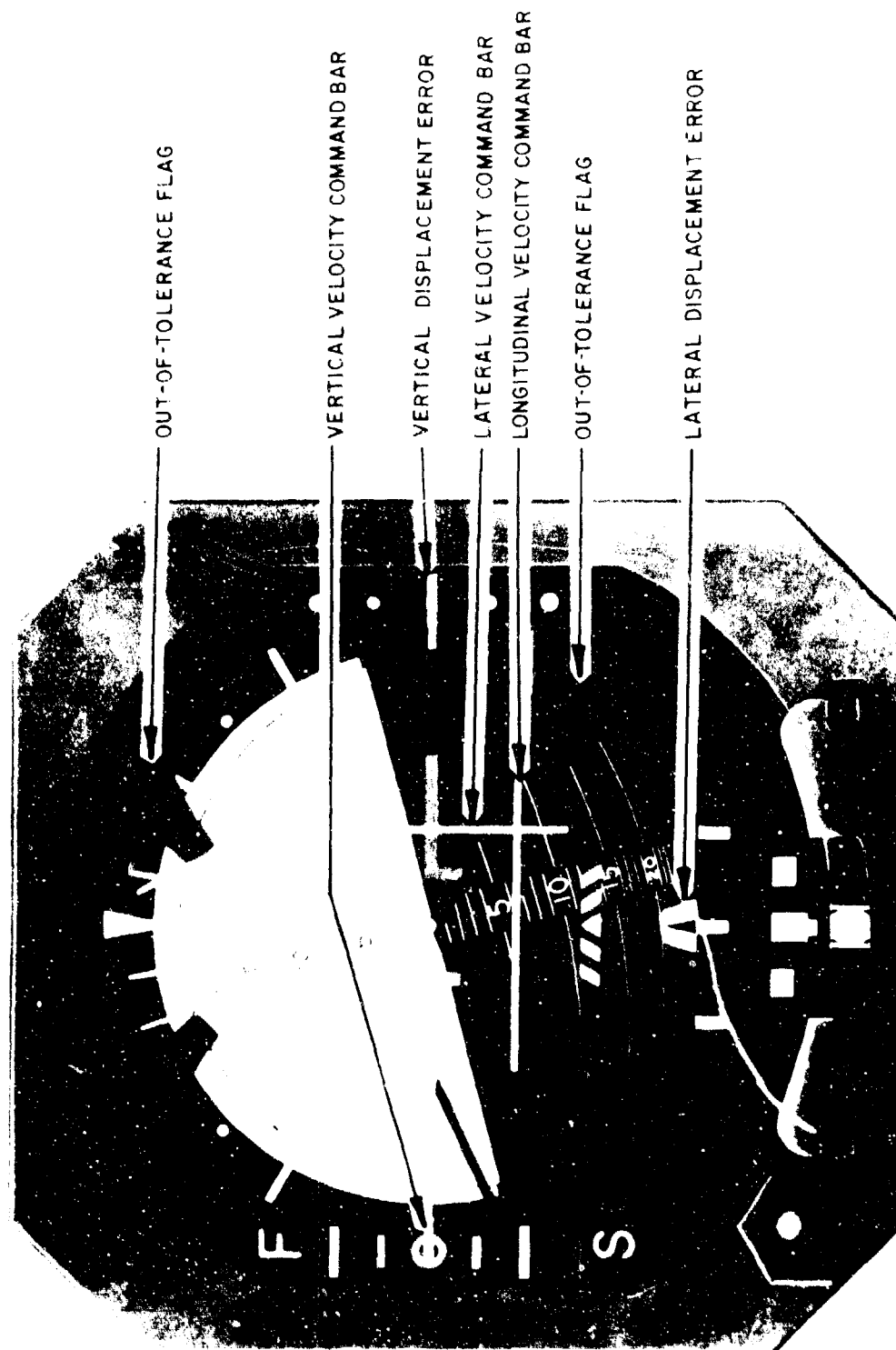
FIGURE 91.
FLIGHT DIRECTOR DISPLAY

## 2.1.6.3.2  Lateral Control Loops

The lateral control loops are shown in Figure 90. These maintain helicopter track by determining cross-track velocity, $F_{VYTRR}$ and feeding it back through proportional and integral gains $K_{SYV}$ and $K_{SYD}$, respectively.

## 2.1.6.3.3  Vertical Control Loops

The vertical control loops which provide the desired descent rate and altitude profiles are shown in Figure 90. The functions $F_{CZV}$ and $F_{CZD}$ represent the desired rate of descent and altitude profiles, respectively. $F_{CDC}$ represents the collective lever displacement which approximates the desired profile. The rate limits $L_{Z6}$ and $L_{Z7}$ are included to soften the step changes on $F_{CZV}$ and $F_{CDC}$. Rate of descent information is provided by a complementary filter which uses a heavily filtered radar rate for low frequency data and vertical acceleration for high-frequency, short-term data.

The altitude feedback signal utilizes barometric altitude from approach initiation to 1000 feet from the hover point. It is assumed that at 1000 feet from the hover point, the aircraft is over relatively flat terrain and the altitude signal switches transient-free to radar altitude. The difference between baro and radar altitude at the time of switching is ramped in at a rate of 4 feet/sec. The transient-free switch insures a smooth transition from baro to radar and an absolute hover altitude of 100 feet.

Compensation for the collective trim shift, associated with the aircraft power required curve is provided through the collective trim compensation function, $F_{CAS}$, and the low airspeed collective bias loop. $F_{CAS}$, mechanized in the basic vertical SCAS, provides compensation for airspeeds greater than 40 knots. The low airspeed collective bias loop provides additional compensation for airspeeds below 40 knots.

This loop functions by generating an approximate airspeed signal, and stepping in .5 inches of "up" collective stick through a lag whenever the approximate airspeed drops below 25 knots. As reliable airspeed measurement is not available below 40 knots, the airspeed approximation is generated by determining the difference between airspeed and longitudinal groundspeed. This difference is stored when $D_X$ becomes less than 2290 feet. The approximate airspeed is equal to the sum of longitudinal groundspeed and the above stored difference.

2.1.6.3.4   Basic SCAS Modifications

The following basic SCAS modifications were required for automatic approach operation.

- Increased pitch attitude gain, $K_{MAD}$, to .45 in./deg to provide tighter pitch attitude control.

- Removed lateral control response quickening loop in order to reduce lateral control sensitivity.

- Modified longitudinal asymetrical limiter, LM8, to 2 inches forward and 4 inches aft, and added a longitudinal stick bias equivalent to 2 inches of aft stick. This was required to prevent the longitudinal AFCS from bottoming the asymetrical limit and causing the loss of pitch attitude feedback.

- Added a complementary vertical rate feedback loop to the differential vertical AFCS output with a gain of .135 in./fps, $K_{ZLV3}$.  This provided additional vertical damping and reduced the collective stick sensitivity.

2.1.6.4   Flight Director Display Signal Generation

The flight director allows the pilot to monitor the performance of the auto approach system and, if necessary or desired, to manually fly the helicopter along the approach profile. The information displayed on the flight director (see Figure 91) includes:

Steering Command

- Longitudinal
- Lateral
- Vertical

Flight Path Error Indications

- Lateral
- Vertical

Out-of-Tolerance Indications

The steering commands represent the difference between the required stick command and the actual cockpit control displacement.  This signal is fed to the flight director command with appropriate scaling and dynamic shaping to provide acceptable commands for the pilot to follow.  The following command dynamics and sensitivities provided adequate pilot tracking capability.

273

$$\text{Long Vel Comm} = .60 \ \frac{\text{inches}}{\text{inch}} \ \frac{1}{.75S+1}$$

$$\text{Lat Vel Comm} = .715 \ \frac{\text{inches}}{\text{inch}} \ \frac{1}{.75S+1}$$

$$\text{Vert Vel Comm} = .25 \ \frac{\text{inches}}{\text{inch}} \ \frac{1}{1.5S+1}$$

The vertical and lateral flightpath errors were displayed using the following sensitivities:

$$\text{Vert Error} = \frac{120 \text{ feet error}}{1 \text{ inch displ}}$$

$$\text{Lat Error} = \frac{120 \text{ feet error}}{1 \text{ inch displ}}$$

The FD (Flight Director) and RT (Rate of Turn) flags are driven into view whenever any of the flightpath error tolerances were exceeded. These tolerances are:

for $12300' > D_x > 2290'$

| | |
|---|---|
| Vert Error | $< 40$ ft |
| Lat Error | $< 80$ ft |
| Groundspeed Error | $< \pm 6$ kn |

for $2290 > D_x \geq 0$

| | |
|---|---|
| Vert Error | $< 10$ ft |
| Lat Error | $< 40$ ft |
| Groundspeed Error | $< \pm 4$ kn |

274

## 2.1.7  Hover Trim

The HLH AFCS is configured with a selectable control feature
that automatically corrects the helicopter to a zero ground-
speed condition.  Known as Automatic Hover Trim, this select-
able mode is incorporated to reduce cockpit workload during
the final stages of a manually initiated approach to hover.
It is particularly effective as an approach aid when utilized
in conjunction with Altitude Hold.  Another Hover Trim appli-
cation considers engagement of the mode while recovering from
maneuvers resulting in disorientation or vertigo which occurs
from time to time while flying under IFR flight conditions.

The Hover Trim system operates by slowly backdriving cockpit
longitudinal and lateral controls to a force trim reference
corresponding to zero ground speed.  It may be activated any-
where in the flight envelope by depressing a button on the
pilot's Mode Select panel.

LONGITUDINAL AXIS MECHANIZATION - As illustrated in the longi-
tudinal AFCS functional block diagram (Figure 14), Hover Trim
control laws consist of a single proportional feedback through
which a longitudinal ground-speed signal ($\dot{X}_E$) is passed.  The
signal goes directly into the integral back-drive path to
command parallel stick motion in the cockpit.  L-22 logic
energizes the loop, and it stays engaged as long as the pilot
does not force trim with the mag brake or select the Velocity
OFF mode of operation.

As long as the groundspeed is greater than 10 feet per second,
a constant level signal is sent to the integral drive because
of the LM4 limiter.  This produces a gradual stick input in
the cockpit which slows the aircraft toward hover.  Stick in-
puts continue until velocity is completely nulled through the
integral control drive.

A dual gain network is provided to increase longitudinal stick
backdrive gain above 45 knots airspeed.  When Hover Trim is
selected in high-speed flight, the aircraft decreases velocity
at a moderately rapid pace initially, and then more slowly as
hover is approached.

LATERAL AXIS MECHANIZATION - Figure 23 shows a similar ground-
speed feedback and integral backdrive mechanization for the
lateral Hover Trim network.  L-24 logic switching controls the
mode.  This feedback begins to zero lateral velocity when the
aircraft has slowed to the point that groundspeed reference
(as defined by Velocity Mode controlling logic) is being used.
A single gain level is incorporated in the lateral loop since
the mode is not required to operate at high speed.

During the HLH AFCS demonstration program, customer evaluation pilots typically found Hover Trim most useful for stabilizing the final segment of manually-executed IFR-type approach maneuvers. From a 500-foot-per-minute descent at around 80 knots, the Altitude Hold mode was employed first to level the flight path at 150 to 200 feet above the ground. The pilot then pitched the nose up to initiate a longitudinal deceleration. At approximately 25 knots, Hover Trim was engaged and the remainder of the approach was accomplished automatically.

## 2.2  NORTHROP FLIGHT SIMULATION

### 2.2.1  Summary

In 1973, two piloted simulator evaluations of proposed HLH AFCS
control laws and logic were conducted at the Northrop Flight
Simulation facility in Hawthorne, California.  Overall simula-
tion objectives were to:

- Refine control law and logic mechanization developed for
  demonstration on the 347 Flight Research Vehicle so as to
  minimize expensive and time-consuming hardware and soft-
  ware changes on the flight test program, and

- Ensure adequacy of vehicle handling qualities for meeting
  the requirements of the HLH mission through continued
  AFCS development.

The first simulation was accomplished in April on the LAS/WAVS
(large amplitude - wide angle visual) "big beam" simulator
illustrated at the top of Figure 92.  The principal purpose of
this testing was to evaluate basic SCAS performance throughout
the flight envelope from the pilot's cockpit flight station.
Hover Trim and Automatic Altitude Hold selectable mode fea-
tures were also looked at along with aircraft behavior result-
ing from simulated AFCS and DELS failures.

A second phase of testing was completed in late December and
utilized the Low Speed "Rotational" simulator (shown at the
bottom of Figure 92) to represent the rearward facing load
crewman's station.  Hover Hold control laws were explored in
conjunction with evaluations of the "Prototype" LCCC unit.

Separate comparisons of the finger/ball and grip-type LCC
controller configurations were also made by customer pilots
and engineering representatives.  Additional testing assessed
the effect of external loads on vehicle handling qualities with
the Hover Hold mode engaged.

The math model driving both simulations represented the 347
helicopter.  This full envelope "total force" model was exten-
sively checked out and validated against flight data in the
Vertol Hybrid Simulation Laboratory (and on the Nudge simulator),
prior to being programmed at Northrop.  AFCS modeling was accom-
plished with General Electric ICP-002 incremental digital com-
puters which were similar in principle to the ICP-733 models
used on the demonstration aircraft.

Major simulation results are summarized in Figures 92 and 93.
As shown on the first figure, 66 hours of productive piloted
flight simulation time were "flown" during the program.
Requirements for ease software control law modifications were

# FULL MANEUVERING MATH MODELS —
## COMPLETE AFCS FUNCTIONS

PILOT

LARGE AMPLITUDE/
WIDE ANGLE VISUAL
SIMULATOR

BEAM VERTICAL MOTION
± 10 FT AT COCKPIT

BEAM LATERAL
TRANSLATION
± 10 FT AT COCKPIT

PILOT HOURS 35
AFCS MODS
10 LOGIC
28 SOFTWARE

VISUAL HEMISPHERE
WITH PROJECTED SKY,
EARTH & MOUNTAINOUS HORIZON

BEAM

± 20
DEGREES
ROLL

± 20 DEGREES
YAW

± 20
DEGREES
PITCH

COCKPIT

ROTATIONAL/POINT
LIGHT SOURCE
SIMULATOR

LOAD-CONTROLLING CREWMAN

PILOT HOURS 31
AFCS MODS
5 LOGIC
20 SOFTWARE

HORIZONTAL FIELD OF VIEW
±100° FROM AIRCRAFT $\mathbb{C}_L$

-100°

POINT LIGHT SOURCE
DISPLAY PROJECTION
SYSTEM

$\mathbb{C}_L$

LCC CONTROLLER

100°

107° VERTICAL FIELD OF VIEW
30° ABOVE HORIZON
77° BELOW HORIZON

FIGURE 92.

# FLIGHT SIMULATION

278

NORTHROP FLIGHT SIMULATION

| Pilot Rating | Pilot/Copilot | Load Controlling Crewman | Aircraft Characteristics | Impact on the Pilot |
|---|---|---|---|---|
| 10 | | | Unable to Fly | Control will be lost during some portion of required operation |
| 9 | | | Major Deficiencies | Intense pilot compensation required to retain control |
| 8 | | | Major Deficiencies | Considerable pilot compensation required for control |
| 7 | | | Major Deficiencies | Adequate performance not attainable with maximum tolerable pilot compensation. Controllability not in question |
| 6 | | | Very Objectionable but Tolerable Shortcomings | Adequate performance requires extensive pilot compensation |
| 5 | | | Moderately Objectionable Shortcomings | Adequate performance requires considerable pilot compensation |
| 4 | | | Minor but Annoying Shortcomings | Desired performance requires moderate pilot compensation |
| 3 | | | Fair – Mildly Unpleasant | Minimal pilot compensation required for desired performance |
| 2 | | | Good – Desirable | Pilot compensation not a factor for desired performance |
| 1 | | | Excellent – Highly Desirable | Pilot compensation not a factor for desired performance |

Pulse and Step Response | Trimability | Velocity Reference Switch | Lateral Reversals | Turns in Winds | Control Gradients | Altitude Hold | Position Acquisition and Hold | Load Shuttle

*Based on Cooper-Harper Handling Qualities Rating Scale (NASA TND-5153) and definitions in accordance with AR 310-75

FIGURE 93. PILOT RATING OF HANDLING QUALITIES WITH HLH CONTROL SYSTEM NORTHROP FLIGHT SIMULATION

identified in Phase I testing, and 20 in the Phase II.  A
total of 15 logic changes were also identified.  These logic
revisions were of particular importance because of the diffi-
culty associated with modifying the "hard wired" logic modules
on the 347 flight test aircraft after they were once installed.

A summary assessment of handling qualities with the final AFCS
control laws programmed in the simulation is presented in
Figure 93.  Pilot Cooper-Harper ratings of between 1.0 and 2.0
(in the desirable to highly desirable range) were achieved
for virtually all test maneuvers with the AFCS engaged.  Simu-
lated triplex AFCS computer hardover failures were found to be
readily recoverable, as were DELS failures for the 347 demon-
strator with reversion to the Mechanical Backup Units.

Both simulations were considered by pilot evaluators to repre-
sent a high level of fidelity in reproducing expected aircraft
and control system characteristics.  As a direct result of
this, when the AFCS was finally evaluated on the 347 test air-
craft, pilot ratings of handling qualities were quite similar
to those found in the simulator the year before.

In the evaluation that follows, the Northrop simulation program
is discussed in three segments.  The first covers development
of the math model and simulator representations of the test
aircraft and control system (Section 2.2.2).  This description
is followed by a discussion of the Phase I full envelope SCAS
evaluation from the pilot's station (Section 2.2.3).  The load
crewman/LCCC Phase II simulation is reviewed last in Section
2.2.4.

## 2.2.2  Simulation Development

### 2.2.2.1  Mechanization and Validation of the Math Model

The math model used in both phases of the Northrop simulation
was developed in the Vertol Hybrid Simulation Laboratory dur-
ing 1971 and 1972.  A complete description of this model and
its Vertol computer mechanization is included in Vertol Docu-
ment D301-10148-1, titled "Full Flight Envelope Math Model for
347/HLH Control System Analyses - Control Document" (Reference
7).

A brief synopsis of the more important features of the model
is presented in this section of the report.
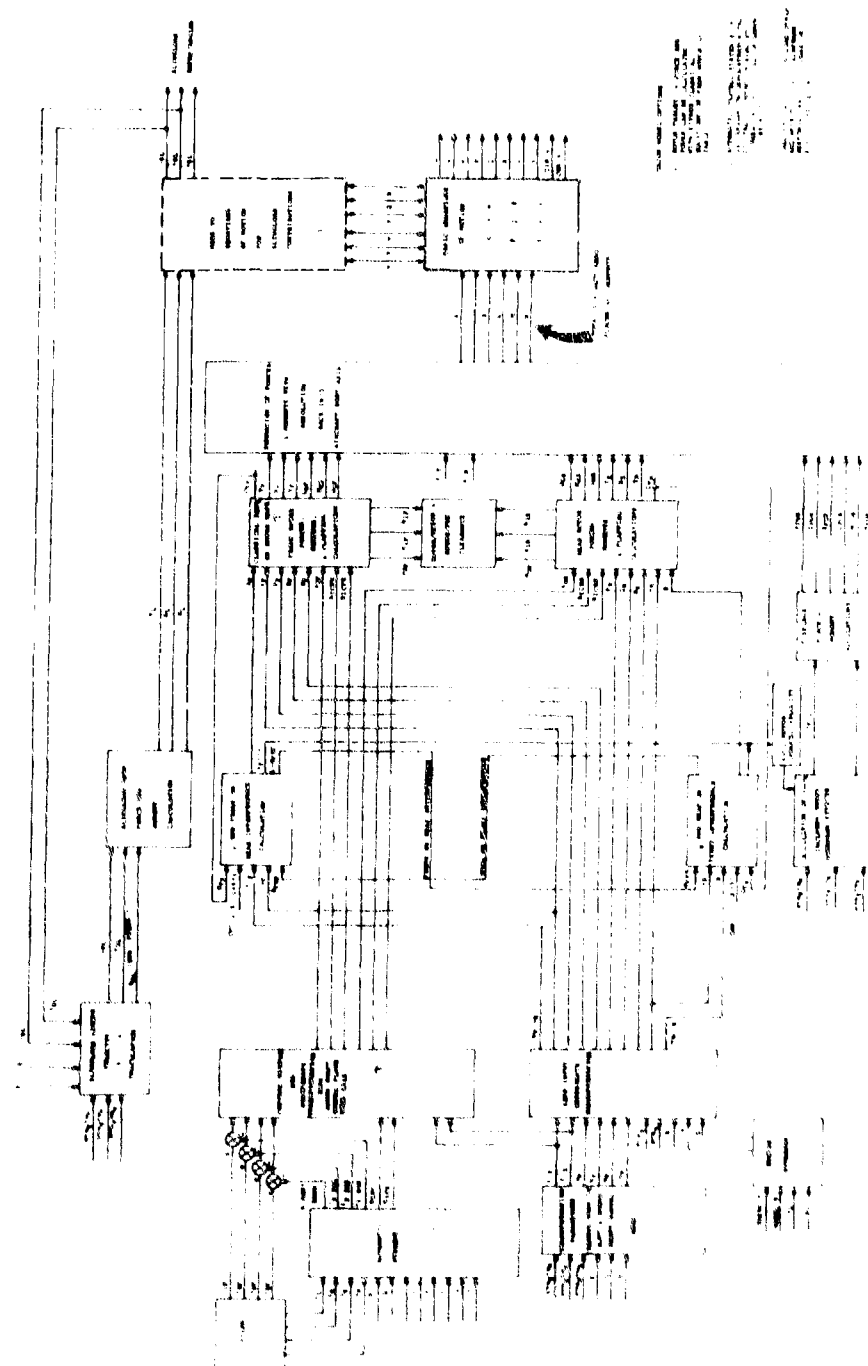
Figure 94. 347/HLH Tandem Helicopter Aircraft Mathematical Model

## 2.2.2.1.1  Math Model Features

AIRFRAME AND EQUATIONS OF MOTION - The total force tandem
helicopter airframe math model shown in Figure 94 (and de-
scribed in Reference 7) is based upon a set of six fully
coupled rigid body equations of motion.  These equations cal-
culate body axis linear and angular airframe accelerations from
a summation of rotor and fuselage forces and moments.  Accel-
erations are integrated, and then resolved to produce body and
rotor system linear and angular velocity components, and
fuselage Euler angle rotations.  Angle of attack and sideslip
values are computed next for both rotors and the fuselage.

These are used, in turn, along with rotor inflow and advance
ratio information (and control system inputs) to determine
rotor and fuselage forces and moments.  The forces and moments
are summed, resolved back into the aircraft body axis system,
and then the computational cycle again repeats itself with
calculation of the acceleration set.

Rotor forces and moments may be determined in two ways.  The
simplest utilizes classical theory to compute the six forces
and moments generated by each rotor.  A linear section lift
slope and parabolic drag variation is assumed in the classical
approach.  First harmonic flapping assumptions are also made
in the determination of coning and longitudinal or lateral
flapping.

An alternative (and more accurate) rotor solution involves the
use of pre-computed forces and moments in the form of "Rotor
Maps".  These maps are derived with a comprehensive rotor
analysis which considers the effects of compressibility and
stall.  Map data are expressed in the rotor wind axis, and are
stored in digital tabular form in the computers.

In addition to basic aircraft calculations, the equations of
motion also accommodate forces and moments produced by an
external sling load.  Two-point inverted-Y and -V suspension
systems may be used, and the effects of quasi-static load
ae dynamics can also be considered.

Other airframe math model features include the capability for
imposing either steady winds or a random gust sequence on the
helicopter.  An engine governor and rotor dynamic shaft system
is also modeled to provide a rotor speed degree of freedom
which can respond to changes in aerodynamic torque requirement
and engine power available.

CONTROL SYSTEM - A rather complete representation of the mechanical and automatic flight control systems is included in the simulation math model. Mechanical control runs from the cockpit to the rotor system are provided. Control mixing and upper boost dynamic characteristics are simulated as are interconnections for the 347 SAS or SCAS systems. Interfacing of the AFCS and DELS through a series of "frequency splitters" was modeled along with the dynamic characteristics of cockpit control backdrive actuator for each AFCS axis.

2.2.2.1.2 Mechanization and Validation of Simulation

VERTOL EFFORT - The math model just described and illustrated in Figure 94 was programmed at Vertol on four AD-4 analog computers coupled to an IBM 360-44 digital processor. Rotor maps and selected control systems or airframe functions were stored in twin BCA digital mini computers.

A "checkout" 347 SAS was mechanized on one of the AD-4 computers, and the HLH demonstration AFCS for the 347 in the 360-44. The AFCS control law model was programmed using the VECEX (Vector Execution) system, which permits control law "patching" in the digital computer, using techniques similar to those applied on an analog computer. AFCS logic was programmed on three AD-4 computer consoles.

Initial model validation consisted of comparing unpiloted trim, derivative, and dynamic response results (for both augmented and unaugmented flight conditions) with predicted data. Programs used to generate the validation predictions had previously been verified with flight test results.

When the simulation model checked against the theoretical predictions, a series of runs were made using actual control inputs generated in an earlier 347 flight test program. Helicopter responses, both with and without external sling loads attached, were checked against the flight results. An example of this simulation validation against test data is presented in Figure 95. Good correlation was shown to exist for virtually all test points compared.

In preparation for mechanizing the math model at Northrop, a decision was made to program the AFCS simulation model on two GE ICP-002 incremental computers at Vertol. The purpose of this was to provide familiarity in programming by using flight control computers similar to those that would be installed on
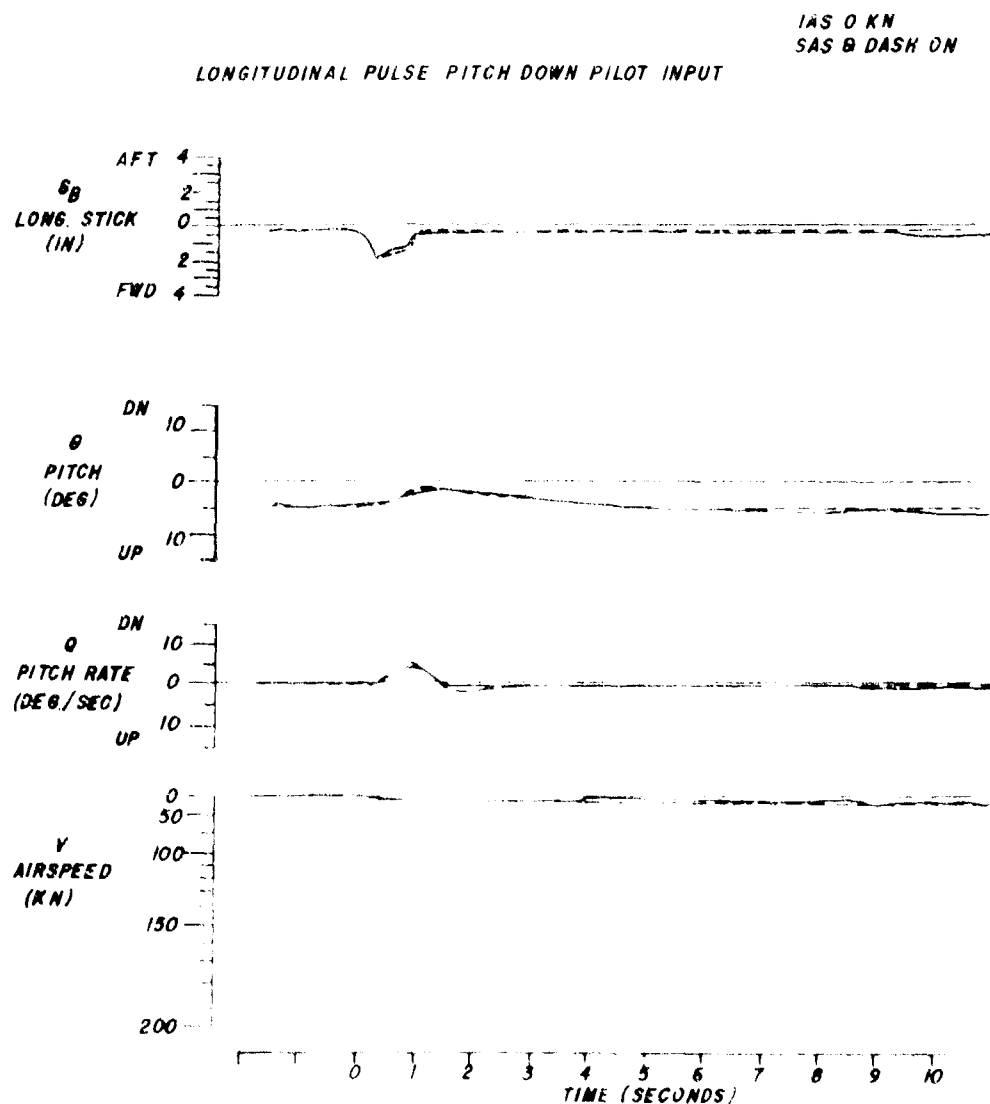
LONGITUDINAL PULSE PITCH DOWN PILOT INPUT



FIGURE 95 HYBRID MODEL VALIDATION WITH 347 FLIGHT TEST DATA

the 347 Flight Research Vehicle.  An additional objective was
to eliminate the necessity for programming the detailed AFCS
control laws on the Northrop computers, thereby saving a sub-
stantial amount of time and money at the contractor simulation
facility.

Unpiloted validations of the GE computer programmed control
laws were made against VECEX results by comparing aircraft
pulse control responses for both AFCS models.  Typical data
from this comparison are illustrated in Figure 96.
Correlation between the two AFCS modeling approaches is shown
in the figure.

As expected, the GE modeled AFCS produced aircraft responses
which were very slightly more damped than the VECEX associated
runs.  This characteristic was due to a substantially reduced
simulation time frame permitted by the incremental computers.
The lower time frame more closely approximated actual con-
ditions on the 347 test aircraft.

A limited Nudge simulator validation of the AFCS control laws
and logic was flown by Vertol pilots just before the GE com-
puters were shipped to Northrop.  Final AFCS updates were pro-
grammed at this time.

NORTHROP MATH MODEL MECHANIZATION AND CHECKOUT - The mechani-
cal control system and checkout AFCS math models were pro-
grammed on an EAI 8900 hybrid computer (consisting of Model
8400 digital and Model 8800 analog components), and on two
high-capacity Comcor 5000 analog computers.  A PDP-9B digital
minicomputer was used for rotor map storage.  These computers
were trunked together (and to the simulator) as shown in the
Figure 97 block diagram schematic.

AFCS logic was patched on the Model 8800 analog console.  A
small analog Comcor 175 computer was utilized to model the
cockpit longitudinal/lateral stick and rudder pedal force-feel
systems (and CCDA actuator characteristics) for the 347 air-
craft.  Another 175 provided motion monitoring capability for
the large amplitude simulator.  A third 175 analog was pro-
grammed with the Load Stabilization System control laws.

Motion and visual drive equations for both simulators were
programmed (in assembly code) on the EAI 8400 digital computer.
The LAS/WAVS drive equations were already in existence and
checked out when 347/HLH math model programming was started.

Drives for the rotational simulator, on the other hand, had to
be rederived and revalidated because of a requirement to pro-
gram them digitally, instead of using an analog computer as in
previous simulations.  The digital mechanization was dictated
by a lack of analog computing capacity at the facility, and

285
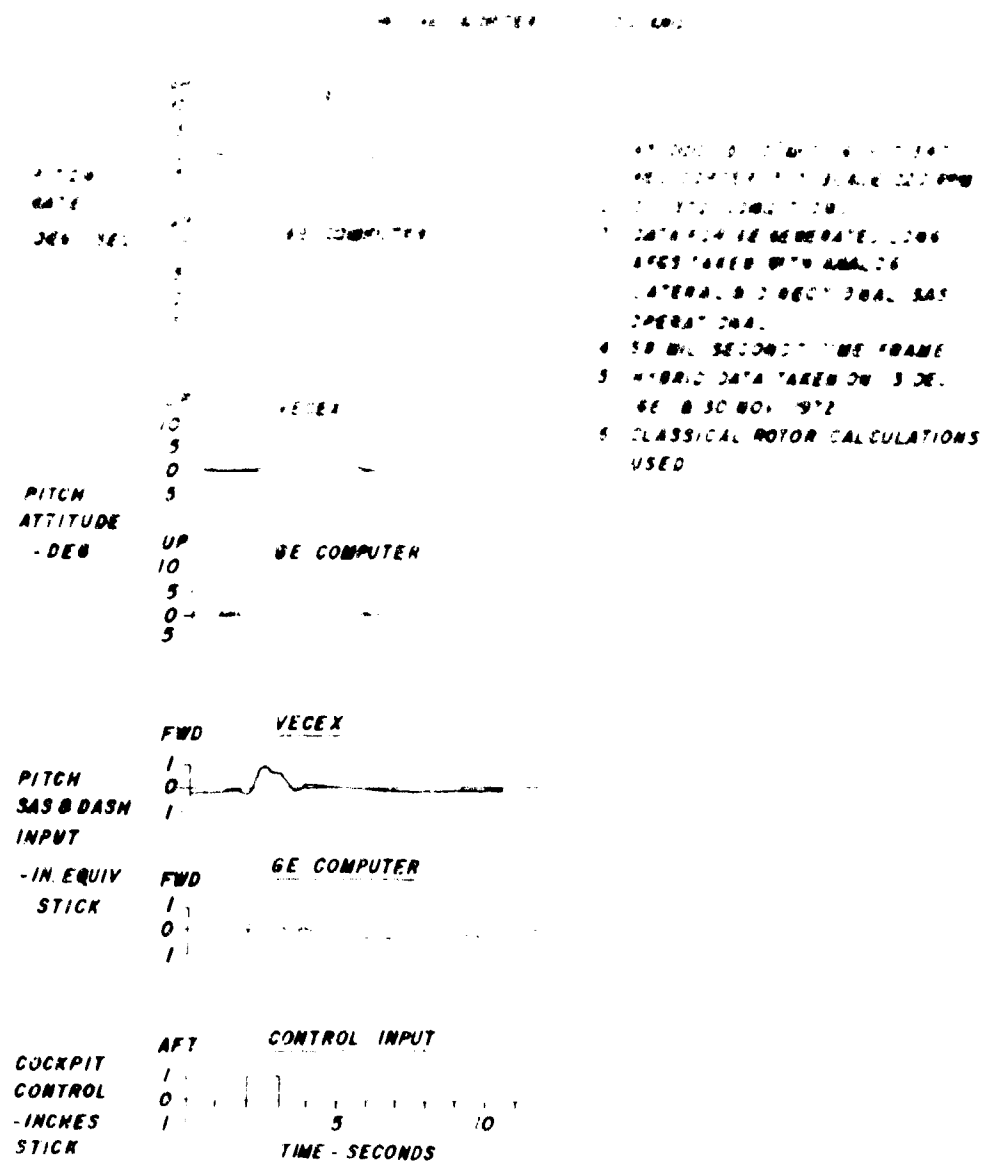
FIGURE 96. PITCH RESPONSE USING VECEX & GE. COMPUTER
GENERATED SAS INPUTS
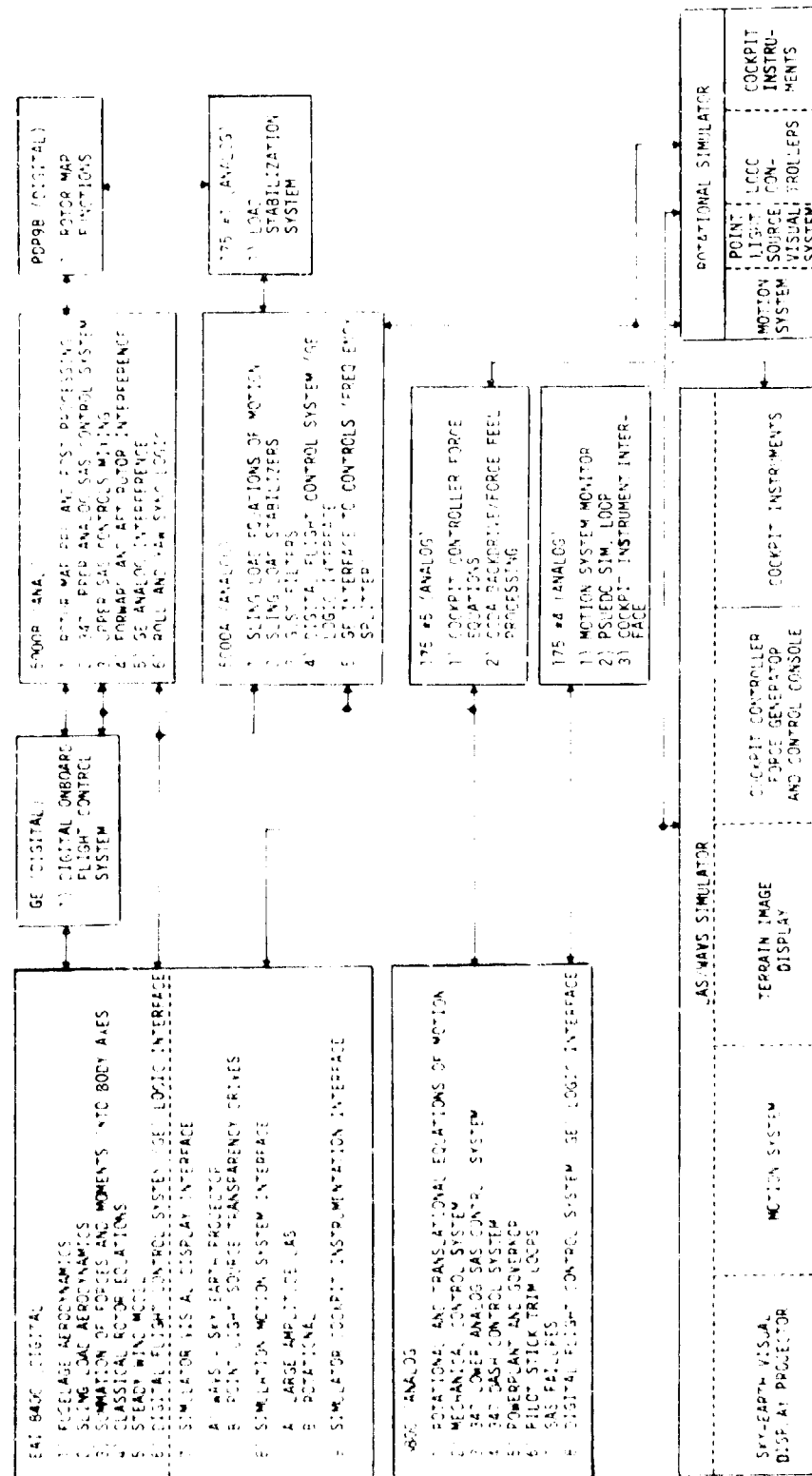
FIGURE 97. XCH-62F 347 HLH FLIGHT SIMULATION
COMPUTER/SIM LAYOUT

because the rearward facing load crewman orientation required several axis transformations which were more easily handled in the digital computer.

Validation of the math model at Northrop was accomplished in essentially the same manner as at Vertol. Also validated before the Phase I program were the cockpit stick and rudder pedal force feel and CCDA characteristics.

## 2.2.2.2  Simulator Description and Checkout

### 2.2.2.2.1  LAS/WAVS Phase I Simulation

The large amplitude Northrop five-degree-of-freedom simulator utilizes a cockpit module suspended on the end of a beam as shown in Figure 92. The cockpit is free to roll, pitch and yaw and move sidewards or up and down to emulate motion of the aircraft being simulated. No longitudinal translation capability is provided, but accelerations along this axis are simulated with cockpit postular tilt.

VISUAL DISPLAY -- The visual representation is generated for the pilot by projection of a sky-earth-mountain panorama on a spherical screen mounted around the cockpit module. This visual scene is adequate for VFR maneuvering throughout the cruise and low-speed range of the flight envelope. Precision hovering cannot be performed with accuracy, however, due to a lack of terrain detail. For this reason, testing was shifted to the Rotational simulator with its superior "point light source" visual system for the Phase II Hover Hold/LCCC simulation program.

MOTION DRIVES - The approach to motion simulation developed by Northrop and utilized in both simulators is described in depth in References 8 and 9. Basically, an attempt is made to create for the pilot an illusion of motion associated with flight which produces angular velocity and "specific force" sensations similar to those of the real world; without causing the simulator to "bottom" on its motion stops or to generate invalid force or velocity cues. Specific force is the apparent force at the pilot's station, and is the quantity felt when pressure is applied to the body surface or joints. It is defined in Reference 8 as the "sum of the vehicle's external forces divided by vehicle mass, less the gravitational components" (which the pilot does not normally perceive).

In the LAS motion drive mechanization, angular rate of the simulated aircraft is high pass filtered initially and is then integrated to form an attitude command for the cockpit. Prior to integration, specific force is added to the angular rate signal (in the form of longitudinal or lateral acceleration corrected for gravity) through use of a "coordinating" lead-lag circuit. The combined network attenuates the computed

288

aircraft attitude to an angle which results in the formation of correct steady state lateral and longitudinal accelerations using only gravity components (in the form of postural tilt). The "coordinating" circuit facilitates wide band specific force recovery, and at the same time, limits simulator travel because of the nature of its overall transfer function.

The rotational simulator motion drive mechanization is similar to the one just described, but it utilizes low-pass filters in place of the "coordinating" circuit. This first order filter minimizes the false angular velocity sensations accompanying rotation to an attitude which produces the desired preception of longitudinal and lateral acceleration.

COCKPIT SETUP - The simulator cockpit cab layout for the Phase I evaluation was configured to represent the right hand pilot's station in the 347 cockpit. A conventional arrangement of stick and pedals was included in the basic simulator cab, and the force feel characteristics for these controls were provided by a set of rotary hydraulic servo actuators mounted under the floor. The 347 breakout and linear force gradients (with hysteresis included) were simulated as were the mag brake and beep trim systems. CCDA backdrive actuator characteristics were also modeled.

The collective stick installed in the cockpit was a standard CH-47B component with electromechanical servo trim actuator and magnetic brake attached. This actuator was similar to the one used in the 347 aircraft during the HLH AFCS demonstration program.

The arrangement of the simulator panel instruments duplicated the right-hand quadrant and glare shield in the 347 Flight Research aircraft. Basic flight instruments, engine and rotor gauges, and special instrumentation associated with the HLH AFCS evaluation were installed on the panel. During the Phase I program, the following instrumentation was operational:

  Basic Flight Instruments

  - Airspeed, barometric altitude, vertical speed, radar altitude, turn and slip

  - ADI (attitude director indicator) and HSI (horizontal situation or heading indicator)

  Aircraft Instruments

  - Rotor speed, combined engine torque

289

HLH/347 AFCS Associated Instrumentation

- Longitudinal groundspeed (vertical strip indicator), lateral groundspeed (horizontal strip indicator)

- 347/HLH mode select panel

SIMULATOR CHECKOUT - All trunking to and from the simulator complex was checked to verify the signs of motion and visual drive signals, etc. Cockpit instrumentation was calibrated and exercised open loop, as were the various mechanical control force feel drives and CCDA actuator mechanizations. The force feel/mag brake system was verified by a Vertol test pilot to ensure characteristics similar to those on the 347 aircraft. Beep trim motoring of the sticks was also validated.

2.2.2.2.2   Low-Speed Rotational Phase II Simulation

The rotational flight simulator is a five-degree-of-freedom device which provides pitch, roll, and yaw angular motions along with capability for limited vertical and longitudinal movement. No lateral translation is incorporated in the motion base, but lateral accelerations are simulated with postular tilt as described in the previous section.

MOTION DRIVES - The primary servo drive actuators for the simulator cockpit cab are arranged in pairs with two oriented horizontally and two vertically. A separate actuator system rotates the cab about its Y-Y axis to provide pitching motion.

Rotation of the cockpit about its yaw axis is facilitated by differential operation of the horizontal actuators. Although these two actuators can be operated together to provide longitudinal X motion, this capability was not utilized during the Hover Hold simulation in order to preserve actuator authority for the yaw degree of freedom.

Rolling motion is developed by differential extension of the vertical actuators. A small amount of simultaneous vertical actuator travel is permitted to generate a vertical motion cue for the pilot. The vertical authority is deliberately maintained at a low level to prevent degradation of roll axis motion.

As indicated earlier, cab orientation for the Hover Hold Phase II simulation represented a rearward facing load crewman's station which is located substantially forward of and below the aircraft center of gravity. Correction terms were incorporated in the digital motion drive equations to account for the moment arms of the LCC cab.

POINT LIGHT SOURCE VISUAL DISPLAY - The visual display for the Rotational simulator is one of the most realistic available for low-speed and hover operations. It consists of a transparent terrain model mounted above the pilot's head, through which light from a very bright point source (located above the transparency) shines, to develop an image on a spherical screen. Figure 92 shows how the 200-by-107-degree screen is positioned relative to the cockpit cab.

Mechanical drives for the transparency are provided by a six-degree-of-freedom servo actuator complex which permits continuous rotation of the model (in the X-Y plane) during extended yaw maneuvering. The software equation drives for the visual display are set up to move or rotate the transparency in conjunction with cab motion, so as to produce the correct apparent aircraft attitude and location within the confines of the transparency visual field of view.

For the Hover Hold/LCCC simulation, a 750-to-1 scale model of an airport with surrounding countryside was utilized. A number of prominent features, such as runways, hangars, trucks, trees, etc. were simulated.

Because of the presence of these items, excellent visual peripheral cueing was available to the load crewman pilot for low-speed and hover maneuvering. The operational area available within the VFR range of the 750:1 transparency was approximately 1500 feet by 1500 feet (full scale), and altitudes up to 625 feet above the surface were usable.

COCKPIT CONFIGURATION - The rotational simulator cockpit was configured as a load crewman's station with the Phase I instrument and Mode Select panels installed for test purposes. Also provided on the left hand top side of the LCC panel was a CRT tracking scope which simulated the visual augmentation display on the demonstrator aircraft. Its purpose was to aid the simulation pilot in evaluating precision hover tracking and position hold tasks. The "inside out" fly-to horizontal display depicted a T-shaped target as if it were being viewed from a window in the bottom of the helicopter. A variable scale grid (representing $\pm$ 5, 50, or 500 feet) was superimposed on the CRT face along with simulated reference marks for the tracking exercises. Pilot selectable scale changes were made possible by turning a selector knob.

The prototype LCC controller (later used on the 347 flight program) was installed along with an adjustable arm rest. This is the finger/ball unit described in Section 2.1.4. For the BOA #12 tests, another controller was also installed for comparative evaluation with the finger/ball configuration. This four-axis, right-hand grip-type controller (known as the mockup LCCC) was configured with a thumb yoke for

proportional control of the vertical axis. It was used in an earlier LCCC design review at Vertol and was specially modified with rotary potentiometer transducers for the Northrop simulation.

A complete in depth description of both LCC units is presented in the BOA #12 report (Reference 10).

SIMULATOR CHECKOUT - To prepare the simulator for the Phase II program, a comprehensive calibration and frequency response test was performed on all motion and visual drive actuators. Actuator servo valves and feedback transducers were overhauled as necessary, and special actuator compensation networks were developed and validated to ensure motion and visual drive fidelity.

Calibration tests with both LCC units installed in the cockpit were performed, as were open loop drive tests with the tracking scope. Normal testing of simulator trunking, including checks on the signs of analog signals and sense of logic discretes, etc., were carried out prior to piloted validation of the simulation.

## 2.2.3 Northrop Phase I 347/HLH AFCS Pilot's Simulation

Phase I simulation activities are described in four segments, including major program objectives, pre-test preparations, test program, and principal results.

### 2.2.3.1 Objectives

In addition to the general goals stated at the beginning of this section, a number of specific objectives were also set for each simulation phase. Detailed objectives adopted for the Phase I program are listed below:

(1) Optimize AFCS control law and logic concepts for the basic high- and low-speed SCAS (including determination of proper frequency splitter settings) to produce the desired level of handling qualities for the HLH mission.

(2) Conduct static and dynamic stability evaluations in all axes. Assess maneuverability and controllability with final control pickoff, beep trim, and "security blanket" settings incorporated.

292

(3) Refine and evaluate the following selectable modes
     and or automatic control features:

   ● Automatic Hover Trim

   ● Automatic Altitude Hold

   ● Velocity Mode Transfer Switching

   ● Ride Qualities at the Pilot's Station with the
     PHS Engaged

(4) Investigate aircraft transient behavior subsequent to
     the following types of simulated AFCS or DELS failure:

   ● AFCS Engagement and Disengagement

   ● Triplex AFCS Computer Hardovers (Individual and
     Multiple Axis)

   ● Reversion from DELS to Mechanical Backup Units

## 2.2.3.2  Pre-Test Preparations

A limited fixed-base checkout was run by Engineering and
Test Pilot personnel, where the sky/earth visual projection
system was operating along with the airframe and AFCS.
Visual drives were verified at this time.  Concurrent with
the fixed-base activity, calculations were performed using
Model 347 stability derivative data to define a preliminary
set of coefficients, gains, time constants, etc., for use
in the motion drive mechanization.

## 2.2.3.3  Phase I Test Program

The entire Phase I simulation test effort is outlined in
Table 9.  Detailed are the principal piloted and unpiloted
evaluations carried out to meet program objectives.  Eight
test flights were conducted over a period of 19 days, during
which time 34-1/4 hours of simulator flight time were
acquired.  In addition, 60 hours of nonpiloted testing were
accomplished to validate the math model and AFCS (as described
previously) before piloted testing started.  After commence-
ment of flight activities, an additional 11-1/2 hours of
nonpiloted computer evaluations were performed as the AFCS
was updated and refined.

293

TABLE 9. NORTHROP FULL FLIGHT ENVELOPE/LARGE MOTION BASE SIMULATION
PHASE I HLH AFCS PILOTED/NONPILOTED EVALUATION SUMMARY

| FLT NO. | DATE | NONPILOTED EVALUATION | SIMULATOR/ COMPUTER TIME | PILOTED EVALUATION | SIMULATOR FLIGHT TIME |
|---|---|---|---|---|---|
| | 3/22 TO 4/3 | GE/Airframe/AFCS/Simulator Integration & Checkout | 60 | | |
| 1 | 4/6 | Final AFCS Checkout with Fixed Base | 5 | Initial motion evaluation | 1 |
| 2 | 4/9 | | | ● Motion evaluation<br>● Preliminary AFCS checks | 4 |
| 3 | 4/12 | Motion study with & without simulator in loop | 3 | ● Final motion verification<br>● Studied AFCS backdrive of pilot controls | 4 |
| 4 | 4/13 | Nonpiloted study of AFCS backdrives with simulator in loop | 2 | Pulses & steps (all axes), lateral maneuvers & static trim, beep trims, auto hover trim | 3-3/4 |
| 5 | 4/14 | | | Lateral maneuvers & trim, altitude hold mode, auto hover trim, precision hover system. | 5-3/4 |

294

TABLE 9. (CONTINUED)

| FLT NO. | DATE | NONPILOTED EVALUATION | SIMULATOR/ COMPUTER TIME | PILOTED EVALUATION | SIMULATOR FLIGHT TIME |
|---|---|---|---|---|---|
| 6 | 4/18 | o Collective CCDA Frequency Response<br>o Altitude Hold Modifications | 1-1/2 | Lateral maneuvers to evaluate logic revisions & AFCS changes, altitude hold, longitudinal acceleration/deceleration, velocity mode transfers, beep trims, AFCS engage/ disengage, triplex failures | 4-1/2 |
| 7 | 4/24 | --- | --- | Pulses & steps (all axes) beep trims, velocity mode transfers, triplex failures lateral & directional pickoff optimization | 5-1/4 |
| 8 | 4/25 | --- | --- | Automatic hover trim, mechanical backup reversion failures, differential pulses and steps, precision hover system | 6 |
| | | TOTAL HOURS | 71-1/2 | TOTAL HOURS | 34-1/4 |

295

Portions of three flights were utilized at the start of the flight program to sort out motion drive problems. Simulator roll axis drive coefficients were modified several times to produce satisfactory response characteristics, and minor changes were made in other axes. Once a realistic simulation of aircraft motion was achieved, a static and dynamic stability evaluation of the basic 347 was made to compare with previous experience in this test aircraft.

Pilot comment indicated that a very realistic and representative model of the 347 helicopter existed in the simulation. The unaugmented roll rate damping was, however, felt to be lower than in the actual aircraft.

## 2.2.3.4 Principal Simulation Results

The preliminary evaluation phase of AFCS testing revealed a number of problems associated with operation of the high-speed limited roll attitude lateral stick gradient ("security blanket"), roll and yaw beep trim characteristics, and the altitude hold and hover trim selectable modes. Problem areas were quickly identified, and modifications to AFCS design parameters and logic were made to improve system performance based on pilot comments and ratings.

A summary of the changes required in each AFCS axis is given next. In general, reference to the four AFCS block diagrams presented earlier in the design analysis (Figures 14, 23, 28, and 30), will clarify the reasoning behind any control law and logic changes described. Although these diagrams represent the final flight test AFCS configuration, they are sufficiently close to those utilized in the simulation to be of value in understanding the system modifications.

## 2.2.3.4.1 AFCS Modifications

LONGITUDINAL AXIS

a. The low-speed LCP control schedule was phased in over a lower groundspeed region (25 to 40 knots). Hover gain was lowered to improve low-speed longitudinal response characteristics to pilot control inputs, and to prevent saturation of the authority limits.

296

b. Automatic hover trim acquisition control loops were modified to provide an acceptable deceleration rate and pitch attitude response during transition from high to low speed, and to minimize overshoot in groundspeed as the aircraft approaches hover.

c. Longitudinal stick feed forward gains were changed to provide an acceptable pitch attitude response when velocity feedbacks are off. The longitudinal stick gain, which was originally summed in before the track-store element, was eliminated and the entire amount added in after the track-store element.

LATERAL AXIS

a. Lateral velocity control gradient at low speed was increased to 53 knots/inch to improve harmony with the longitudinal velocity gradient.

b. Lateral control response at high speed was desensitized by reducing the lateral stick pickoff gain.

c. The parallel lateral control backdrive gain in the lateral velocity mode bias eliminator was reduced to satisfactorily backdrive at low airspeed. An additional path was also added to increase the backdrive gain at high airspeed.

d. Scheduled roll attitude gain (FLAD) was replaced with a fixed value gain (.05 inch/degree), to provide a constant 10.0-degree limitation to the roll attitude/ lateral stick gradient at high speed. (Note that the 10-degree limitation was reduced to 5 degrees in the flight test program to improve sluggish rollout response characteristics.)

e. Logic L-43 was modified to provide acceptable operation of the lateral "security blanket" function over the entire high speed range. The position of the lateral stick reference synchronizer activated by the logic L-43 was also relocated to track the error difference between the lateral stick position and roll attitude response, rather than absolute stick position only.

This new mechanization improved the accuracy of the roll attitude/lateral stick relationship within the limited roll attitude gradient region, and resulted in smaller deviations from reference roll attitude when the aircraft was allowed to retrim after release of

297

lateral control forces. Figure 98 shows the improved L-43 logic. Figure 99 illustrates a typical roll maneuver time history with the revised logic, where the pilot stabilizes at a roll attitude without retrimming the stick forces, and then releases the stick to return it to a zero force reference condition.

f. Bank Angle Synchronization L-3 logic was changed to provide differential roll attitude beep capability past the 10.0-degree limited roll attitude gradient region. Prior to the change, the bank angle synchronization loop latched in a "sync" condition and prevented roll attitude beep trimming outside the 10.0-degree limited roll attitude control gradient region. Figure 98 shows the revised L-3 logic at the top. A time history showing lateral beep trim characteristics after the logic change is presented in Figure 100. In addition to the logic modification, the differential roll attitude beep trim rate was increased to 3.2 degrees/second.

g. Transient-free switching of the lateral velocity reference when accelerating with the lateral stick in detent at steady bank angle required the addition of a velocity mode change discrete to L-3 logic. The one-shot discrete forces the bank angle synchronizer into a stabilize condition when switching from a groundspeed to airspeed reference and causes the bank angle to hold throughout the transition. Figure 98 shows the additional discrete added to the L-3 logic network.

DIRECTIONAL AXIS

a. Directional control response at low speed was desensitized by reducing the pedal pickoff gain by a factor of four.

b. Yaw acceleration response to parallel beep trim of the pedals was found unacceptable in low speed. A differential heading beep trim input to the heading hold synchronizer was found necessary to provide precise heading adjustments at low speed. A modification to the heading hold logic L-5 was also necessary to accomplish this function.

## L-3 BANK ANGLE SYNCHRONIZATION

GROUND CONTACT(L-I)
VELOCITY REFERENCE(QL 366)
COUPLED AUTO APPROACH/NAV GUIDANCE MODE
LATERAL AFCS ENGAGE — INV

OR → [SYNC BANK ANGLE]

LATERAL STICK OUT OF DETENT

DIFF ROLL ATTITUDE BEEP TRIM — INV

AND

AND

LAT STICK BEEP TRIM
CYCLIC MAG BRAKE DEPRESSED

AND

OR

IROLL RATEI >I O DEG/SEC
ROLL ATTITUDE THRESHOLD(IEI > .15)
VELOCITY REFERENCE MODE CHANGE [1] — INV

OR

AND

DIFF ROLL BEEP TRIM [1]
LAT STICK BEEP TRIM [1]

AND

(1) INDICATE CHANGE TO LOGIC

## L-43 LATERAL STICK REFERENCE SYNCHRONIZER (SECURITY BLANKET)

LATERAL STICK OUT OF DETENT
LATERAL STICK BEEP TRIM
CYCLIC MAG BRAKE

OR → INV → [OPERATE BANK ANGLE ERROR SIGNAL FROM REFERENCE]

IROLL ATTITUDEI > I.ODEG

AND
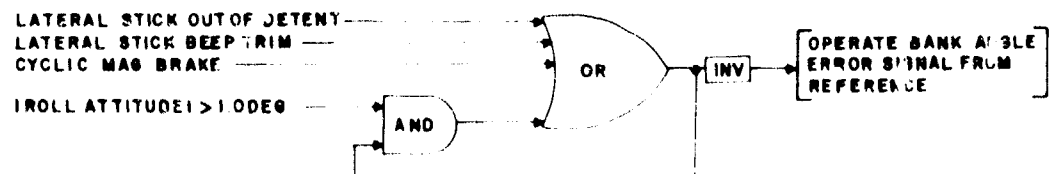
FIGURE 98.

HLH AFCS SIMULATION LOGIC RECOMMENDED REVISION

299
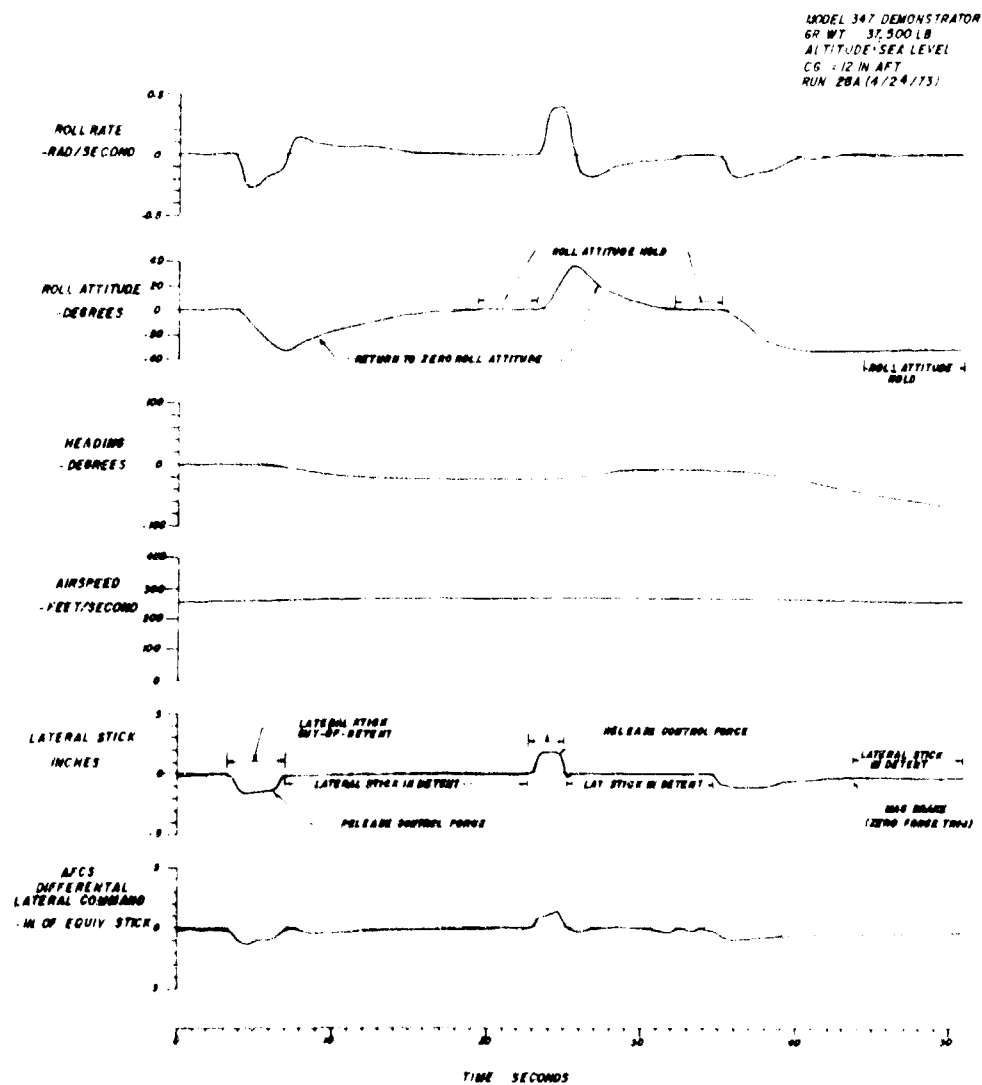
FIGURE 99.

HLH/ATC FLIGHT CONTROL / LARGE MOTION BASE SIMULATION

HIGH SPEED LATERAL RESPONSE CHARACTERISTICS

FIGURE 100.

HLH ATC FLIGHT CONTROL/LARGE MOTION BASE SIMULATION

HIGH SPEED FORWARD FLIGHT EFFECT ON TRIM CHARACTERISTICS

301
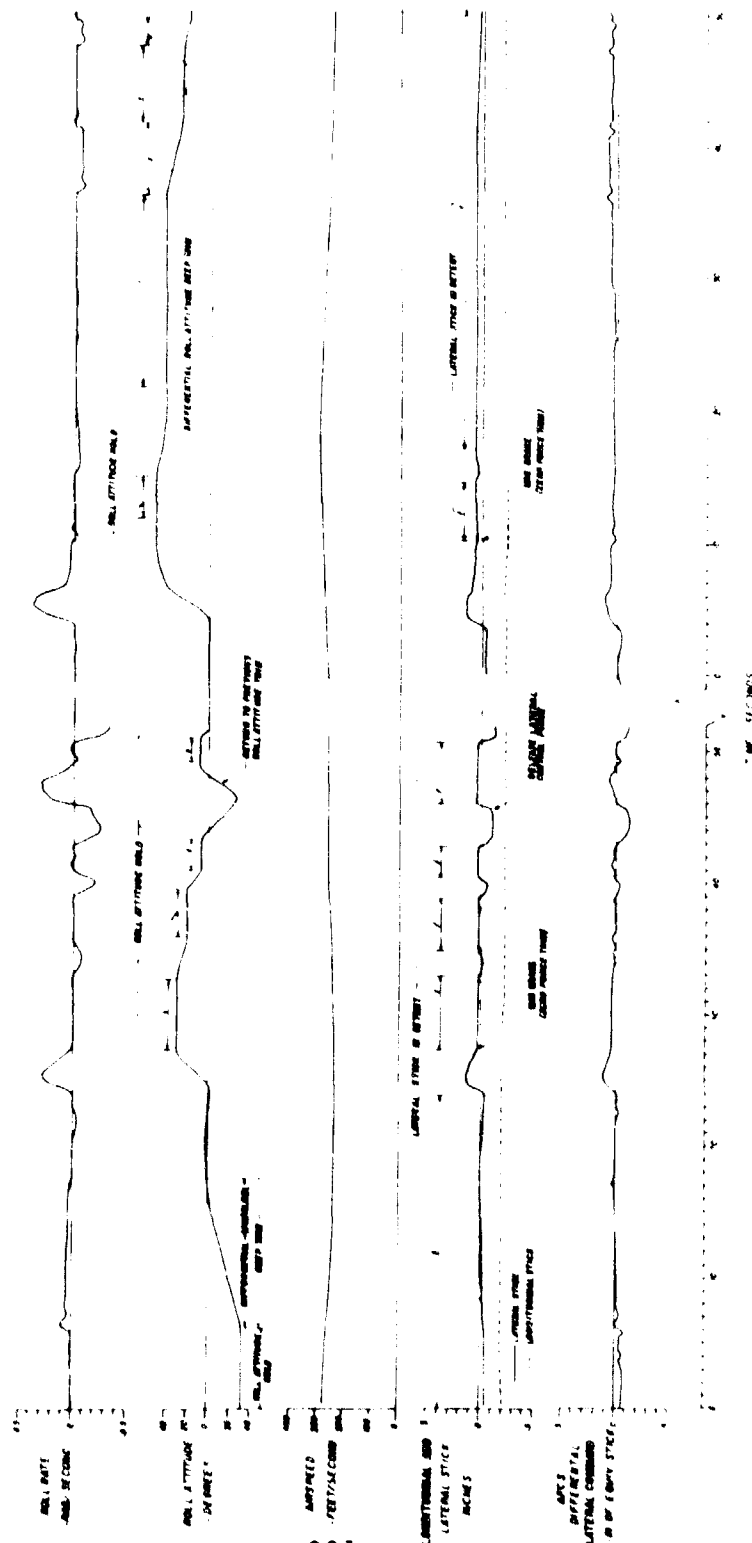
VERTICAL AXIS

a. The collective CCDA rate limit (0.66 inch/second) was found to be unacceptably slow to obtain a satisfactory altitude hold, particularly for the high gain radar mode. In addition, approximately 0.25 inches of dead zone in the collective actuator linkage allowed some drift and long-term limit cycle in the altitude response.

A differential output command path was added to the vertical AFCS to obtain an acceptable altitude hold mode. Also, the vertical acceleration gain was increased by a factor of four to provide additional vertical damping.

b. As a result of the Phase I simulation, further study of the vertical axis was indicated prior to the flight test program, to define limitations imposed by actuator dynamic response characteristics. Alternate gain, shaping, and differential authority configurations to improve the radar hold mode were to be evaluated.

2.2.3.4.2  Pilot Evaluation Results

Table 10 presents a pilot rating summary for tests and maneuvers flown with the final AFCS configuration. Virtually all pre-test handling qualities objectives were either met or exceeded, as indicated by the Cooper-Harper ratings given most maneuvers and control system features. The vertical axis/CCDA deficiencies identified in the simulation were analyzed and solutions were later proposed for the flight test program.

SIMULATED AFCS AND DELS FAILURES

Authority and rate limiter settings for the frequency splitters (described in Section 2.1.3.1.5) were developed during the AFCS preliminary evaluating test phase. In the latter part of the simulation, the effectiveness of these splitters for attenuating aircraft transient response resulting from AFCS hardover failures was evaluated.

TABLE 10.

PHASE I -- NORTHROP FULL FLIGHT ENVELOPE/
LARGE MOTION BASE SIMULATION

FLYING QUALITIES RATING SUMMARY

| Evaluation Items | Pilot Cooper-Harper Rating |
|---|---|
| (1) Pulse and step response characteristics (all axes)- well damped at all airspeeds. | 1.5-2.0 |
| (2) Beep rates and trimmability – capability for precise adjustment of aircraft pitch, roll, and yaw at all speeds | 1.0-1.5 |

|  | PITCH | ROLL | YAW |
|---|---|---|---|
| Low Speed – Parallel | Parallel | Differential Heading |
| High Speed -Parallel | Parallel ($\phi<10°$) Differential ($\phi>10°$) | Parallel |

| Evaluation Items | Pilot Cooper-Harper Rating |
|---|---|
| (3) Longitudinal Acceleration/Deceleration in headwinds and crosswinds – <br> (a) No unacceptable transients at velocity mode switchover. <br> (b) Backdrive of longitudinal and lateral control smooth and hard to detect. | 2.0 |
| (4) Lateral Reversals to bank angles of 60 degrees – No unacceptable characteristics. | 2.0 |
| (5) Turns in winds to 50 deg of bank angle – <br> (a) Small loss in airspeed <br> (b) Tight bank angle hold | 1.5-2.0 |

303

TABLE 10. (CONTINUED)

| Evaluation Items | Pilot Cooper-Harper Rating |
|---|---|
| (7) Longitudinal and lateral velocity control gradient at low airspeed (groundspeed reference) --<br>(a) Excellent low speed maneuvering characteristics.<br>(b) Good control harmony between axes | 1.5-2.0 |
| (8) Altitude hold in level flight, turns, and acceleration and deceleration maneuvers --<br>(a) Baro mode is satisfactory<br>(b) Radar mode requires more study due to nonlinear effects of collective actuator. | 2.0-3.0 |
| (9) Selectable Modes<br>(a) Airspeed -- Basic 347 characteristic acceptable.<br>(b) Velocity Disable/Decay -- Provides attitude control system and capability to ramp out velocity control bias.<br>(c) Automatic Hover Trim -- Mode acceptable, but has slow deceleration rate. | 1.5<br><br>3.0 |

Simulated triplex computer hardovers (in both directions) were introduced separately into each AFCS axis, and then in combination with one another. With the final frequency splitter authority limits incorporated, all failures were determined to be recoverable. A summary of failure types, and an estimate of delay time between the failure and initiation of pilot corrective action is presented in the table below.

| TYPE FAILURE | AXIS | FLIGHT CONDITION | DELAY TIME |
|---|---|---|---|
| Single Axis | Longitudinal | VFR @ 140 kn | 2 Seconds Nose-Up 1.5 Seconds Nose-Down |
| | Lateral Directional Vertical | VFR @ 165 kn VFR @ 145 kn VFR @ 165 kn | }>1 Second |
| Multiple Axis | All Combined | VFR & IFR @ 160/165 kn | }>1 Second |
| | Lateral (+) Opposite Directional | VFR & IFR @ 160/110 kn | |

In addition to AFCS hardover failures, DELS malfunctions were also simulated. For the initial fly-by-wire flight testing of the 347, a mechanical backup system was to be installed in the aircraft. In the event of a DELS failure, control was immediately transferred from the DELS to the mechanical backup units. Reversion to the MBU while flying on basic aircraft (AFCS not engaged) was simulated at the end of the Phase I Program with a variable length differential control step input. Recovery from these simulated control reversions was found to be no problem.

Aircraft transients associated with AFCS engagement and disengagement were also determined to be mild when evaluated in the first simulation.

### 2.2.4  Phase II Load Crewman/LCCC Simulation

Discussion of the Phase II load-controlling crewman and LCCC simulation is organized like the Phase I writeup, with background and objectives, pre-test preparations, and test results reviewed.

#### 2.2.4.1  Background and Objectives

Objectives were to:

(1)  Evaluate hover hold control and stabilization laws for both the Hover Hold/PHS and IMU/Radar modes of operation.

- Assess the effects of Precision Hover Sensor physics on hover hold performance.

- Check pilot's station ride qualities for hover hold operations.

(2)  Evaluate the prototype LCCC with respect to meeting hover mission requirements with the hover hold mode engaged.

(3)  Compare the finger/ball (prototype) and "grip with thumb yoke" (mockup) LCCC controllers for performing VFR and IFR precision hover and load shuttle maneuvers (under separate BOA).

(4)  Evaluate load damping and position hold characteristics for the hover hold mode with the LSS engaged.

During final preparation for the hover hold simulation, a decision was made to eliminate precision hover ride qualities testing (at the pilot's station) in the LAS/WAVS simulator. This decision was based upon intermittent schedule conflict problems with Northrop in-house flight simulations, and on the necessity to concentrate maximum effort in bringing the rotational simulator up to an operational status. This simulator had not been utilized for serious simulation work in the two years preceeding the HLH program; and as a consequence, required extensive refurbishment, calibration, and updating of its motion and visual drive mechanizations before hover hold testing could start.

## 2.2.4.2 Pre-Test Preparations

The various tasks accomplished in bringing the math model up to date and refurbishing the simulator for the Phase II program are outlined in Table 11. In addition to the simulator and LCCC calibration and checkout procedures described in Section 2.2.2.2.2, a substantial effort was also directed toward reprogramming the GE computers for the updated hover hold control laws. Analog logic associated with this mode was also modified to reflect the final Vertol pre-test hover hold configuration.

Precision Hover Sensor modeling (as described in the hover hold design analysis) was programmed in the EAI 8400 Digital Computer, and checks were run to ensure its proper operation. Models of the Drift Clear and PHS-IMU velocity switching networks were also programmed and verified.

During the Phase I program (and followup Northrup/Vertol advanced tandem helicopter simulation flown in early summer), the external sling load model was programmed and validated with theoretical response predictions and flight test results. Load damping and position hold loops in the load stabilization system were also patched on a Comcor 175 analog computer and PDP-9B combination in preparation for Phase II testing.

Approximately 250 hours of unpiloted computer or simulator time were utilized in preparation for the Phase II simulation. A substantial portion of this time (115 hours) was utilized in updating simulator hardware and drive mechanizations for the motion base and visual systems.

## 2.2.4.3 Test Program

The principal activities conducted during piloted and un-piloted Hover Hold/LCCC evaluations are summarized in Table 11. Six test flights were made along with a preliminary validation checkout of the simulator and 347 aircraft model. A total of 31-1/4 simulator flight hours were flown in the test program, and approximately 38 hours of unpiloted compu-ting time were utilized after testing started for ongoing AFCS analysis, daily simulator checkouts, etc. The primary focus of the unpiloted AFCS work was to determine the effects of external sling load dynamics on the Hover Hold mode, and to check out the LSS model.

## TABLE 11.

SECOND PHASE NORTHROP FULL FLIGHT ENVELOPE/ROTATIONAL FLIGHT SIMULATION
HLH AFCS PILOTED AND NONPILOTED EVALUATION SUMMARY

| DATE | FLT NO. | NONPILOTED SIMULATION PREPARATION AND VALIDATION | SIMULATOR & COMPUTER UTIL HR | PILOTED EVALUATION | ROTATIONAL SIMULATOR FLT TIME |
|------|---------|---------------------------------------------------|------------------------------|---------------------|-------------------------------|
| 8/18 thru 9/29 | -- | Basic 347 simulation model & Task II logic refurbishment & revalidation. | 42 | | |
| 10/30 thru 11/9 | -- | Patching & open loop checkout of hover hold, PHS/LSS/LCCC logic & PHS sensor model. | 35 | | |
| 11/10 thru 11/15 | -- | Rotational simulator actuator calibration & testing to define compensation requirements. | | | |
| 11/9 | -- | Open-loop G.E. testing & final logic checks. | 10 | | |
| 11/10 thru 11/17 | -- | Closed-loop combined G.E. AFCS/347 airframe checkout. | 47 | | |
| 11/15 thru 12/5 | -- | Static/dynamic checkout of simulator motion and visual drive interface transformation and shaping networks. | 54 | | |
| 11/16 thru 12/6 | -- | Simulator/cockpit hardware checkout and final airframe/AFCS simulator interfacing. | 28 | | |

308

| DATE | FLT NO. | NONPILOTED SIMULATION PREPARATION AND VALIDATION | SIMULATOR & COMPUTER UTIL HR | PILOTED EVALUATION | ROTATIONAL SIMULATOR FLT TIME |
|---|---|---|---|---|---|
| 12/6 | X-0 | | | Evaluation of motion & visual cues with final 347 aircraft validation. | 1.5 |
| 12/7 | X-1 | Closed-loop airframe/AFCS dynamic checks with LCCC mounted in lab. | 3 | Initial hover hold/ "Prototype" LCCC evaluations using continuous and noncontinuous PHS sensor model – no –no turbulence. | 4.5 |
| 12/8 | X-2 | Daily airframe/AFCS setup and model revalidation. | 2 | Hover hold/PHS/"Prototype" LCCC evaluations with & without atmospheric turbulence & steady winds applied. Hover hold/IMU-Radar evaluation, including engagement study. Frequency splitter analysis. | 6.0 |
| 12/12 | X-3 | ●Daily setup/revalidation of simulation. ●Slingload math model checkout and validation. | 2  1 | ● PHS/Hover Hold/LCC optimization with turbulence/steady winds. ● Further frequency splitter assessment. | 3.5 |

| DATE | FLT NO. | NONPILOTED SIMULATION PREPARATION AND VALIDATION | SIMULATOR & COMPUTER UTIL HRS | PILOTED EVALUATION | ROTATIONAL SIMULATOR FLT TIME |
|---|---|---|---|---|---|
| | | • Basic pulse dynamics with & without frequency splitters. | 1 | • Evaluation of drift-clear function. | |
| | | • Drift-clear investigation. | 2 | • BOA LCC evaluation with prototype finger/ball controller using both visual reference & tracking scope–PHS engaged.<br>–2 pilot evaluators*<br>–3 engineering evaluators*<br>*Representing U.S.Army | 2.0 |
| 12/13 | X-4 | • Daily setup & revalidation of simulation. | 2.75 | • Continued Hover Hold PHS, Hover Hold/IMC, Prototype LCCC, frequency splitter & drift clear evaluations. | 3.5 |
| | | • Pulse dynamics with external load – basic G.E. AFCS also with PHS/Hover Hold engaged. | 2.0 | • Gust evaluation conducted with PHS engaged. | |
| | | • Removed prototype controller & installed mockup LCCC (calibrated mockup) for BOA. | 3.0 | • BOA mockup thumb/grip controller evaluation– PHS on:<br>–2 pilot evaluators*<br>–1 engineering/pilot evaluator*<br>*Representing U.S.Army | 2.0 |

310

| DATE | FLT NO. | NONPILOTED SIMULATION PREPARATION AND VALIDATION | SIMULATOR & COMPUTER UTIL HR. | PILOTED EVALUATION | ROTATIONAL SIMULATOR FLT TIME |
|---|---|---|---|---|---|
| 12/16 | X-5 | ● Daily setup & validation of simulation. | 2.75 | | |
| | | ● Baseline pulse dynamics with 7500-lb slingload (37,500-lb a/c)-No LSS<br>-Inverted-Y & -V load suspension (20-ft cable length).<br>-With & without PHS engaged. | 1.25 | | |
| | | ● Checkout of Load Stabilization System (LSS) initiated. | 6.0 | | |
| 12/18 | X-6 | ● Daily setup and model revalidation. | 2.75 | ● Optimization of Hover Hold/PHS & IMU/LCCC including:<br>-Assessment of LCCC input lags & reduced lateral sensitivity.<br>-Effect of external slingload (inverted Y & V type suspension).<br>-PHS engagement characteristics. | 4.5 |
| | | ● LSS model mechanization checkout completed for longitudinal & lateral axes. | 2.0 | ● BOA prototype LCC controller evaluation with 2d group of customer pilots - PHS on. | 1.5 |

| DATE | FLT NO. | NONPILOTED SIMULATION PREPARATION AND VALIDATION | SIMULATOR & COMPUTER FLT HR | PILOTED EVALUATION | ROTATIONAL SIMULATOR FLT TIME |
|---|---|---|---|---|---|
| | X-7 | • Basic step revalidation | 1.0 | -2 Pilot evaluators U.S. Army -1 Pilot evaluator,MIT | 1.5 |
| | | • Lateral & longitudinal LCCC input schedules plotted for old & revised values as programmed in G.E. | 3.0 | • Evaluation of lateral & longitudinal LCCC schedules with reduced velocity command threshold levels & increased sensitivity for small controller motion. | |
| | | • Mockup controller installed for BOA (Prototype LCCC removed). | .75 | • BOA mockup thumb/grip controller evaluation for 2nd group of pilots - PHS ON. -1 Pilot evaluator- U.S. Army -1 Pilot evaluator-MIT | .75 |

312

AFCS/Prototype LCCC Evaluation - On Flights 1 and 2, stability and controllability evaluations of the Hover Hold mode and prototype LCCC were made while using a continuous or "locked" PHS sensor. During the second flight, normal sensor locking and unlocking characteristics were introduced along with steady and turbulent wind conditions. Hover Hold/IMU maneuvers were accomplished, along with an analysis of the effects of differential output frequency splitter on hover hold performance.

Flight 3 continued the Hover Hold/PHS and IMU testing, and the drift clearing feature was assessed for the first time. Analysis of both Hover Hold modes continued on Flight 4 as shown in the table. On this flight, the effects of gusts on automatic hover hold performance with the PHS engaged were evaluated.

Flight 5 was an unpiloted assessment of external load performance with and without the two Hover Hold modes engaged. Extensive LSS checkouts were performed and this unpiloted analysis continued over into flight 6.

During the piloted portion of the sixth flight, two configurations of external slingloads were flown and evaluated. In addition, LCCC input lags and control sensitivities were adjusted to improve an aircraft control response. Controller sensitivity and threshold levels were further modified on Flight 7 to achieve harmonious control response characteristics.

BOA Controller Evaluation - Portions of Flights 3, 4, 6, and 7 were utilized by customer pilots and engineers to compare finger/ball and "grip" LCCC controller characteristics, while executing simulated VFR and IFR hover hold tracking and station keeping tasks. Table 12 summarizes the flight time for each participant (totaling about 6 hours) with the two candidate controllers. Customer evaluators "flew" the basic 347 with Hover Hold/PHS engaged (including a fully operational sensor).

Five pilots checked both controller configurations (illustrated in Figure 101) and three engineering evaluators assessed the finger/ball LCCC only. Evaluation tasks included:

● About 5 to 10 minutes of VFR familiarization maneu- euvers with the controller being evaluated, followed by practice precision tracking tasks between two "targets" superimposed on the tracking scope grid.

| TABLE 12.LCCC EVALUATORS AND SIMULATION FLIGHT TIME | | | |
|---|---|---|---|
| CUSTOMER EVALUATORS | PILOT DESIGNATION | CONTROLLER EVALUATION FLIGHT TIME ~ MINUTES | |
| | | FINGER/BALL PROTOTYPE | THUMB/GRIP MOCKUP |
| EXPERIMENTAL TEST PILOTS | | | |
| H. Chambers - AVSCOM | (A) | 45 | 20 |
| D. Simon - AMRDL | (B) | 40 | 50 |
| ENGINEER/PILOTS | | | |
| J. Terry - AMRDL | (C) | 15 | 40 |
| J. Dunbar - MIT | (D) | 25 | 10 |
| LINE ASSIGNED U.S. ARMY PILOT | | | |
| W. Gault - CW3,USA | (E) | 40 | 20 |
| ENGINEERING EVALUATORS | | | |
| F. Cappetta-AVSCOM | | 15 | - |
| J. Savage -AMRDL | | 10 | - |
| D. Hubble -AVSCOM | | 10 | - |
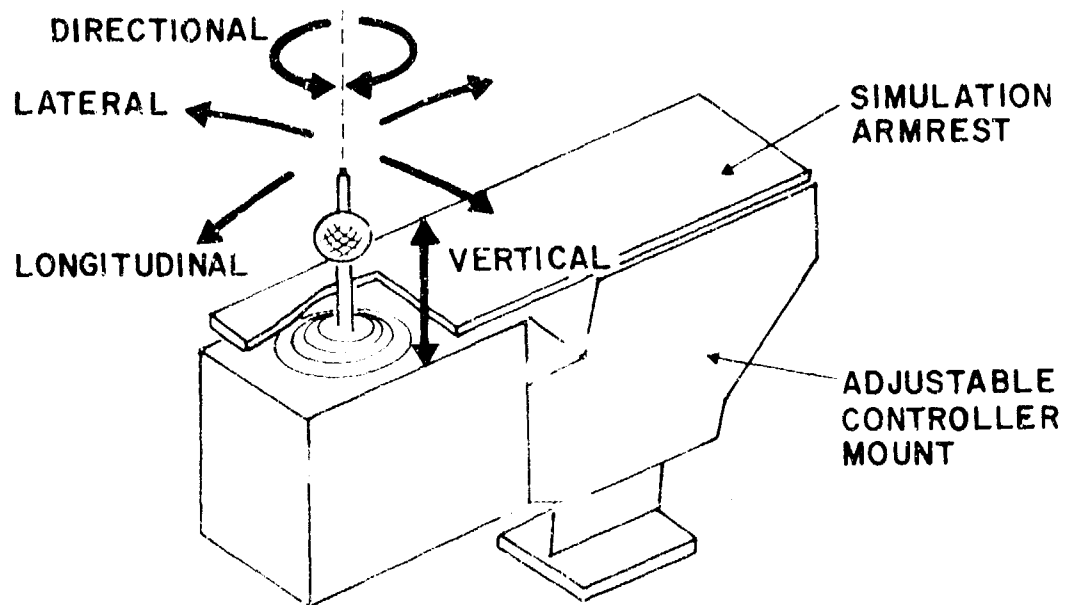
FINGER/BALL LCC "PROTOTYPE" CONTROLLER
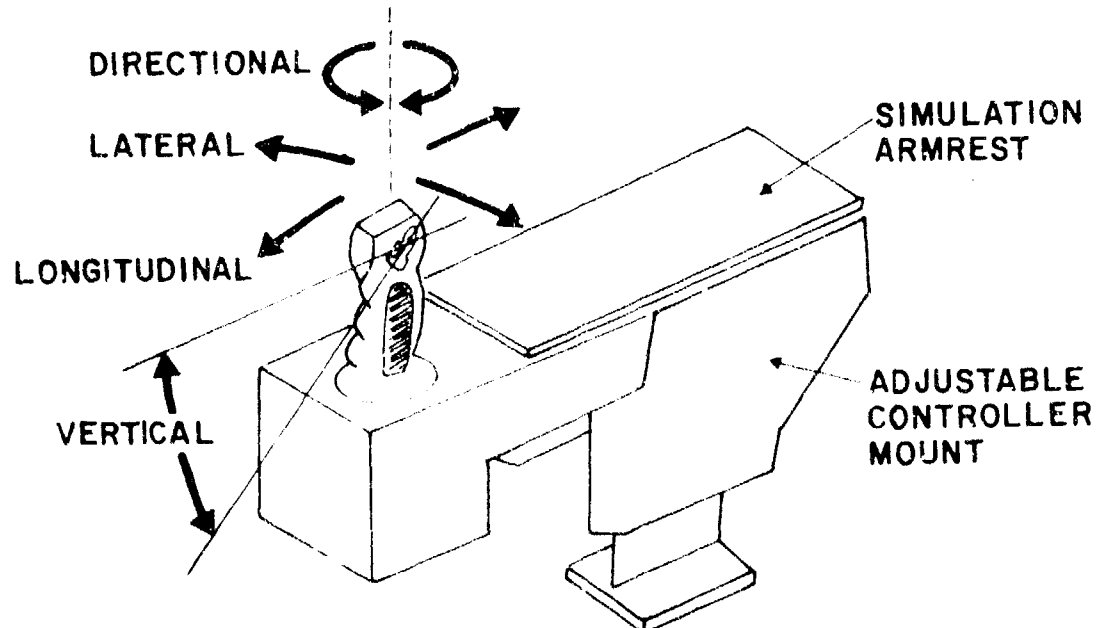
THUMB/GRIP LCC "MOCKUP" CONTROLLER

FIGURE 101.
LOAD-CONTROLLING CREWMAN CONTROLLERS USED
IN BOA EVALUATION

- A visual load shuttle maneuver was then executed, where the aircraft was translated VFR from the airport center to a helipad. Approaching the pad, a turn and descent were initiated, followed by visual hover over the pad, and by subsequent return to the center of the airdrome.

- Nearing the site where maneuvering began, the pilot transitioned from VFR to the tracking scope, at which time a precision acquisition and positioning maneuver was accomplished.

All maneuvers were performed in calm air, then with steady 25-knot winds, and finally with steady winds and a 5 fps RMS gust condition applied as time permitted.

Significant pilot comments regarding the controller being evaluated were recorded.

2.2.4.4  Results of the Phase II Simulation

In the second phase simulation, just as in the first, a number of AFCS control law and logic modifications were required in order to produce the desired level of handling qualities. Nearly all simulation objectives were success- fully achieved; especially those related to vehicle handling qualities with the hover hold mode engaged. Prototype LCCC performance was also highly rated with respect to accomplish- ment of the load shuttle or position hold LCC missions. Vehicle performance with external loads attached was adjudged to be satisfactory for the hover and shuttle tasks, but no piloted assessment of LSS characteristics was possible due to insufficient time available on the final simulator flight.

2.2.4.4.1  AFCS Modifications

Twenty software and five logic changes were developed and evaluated during the second simulation. A summary of the more important of these modifications is given below:

LONGITUDINAL AXIS

o  The longitudinal velocity error limiter (LX1) was opened to 1.0 degrees to improve longitudinal acceleration response for LCCC commands. (Reference to the indivi- dual axis AFCS block diagrams presented earlier in the design analysis will be helpful in assessing the impact of modifications discussed in this section.)

- Longitudinal and lateral LCC controller input command lags (TY5 and TY9) were reduced to 0.25 and 0.5 seconds respectively, so as to quicken response time for both small ("creep") and large ("leap") velocity inputs.

LATERAL AXIS

- The lateral parallel backdrive command path from the lateral velocity error signal was modified to correct an under-damped lateral response characteristic, particularly when making large and rapid LCC control reversals. The lateral response would get out of phase with LCC commands due to excessive motion of the primary cockpit control. This lateral LCC control deficiency was corrected by elimination of long term washout ($T_L6$) in the lateral differential command, and by limiting the integral backdrive signal using the LL3 limiter.

- Roll attitude and roll rate gains ($K_{LAD2}$ and $K_{LAR}$) were increased to reduce initial roll attitude response for small LCC controller commands, and also to soften the roll attitude response upon recovery to zero lateral velocity when the LCC controller is placed in the detent position.

DIRECTIONAL AXIS

- Yaw response was increased by elimination of the parallel command path ($KRLC = 0.0$), and removal of the washout ($T_{N8}$) in the differential command path. This change corrected the long-term reduction of yaw rate response caused by washout of the LCC differential command.

GENERAL

- Drift Clear (L-34)/Hover Hold (L-11) logic was modified to provide acceptable IMU drift clear operation when Hover Hold is engaged. It was necessary to input the Drift Clear logic discrete (L-34) into Hover Hold engage logic L-11 to momentarily disengage Hover Hold while drift clearing. Otherwise, the aircraft responds to the IMU synchronization transient and any controller out-of-detent command.

317

## CONTROLLER COMMAND SCHEDULING

- LCC velocity command functions in all axes ($F_{XLC}$, $F_{ZLC}$, $F_{LLC}$, $F_{NLC}$) were modified to reduce controller dead-band and velocity command threshold levels. The old pre-simulation velocity command functions (primarily in the longitudinal and lateral axes) were found to be unacceptable in the Hover Hold/IMU mode with only IMU velocity feedback, and no position hold engaged (PHS disabled).

  Reduction of controller deadband provided an increase in controller velocity response and quicker response time for small inputs. This enabled the LCC pilot to precisely maneuver the aircraft and hold a ground position without overcontrolling, particularly in gusty conditions. Figure 102 shows the original $F_{XLC}$ and $F_{LLC}$ velocity command functions, as well as the modified schedules synthesized in the simulation.

### 2.2.4.4.2 Pilot Handling Qualities Ratings

A complete tabular summary of pilot handling quality ratings for the Phase II simulation is given in Table 13. Two modes of operation were rated. The first of these includes precision position acquisition and hold maneuvering, using "beep" and "creep" controller commands and the tracking scope for positional reference. As shown in the table, when this type of task was accomplished with the PHS enabled, a rating of 0.5 was given the system to indicate superior performance.

Beneath the PHS score is a buildup of pilot ratings reflecting continued system improvement, as the simulation AFCS/LCCC design synthesis progressed for the Hover Hold/IMU mode. Note that a rating of 1.0 was finally possible after refinement of the control laws and LCCC scheduling. Very good Cooper/Harper ratings were also given for higher velocity reference maneuvering under VFR conditions, (both with and without a valid PHS).

It is interesting to note that Hover Hold/PHS performance was degraded only slightly when the aircraft picked up an external slingload. Scores for the slingload configured aircraft maneuvers are shown at the bottom of the Table.
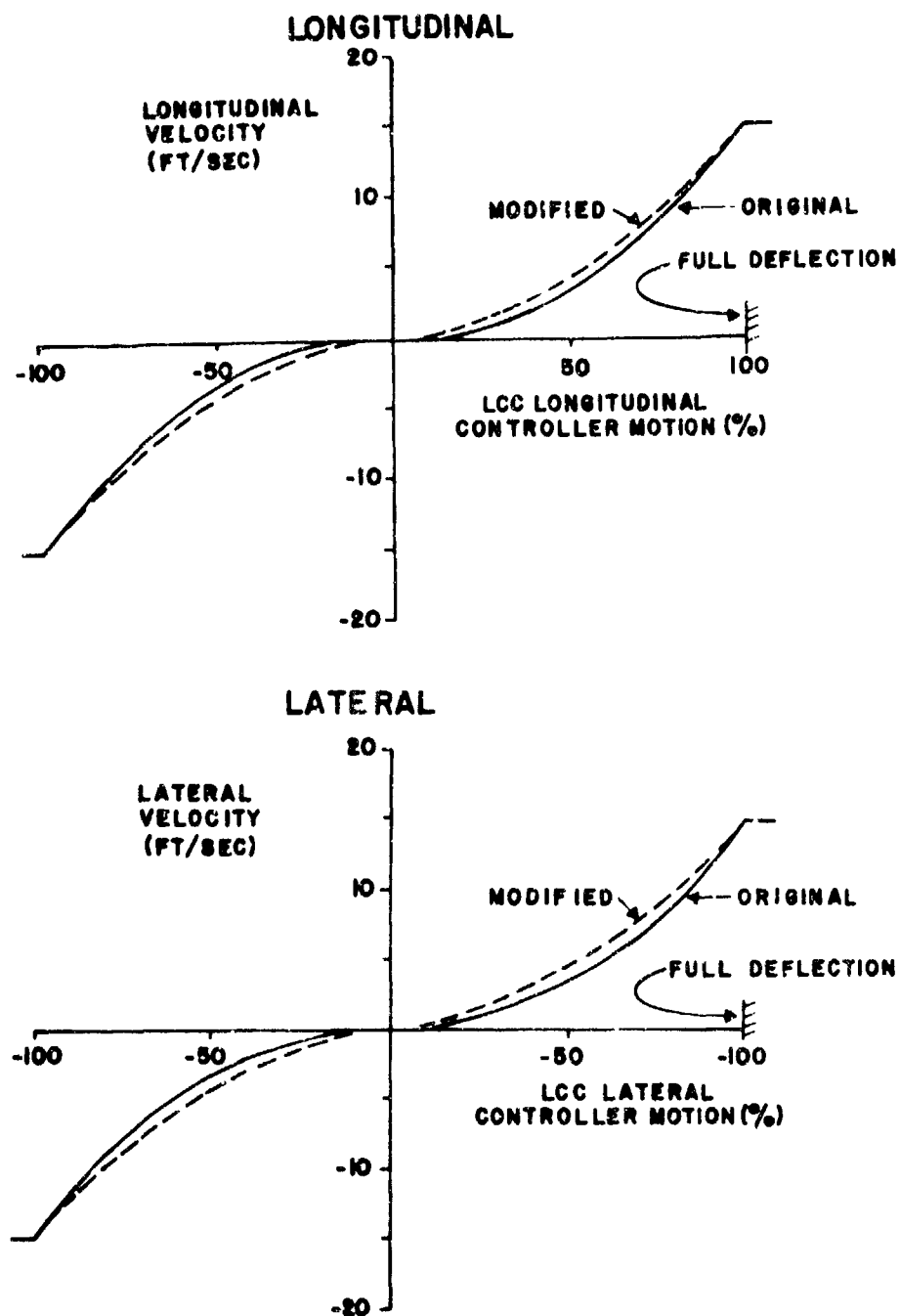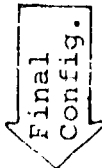
318

LONGITUDINAL



LATERAL



FIGURE 102.

LCC VELOCITY COMMAND FUNCTIONS

319

**TABLE 13. FLYING QUALITIES RATING SUMMARY – SECOND PHASE SIMULATION**

| AFCS OPERATING MODE | PILOT COOPER-HARPER RATINGS | |
| --- | --- | --- |
| | PRECISION POSITION ACQUISITION/HOLD "CREEP/BEEP" MANEUVER USING SCOPE | LOAD SHUTTLE NORMAL MANEUVERING MANEUVER USING VISUAL REFERENCE |
| - AIRCRAFT ONLY - | | |
| PHS ON (PRECISION HOVER SENSOR) | 0.5 | 1.0 to 2.0 |
| HOVER HOLD (IMU VELOCITY ONLY) | | |
| A. AS TESTED INITIALLY | | |
|   . In Calm Air | 2.0 | |
|   . With 5 FPS RMS Gust | 2.5 | |
| B. WITH IMPROVED LCCC INPUT SHAPING | | |
|   . 5 FPS Gust | 2.0 | |
| C. SAME AS B WITH REDUCED LCC INPUT THRESHOLDS | 1.5 | |
| D. SAME AS C WITH | | |
|   . Long./Lat.LCCC Input Sensitivity Reduced 20% | | |
|   . Increased Lat. Rate Damping & Attitude Gain | 1.0 ⇦ Final Config. | 1.0 to 2.0 |
| - AIRCRAFT PLUS SLINGLOAD - | | |
| PHS ON | 0.5 to 1.0 | 1.0 to 2.0 |

PILOTED FLIGHT TIME: 31 HOURS

AFCS MODS IDENTIFIED
20 Software
5 Modal Logic

### 2.2.4.4.3   BOA LCC Controller Evaluation Results

Results of the Basic Ordering Agreement controller comparison are summarized in Table 14.   Listed in the table are the principal LCCC features evaluated, and the types of tasks used to assess controller performance.   A synopsis of controller improvements suggested by the pilot evaluators is also included, along with an overall controller rating preference.

Based upon pilot evaluation comments, a consensus favoring the finger/ball configuration was expressed.   This conclusion substantiated earlier controller test results acquired during the Vertol Nudge Simulation in December 1972 (described in Hover Hold Key Developments, Section 2.1.4.2). Nearly all of the BOA LCCC evaluators preferred the finger/ball controller for precision target acquisition and hold maneuvering; and this is the flight mode around which HLH/347 LCCC design has been optimized.   A preference for the thumb yoke method of controlling vertical aircraft motion was also expressed.

While most of the evaluators stated that either controller would be acceptable, specific suggestions to improve various features of both were made.   Finger/ball suggestions included reduced yaw forces and adjusted vertical detent breakouts for improving control harmony.   These changes were incorporated in the unit before the 347 Flight Program, and the results as expected were very favorable.

BOA recommended modifications of the grip controller included addition of a mag-brake locking mechanism, and viscous dampers similar to those on the prototype finger/ball device.

## 2.3 HLH AFCS SYNTHESIS

### 2.3.1 Summary

The philosophy adopted in design of the HLH AFCS was to
develop a set of control law and logic mechanizations suitable
for meeting HLH mission requirements and goals, and then dem-
onstrate the validity of these laws on the 347 Flight Research
Aircraft. With the AFCS verified in flight test, the stabili-
ty and control concepts would then be directly transferable
to the HLH after minor modification of gains, time constants,
etc., to account for vehicle size and gross weight effects.

The analysis described in this section provides final sub-
stantiation that control concepts developed for, and demon-
strated on the 347, will provide the same superior handling
qualities when applied in the HLH aircraft.

Using the ATC full envelope Vertol Hybrid Simulation model
described in Section 2.2.2.1, an assessment of vehicle sta-
bility and controllability characteristics was made for the
HLH airframe and rotor dynamic system configuration. AFCS
control laws and logic were those developed earlier for the
347. Preliminary analysis indicated that HLH control sensi-
tivity and system gain levels should be about the same as
those used in the 347 program when both aircraft were flown
at their respective design weight conditions. Accordingly,
the HLH was evaluated at its design weight (118,000 pounds)
using 347 AFCS parameter values. The objective was to adjust
gain levels, etc., if required, in order to develop response
characteristics comparable to those of the 347. Very few
changes were necessary to produce the desired results.

Pulse and step responses in hover and forward flight were
generated for all axes of the basic SCAS. These runs were
made with and without the Automatic Altitude Hold mode
engaged. Transitions through the velocity mode transfer
switch were accomplished, and the effect of control back
driving was assessed. In addition, low-speed responses,
including external load dynamics and Load Stabilization System
characteristics, were also evaluated.

Comparison of unpiloted HLH simulation results with previous
347 data showed the effect of configuration to be minimal,
and the control concept directly transferable to the HLH
vehicle as expected.

### 2.3.2 Background

Original ATC AFCS development plans called for a piloted
simulation of the HLH aircraft. The simulation was to include
assessment of HLH handling qualities, and evaluation of a

323

variable Programmable Force-Feel Unit (PFFU) for the primary
cockpit controller. This PFFU was developed for the HLH
aircraft under a separate ATC program element to provide
maneuver cueing for the pilot.

Maneuver cueing requirements are strongly dependent upon the
stability and maneuverability characteristics of the aircraft
involved. Use of the variable force-feel approach to improve
apparent stability levels (e.g., bobweight effects); or to
improve response feel characteristics of nonconventional
controller qualities had been demonstrated successfully in
the past on other helicopters. Its application in the HLH
program would depend upon the results of handling quality
evaluations in the 347 ATC simulation and flight test programs.

As indicated in the previous report section, Northrop-piloted
simulation efforts in 1973 were highly successful in develop-
ing and validating the HLH concept of complete hands-off
stability, and linear velocity response characteristics for
the demonstrator aircraft. On the basis of the simulator
results, it was decided that a further piloted evaluation of
HLH handling qualities would not be required in view of having
already demonstrated the characteristics necessary for the
Heavy Lift AFCS.

The follow-on 347 flight program confirmed the favorable simu-
lation outcome, and permitted further refinement of AFCS SCAS
and selectable mode features. In addition, pilots commented
that the Model 347 fixed force-feel system (when used in con-
junction with the HLH control laws) was adequate for meeting
requirements of the Heavy Lift mission as had been anticipated
when requirements for PFFU simulation were dropped earlier.

The unpiloted HLH simulation analysis documented in this
section was substituted for the original piloted program in
order to assess vehicle size effects (if any), and AFCS
parameter settings.

2.3.3   HLH Math Model and AFCS Development

AIRFRAME AND ROTOR - Prior to starting analysis of the HLH
AFCS, the full envelope total force math model was updated
with HLH airframe and mechanical control characteristics.
Changes to the 347 model included:

● Incorporation of HLH parameters, such as rotor radius and
   solidity, cg moment arm relationships, rotor and fuse-
   lage inertia values, fuselage force and moment data, and
   longitudinal cyclic trim schedules for both rotors.

124

- Development, checkout, and programming of new rotor maps for both HLH rotors based on VR-7 and VR-8 airfoil technology. The effects of Mach number (compressibility), rotor stall, and unsteady lift aerodynamics were all considered in preparation of the map package. The available range of advance ratios extended from $\mu = 0$ (in hover to) $\mu = .5$ (in high-speed cruise).

- Development and incorporation of a simulated HLH engine and dynamic rotor shaft system model.

- Incorporation of HLH mechanical control mixing and integrated upper boost dynamic characteristics.

After configuring the math model with the HLH parameters mentioned above, a series of verification trim sweeps in level flight and climb were made, and then compared with predicted performance. Correlation was good as in the earlier 347 trim validation. A sample of the level-flight trim results is presented in Figures 103 through 108.

Plotted simulation trim data reflect an application of classical theory to the determination of rotor forces, moments and flapping. For comparative purposes, rotor map results are also shown in Figure 106 for the forward and aft rotor aero torque required. Improved high-speed correlation is shown for the map data, and this is due primarily to the more rigorous interpretation of nonlinear aerodynamic effects, such as rotor stall, compressibility, etc.

In addition to the trim comparisons just described, a series of stability derivatives were also generated with the simulation math model to further confirm its validity. These results compared favorably with expected performance.

325
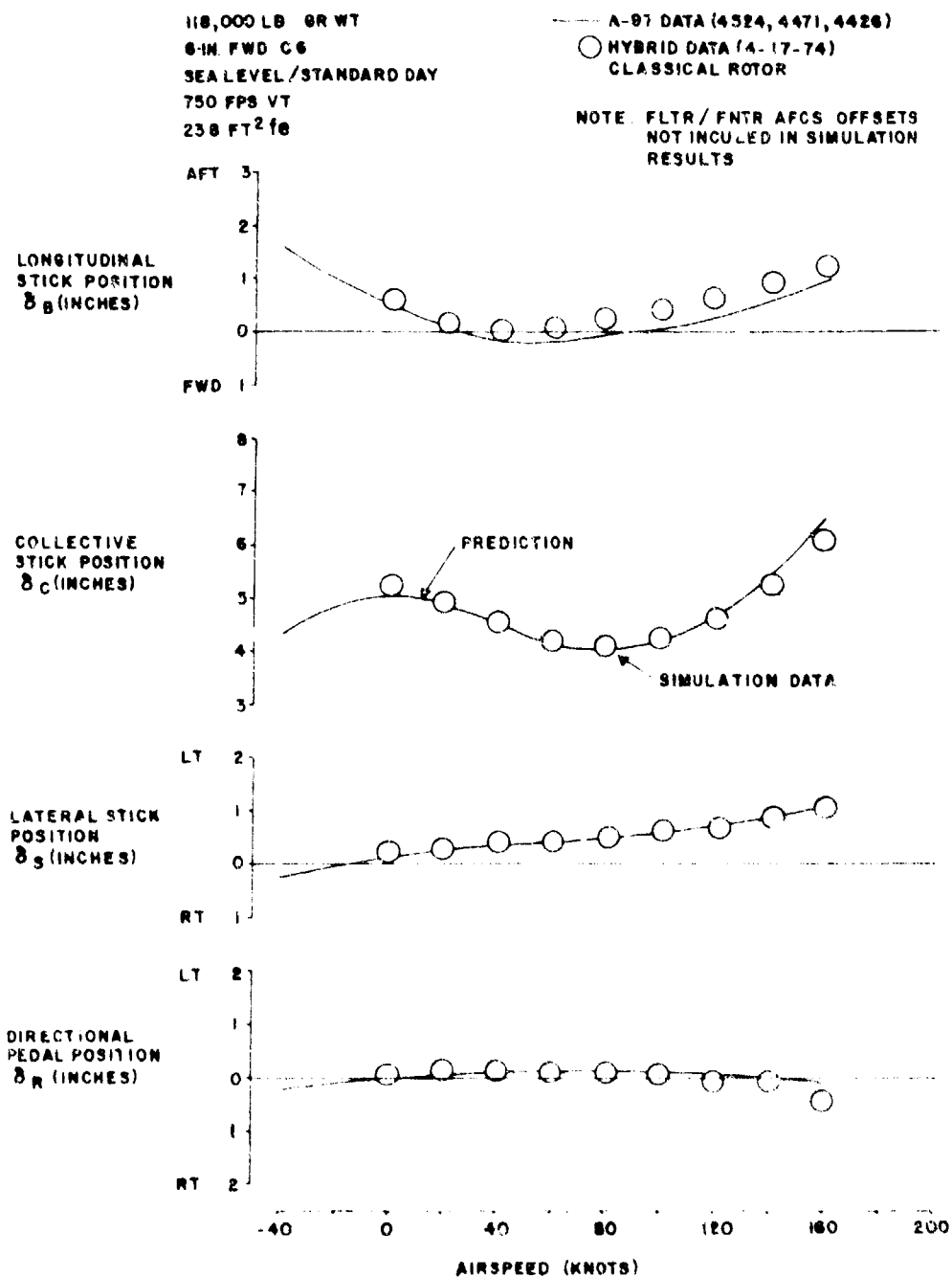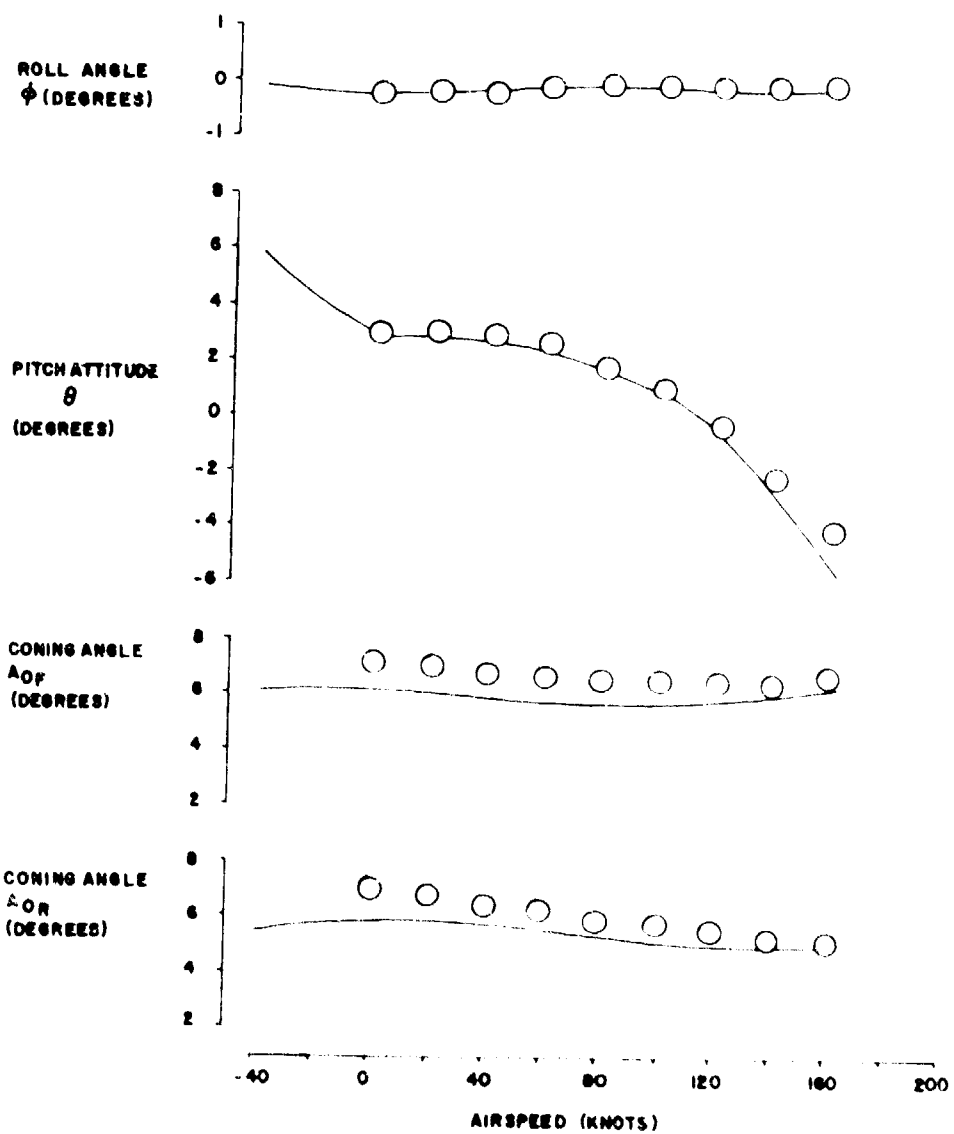
FIGURE 103. MODEL 301 HLH TRIM VALIDATION

118,000 LB  GR WT
6-IN. FWD C G
SEA LEVEL/STANDARD DAY
750 FPS VT
238 FT² fe

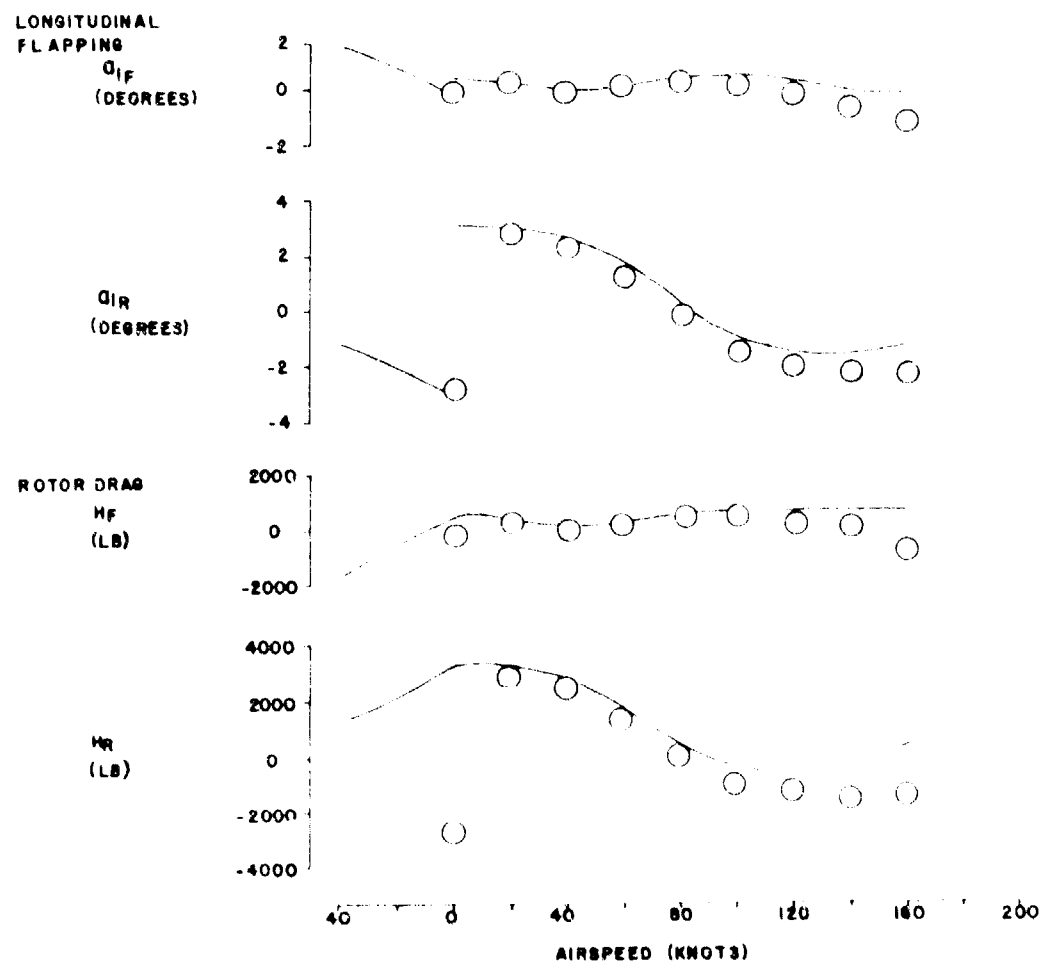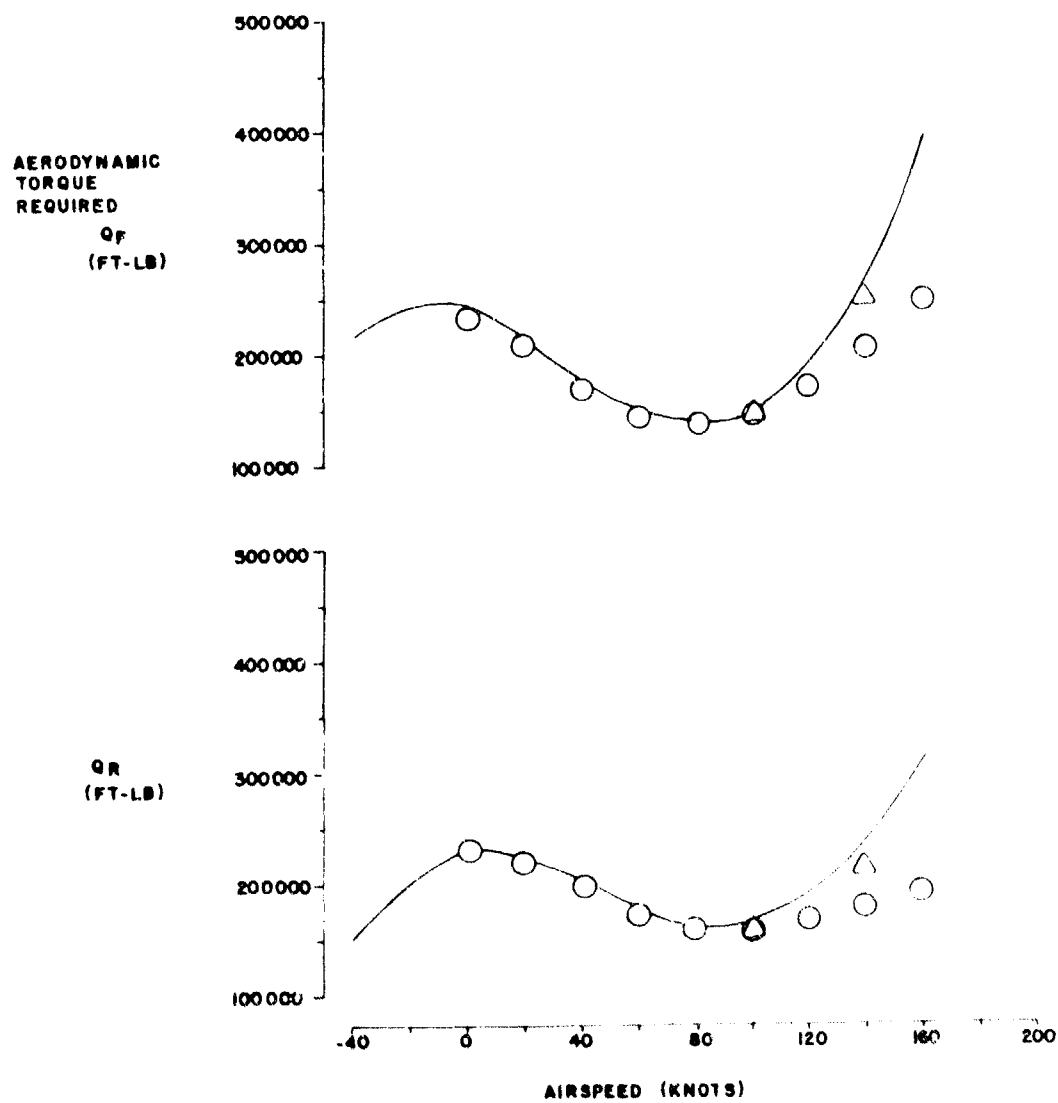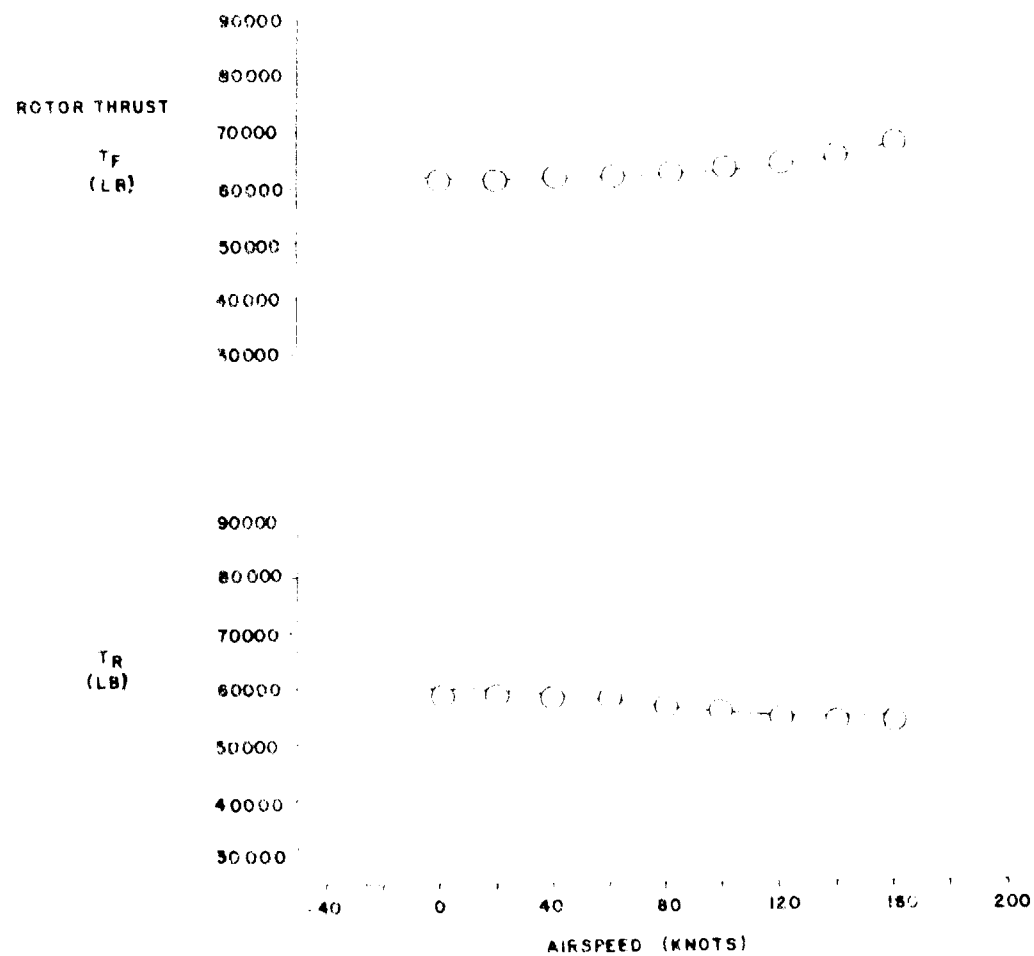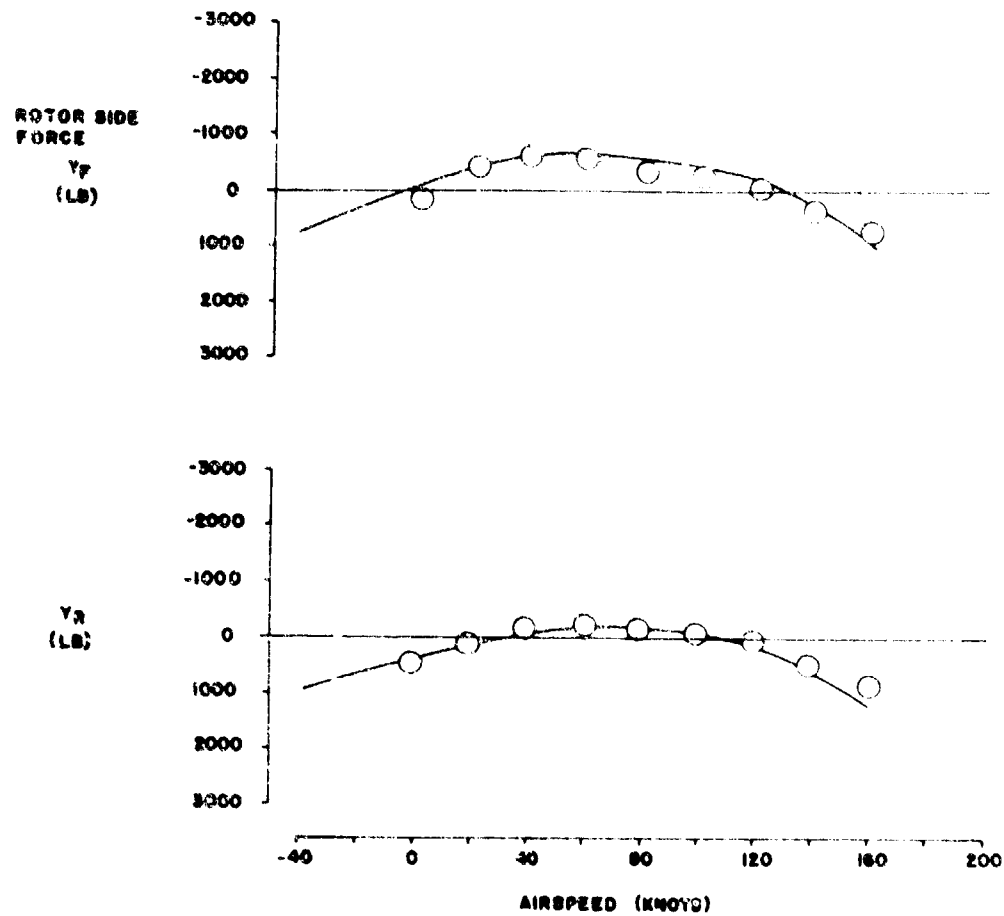A-97 DATA (4524,4471,4426)
HYBRID DATA (4- 17- 74)
CLASSICAL ROTOR

FIGURE 104.  MODEL 301 HLH TRIM VALIDATION

327

FIGURE 105. MODEL 301 HLH TRIM VALIDATION

FIGURE 106. MODEL 301 HLH TRIM VALIDATION

118,000 LB GR WT
6 IN FWD C G
SEA LEVEL/STANDARD DAY
750 FPS VT
238 FT² fe

-A-97 DATA (4524 4471, 4426)
( ) HYBRID DATA (4-17-74)
    CLASSICAL ROTOR

FIGURE 107  MODEL 301 HLH TRIM VALIDATION

330

FIGURE 108. MODEL 301 HLH TRIM VALIDATION

331

AFCS - Preliminary estimates of required HLH rate and attitude gain factors for the SCAS were made and these were then inserted into the simulation AFCS model to act as a starting point for the analysis. Assumptions in this preliminary work were that the desired HLH response frequencies (for the various longitudinal, lateral, directional and vertical modes) should be proportional to those on the 347, but factored down to reflect the lower HLH rotor operating speed (i.e., 23 radians/second for the 347 vs. 16 radians/second for the HLH). Desired damping levels were assumed to be identical to the 347 values. Required rate feedback gains for the lateral and directional axes (at vehicle design weight of 118,000 pounds) were estimated to be essentially unchanged from the 347, but the attitude gain requirement for the directional axis was reduced by about 1/3 from its 347 level. A lowered acceleration gain in the vertical axis was also indicated.

## 2.3.4 Results of Unpiloted HLH Hybrid Simulation Analysis

The principal objective of the HLH unpiloted hybrid simulation was to develop response data for this aircraft which closely resembled the characteristics of the 347. As indicated in the previous section, an attempt was made to duplicate the 347 damping levels with a slightly lower response frequency for the larger aircraft.

The only stability feedback gain changes required to produce the desired results were those discussed earlier. It is anticipated that minor modification of these (and other) gains, time constants, etc., will be required in the future to fine-tune the AFCS for installation in the Prototype or any potential production HLH aircraft. The basic control laws for these aircraft, however, are expected to remain essentially the same as those demonstrated on the 347.

A series of control pulses and steps in all axes were introduced into the HLH simulation model to evaluate aircraft controllability and stability. These control inputs were made with the cockpit sticks and pedals in order to include pick-off feedforward characteristics in the resulting aircraft response. Steps and pulses were run in high-speed cruise at 120 knots, and in hover with 5-knot winds. Typical HLH pulse and step responses are illustrated in Figures 109 through 116 along with comparable 347 runs based on the same control inputs.

Figures 109, 110, 111, and 112 compare stability response data for pulse inputs in the four control axes at 120 knots. Excellent correlation with the 347 baseline is shown for all cases. Attitude responses are virtually identical for both aircraft, and only minor variations in angular rate or SCAS input were observed. The effect of vehicle size on stability is minimal
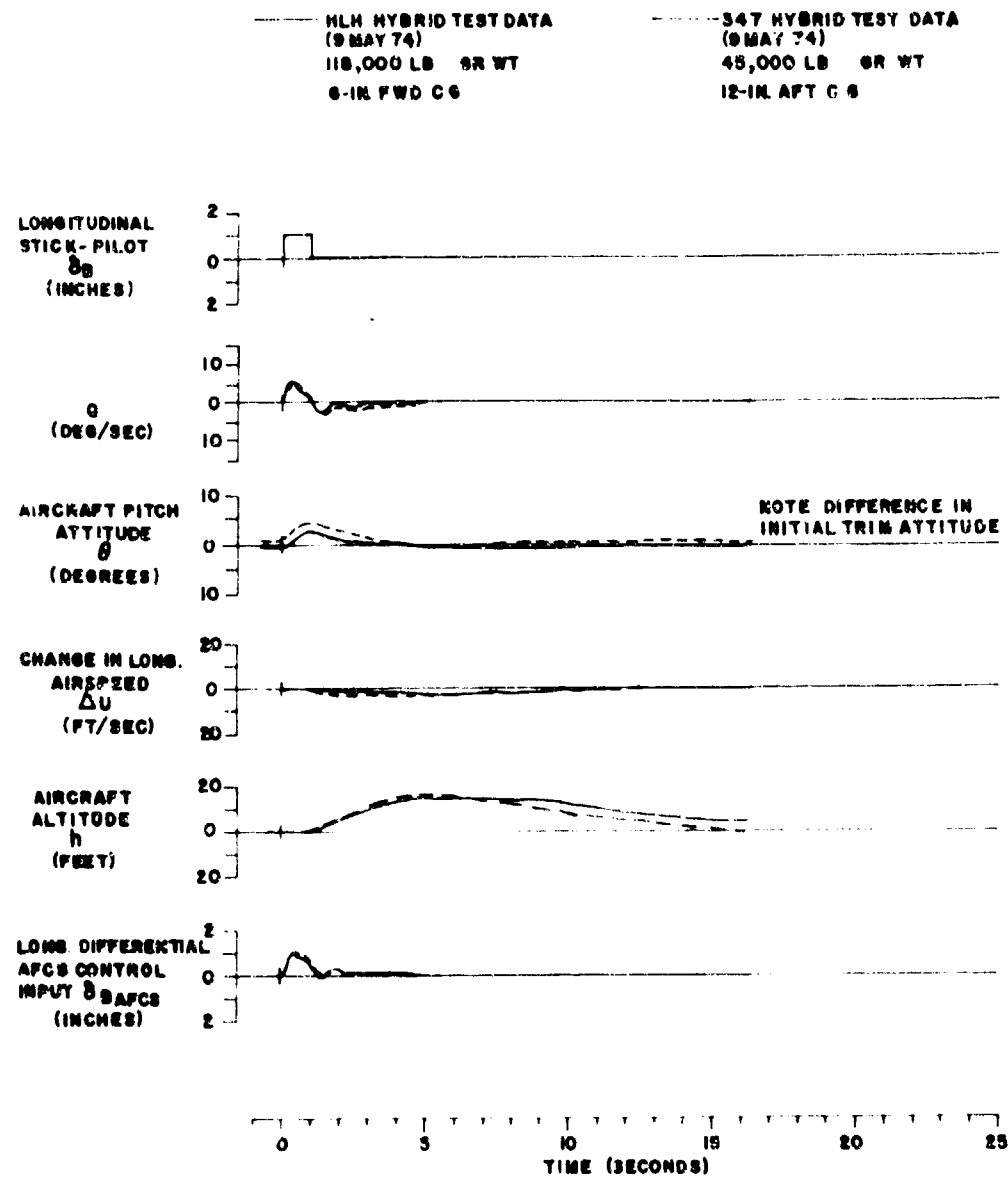
120 KNOTS - SEA LEVEL / STANDARD DAY - ALTITUDE HOLD OFF

---------- HLH HYBRID TEST DATA          --------- 347 HYBRID TEST DATA
(9 MAY 74)                                (9 MAY 74)
118,000 LB   GR WT                        45,000 LB    GR WT
6-IN FWD CG                               12-IN AFT CG



LONGITUDINAL
STICK- PILOT
$\delta_B$
(INCHES)

Q
(DEG/SEC)

AIRCRAFT PITCH
ATTITUDE
$\theta$
(DEGREES)

NOTE DIFFERENCE IN
INITIAL TRIM ATTITUDE

CHANGE IN LONG.
AIRSPEED
$\Delta u$
(FT/SEC)

AIRCRAFT
ALTITUDE
h
(FEET)

LONG. DIFFERENTIAL
AFCS CONTROL
INPUT $\delta_{BAFCS}$
(INCHES)

TIME (SECONDS)

FIGURE 109.
HLH RESPONSE TO PULSE
CONTROL INPUT - LONGITUDINAL AXIS

333

————— HLH HYBRID TEST DATA
(9 MAY 74)
118,000 LB   GR WT
6 IN. FWD  C G

— - — · 347 HYBRID TEST DATA
(9 MAY 74)
48,000 LB    GR WT
12 IN. AFT C G



**FIGURE. 110
HLH  RESPONSE TO PULSE
CONTROL INPUT - LATERAL AXIS**

120 KNOTS - SEA LEVEL / STANDARD DAY - ALTITUDE HOLD OFF

———— HLH HYBRID TEST DATA (9 MAY 74)    ————— 347 HYBRID TEST DATA (9 MAY 74)
118,000 LB   GR WT                        45,000 LB   GR WT
6-IN. FWD C G                             12 IN. AFT C G
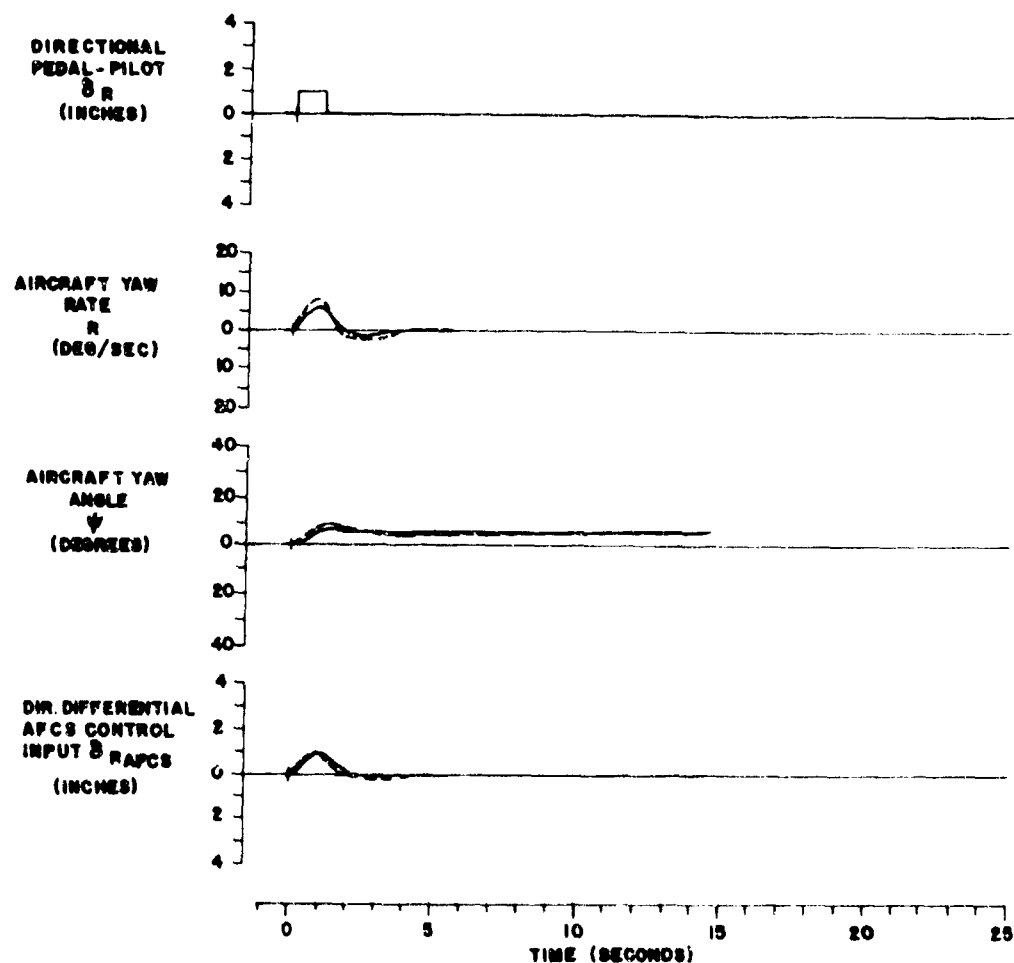
FIGURE 111.
HLH RESPONSE TO PULSE
CONTROL INPUT - DIRECTIONAL AXIS

335

120 KNOTS - SEA LEVEL/STANDARD DAY - ALTITUDE HOLD OFF

HLH HYBRID TEST DATA
(9 MAY 74)
119,000 LB  GR WT
6 IN. FWD C G

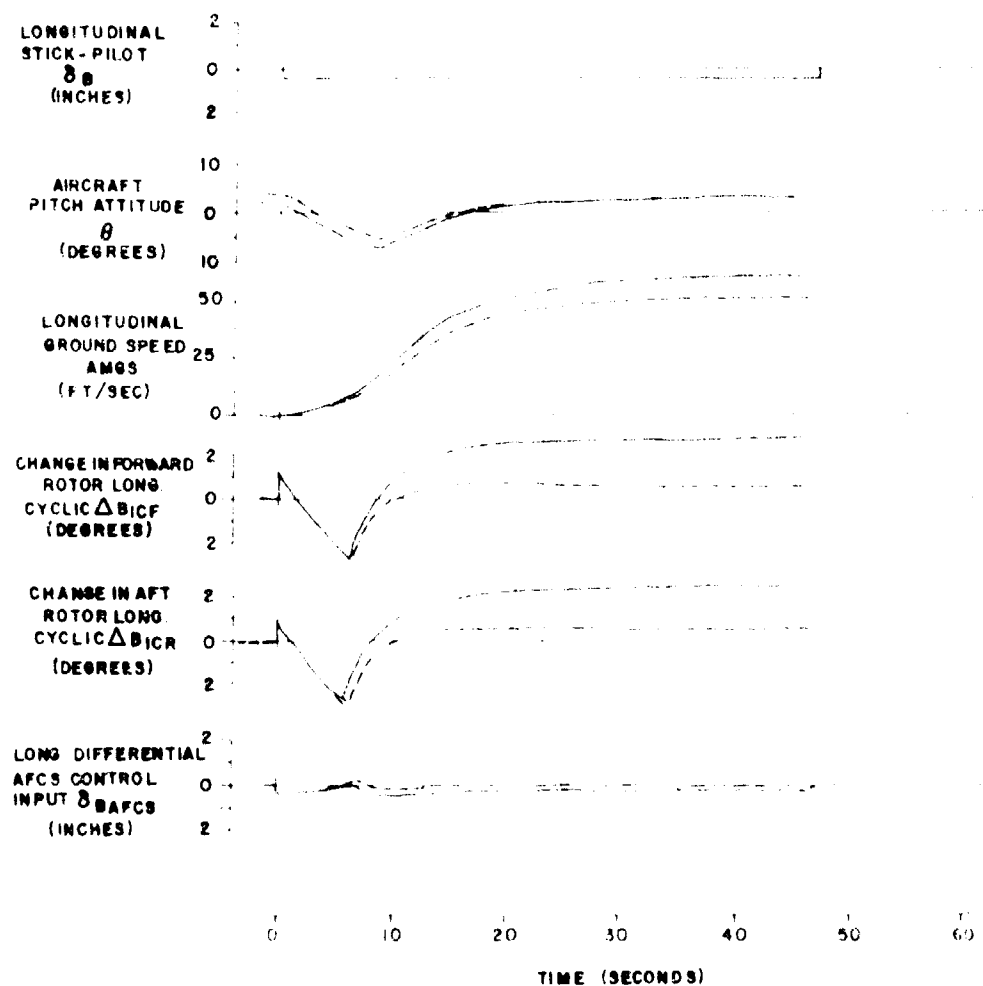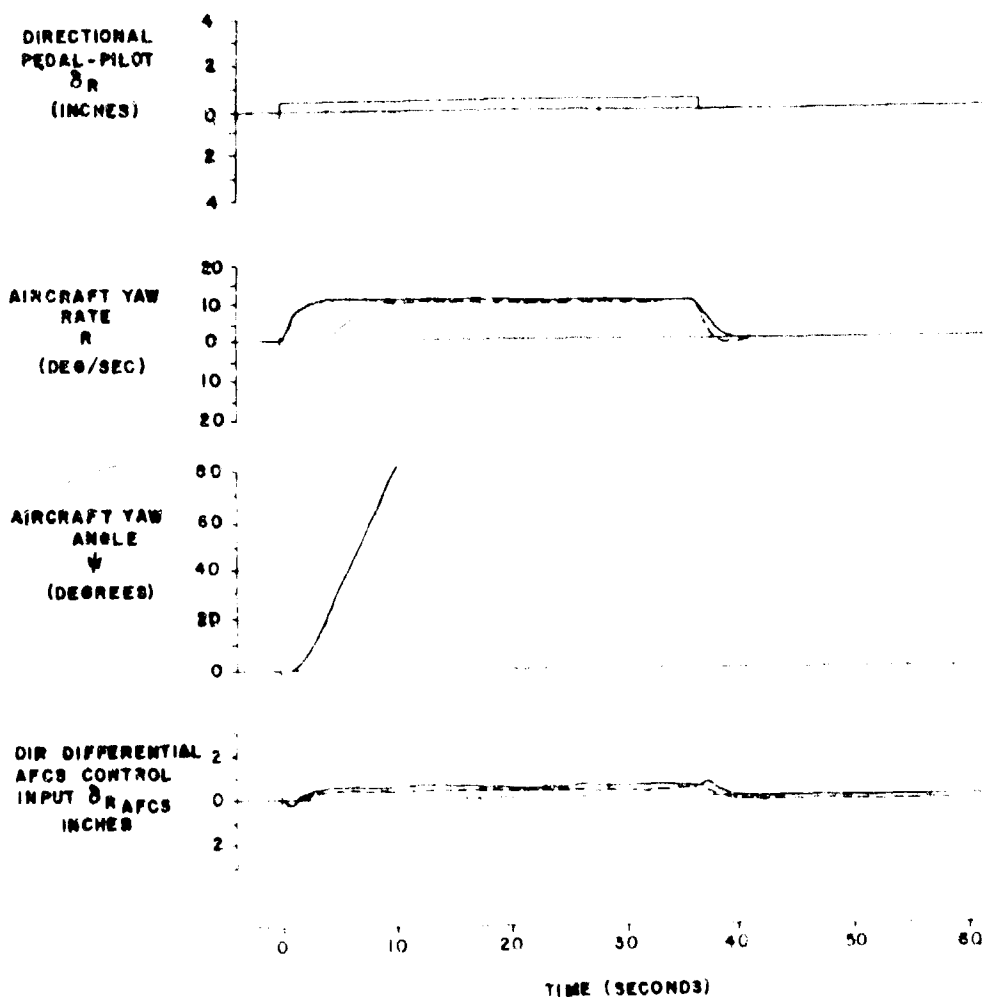347 HYBRID TEST DATA
(9 MAY 74)
45,000 LB  GR WT
12 IN. AFT C G

WITH ALTITUDE HOLD OFF NO VERTICAL SCAS INPUTS ARE MADE
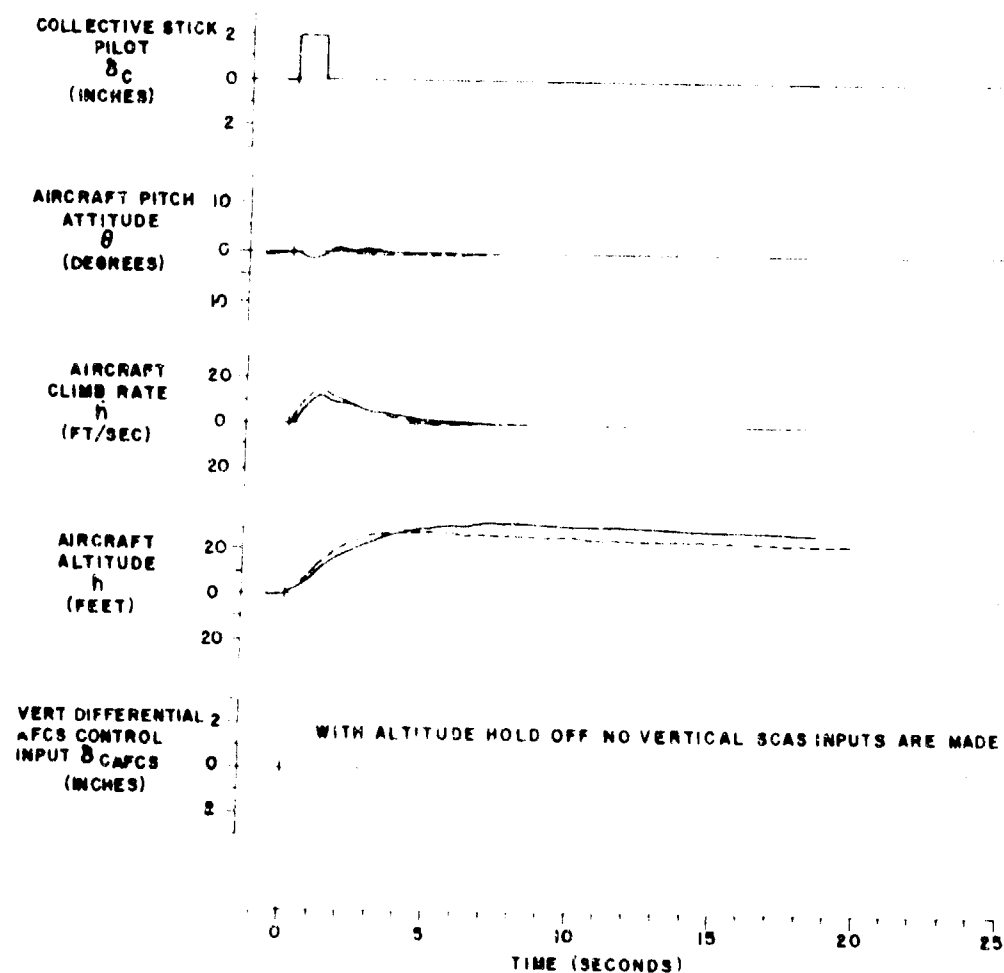
FIGURE 112.
HLH RESPONSE TO PULSE
CONTROL INPUT-VERTICAL AXIS

336

as shown in the figures. Duplicate runs were also made with the Altitude Hold mode engaged, and these showed good correlation with the 347 results as well.

Low-speed controllability is demonstrated on the step response data at zero groundspeed with 5-knot winds applied (Figures 113 through 116). Aircraft steady state velocity response to the various control inputs was found to be about the same for both aircraft indicating similar levels of controllability for the low-speed linear velocity groundspeed mode of AFCS operation.

Transitions between the low- and high-speed modes of flight were explored to validate operation of velocity mode transfer switching in the HLH AFCS. A typical result of this testing is shown in Figure 117 which depicts an acceleration from hover in 30-knot winds to a steady state 110-knot airspeed in forward flight.

This maneuver is followed by removal of the step control input, and deceleration back to the original hover condition. Longitudinal stick backdriving (for removal of the groundspeed/airspeed bias) is simulated by leaving the magnetic brake depressed until reaching steady state conditions after passing through the velocity mode switch.

As expected, the HLH time history data shown in Figure 117 indicate that transitions from low- to high-speed flight (and back again) are very similar to those made with the 347. Acceleration and deceleration characteristics of the two helicopters were virtually identical throughout the maneuver, and no undesirable transient control inputs or aircraft responses were observed for the HLH as it passed through the transition switching region.

Additional assessment of the HLH AFCS was made in low-speed flight with an external load attached to the aircraft. Load Stabilization System damping loops were engaged for these runs. Cockpit pulse inputs were introduced to excite the aircraft (and load) in the longitudinal, lateral and directional axes. Aircraft and load response characteristics were found to be quite similar to those of the 347 when comparable load suspension cable lengths were used.

On the basis of the HLH simulation responses evaluated, it is concluded that control system concepts developed and demonstrated on the 347 are directly transferable to the HLH aircraft, and should produce the same level of superior handling qualities for the Heavy Lift mission.

337

| HLH HYBRID TEST DATA | 347 HYBRID TEST DATA |
|---|---|
| (29 MAY 74) | (9 MAY 74) |
| 118,000 LB  GR WT | 45,000 LB  GR WT |
| 8 IN FWD C G | 12 IN AFT C G |

LONGITUDINAL
STICK - PILOT
$\delta_B$
(INCHES)

2

0

2

AIRCRAFT
PITCH ATTITUDE
$\theta$
(DEGREES)

10

0

10

LONGITUDINAL
GROUND SPEED
AMGS
(FT/SEC)

50

25

0

CHANGE IN FORWARD
ROTOR LONG.
CYCLIC $\Delta B_{1CF}$
(DEGREES)

2

0

2

CHANGE IN AFT
ROTOR LONG.
CYCLIC $\Delta B_{1CR}$
(DEGREES)

2

0

2

LONG DIFFERENTIAL
AFCS CONTROL
INPUT $\delta_{BAFCS}$
(INCHES)

2

0

2

TIME (SECONDS)

0    10    20    30    40    50    60

FIGURE 113.
HLH RESPONSE TO LONGITUDINAL STEP
CONTROL INPUT

338

——— HLH HYBRID TEST DATA      – – – 347 HYBRID TEST DATA
(29 MAY 74)                         (9 MAY 74)

(118,000 LB   GR WT              45,000 LB    GR WT

6-IN. FWD CG                   12-IN. AFT CG



FIGURE 114.
HLH RESPONSE TO LATERAL STEP
CONTROL INPUT

339

O KNOTS GROUND SPEED - 5 KNOTS HEADWIND - ALTITUDE HOLD OFF
SEA LEVEL/STANDARD DAY

FIGURE 115.
HLH RESPONSE TO DIRECTIONAL STEP
CONTROL INPUT

340

COLLECTIVE STICK
FROM TRIM-PILOT
$\delta_c$
(INCHES)

AIRCRAFT
CLIMB RATE
$\dot{h}$
(FT/SEC)

AIRCRAFT
ALTITUDE
$h$
(FEET)

VERT DIFFERENTIAL
AFCS CONTROL
INPUT $\delta$ CAFCS
(INCHES)

TIME (SECONDS)
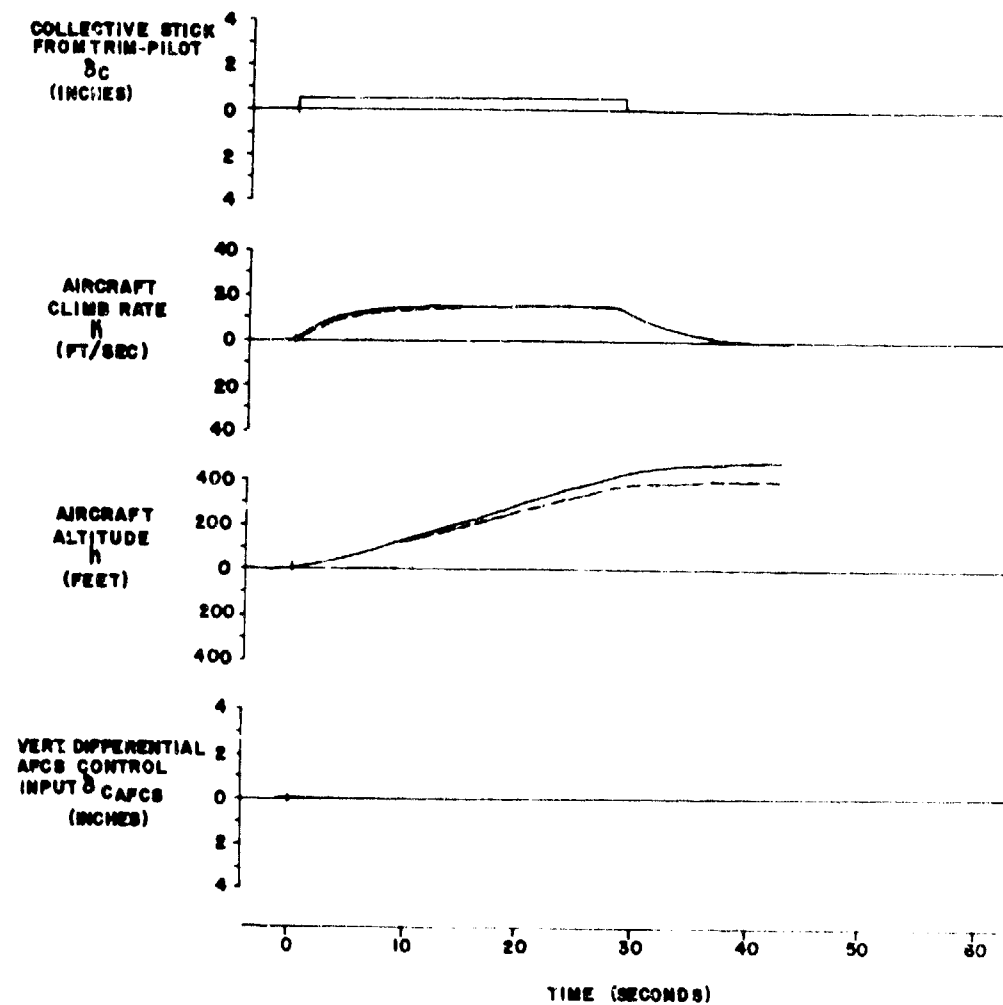
FIGURE 116.
HLH RESPONSE TO VERTICAL STEP
CONTROL INPUT

341
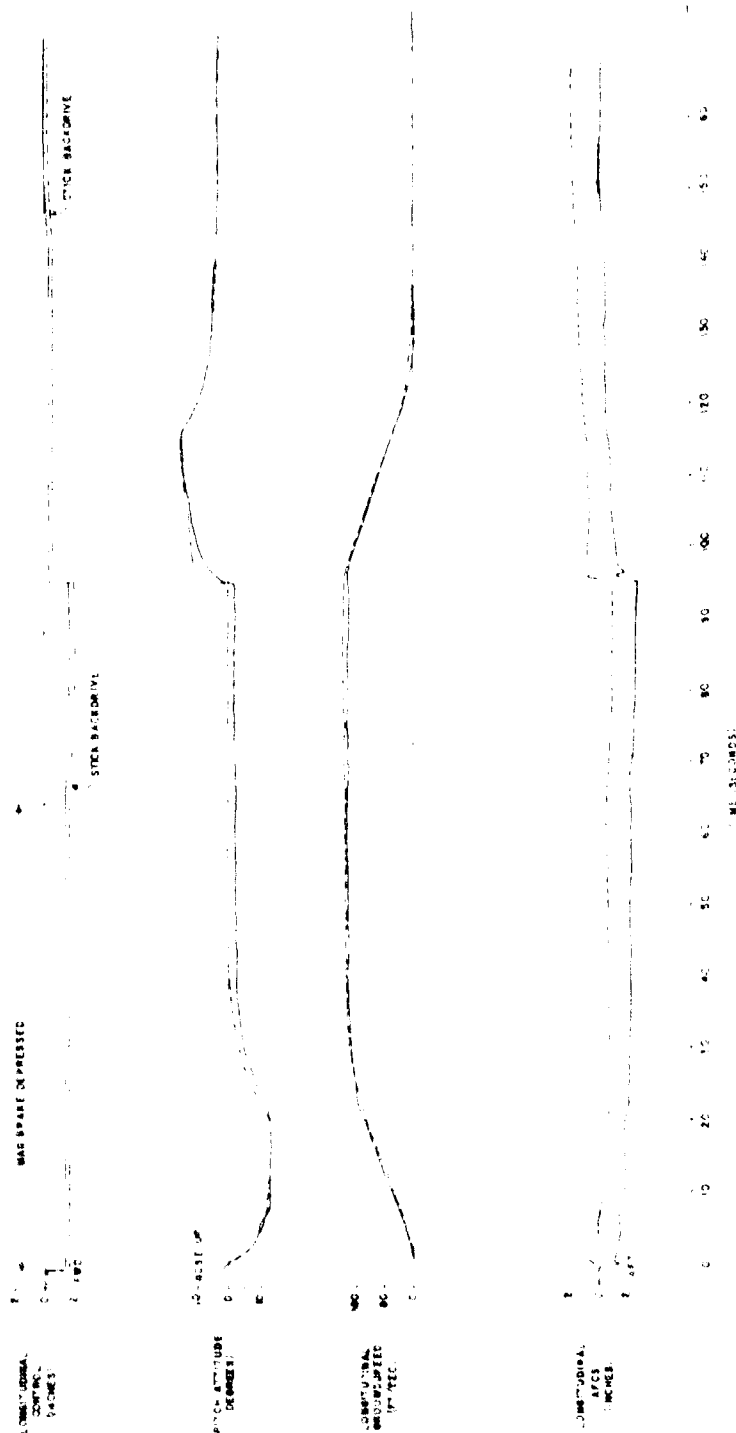
FIGURE 117.
LONGITUDINAL ACCELERATION & DECELERATION FROM HOVER
WITH 30-KNOT HEADWIND

342

## 2.4 AFCS PRE-FLIGHT TESTING AND SOFTWARE CONTROL

A procedure for AFCS logic and software control was essential
due to control law complexity. All programming of the digital
computers was performed by General Electric personnel. Boeing
Vertol responsibilities included design specification, software
and logic verification, and documentation of program changes.

AFCS flight testing was accomplished in a sequential manner
using four software program phases: (1) Basic SCAS, (2) Basic
SCAS and Hover Hold, (3) Basic SCAS, Hover Hold, and Load
Stabilization, and (4) Basic SCAS and Automatic Approach to
Hover. Thirteen reprograms of the basic four computer programs
were necessary during the flight test program for incorporation
of parameter changes.

Laboratory and aircraft ground tests verified all AFCS hard-
ware logic software programming. The laboratory checkout used
an integrated FCS test stand complete with cockpit controls,
DELS, rotor actuators, and AFCS triplex computers and input/
output processors. Open loop testing was performed by insert-
ing test input signals and observing the appropriate AFCS or
DELS output response. The thorough laboratory testing reduced
aircraft ground test requirements.

Success of the program control procedures was demonstrated on
the first AFCS flight. All axes of the basic SCAS and radar
altitude hold modes functioned as designed. All additional
checkout flights after each major reprogram were trouble-free
with one exception when the complete laboratory verification
procedure was not followed. Flight test time was mainly used
to optimize handling qualities for HLH mission tasks and to solve
hardware interface problems. No major changes to the AFCS
design or concept were required.

Software control on this program was in informal rather than a
formal procedure involving a lot of paper work. Software
changes were often transmitted verbally to offsite G.E. personnel
and documented after the fact because of the tight flight test
schedule. Control was maintained through close coordination
between only a few G.E. and Vertol engineers who had a detailed
knowledge of system operation. Complete laboratory testing
was essential to the success of software control.

# 3.0  AFCS HARDWARE

## 3.1  INTRODUCTION

The digital AFCS is designed to provide stability and control augmentation to the primary electrical flight control system of the HLH/ATC program demonstrator aircraft.  The AFCS is implemented as a triple redundant system with active parallel elements designed to provide fail-operative/fail-safe performance.

The AFCS receives command, sensor, and discrete inputs from other aircraft systems, as well as its own equipment, which it then combines and operates upon according to prescribed control laws represented by equations involving the input variables and selected constants.  The control law outputs are then routed to the primary flight control system – consisting of the Direct Electrical Linkage Subsystem (DELS), the Cockpit Control Driver Actuators (CCDA), and the Longitudinal Cyclic Pitch Trim System (LCP) (see Figure 118).  These outputs are conveyed through the forward and aft swashplates to the rotors to affect aircraft stability and control response.

The AFCS further provides displays to the flight crew indicating system operational mode status and subsystem failure status information.

Figure 119 shows the Flight Control Computer (FCC) subsystem with connection to the control and display panels in a simplified form.  Three digital computers perform the computations to solve the control law equations.  Each operates independently but in synchronism.  The three computers are connected to a parameter change/display unit (PCDU) which provides a memory interrogation and change capability for test purposes.

The PCDU addresses the memory locations in the computer and allows the flight program contents to be displayed and altered on-line if required.

All interfacing between the computers and aircraft systems is achieved through the Input/Output Processor (IOP) units. These units condition, select, monitor, and vote on the inputs so that all three computers operate on the same input data. The IOPs also monitor and vote on the computer outputs, and generate the timing signals that keep all three computers operating synchronously.  The IOPs decode, and perform
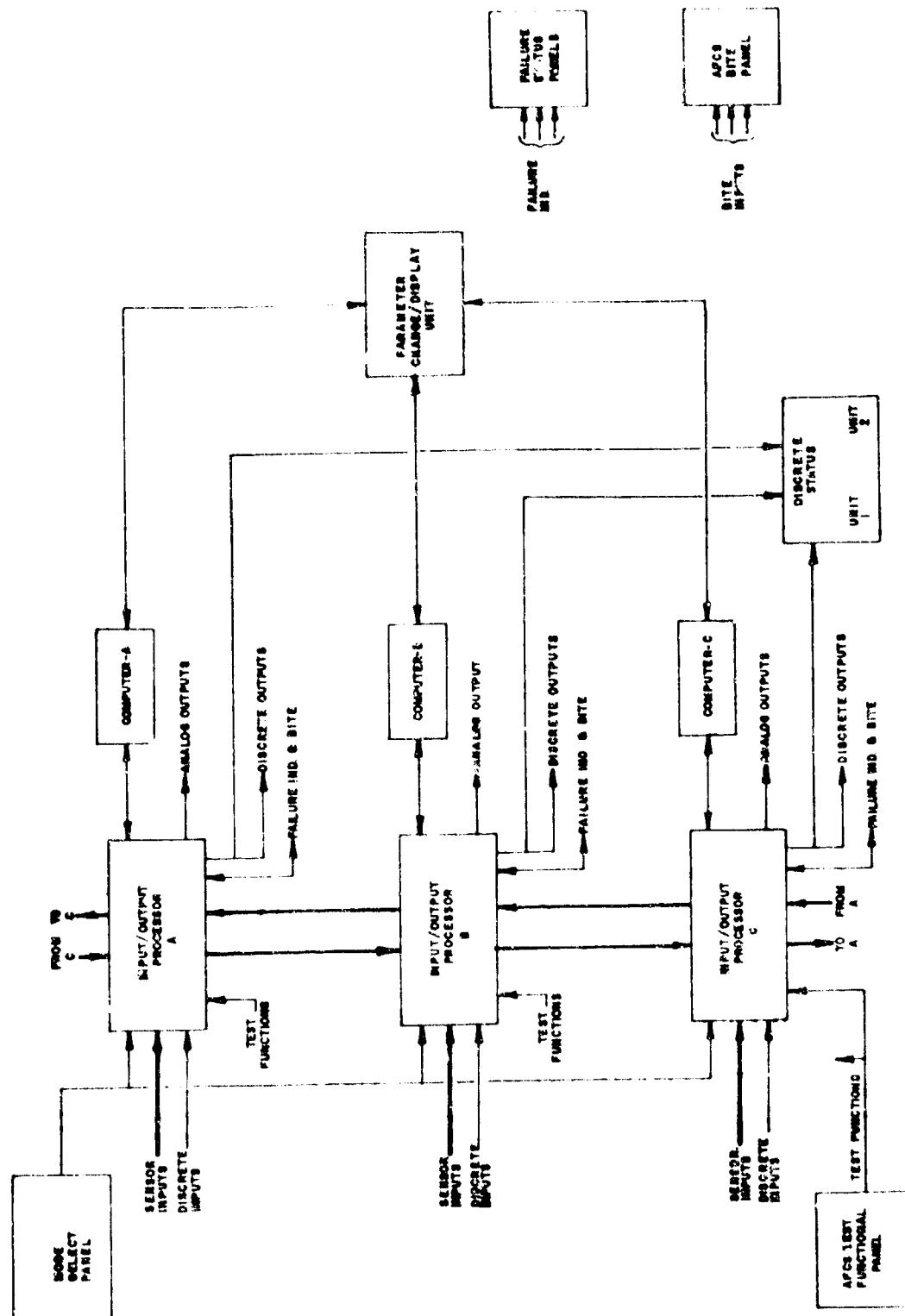
344

FIGURE 118. FLIGHT CONTROL SYSTEM BLOCK DIAGRAM

FIGURE 119. AFCS BLOCK DIAGRAM

346

logical operations on the mode select panel inputs, as well as other inputs affecting the mode of computer operation. The IOPs provide discrete signals (some of which are inputs and some of which are computed or developed within the IOP) to the discrete status panels for display. The IOPs provide failure and system status indications (the result of continuous failure monitoring) to the AFCS and sensor failure status panels. The IOPs also interface with the BITE panel, providing test in progress and go/no-go information as determined by BITE circuits within the IOPs. Finally, the IOPs accept test function inputs from the AFCS test function panel.

The IOPs receive multiple sensor inputs which may be simplex, duplex or triplex. The IOPs exchange information and voter circuits decide which inputs are to be used for further stages of signal processing. Median value selection is adopted for triplex information and average value for duplex information. Single failure of triplex signal inputs causes the system to switch to averaging of the remaining two signals.

The pilot has control of the AFCS through the mode select panel and the system test function panel. These two panels permit the pilot to engage the AFCS in all or any combinations of the four control axes: longitudinal, lateral, directional and vertical; and to select operational modes, for example, hover hold, auto approach coupler, auto load stabilization, and altitude hold. The ability to insert test function inputs to facilitate evaluation of system stability or control response is provided.

The flight test engineer is provided with an engineering evaluation of system performance through the use of the PCDU, discrete status, and failure indication panels. BITE permits a system functional checkout prior to flight and is locked out in flight via the throttle quadrant switches.

The following sections describe the various AFCS hardware components, present major performance characteristics and performance evaluation based on ATC flight testing.

## 3.2  FLIGHT CONTROL COMPUTER SUBSYSTEM

### 3.2.1  Equipment Structure

The ICP-733 Digital Computing Subsystem, built by the General Electric Company, consists of an integrated set of hardware

and software elements specifically designed for real-time airborne control applications. The design is based upon the incremental computing technique using an arithmetic unit organized as a general algorithm which provides for high-speed processing combined with precise computational accuracy and programming flexibility.

The airborne equipment consists of two units for each AFCS channel:

- ICP-733 Computer (Flight Control Computer - FCC)
- System Interface Unit (Input/Output Processor - IOP)

The FCC performs all the computations necessary for the flight control laws and the IOP performs all of the signal conditioning necessary to communicate between the computer and the other elements of the flight control system. The IOP also performs additional tasks related to system logic and redundancy management.

The ICP-733 computer and IOP hardware functional and modular organization is an expanded version of the ICP-710 system with state-of-the-art packaging, and off-the-shelf standard integrated circuit components. All parts utilized in the fabrication of the units were built and tested to military specifications. No custom-made circuits were fabricated for the HLH-ATC AFCS application.

A programmable Read Only Memory (ROM) device was chosen for the flight control computer program memory. This device is the interim step between the core memory which is utilized for laboratory test purposes and the solid state ROM recommended for the production system, the program of which is fixed by fabrication of the mask at the device production stage. The programmable ROM is electrically alterable, permitting program changes with the aid of ground support equipment, while retaining the advantage of not being susceptible to electrical transients causing memory scramble - a flight safety consideration.

The flight control computer retains the capability to operate with an external core memory unit simply by removing the programmable ROM printed circuit cards and substituting buffer cards to interface with the external memory. The core memory unit finds substantial use in laboratory development of the computer and later on in simplex system flight control law debug operations.

348

### 3.2.2  Development History

The ICP-733 digital computing system represents the third generation in a line of incremental computers developed specifically for flight control and weapons system applications.  General Electric has developed the incremental computing system over a period of 10 years and has proven the concept in several flight test programs.

The first incremental control processor developed (ICP-001) had a limited memory of 64 algorithms programmed on prewired program boards.  This machine was flown to prove that it could match the performance of a comparable analog system with regard to control stability and accuracy for an automatic landing system on the Boeing prototype 707 aircraft.

The ICP-002 series expanded memory to twice that of the first machine and was developed in a triplex configuration to validate the redundant digital interface system concept under flight conditions.

The ICP-710 system was designed to perform ballistic computations for a helicopter weapon delivery system.  The design of this equipment was directed toward producing an efficient cost-effective computer using modular construction and standard off-the-shelf components.  The equipment was developed and tested to military specifications.  The computer unit was designed to accept two boards of solid state ROM devices which form the program memory for use with a production system. However, for development purposes, an external electrically alterable core memory unit was fabricated to facilitate ease of software reprogramming.  The computer unit operates with the same iteration rate as the series 002, and has the same computational capacity.  Ground support equipment in the form of a Program Loader unit and Program Monitor unit function to change the program in core memory and check out the system operation.

The ICP-733 system retained the features of the 710 system with expansion in program memory and a decrease in the iteration rate.  Capabilities to test the system preflight and to monitor and to change the software in flight were added.  The input/ output processor, built on the same design principles as for the 710 system, was largely expanded to handle the numerous sensor and logic system interfaces while also incorporating sensor failure detection and system shutdown capability.

349

### 3.2.3   Flight Control Computer Description

The LCP 733 variable-increment computing system has been designed for use in a relative closed-loop control system application.   The operating characteristics of the computer are such that the discrete nature of the computation has negligible effect upon the control law mechanization which permits design of the system control laws by conventional means.

In evaluating the ICP 733 system for use in the HLH AFCS application, several characteristics were considered.   These were:

- Solution rate – band width
- Computational efficiency
- Computer memory
- Accuracy
- Redundant system operation
- Interfacing requirements
- On-line internal monitoring capability

### 3.2.3.1   Solution Rate – Bandwidth

The computer timing is under hardware control.   The timing signal is generated from a 1.288 MHz crystal-controlled clock. The computer uses serial arithmetic elements operating at the clock frequency bit rate.   All inputs are sampled, all outputs are updated and all computations are performed at a rate of 101.725 times per second.

The ICP 733 computer is a variable increment machine where the increment variables are represented by a four-bit coded number corresponding to integer powers of two in the range 0, $\pm 1$, $\pm 2$, $\pm 4$, up to $\pm 64$ machine units.   The slew rate limit is a characteristic of the incremental computer as differentiated from a whole-word computer, and is defined as the maximum rate at which any internal variable can change.   Since the largest increment is 64 machine units, and since the solution or iteration rate is 101-725 iterations per second, the computer slew rate limit is thus 6510 machine units/sec.   This translates to 0.32 sec. and 5.03 sec. for computer inputs or outputs and arithmetic unit parameters to slew half range, respectively.

The basic bandwidth of the computer is established by the slew rate limit. The maximum rate of change of a sinusoidal signal defined by A sin wt is $A\omega$. The system control band width is established by the inner loop high-frequency mode stabilization requirements typically satisfied by the aircraft acceleration and rate gyro sensors. Sufficient stabilization is achieved with excursions within 10 percent of full-scale range. Full-range signal inputs and outputs are established by the analog-to-digital conversion (and vice versa), which is set to $\pm2048$ machine units. Weighing these factors together establishes a realistic control band width upper limit of approximately 5 Hz. This upper limit, of course, is variable depending on how the control loops are scaled within the computer, since the slew rate limit may be reached anywhere in the computational process. A further factor to be considered is the signal conditioning applied to each sensor input, as well as minor contributions yielded by holding period in the input shift register, computational delay, and pulse-width-modulated D/A converter signal shaping. These latter factors, however, appear small in comparison to the major limitations of slew rate limiting and individual signal conditioning in determining the computational bandwidth constraints.

The bandwidth characteristics of the incremental computer have been demonstrated to be more than adequate for the AFCS requirements.

### 3.2.3.2 Computational Efficiency

The arithmetic section of the computer is a mechanization of a general algorithm, which is particularly suited for the solution of algebraic and differential equations in real time. An "algorithm" is a name for the computational operations that are performed by the time-shared incremental arithmetic section during a specified time interval within each computer iteration. Those operations performed most efficiently are summation, multiplication, division, integration, filtering, and square root. Logic and nonlinear functions are performed much less efficiently.

For this reason, most of the logic operations, which appear to a large degree within helicopter control system laws, are separated from the computer software and performed in hardware within the input-output processor unit.

351

### 3.2.3.3 Computer Memory

Program Memory. The computer is a stored program machine with program storage capacity for 512 algorithms of instructions of which 256 can be computed during one computer iteration. The program memory provides sequential control of the incremental arithmetic unit. A conditional branch test is utilized to control the selection of program instructions for these algorithms; thus, the problem being executed at any given time may be varied as a function of mode control logic or of computed variables.

Initial program memory estimates permitted approximately 80% growth capability, including the approach to hover mode for the 512 algorithm capacity.

The basic program memory consists of four boards, each board containing twelve erasable/reprogrammable MOS-ROM (metal oxide semi-conductor - Read Only Memory) devices. These devices are erased by means of ultraviolet light and are programmed through the application of a high voltage level.

The four boards are all keyed differently so as to fit only in the proper location in the computer. The Read Only Memory is organized such that each of the four boards contains 128 algorithms. Each board contains 1536, 16-bit words or 24,576 bits per board. Total program memory contains 98,304 bits.

In order to facilitate software checkout and verification. an external alterable memory unit (8K x 18-bit core) can be used. Two interface modules are used in place of the program storage modules (four ROM boards) when using the memory unit. The four ROM boards and the program storage control board are removed when using the external program memory unit.

Variable Memory. Four working shift registers (Y, U, V, X) are used to store the 16-bit whole-word variables that are computed by the incremental arithmetic unit. A fifth shift register (rho), containing 40 bits, is used as an accumulator for products and additions of the whole-word variables and incremental changes in variables. The size of the rho register permits computational surge to insure that there is no loss of information.

Increment Memory. The result of each algorithm computation is a four-bit increment that is stored in a preassigned location of a random access increment memory. This increment result can be accessed at any algorithm time to be used in the computation as an input to any of the 256 algorithm functions. Thus, a total of 512 four-bit words are required for increment storage.

Parameter Change Memory. All parameter changes to be made inflight are stored in a random access memory, which is accessed through the Parameter Change/Display unit on the cockpit center console. The values stored in the parameter change memory are summed with the Sp/Sq constants located in program memory to form new parameter values for computational use; however, the basic program memory constants remain unaltered.

3.2.3.4 Accuracy

The ICP-733 system is a highly accurate control computer system. The analog-to-digital and digital-to-analog converter word lengths are 12 bits and the internal word length is 16 bits including sign. The digital-to-analog conversion is done by setting a sample and hold from the output of a digital-to-analog converter. Because of the high refresh rate and the quality sample and holds used, the dc outputs are held within .1 percent of nominal and the ac outputs are held within .2 percent of nominal.

In the arithmetic section of the computer, a 40-bit register (rho register) is used to sum up partial products and to retain the residual after each algorithm output increment has been generated. The combined characteristics of the rho register used to sum up the partial products and the increment selector characteristic yields an accuracy for the 16-bit internal variables equivalent to using a 16-bit representation in a whole word computer and rounding after each computation. The rho register also serves as a surge register, insuring no loss of information when the machine momentarily reaches slew rate limit. The accumulation of partial products, which are formed when mechanizing a digital filter, is achieved by the rho register. This permits pole placement accuracy greater than that offered by a 16-bit whole-word computer using double precision arithmetic.

353

### 3.2.3.5  Redundant System Operation

The triplex, digital AFCS is designed to provide fail-operative/fail-safe performance.  This requirement is mechanized with an active triple-redundant system and all failures are considered to be within the definition requirement for fail operational performance.  The system is described as an "active parallel redundant" system in the sense that each computer channel is powered, online, and performs identical functions.  The system is also "active" in the same sense that it has the capability of detecting the isolating faults and inhibiting their propagation as control output commands.

Two of the most important features for simplification of the redundant interface design is median sensor input selection and identical, time-synchronized computations.  The input/output processor contains the key hardware elements which provide for the median selection of all input signals and the triple redundant clock mechanization which permits synchronization of three computers on a bit-by-bit basis.  This subject is treated further in redundancy management within the IOP. The advantage of providing coherent data inputs and timing to each computer channel are rewarded by identical dynamic tracking of the real time processed outputs.  This is of particular significance when the software processing requires integrations.

### 3.2.3.6  Interfacing Requirements

Power.  The computer unit operates from dual 115 Vac, 400 Hz aircraft power sources which comply with the requirements of MIL-STD-704A.

The regulated dc voltages required by the computer unit are generated within the unit from the 115 Vac line.  Loss of a single ac source will not cause the loss of the computer operation.

Internal failure monitoring is contained in the supply to annunciate the loss of either primary input power source or an out-of-tolerance condition on any regulated supply output.

28 Vdc power is also supplied to the computer to operate the BITE flag.

<u>Signal Inputs/Outputs</u>.  All variable and discrete computer inputs/outputs are made through the IOP.  The computer is timed to receive and transmit inputs/outputs within two distinct cycle times of one iteration period.

<u>Computer Inputs</u>

- 48 serial-digital, 16-bit 2's complement binary

- 64 discretes or 64 4-bit serial increments

Table 15 lists the computer variable inputs in cycle 1 and cycle 2.  Note that the algorithm numbers indicate when the input is received by the computer.  Processing in the IOP occurs two algorithm times earlier.  Inputs, including those that do not require conversion are listed.  Table 16 lists all the computer discrete inputs.  There is no algorithm delay on discrete processing.

<u>Computer Outputs</u>

- 32 serial-digital, 16-bit 2's complementary binary

- 64 discretes or 64 4-bit serial increments

Table 17 lists the computer discrete outputs.  The variable outputs are reflected in Table 21.

<u>Data Address/Display and Change</u>.  Each computer directly interfaces with the Parameter Change/Display unit which allows the pilot or engineer to display the value of any input/output variable, the contents of any program memory location, and any internal computer variable associated with each computer.  The capability is also provided to input delta changes to program memory contents without directly altering the basic programmed values.

<u>Data Recording</u>.  Each computer directly interfaces with the Digital In-flight Recording System.  Timing is provided only by computer A to the recording system.  Raw sensor, voted algorithm X and Y register information and selected memory constant parameter data can be recorded.

355

Table 15.   Computer Variable Inputs

| | | | | | | | |
|---|---|---|---|---|---|---|---|
| 57 | Source | AC | Volts | | | 107 | 25 |
| 38 | Aux Cord Tension | AC | Lbs. | | | 104 | 26 |
| 39 | | | Ft | | 14.024 | | 27 |
| 40 | | | Ft/Sec | 250.325 | 26.0 | | 28 |
| 41 | | DC | Volts | 984.0 | | 175 | 29 |
| 42 | Fwd Cable Tension | AC | Lbs. | 0.256 | 25629.68 | 177 | 30 |
| 43 | Aft Lat Cable Angle | AC | Deg | 40.0 | 192.603 | 179 | 31 |
| 44 | Fwd Lat Cable Angle | AC | Deg | 40.0 | 192.603 | 181 | 32 |
| 45 | Lat ICCC | AC | Deg | | | 183 | 33 |
| 46 | Lat ICCC | As | In | 11.7 | | 185 | 34 |
| 47 | Lat Pedal Position | DC | In | 720.0 | 8.24 | 187 | 35 |
| 48 | Lat Stick Position | DC | In | 40.0 | 14.224 | 189 | 36 |
| 49 | Not Used | | | | | 191 | |
| 50 | Not Used | | | | | 193 | |
| 51 | Not Used | | | | | 195 | |
| 52 | Not Used | | | | | 197 | |
| 53 | * | | | | | 199 | 37 |
| 54 | * | | | | | 201 | 38 |
| 55 | * (SA) | | | | | 203 | 39 |
| 56 | * (SA) | | | | | 205 | 40 |
| 57 | Airspeed | As | Knots | | 6011 | | 41 |
| 58 | Diff Pressure | DC | lb-in2 | 2658.6 | 2.647 | 209 | 42 |
| 59 | Sin θ | Sync | Unit | 1702.14 | 614.101 deg/sec | 211 | 43 |
| 60 | Cos θ | Sync | Unit | 1702.14 | 219.181 deg/sec | 213 | 44 |
| 61 | Sin ψ | Sync | Unit | 1702.14 | 219.101 deg/sec | 215 | 45 |
| 62 | Cos ψ | Sync | Unit | 1702.14 | 219.181 deg/sec | 217 | 46 |
| 63 | Pitch Rate | AC | Deg/sec | 34.00 | 191.465 | 219 | 47 |
| 64 | Yaw Rate | AC | Deg/sec | 34.00 | 191.423 | 221 | 48 |

No Computer Input operations — converted only

356

Table 16.   Computer Discrete Inputs   (CDI)

COMPUTER DISCRETE INPUTS  (CDI)

| Number | Algorithm | Logic No. | Variable - True State (-1) | |
|---|---|---|---|---|
| | | | | CYCLE 1 |
| 1 | 0 | L2B | Coupler Engage | |
| 2 | 2 | L2A | FDI Eng | |
| 3 | 4 | L32 | Velocity Norm | |
| 4 | 6 | L33 | Velocity Decay | |
| 5 | 8 | L37A | Long Engage | |
| 6 | 10 | L37B | Vert Engage | |
| 7 | 12 | L37D | Dir Engage | |
| 8 | 14 | | Long Beep Trim - Pos | |
| 9 | 16 | | Long Beep Trim - Neg | |
| 10 | 18 | L30D | CCDA Vert Sync | |
| 11 | 20 | L30C | CCDA Dir Sync | |
| 12 | 22 | L30B | CCDA Lat Sync | |
| 13 | 24 | L30A | CCDA Long Sync | |
| 14 | 26 | L37C | Lat Engage | |
| 15 | 28 | | Diff Test | |
| 16 | 30 | | LCP Test | |
| 17 | 32 | | Dir Beep Trim - Neg | |
| 18 | 34 | | Dir Beep Trim - Pos | |
| 19 | 36 | L28 | Stick Beep Trim Disconnect (Lat/Long) | |
| 20 | 38 | L1 | Ground Contact | |
| 21 | 40 | L23 | Auto Lat. Hover Trim Engage | |
| 22 | 42 | L22 | Auto Long. Hover Trim Engage | |
| 23 | 44 | L3A | Bank Angle Sync | |
| 24 | 46 | L4B | Dir and Long Contr. Resp. | |
| 25 | 48 | L5A | Heading Sync | |
| 26 | 50 | | Lat Beep Trim - Pos | |
| 27 | 52 | | Lat Beep Trim - Neg | |
| 28 | 54 | L41 | Lat Stk Offset Compensation | |
| 29 | 56 | L39B | Lat TFS Bias Elim | |
| 30 | 58 | L38A | Lat Vel Mode Transfer | |
| 31 | 60 | L38B | Long Vel Mode Transfer | |
| 32 | 62 | | BITE No 1 | |
| | | | | CYCLE 2 |
| 33 | 192 | L19 | Prec Hov Hold Vel Ref | |
| 34 | 194 | L27C | Load Centering Mode | |
| 35 | 196 | L11 | Hover Hold Engage | |
| 36 | 198 | L20 | LCC Controller Enable | |
| 37 | 200 | L39A | Long TFS Bias Elim | |
| 38 | 202 | L9C | Vert PHS Position Stab | |
| 39 | 204 | L8B | Lat PHS Position Stab | |
| 40 | 206 | L8A | Long PHS Position Stab | |
| 41 | 208 | L34B | Reset KX5N4, KY5N4 Int Output | |
| 42 | 210 | L7A | Convert to Rad Alt Ref | |
| 43 | 212 | L6A | Altitude Hold | |
| 44 | 214 | L27D | Lead Centering Mode | |
| 45 | 216 | L46 | Rad Rate Operative | |
| 46 | 218 | L34A | IMU Drift Clear | |
| 47 | 220 | | Neg Amplitude | |
| 48 | 222 | | Airspeed 2F | |
| 49 | 224 | L36 | Prec Hov Relock Comm | |
| 50 | 226 | L27B | Load Position Hold Mode | |
| 51 | 228 | L27K | | |
| 52 | 230 | L27F | | |
| 53 | 232 | | Disc Input - Dis Fail No. 1 | |
| 54 | 234 | | Hi Amplitude + V/V Ovfl | |
| 55 | 236 | | Mid Amplitude + Dis Fail No. 2 | |
| 56 | 238 | | Lo Amplitude + X/Y Ovfl | |
| 57 | 240 | | Step Input | |
| 58 | 242 | | Ramp Input | |
| 59 | 244 | | Pulse Input | |
| 60 | ? | | Parallel Test | |
| 61 | 248 | | Vert Axis Test | |
| 62 | 250 | | Dir Axis Test | |
| 63 | 252 | | Lat Axis Test | |
| 64 | 254 | | Long Axis Test | |

357

## Table 17   Computer Discrete Outputs (CDO)

**COMPUTER DISCRETE OUTPUTS (CDO)**

| Number | Algorithm | Variable — True State (1) | CYCLE |
|---|---|---|---|
| 1 | 1 | Nav Valid | CYCLE 1 |
| 2 | 3 | Drift Clear Engage | |
| 3 | 5 | IMU G/s < 70 ±5 kts | |
| 4 | 7*9(3) | A/S > 45 Knots | |
| 5 | 9 | Vert Pir Velocity < 5 fps | |
| 6 | 11 | Long Vel > 30.5 in | |
| 7 | 13 | Long Vel Ref Mode Change | |
| 8 | 15 | Long Ramp Bias < 0.05 in | |
| 9 | 17 | Rad Alt < 360 ft | |
| 10 | 19 | Rad Alt < 400 ft | |
| 11 | 21 | Vert Int Pos > THSH | |
| 12 | 23 | Long 0.3 < 3 kts | |
| 13 | 25 | Lat 0.3 > 15 kts | |
| 14 | 27 | Long > 5 > 17 kts | |
| 15 | 29 | Long PHS Velocity < 5 fps | |
| 16 | 31 | Long Int Pos > THSH | |
| 17 | 33 | Vert PHS Pos Error < 0.2 ft | |
| 18 | 35 | Long PHS Pos Error < 0.5 ft | |
| 19 | 37 | Long RCDA sys | |
| 20 | 39 | Vert RCDA sys | |
| 21 | 41 | Long Ramp Bias < 0.05 in | |
| 22 | 43 | Rad Alt Rate = 0 ±200 ft | |
| 23 | 45**(65) | Vert Int Detent | |
| 24 | 47 | Long Int Detent | |
| 25 | 49 | *Not Decoded | |
| 26 | 51 | *Not Decoded | |
| 27 | 53 | *Not Decoded | |
| 28 | 55 | *Not Decoded | |
| 29 | 57 | *Not Decoded | |
| 30 | 59 | *Not Decoded | |
| 31 | 61 | *Not Decoded | |
| 32 | 63 | *Not Decoded | |
| 33 | 129 | Diff Pressure > 0.058 | CYCLE 2 |
| 34 | 131 | Velocity Scale Phase | |
| 35 | 133 | Lat Velocity Ref Mode Change | |
| 36 | 135 | Roll Attitude Threshold T > .15 | |
| 37 | 137 | Roll Rate > 1.5 deg/sec | |
| 38 | 139 | Roll Attitude Limit Detect | |
| 39 | 141 | | |
| 40 | 143 | A/S > 45 Knots | |
| 41 | 145 | Roll Attitude > 1 deg | |
| 42 | 147 | Yaw Rate > 1 deg/sec | |
| 43 | 149 | Dir Int Pos > THSH | |
| 44 | 151 | Lat Vel > 02 in | |
| 45 | 153 | Lat Ramp Bias < .05 in | |
| 46 | 155 | Lat Int Detent | |
| 47 | 157 | Lat RCDA sys | |
| 48 | 159 | | |
| 49 | 161 | Lat Int Pos > THSH | |
| 50 | 163 | Lat Int Velocity < 3 fps | |
| 51 | 165 | Lat PHS Pos Error < 0.5 ft | |
| 52 | 167 | Lat AS | |
| 53 | 169 | Servo Valve Position R-Focus | |
| 54 | 171 | Lat RCDA sys | |
| 55 | 173 | Large Int Detent > ±50 in | |
| 56 | 175 | Mid Int Detent > 75 in | |
| 57 | 177 | *Int Decoded | |
| 58 | 179 | *Not Decoded | |
| 59 | 181 | * | |
| 60 | 183 | * | |
| 61 | 185 | * | |
| 62 | 187 | * | |
| 63 | 189 | * | |
| 64 | 191 | * | |

* Not a Computer Discrete Output in Test Tape.

358

### 3.2.3.7 On-line Monitoring Capability

The computer contains extensive on-line internal monitoring.
Parity checks and timing monitors are used to provide a com-
prehensive failure detection capability. In addition, com-
putational overflow monitors are provided. This monitoring
contributes significantly to the fault isolation performance
of the entire system.

One of the computer boards is dedicated to BIT. Continuous
BIT consists of the following:

- Continuously on-line computational test problems
  (executed through the IOP).

- Parity check on program instruction readout and all
  variable storage.

- Read/write check on increment storage.

- Timing and power supply monitors.

- Memory overflow monitor.

Storage Memory Protection. Storage memory protection is pro-
vided for all program memory instructions, parameter constants
and machine instructions. All parameter data, program control
instructions and address instructions are stored in the
Erasable ROM, and as a result, are protected from any type of
electrical transient, etc. The machine operating instructions
are mechanized as the general algorithm and as such are hard-
wired in the computer. System and program variables are the
only parameters that are not protected in the event of power
failures, etc.

Overflow Protection. The computer program is written such
that maximum input combinations of all variables do not cause
an overflow. Functions, such as integration have software
limiters programmed for overflow protection. A hardware
monitor is provided such that in the event an actual overflow
occurs, the system is protected and the overflow is treated
as a computer failure.

### 3.2.4    Input/Output Processor Description

The input/output processor provides all interface require-
ments between the computer unit and the flight control system
sensors, stick pick-offs, cockpit-control driver actuators,
speed trim system, flight director and ground velocity indi-
cator, mode select and system test function panels, failure
and discrete status panels, and the direct electrical linkage
subsystem. The IOP also provides all of the basic require-
ments for redundancy management, failure detection, failure
protection circuitry, timing, and BITE. A block diagram of
the IOP is shown in Figure 120.

### 3.2.4.1    Analog Input Processing

A total of 36 analog inputs to the IOP must be
transformed into a dc signal before being applied to the A/D
converter. Sixteen ac inputs are first demodulated
using the appropriate reference phase supply and then signal
conditioned. Four synchro inputs are applied to trans-
former modules which convert the three-wire input information
into two components in quadrature by means of a Scott-T
transformer. The outputs, sine and cosine two-wire ac sig-
nals, are then demodulated and signal conditioned. Sixteen
dc inputs are applied to the signal conditioner circuits,
which act as buffer/gain blocks between the sensor inputs and
the A/D converter. All analog inputs to the IOP are listed
in Table 18.

In the IOP, there is a single A/D converter to which 48 chan-
nels of dc information is multiplexed. The multiplex switches
are closed at the beginning of an even-numbered algorithm;
the signal is then allowed to settle for 13.6 microseconds,
after which a convert command is given, and the A/D converter
module converts the analog signal to a 12-bit digital word in
25 microseconds using successive approximation. Conversion
is completed in one algorithm time. The digital data is
shifted out of the A/D converter into a shift register on the
sensor comparator card with the converted data loaded in the
lower 12 bits of the 16-bit serial word.

### 3.2.4.2    Signal Input Conditioning

Ac and dc sensor signals are input differentially to opera-
tional amplifiers to reduce signal noise. The amplifiers
also act as active filter networks providing two first order

FIGURE 120. IOP BLOCK DIAGRAM

361

## Table 18. IOP Variable Inputs

**DC INPUTS**

| No | Variable *Limited at 1100 ft | Max Volt | Units | Max Input Scale @ Units | Time Constant $T_1$ | $T_2$ | Comp Alg | Computer Scaling MU/Unit | ** V. | ** Scaling MU/V |
|----|----|----|----|----|----|----|----|----|----|----|
| 1 | EPS Vert Position | ±5.0 | ft | 4.147 | | 0.01045 | | | | |
| 2 | EPS Vert Velocity | ±5.0 | ft/Sec | 7.67 | | 0.01045 | 41 | 50.125 | | 184.0 |
| 3 | EPS Long Position | ±5.0 | ft | 4.147 | | 0.01045 | 43 | 460.763 | | 184.0 |
| 4 | EPS Long Velocity | ±5.0 | ft/Sec | 7.67 | 0.015 | 0.01842 | 47 | 50.125 | | 184.0 |
| 5 | Altitude Rate | ±10.0 | ft/Sec | 50.0 | 0.015 | 0.0164 | 43 | 46.5 | | 184.8 |
| 6 | Radar Altitude | ±25.0 | ft | 5000 | | 0.01045 | 44 | 1.92 | | 184.0 |
| 7 | Long Stick Position | ±5.018 | in | 65 | | | 48 | 243.143 | | |
| 8 | Vert Acceleration | ±12.0 | g | 2.0 | 0.0174 | | 61 | 1024.0 | | |
| 9 | Baro Altitude HP | 10.0 | ft | 250 | 0.014 | 0.014 | 75 | 8.192 | | |
| 10 | Baro Altitude (2x) | ±10.0 | ft | 1500 | 0.012 | 0.0164 | | 1.365 | | |
| 11 | EPS Lat Position | ±5.0 | ft | 4.147 | 0.015 | 0.01845 | 171 | 460.763 | | 184.0 |
| 12 | EPS Lat Velocity | ±5.0 | ft/Sec | 7.67 | 0.015 | 0.01845 | 173 | 250.125 | | 184.0 |
| 13 | Col Brake Pressure | ±1.4 | Volt | | 0.015 | 0.01845 | | 500.0 | | |
| 14 | Vert Stick Position | ±5.018 | in | 2.5 | 0.015 | 0.01845 | 181 | | | 184.0 |
| 15 | Lat Stick Position | ±5.018 | in | 4.28 | 0.015 | 0.01845 | 189 | 457.315 | | 184.0 |
| 16 | DLC Pressure | ±10.0 | lb/in² | | 0.016 | 0.0164 | 209 | | | 204.8 |

**AC INPUTS**

| No | Variable *Limited at ±50° | Max VRMS | Units | Max Input at @ Units | Time Constant $T_1$ | $T_2$ | Comp Alg | Computer Scaling MU/Unit | | Scaling MU/VRMS |
|----|----|----|----|----|----|----|----|----|----|----|
| 1 | Aft Long Cable Angle* | 18.0 | Deg | ±90.0 | 0.0117 | 0.0195 | 51 | 40.024 | FWD | 200.1 |
| 2 | Fwd Long Cable Angle* | 18.0 | Deg | ±90.0 | 0.0117 | 0.0195 | 53 | 40.024 | FWD | 200.1 |
| 3 | Long LCCC | 10.4 | | | 0.0117 | 0.0201 | 55 | 1077 V. | AFT | 196.2 |
| 4 | Vert LCCC | 10.4 | | 5 | 0.0117 | 0.0201 | 57 | 4096 | UP | 196.2 |
| 5 | Pitch Rate | 6.0 | Deg/Sec | ±60.0 | 0.0117 | 0.0201 | 61 | 34.000 | UP | 140.0 |
| 6 | Spare No 1 | 10.4 | Volts | | 0.0117 | 0.0201 | 69 | 148.224 | | 196.2 |
| 7 | Spare No 2 | 10.4 | Volts | | 0.0117 | 0.0201 | 167 | 196.224 | | 196.2 |
| 8 | Left Cable Tension | 10.4 | lbs | 8000 | 0.0117 | 0.0201 | 169 | 0.256 | INCR | 196.2 |
| 9 | Right Cable Tension | 10.4 | lbs | 8000 | 0.0117 | 0.0201 | 177 | 0.256 | INCR | 196.2 |
| 10 | Aft Lat Cable Angle* | 18.0 | Deg | ±90.0 | 0.0117 | 0.0195 | 179 | 40.024 | LEFT | 200.1 |
| 11 | Fwd Lat Cable Angle* | 18.0 | Deg | ±90.0 | 0.0117 | 0.0195 | 181 | 40.024 | LEFT | 200.1 |
| 12 | Lat LCCC | 10.4 | Deg | 115.0 | 0.0117 | 0.0201 | 183 | 136.5 | CLOCKW | 196.2 |
| 13 | Lat LCCC | 10.4 | in | ±1.74 | 0.0117 | 0.0201 | 185 | 4177 | LEFT | 196.2 |
| 14 | Airspeed | 11.0 | Knots | 300 | 0.0117 | 0.0201 | 207 | 10.83 | INCR | 187 |
| 15 | Roll Rate | 6.0 | Deg/Sec | ±60.0 | 0.0117 | 0.0201 | 219 | 34.000 | RIGHT | 340.0 |
| 16 | Yaw Rate | 6.0 | Deg/Sec | ±60.0 | 0.0117 | 0.0201 | 221 | 34.000 | LEFT | 340.0 |

**SYNCHRO INPUTS**

| No | Variable | Variable Range | Max | $T_1$ | $T_2$ | Computer Algorithm | | |
|----|----|----|----|----|----|----|----|----|
| 1 | Pitch Attitude $s/c \cdot T/P \begin{cases} \sin\theta \\ \cos\theta \end{cases}$ | ±180° | 11.8 / 11.75 | 0.007 | | 63 / 65 | | NOSE UP |
| 2 | Spare $s/c \cdot T/P \begin{cases} \sin\phi \\ \cos\phi \end{cases}$ | ±180° | 11.8 / 11.75 | | | 71 / 73 | mv/deg at 90° | |
| 3 | Roll Attitude $s/c \cdot T/P \begin{cases} \sin\phi \\ \cos\phi \end{cases}$ | ±180° | 11.8 / 11.75 | 0.007 / 0.0201 | | 211 / 213 | mv/deg at 0° | RIGHT |
| 4 | Heading $s/c \cdot T/P \begin{cases} \sin\psi \\ \cos\psi \end{cases}$ | 0 → 360° | 11.8 / 11.75 | 0.007 / 0.0201 | | 215 / 217 | | RIGHT |

**DIGITAL INPUTS** — Word Length 16 bits

| No | Variable | Resolution | Units | Range | Computer Algorithm | Computer Scaling MU/Unit | Sense |
|----|----|----|----|----|----|----|----|
| 1 | N-S Velocity | 0.016 | ft/Sec | ±512 | 33 | 64 | FWD |
| 2 | E-W Velocity | 0.016 | ft/Sec | ±512 | 35 | 64 | RIGHT |

362

lags. The filter time constants are designed to attenuate sensor noise and undesirable harmonic frequencies attributed to airframe vibration and rotor downwash effects upon the pitot static system without compromising control loop stability and performance appropriate to the individual sensor.

### 3.2.4.3 Serial-Digital Data Processing

The IOP is designed to receive two serial-digital asychronous 32-bit whole words, although the computer is computer is timed to receive a total of six serial digital transmissions. Serial data from the Inertial Navigation Unit containing N-S, E-W velocity information is transmitted to the IOP. Each word, 32 bits in length, is updated every 50 m sec. Data transmission being used for HLH/ATC differs from the ARINC 561-2 standard in that the MSB (most significant data bit) is bit 30, rather than 29, thus making the sign bit 31 and parity bit 32.

### 3.2.4.4 Discrete Input/Output Processing

The discrete inputs to the IOP are listed in Table 19. These primarily consist of functional commands from the mode select panel and the system test function panel plus cockpit control functions. Some operational discretes are issued from sensor subsystems. The IOP accepts logic levels of 28 Vdc, 5 Vdc and ground-to-open which are buffered to operate high-level NAND logic gates.

Discrete and logic inputs are fed to four I/O discrete and mode logic circuit cards as shown in Figure 121. On each card, 16 discrete signals are multiplexed onto one output line. Logical operations are performed on the discrete inputs before multiplexing. The four discrete data lines are gated on the timing three-circuit card, generating a signal that is combined with digital and converted analog input data. The combined data signal is sent to the median selection and voting circuits, where the sensor input information is processed as described in Section 3.2.4.10, and to the discrete voters and failure monitors. The voted discretes are recombined with the sensor inputs in the circuits which drive the data bus to the computer. The computer discrete inputs are processed during even algorithm times 0 through 62 and 192 through 254.

Discrete outputs are received from the computer in odd algorithm times 1-49 and 129-175. These outputs are fed to a

363

Table 19.  IOP Discrete Inputs (PDI)

| No. | Discrete Signal | Source | Type |
|---|---|---|---|
| 1 | Drift Clear | Mode Select Panel | 28 vdc/open |
| 2 | AFCS Select | Mode Select Panel | 38 vdc/open |
| 3 | Coupled Approach Select | Mode Select Panel | 28 vdc/open |
| 4 | Hover Hold Select | Mode Select Panel | 28 vdc/open |
| 5 | Hover Trim Select | Mode Select Panel | 28 vdc/open |
| 6 | Vel Mode (Off) Enable | Mode Select Panel | 28 vdc/open |
| 7 | Vel Decay Select | Mode Select Panel | 28 vdc/open |
| 8 | A/S Select | Mode Select Panel | 28 vdc/open |
| 9 | G/S Select | Mode Select Panel | 28 vdc/open |
| 10 | Radar Alt Select | Mode Select Panel | 28 vdc/open |
| 11 | Baro Alt Select | Mode Select Panel | 28 vdc/open |
| 12 | Load Stab On | Mode Select Panel | 28 vdc/open |
| 13 | Error Reset | Mode Select Panel | 28 vdc/open |
| 14 | System Reset | Mode Select Panel | 28 vdc/open |
| 15 | BITE Arm | Mode Select Panel | 28 vdc/open |
| 16 | AFCS 2F | Mode Select Panel | 28 vdc/open |
| 17 | Alt Hold Select | Mode Select Panel | 28 vdc/open |
| 18 | LCCC Select | Mode Select Panel | 28 vdc/open |
| 19 | Eng/FDI Select | Mode Select Panel | 28 vdc/open |
| 20 | Long Axis Test | System Test Function Panel | 28 vdc/open |
| 21 | Lat Axis Test | System Test Function Panel | 28 vdc/open |
| 22 | Dir Axis Test | System Test Function Panel | 28 vdc/open |
| 23 | Vert Axis Test | System Test Function Panel | 28 vdc/open |
| 24 | LCP Test | System Test Function Panel | 28 vdc/open |
| 25 | Neg - Amplitude | System Test Function Panel | 28 vdc/open |
| 26 | LO - Amplitude | System Test Function Panel | 28 vdc/open |
| 27 | MED - Amplitude | System Test Function Panel | 28 vdc/open |
| 28 | HI - Amplitude | System Test Function Panel | 28 vdc/open |
| 29 | Pulse Input | System Test Function Panel | 28 vdc/open |
| 30 | Ramp Input | System Test Function Panel | 28 vdc/open |
| 31 | Step Input | System Test Function Panel | 28 vdc/open |
| 32 | Diff Test | System Test Function Panel | 28 vdc/open |
| 33 | Parallel Test | System Test Function Panel | 28 vdc/open |
| 34 | Gust Input | System Test Function Panel | 28 vdc/open |
| 35 | Long Axis Enable Select | System Test Function Panel | 28 vdc/open |
| 36 | Vert Axis Enable Select | System Test Function Panel | 28 vdc/open |
| 37 | Lat Axis Enable Select | System Test Function Panel | 28 vdc/open |
| 38 | Dir Axis Enable Select | System Test Function Panel | 28 vdc/open |
| 39 | Cyclic Mag Brake | CCDA Electronics | 28 vdc/open |
| 40 | Collective Mag Brake | CCDA Electronics | 28 vdc/open |
| 41 | AFCS Warning | DEL | 28 vdc/open |
| 42 | BIT Override | DEL | 28 vdc/open |
| 43 | Lat Beep Trim - Pos (Right) | Pilot's Cyclic Control | 28 vdc/open |
| 44 | Lat Beep Trim - Neg (Left) | Pilot's Cyclic Control | 28 vdc/open |
| 45 | Long Beep Trim - Pos (Aft) | Pilot's Cyclic Control | 28 vdc/open |
| 46 | Long Beep Trim - Neg (Fwd) | Pilot's Cyclic Control | 28 vdc/open |
| 47 | Dir Beep Trim - Pos (Right) | Pilot's Coll Control | 28 vdc/open |
| 48 | Dir Beep Trim - Neg (Left) | Pilot's Coll Control | 28 vdc/open |
| 49 | Dir Pedal Out Detent | Pilot's Dir Control | 28 vdc/open |
| 50 | Long Stick Out Detent | Pilot's Cyclic Control | 28 vdc/open |
| 51 | Lat Stick Out Detent | Pilot's Cyclic Control | 28 vdc/open |
| 52 | AFCS Release (FDS) | Pilot's Cyclic Control | 28 vdc/open |
| 53 | Ground Contact Aft No. 1 LEFT | Gear Switch | Gnd/open |
| 54 | Ground Contact Aft No. 2 LEFT | Gear Switch | Gnd/open |
| 55 | Ground Contact Aft No. 1 RIGHT | Gear Switch | Gnd/open |
| 56 | Ground Contact Aft No. 2 RIGHT | Gear Switch | Gnd/open |
| 57 | Mechanical Backup | FDTA | 28 vdc/open |
| 58 | PHS Lock | PHS | 0 vdc/open |
| 59 | LCC Drift Clear | Load Control Crewman | 28 vdc/open |
| 60 | *Disc Warning | IMU | 28 vdc/open |
| 61 | *Attitude Warning | IMU | 28 vdc/open |
| 62 | *Heading Warning | IMU | 28 vdc/open |
| 63 | Radar Rate Reliability | Radar Rate Adapter | 4.5 vdc/open |
| 64 | Pilot Enable PHS | Pilot PHS Enable Switch | Gnd/open |
| 65 | Load Pos Hold Sel | Load Pos Hold Rel Sw. | Gnd/open |
| 66 | PHS Internal R Lock | PHS | 9 vdc/open |

* Not Used.
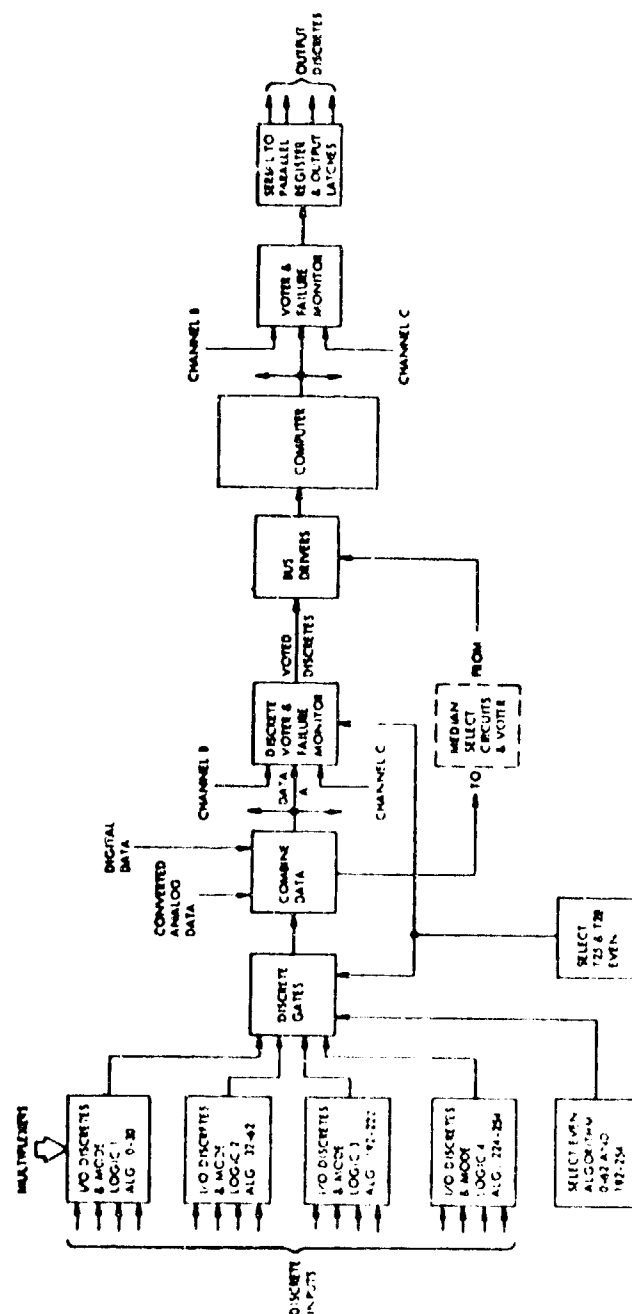
FIGURE 121. DISCRETE INPUT/OUTPUT PROCESSING

voter and failure monitor. The voted outputs are clocked
serially into a register. When all discretes within an
iteration have been received from the computer unit, the
shift register transfers the data to a holding register
which is directly coupled to output drive circuits.

The majority of IOP discrete outputs drive lamps in the mode
select, AFCS failure status, sensor failure status and dis-
crete status panels. A list of these outputs is given in
Table 20.

3.2.4.5 Sensor Signal Processing

The circuits that process sensor input signals are located
in the IOPs. These circuits have a threefold purpose:

- To ensure that the computers receive a valid input in
  usable form.

- To ensure that all three computer units receive identi-
  cal inputs so that the computations performed by all
  computers will be identical.

- To monitor the inputs for failure and provide failure
  status information to the other circuits that require it.

The processing of sensor inputs differs slightly, depending on
whether the input is triplex, dual or nonredundant. Figure
122 shows the signal flow for triplex sensors. Dual sensor
inputs are processed as if they were triplex with one channel
failed, and are connected to channels A and C. Nonredundant
(simplex) inputs are fed to all three channels and processed
like triplex inputs, however, it is to be noted that:

- No failure of a nonredundant sensor will shut down the
  system.

- Failure indications apply only to input signal con-
  ditioning circuits since all channels receive the
  same signal.

366

## Table 20.  IOP Discrete Outputs  (PDO)

IOP DISCRETE OUTPUTS (PDO)

| No. | Discrete Signal | Destination | Type |
|---|---|---|---|
| 1 | System 2nd Fail | AFCS Failure Status | Ground/Open |
| 2 | Computer First Fail | | |
| 3 | Computer Input Data | | |
| 4 | Computer Clock | | |
| 5 | Computer Iteration Reset | | |
| 6 | Computer ROM | | |
| 7 | Computer RAM | | |
| 8 | Computer Shift Register | | |
| 9 | Computer Power | | |
| 10 | Computer Overflow | | |
| 11 | IOP First Fail | | |
| 12 | IOP Output Data | | |
| 13 | IOP Input Discrete | | |
| 14 | IOP Iteration Reset | | |
| 15 | IOP Clock Switchover | | |
| 16 | IOP Primary Clock | | |
| 17 | IOP Secondary Clock | | |
| 18 | IOP Power | | |
| 19 | Longitudinal Rate | AFCS Sensor Failure Status | |
| 20 | Longitudinal Attitude | | |
| 21 | Longitudinal Airspeed | | |
| 22 | Longitudinal Control Position Transducers | | |
| 23 | Lateral Rate | | |
| 24 | Lateral Attitude | | |
| 25 | Lateral CPT | | |
| 26 | Directional Rate | | |
| 27 | Directional Heading | | |
| 28 | Directional Sideslip | | |
| 29 | Directional CPT | | |
| 30 | Vertical Acceleration | | |
| 31 | Vertical Baro Altitude | | |
| 32 | LCCC | | |
| 33 | Simplex I-3 | | |
| 34 | IMU/Groundspeed | | |
| 35 | Gear Switch | | |
| 36 | Ground Contact | Discrete Status #1 | |
| 37 | Long. Out of Detent | | |
| 38 | Lat. Out of Detent | | |
| 39 | Dir. Out of Detent | | |
| 40 | Long. CCDA Sync | | |
| 41 | Lat. CCDA Sync | | |
| 42 | Dir. CCDA Sync | | |
| 43 | Vert. CCDA Sync | | |
| 44 | Roll Stabilized | | |
| 45 | Heading Stabilized | | |
| 46 | Beep Disconnect | | |
| 47 | Long. Bias | | |
| 48 | Lat. Bias | | |
| 49 | Roll Rate | | |
| 50 | Roll Attitude | | |
| 51 | Roll Attitude Error | | |
| 52 | Roll Limit Detector | | |
| 53 | Diff. Pressure | | |
| 54 | Heading Rate | | |
| 55 | Airspeed Reference | | |
| 56 | Long. Position Stabilize | Discrete Status #2 | |
| 57 | Lat. Position Stabilize | | |
| 58 | Vert. Position Stabilize | | |
| 59 | Long. LCCC Detent | | |
| 60 | Long. LCCC Threshold | | |
| 61 | Lat. LCCC Detent | | |
| 62 | Lat. LCCC Threshold | | |
| 63 | Vert. LCCC Detent | | |
| 64 | Vert. LCCC Threshold | | |
| 65 | PHS Internal Relock Threshold | | |
| 66 | PHS Relock Command | | |
| 67 | Flasher Group 1 | Mode Select Panel | 5 VDC/Open |
| 68 | Flasher Group 2 | | |
| 69 | Flasher Group 3 | | |
| 70 | Flasher Group 4 | | |
| 71 | Flasher Group 5 | | |
| 72 | Flasher Group 6 | | |
| 73 | Flasher Group 7 | | |
| 74 | Flasher Group 8 | | |
| 75 | Flasher Group 9 | | |

Table 20 (Continued)

| No. | Discrete Signal | Destination | Type |
|-----|-----------------|-------------|------|
| 76 | AFCS DEL Engage | Mode Select Panel | 28 vdc/open |
| 77 | AFCS Engage | Mode Select Panel, 28 vdc bulb | Gnd/open |
| 78 | Engage FD1 | | |
| 79 | CPLR Engage | | |
| 80 | LCCC Enabled | | |
| 81 | Hover Hold Engage | | |
| 82 | Baro Alt. Hold Engage | | |
| 83 | Radar Alt. Hold Engage | | |
| 84 | Hover Trim Engage | | |
| 85 | Drift Clear Engage | | |
| 86 | Baro Altitude Hold | Baro Altitude Sensor | 28 vdc/open |
| 87 | PHS Relock CMD | PHS | 5 vdc/open |
| 88 | PHS Operate CMD | PHS | 5 vdc/open |
| 89 | Vert CCDA Engage | CCDA Electronics | 28 vdc/open |
| 90 | Long CCDA Engage | | |
| 91 | Lat CCDA Engage | | |
| 92 | Dir CCDA Engage | | |
| 93 | AFCS 2F | DEL | 28 vdc/open |
| 94 | AFCS I/O Reset | DEL | 28 vdc/open |
| 95 | Stick Command Wrn Flag | Flight Director | 28 vdc/open |
| 96 | Position Error Wrn Flag | Flight Director | 28 vdc/open |
| 97 | (MAP) Long Axis Off | Mode Advisory Panel | Gnd/open |
| 98 | (MAP) Lat Axis Off | | |
| 99 | (MAP) Dir Axis Off | | |
| 100 | (MAP) Vert Axis Off | | |
| 101 | Velocity Scale Change | Ground Vel. Indicator | 28 vdc/open |
| 102 | LCC Armed | LCC Armed Light (LCC Capsule) | 28 vdc/open |
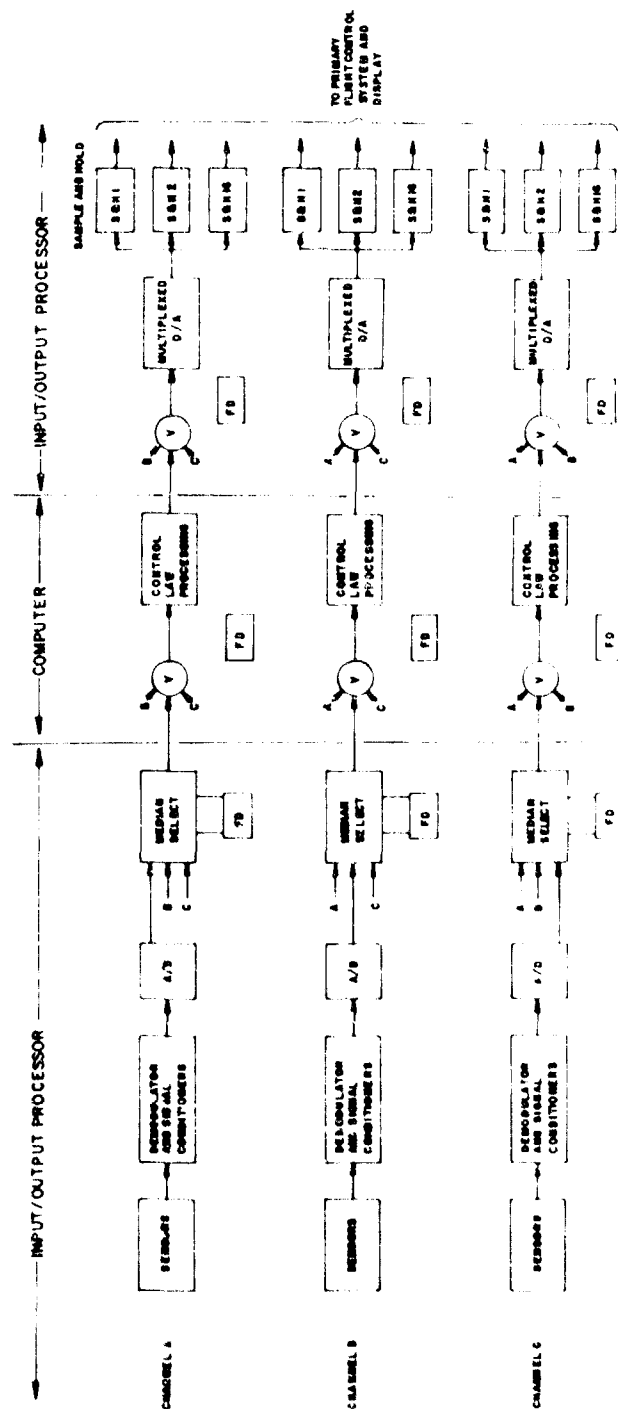
FIGURE 122. SIGNAL INTERFACE FLOW FOR TRIPLEX SENSORS

### 3.2.4.6  Analog Output Processing

The IOP has a 32-channel digital/analog (D/A converter) but only 16 sample-and-hold circuits are mechanized.  The analog outputs of the AFCS are listed in Table 21.

The computer outputs are fed to majority logic voters in each IOP.  The voted outputs are loaded into a register during time slots T1 - T16 of even algorithms 0 - 20 and 128 - 138. While an output is stored in this register, it is tested for overflow.  In the next succeeding even algorithm, the output is shifted out of the register into the input register of the D/A converter, while the next output is shifted into the over-flow detection register.  The D/A converter output is allowed to settle for the remainder of the algorithm time.  The ladder summing network and its current drive amplifier are allowed 12 microseconds for settling after the D/A register is loaded. This is about twice the time required for the amplifier to settle within 1/2 LSB.

Sixteen sample-and-hold circuits are connected to the D/A converter output.  The sample-and-hold circuits are supplied with a D/A strobe signal and a gate signal from one of three demultiplexers.  When both of these logic signals are low, the sample-and-hold switch is closed, and the multiplexed sample and hold is then placed into the sample mode for 24 microseconds and the D/A converter output is acquired.  It is then returned to the hold mode.  A typical droop for the circuit is 100 M V/sec.

All output signals are scaled for $\pm 10$ Vdc and drive into high impedance loads except for the flight director signals.  The output impedance of the sample-and-hold circuit is low and the output buffer resistor values associated with the flight director are chosen to give proper indicator deflection. Longitudinal groundspeed output is mechanized only in Channel A.  Lateral groundspeed output is mechanized only in Channel C.  This permits the total number of dc outputs per IOP to be 6.

### 3.2.4.7  Clock System and Timing (Figure 128)

Bit time synchronization of the three redundant channels is accomplished by driving each from the same oscillator refer-ence.  The fail-operational requirement is handled by using two oscillators and switching to the second in a transient-

**TABLE 21.**   **ICP ANALOG DC OUTPUTS**

**Range:** ± 10 vdc; ± 2048 Machine Units (MU)

| No. | D/A No. | Variable | Units | Range | Max. Output | Computer Scaling MU/Unit | Comp. Algorithm | Resistor ohms | +VDC Sense |
|---|---|---|---|---|---|---|---|---|---|
| 1 | 1 | Long. CMD-DEL | in. | ±4.0 | 4.0 | 512 | 0 | 150 | Nose Dwn |
| 2 | 2 | Vert. CMD-DEL | in. | ±1.5 | 1.5 | 1365.33 | 2 | 150 | Down |
| 3 | 3 | Long. CMD-CCDA | in. | ±4.0 | 4.0 | 512 | 4 | 150 | Aft Stk |
| 4 | 4 | Vert. CMD-CCDA | in. | ±4.0 | 4.0 | 512 | 6 | 150 | Down |
| 5 | 5 | Fwd LCP | deg | ±4.0 | 4.0 | 512 | 8 | 150 | Tilt Aft |
| 6 | 6 | Aft LCP | deg | ±4.0 | 4.0 | 512 | 10 | 150 | Tilt Fwd |
| 7 | 7 | Vert. Pos Error | μa | ±150 | 550 | 3.724 | 12 | 16.9K | Up |
| 8 | 8 | Collective Stk Comm. | ma | ±2.2 | 4.115 | 497.691 | 14 | 1430 | Up |
| 9 | 9 | Long. Stk Comm. | μa | ±275 | 15.0 | 1.356 | 16 | 5620 | Up |
| 10 | 10 | Long. Ground Speed | ad | ±150 | 151 | 13.563 | 18 | 64.9K | Down |
| 11 | 11 | Lat. Ground Speed | μa | ±150 | 151 | 13.563 | 20 | 54.9K | Right |
| 12 | 12 | Lat. CMD-DEL | in. | ±1.5 | 1.5 | 1365.33 | 128 | 150 | Right |
| 13 | 13 | Dir. CMD-DEL | in. | ±1.5 | 1.5 | 1365.33 | 130 | 150 | Right |
| 14 | 14 | Lat. CMD-CCDA | in. | ±1.5 | 1.0 | 2048 | 132 | 150 | Right |
| 15 | 15 | Dir. CMD-CCDA | in. | ±1.5 | 1.5 | 1365.33 | 134 | 150 | Left |
| 16 | 16 | Lat. Pos Error | vac | −0.02 | 0.05 | 40960 | 136 | 200K | Left |
| 17 | 17 | Lat. Stk Comm | μe | ±390 | 1510 | 1.356 | 138 | 5620 | Right |
| | | | | | | | 140 | | |
| | | | | | | | 142 | | |
| | | | | | | | 144 | | |
| | | | | | | | 146 | | |
| | | | | | | | 148 | | |

372

FIGURE 123 SYNCHRONIZED REDUNDANT CLOCK SYSTEM

free manner upon the failure of the first. Primary and sec-
ondary oscillator monitoring circuitry and switchover logic
is repeated in each channel so monitoring circuitry and switch-
over logic is repeated in each channel so that failures of the
switchover circuitry in one channel cannot affect the other
two channels. The switchover command generated in each channel
is voted with the other two channels to affect all three
channels, switching over to the secondary oscillator simultan-
eously when two channels have detected a failure of the primary
oscillator. A simple monitor is used that essentially compares
the oscillator signal with itself, delayed 1/2 the nominal
period. A pulse is generated whose width is proportional to
the difference of the oscillator period from nominal. If the
width of the generated pulse is greater than a given time
delay (this sets the tolerance), an oscillator failure pulse
is generated and a failure latch is set.

### 3.2.4.8  Power

The IOP operates on dual source 115 VAC, 400 Hz single-phase
power and single source 28 volts DC. The regulated DC voltage
required by the IOP circuitry is generated within the unit
from the 115 VAC line, and is arranged such that loss of a
single AC supply will not cause the loss of IOP operation.
The 28 VDC is used for control logic and BITE flag drivers.

### 3.2.4.9  Built-In-Test Equipment (BITE)

This constitutes an important part of the IOP design. The
BITE system is semi-automatic and is used to detect failures
within the system failure detection circuits. The principle
used is that if during preflight test it can be determined that
all failure monitors are working properly, then the probability
of an undetected failure occurring in flight is greatly reduced.
Thus, the BITE system can only be armed when the engine throttle
levers are in the OFF position, otherwise BITE is inhibited.

The BITE function is separated into simplex channel and tri-
plex system tests. The channel test consists of 32 time slots
which check all the failure monitors in one channel while the
whole system is operating. This is run through for each
channel. The system test checks the operation of the triplex
failure monitors in 15 time slots and is run once. An outline
of the test sequence is given in Table 22.

Table ... ... Test ... Sequence

| Test Number | Failure Monitored | | |
|---|---|---|---|
| T01 | No computer connect (1st, 2nd Pass) No system shutdown | | |
| T02 | Computer ... Computer local | | |
| T03 | Computer and System shutdown | Input data ... simulated ... another ... Error rate | |
| T04 | No computer connect | | |
| T05 | Computer set Comp no local | Local ... Reset fail | |
| T06 | | Active ... | |
| T07 | | | |
| T08 | | | |
| T09 | | | |
| T10 | No IOP failure | | |
| T11 | IOP set IOP local | | |
| T12 | IOP ... | | |
| T13 | | | |
| T14 | IOP set IOP local | | |
| T15 | | | |
| T16 | No IOP failure | | |
| T17 | IOP set IOP local | | |
| T18 | IOP set | | |
| T19 | No IOP failure | | |
| T20 | IOP first IOP two Primary stuck | | |
| T21 | | | |
| T22 | | | |
| T23 | | | |
| T24 | | | |

Table 22 (Continued)

| Test Number | Failure Monitored | Signals Activated | Test Description |
|---|---|---|---|
| T25 | .... | Error reset Computational reset | Reset the discrete errors |
| T26 | No rate gyro failures | .... | Check for no initial failures |
| T27 | | Rate gyro test positive | Sensor Failure Engage relays to torque all three rate gyros positive |
| T28 | Pitch Rate Roll Rate Yaw Rate | Error reset Computational reset | Sensor Failure Check that failures have occurred and reset errors |
| T29 | No rate gyro errors | .... | Check for no initial failures |
| T30 | .. | Rate gyro test negative | Sensor Failure Engage relays to torque all three rate gyros negative |
| T31 | Pitch Rate Roll Rate Yaw Rate | Error reset Computational reset | Sensor Failure Check that failures have occurred and reset errors |
| T32 | .. | .. | Stop sequencer Illuminate GO light on BITE Panel |
| ST01 | No axis second failures | Error reset Computational reset | System Tests Initialize system test sequence with a system reset Check for no residual failures |
| ST02 | .. | Rate gyro test channel A negative channel C positive | Axis Failures Torque channel A gyros negative Torque channel C gyros positive |
| ST03 | Lateral axis Longitudinal axis Directional axis 2nd failures | Error reset Computational reset | Axis Failures Check that failures have occurred then reset the errors |
| ST04 | .... | .... | Spare |
| ST05 | .... | .. | Spare |
| ST06 | .... | .. | Spare |
| ST07 | Analog output | Analog input | Analog I/O Insert analog bias and monitor analog output |
| ST08 | No IOP failures | .... | Check for no initial failures |
| ST09 | Discrete 1st | Channel A discrete input failure | Discretes Fail a signal in channel A only check for first failure |
| ST10 | Discrete 2nd | Channel B discrete input failure Error reset | Discretes Fail a signal in channel B only check for second failure then reset the errors |
| ST11 | No computer overflow No system shutdown | . | Check for no initial failures |
| ST12 | Computer overflow System shutdown | X/Y overflow test Error reset Computational reset | Computer Overflow Overflow the X, Y register and check for failure and system shutdown then reset the errors |
| ST13 | Computer overflow | $U_o$, $V_o$ overflow test Error reset Computational reset | Computer Overflow Overflow the $U_o$, $V_o$ register and check for failure indication then reset the errors |
| ST14 | .... | .... | Spare |
| ST15 | .... | .... | Stop sequencer Illuminate the GO light on the BITE Panel |
| ST16 | .. | .... | Spare |

A general block diagram of the BITE system is given in Figure
124. The operation of the system is controlled and timed by
the sequencer. The reset, stimulation, and monitor sections
perform their functions under that control. In the system
test mode, interchannel communication is necessary to keep the
three BITE systems running synchronously. The failure monitors
are tested by first inserting FAIL signal into the input of the
voter-monitor. This should cause the monitor to latch in a
first-failure indication. This indication is monitored by
the BITE circuitry. This FAIL signal is removed and another
input is failed. This should cause second-failure indication,
which is also checked. Note that testing does not affect the
output of the voter because no more than one input is in a
failed state at any particular time.

In the case of the sensor failure monitors, the rate gyros
are stimulated in a manner such that a simulated gyro failure
is detected by the failure monitor. The sensor failure moni-
tor is time shared and so is checked for any type of sensor
failure. At the completion of each test time slot, the fail-
ure latching networks must be unlatched and so the BITE per-
forms an ERROR reset or system (computational) reset
automatically.

3.2.4.10   Redundancy Management

Redundancy management pertains to the reconfiguration of a
malfunctioning system in order to preserve safe flight condi-
tions. The basic requirements of the AFCS performance in the
event of equipment failures are that the system be:

a.   Fail-operational in the event of a system first-failure
     condition. Fail-operational performance is defined
     such that no system performance degradation is experi-
     enced with a system first failure.

b.   Fail-safe in the event of a system second-failure con-
     dition. Fail-safe performance is defined by the con-
     dition that any transient signal commanded to DELS or
     speed trim or CCDA upon a failure can be safely compen-
     sated for by pilot action.

The system provides fail-operational, fail-safe performance for
triplex sensors, fail-safe performance for dual sensors and
fail-limited performance for single sensors. Fail-limited is
defined as a condition where a failure of a nonredundant
sensor associated with a selectable mode is limited to a
magnitude such that the pilot can override and or switch off
the affected mode to allow safe recovery of the aircraft.
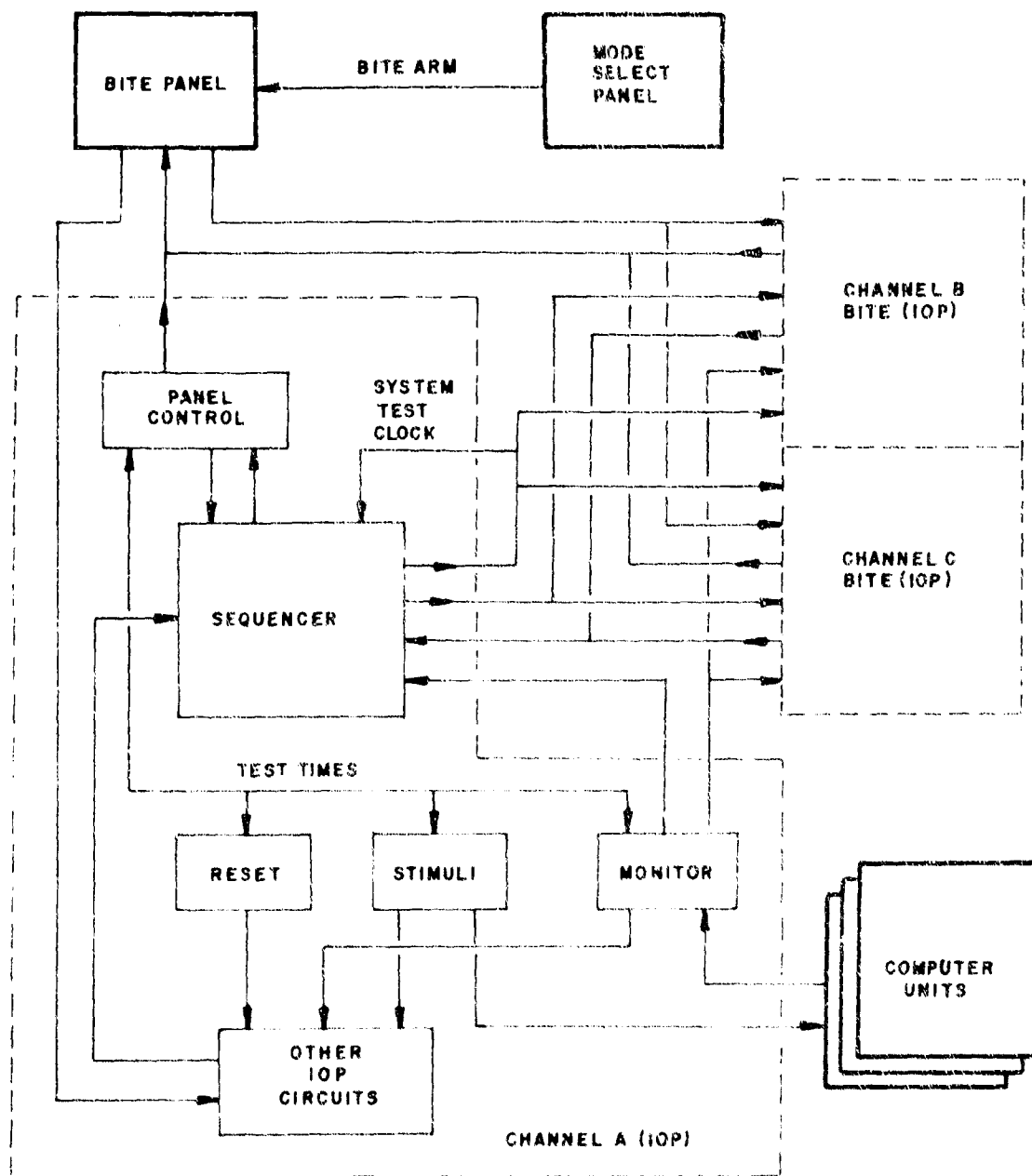
FIGURE 124. BITE CIRCUIT BLOCK DIAGRAM

The AFCS, while not considered critical to safety of flight, is categorized into three regimes regarding degree of criticality and consequent functional capability following loss or degradation of the flight control function. These are:

a.  System level failures are deemed most critical when requiring total AFCS shutdown and reversion to unaugmented flight.

b.  AFCS axis failures require the shutdown of individual or multiple combination of axes.

c.  Selectable mode failures deemed least critical require manual disengagement or pilot override of the selected mode.

In order to fulfill the specification requirements for fail-operational capability on a system level, a triplex system configuration was chosen for the AFCS. The following redundant connections were adopted to maintain complete channel independence on the system level basis:

*   All IOP and computer units are identical and therefore interchangeable between channels.

*   All cross-channel data transfer is performed between the IOP units and is isolated such that failure of one channel cannot propagate into another channel. This implies that all signal transmissions between IOPs are accomplished in two separate cables carrying information in opposing directions.

*   Each computer operates in conjunction with and communicates only with its own IOP. All signal transmissions between the two units are carried in one cable.

*   All information prior to first stage voting in each IOP is manipulated into triplex format.

*   All voting and signal selection is performed digitally.

The redundancy management scheme for the HLH-ATC AFCS is a software function primarily contained within the IOPs. The scheme involves the appropriate selection of sensor inputs and the detection of sensor failures, the control and monitoring of strategically located voters throughout the system input to output computational process and the appropriate logic control to handle axis and system level shutdown automatically with suitable indication to the pilot.

## 3.3  AFCS SENSORS

### Sensor Signal Selection and Failure Detection

All the redundant signals are selected in the IOP. The sensor
selector selects the median of three signals until an indi-
vidual sensor has failed. If one of the three sensors fail,
the two remaining good signals are averaged and the average
value is sent to the computer. At a sensor second failure,
the selector continues to use the average of the two signals
that were used after the first failure. The sensor selector
will not switch back to the median value if the first failure
heals itself. Only a system reset (computational reset)
unlatches the selector mechanism to permit median selection
again. The same functions are used for dual sensors such
that the system is forced to average the dual signals. A
signal second failure requires various types of action depend-
ing on which signal has failed. A failure decoder is used
for this purpose which is based upon the sensor redundancy
level. The sensor signal selector mechanism is a time-shared
device which can be used for up to a maximum of 64 input
variables.

The sensor failure monitor is designed to provide a high
degree of flexibility. The scheme is shown in Figure 125.
The two sensor failure detection paths are used to improve
the probability of detecting all types of sensor failure
modes.

The cross-channel monitor compares each sensor channel with
the other two sensor channels. When the difference between
any two channels exceeds a preset value for a preset time
period, a failure of one of the two particular channels is
said to have occurred.

The low-pass filter removes the high frequency noise in order
to reduce the detection level, which must be set low enough to
satisfy maximum aircraft failure transient response levels,
yet must be high enough to avoid nuisance or false failure
indications. The low-pass filter is used to detect slow drift
and hardover-type failures.

The band-pass filter path (washout) is used such that the
detect level can be reduced for detecting passive type fail-
ures. The band-pass filter removes the null error and the
high frequency noise from the sensor signals being monitored.

379
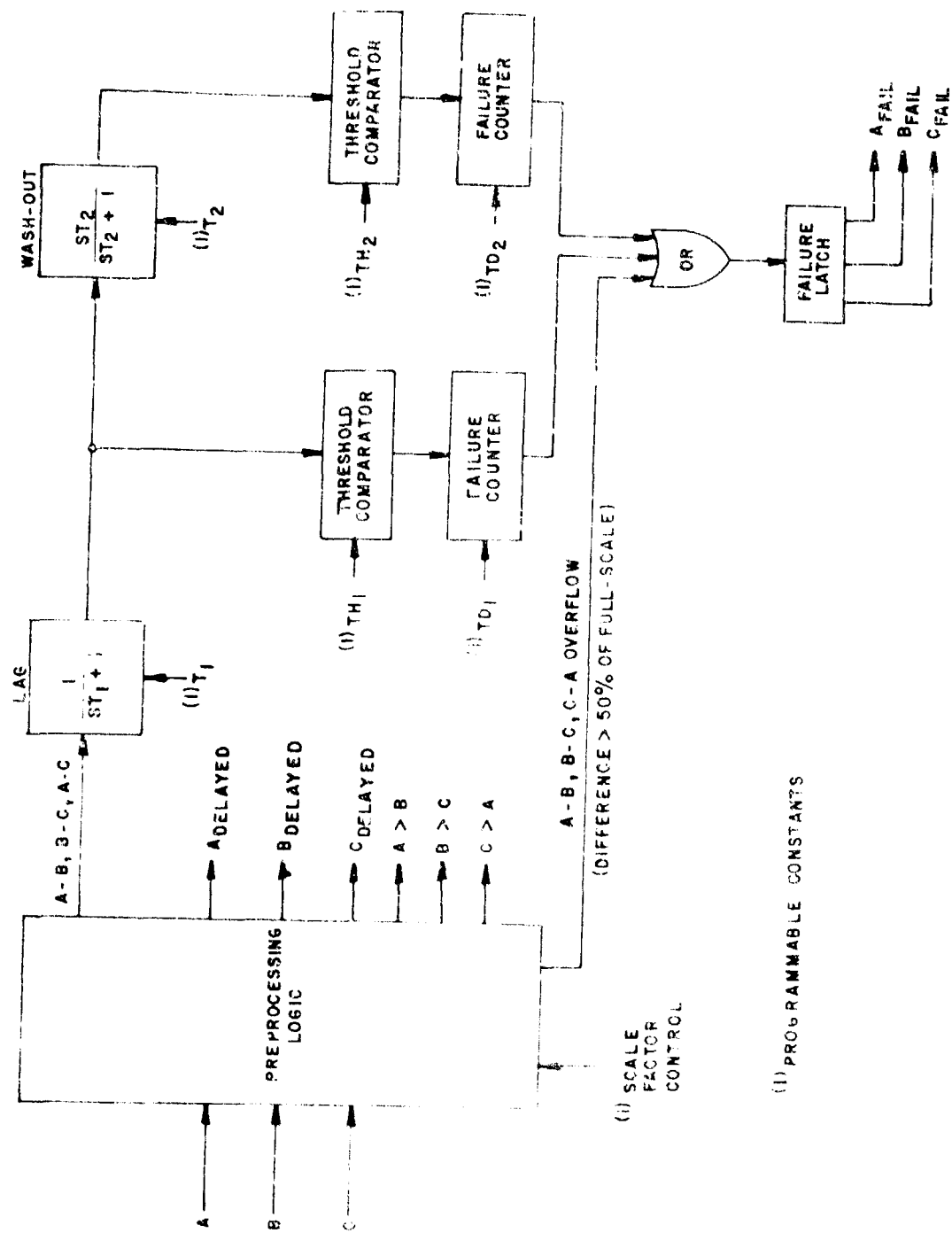
FIGURE 125. SENSOR FAILURE MONITOR BLOCK DIAGRAM

The frequency content of the signals that exist even when the sensor is operating around null can be used to detect failures if the null offset is eliminated from the threshold detection. The optimum bandpass characteristics depend upon the sensor characteristics.

The failure counters are used to delay failure indications that would occur because of transient conditions that could be caused by sensor switching and power transients. The failure counter in the lag path will typically be programmed for a shorter time than the failure counter in the washout path, such that the shorter time delay in the low-pass filter path permits time to shut down to be a function of the hardover amplitude.

All the time constants, threshold levels and time delays are programmed in the IOP Programmable Read Only Memory (PROM) for each of the input variables.

## Voting and Failure Monitoring

Majority logic voters and failure monitor circuits are placed at strategic points in the computers and IOP.

### Input/Output Data Voters

The computer input/output data voters provide redundant path isolation between the computer and IOP units. This means that a failure of a computer in any one channel does not cause the loss of the IOP unit in the same channel and vice versa. The processed sensor signal is sent from each IOP to all three computers, as shown in Figure 122. In each computer, an input voter compares the three inputs by pairs, bit by bit and outputs a signal corresponding to two out of three inputs. The voter and associated failure monitor is shown in Figure 126. If one input differs from the other two, a first failure output is generated. If, subsequent to a first failure, the two previously non-failed inputs should differ, a second failure output is generated. A local failure is indicated only if there is a fault in the failure monitor.

The computed signal outputs are majority logic voted in each IOP and then fed to overflow detection circuits before being processed through the D/A converter and output sample-and-hold circuits.
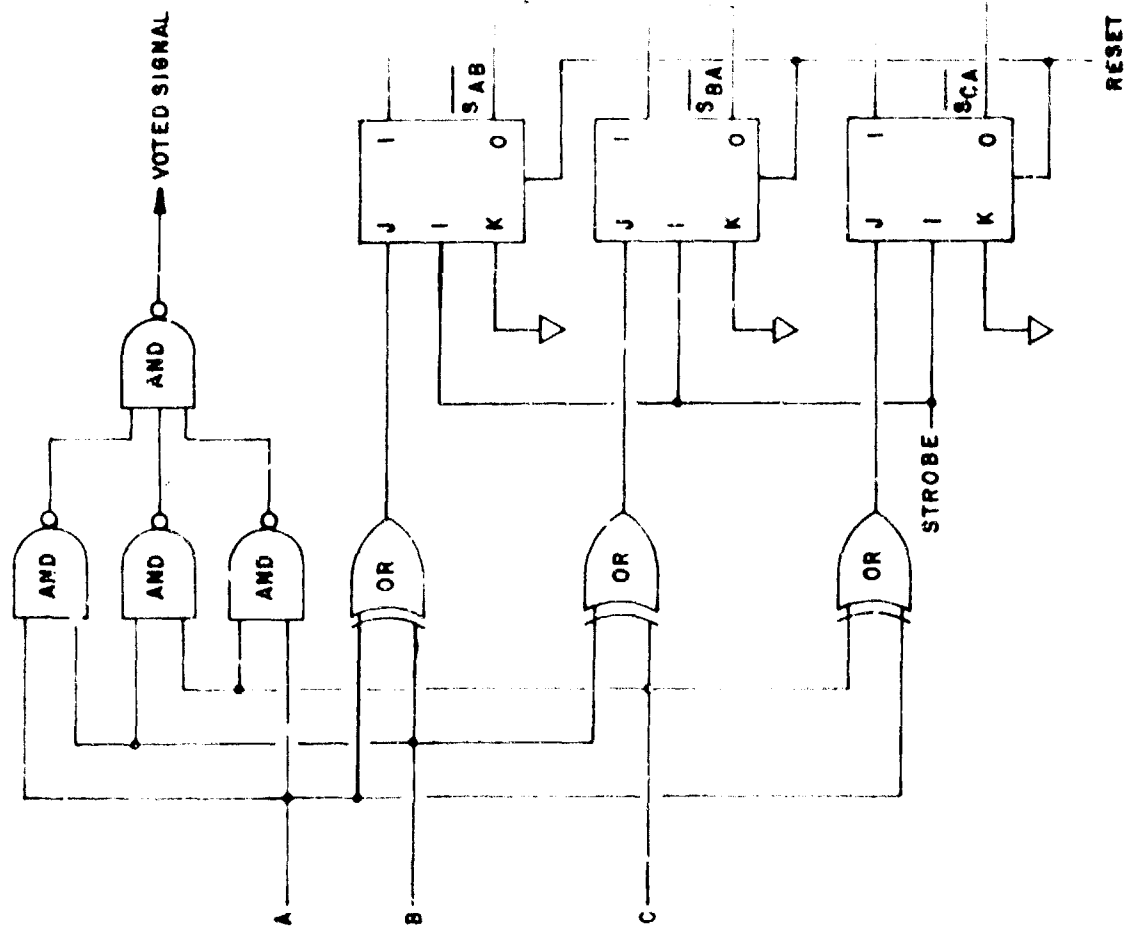
FIGURE 126. MAJORITY LOGIC AND MONITOR SCHEMATIC

## Iteration Reset and Clock Voters

The iteration reset, clock, and clock switchover voters are required to provide bit synchronous operation between channels.

## Discrete Input Voter

The discrete input voter is required to synchronize asynchronous data caused by delays such as switch contact closure. Failure tripout can be delayed by any number of counts up to a register maximum of 15. The timing may be selected such that the discretes are sampled once every eight iterations and if any incompatibility exists for eight consecutive samples, a failure is announced. This would account for a period of approximately 640 ms. Alternatively, one could sample 15 consecutive iterations, which would account for a period of approximately 150 ms.

## 3.3.1   Airspeed Sensor

Airspeed for the AFCS is provided by three precision airspeed trim (PAST) units which convert pitot-static pressure inputs to linearized indicated airspeed outputs. The AFCS uses airspeed data for velocity command in the longitudinal axis, lateral stick trim, pedal position, and collective position compensation. PAST was developed by Boeing for the Model 347 flight test program which used two PAST units. One additional unit was added to meet the HLH/ATC triplex requirement.

The PAST utilizes a feedback servo loop which renulls the force exerted by pitot pressure on the airspeed transducer diaphragm. This is accomplished by integrating the error through a motor, which runs a main cam proportional to pitot pressure (a "q" or squared function) and a force through a spring is fed back to renull the force on the diaphram (see Figure 127). On the servo motor output shaft, there are several programmed cams which provide linear or schedule position motion signals through spring-loaded LVDTs. One of these cams provides the linearized airspeed output to the FCCS. Two additional cams in the A & C channels provide the airspeed scheduling to the longitudinal cyclic pitch speed trim electronic units.

Total pressure is supplied to each PAST unit via dedicated pitot heads. Static pressure inputs are paralleled from a

STATIC
PRESSURE

BELLOWS

LVDT

EXCITATION

POWER
AMP

SPRING

PROGRAMMER
CHMS

Q SHAPED
CAM

BELLOWS

PITOT
PRESSURE

SERVO
MOTOR

LVDT
XDCR

40 KNOT
SWITCH

LVDT
XDCR

LINEARIZED
IAS

MECHANICAL SYSTEM

AIRSPEED
LINEARIZED

$\dfrac{K}{S}$

$Y = X^2$

BLOCK DIAGRAM
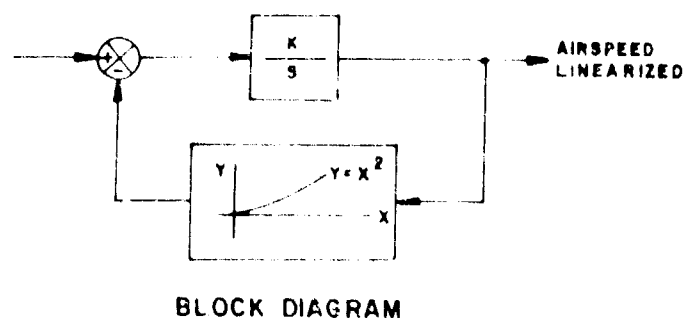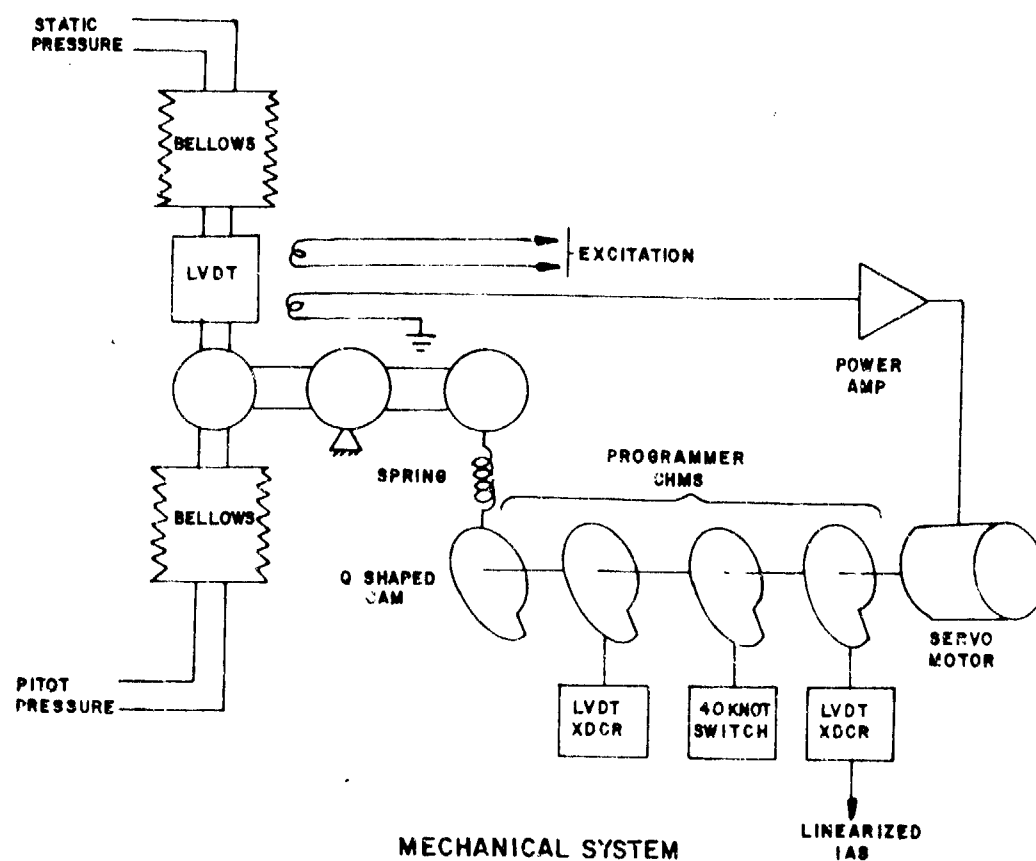
FIGURE 127. PRECISION AIRSPEED TRIM BOX

single pair of static ports.  The units have a manually slewed
test inject feature which simulates airspeed output over the
entire operating range for preflight and bench checkout.  Per-
formance characteristics are summarized below:

| | |
|---|---|
| Differential pressure range | 2 psi |
| Burst pressure range | 5 psi |
| Linearity | 0.3 percent of full-scale output voltage |
| Resolution | 0.1 percent of full-scale output voltage |
| Accuracy (overall) | 0.5 percent |
| Bandwidth | Flat to at least 6 Hz |
| Voltage Output | 11 VRMs (0 to 1.5 psi) |

### 3.3.2  Sideslip Sensor

Lateral differential pressure (i.e., sideslip) is required by
the AFCS to augment the directional stability of the aircraft
and to provide a positive pedal control gradient.

Each of the three sideslip sensing systems consists of a set
of pressure ports, a differential variable-capacitance trans-
ducer, and conditioning electronics.

Two sideslip transducers measure differential pressure through
the existing SAS sideslip pressure ports and plumbing. ımbing.
A similar set of components was installed to provide the third
channel of data for the ATC system.  The pressure ports
mounted on either side of the lower forward fuselage are
electrically heated.

Performance characteristics of the transducer and electronics
are:

- Differential air pressure range of transducer $\pm 0.75$ psi

- Burst pressure range of transducer $\pm 1.0$ psi

- Resolution   0.05 percent of FS

- Linearity  0.1 percent of FS

- Accuracy (overall)  0.2 percent of full scale

- Bandwidth  6 Hz

- Output signal range $\pm$10 Vdc

### 3.3.3  Reference Barometric Altitude

The reference barometric altitude sensor (sometimes referred to as altitude synchronizer) provides high and low sensitivity differential barometric altitude output signals to the AFCS:

- The high-gain signal has a range of $\pm$250 feet for $\pm$10.0 Vdc and is used for Altitude Hold and Hover Hold modes.

- The low-gain signal has a range of $\pm$1500 feet for $\pm$10.0 Vdc and is only used for Automatic Approach to Hover mode.

A pair of static pressure ports, one mounted on either side of the fuselage at station 240, are manifolded together to feed two barometric altitude sensors, which are mounted close together on the right side of the aircraft cabin.  The dual sensor output signals are transmitted to AFCS channels A and C.  Each sensor has a manual self-test capability, which is only operable when the appropriate AFCS modes have been selected.  The sensor signal outputs normally remain in an altitude synchronizing (tracking) mode which results in a zero signal output until an altitude stabilizing discrete is issued from the AFCS mode logic.  Upon command, the sensor references to the local aircraft barometric altitude and the output signals indicate deviation in altitude from the selected reference point.  The sensor is designed to operate over a pressure altitude range of -1000 ft  to $\pm$15,000 ft.

The reference barometric altitude sensor used on the HLH-ATC 347 demonstrator aircraft uses virtually the same components as the altitude sensor designed for the Canadian CH-147 AFCS, with some signal scaling modifications.  The sensor consists of two major elements; the pressure sensing transducer and the signal conditioning electronics.

386

The static-pressure sensing transducer is of the variable resistance type; i.e., unbonded strain gage windings from two arms of a Wheatstone bridge. Pressure against the diaphragm produces a displacement of the sensing element changing the resistance of the active arms and causes an electrical output precisely proportional to applied pressure. Acceleration and vibration have little effect on bridge output, being cancelled by the geometry and winding arrangement of the star spring-type sensing element. Compensation for the effects of wide ambient temperature variations is provided by locating the two inactive arms close to the active windings and through careful selection of materials in manufacturing.

The signal conditioning electronics is split into two stages; the first stage comprises a closed-loop analog/digital servomechanism to re-reference the bridge output to provide a limited altitude range about a selected absolute altitude. The bridge signal output is first amplified and passed to a threshold detector. When the signal exceeds a specified level, a pulse is produced and fed to a register which drives a digital-to-analog converter. The ladder resistor chain is in parallel with the bridge inactive arms, and thus acts to vary the resistance to rebalance the bridge output. The altitude hold logic discrete acts to inhibit pulse outputs when the stabilize mode is requested.

The second stage comprises an analog synchronizer followed by two output signal drives, one for low sensitivity, and the other for high sensitivity. The analog synchronizer consists of a capacitor, field effect transistor, and a relay, all contained within a sealed can for humidity protection. The synchronizer provides a zero output signal reference in the altitude tracking mode during the time that the first stage is continually rebalancing the bridge output. When the stabilize discrete is issued from the AFCS, there is an initial delay to acquire bridge balance, followed by the analog synchronizer delay in acquiring a stabilized output. The total time to stabilize can be as much as one second.

### 3.3.4  Rate Gyros

Rate gyros provide the AFCS control loops with effective body-referenced rate data. The rate gyros used are the General Electric RR-15 which were designed and fabricated for the F-15 AFCS. Each rate gyro unit consists of three mutually orthogonal rate sensors which sense rate of angular motion

about the pitch, roll, and yaw axes of the aircraft. Each
sensor contains a motor speed detector for self test. Also,
the unit incorporates circuitry to torque the gimbal output
axis during preflight BITE. Major performance characteristics
are: range $\pm 60$ deg/sec, resolution of $\pm .01$ deg/sec, accuracy
and linearity of 0.5 percent of full scale.

### 3.3.5    Inertial Measurement Unit

The Inertial Measurement Units are Delco Carousel IV Inertial
Navigation systems. The IMUs supply earth-referenced veloci-
ty, acceleration, and attitude information to the AFCS con-
trol loops. The Carousel IV consists of a navigation unit, a
mode select unit, a control display unit, and a battery unit,
as shown in Figure 128.

### 3.3.5.1    Navigation Unit

The navigation unit contains an inertial reference unit and a
general purpose digital computer. The inertial reference unit
is a four-gimbal stable platform, referenced to local vertical.
Horizontal sensors on the stable platform, gyros and accel-
erometers for the X and Y axes, are rotated at a controlled
rate of 1 rpm. The platform, therefore, behaves as a free
azimuth unit. North reference is obtained with the navigation
computer, based upon precise knowledge of platform azimuth
position established during alignment and the controlled rate
of rotation. The navigation computer is a binary-serial pro-
cessor which performs the computations required for:

- Rate gyro and linear accelerometer integration and
  coordinate transformations

- Gyro platform erection, alignment and drive

- Navigation computations

- Display signal generation

- Self test and system health

### 3.3.5.2    Mode Select Unit

The Mode Select Unit enables selection of the system operating
modes: OFF, STBY, ALIGN, NAV, and ATT. The STBY and ALIGN
modes are used during ground operations to facilitate azimuth

388
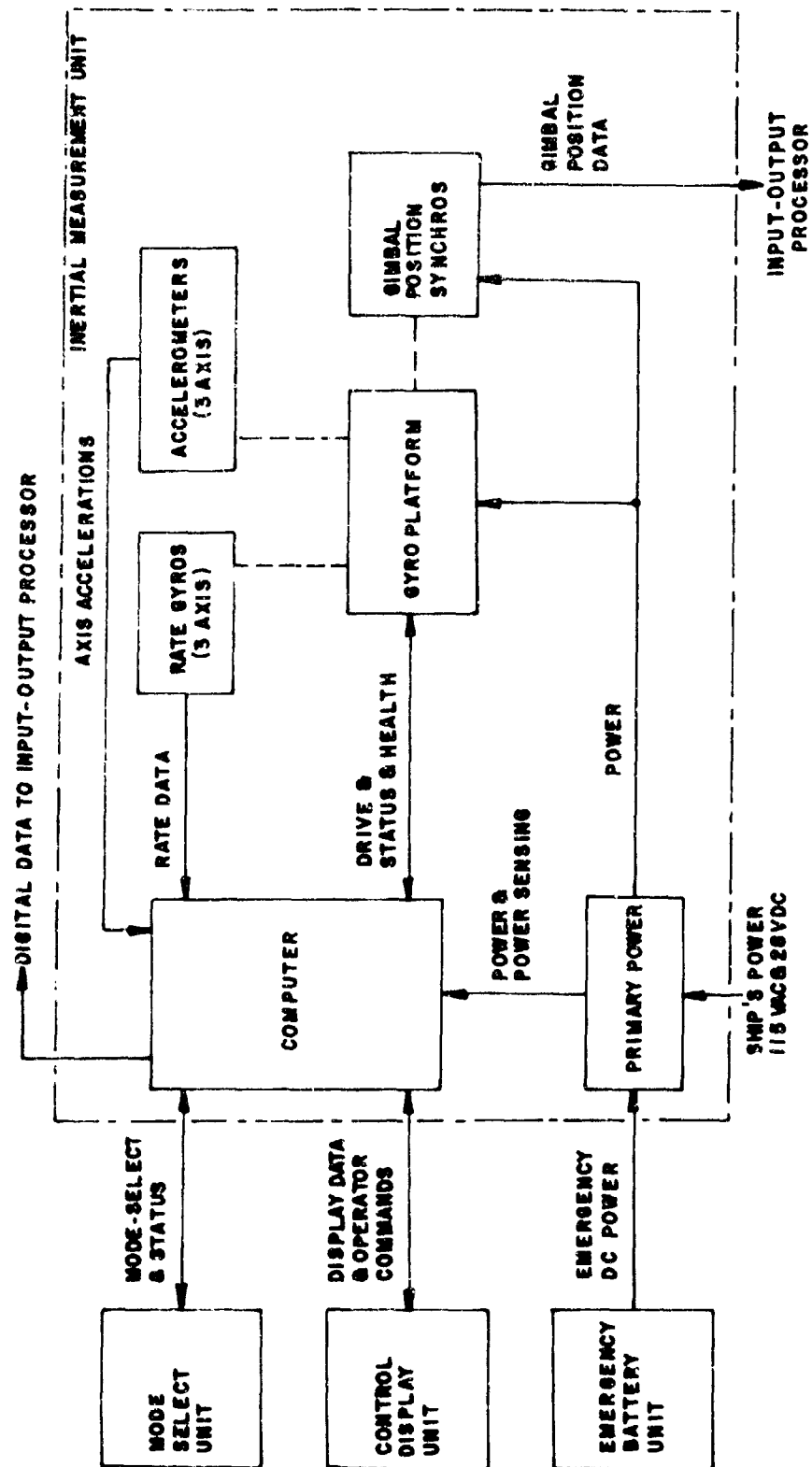
FIGURE 128. INERTIAL MEASUREMENT UNIT BLOCK DIAGRAM

389

initialization and alignment of the system. The NAV mode is used during normal flight operations to provide flight control parameters to the AFCS. The ATT mode is used to provide attitude signals for reference purposes; this mode is normally used only on occurrence of failures within the navigation computer. The unit also contains status - indicator lamps that indicate the operational capability of the battery unit and the state of readiness of the system to enter the NAV mode.

### 3.3.5.3 Control Display Unit

The control display unit contains a keyboard and selector switches for insertion of present position in the form of latitude and longitude inputs. The control display unit also contains displays and indicators for alignment status, computer memory call-up, and malfunction information.

### 3.3.5.4 Battery Unit

The battery unit powers the system during momentary interruption in the prime power supply. Battery unit power is coupled to the power circuits so that it will sustain system operation in any mode for periods of up to 15 minutes when the 115-Vac, 400-Hz, single-phase input power is interrupted or drops below the required voltage.

### 3.3.6 Attitude Heading Reference System

The attitude heading reference system, AN/ASN-76, provides pitch and roll attitude and magnetic heading information to Channel B of the AFCS. The Carousel IV IMUs supply similar information to Channels A and C.

Major components are:

- Displacement Gyroscope

- Reference Set Controller

- Electronic Control Amplifier

- Flux Valve

- Magnetic Heading Adapter

390

The displacement gyroscope is a pendulously erected two-gyro, multiple gimbal stable reference from which vehicle direction changes and attitude are measured. Heading, roll,and pitch signals are supplied to the IOPs through the electronic control amplifier. The electronic control amplifier provides multiple heading outputs representing gyro-stabilize magnetic heading in the slaved, free gyro, or compass modes. The reference set controller contains the indicators and controls necessary to operate the system. The flux valve supplies an electrical indication of vehicle heading with respect to the horizontal component of the earth's magnetic field. The magnetic heading adapter, designed by Boeing Vertol specifically for the HLH ATC. is a differential synchro which converts magnetic heading to the equivalent of true heading by adjusting the synchro device to the local variation angle. This makes the heading from the ASN-76 compatible with the true heading supplied by the IMUs.

Performance characteristics include:

- Attitude gyro accuracy $\pm14$ minutes of arc
  (maximum error spread)

- Latitude operational range $\pm82$ degrees

- Sensitivity 206 mv/degree (+5 percent)

- Output voltage 11.8 Vrms

3.3.7 Radar Altimeter

The AN/APN-194 Radar Altimeter is a high-resolution pulse radar operating at 4300 MHz that indicates absolute clearance over land or water from 0 to 5000 feet. The AFCS uses this information in the radar altitude hold, hover hold, and auto approach to hover modes. In addition to providing altitude, the signal is differentiated through a rate adapter unit developed by Honeywell for the ATC program to provide a high sensitivity altitude rate signal to the AFCS. The vertical rate signal is used as backup for the precision hover hold velocity reference. Signals from the simplex radar altimeter and rate adapter are paralleled to provide inputs to the tri-plex AFCS channels. Operation is based on precise measurement of the time required for an electromagnetic energy pulse to travel from the aircraft to the ground terrain and return. The tracking circuitry detects the leading edge of the re-flected signal and after "lock on", rejects all other signals

391

until the next pulse is received. The time of pulse arrival is compared with the time of pulse transmission and the resultant time differential is processed to provide the range information in both digital and analog form. The characteristics of closed-loop, leading-edge tracking, combined with extremely short pulse duration, is basic to the accuracy of the system.

The computing circuitry and use of separate transmitting and receiving antennae permits altitude measurement to touchdown. This is accomplished by providing sufficient electromagnetic isolation between the transmitter and receiver antennae which allows reception of early reflections from the ground while the transmitter pulse is still being radiated.

The electronic altimeter set is composed of one receiver-transmitter, a rate adapter, an interference blanker unit, two identical antennae, and one cockpit indicator. A simplified block diagram of the APN-194 system as installed in the Model 347 aircraft is shown in Figure 129.

The indicator controls system power, converts the analog altitude signal to a visual display, and provides an adjustable low altitude warning and flag alarm. System self-test, with a 100-foot readout on the indicator is also initiated from the indicator.

Loss of receiver track is indicated by a 4 Vdc discrete. Valid rate data is indicated by the presence of a 4.5 Vdc discrete.

Principal performance characteristics are summarized below:

### ALTIMETER

Range 0-5000 feet (use only 250 feet for AFCS)

Accuracy ±3 feet or 4 percent of actual range

Response time 0.1 ±0.025 second (first-order system)

Voltage output 0 to +25 volts
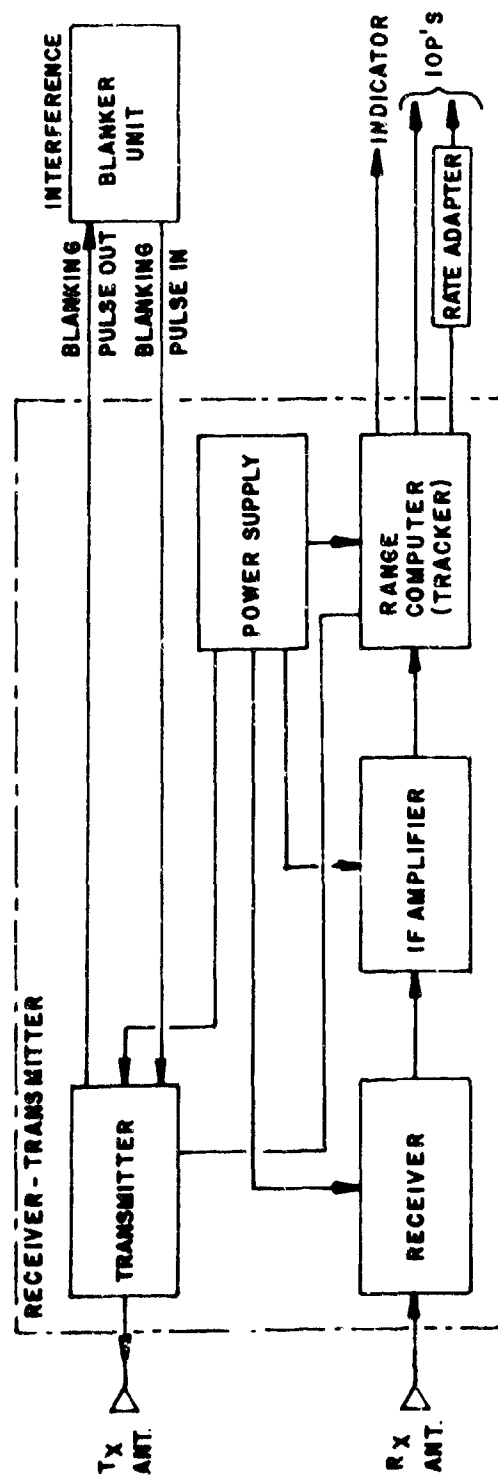
FIGURE 129. APN-194 RADAR ALTIMETER RECEIVER/TRANSMITTER
BLOCK DIAGRAM

ALTITUDE RATE ADAPTER

Range ±50 ft/sec

Accuracy ±(0.1 ft/sec +0.5 percent of reading)

Voltage Output ±10 Vdc

### 3.3.8 Precision Hover Sensor

Under the HLH/ATC Program, an element of the Flight Control
System was the development of a Precision Hover Sensor. The
goal of the Precision Hover Sensor is to provide accurate
ground referenced position information such that aircraft
position can be maintained in reference to a known point on
the ground within ±4 inches longitudinally, laterally, and
vertically. It was further desired that the sensor be self-
contained and be capable of operation in all-weather IMC
conditions.

The Precision Hover Sensor developed under the HLH/ATC program
was designed and fabricated by RCA of Camden, New Jersey,
under a subcontract from the Boeing Vertol Company. The sen-
sor utilizes two newly developed sensor techniques; namely,
image-correlation tracking and pulse sine-modulated laser
ranging, using pulsed-laser-illuminated gated imaging to mea-
sure position offsets and velocities.

The Precision Hover Sensor is located on a supporting mount in
the rear of the Model 347, as shown in Figure 130.

The type of sensor system chosen for the development resulted
from Boeing contracted design studies with RCA, Camden, New
Jersey; General Electric, Utica, New York; and Martin Marietta,
Orlando, Florida.

The development of the PHS was initiated as design and fabri-
cation of a feasibility demonstration model to be flown on
the Model 347 aircraft. The development was geared to the
use of existing off-the-shelf subsystems or components where-
ever possible to minimize costs and schedule. The use of off-
the-shelf components has resulted in a system that is larger
and heavier than a PHS specifically designed for a prototype
or production HLH aircraft, resulting from development of
subsystems to optimize size and weight. The functional dia-
gram of the PHS is shown in Figure 131 and the PHS character-
istics are stated in Table 23.

394

TABLE 23.  PHS CHARACTERISTICS

| | |
|---|---|
| Hover Precision | ( X,  Y,  Z)......$\pm$0.6 in. |
| Detectable Velocity | (X, Y, Z)   ......$\pm$1 in/s |
| Data Bandwidths | B     ......10 Hz |
| Maximum Displacement | X, Y, Z   ......$\pm$4 ft |
| Altitude | 25 to 125 ft |
| Loss Margin | 1000 |
| Lock-on Time | 0.6 s max |
| Reacquisition Time | 0.8 s |
| Temperature Range | -20°C to +55°C |

| POWER | 28 V dc | 110V, 3A, 400 Hz |
|---|---|---|
| Sensor Head | 360 W 420 W peak | 100 W |
| Stabilization Platform | 280 W 400 W peak | 60 W |
| Total | 640 W 820 W peak | 160 W |

| WEIGHT | |
|---|---|
| Sensor Head & Mount | 355 lb |
| Stabilization Platform | 185 lb |
| Total | 540 lb |

| DIMENSIONS (irregular) | |
|---|---|
| Sensor Head | 22 in. dia x 53 in. |
| Platform | 41 x 25 x 16 in. |
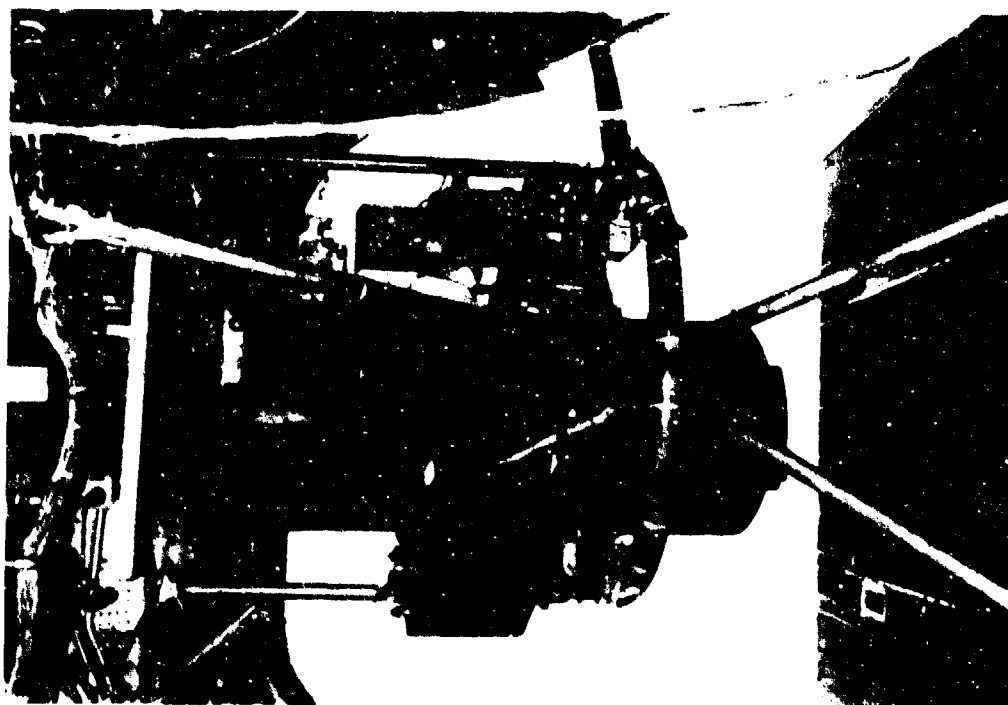
LOOKING FORWARD

LOOKING AFT
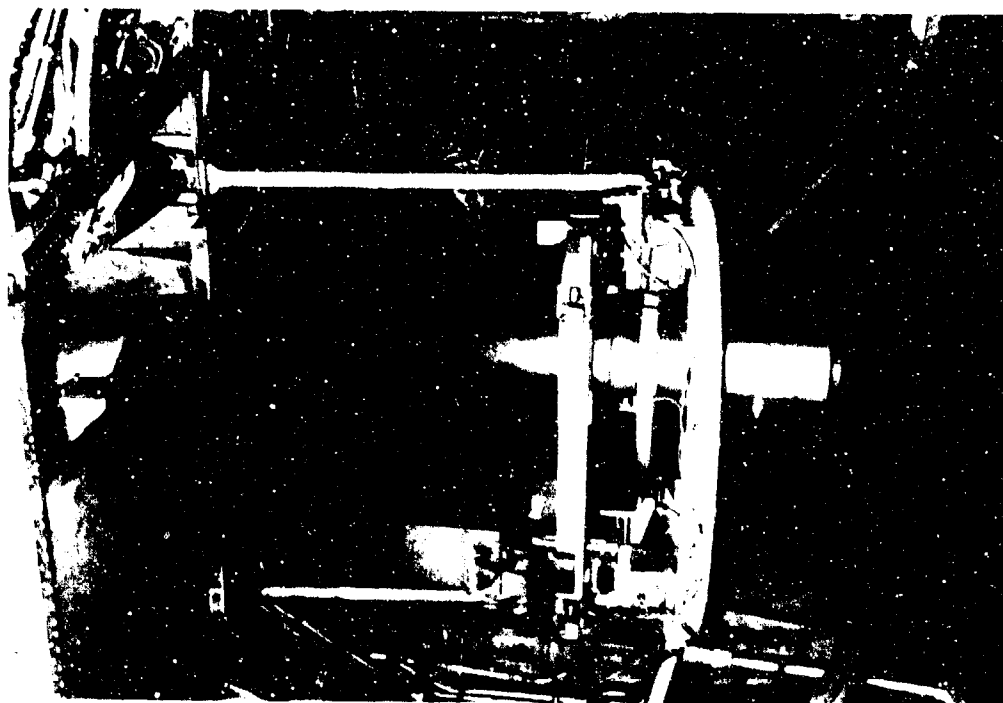
FIGURE 130. PRECISION HOVER SENSOR INSTALLED IN MODEL 347 HELICOPTER
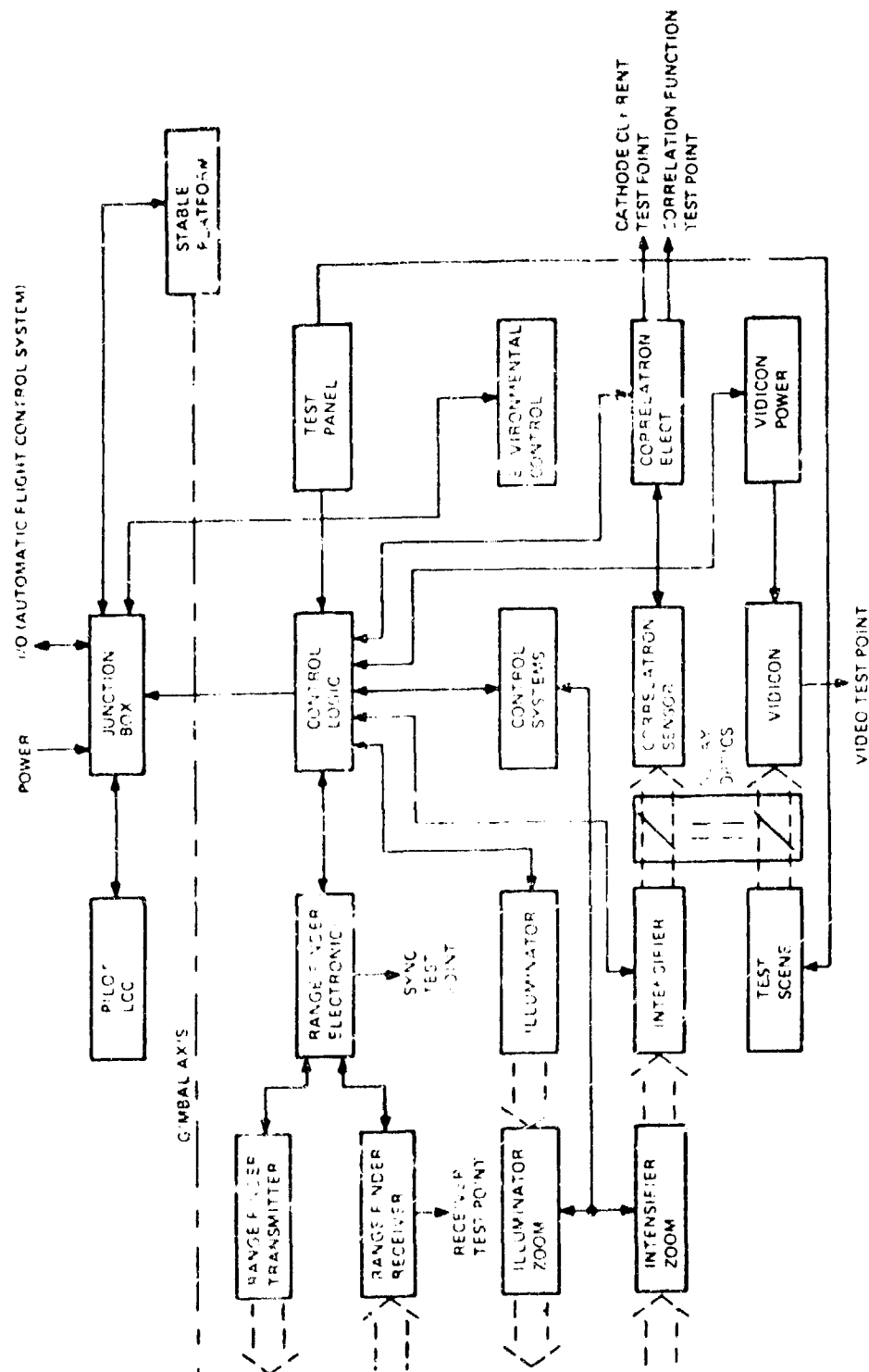
FIGURE 131. FUNCTIONAL BLOCK DIAGRAM OF PHS SYSTEM

### 3.3.8.1 Stable Platform

The main sensor subsystems are contained in one package and are mounted to a two-axis stabilized platform. The stabilized platform is a mass balanced torque driven gyro-stabilized vertical mount and is a modification of a standard Aeroflex Type 28A aircraft camera mount. The mount provides vertical stabilization within the limits of the mount gimbal ($\pm 10^\circ$ roll and $+10^\circ$ pitch) to the reference of the self-contained gyro.

The platform structure consists of three major components; the frame, the pitch gimbal, and the roll gimbal.

A circular opening in the roll gimbal (inner) accepts and supports the cylindrically shaped PHS sensor. Attached to the roll gimbal are also the roll trunnions. Limit stops restrict the freedom of the roll gimbal to $\pm 10^\circ$. Limit switches provide status information to the control logic.

The pitch gimbal girdles the roll gimbal, and supports the pitch trunnions, roll torquer, and an automatic caging mechanism. A gyro leveling plate at one end of the pitch gimbal provides space for mounting the ARG-5C vertical gyro. Limit stops and limit switches are provided for the same purpose as on the roll gimbal.

The frame girdles the pitch gimbal and supports the pitch torquers, all torque amplifiers, and an electronic chassis with connectors for interconnecting cables. Cable-type vibration isolators are provided between the stable platform frame and the aircraft frame. Also mounted on the frame is a rate of turn switch.

### 3.3.8.2 Range Finder

The ranging system of the Precision Hover Sensor combines the advantages of both a CW ranging system (high resolution) and a pulse ranging system and multiple scene discrimination capability. The signals from the range transmitter and receiver are processed in the range electronics to obtain absolute altitude (z), altitude change ( Z) and vertical velocity (Z). The system timing and status signals are also generated in the range electronics. The range transmitter generates a sine-wave modulated pulse of light which is collimated into a narrow beam and directed towards the ground. The transmitter

398

also generates an electrical signal to the range electronics corresponding to the time of transmission of the optical pulse.

Light from the range transmitter laser beam is reflected from the ground and detected by the range receiver. The receiver in turn generates electrical signals to the range electronics corresponding to the phase and arrival time of the return pulse.

Fine-range information is obtained by comparing the phase of the transmitted sinusoidal modulation to the phase of the received sinusoidal modulation. The signal detector amplifier output is first passed through the 100-MHz phase locked loop to derive a continuous waveform for determining phase. The resultant signals are then mixed with the local oscillator frequency of 99,950 MHz to produce two 50-kHz signals, whose phase difference is the same as the phase difference between the transmitted and received 100-MHz signals.

The phase detector provides a dc voltage output which is linearly related to the phase difference, and thus to the fine range. The fine-range information is accurate to 1 inch with a resolution of 0.1 inch over an unambiguous range of 5 feet.

The dc output of the phase detector is fed into an A/D converter to obtain the fine-range information in digital form for combination with coarse-range information. The two measurements are combined in the output register to yield a 1000-foot scale range reading with an accuracy of 1 inch and a resolution of 3/16 inch.

A reason for converting the fine-range information to digital form is to provide an accurate stored reference for deriving the hover error signals. When the operator wants to put the helicopter into automatic hover, he pushes a button on his control which generates the hold command. This causes the fine range information in the A/D converter to be stored in a separate digital register.

This stored fine range is then converted back to analog form in the D/A converter and compared to updated analog fine-range data coming out of the phase detector. The result of this comparison is an analog error signal corresponding to any small changes in altitude of the helicopter. This signal is then differentiated to yield the rate at which altitude changes are occurring.

399

The coarse-range information is obtained by measuring the time
delay between the leading edge of the transmitted pulse and
the leading edge of the received signal. The 100 MHz trap is
used to remove the high-frequency modulation from the received
waveform and to provide a clean leading edge to the threshold
detector. The outputs from the threshold detectors are digital
pulses which are delayed by the same amount of time as the
transmitted and received laser signals. This delay is measured
in the time-interval counter.

The time-interval counter will range on the last valid return
received during a total maximum range interval of 1000 feet;
this allows the system to range through obstacles, such as
trees. A multiple scene indication will be generated if more
than one valid scene is encountered during the range interval.
One hundred range measurements will be summed and averaged in
the time-interval counter to produce a coarse-range measure-
ment with an accuracy of 5 feet and a resolution of 0.5 feet.

3.3.8.3  Correlatron

The measurement of the  X, X,  Y, and Y incremental position
and velocity parameters is accomplished by utilizing a Correla-
tron tracker. The Correlatron is used as a closed-loop system
and requires three modes of operation:

(1) A write mode, where the initial image position is
    stored as a charge pattern

(2) A read mode, where the input image and the previously
    stored reference are correlated

(3) An erase mode, where the previously stored reference
    charge pattern is removed.

The Correlatron subsystem consists of a sensor package and
an electronic assembly.

The system, with the exception of one test relay, has no moving
parts and contains no hot cathodes. Internal switches are
transistors. Components are all hard wired with no transistor
or amplifier sockets. The circuit boards in the sensor are
coated against moisture, fungus, etc.

Both the sensor and electronics assemblies were constructed to
be completely shielded for EMI. The optical input port of the

sensor utilized a conductive window to accomplish the shielding, as well as to prevent dirt from reaching the Correlatron photo-cathode.

During the read mode, the photoelectron image is nutated in x and y with a sine wave. This is a multiplex nutation; x is blanked for one cycle, and then y is blanked for one cycle. The output of the buffer amplifier is switched synchronously to separate the x and y signals. These signals are amplified separately and the gain is automatically controlled to provide a replica of the x and y error signal without distortion or phase shift.

During the closed-loop match condition, the Correlatron signal appears as a full-wave rectified sine wave. When the Correlatron senses the input image drift by "distorting" the full-wave rectified signal form factor, the phase discriminator determines magnitude and direction to correct the loop and to maintain the proper form factor.

The loop is closed through the integrators and deflection amplifiers. This closed loop maintains the optimum position match between the photoelectron image and the stored image.

The output of the integrator represents position and the input to the integrator represents angular rate. The stored image in the Correlatron may be updated periodically or when the S/N drops below a prescribed level. In the erase mode, a uniform flood of photoelectrons drives the front surface (dielectric) of the storage element to cathode potential since operation is below the first crossover of the secondary emission curve. The backing electrode is typically at 15 V with respect to the photocathode.

In the write mode, the photocathode is typically switched to -600 V. The representation is of a spot of light on the photocathode giving a beam of photoelectrons. These electrons hit the dielectric with energy above the first crossover, and the secondaries are collected mesh. Thus, the written areas are charged positive, say +0.5 V.

3.3.8.4   Intensifier Subsystem

The intensifier subsystem provides light amplification for boosting the low-level illuminator light reflected from the ground scene to the level required by the Correlatron.

401

This subsystem contains three image-intensifier stages. The first stage consists of a micro-channel plate intensifier tube which converts the 8500 Å illuminator light to a P-20 output phosphor. This stage is gated with a 140 V 50-ns pulse which allows only light arriving from the pulsed illuminator to be amplified.

The next stage in the intensifier string is a second micro-channel plate tube which provides both gain and automatic light control. This stage allows the gated first stage to be operated at a safe bias level and its resulting moderate gain. The second stage provides a constant scene output brightness to the third stage over the range of scene illuminations encountered by the PHS system.

The third stage in the intensifier string is a diode-type gain stage which amplifies the output of the second stage and provides the high output brightness needed to produce the required Correlatron cathode current for lock-on.

3.3.8.5   Illuminator Subsystem

An AlGaAs laser illuminator is utilized and provides pulsed illumination of the ground scene, which, in conjunction with the range-gated intensifier chain, permits rejection of significant amounts of scattering from atmospheric particles, which would degrade the image of the ground scene. The illuminator also permits night operation.

The laser illuminator utilizes thermoelectrically temperature-controlled AlGaAs injection lasers to provide the pulsed illumination. AlGaAs is utilized to achieve 8400 Å wavelength of emission where the first photocathode of the intensifier has high responsitivity. Temperature control of the AlGaAs is utilized to stabilize the emission wavelength of the laser within the passband of the intensifier spectral filter.

A motorized zoom lens provides a collimated circular beam which matches the Correlatron format. A zoom capability of 5.5 to 1 from 9 degrees to 45 degrees full angle divergence enables a constant scene diameter to be illuminated while the range is varied from 25 to 125 feet.

The laser illuminator is a single self-contained package requiring only 28 Vdc prime power and a 20-kHz sync pulse train for operation. All power conversion and heat exchange are performed within the package.

### 3.3.9  Load Stabilization Sensors

Implementation of the external load stabilization modes in the flight control computer requires the sensing of cable angles and tension.

### 3.3.9.1  Cable Angle Sensing

Four synchro-rotary transformers were utilized to sense cable angles; i.e., two transformers located at the forward and aft cable securing mounts, respectively - one to sense longitudinal, and the other to sense lateral angles.  The transducers were mounted between aircraft structure and the cable hook assemblies.  These sensors, manufactured by Clifton Division of Litton Systems, Inc., provide ac outputs up to $\pm 90°$ of rotation with a sensitivity of 200    VRMS per degree. The signal range was limited in the IOP signal conditioning circuitry to $\pm 50°$ in both axes.  The cumulative effect of resolution, null offset, and hysteresis is less than 10 minutes of arc for the transducer devices themselves.  The principal contributors to hysteresis were anticipated to be the Teflon/steel load hook bearings.  Flight test results, however, indicated the actual values to be less than the analytical estimates of $\pm 5.4$ minutes of arc longitudinally and $\pm 4.2$ minutes laterally.  The actual values had no appreciable degrading effects on LSS performance.  (Refer to Section 2.1.5.3.3 for discussion of CSMP hysteresis evaluation).

### 3.3.9.2  Cable Tension Sensing

Strain gages were installed in both the forward and aft cargo hook bolts to provide a measure of load weight on each cable. This information was required for implementation of the automatic load-centering mode.  The strain gage signals were fed into bridge networks whose outputs were amplified prior to signal transmission to each of the IOPs.  The cable tension electronics were scaled for 0 to 8000 pounds each.  The full-scale output was adjusted to 10.4 VRMS, equivalent to 8,000 pounds.

403

## 3.4 LOAD CONTROLLING CREWMAN's CONTROLLER (LCCC)

### 3.4.1 Introduction

The LCC controller provides inputs to the AFCS for the control
of the aircraft by the load-controlling crewman during flight
with the hover hold mode engaged. The LCCC controls flight
in the longitudinal, lateral, directional, and vertical axes
by means of a four-axis finger ball. The authority of the
controller is limited by the control laws implemented in the
AFCS computers which also provide for pilot override of LCC
control inputs at any time.

The LCC controller was developed and manufactured by
Honeywell, Inc., Minneapolis, Minnesota. The controller uses
basic mechanism concepts that were developed for the Apollo
hand controllers and for recent fly-by-wire sidesticks. The
development program began with a human factors study of hand-
control and sidestick concepts which considered one-, three-,
and four-axis grip and finger controllers. The development
phase of the program culminated in a four-axis mock-up con-
troller which could be modified to have various force break-
outs, force gradients, displacements, and different kinds of
grips. The mockup was evaluated to determine the final LCCC
configuration. The design selected is portrayed in Figure
132. The controller is used by holding the ball with the
thumb and finger tips of the right hand. A special arm rest,
not shown, is provided for the controller.

### 3.4.2 LCCC Description

3.4.2.1 Major Functional Components are the control stick,
force feel springs, force feel dampers, and triple-
redundant position transducers. Also included is a
trim switch and magnetic brakes to hold the stick in
any longitudinal and lateral position with hands off.
No brakes are provided for the directional and verti-
cal axes.

404
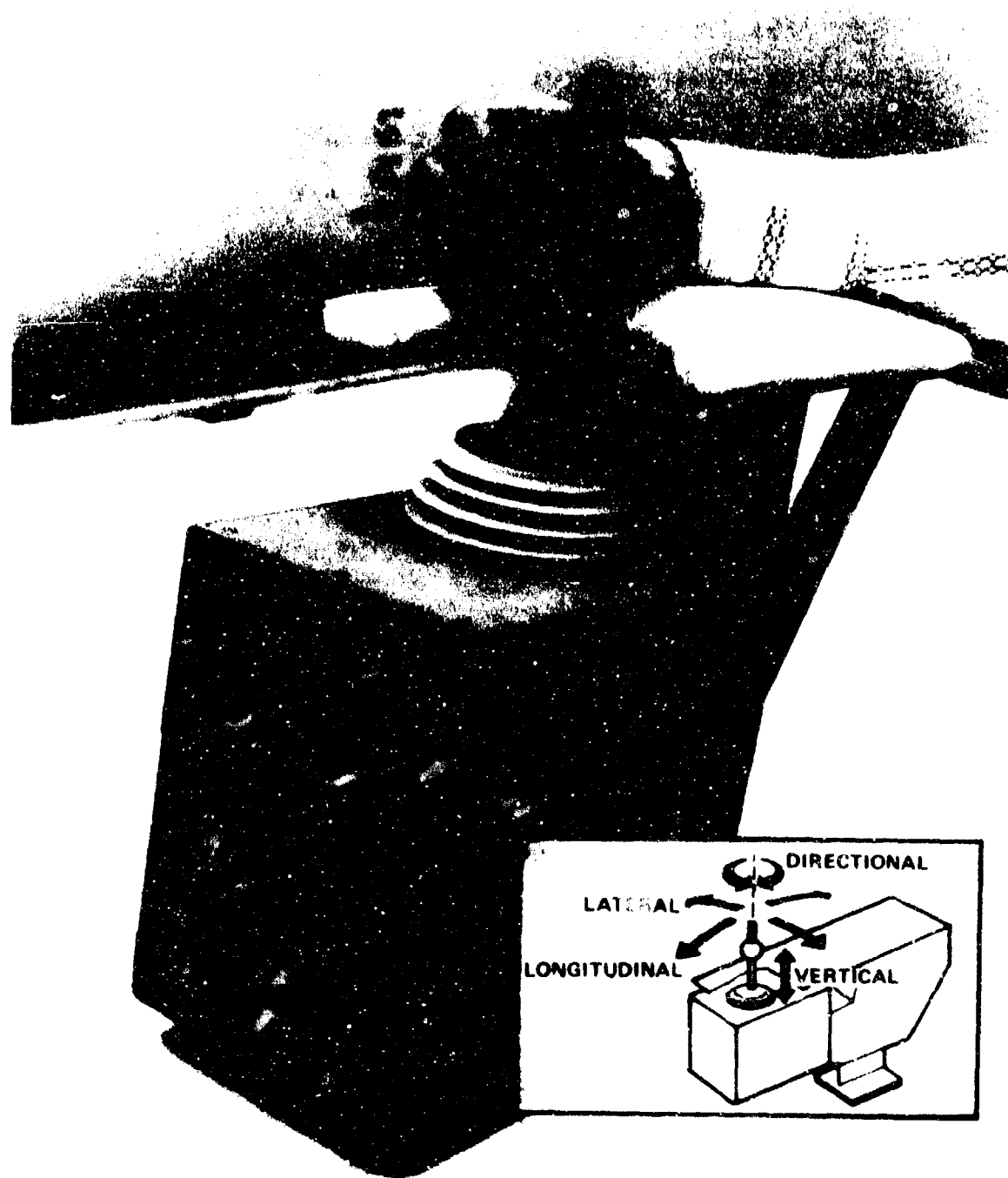
FIGURE 132. FOUR-AXIS FINGER/BALL CONTROLLER

3.4.2.2  Operating Characteristics

o  The control motions are:

   - Fore/aft stick rotation for longitudinal

   - Left/right stick rotation for lateral

   - Up/down stick translation for vertical

   - Left/right ball rotation for directional

o  Force breakout and a force gradient, proportional to
   stick displacement, are provided in each axis.  Dampers
   are incorporated to smooth control motions and to provide
   a smooth deadbeat return to the neutral position should
   the stick be released at any displacement.

o  Electrical Outputs are ac analog signals from triple-
   redundant rotary variable differential transformers
   (RVDT's) in each axis.  One output signal from each
   axis is fed into each of the AFCS input-output
   processors.

3.4.2.3  Performance Characteristics

o  Control stick displacements are limited by mechanical
   stops adjustable between:

      ±8 degrees and ±12 degrees in longitudinal
      and lateral axes

      ±15 degrees ±1 degree in directional axis

      ±0.5 inch in vertical axis

   The pivot point is 7.17 inches below the center of the
   finger ball, and the translation of the ball in the
   longitudinal and lateral axes is between 1.0 and 1.5
   inches.

● Force breakouts and gradients are as follows:

| Axis | Force Breakout (lb) | Force Gradients (lb/in. or degree) |
|------|------|------|
| Longitudinal | 0.75 | 1.0 lb/inch |
| Lateral | 0.60 | 0.79 lb/inch |
| Directional | 0.70 | 0.117 lb/degree |
| Vertical | 1.00 | 1.05 lb/inch |

● Damping Ratio is 0.7 in each axis

● Analog Output Voltages, obtained from triply redundant rotary variable differential transformers provide 10.0 volts RMS at the maximum stop settings and track within 2 percent.

## 3.5 CONTROL/DISPLAY PANELS AND INSTRUMENTS

The AFCS control and display panels are separated into two categories: that equipment which is required for a fully operational production aircraft; and that additional equipment necessary to the conduct of developmental flight test.

The production-oriented equipment includes an AFCS mode select panel, a PHS control panel, flight director indicator, radar altimeter indicator, groundspeed indicator, and pilot caution/advisory panels all located in the cockpit, as shown in Figures 133 and 134. The two IMU control/display units, and BITE, AFCS failure stations, and sensor failure status panels were located on the right side of the fuselage aft of the main entry door in the main cabin as shown in Figure 135. An LCCC-enabled light, IMU drift clear switch, and a second PHS control panel were located in the LCC station.

The flight-test-oriented equipment includes a system test function panel and parameter change/display unit mounted in the cockpit center console and shown in Figure 133. The discrete signal status panels numbers 1 and 2 located in the main cabin are shown in Figure 135.

407
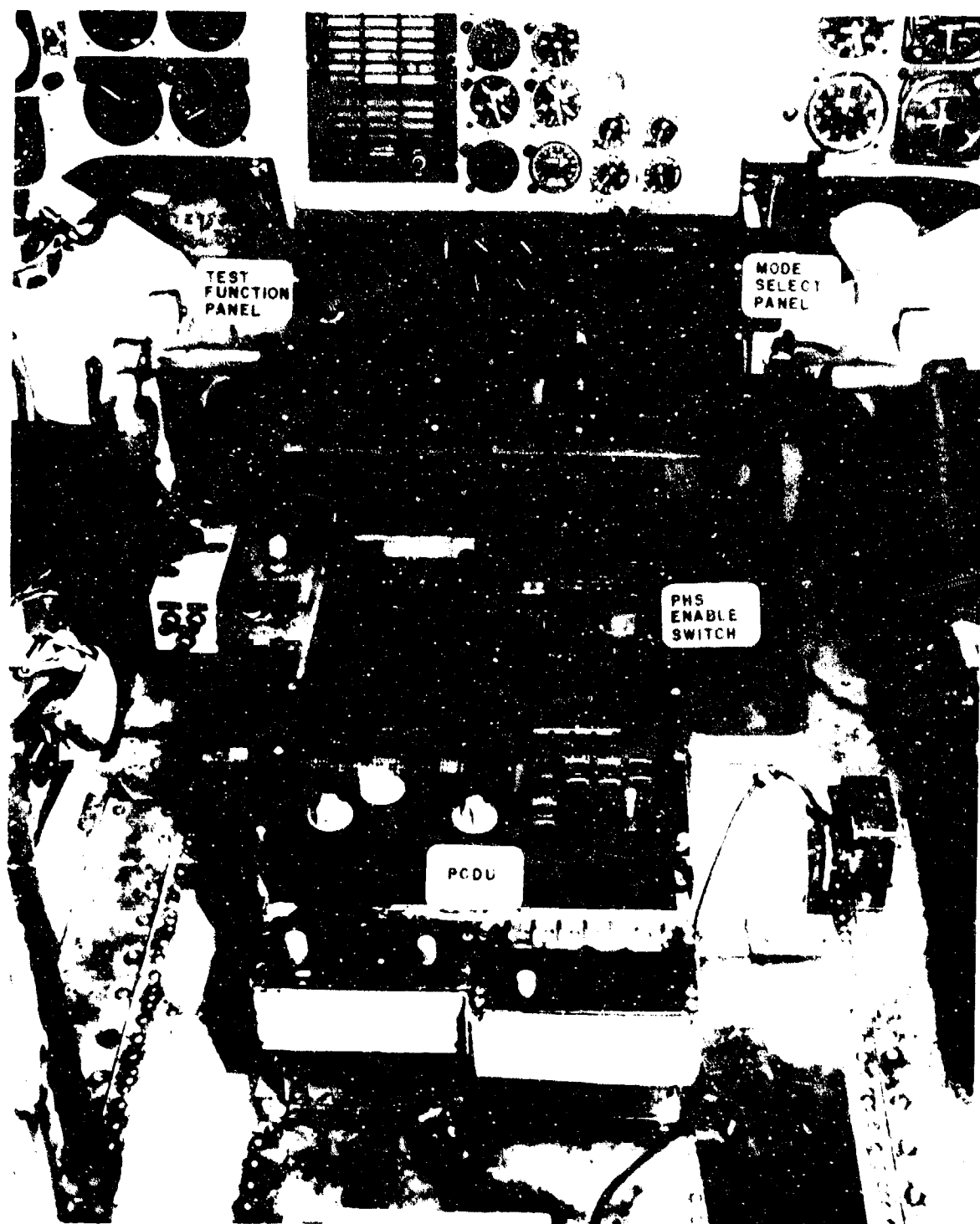
FIGURE 133 COCKPIT CENTER AND CANTED CONSOLES

FIGURE 134. PILOT'S PANEL

AAH CUE INDICATOR

ASN-78 HEADING DISPLAY

INS CONTROL DISPLAY UNIT

INS MODE SELECTOR UNIT
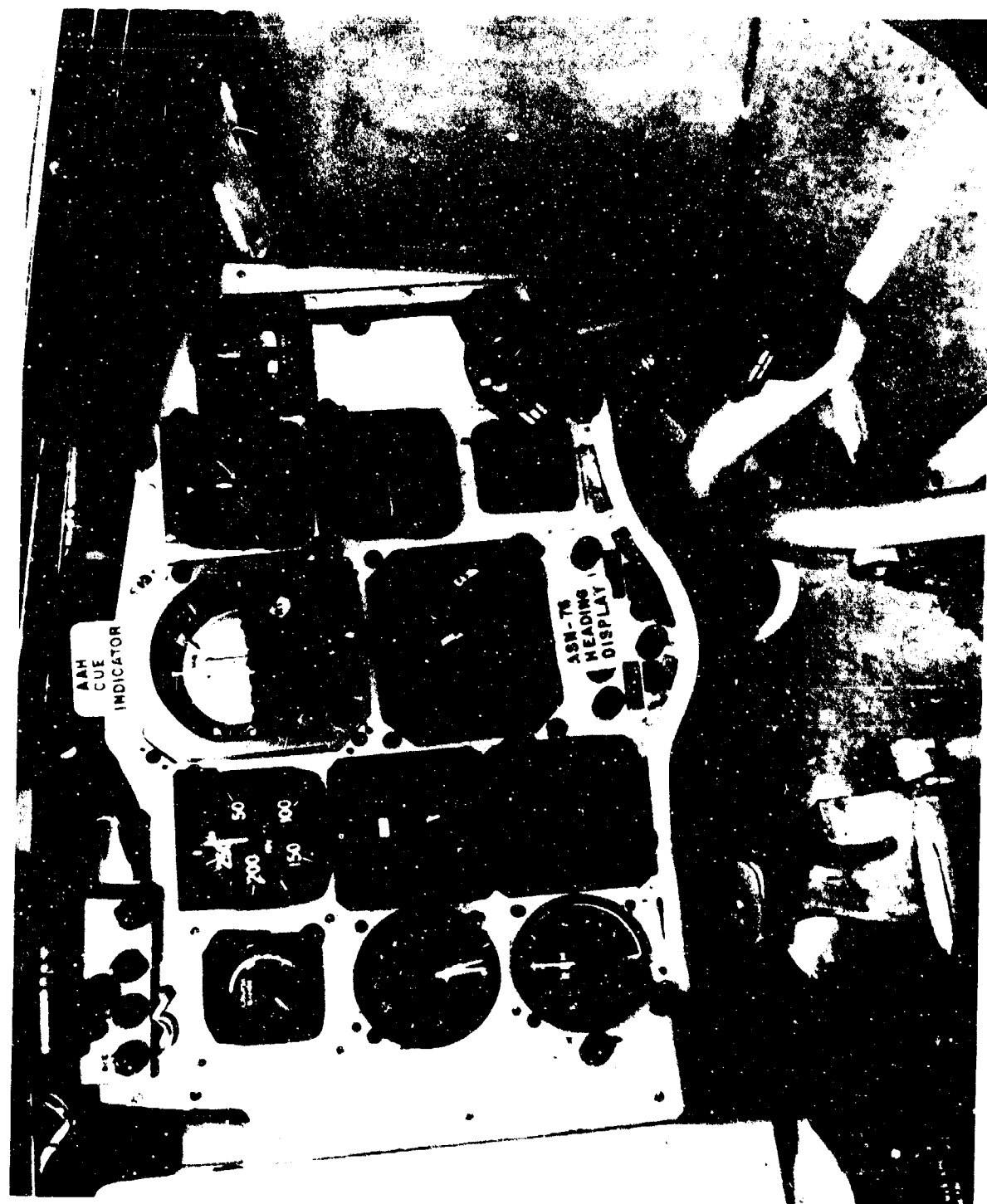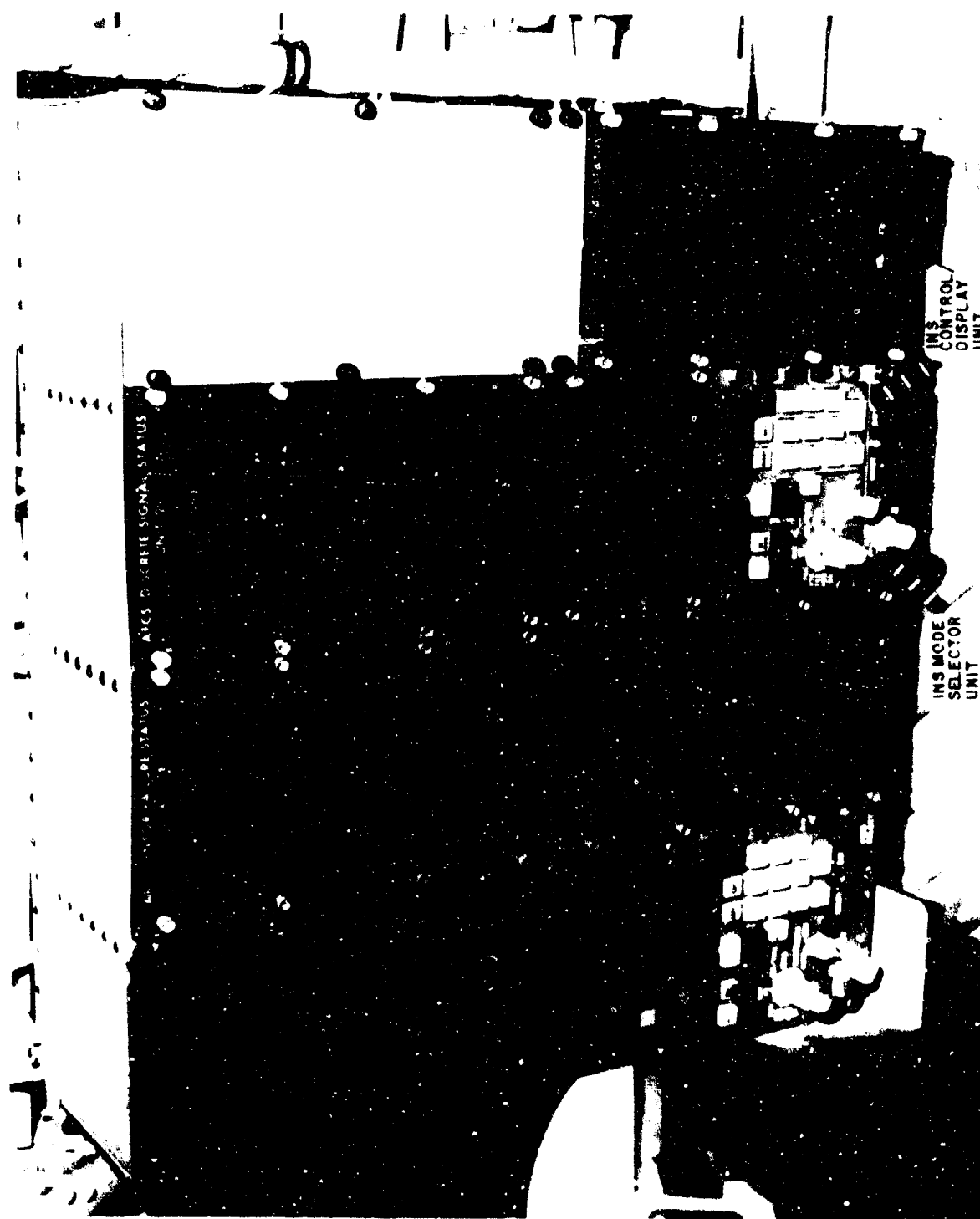
FIGURE 135. FLIGHT ENGINEER'S STATUS PANEL

410

### 3.5.1  Production Flight Equipment

#### 3.5.1.1  Mode Select Panel

The Mode Select Panel provides normal control of pilot-select-
able AFCS modes, as well as BITE and reset functions.  Figure
136 shows the panel layout.  The front panel is lighted and
contains switches defined in Table 24.  This panel interfaces
with the FCCs through the IOPs.  The mode select panel also
contains the electronic logic for 27 failure signals that
flash the master caution and AFCS warning lights in the
cockpit.

#### 3.5.1.2  PHS Control Panel

The pilot and LCC PHS control panel's are identical units
(Figure 137).  The pilot's unit is installed in the right side
of the center console, while the second unit is located on the
LCC cargo handling panel to the operator's left side.  Each of
these control panels contain:

- Power ON/OFF switch

- STANDBY Light - indicates that the PHS equipment is ready
  to operate as soon as the OPERATE COMMAND is received
  from the modal logic in the IOPs.

- LOCK Light - indicates that the correlation is locked on
  to and is tracking its observed field.

- NO LOCK Light - indicates that the range finder and/or
  correlation has lost lock - for a period in excess of
  0.7 to 0.8 seconds - and is attempting a relock in the
  presence of the READY and LOCK COMMANDS.

- FAIL Light - indicates the loss of intensifier switch on,
  rangefinder counter start, illuminator system OK, or a
  platform limit stop while a ready command is present.
  Sensing illuminator or intensifier zoom movement during
  lock-on will also generate a FAIL.  Further, an excess
  temperature, a loss of platform ac power, or lack of
  continuity in the PHS interlock path will also generate
  a FAIL.
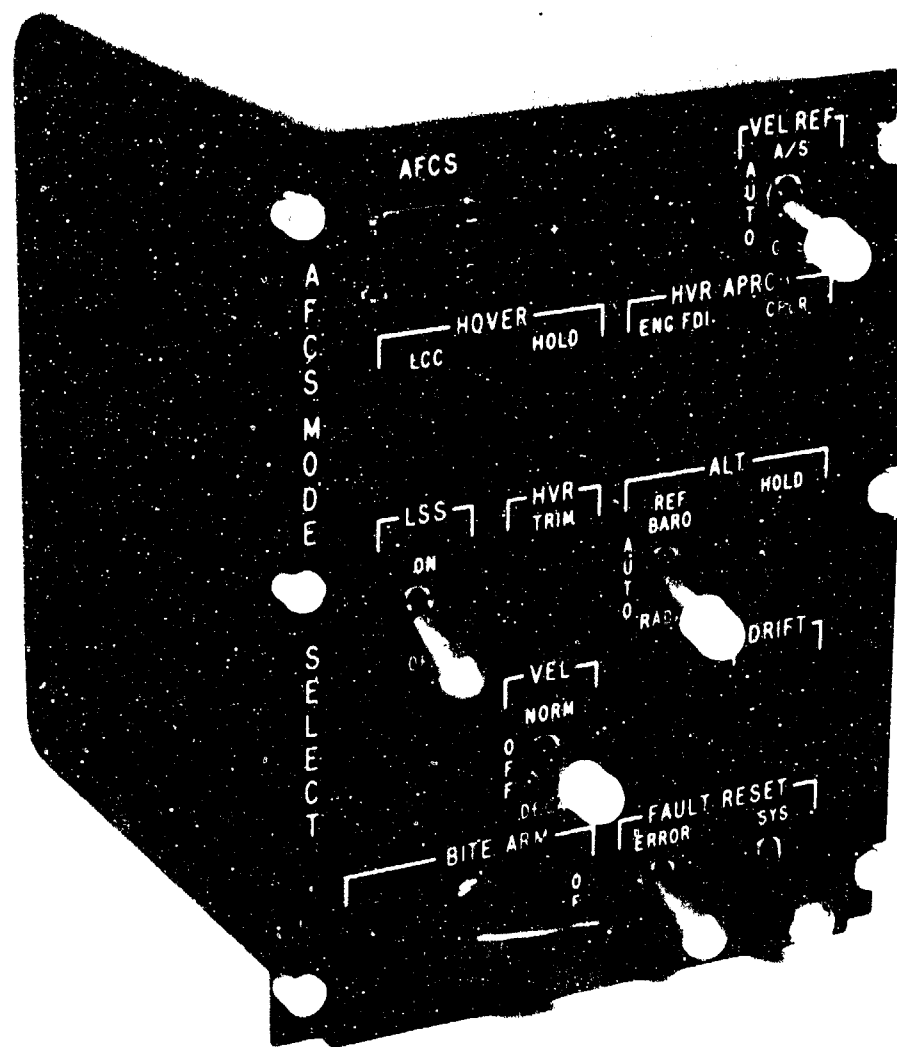
FIGURE 136. MODE SELECT PANEL

TABLE 24. DESCRIPTION OF SWITCHES ON MODE SELECT PANEL

| SWITCH IDENT. | TYPE | FUNCTION |
|---|---|---|
| AFCS | Lighted Pushbutton | Engage or disengage AFCS. |
| LCC | Lighted Pushbutton | Transfers control of aircraft during hover to LCC. |
| Hover Hold | Lighted Pushbutton | Engage or disengage hover hold mode. |
| ENG FDI | Lighted Pushbutton | Energizes the auto approach processing and flight director. |
| CPLR | Lighted Pushbutton | Couples the auto approach guidance commands into the CCDAs. |
| LSS | 2-Position Toggle | Selects the load stabilization mode. |
| HVR Trim | Lighted Pushbutton | Engage or disengage auto trim. |
| ALT HOLD | Lighted Pushbutton | Engage or disengage altitude hold whether radar or baro is controlling. |
| VEL REF | 3-Position Toggle | Selects between airspeed (A/S) groundspeed (G/S) or automatic (Auto) velocity reference. |
| DRIFT CLEAR | Lighted Pushbutton | Clears effects of IMU velocity drifts. |
| BITE ARM | 2-Position Toggle (Guarded) | Energizes the BITE Panel. |
| ERROR RESET | 2-Position Lever Spring Loaded OFF | Two switches to attempt fault reset. |
| SYSTEM RESET | 2-Position Lever Lock | Performs a computational reset function which automatically disengages AFCS; used with Error Reset to completely reset all LEDs on failure status panels. |
| ALT REF | 3-Position Toggle Switch | Select between radar, baro or auto altitude hold reference. |
| VEL | 3-Position Toggle | Switches off or decays out the velocity feedback loops. |

413

FIGURE 137. PHS CONTROL PANEL

414

3.5.1.3   Flight Director Indicator

The Flight Director Indicator, a Sperry Model HZ-6F, displays
in a single instrument, aircraft attitude information and
direct flightpath guidance control commands as shown in
Figure 91.   In addition, appropriate warning indications for
each aircraft attitude and velocity axis are available.   The
FDI is coupled to the AFCS by manually selecting either the
ENGAGE FDI or COUPLER modes on the AFCS Mode Select panel.

Three steering commands and two displacement error signals are
presented on the flight director for the auto approach to
hover guidance.

*   Lateral Command - indicated via the vertical command bar

*   Longitudinal Command - indicated via the longitudinal
    command bar

*   Vertical Command - indicated via the doughnut on left
    side of the altitude ball

*   Lateral Deviation - indicated via localizer pip

*   Vertical Deviation - indicated via glide-slope pip

*   Out-of-Tolerance Indication - via FD warning flag

3.5.1.4   Radar Altitude Indicator

The radar altitude indicator, ID-1760A/APN-194, displays the
aircraft's absolute altitude in feet, as shown in Figure 134.
The operating control on the height indicator serves as a
push-to-test switch, a set control for the low-level warning
index and a system ON/OFF power switch.   The low-level warning
index is a white edge marker.   This is set by the control to
any desired low altitude limit.   With the pointer in line with
or below the marker, a LOW caution lamp on the lower right-
hand corner illuminates to show that the helicopter is below
the set low-altitude limit.   A black and yellow striped OFF
flag appears when system power fails or when the unit loses
track.

### 3.5.1.5 Ground Velocity Indicator

Aircraft longitudinal and lateral ground velocities are displayed to the pilot on a standard ID-351 course indicator. The IMUs supply the velocities in terms of $V_N$ and $V_E$. A computer subroutine transforms these velocities to longitudinal and lateral ground velocities as measured at the aircraft cg. Velocities are displayed over two sensitivity ranges; low sensitivity range $\pm 15$ knots, both axes; high sensitivity range $\pm 100$ knots longitudinal, and $\pm 50$ knots lateral. The low sensitivity range is used when the hover hold mode is selected.

### 3.5.1.6 Caution and Advisory Panels

Three caution and advisory panels are available to the pilot:

* Master Caution/Advisory Panel

* Master Caution Light

o Auxiliary Caution Panel

AFCS failure status is displayed to the pilot via the AFCS warning and AFCS OFF lights on the master caution/advisory panel. With no AFCS failures, the warning light is out. The first failure causes the AFCS warning light to flash. The pilot can reset the flasher by pressing the master caution light and it will stay on, but not flash. Any succeeding failure will cause it to flash until reset again. There are nine flasher groups:

1. Computer First Failure
2. Interface Unit First Failure (or) DEL Warning
3. Pitch (or) Roll (or) Yaw Rate Gyro First Failure
4. Pitch (or) Roll (or) Heading Attitude First Failure
5. Long (or) Lat (or) Dir Control Position Transducer First Failure
6. LCCC (or) Baro Alt (or) Nonredundant I/O Failure
7. Vert Acceleration (or) Gear Switch (or) INS Velocity Fail (or) Sensor Warning
8. Differential Pressure First Failure
9. Airspeed First Failure

416

System level second failures will cause the AFCS OFF light to come on indicating AFCS disengagement. The master caution light gives a heads-up indication to the pilot that the status of the master caution advisory panel has changed.

The auxiliary panel, mounted on the glare shield, displays the engage/disengage status of the individual AFCS control axes.

3.5.1.7  BITE Panel

The BITE panel, designed and developed by General Electric for ground and preflight checkout of the FCCs, IOPs, and rate gyros, performs the following functions:

- Provides a means to initiate and select the self-test sequence

- Indicates testing in progress and all test failures

- Provides a "GO" indication for each individual channel

(The BITE Panel is shown in Figure 135. A rotary detent selector switch is used to select the channel to be tested. Positions include the following:

- OFF

- Channel A

- Channel B

- Channel C

- System

A series of six LEDs are used to indicate, in binary form, the number of the test in progress. A test initiate momentary pushbutton initiates the test sequence which continues automatically to completion and terminates with a "GO" light. If a test failure is encountered, the sequence stops, indicating the failed test number. When the fault is corrected, the sequence may be reinitiated to identify additional failures by actuating the switch again.

417

The BITE system is entirely dormant when the BITE ARM switch
on the MODE SELECT panel is off.  When this guarded switch is
thrown into the ARM position and both engine condition levers
are in the off position, power is applied to the AFCS BITE
panel.

When the BITE is enabled, the ARMED light will illuminate.
(The four green GO lights, the red FAIL light, and the amber
TEST light can be illuminated by depressing the LAMP TEST
button.)  The channel to be tested is selected by turning the
TEST SELECT rotary switch to either A, B, C, or SYS.  The
test sequencer will start when the INITIATE button is pushed.
As the sequencer steps through the tests, the TEST light will
remain on and the TEST NUMBER lights will indicate the test in a
binary code.  The sequence of tests is listed in Table 22,
Section 3.2.4.9.

If all tests pass, the green GO light for the channel selected
will go on, and the TEST NUMBER lights will show the last test
in that sequence.  The TEST light will remain on.  The BITE
system is now ready to test the next channel.  Select another
channel and proceed as above.  If any test fails, the FAIL
light will go on, and the TEST NUMBER lights will indicate the
test which failed.  This knowledge will aid the operator in
diagnosing the cause of the failure.  The test sequence cannot
proceed beyond a failed test.  If the INITIATE button is de-
pressed, the sequencer will be reset and all lights will go
out.  When all tests in all channels have passed, the TEST
SELECT switch should be turned to OFF, and the BITE ARM
switch should be turned off.  It is not necessary to reset
the system before or after the test sequence; this is done
automatically.

3.5.1.8  AFCS Failure Status Panel

The failure status panel, shown in Figure 135, provides an
indication of failures within the computers and IOPs on an
individual channel basis.  A total of 48 monitor points are
displayed.  Grounding of a given circuit energizes a light-
emitting diode (LED) for the respective monitor point.  The
panel, in addition to displaying first-failure information,
provides an explicit indication of system second failures via
the top row of lights, as well as by the LEDs associated with
the individual monitor point failures.

418

### 3.5.1.9  Sensor Failure Status Panel

The sensor failure status panel, shown in Figure 135, provides an indication of sensor failures as detected by the IOP sensor monitors. The grounding of a given circuit energizes the LED for the respective monitor point. The bottom row of LEDs, which are not labeled, indicate sensor comparator trips. The panel incorporates three pushbutton switches, located on the front panel, for testing the operation of the LEDs. A 28-volt dc to 5-volt dc power converter is incorporated in the panel to energize the LEDs. The 5-volt dc power is also fed to Discrete Status Panel I to drive its LED circuits.

### 3.5.1.10  LCC Station Control/Display Devices

An LCC-enabled light and drift clear switch are located on a vertical panel to the operator's left front. The enabled light indicates that the pilot has armed the LCC controller for hover maneuvering and load positioning. Operation of the drift clear pushbutton switch provides the LCC with the ability to momentarily resynchronize the IMU hover hold velocity control loops. This function is needed to correct for accumulated sensor drift at those times when the PHS is not operating, thus automatically updating the IMU velocity data.

The LCC's PHS control panel is located on the aft portion of the left side control panel. This unit is an exact duplicate of the pilot's panel which is described in Section 3.5.1.2.

### 3.5.2  Test-Oriented Equipment

### 3.5.2.1  System Test Function Panel (STFP)

The System Test Function Panel shown in Figure 133 is located on the left front of the center console within reach of the pilot, copilot, or test engineer. The panel was developed by General Electric as a piece of ground- and flight-test equipment and would not be part of a production AFCS. This equipment provides disturbances of preselected amplitude and of automatic or manual time duration for AFCS evaluation. In addition, the panel provides the capability to disable any or all AFCS axes. The panel is backlighted for night operations.

419

### 3.5.2.1.1  Axis Disabling

The lower portion of the panel contains four switches used to disable the AFCS control axes.  Displacing the switch to the disable position, results in that axis being disabled.  Any output signals on that axis are ramped to '0' at a rate between .07 and .2 inches equivalent pilot control grip movement per second.  Returning the switch to the enable position causes the axis to be reenabled at the same ramp rate.

### 3.5.2.1.2  Aircraft Disturbances

To disturb the aircraft automatically, the upper and middle sections of the unit marked "Function Input", "Excitation", and "Location", are used in various combinations.  The detail usage is described below.  The panel switches input discretes to the IOP, but the actual functions are generated in the computer software.

### 3.5.2.1.3  Function Input

<u>Axis Selection</u>.  The upper left-hand switch is used to select the axis to be disturbed.  Choices are:

- OFF  - No axis can be disturbed

- LONG - Enables automatic inputs to be selected for the longitudinal axis only

- LAT  - Enables automatic inputs to be selected for the lateral axis only

- DIR  - Enables automatic inputs to be selected for the directional axis only

- VERT - Enables automatic inputs to be selected for the vertical axis only

- LCP  - Enables automatic inputs to be selected for the longitudinal cyclic pitch only

420

Amplitude Selection.  The upper right-hand portion of the
panel is used to select disturbance magnitude and direction.
Selections available are:

- OFF – Inhibits any automatic disturbances from being
  passed through the control system

- LO – Produces smallest amplitude of disturbance

- MED – Produces intermediate level of disturbance

- HI – Produces largest level of disturbance

- RIGHT (UP) OR LEFT (DOWN) – Rotating the switch clockwise
  or counterclockwise determines disturbance
  polarity.

The table below lists the individual axis amplitudes corres-
ponding to the selections available.

AMPLITUDE
| SWITCH POSITION | LONG | VERT | LAT | DIR | LCP |
|---|---|---|---|---|---|
| High | 1.0 | 1.5 | 0.75 | 0.66 | 1.5 |
| Medium | .67 | 1.0 | 0.50 | 0.44 | 1.0 |
| Low | .33 | 0.5 | 0.25 | 0.22 | .5 |

All inputs are symmetrical for right (up) or left (down).
All values are inches of cockpit grip motion except LCP,
which is in terms of cyclic pitch blade angle at both rotors.

Excitation – Pulse, Ramp, Step.  The excitation panel section
is used to insert a pulse, step, or ramp-type disturbance to
the aircraft.

- Pulse.  A momentary depression of the button causes a
  1-second pulse to be passed through the AFCS to the
  aircraft.

- Step-Ramp.  Selecting the step-ramp switch to the step
  position provides a step input to the AFCS.  This switch
  is spring loaded such that the input will be held in the
  AFCS only so long as the switch is depressed.  Selecting
  the ramp position causes the signal selected to ramp up
  to the steady state selected amplitude in 4 seconds.

421

## Location - OFF, DIFFERENTIAL, PARALLEL

The location switch is used to select a differential or parallel automatic disturbance to the aircraft control system as described below.

- **OFF Location.** In the OFF position, no automatic disturbance can be passed to the aircraft.

- **Parallel Location.** Ramps or steps are introduced to move the appropriate cockpit controls directly. This is analogous to the pilot inserting the same input manually. The parallel inputs move the cockpit control through the Cockpit Controls Driver Actuators which have a maximum velocity limit of approximately 1 inch per second. Therefore, the parallel step selection causes the leading and trailing input demands not to be sharp edged. The parallel inputs are intended to simulate repeatable accurate maneuver demands by the pilot.

- **Differential (DIFF) Location.** Pulses or steps are introduced to the Direct Electrical Linkage System and longitudinal cyclic pitch without moving the cockpit controls. AFCS logic inhibits differential ramps from being input to the control system. The differential inputs are used to evaluate stability and wind-type sharp edge disturbances.

- **Gust - ON, OFF.** This function was disabled for Model 347 flight testing.

### 3.5.2.2 Parameter Change/Display Unit

The Parameter Change/Display Unit (PCDU) provides two essentially independent functions. These are parameter display and parameter change. The panel is furnished primarily for the flight-test phase. Figure 138 shows the panel layout.

### 3.5.2.2.1 Parameter Change

The parameter change function provides a means of varying the $S_p$ and $S_q$ constants of any algorithm in program storage by adding net increments to the constants as they are used. The value in program storage remains unchanged (program storage is not alterable in flight). This function has its own display for monitoring the values of $S_p$ and $S_q$ net increments.
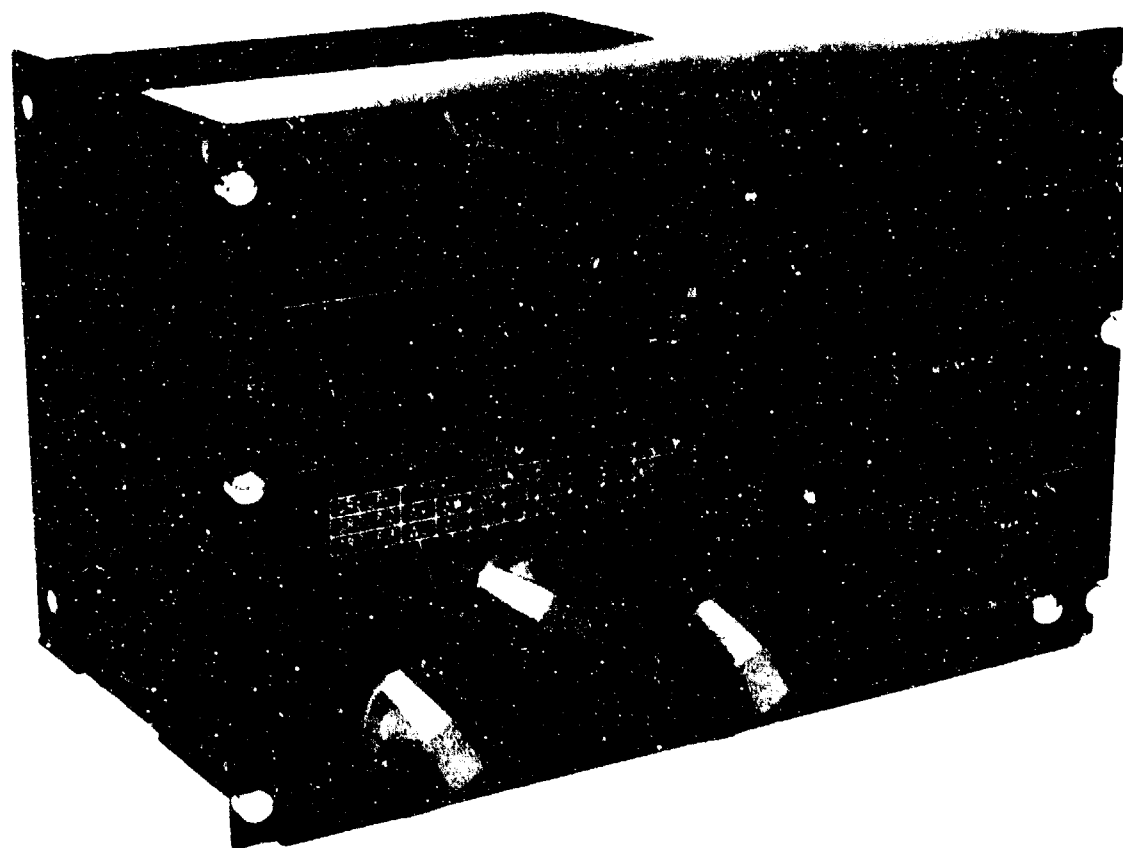
FIGURE 138. PARAMETER CHANGE / DISPLAY PANEL

## Change Capability

The value of Sp and Sq for all 512 stored algorithms can be changed in steps of $\pm1$, $\pm10$, $\pm100$, and $\pm1000$ machine units. The net change is displayed in a digital readout. In each algorithm time, net increments for the Sp and Sq constants are selected by means of the program instruction address for that algorithm time. The net increments are serially added to the constants as they are shifted into the arithmetic unit.

Changing the Sp and Sq net increments for an on-line algorithm is accomplished by the following procedure:

- Select memory location, including designation of Sp and Sq

- Select + or - sign

- Select ENABLE (if not in that position already)

- Depress desired increment value pushbutton (one only)

At the time when the selected Sp or Sq net increment is added to the Sp or Sq constant, the new increment selected at the panel ($\pm1$, $\pm10$, $\pm100$, $\pm1000$) is added to the old net increment and the new net increment is stored in place of the old net increment. The INCREMENT switches are interlocked so that only one increment value at a time can be added to a net increment.

The panel display monitors the selected Sp or Sq net increment at the time it is used. If the selected net increment belongs to an algorithm which is not on-line, it will not be displayed and the display will be blanked.

The limits on the permitted range of values for the net increments are +8191 and -8192. If an increment would cause the value of a net increment to exceed these limits, an overrange condition is detected and the old net increment value is preserved. Depressing CLEAR or another INCREMENT VALUE switch will clear the overflow condition in addition to the normal operation of these switches.

Throwing the ENABLE/DISABLE switch to DISABLE inhibits the changing of any net increments. The display remains active.

424

Indicators on the STATUS switch monitor the clock and itera-
tion sync voters. First fail on the clock illuminates the C.
Second failure of the clock illuminates the ? under the C and
causes the parameter change function to be disabled. The
same sequence applies to the sync portion of the switch.
Depressing the switch resets the failure latches.

When the system is in the reset mode, the parameter change
function is not limited to constants corresponding to on-line
algorithms. In reset, any of the 512 Sp or Sq values can be
changed.

3.5.2.2.2  Parameter Display

The parameter display function provides a passive display of
all sensor inputs, increment data words, Sp and Sq constants,
and whole-word data registers U, V, X, and Y. Any of the
three computer channels can be monitored during any algorithm
time.

The display is a five-digit decimal plus sign. A digital-to-
analog channel is available for external meter. The analog
output is ±10 volts dc and is derived from the 12 most sig-
nificant bits of the displayed data word.

On command from the display interface, the panel transmits an
address and a request code, based on the selected algorithm
time (thumbwheel switches) and the desired parameter
(PARAMETER and GROUP switches). On the basis of this informa-
tion, the interface logic waits until the correct data is
available and sends it back to the panel to be displayed.
The display is normally updated once per iteration.

Discrete sampling of input data is possible in the event the
data changes too quickly to be observed easily. Depressing
SAMPLE will cause the next data word to be held in the input
register (indicator lit) until SAMPLE is depressed again
(indicator dark). The channel to be monitored is selected by
means of the CHANNEL switch.

3.5.2.3  Discrete Status Panels #1 and #2

Each Discrete Status panel provides a display of the status of
up to 28 signals originating in the Input/Output Processor
units A, B, and C. The information displayed on these panels
is provided to facilitate on-line analysis and trouble

shooting of the principal AFCS modal logic input switching and threshold states, as well as function output states. The LEDs on Panel #1 are driven from IOPs A and C and the LEDs on Panel #2 are driven from IOPs A and B. The grounding of each circuit energizes a LED with the adjacent legend. Each panel incorporates two pushbutton switches located on the front of the panel to test the operation of the LEDs. Figure 135 shows the panel layouts.

## 3.6  GROUND SUPPORT EQUIPMENT

The intention of this section is to familiarize the reader with those items of equipment necessary for the test and programming support necessary in the AFCS program development effort. This does not necessarily indicate the type of ground support equipment required for equivalent production hardware.

The ground support equipment is divided into two classes; that specifically used to program and check out the computer software, and that used for hardware checkout and troubleshooting purposes.

### 3.6.1  Software Support Equipment

The following items of equipment are essential to the simplex system program validation phase and subsequent programming of the computer program memory boards, prior to conducting a full triplex system checkout.

- o  Program Loader Unit
- o  Core Memory Unit
- o  ROM Programmer Unit
- o  Program Monitor Unit (utilized by General Electric Co. only in both software development and hardware checkout)

### 3.6.1.1  Program Loader Unit

The Program Loader Unit (see Figure 139) is used to load the Program Memory or the ROM Programmer with the software program and to indicate the status of those units. Provision is made for either automatic loading with a punched paper tape or manual loading via a switch panel. Sixteen binary indicators read out programmed data to permit visual program verification. An automatic verification mode is used to check the

426
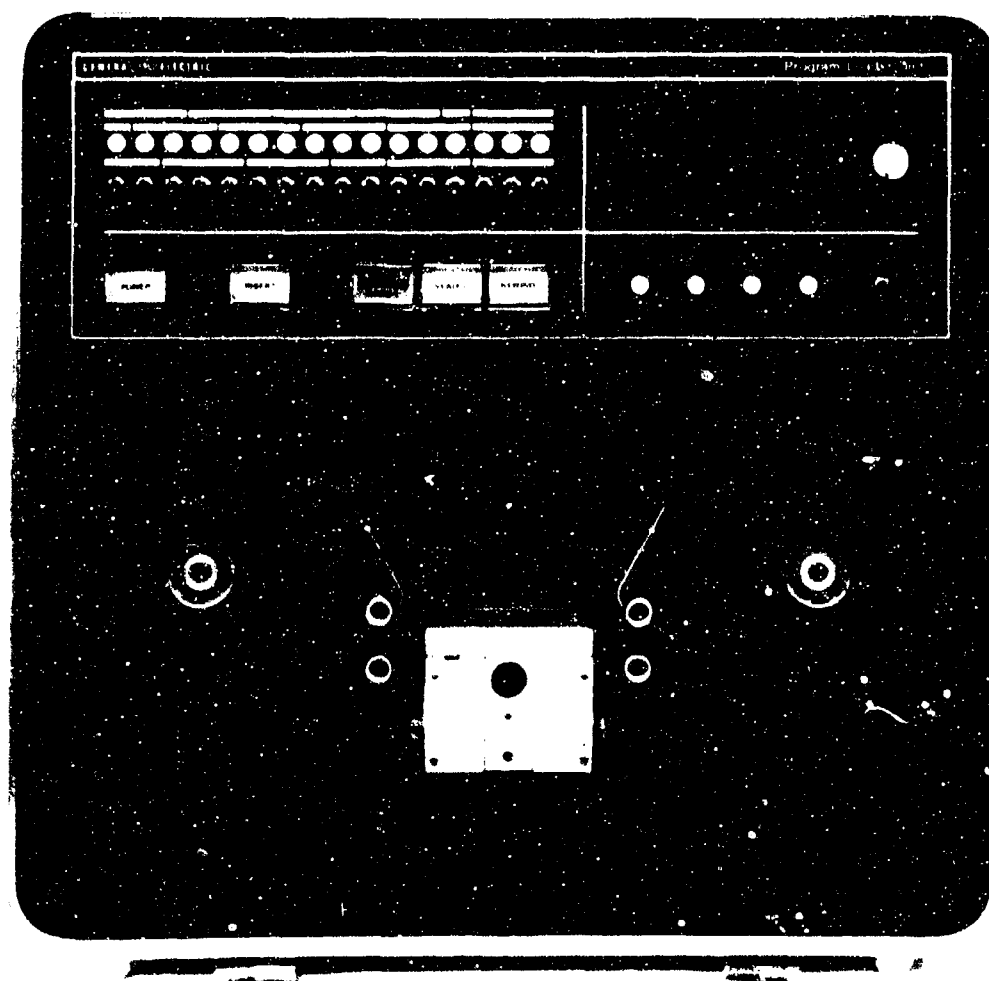
FIGURE 139.  PROGRAM LOADER UNIT

loaded program against the tape. The program tape is made by the Variable Increment Computer Assembler Program (VICAP) assembler on a laboratory computer. The program is put on four tapes, each one corresponding to a MOS Program Storage Board.

## Operating Modes

The Program Loader Unit has four operating modes:

1. LOAD/MODIFY - Inputs data read from tape to memory. LOAD will clear the memory to a setable bit pattern while MODIFY affects only the locations on the tape.

2. VERIFY - Compares data read from tape to data already stored in memory. The VERIFY mode has two functions. First, it allows the Program Loader Unit to check that the information has been loaded correctly. The second is a documentation technique for keeping track of manual changes made to the stored program.

3. VERIFY ERROR - The VERIFY ERROR light has a triple function. In the VERIFY mode, it will indicate a difference between the tape and the memory. When the PLU is in the display service mode, it shows the results of an odd parity check on the incoming data. When the ROM Programmer is being loaded, it will light if the read/write check in the programmer fails.

4. MEMORY NO GO - The MEMORY NO GO light indicates the status of a memory monitor which checks memory parity, timing, and power supply voltages.

## 3.6.1.2 Core Memory Unit

The Memory Unit is used to provide an electrically alterable program storage. It is used for simulation and software development effort on the HLH-ATP AFCS program.

## Memory Capacity/Timing

The Memory Unit is loaded by the Program Loader Unit and contains an 8K x 18 bit core memory which provides 512 algorithms of non-volatile program storage. Timing and control, and input/output buffering are provided for transfer of data to the computer, and also for read/writer operations

428

with the Program Loader Unit. The Memory Unit is in a read-only mode when operating with the computer only.

The memory is a 3-dimension, 3-wire, destructive readout core. It is non-volatile and electrically alterable. Full cycle time for read/restore is 2.5 microseconds. An internal 1 MHz crystal controlled oscillator is used for independent memory unit operation.

BITE Provisions

Internal monitoring is provided so that a continuous parity check is performed on every memory location, independent of the computer requests. The Memory Unit may be operated by itself with the Program Loader Unit in order to accomplish program editing or other program loading functions.

The following built-in tests are provided in the Memory Unit:

- o Parity check on every word read from memory
- o Timing status monitor
- o Power status monitor
- o Data transmission parity check

3.6.1.3 ROM Programmer

The ROM Programmer (see Figure 140) is used to load the software program into the computer ROM program storage modules and to load the IOP ROM sensor monitor modules. The Computer Unit has four ROM program storage modules and the IOP has one ROM sensor monitor module.

The ROM Programmer is used with the Program Loader Unit to accomplish automatic program loading and automatic verification against the tape. The tape assembly is part of the Program Loader Unit.

The function of the ROM Programmer is divided into three main modes of operation.

LOAD Mode

Under control of the PLU, data from the tape is loaded into the RAM in the ROM Programmer. A read/write check is performed on all data; a read/write error activates the VERIFY

429
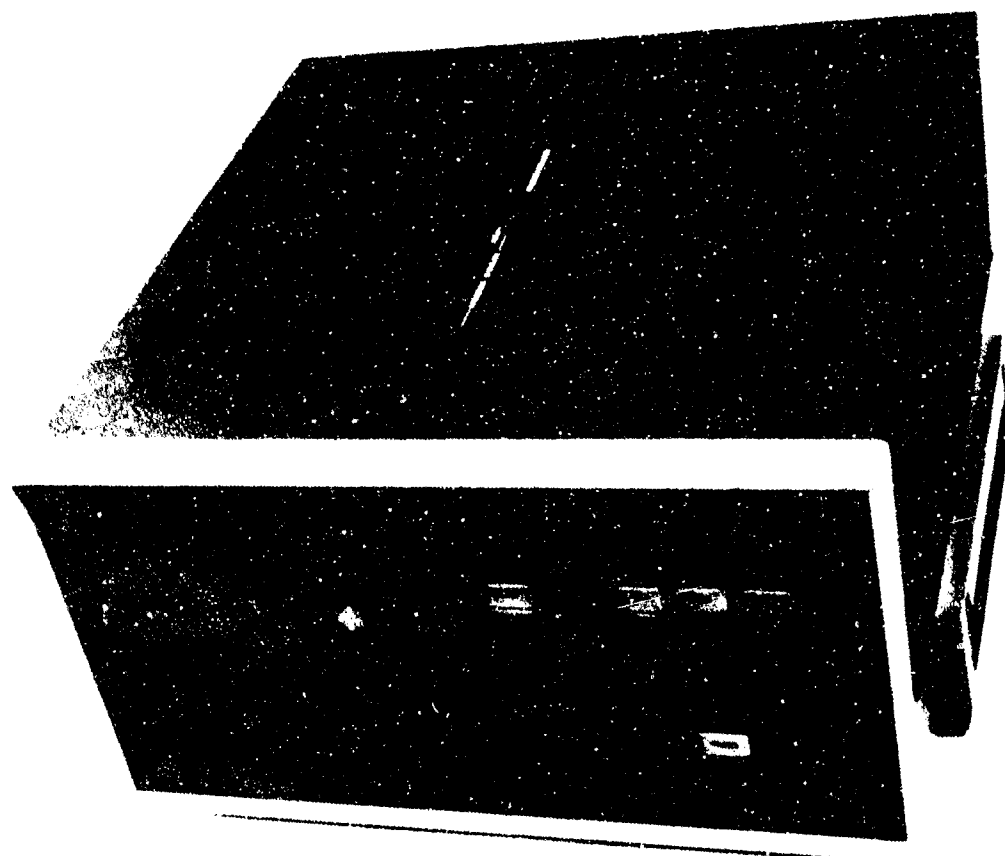
FIGURE 140. ROM PROGRAMMER

430

ERROR light on the PLU and stops the tape. The entire RAM
will be cleared to the bit pattern of the first data word on
the tape.

PROGRAM Mode

A programmed counter generates addresses such that the ROMs
are programmed one at a time in sequence and at a rate that
insures operation within the maximum duty cycle permitted. A
regulator on the output of the power supply allows control of
voltage switching by the timing logic. No high voltages are
applied to any programming sockets unless the programming
cycle is in progress. The PLU controls have no effect on
programming cycle.

VERIFY Mode

VERIFY control functions and logic are independent of those
for PROGRAM: therefore, a board can be verified while other
boards are being programmed. Control is originated by the
PLU.

As with core memory, the PLU compares the output data with
the data on the tape; an invalid comparison stops the tape
and enables a display of the address of the faulty location.
If an error is found, however, the ROM involved must be
reprogrammed.

3.6.2   Hardware Support Equipment

The following items of equipment are essential to the triplex
system validation at the integration test stand and system
functional checkout on the test aircraft, as well as for any
troubleshooting tasks at either location:

- o   AFCS Test Set
- o   IMU Velocity Simulator
- ●   Breakout Cable Sets

3.6.2.1   AFCS Test Set

The test set serves two functions. It is primarily designed
for use with the Model 347 demonstration aircraft for func-
tional system checkout and troubleshooting purposes. It also
serves as a sensor/discrete simulator for use with the systems
integration test stand. The Test Set, shown in Figure 141,
provides the following capabilities:

431
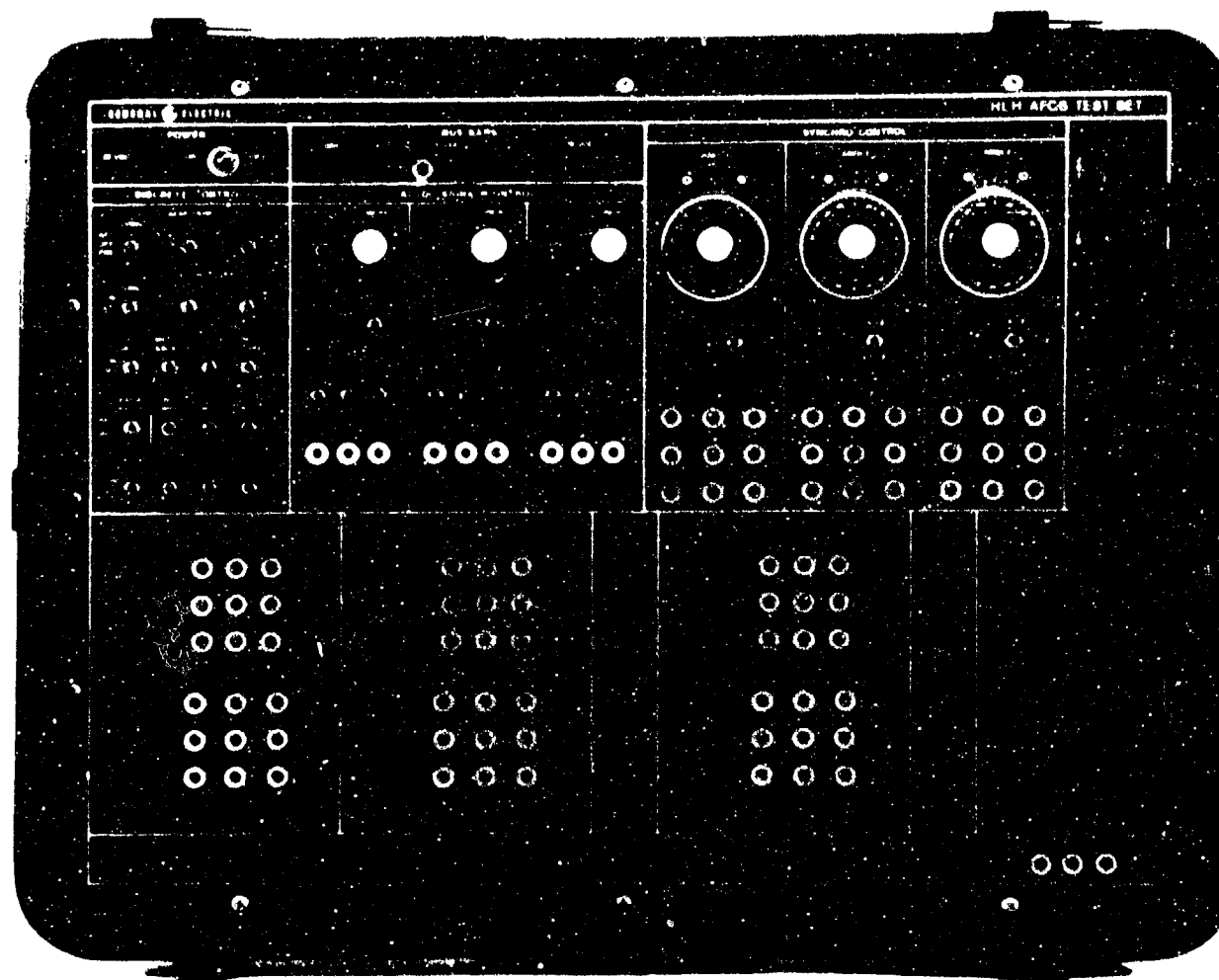
FIGURE 141. AFCS TEST SET

1. Control and monitor of all IOP discrete inputs

2. AC/DC signal control (triplex)

3. AC synchro control (triplex)

4. Monitor patch panel of IOP J6 signals

5. Provides bus bar power (28 Vdc and 5 Vdc) for external use

## Discrete Control

A 32-pin patch panel J9T enables either the simulated discrete and/or aircraft sensor discrete output to be monitored. The aircraft sensor discretes are simulated by toggle switches situated above the patch panel.

## AC/DC Signal Control

The three independent ac/dc panels permit triplex system testing of either ac or dc signals or any combination of dual- and single-channel signals. The high and low signal source output jacks are patched to the appropriate HI and LO jacks on the J6I, II, or III panels.

When operating from external ac reference, the signal is controlled and patched similarly to that for dc control. The significant difference is that of providing the correct phasing for IOP demodulation. The EXT AC reference jacks may be patched to any one of the system supplied AØ, BØ, CØ 26 Vac via the appropriate panels J6I, II, III, depending upon which IOP the J6I, II, III cables are connected to.

## AC Synchro Control

Each synchro control panel is supplied with 26 Vac excitation from panels J6I, II, or III, or any other source, as required. Three parallel outputs are available for each of the stator windings (X, Y, and Z) on each panel. The excitation voltage may be reversed in phase by the switch labeled INØ/OUTØ, without repatching.

## Monitor Patch Panel (IOP J6)

Each patch panel labeled J61, II, III is connected to the designated cable set labeled J61, II, III, respectively. Patch panel III contains the total number of active system wires contained within J6 (IOP) cable listing. All spare wires in J6 are not brought out in the test set. Thus, access via patch panel III permits any simplex, duplex,or triplex signals to be monitored by connecting to the desired IOP. Degraded capability exists on Panel II in that no simplex signals are available. Panel I only contains triplex signal lines for monitoring.

The 26 Vac Ref. on each of the triplex J6 panels has two patch jacks labeled IOP and XMFR. The XMFR jack is the system 115/26 Vac output line which feeds the IOP jack input to provide a reference for demodulation within each IOP.

Normally, the XMFR and IOP jacks are numbered to provide line continuity; however, provision to break this line makes it possible to supply each IOP with any phase 26 Vac supply.

## Bus Bar Power

Provision is made for 28 Vdc and 5 Vdc bus bar supplies and chassis ground to be available at patch points at the top of the test set. This provides capability to permit monitoring of the internal supplies and also to provide discrete signal voltage levels available for test purposes.

### 3.6.2.2 IMU – Velocity Simulator

The IMU Velocity Simulator provides serial-digital signals to both IOPA and IOPC, representing the velocity information normally provided by both INS #1 and INS #2. This simulation device serves both the test integration stand and the Model 347 demonstration aircraft for functional system checkout. The IMU velocity simulator panel shown in Figure 142 is configured with two banks of 16 toggle switches which represent the binary channel, data word, sign,and parity bits. Four momentary pushbutton switches are used to load data from channel A (N-S and E-W) to IOPA and from Channel C (N-S and E-W) to IOPC.

The required velocity is set up in binary format with the appropriate sign and odd parity (this is necessary in all

434
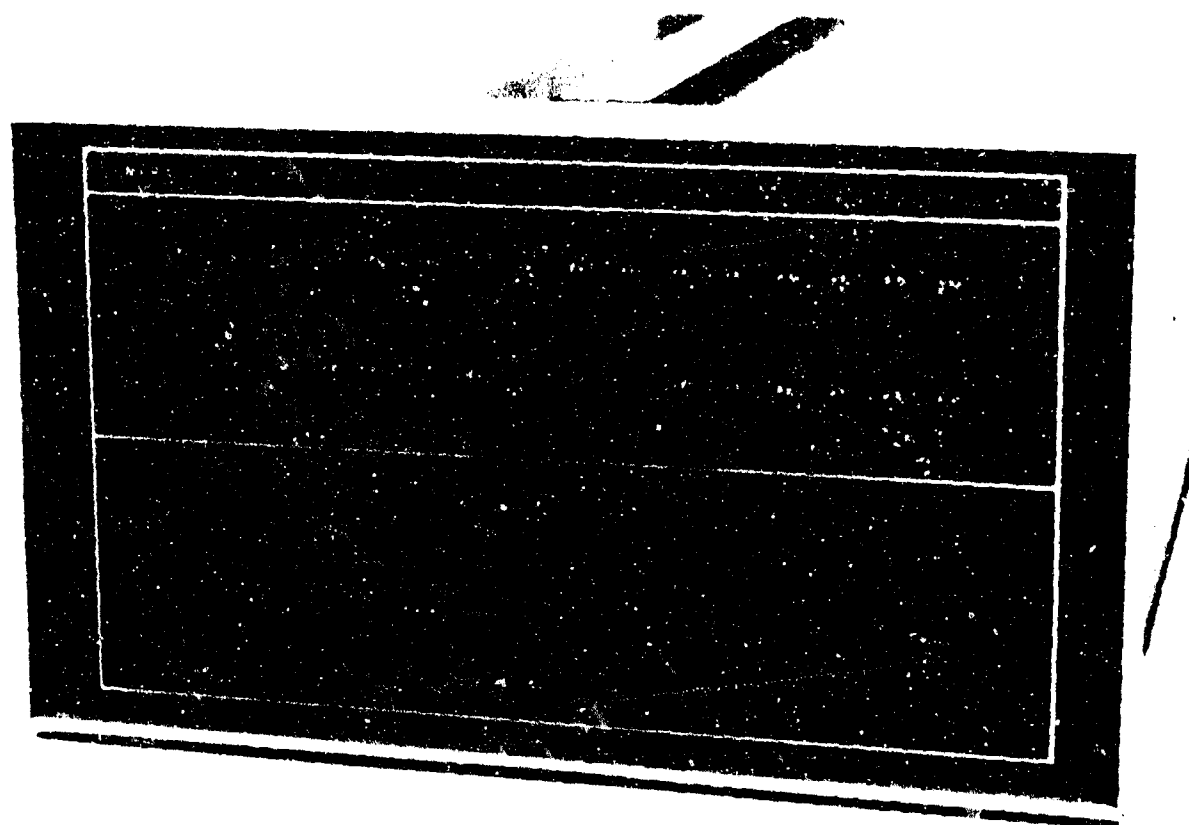
FIGURE 142. HLH-IMU VELOCITY SIMULATOR

435

binary data messages) by the toggle switches. Depressing a pushbutton enters the data set up by the toggle switches into the N-S or E-W register of the channel selected. The data in each N-S and E-W register is then transmitted in a serial manner each time frame to the appropriate IOP. Each of the four output registers may be reloaded with an update velocity by reselecting the toggle switches and depressing the appropriate pushbutton for that register.

The IOP receives the full 32-bit word and then translates the 22 bit + sign data to 15 bit + sign data to be compatible with the computer digital data format. This essentially provides a velocity maximum available range of ±512 ft/sec with a resolution of 0.016 ft/sec, adequate for the AFCS performance.

Timing

The simulator utilizes a single clock generator which is common to both channels A and C. The simulator clock rate provides a bit rate of 9.6 kHz. The clock runs asynchronously from the computer clock.

The transmission of two serial 32-bit words is completed in a 50-msec time frame. Clock and sync pulses are transmitted to each IOPA and C.

3.6.2.3   Breakout Cables

Two breakout cable sets are for use with the IOP connectors J8 and J10.

The use of these two breakout cable sets with the AFCS pre-flight test set provides the capability to monitor and troubleshoot any signal interface between the IOP and the outside signal domain of the AFCS. Transmission lines between IOP to computer and IOP to IMU are serial digital links and are not served by any breakout cable.

## 2.7  HARDWARE CONTROL

The process of integrating the AFCS hardware with the fly-by-wire control system demands close hardware configuration control for activities conducted between the vendor's facility, the integration test stand and the flight line.

Quality assurance provisions at the vendor's facility maintains configuration control of delivered hardware and subsequent modification thereof.  Operating procedures defined for the DELS Flight Test Program were maintained throughout the AFCS test program at the flight line.  The following informal documentation procedures were adopted for the period of system tests at the integration test stand through to the flight line.  These were designed to keep track of hardware-related problems and to keep a historical record of activities conducted.

Daily Activity Log.  The Daily Activity Log maintains a record of all work accomplished on a daily basis for whatever period of testing is in progress on the AFCS, either at the test stand or the aircraft.  The engineer responsible for the system testing on a particular shift enters brief descriptions of tasks accomplished, problems identified for further analysis, and personnel responsible for taking further action.

Problem/Resolution Log.  The Problem/Resolution Log describes briefly, all problems encountered during integration tests, identifying the problem whenever possible to a specific locality.  For example, a problem may be identified to a computer unit, however, the cause may not be identified until further investigation by the vendor.

Each problem identified is logged by number and a parallel resolution log is kept to track the findings of each investigation and subsequent solution thereof.  A summary sheet identifies the problem by number, locality affected, date first observed, and responsibility for action.  The resolution column remains open until such time as a solution is found.

AFCS Equipment Status Log.  The AFCS equipment status log maintains record of all work conducted on each line-replaceable unit (LRU).  This may constitute removal and repair of circuit board elements, repair to internal wiring or connectors, etc. Each configuration change or part replacement must be stated along with the unit serial number and part number affected.

437

This log accounts for work carried out at vendor's facility to maintain an accurate historical record.

The following formal documentation instruments were adopted to handle the movement of AFCS equipment on the flight test aircraft.

### Test Unit Release (TUR)

The Test Unit Release form provided the engineering authorization to install new equipment on the aircraft or to modify equipment already installed, including such items as electrical wiring modifications or details of mechanical changes. It also provided authorization to the vendor to conduct equipment modifications as a result of flight test experience, that generally involved additional cost to the contractor.

### Flight Test Work Log

The Flight Test Work Log maintains an accurate record of equipment installation and removal on the flight test aircraft. Through entries into the flight test work sheet, control of AFCS-related equipment is maintained. The Daily Activity Log pertinent to AFCS maintains an account of tests conducted and observations made on the flight control system.

### Rejection Report

The Rejection Report form provides a means of conveying information pertinent to the failure of any equipment aboard the aircraft. All hardware removed from the aircraft is assigned a disposition. Corrective action may be taken at the Boeing plant or at the vendor's facility. Boeing Vertol Quality Control Group buys the rework acceptance before the equipment is reinstalled in the aircraft. This form was used for all AFCS-related problems.

## 4.0 FLIGHT CLEARANCE TESTING

### 4.1 LABORATORY TESTING

#### 4.1.1 Acceptance Tests at General Electric

AFCS functional tests at the component and system level were
conducted at the supplier's facility before delivery. The
tests were performed at ambient conditions to demonstrate
compliance with S301-10017, Critical Item Development Speci-
fication for AFCS Tasks II and III Demonstrator. Each AFCS
system element was tested under conditions simulating an
interface with the total system. These tests were followed
by system tests which combined all elements and demonstrated
acceptable operation in each of the system operational modes.

#### Acceptance Test Procedures

Specifications were developed by the supplier based on Boeing
Vertol Critical Item Development Specification. The specifi-
cations were used to establish requirements for supplier-
procured components, AFCS subassemblies, and AFCS system
operation. Based on these requirements, Acceptance Test Pro-
cedures were prepared and submitted to Boeing Vertol for re-
view and approval. The procedures detailed all the functional
tests necessary to demonstrate acceptable operation of the
computer unit, Input/Output Processor (IOP), system panels,
and the total AFCS system. Test procedure revisions were
required during testing due to the developmental nature of
the program. All revisions were reviewed and approved by
Boeing Vertol.

#### Computer Unit Acceptance Tests

Each computer unit was tested to demonstrate (1) MOS program
storage capability, and (2) operation in the simplex mode.
The latter test was conducted with the computer interfaced
with an IOP and the system panels.

MOS program storage was checked by verifying that all bits
could be programmed to the zero state and reprogrammed to
the one state.

Simplex operation was verified by inserting a test program,
computing test problems, and displaying the parameters with the
Parameter Change Display Unit (PCDU). The parameter change

439

function of each computer was checked by inserting changes via the PCDU and verifying the correct display of the parameters.

All specification requirements were met by each of the computers.

### IOP Acceptance Tests

Each IOP was operated in simplex to demonstrate compatibility with the computer, panels, and sensor subsystems. Special test equipment was used to apply simulated sensor inputs to the IOP; response to the input conditions was verified by monitoring the data displayed by the PCDU.

Frequency response and phase shift of each signal path was measured.

The simplex channel was operated in each of its operating modes to verify mode logic operation and correct responses to computer discrete inputs and outputs.

All specification requirements were met by each IOP.

### AFCS Panels Acceptance Tests

Acceptance tests were conducted to demonstrate the electrical continuity and proper functioning of lamps and switches for each of the system panels.

In addition to the above tests, the PCDU was functionally tested while interfaced with a computer/IOP and other system panels. The tests demonstrated its capability to change and display computer parameters.

The system panels functioned acceptably.

### AFCS System Acceptance Tests

AFCS components were integrated into the system configuration and tests were conducted to demonstrate specification compliance in each of the operating modes. Sensor inputs were applied to the system in a manner which simulated flight conditions; response to the simulated conditions was monitored to evaluate system operation.

Failure detection capability was determined by performing automatic BITE tests and by evaluating responses to induced system failures.

The two AFCS systems used in the ATC Program met all the acceptance test requirements.

### 4.1.2   Flight Qualification Tests at General Electric

Environmental tests were performed to demonstrate that AFCS components function safely at design operational environments and after exposure to the environments.  Satisfactory operation at the environmental conditions specified in the Critical Item Development Specification was used as a basis for granting flight clearance before entering the Task III flight test program.

Tests were performed on the computer, IOP, and PCDU; other system components are similar to those environmentally tested in the DELS program, therefore, no additional tests were necessary.  A summary of the tests performed is given below.

### 4.1.2.1   PCDU Flight Qualification Tests

The PCDU was tested in accordance with the temperature-altitude conditions of MIL-STD-810B, Method 504.  An operational test was performed to continuously monitor operation during exposure and a performance test was conducted to evaluate operations after the environmental exposure.

All specification criteria were met with one exception: At low temperature (-25°C), the parameter change numeric display failed to illuminate while operating at the low voltage limit (22.5 Vdc, 102 Vac).  The numeric display was regained when the input voltage was increased to 24 Vdc. It was noted that the normal low voltage limit for Category B per MIL-STD-704A is 24 Vdc.

The PCDU was exposed to the vibration resonance search test of MIL-STD-810B, Method 514.1, Procedure I.  Each axis was swept through the required frequency range in a 20-minute time interval.  No discrepancies resulted from the vibration tests and the unit showed no sign of physical failure upon completion.  The unit satisfactorily passed the tests specified in the acceptance test procedure.

441

4.1.2.2  Computer/IOP Flight Qualification Tests

Temperature-altitude, vibration, and humidity tests of
MIL-STD-810B were conducted with the computer and IOP inter-
faced and functioning in the simplex mode.  Operational tests
were made to provide a continuous internal monitor during each
of the environments.  Performance tests were made at signifi-
cant points to determine equipment response to special input
conditions.

The computer/IOP functioned as required during temperature-
altitude tests.  No evidence of physical damage was present
after the tests.

Vibration tests were conducted with the computer/IOP shock
mounted and with the units rigidly mounted to the vibration
test fixture.  No failures occurred during resonance search
or resonance dwell at the frequency selected by Boeing Vertol.
Three failures occurred during the rigid-mount vibration
endurance test:  One ROM and two microcircuits failed and were
replaced.  Inspection of each of the three failed devices
revealed no evidence of mechanical damage.

The computer and IOP were subjected to the 10-day humidity
cycling test of MIL-STD-810B, Method 507, Procedure I.  Two
types of failures were recorded.  Failure of several metal
film resistors was experienced; however, their failure rate
was within the acceptable MIL-Spec limit.

A number of read-only-memory (ROM) device failures also
occurred.  In an attempt to assess the degrading effects of
humidity on the ROM's, a random sample of three devices was
selected from new stock to be subjected to identical condi-
tions present during test of the computer.  At the end of the
10-day cycle, the three ROM devices were taken from the test
chamber and memory contents were immediately verified.  No
discrepancies were found on any of the devices.

Examination of the printed circuit boards on which the ROM's
are mounted indicated considerable moisture penetration of the
conformal coating.  The probability of line-to-line conduction
paths existing at the time of power turn-on may have resulted
in the transmission of excessive currents to some of the ROM
elements.  The position agreed to for completion of the ATC
program  as to continue operation with the existing board
configuration, as no device failures attributable to humidity

442

were experienced either prior to or subsequent to the humidity
tests. Also, full qualification of components was not the
purpose of the ATC program as was evaluation of demonstration
system performance. Furthermore, the rapid advance in whole
word relative to incremental computer technology would tend
to indicate use of the former type in a production HLH system.

## 4.1.3 Integration Test Stand

The integration test stand provides for a spatial installation
of the pilot and copilot controls, force feel, mechanical
linkages, DELS actuators, swashplate driver actuators, and up-
per boost actuators. The test stand has found substantial use
in the integration tests of the fly-by-wire control system -
DELS and AFCS, in completion of the HLH-ATC Task II and III
requirements.

The disposition of electronic equipment pertinent to AFCS in
the stand is as follows:

- AFCS computers, IOP, and Rate Gyro units are installed on
  the same pallets as the DELS units, identical to the
  aircraft configuration.

- Mode Select, System Test Function, PCDU, BITE and Failure
  Status, and Discrete Status Panels are mounted on the
  engineer's panel at the side of the stand to permit ease
  of control and status monitoring.

- The AFCS Discrete Junction Box is mounted on Pallet B
  and 28 Vdc power supplies are provided on the same pallet
  for the GSE AFCS test set and IMU velocity simulator unit,
  identical to the aircraft configuration.

- Miscellaneous control functions, synchros, beep trim, mag
  brake, detents, AFCS release, and indicators such as
  Master Caution, AFCS Warning, and AFCS OFF are installed
  at the cockpit station.

- Wire harness for AFCS is identical to the aircraft con-
  figuration except that some bundles do not terminate in
  connectors, which are specifically for equipment not be-
  ing installed in the stand; for example, PHS, IMU, etc.
  The length of wire bundles and separation of redundant
  channel wire runs have been maintained to approximate
  the aircraft arrangement.

Electrical power supply for the test stand is generated from a Hobart unit located in a room adjacent to the test stand. The simple source supply is split up to represent the aircraft dual bus bar system and the bus control circuitry permits simulated failures of either bus and provides a representative power transfer from one bus to the other. The power monitor unit affords protection for phasing, under/over voltage and frequency variation of the supply source. All contactors, relays, etc., are identical to those used in the aircraft. The circuit breaker panel for distribution of power to the AFCS components and bus control is provided on the engineer panel at the side of the test stand. The 115/26 Vac excitation transformers used for IOP sensor demodulation references are located behind the AFCS circuit breaker panel. Single source 28 Vdc is supplied from a T-R unit which derives power from the laboratory 115 Vac 60 Hz supply.

### 4.1.4 AFCS Integration Tests

System integration testing was conducted at the Boeing Vertol Integration Test Stand facility in two phases: hardware integration tests and flight program software validation. The major objectives of these two phases were to:

(1) Evaluate functional performance of the major AFCS components as an integrated unit to insure compatibility with the AFCS Critical Item Design Specification prior to installation in the test aircraft.

(2) Evaluate the redundancy management system operation for failures which result in a loss of AFCS function to insure that fail-operational/safe conditions prevail.

(3) Develop simplex and triplex system software validation techniques to provide sufficient confidence in the flight computer program tapes prior to installation in the test aircraft.

(4) Develop a hardware/software support facility for all activities resulting from flight test program developments.

The two phases were conducted in series following the equipment delivery schedule. Hardware integration tests were conducted on the initial equipment delivered and resulting problems were related to the vendor to permit design changes to be incorporated in the second shipset of equipment prior

444

to delivery. The first ship set was returned to the vendor for refurbishment, and upon redelivery was put through a short checkout before being shipped to the aircraft for installation and subsequent functional and ground tests. The second ship system was delivered to the integration test stand to permit completion of hardware integration tests and eventual triplex validation of the first flight program software. An interim period was devoted to acceptance tests of the digital in-flight recording system.

Considerable use was made of the AFCS Test Set and system test tape during the integration testing. The test tape, previously utilized during the acceptance tests at G.E., was a significant tool, in conducting end-to-end checks in evaluating hardware interfaces from the simulated sensor inputs (generated by the test set) to the commanded outputs, and status display infor- mation. The test tape provides a means of coupling IOP vari- able inputs to variable outputs through the computer with unity gain. It further enables the operator to control dis- crete inputs to outputs which is useful for mode logic checks. In this manner, complete end-to-end checks were made without the complications of the flight program software.

4.1.4.1   Phase 1 - Hardware Integration Tests

The hardware integration tests encompassed several aspects of the AFCS IOP-computer subsystem performance in the triplex configuration. Limitations of the test stand facility with regard to the use of actual sensors did not permit a thorough integration test of all the wiring interfaces that existed in the aircraft. The following aspects of system performance were tested.

Signal Transmission

The tests of signal transmission were designed to examine the signal characteristics at each Line Replacement Unit (LRU) interface and the processing of the signal path through each LRU. Each variable IOP input/output was checked for absolute range, polarity, scaling, and quantization. Discretes were checked for logic state compatibility with the specification. Redundant channel tracking errors were determined using a common source input to the three IOPs, for each variable type. This provided a qualitative assessment of signall spread due to amplifier offsets, linearity, and digital noise.

445

## System Functional Operation

Tests were conducted to determine the system functional integrity when operating in the aircraft environment. The BITE function was designed to provide a preflight self-test capability to determine whether all the voting and failure monitoring circuitry is operating properly, to reduce the risk of undetected failures in flight. Operational checks on the AFCS-DELS interface were designed to check out the transient-free nature of engagement and disengagement of any or all axes of control, and the inhibiting of re-engaging AFCS following detected second system level failures at the DELS interface.

## Redundancy Management

The AFCS redundancy management scheme is designed to recognize the occurrence of a failure, interpret its location, and then take the appropriate action to shut down the part or whole of the system affected, in a predetermined manner. Also implied is the capability for proper signal selection for unilateral computations and command outputs for flight control actuation under normal and failed-state conditions.

The tests conducted to demonstrate specification compliance with the redundancy management scheme consisted of the following:

- Evaluation of the median value and average value signal-selection technique for triplex and duplex sensor inputs, respectively, and subsequent action following first sensor failures.

- Verify decoding of all sensor inputs (discrete inputs are lumped together and treated as a sensor input) and the programming of all sensor failure detection threshold levels and time constants.

- Verify that the system could sustain the loss of any single IOP and computer without degradation in performance.

- Verify appropriate axes shutdown following selected combinations of sensor failures.

446

## Modal Logic Validation

Modal logic validation during Phase I of the integration tests consisted of an end checkout of each logic statement defined in the design specification document. It was necessary to conduct these checks prior to flight software validation since the latter depended upon successful execution of mode logic in checking control loop functions.

Prior to commencing logic checkout, the hardware circuit implementation was checked against the design specification for correct translation of Boolean statements to NAND logic format.

The philosophy adopted for each logic statement checkout was to set up the necessary inputs to obtain a switching of the statement output to a true condition. The inputs were then exercised to create the output to go to a false state. Once each statement was verified, it was then treated as a single input to a succeeding logic statement. It was possible, therefore, to work through each statement from input to output with a minimal number of input operations having to be set up.

This checkout utilized the system test program tape as a tool to manipulate the logic inputs required from the computer to the IOP. The only observable points available for logic checkout were IOP discrete inputs/outputs and computer discrete input/outputs; thus, it was only possible to exercise the logic to a degree which provided confidence in correct operation of each mode.

### 4.1.4.2 Phase II - Software Validation

The second phase concentrated on debug and validation of the flight program software in two successive stages; namely, simplex and triplex mode of operation, to insure proper interpretation of the control laws and logic.

Prior to commencing the simplex software debug process, it was necessary to conduct reviews of the design specification baseline and compiled change requests versus the algorithm maps and mode logic circuitry developed from the specification, to check for correct interpretation and programming.

The simplex mode of operation consisted of an IOP Computer with External Memory Unit, Program Loader Unit, Program Monitor Unit, AFCS Test Panel, and IOP J8 Breakout Panel.

447

This setup was located in the Flight Controls laboratory alongside the Integration Test Stand. System mode control was achieved using patch cords plugged into the J8 breakout panel. The AFCS Test Panel provided all the necessary variable sensor inputs and discrete inputs to the IOP and permitted monitoring of all IOP outputs. The program loader unit permitted programming modifications to the external core memory and the program monitor unit provided the operator with the versatility of controlling the computations to permit algorithm readout, iteration by iteration.

This setup permitted software checkout to be conducted in parallel with triplex system hardware integration tests on the second ship set. Later in the flight test program, it became possible and more efficient to integrate this setup into a single channel of the triplex system, making available the use of the Mode Select, System Test Function, and Discrete Status panels. Two eight-channel brush recorders were available to record test results.

The software debug technique adopted was simply to exercise the control laws for each mode of operation be it basic SCAS, Hover Hold, etc., to determine correct loop gains, transfer functions, and logic operation on an end-to-end basis, working from the simplest to the most complex loop structure, using a building block concept. The hard-wired mode logic had previously been verified on the triplex set so that only the software logic remained to be checked on a closed-loop basis. All programming problems identified were then corrected on the algorithm maps, coded instructions changed, entered into the program external core memory via the program loader unit, and revalidated. Once a satisfactory debug was achieved, a new program tape was compiled. Tape compilation was initially conducted at the vendor's facility on a Xerox Sigma 5 computer which offered fast turnaround. The VICAP assembler program was modified to be compatible with the Boeing Vertol Hybrid Laboratory 360 - Mod 44 computer, to provide an alternate tape compilation facility.

The next stage of validation involved the triplex system mode of operation. The four Read-Only-Memory (ROM) boards for each of the three computers were each initially erased under ultraviolet light source and then programmed in the ROM Programmer Unit with the program tape information compiled at the end of the simplex debug process. The programming of the complete set of ROM boards usually took several hours, and since each

448

group of three boards were programmed at the same time from one source, a high degree of confidence was reached that each computer would receive identical programs.

Triplex software validation offered a more thorough, final evaluation of the flight program than could be efficiently achieved on the simplex test setup. The same test plan format was carried through from the simplex tests, which provided baseline data to the triplex tests. The simplex validation provided enough information to correct the gross programming errors and, therefore, to minimize the number of ROM board reprograms. Triplex testing extended simplex in the area of the PCDU interface with the flight program where this could not previously be checked.

The results of triplex validation usually required one reprogram, sometimes two; however, it was sometimes necessary to reprogram a ROM board due to failure of a single bit to program correctly. This resulted in change of the integrated circuit component, reprogram, and validation.

The software test plan used for the triplex validation was designed for use in completion of the functional tests on the demonstrator aircraft prior to initial AFCS flights where telemetered data obtained at the aircraft could be compared with that obtained in the laboratory.

## 4.2  AIRCRAFT FUNCTIONAL AND GROUND TESTING

Ground testing was conducted to demonstrate that the integration of the AFCS and the flight research vehicle was correctly performed and that all subsystems within the AFCS were functioning satisfactorily. Testing was broken down into the following categories:

- AFCS signal interface

- AFCS functional operation ⟨ Test Tape / Flight Tape

- RFI/EMC effects

449

### 4.2.1  AFCS Signal Interface Checks

Electrical continuity checks were made to verify that AFCS
interconnect wiring was properly installed.  Checks consisted
of a pin-to-pin survey of each wire.

Critical power checks were made with all AFCS equipment
removed.  AFCS power busses were activated and voltages were
measured on all power carrying pins.

Interface compatibility between the IOPs and all command
inputs, sensors, flight control system, and displays encom-
passed within the definition of AFCS was checked using the
system test program Tape #1 in the computers.  This permitted
complete end-to-end checks to be made for all types of inputs/
outputs without the complication of flight program software.

Four means of checking signal transmission were used:

- AFCS test set inputs

- LRU inputs

- IMU velocity simulator inputs

- External voltage inputs

Inputs to the IOPs were observed on either the PCDU, Mode
Select panel, or status panels.  Outputs were observed at the
receiving LRU level, i.e., actuator or meter movement.

### AFCS Test Set Inputs

The AFCS test set was used to simulate sensor inputs and some
discrete inputs to the IOP.  A detailed description and use of
the test set is given in Section 3.6.2.1.  The PCDU was used
to verify that the signal was received correctly into the IOP.

### LRU Inputs

These checks were accomplished by either initiating a discrete
input at one of several LRUs and observing transmission at the
proper Algo time at the PCDU, or by observing discrete outputs
via annunciator lights at the different LRUs.

450

The emphasis on discrete input/output checks concerned itself
with checking the interface between the IOP and the remaining
LRUs. Discrete checks between the IOPs and FCCs were not
fully addressed since these were done during integration
test stand checkout. Wire-by-wire continuity checks were made
on the aircraft between the IOPs and FCCs and it was felt that
this was sufficient to assure proper transmission without
duplicating checks done previously.

IMU Velocity Simulator Inputs

The IMU velocity simulator was used to check the serial-
digital signals to both IOPs. The required velocity was set
up in binary format, with the appropriate sign and odd parity
by the toggle switches.

External Voltage Inputs

Where it was not possible to use the test equipment or LRU
responses, an external voltage source was used to verify
proper signal transmission. This was primarily for discrete
signal checks.

4.2.2  AFCS Functional Operation

AFCS functional operation was checked initially using the
system test tape and then with an actual flight tape loaded
in the computers. Tests in this area ranged from manual
operation of switches selecting specific functions to system
semi-automatic and fully automatic functions dependent upon
certain input states. Wide use was made of the AFCS test set
during this activity. The system functional tests were per-
formed on ground power first, then on aircraft power.

Checks consisted of:

- Proper functioning of sensors - range, polarity tracking,
  and self-test features.

- Pilot's controls with AFCS and DELS engaged - emergency
  disengage, DELS reversion to mechanical backup, mag
  brake operation, beep trim operation, and cyclic controls
  in and out of detent.

- System engage/disengage - checked conditions to permit engagement, single and multiple axis engagements, manual and automatic shutdown.

- LCCC inputs - range, polarity, force and breakout gradients, and brake operation.

- Flight control interface (DELS, Speed Trim, CCDA) - AFCS second-fail override by DELS, BITE, inhibit auto reversion of DELS to MBU with AFCS on, inhibit of command signals to speed trim.

- BITE panel function - lamp test, arm light, throttle quad and emergency disengage inhibit, test select of channels A, B, C, and system and operation of BITE following test fail or test pass.

- Parameter change/display unit - lamp test, display and change capability, parameter change enable/disable, clear data, status lights, group and channel selection.

- System test function panel - test input (axis, amplitude, direction, location, type, excitation, gust input) and axis enable operation.

- Mode Select panel functions - engage AFCS, engagement of selectable modes, selection of velocity reference and decay function, operation of fault reset, selection of altitude hold reference.

- Failure and discrete status panels - lamp tests, exercise modal and failure logic. Observation of panels was made during entire system functional time.

- Pilot displays - operation of flight director, ground velocity indicator, master caution and annunciator panels, including flasher group, and axis select panel.

- Redundancy Management checks - sensor/discrete input failure detection, loss or transfer of power, loss of cable interconnection, sensor signal selection and computation, system shutdown and disengagement, and IOP/ computer hardware failure detection and monitoring (implicitly exercised during BITE check).

### 4.2.3   RFI/EMC Checks

RFI/EMC testing of the AFCS was conducted on the ground with engines runni. , but rotors unbladed, to eliminate the possibility of rotor/fuselage interference in the case of an extraneous input into the controls.

The objective of these checks were:

- To establish that the various components within the AFCS complex are mutually compatible.

- To establish the level of electromagnetic compatibility between the AFCS, the DELS, and the basic aircraft system.

Checks included the functioning of all electronic/electrical equipment associated with the basic aircraft and observing the effects on the AFCS due to RFI.  Similar checks were made with the flight test instrumentation.  In turn, the AFCS was operated to determine the effects on the basic aircraft systems and DELS.  No adverse effects on AFCS, DELS, or other aircraft systems were noted.

### 4.2.4   Preflight Procedures

During ground checkout, procedures were developed for preflight checkout of the AFCS and the supporting equipment to assure flight readiness.  Procedures for DELS checkout were as used during TASK II flight testing.  The AFCS preflight checks which are detailed in Appendix 5 of Reference 11 cover the following areas:

1. AFCS Initial Setup and Power Checks
2. Flight Tape Identification Verification
3. AFCS BITE Checks
4. Sensor Checks
5. Discrete Signal Checks
6. Engage/Disengage Checks
7. System Test Function Panel
8. LCCC Checks
9. Miscellaneous Checks
10. Speed Trim Checks
11. External Load Cable Tension and Angle Sensors
12. Power Down Sequence
13. Aircraft Flight Line Checks

## 5.0  IN-FLIGHT EVALUATION OF AFCS CONTROL LAWS

The Task III flight test evaluation of the HLH/ATC AFCS and
associated systems was conducted on a modified CH-47 helicop-
ter between March 27 and October 30, 1974.  Aircraft test
configurations, equipment, flight logs and test reports,
together with pilot conclusions and recommendations are
detailed in Reference 11, HLH/ATC Flight Controls  Controls
Ground and Flight Test Report.  Quantitative data, with appro-
priate analysis, is included in this section, covering handling
qualities achieved for each mode of AFCS operation.  Key pro-
blems that required system redefinition during testing are
included.  Pilot ratings from Reference 11 are contained in
data presentation.

### 5.1  OBJECTIVES

The objective of the flight program was to demonstrate that
the AFCS, as designed through analysis, provided aircraft
handling qualities compatible with the HLH operational mission
requirements.  From the pilot station, this means all-weather
IFR capability with external loads.  The load-controlling
crewman, on the other hand, requires a precise control capa-
bility for rapid load acquisition and deposit.  The repetitive
nature and short mission times associated with cargo transfer
implies the helicopter must be easy to fly with minimal work-
load from either station (i.e., Cooper ratings better than
3.5).  Specific objectives for each mode are reported in
Section 2.0.

### 5.2  FLIGHT TESTING

### 5.2.1  Test Vehicle

The Boeing Model 347, Figure 143, was used to develop and dem-
onstrate the HLH handling qualities.  A retractable capsule
was installed to simulate the HLH load controlling crewman
station.  The station was equipped with the prototype finger/
ball controller and necessary mode select panels.  A two-point
suspension system is incorporated.  For load acquisition
(MILVAN), a top lift adapter with remote LCC controlled lock-
ing mechanism was available.

Testing was conducted at an aircraft weight of 38,000 pounds
with load weights ranging from 4800 pounds (empty MILVAN) to
8000 pounds.  Sling lengths of 10, 20, 30, and 55 feet were

LOAD CONTROLLING
CREWMAN STATION
(RETRACTABLE)

TOP LIFT ADAPTER

8 ft x 8 ft x 20 ft MILVAN
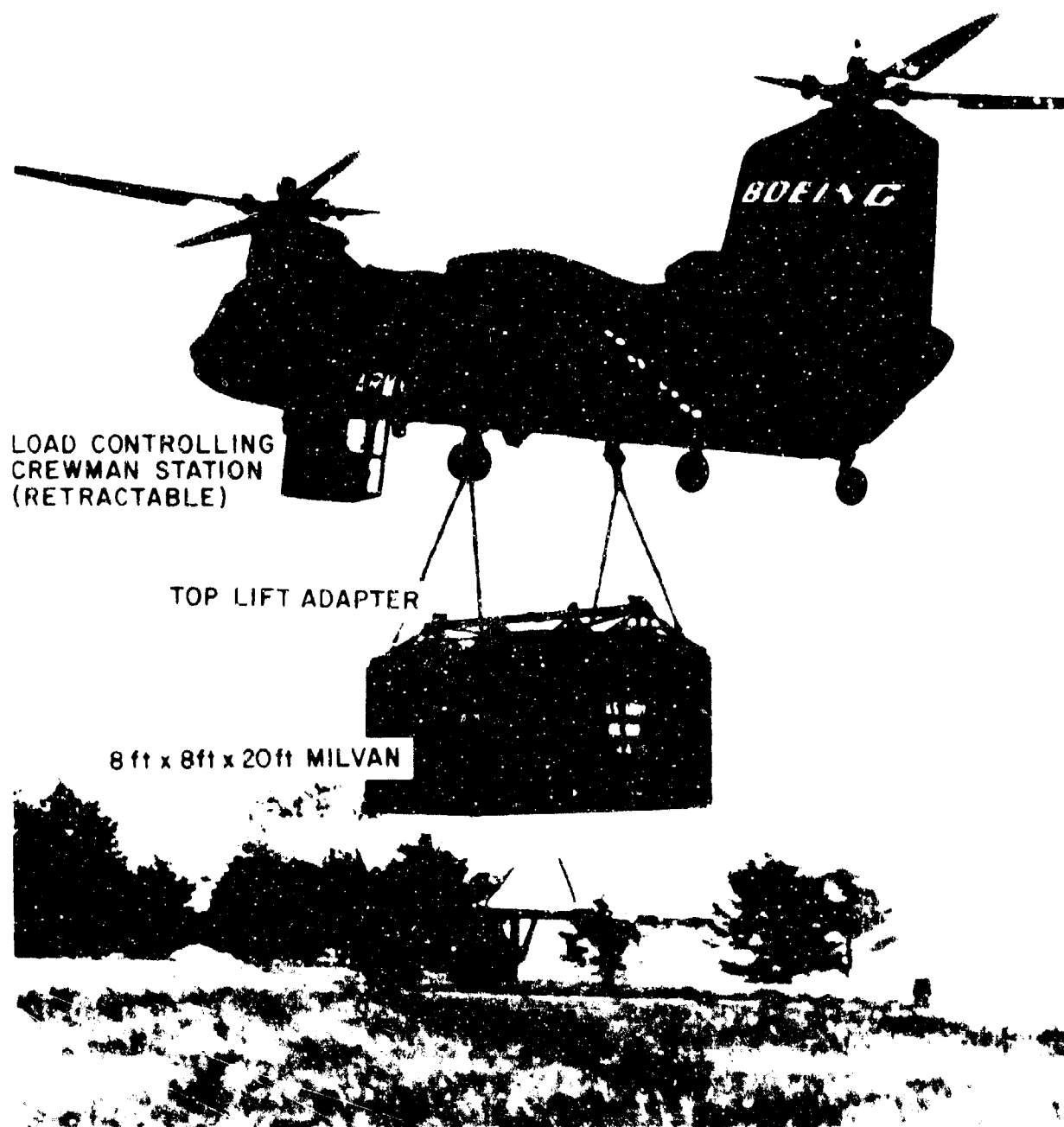
FIGURE 143.
347/ATC DEMONSTRATOR
AIRCRAFT

used with testing concentrated at 10- and 30-foot lengths.
Testing with cables longer than 30 feet was limited due to
load interference with the radar altimeter during longitudinal
motions. Development flights were flown between April and
October of 1974, followed by customer demonstrations in November.
Two U. S. Army Preliminary Evaluations were conducted
during the developmental phase.

5.2.2  Program Sequence

AFCS flight testing was accomplished in a sequential manner
using four software program phases as shown below. Area of
concentration is noted together with approximate flight time.

|  |  | X - Mode Available<br>[X] - Concentrated Testing | | |
|---|---|---|---|---|
|  | Mode Availability | | | |
| AFCS Mode | Tape 1 | Tape 2A | Tape 2B | Tape 3 |
| Basic SCAS | [X] | X | X | X |
| Altitude Hold | X | [X] | X | X |
| Hover Trim | X | X | X | X |
| Hover Hold |  | [X] | [X] |  |
| Load Stabilization |  |  | [X] | X |
| Automatic Approach<br>  to Hover |  |  |  | [X] |
| Reprograms | 2 | 4 | 3 | 4 |
| Flight Hours | 36 | 46 | 64 | 24 |

Thirteen reprograms of the basic four tapes were necessary
to accommodate parameter changes and system redefinitions.
Computer capacity limitations prohibited incorporation of
all modes on one tape. Army Preliminary Evaluations used
Tapes 2A-4, 2B-3, and 3-4.

## 5.3 FLIGHT DEVELOPMENT RESULTS

Flight results are presented below for each AFCS mode. Data
are included covering acceptable and problem areas (both
resolved and unresolved), pilot ratings, and simulator test
comparisons. Recommendations covering problem areas are made
at time of discussion.

### 5.3.1 Basic SCAS

The basic SCAS operation was evaluated throughout the flight
envelope and included assessments of dynamic and static sta-
bility, controllability, and velocity reference mode
switching.

### 5.3.1.1 Dynamic Stability

Dynamic stability evaluations were performed by injecting
pulses and steps into the flight controls by means of the AFCS
Test Function Panel controls (differential pulses and parallel
steps), and also by manual inputs by the pilot. High levels
of damping were achieved under all test configurations as
shown on Figures 144 to 152. The following table identifies
each figure with test configuration.

| Axis | Hover | Transition 40 to 80 Kn | Cruise 80 to 150 Kn |
|------|-------|------------------------|---------------------|
| Longitudinal | Figure 144 | Figure 146 | Figure 150 |
| Lateral | Figure 145 | Figure 147 | Figure 151 |
| Directional |  | Figure 148 Figure 149 | Figure 152 Figure 153 |

Dynamic stability in all axes was very good with a pilot
Cooper-Harper rating of A-1.5. Damping augmentation in the
vertical axis was found to be unnecessary because of high
inherent damping of the basic airframe. The method of incor-
porating damping augmentation also deteriorated vertical con-
trol response. A pseudo-rate signal was formed by lagging
vertical acceleration. In addition, a washout was incorpor-
ated to eliminate steady accelerations. Response to a step

457
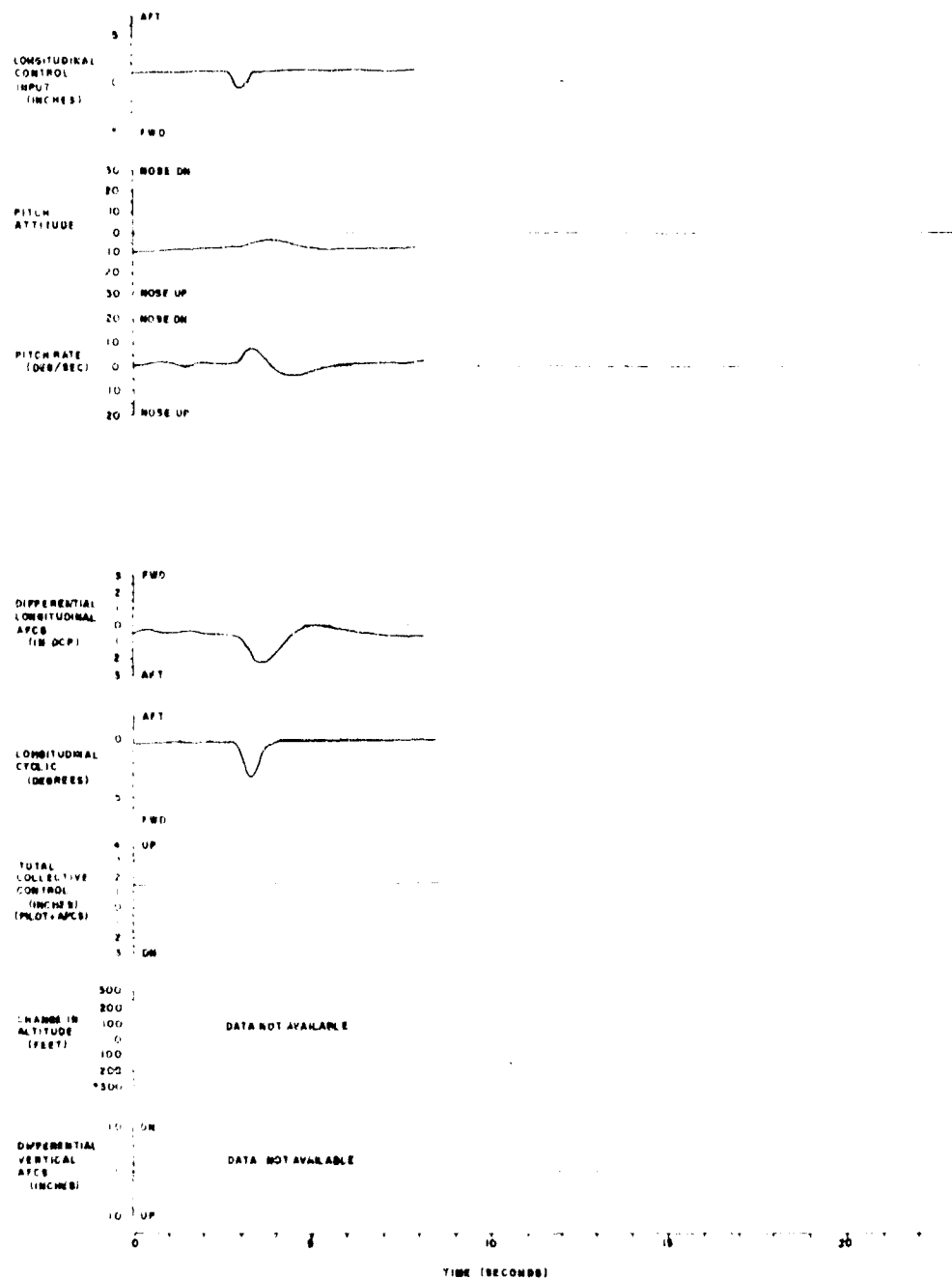
FIGURE 144. AIRCRAFT RESPONSE TO LONGITUDINAL PILOT PULSE - BASIC SCAS — HOVER

458
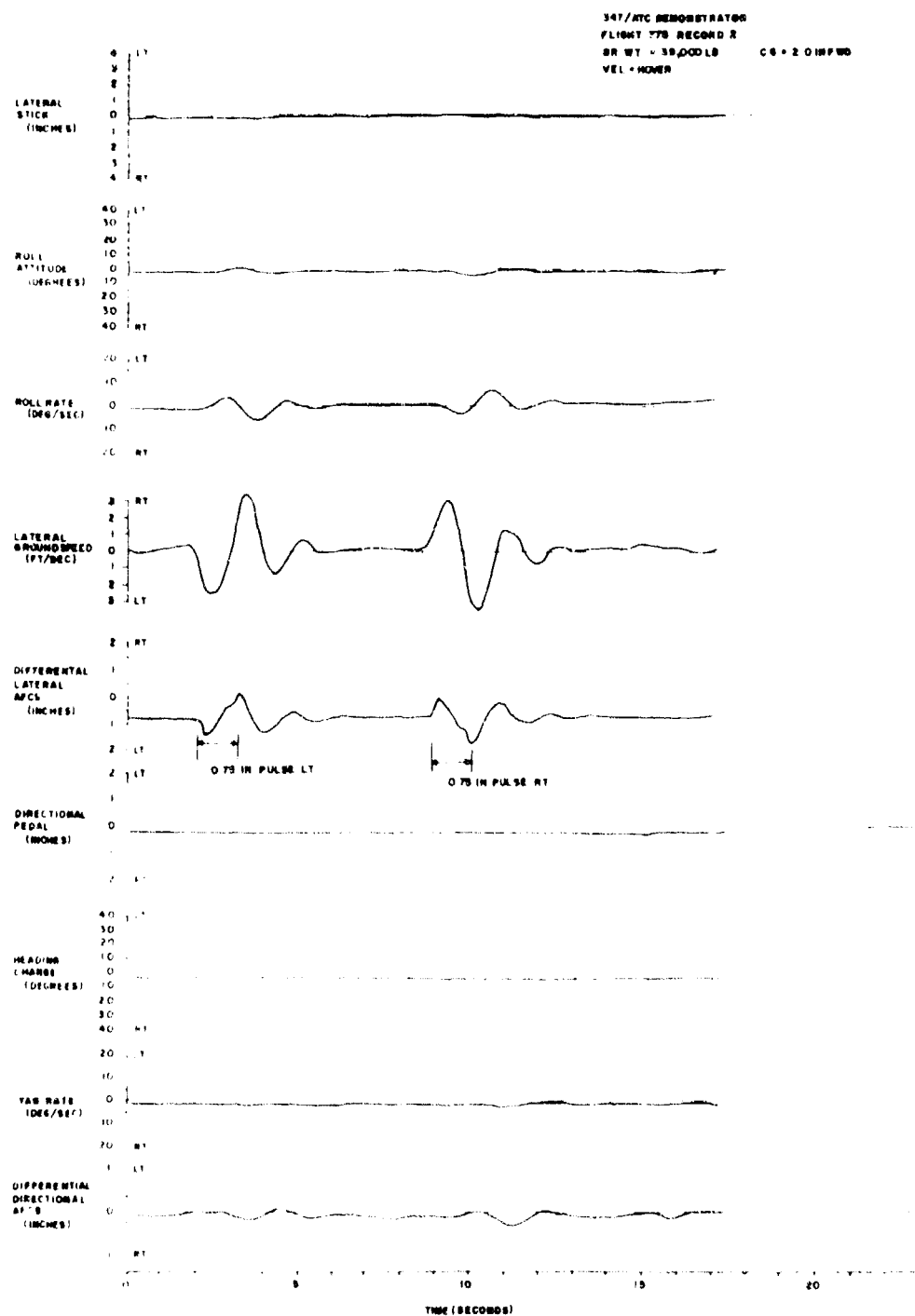
FIGURE 145. AIRCRAFT RESPONSE TO LATERAL DIFFERENTIAL PULSE - BASIC SCAS — HOVER

459
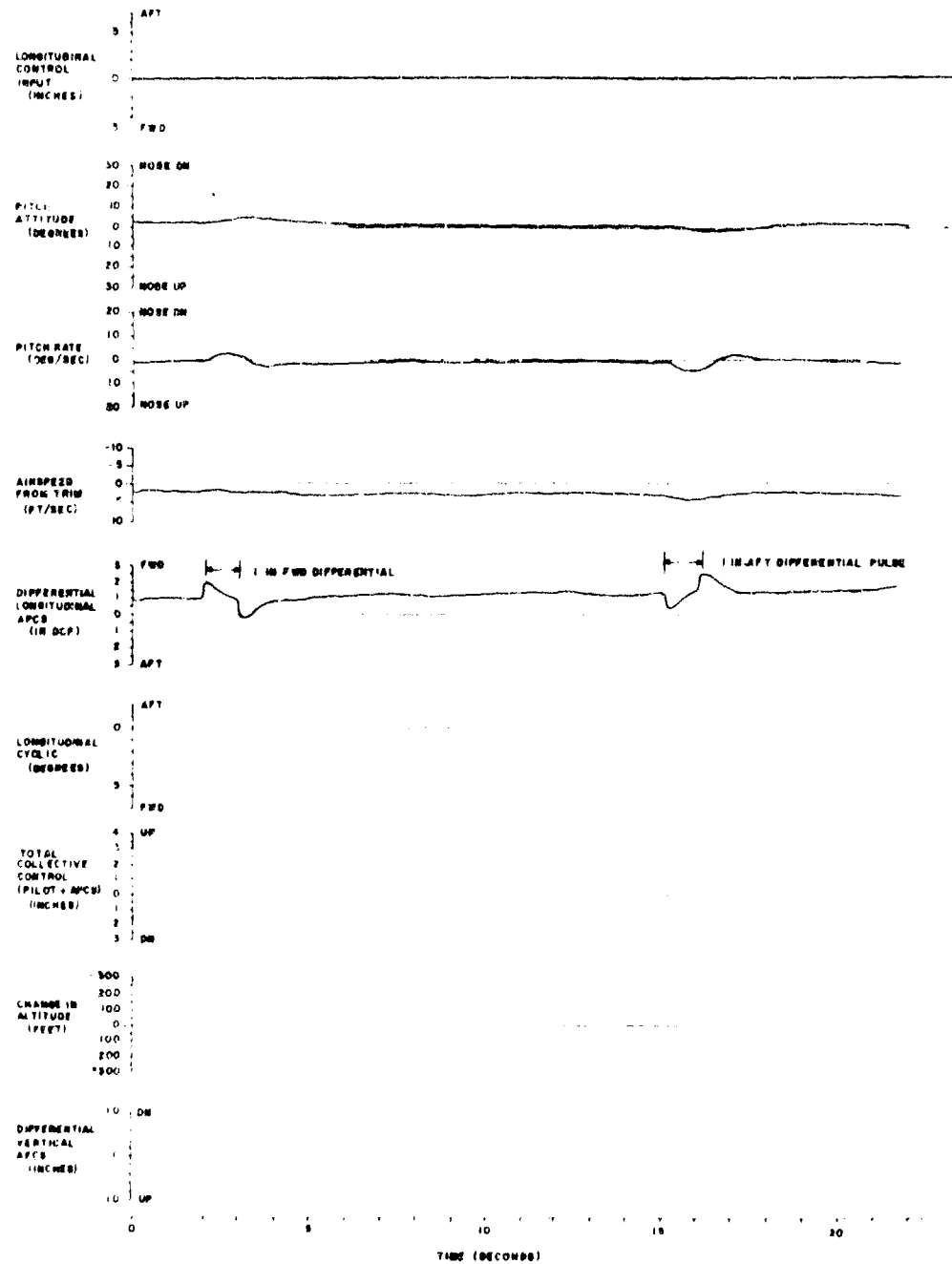
FIGURE 146 AIRCRAFT RESPONSE TO LONGITUDINAL DIFFERENTIAL PULSE — BASIC SCAS — 60 KNOTS
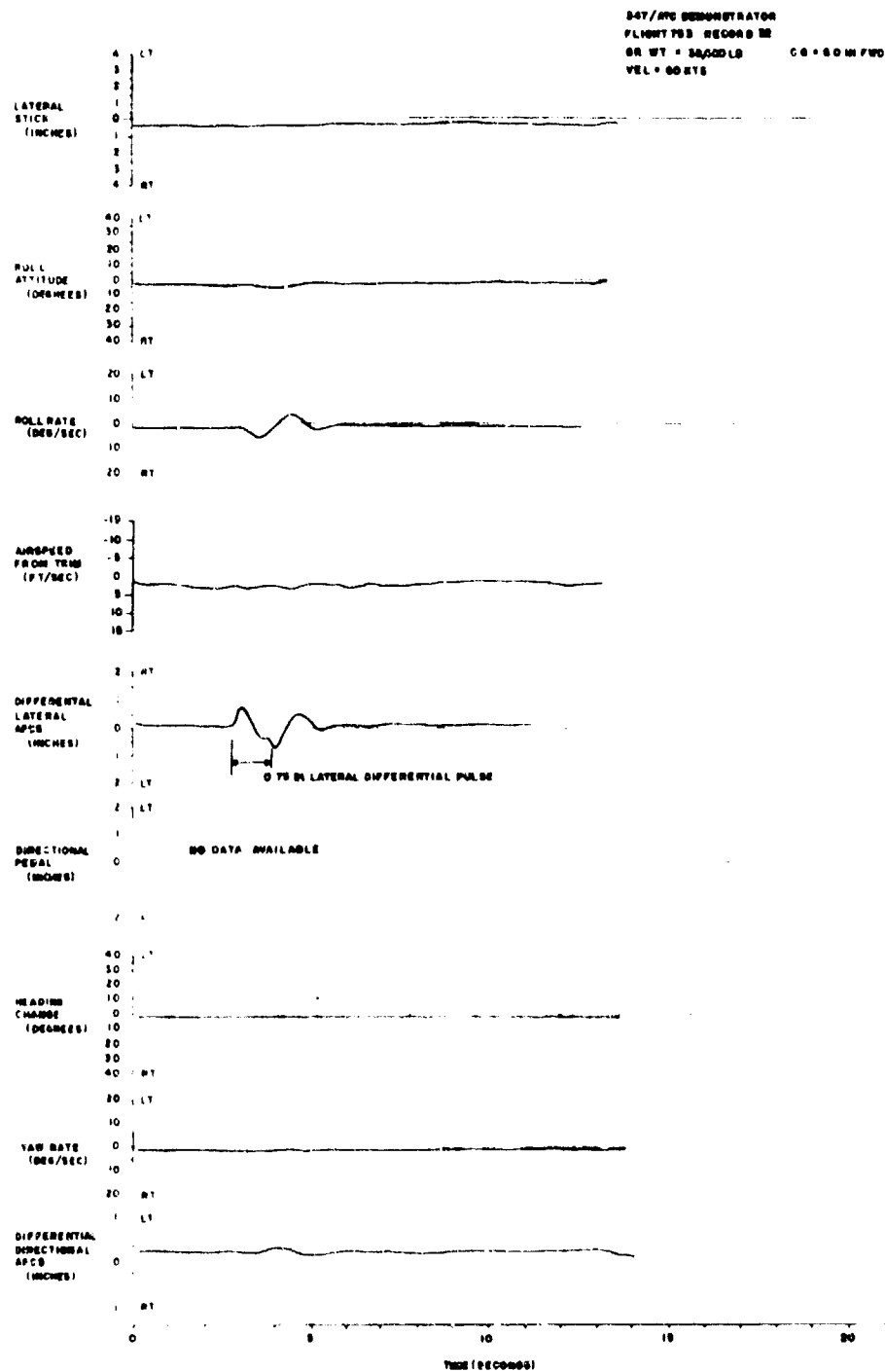
FIGURE 167 AIRCRAFT RESPONSE TO LATERAL DIFFERENTIAL PULSE - BASIC SCAS — 60 KNOTS

461
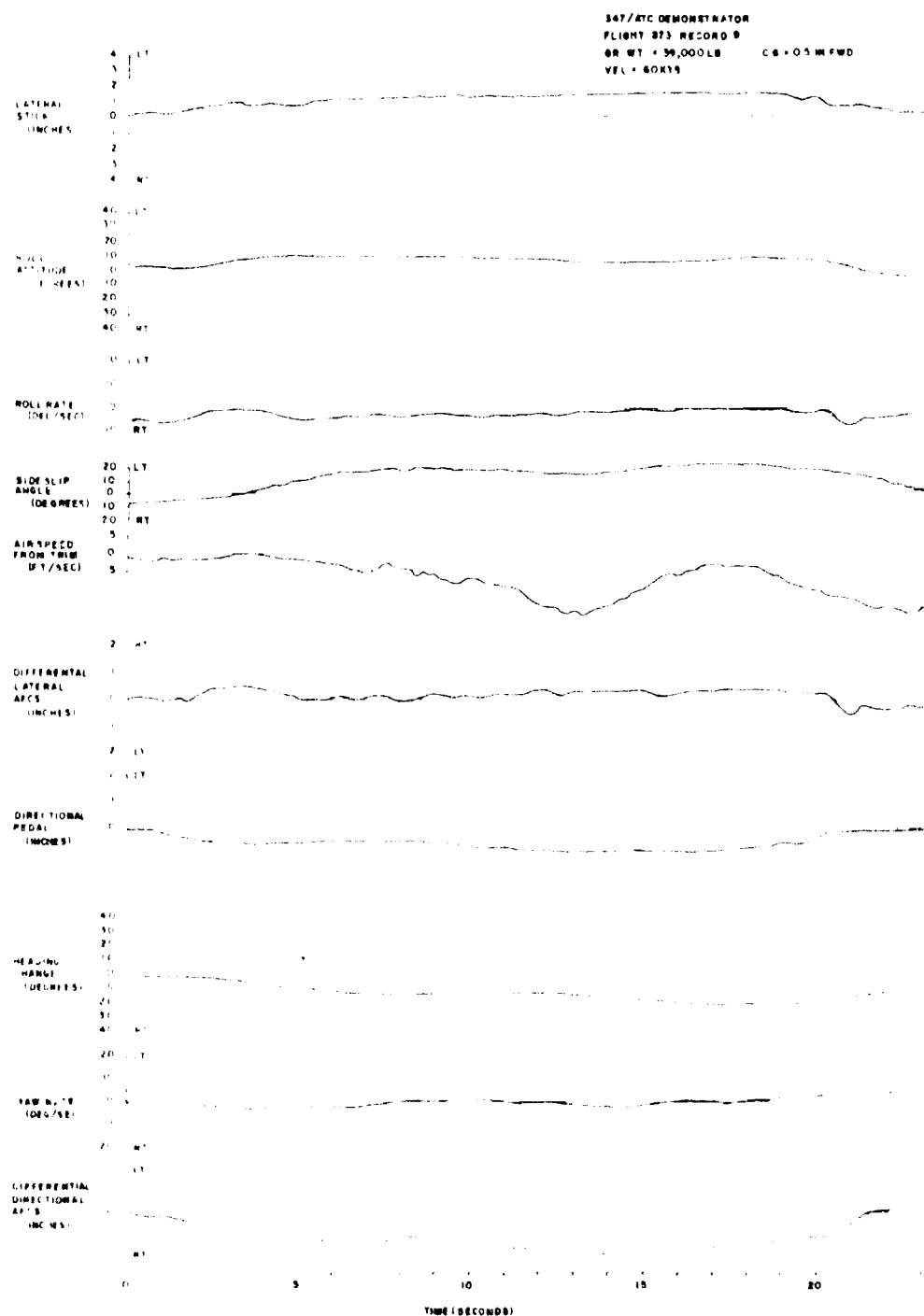
FIGURE 148 AIRCRAFT RESPONSE TO LATERAL DIRECTIONAL STEP-BASIC SCAS — 60 KNOTS
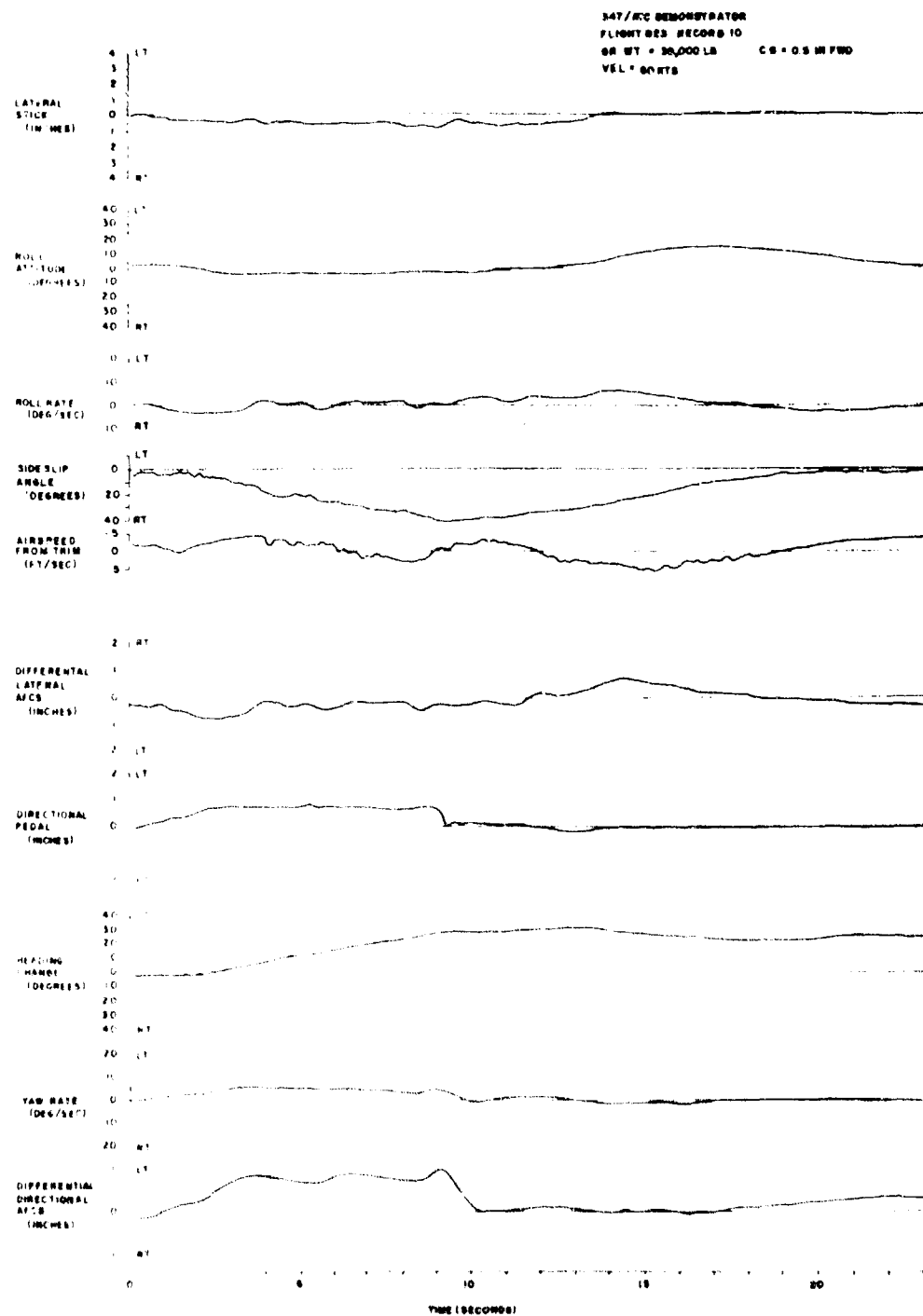
FIGURE 140   AIRCRAFT RESPONSE TO LATERAL DIRECTIONAL STEP - BASIC SCAS — 60 KNOTS
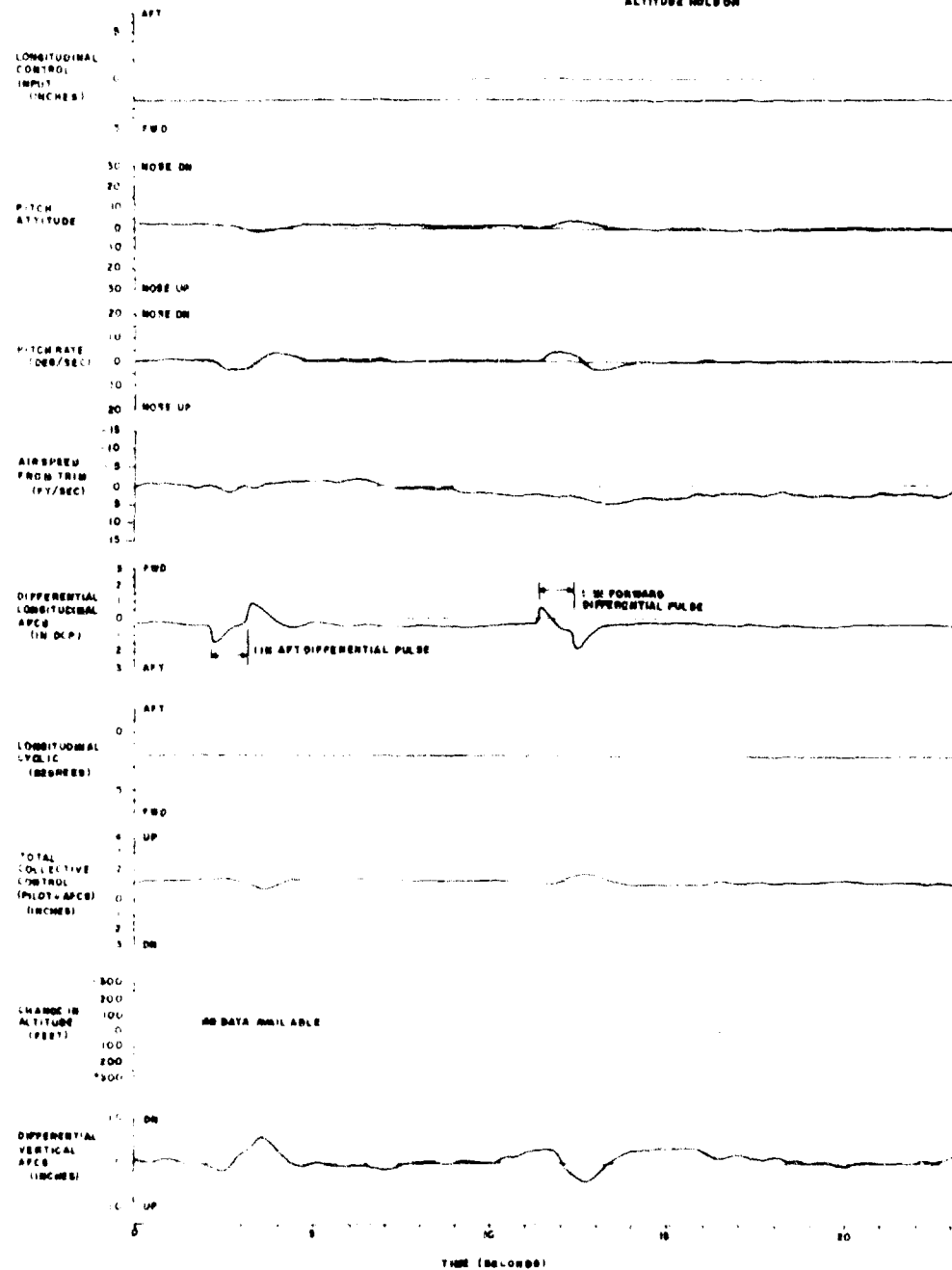
FIGURE 180. AIRCRAFT RESPONSE TO LONGITUDINAL DIFFERENTIAL PULSE - BASIC SCAS — 130 KNOTS

FIGURE 181 AIRCRAFT RESPONSE TO LATERAL DIFFERENTIAL PULSE - BASIC SCAS — 130 KNOTS

465
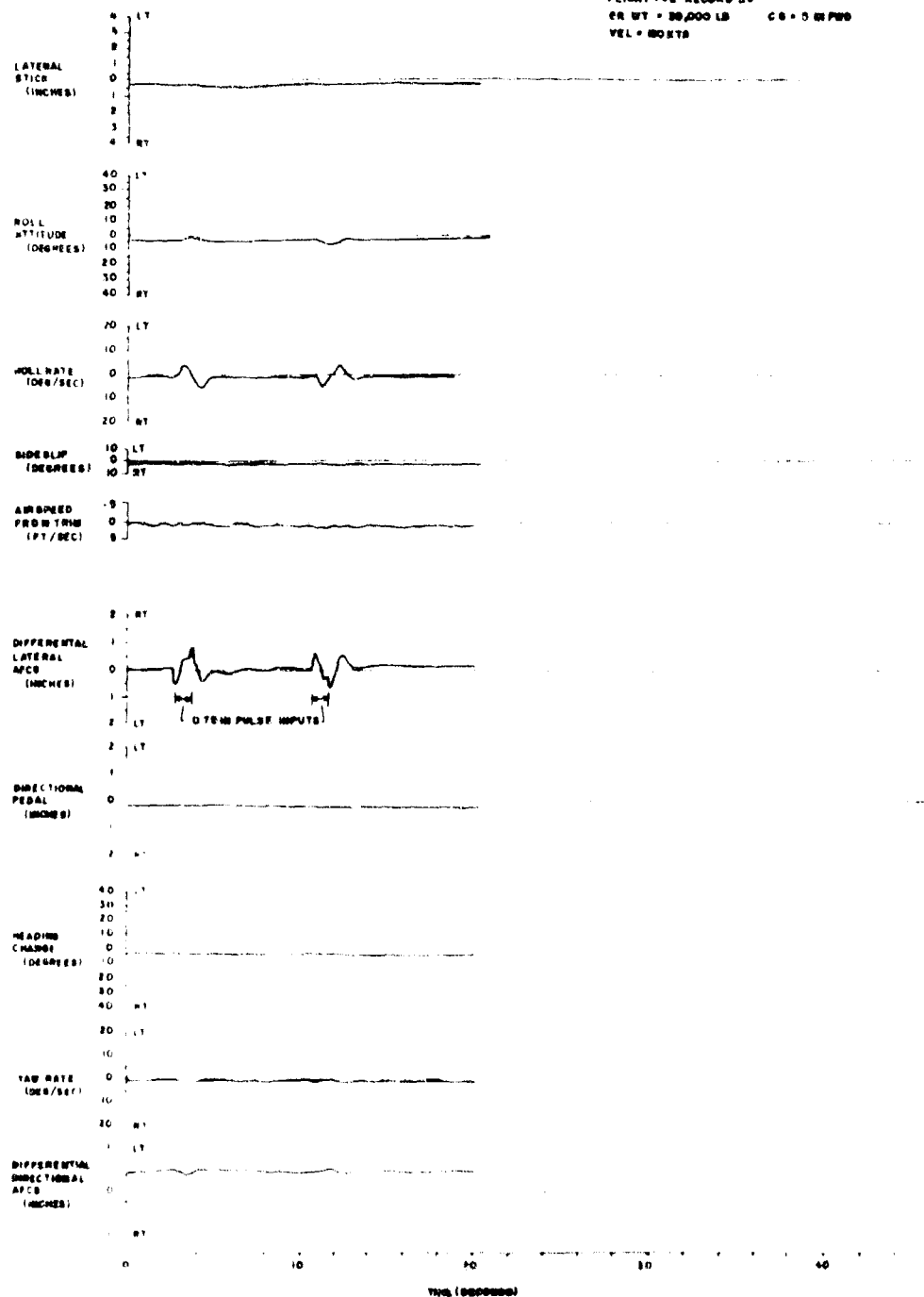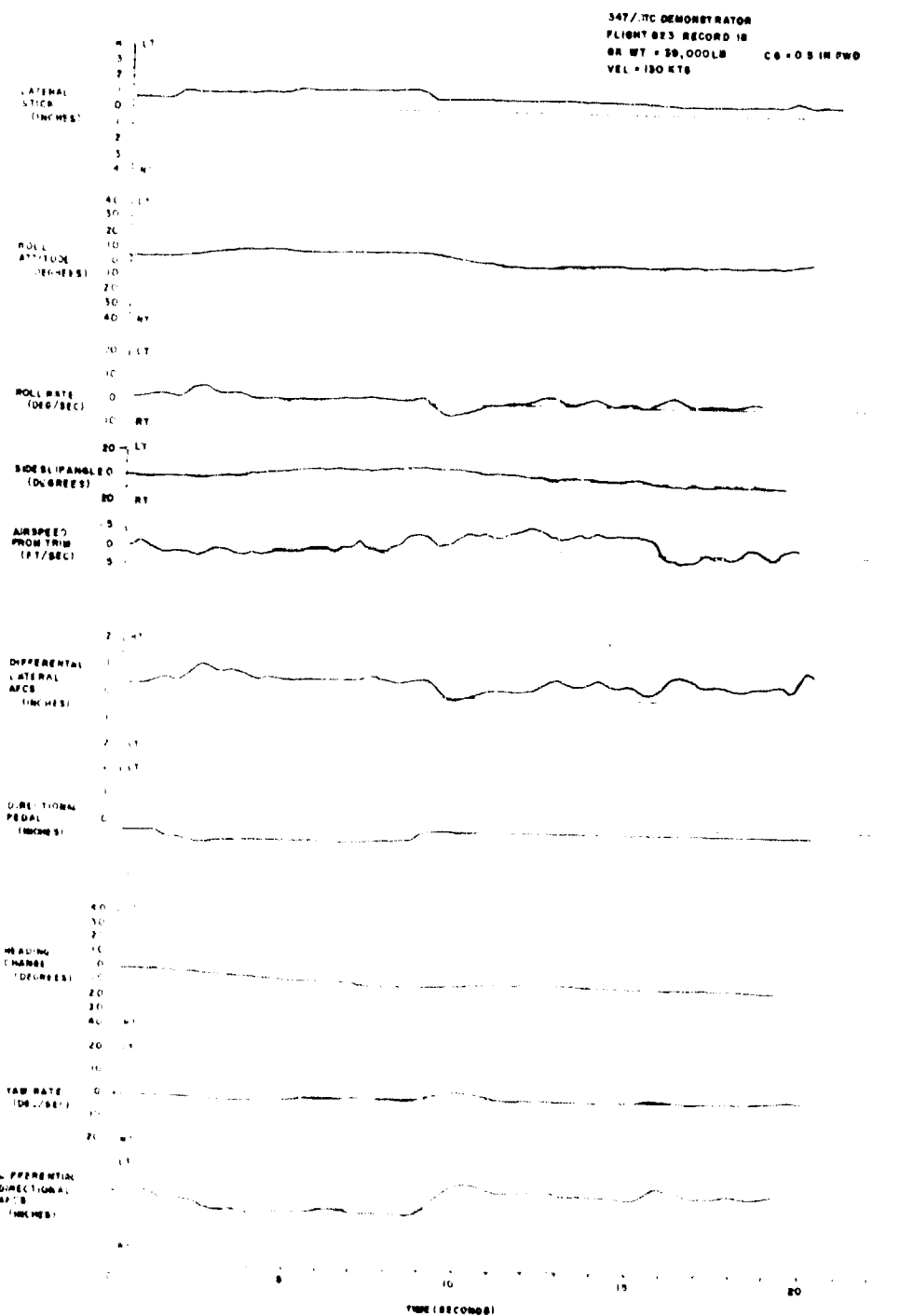
FIGURE 102 AIRCRAFT RESPONSE TO LATERAL DIRECTIONAL STEP · BASIC SCAS — 130 KNOTS
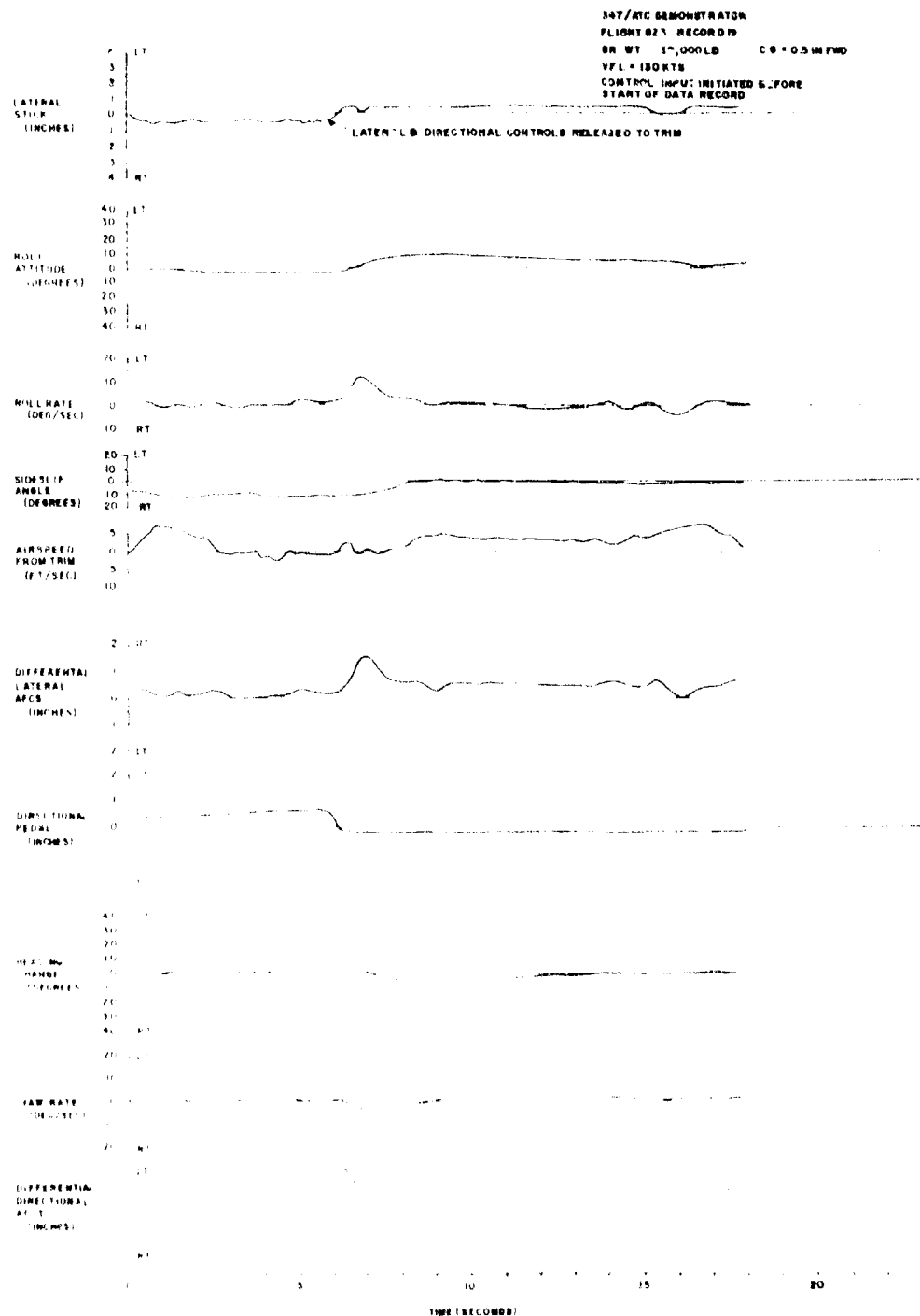
FIGURE 155 AIRCRAFT RESPONSE TO LATERAL DIRECTIONAL STEP BASIC SCAS — 130 KNOTS

of collective was initially well damped, but the climb rate
would continually increase as acceleration was washed out.
The washout and lagged vertical acceleration loop was elimin-
ated during testing of Tape 1, thereby relying totally on the
basic aircraft damping.

5.3.1.2  Static Stability

Static longitudinal and lateral/directional tests were con-
ducted in level flight, turns, climbs, partial power descents,
and autorotation.  Control trim gradients and groundspeed,
airspeed, bank angle, and heading hold characteristics were
assessed.

Longitudinal, lateral and directional control gradient augmen-
tation performed very satisfactorily.  Trim control variations
with speed were as predicted.  No significant lateral-direct-
ional inputs are required.  As examples, a longitudinal
acceleration from hover and deceleration back to hover is
shown in Figure 154.

Airspeed hold above 100 knots was excellent (A-1) in both
stabilized and maneuvering flight.  Airspeed recovery was
evaluated by inputting a differential longitudinal step as
illustrated in Figures 155 and 156 at 130 knots and Figures
157 and 158 at 60 knots.  The high static airspeed gain is
observed wherein only 5 knots of airspeed resulted from the
1-in. differential step.  Airspeed recovery for manual step and
return inputs shown in Figures 159, 160, and 161 exhibit similar
good recovery.  Airspeed hold during turn entry and recovery
is presented in Figures 162 and 163.  Approximately 10 knots
were gained in a right turn and 6 knots lost in a left turn.

In turn maneuvers at slow to moderate speeds (50-80 knots)
airspeed hold was poorer (A-4).  Airspeed increased 15 to
20 knots in right turns and decreased slightly in left turns,
as shown in Figures 164 and 165.

Similar maneuvers presenting the longitudinal axis parameters
are shown in Figures 166 and 167.  Right lateral inputs
create a nosedown basic aircraft moment requiring aft
longitudinal to trim out.  With contols fixed, airspeed
increases to supply this aft trim requirement.  A bank angle
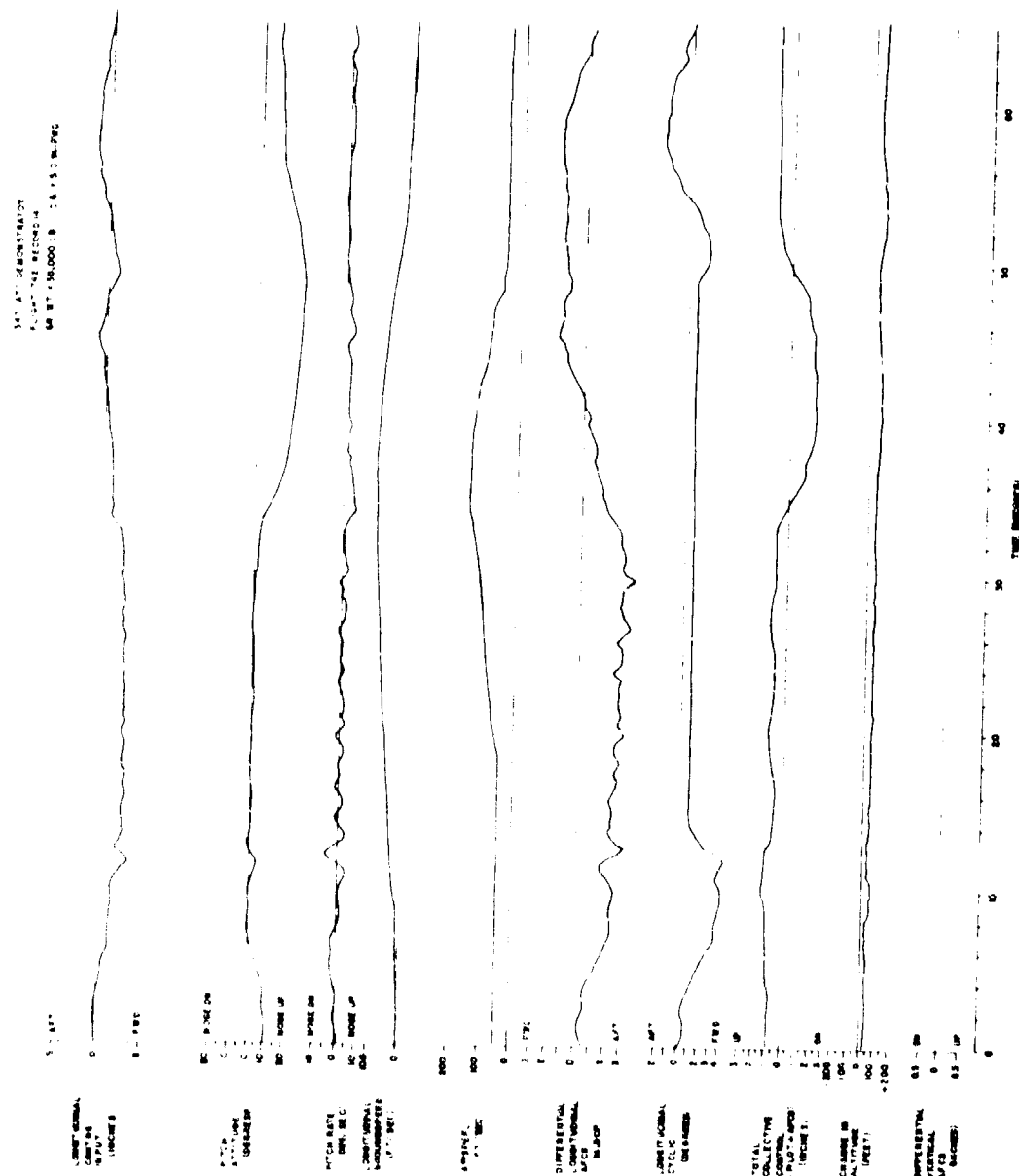
FIGURE B4. (SHEET I)
LONGITUDINAL ACCELERATION & DECELERATION

469
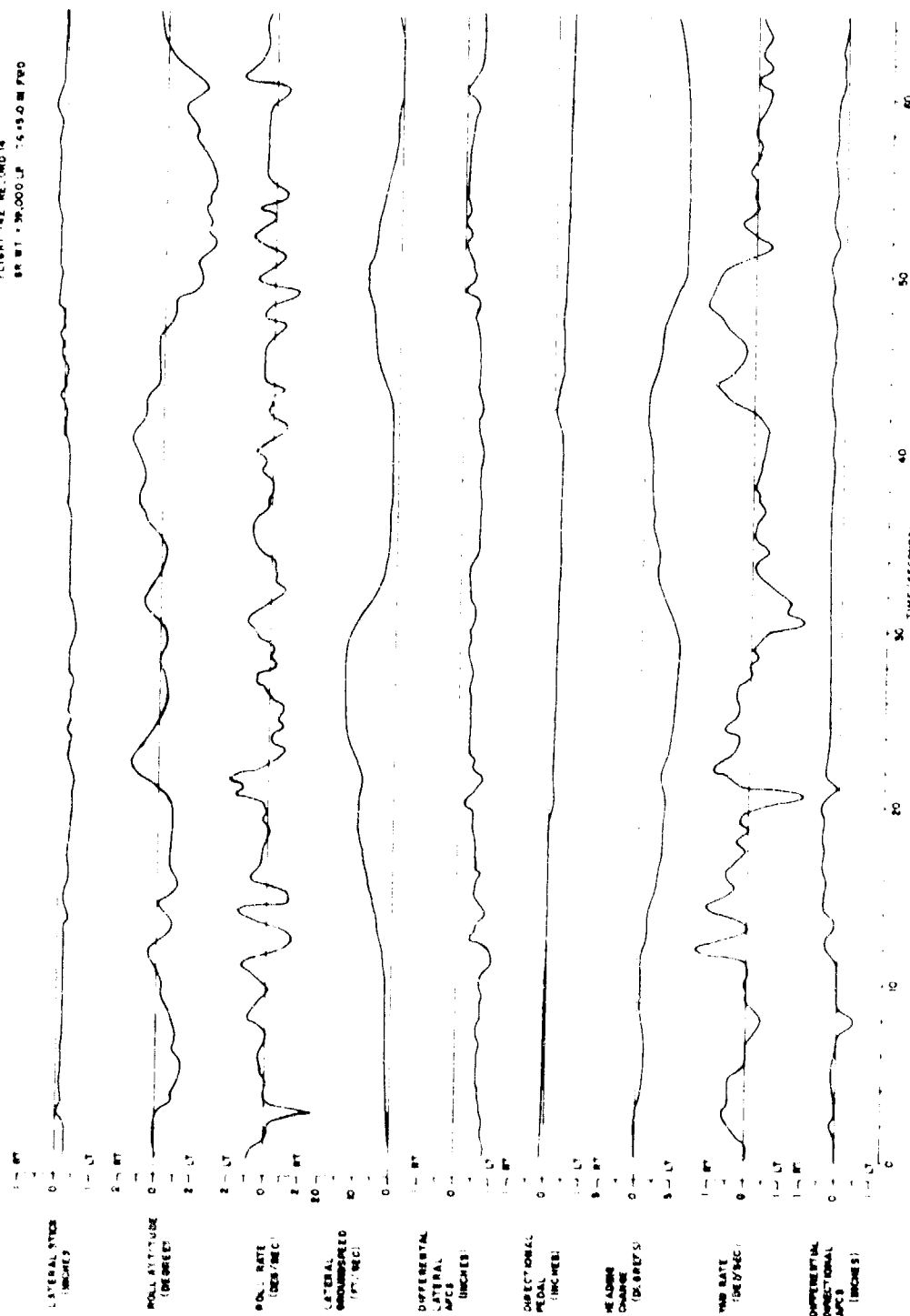
FIGURE 154. (SHEET 2)
LONGITUDINAL ACCELERATION & DECELERATION

FIGURE 155 AIRCRAFT RESPONSE TO LONGITUDINAL DIFFERENTIAL STEP BASIC SCAS — 130 KNOTS

471
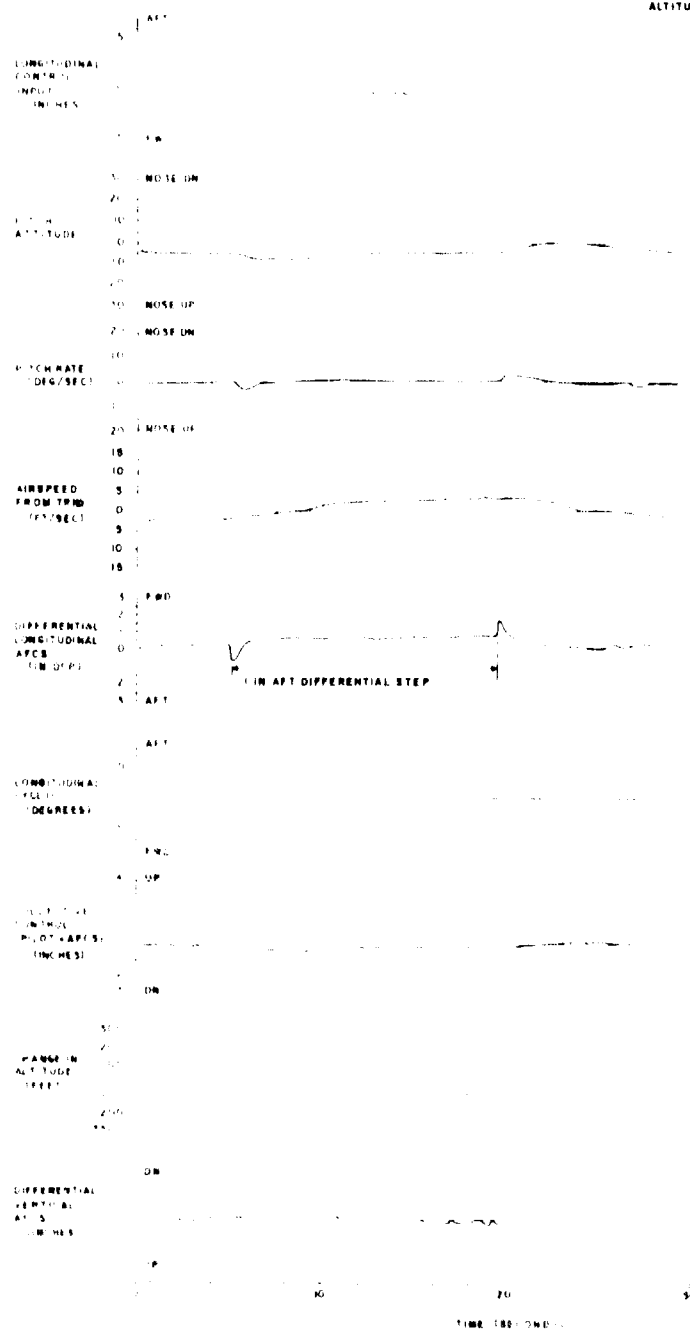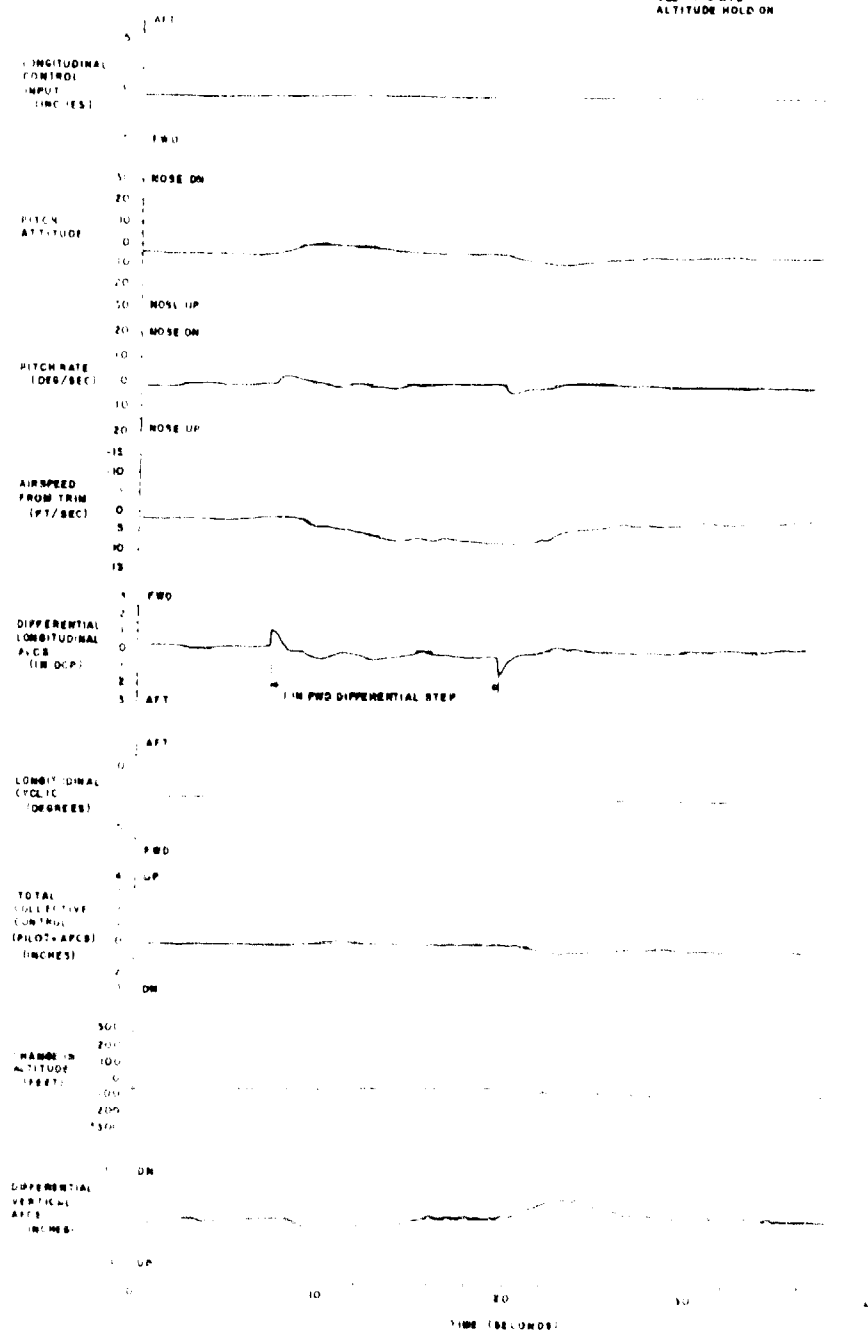
FIGURE 156   AIRCRAFT RESPONSE TO LONGITUDINAL DIFFERENTIAL STEP  BASIC SCAS — 130 KNOTS

472
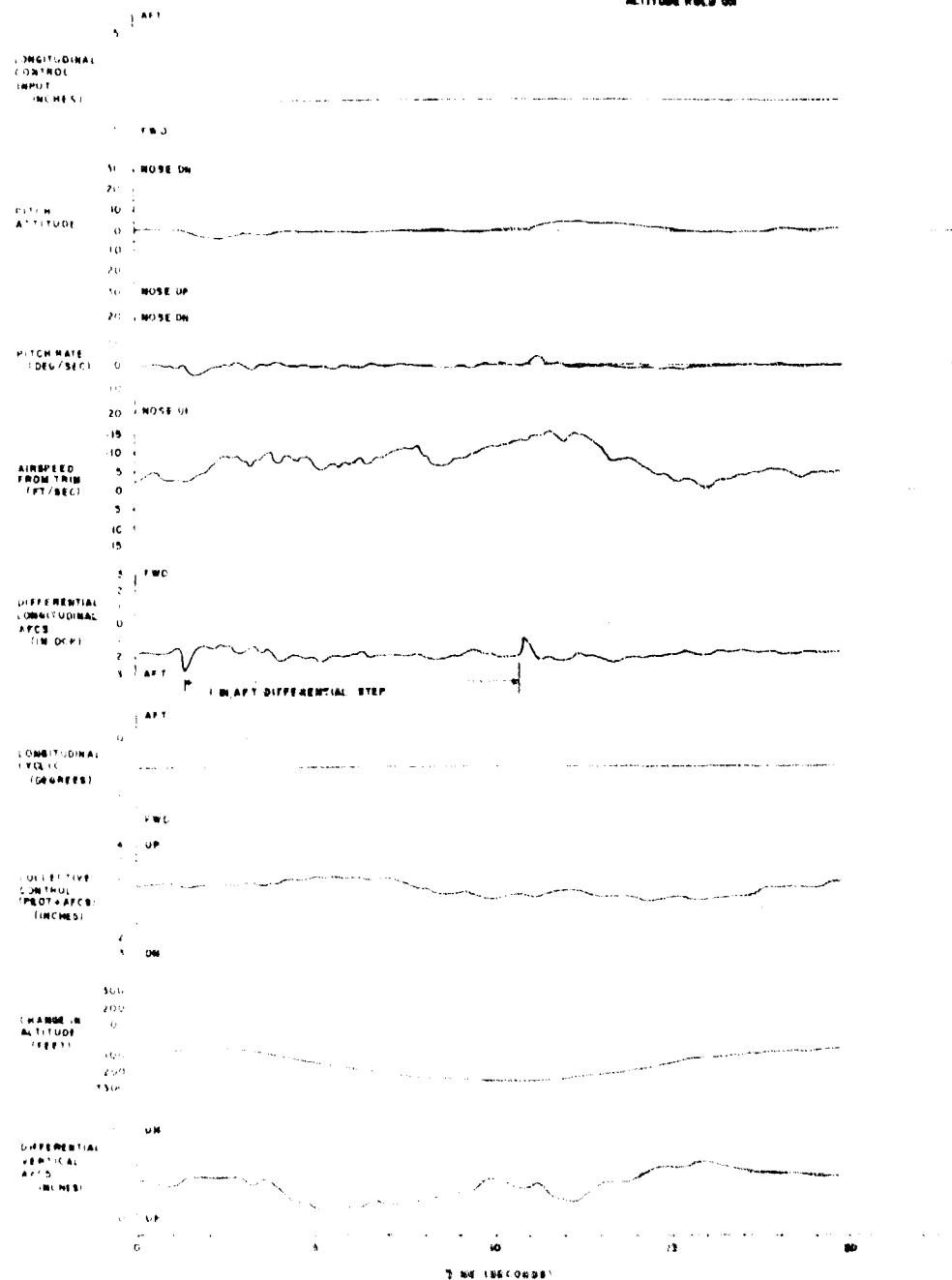
FIGURE 157   AIRCRAFT RESPONSE TO LONGITUDINAL DIFFERENTIAL STEP - BASIC SCAS  —  60 KNOTS

473

FIGURE 58  AIRCRAFT RESPONSE - LONGITUDINAL DIFFERENTIAL STEP  BASIC SCAS  —  60  KNOTS

FIGURE 96. AIRCRAFT RESPONSE TO LONGITUDINAL PILOT STEP & BEYOND — 130 KNOTS
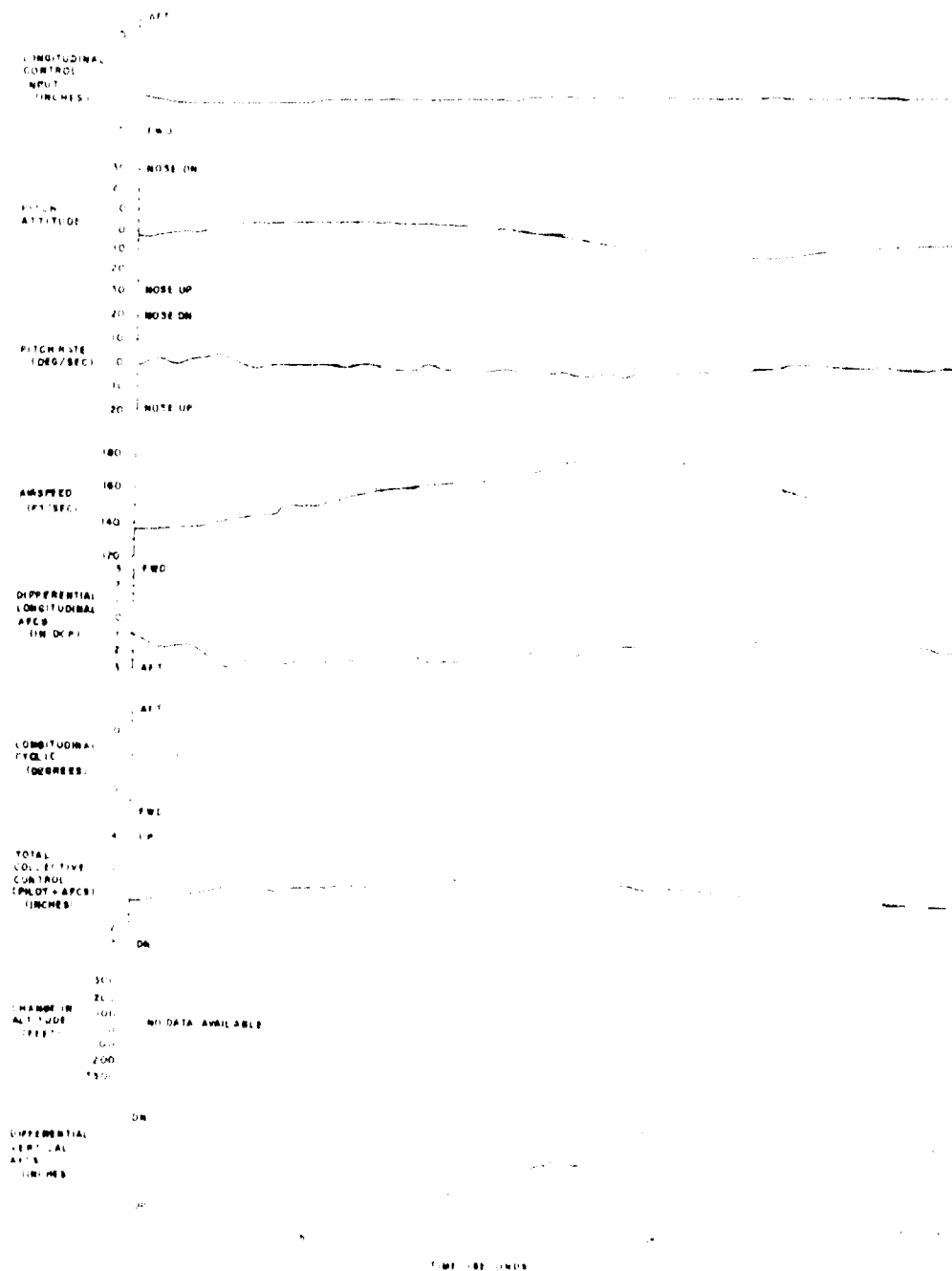
FIGURE 160. AIRCRAFT RESPONSE TO LONGITUDINAL PILOT STEP & RETURN — 80 KNOTS
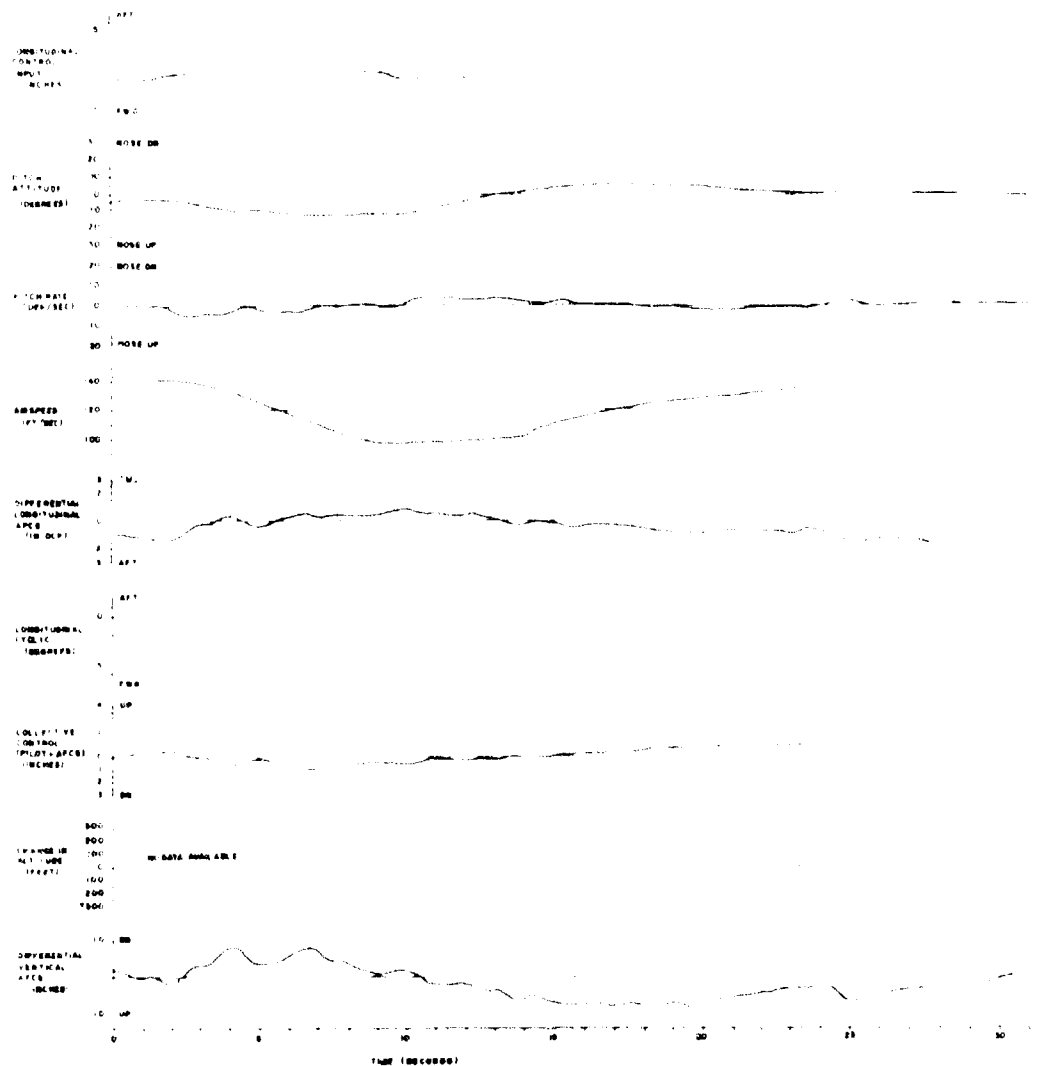
FIGURE 181  AIRCRAFT RESPONSE TO LONGITUDINAL PILOT STEP & RETURN — 80 KNOTS

477
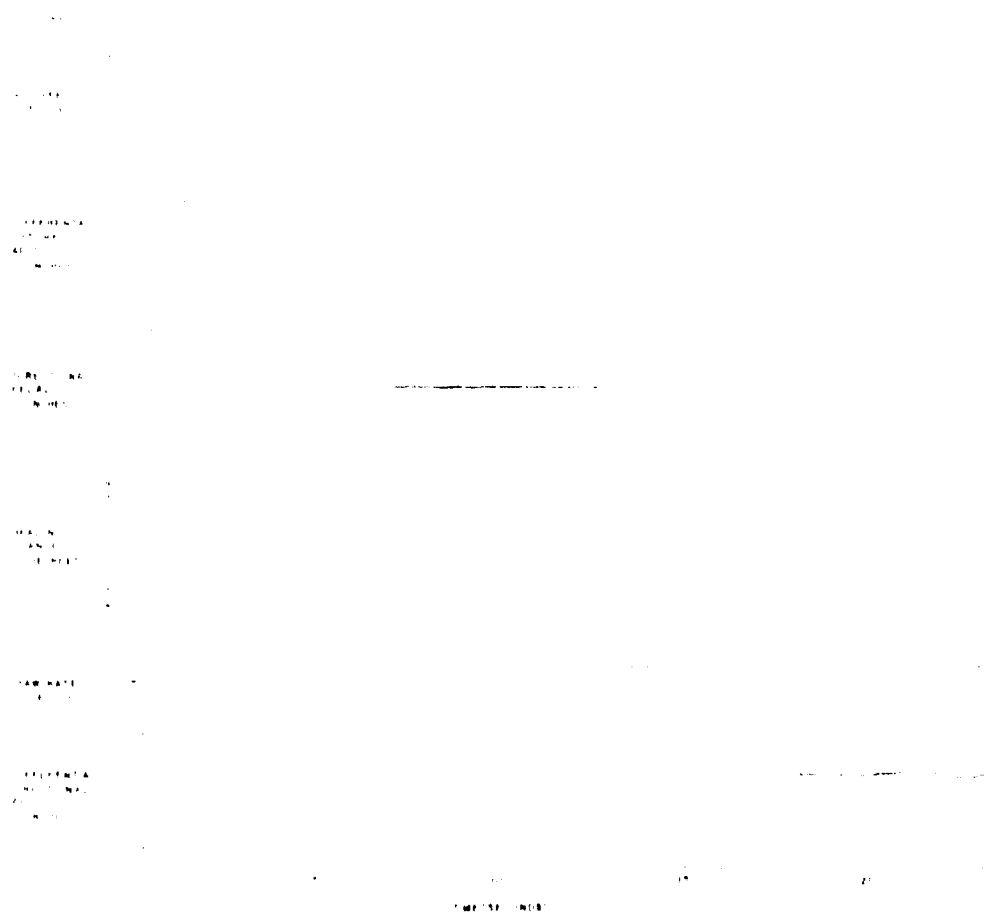
FIGURE 162  AIRCRAFT RESPONSE DURING LEFT TURN MANEUVER — 130 KNOTS
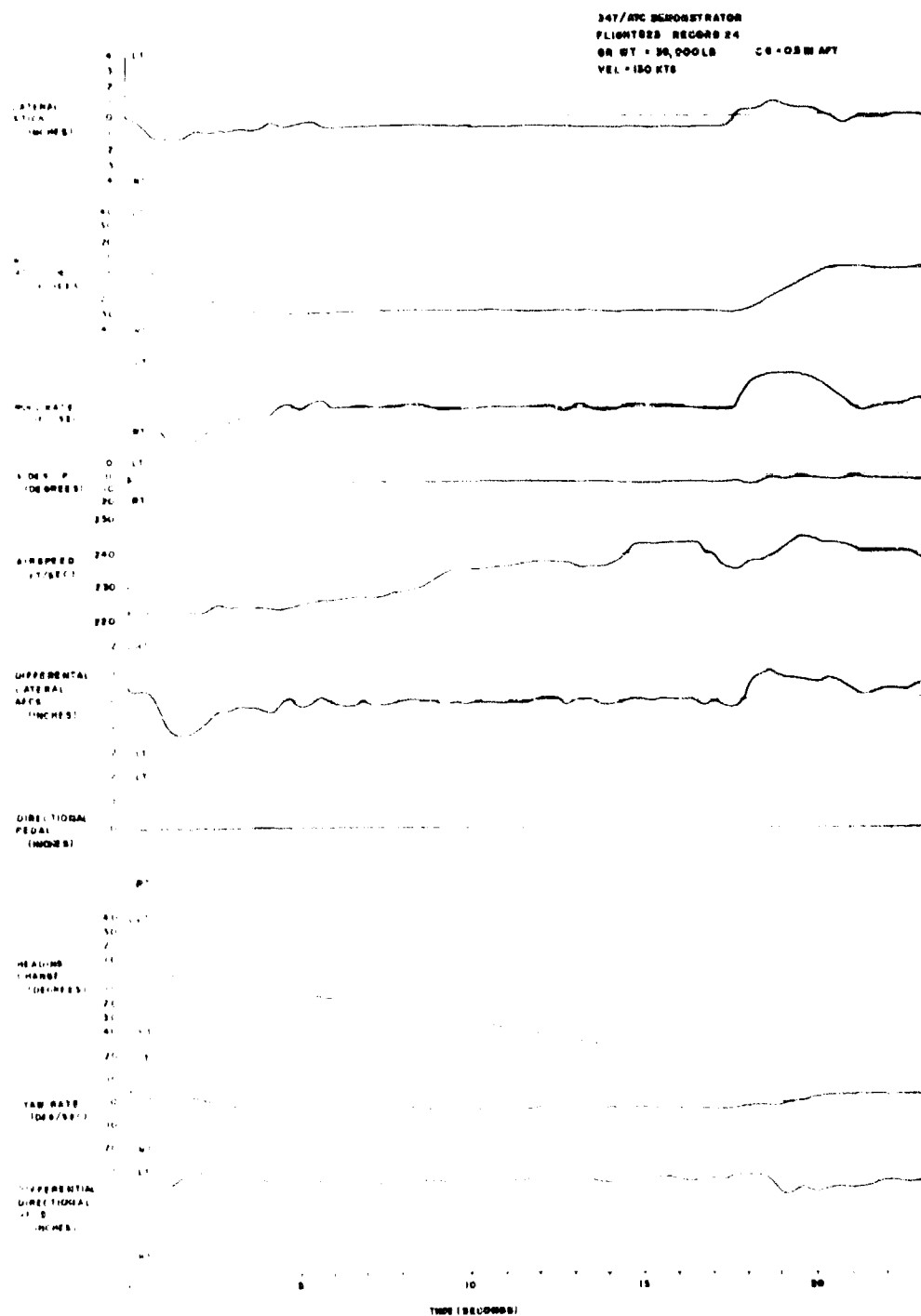
FIGURE 163  AIRCRAFT RESPONSE DURING RIGHT TURN MANEUVER — 130 KNOTS

479
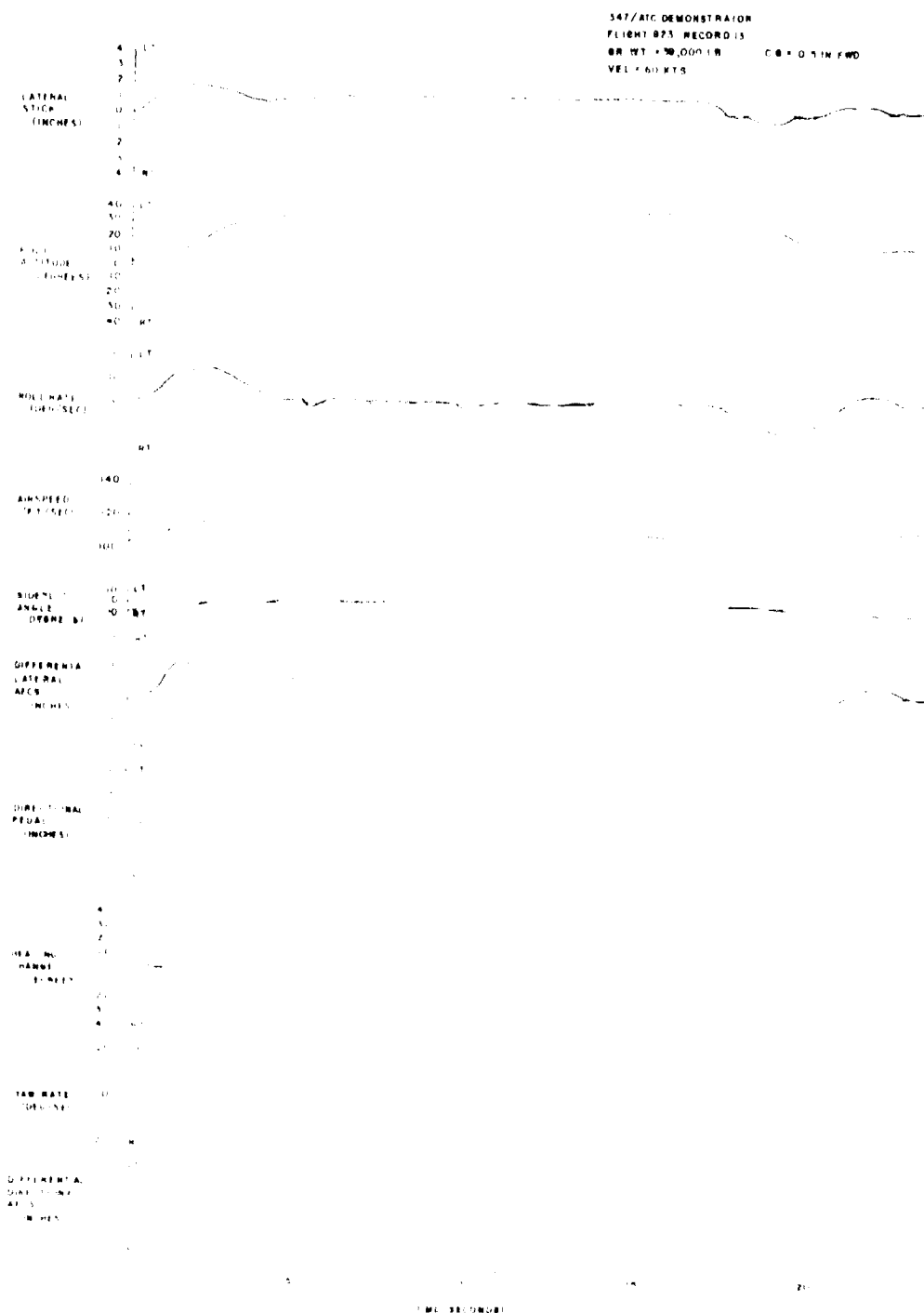
FIGURE 164  AIRCRAFT RESPONSE DURING TURN MANEUVER — 60 KNOTS
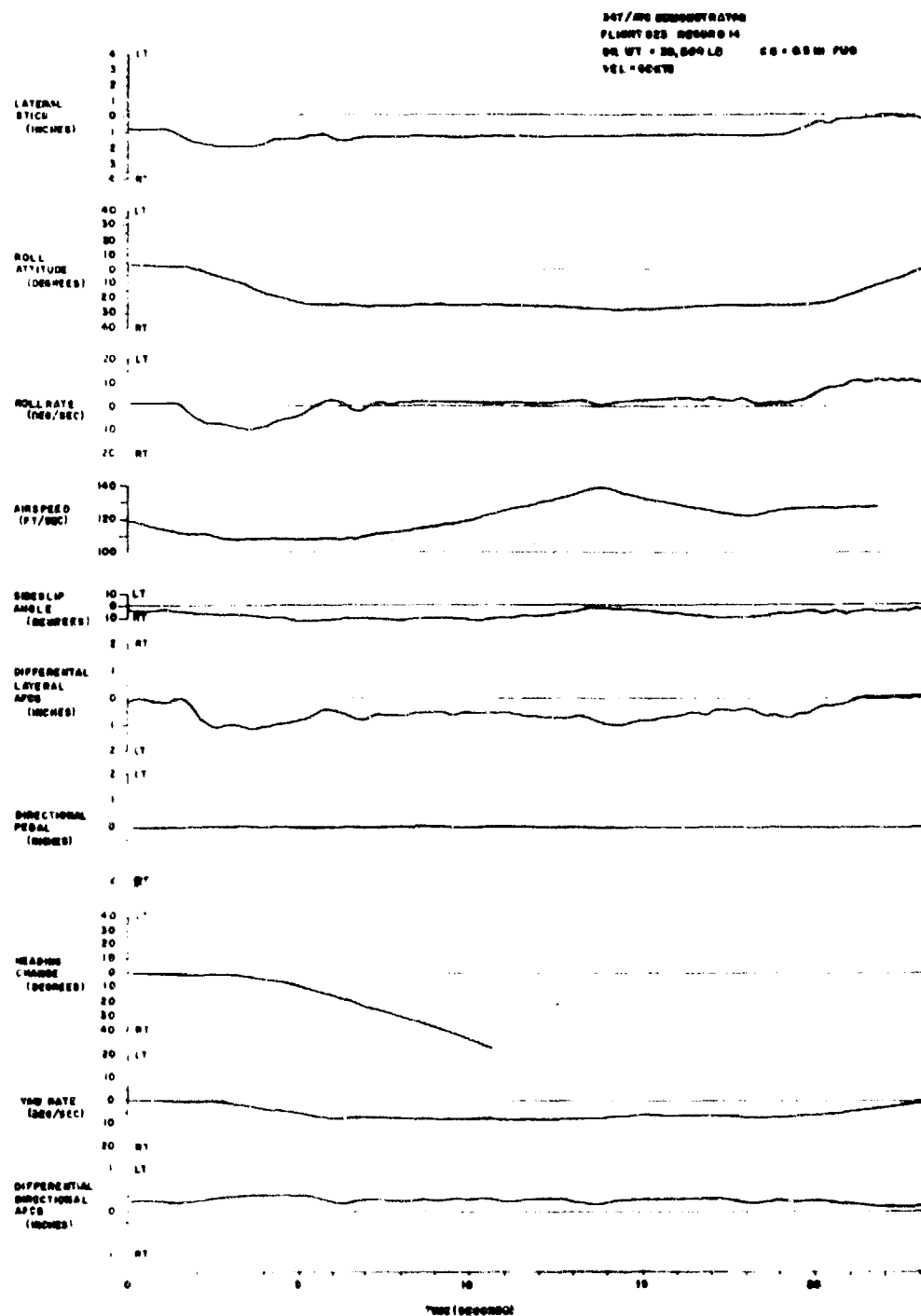
FIGURE 166    AIRCRAFT RESPONSE DURING TURN MANEUVER — 60 KNOTS

481
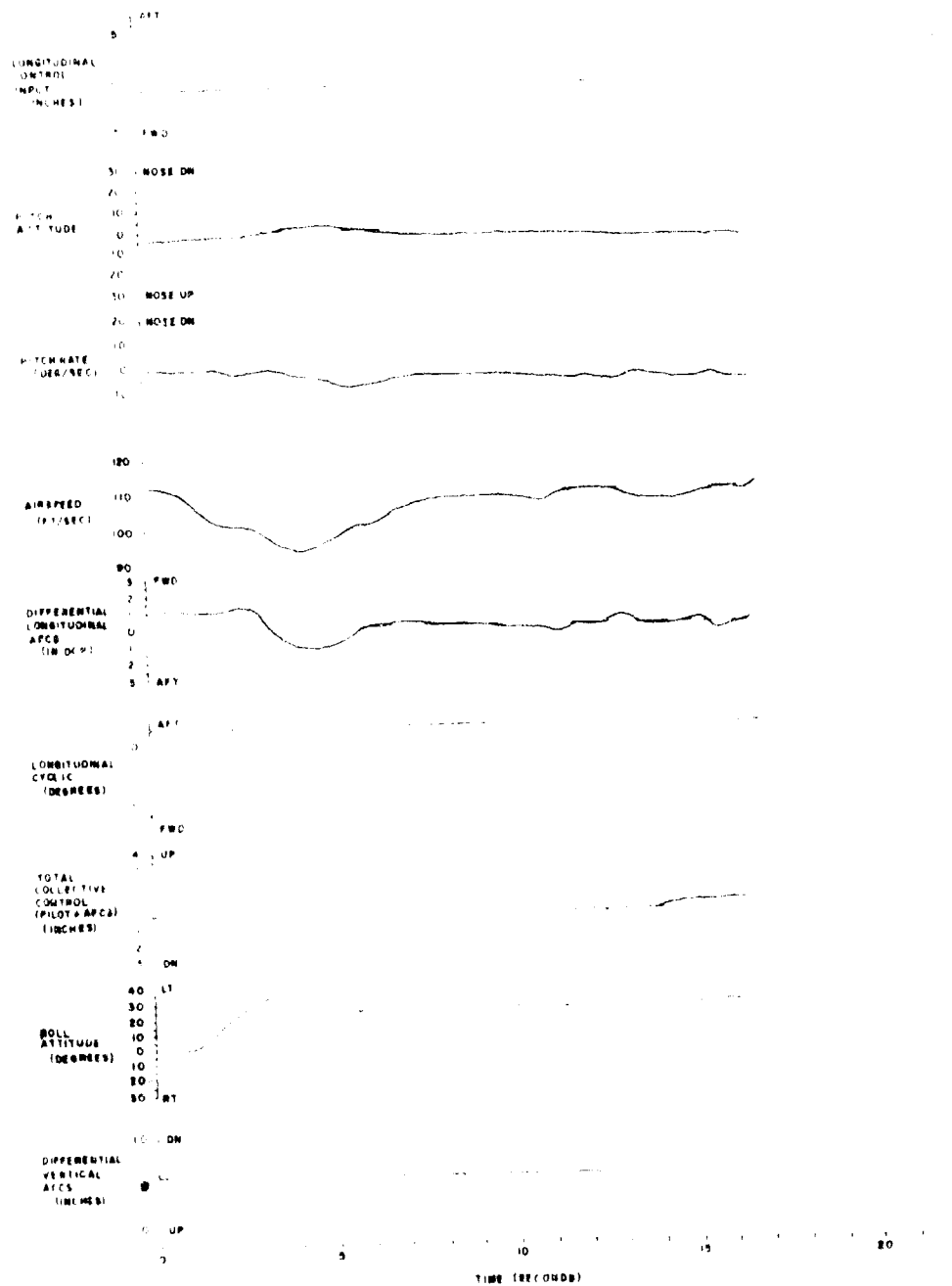
FIGURE 166. AIRSPEED HOLD IN BANK TURN -- 60 KNOTS

482
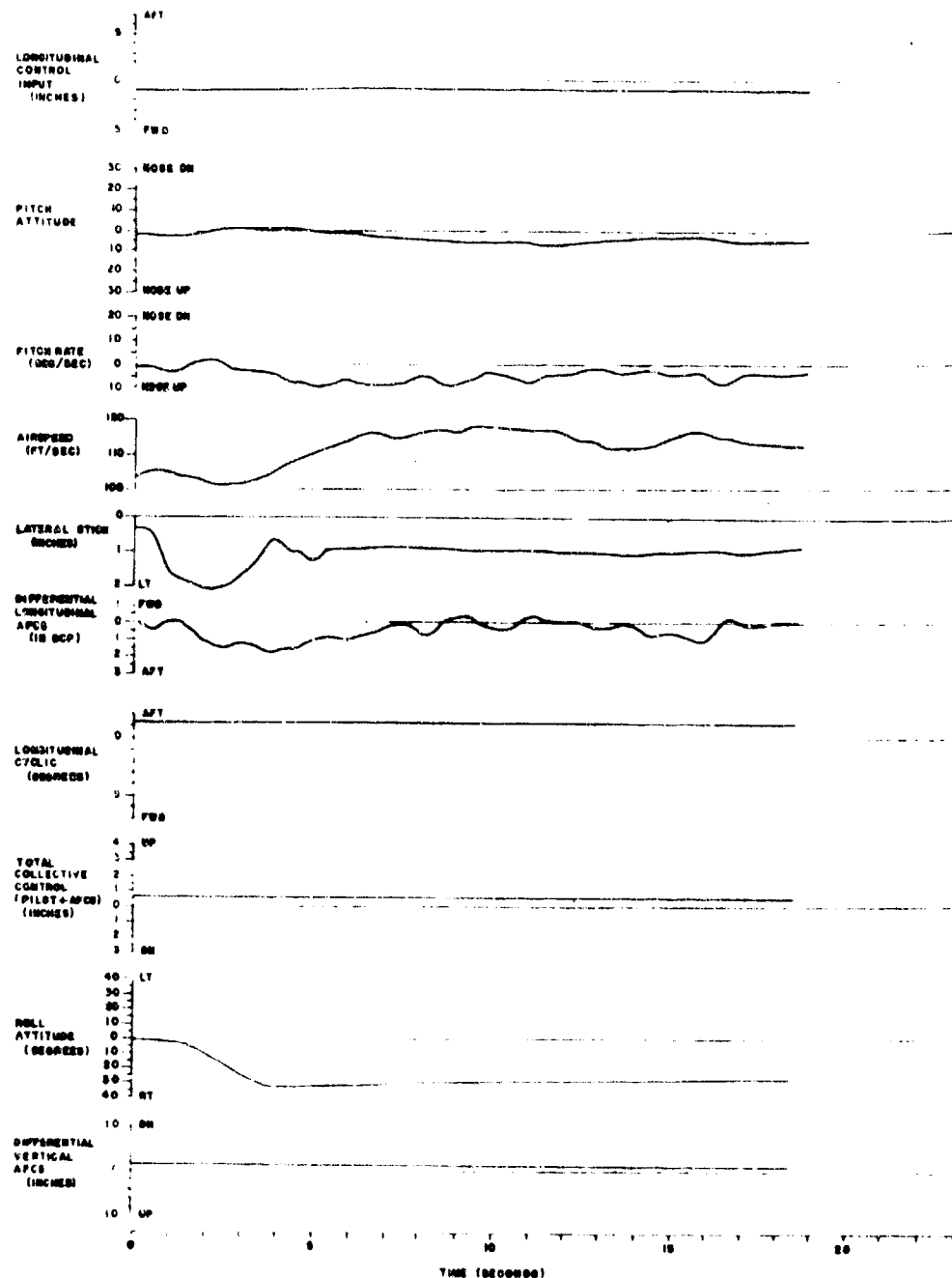
FIGURE 187. AIR SPEED HOLD IN BANK TURN — 60 KNOTS

crossfeed into the longitudinal AFCS was programmed to improve
this on an experimental basis. Initial pitch motion
was suppressed indicating that this approach would work.

However, a washout was in the program causing the airspeed
gain to eventually result.

RECOMMENDATION

Airspeed Hold in Turns (60 to 80 Knots) - Incorporate a bank
angle crossfeed into the longitudinal axis, scheduled with
airspeed to compensate for airspeed deviations.

The simulator-defined airspeed gain was increased in the
flight program by 32 percent between 45 and 120 knots, and by
22 percent at higher speeds.

Groundspeed Hold below 45 knots was acceptable for normal
hover and low speed maneuvering (A-3). The velocity feedback
gains were too low and stick gradients too high, however, to
enable the pilot to precisely acquire and maintain a zero
velocity trim for holding position during cargo operations
(A-4). This was anticipated from earlier simulation studies -
Section 2.1.3.1.3. The longitudinal groundspeed gain was
increased by 60 percent and lateral pickoff gain was reduced by
50 percent during the flight testing to reduce longitudiral con-
trol sensitivity to 80 ft/sec/in. from 130 ft/sec/in. and lateral
sensitivity to 50 ft/sec/in. from 90 ft/sec/in. Trimmability im-
proved significantly. Further sensitivity test reductions proved
increasingly beneficial. However, the higher hover hold gains
(6 x Basic SCAS) and very low sensitivities (1/25th of Basic
SCAS) proved near optimum for meeting these requirements.
Primary control sensitivity shaping, as suggested in Section
2.1.3.1.3, is required to provide this and was not success-
fully developed by analysis in the time available. An alternate
solution is recommended for the HLH.

RECOMMENDATION

Pilot Control in Hover Hold Mode - Provide the pilot a vernier
velocity control capability through stick beep trim when the
hover hold mode is engaged. In addition, incorporate a pilot
override capability of any individual axis when on hover hold.
This permits larger position change maneuvers on Basic SCAS
without disengaging all hover hold axes.

Bank angle and heading hold stability was satisfactory over the complete envelope (A1.5).

5.3.1.3 Controllability

Aircraft response to primary control and beep trim inputs was evaluated during hover, transition, and forward flight. Approach and departure maneuvers, including roll-on landings and running takeoffs, were conducted.

"Beep" trim was acceptable in longitudinal and lateral control (A1 to 1.5); however, the desirability of a variable rate beep trim control in lieu of fixed rate control was indicated. The present compromised gain is too high for vernier beep inputs in hover, and too low for "beep and hold" inputs used to change speed or conduct turn maneuver in cruise. Directional beep trim control operated acceptably. It was judged to be unnecessary in the Model 347 aircraft due to good pedal control characteristics of the augmented aircraft. Note that the lateral beep in forward flight is initially parallel, reflecting the limited bank angle lateral stick gradient, and then differential.

Maneuverability characteristics demonstrated in longitudinal accelerations and decelerations, pedal fixed coordinated turns, and sideslips, etc., were excellent (A1 to 1.5).

Data from a longitudinal acceleration between hover and 80 knots, and deceleration back to hover, Figure 154, demonstrates low control activity requirement.

A significant problem occurred during level flight rapid deceleration maneuvers using high nose up attitudes. The AFCS/DELS interface authority was bottomed at approximately 30 knots and required pilot stability inputs to complete the maneuver.

In the original simulator design, the attitude, velocity, and stick pickoff summation was limited to 2-1/2 inches of equivalent forward stick, which is the same limit as existed in the DELS interface. As the aircraft decelerated through 30 knots, more than 2-1/2 inches of forward AFCS was required to maintain pitch attitude and the pilot had to come forward

485

with the control. This is caused by rotor interference. The combined effect of high nose-up attitude and stick pickoff saturated the AFCS authority. As the aircraft further decelerates, the rotor interference subsides and the aircraft rapidly pitches down. Pitch damping augmentation was not immediately available as the AFCS output was saturated. A rapid aft pilot input was required to stabilize attitude. The system was modified allowing only 1-1/2 inches of authority to attitude, velocity and pickoff summation. This insured 1 inch of pitch rate damping authority available at all times but the resulting maneuver was satisfactory.

The high forward trim authority requirement prohibited a hands-off rapid deceleration and represented a change in handling qualities through this regime.

RECOMMENDATION

Hands-off Steep Flare Controllability - Incorporate a parallel stick backdrive command to provide additional attitude stabilization when the AFCS/DELS interface is approaching saturation.

The limited bank angle lateral stick gradient (security blanket) offered improved trimmability about zero bank angle, as well as a control-free return to "wing level" trim. Security blanket "return to wing level" operation is seen in Figures 168 and 169 and 170 and 171 for 60 and 130 knots. The simulator-defined limited attitude limiter was symmetric, using ±0.5 in. for 10 degrees of bank angle. This was first changed ±0.5 in. for 5 degrees of bank to provide a more rapid rollout. In addition, the basic aircraft required approximately 0.1 in. of left lateral control to stabilize in a left or right bank. This resulted in a trim requirement of 0.6 in. for left turns and 0.4 in. for right turns. Release of controls caused a slower rollout from the right. The attitude limiter was then made assymetric; 0.5 in. of equivalent right stick (left turns) and 0.675 degree of equivalent left stick (right turns) to balance rollout rate.

The forward-flight turn maneuvers are accomplished with cyclic stick only. (Note Figures 168-171). Pedal inputs are not required for turn coordination. Forward flight pedal responses are predominately sideslip as shown earlier in 5.3.1.1.
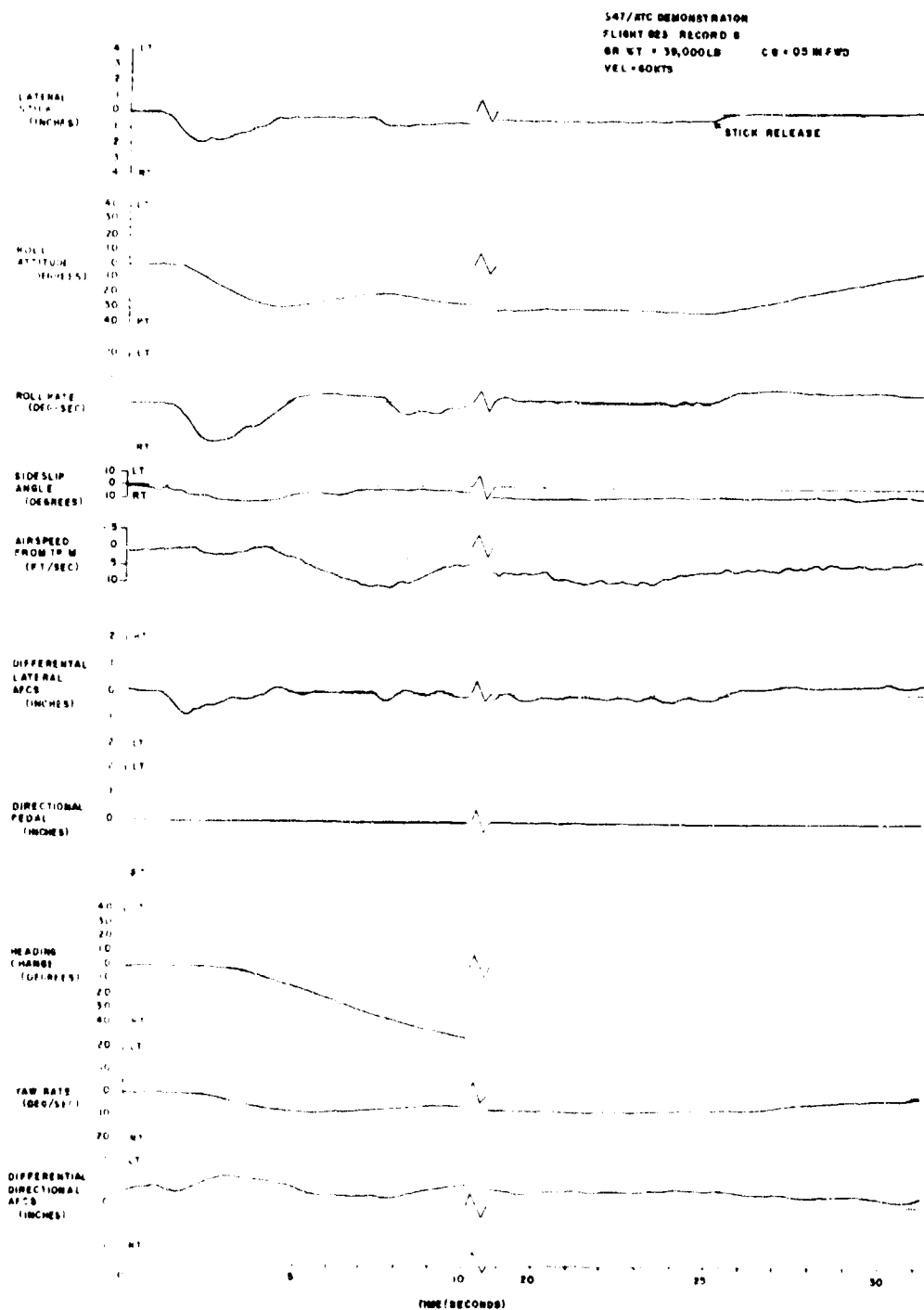
486

FIGURE 188 AIRCRAFT RESPONSE TO LATERAL PILOT INPUT & RETURN —
SECURITY BLANKET · BASIC SCAS — 60 KNOTS

487
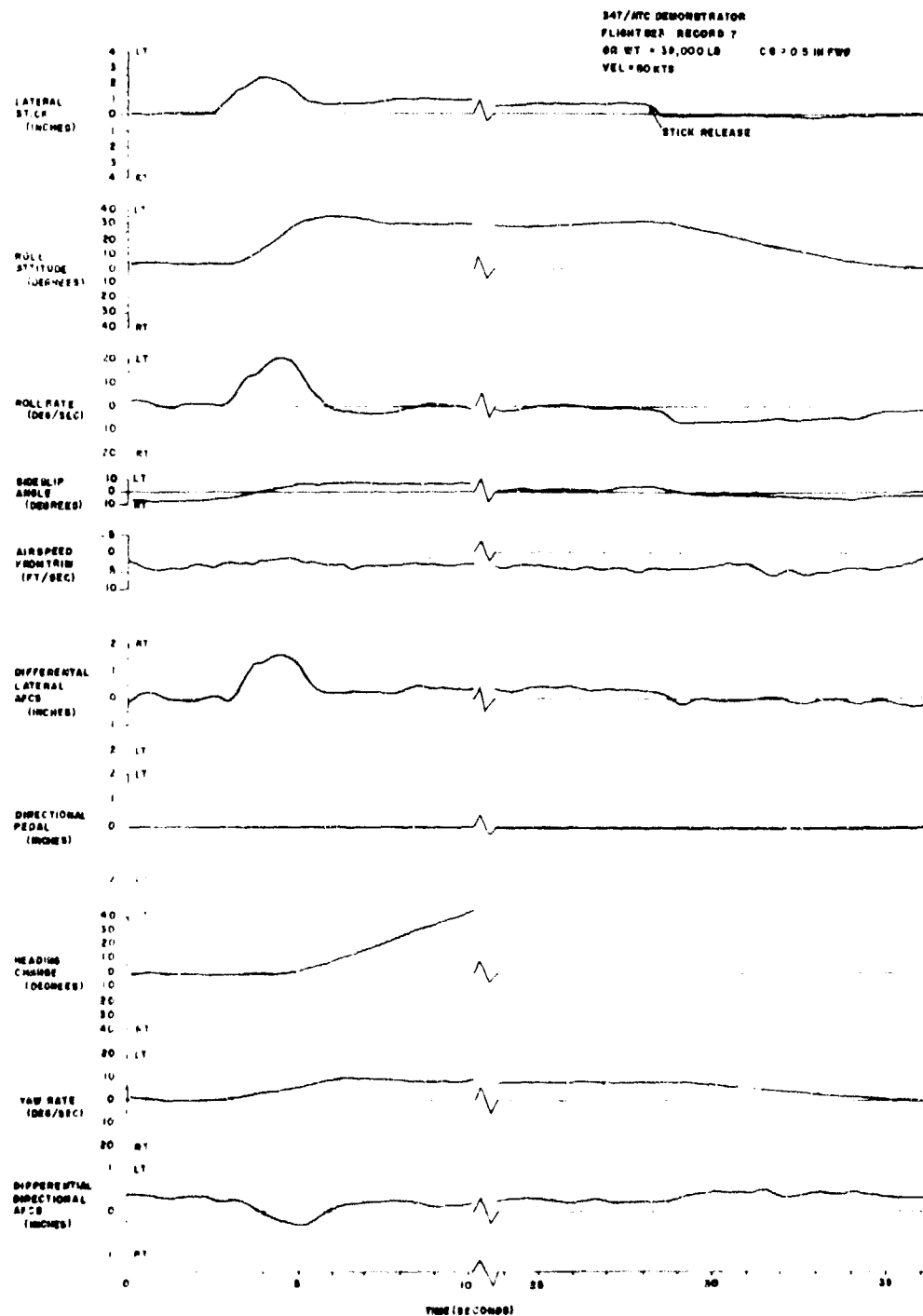
FIGURE 188. AIRCRAFT RESPONSE TO LATERAL PILOT INPUT & RETURN-
SECURITY BLANKET - BASIC SCAS - 60 KNOTS
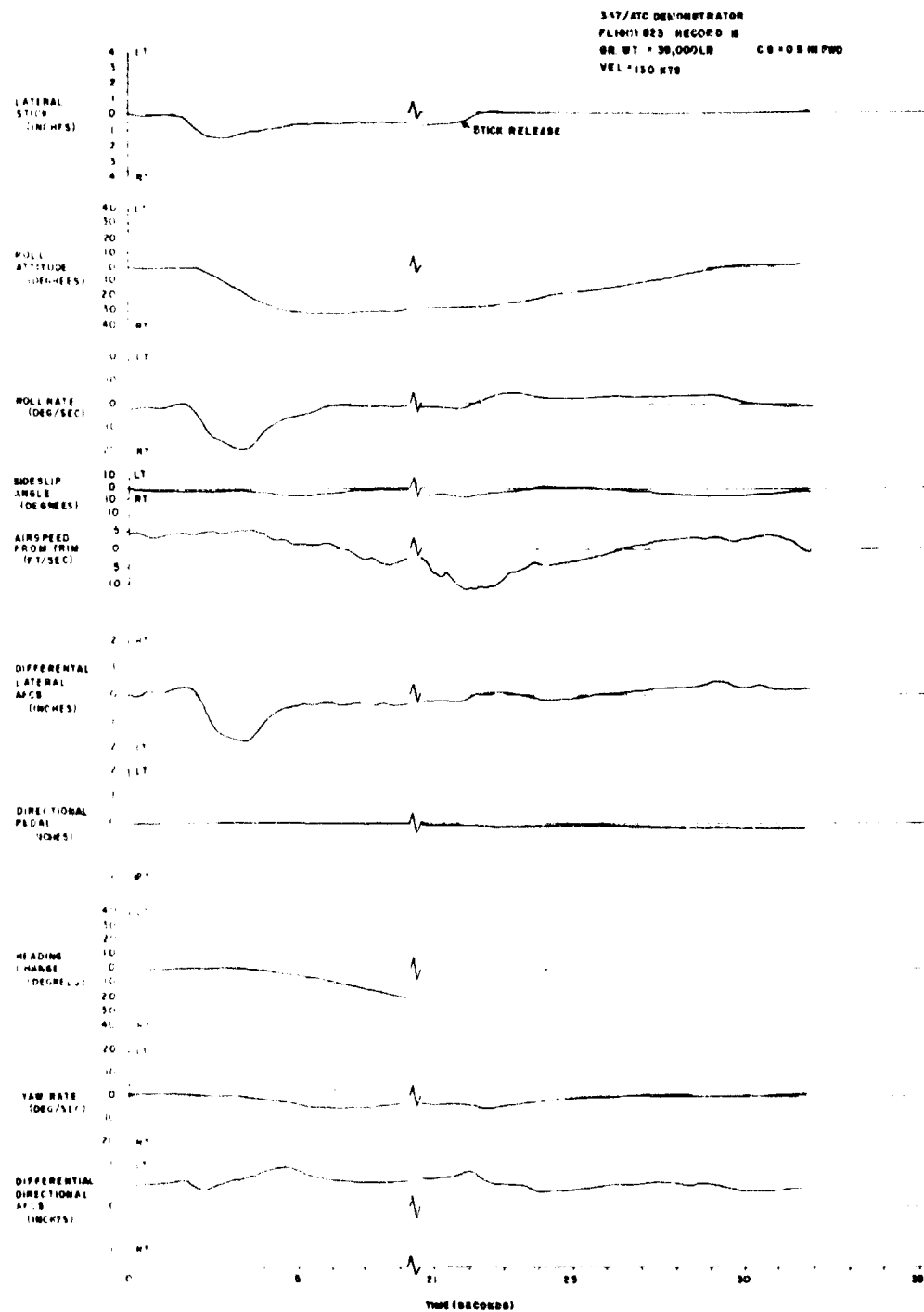
FIGURE 170 AIRCRAFT RESPONSE TO LATERAL PILOT INPUT & RETURN
SECURITY BLANKET - BASIC SCAS — 130 KNOTS
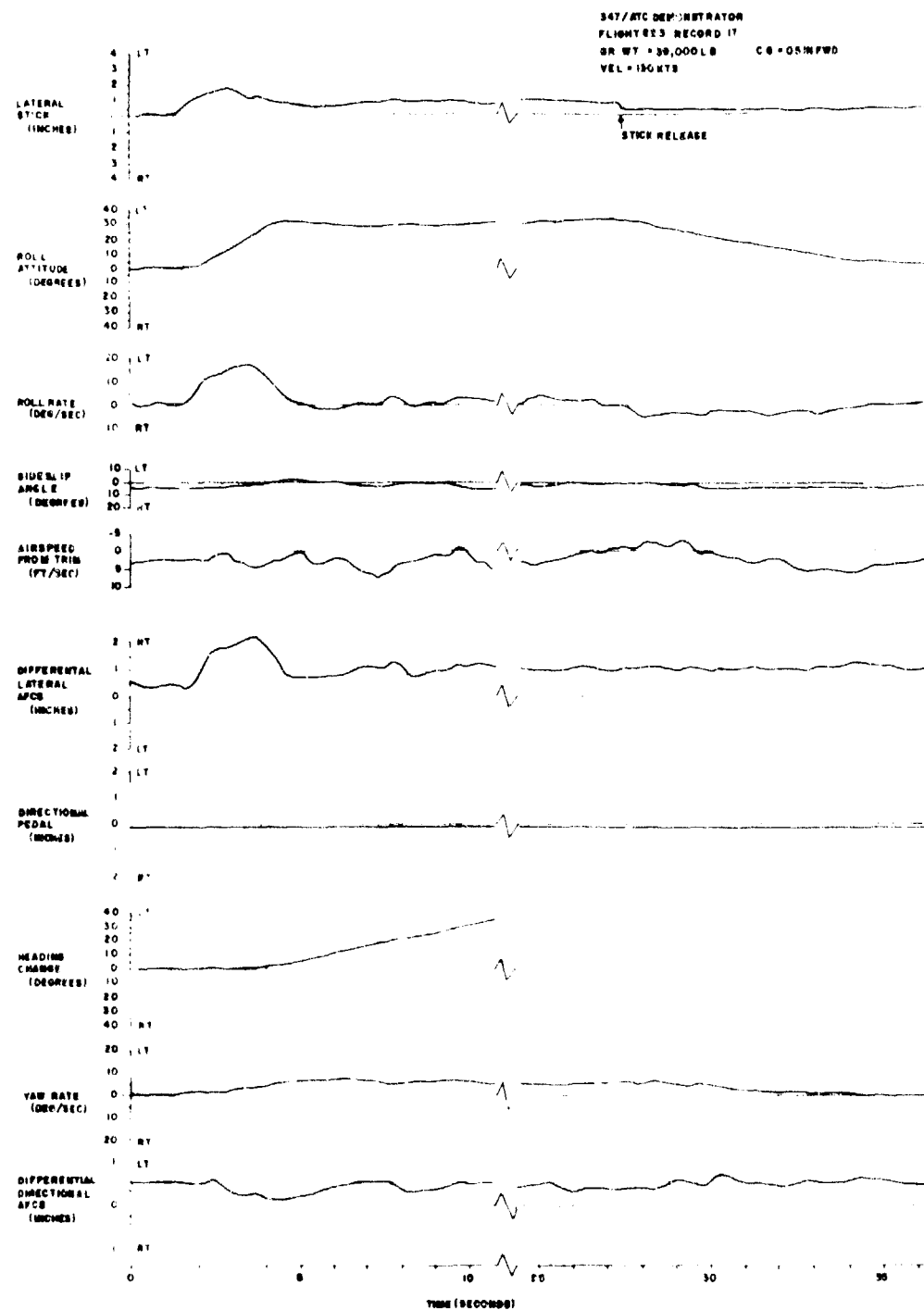
FIGURE 171. AIRCRAFT RESPONSE TO LATERAL PILOT INPUT & RETURN
SECURITY BLANKET - BASIC SCAS - 130 KNOTS

490

A pedal response in hover shows a rapid yaw rate rise time. When the ped. l is returned to trim, the aircraft slowly decelerates to zero yaw rate, wherein heading lock is engaged. The yaw rate feedback on SCAS was increased in flight to be compatible with that required for hover hold. This necessitated an increase in pedal pickoff gain to maintain yaw rate sensitivity.

Takeoff and landing maneuvers were accomplished routinely with no transients. The original landing logic switched the system into an airspeed mode upon touchdown, which created a bias error; the stick would trim forward if not constrained by the pilot. This was modified to eliminate mode transfer on touchdown (Section 2.1.3.1.4.)

5.3.1.4  Velocity Mode Transfer Switching

The automatic transfer between ground-referenced IMU velocities below 45 knots, and airspeed reference (or vice versa) was thoroughly checked by performing straight and turning acceleration and deceleration maneuvers in different effective wind conditions.

For most maneuvers, including combined longitudinal/lateral accelerations, velocity reference transfer was transient free and bias elimination through control backdrive generally went undetected by the pilot (A2 to 2.5). However, during accelerations wherein steep turns were initiated just prior to velocity reference switchover, the lateral bias magnitude was sufficiently large to exceed available AFCS/DELS authority limits, making retrim difficult (U-7). This problem is shown on Figure 172. Due to the lateral AFCS saturation (1-1/2 in.), the pilot must trim the aircraft out with 1-1/2 in. of pilot control in the opposite direction. However, the bank angle/ roll rate stabilization is ineffective as AFCS has bottomed. Thus, when bias elimination begins to occur, the stick is moved without compensating AFCS change and the aircraft rolls, requiring retrim. Eventually, the bias gets small enough to permit retrim with bank angle hold working and bias elimination proceeds normally.
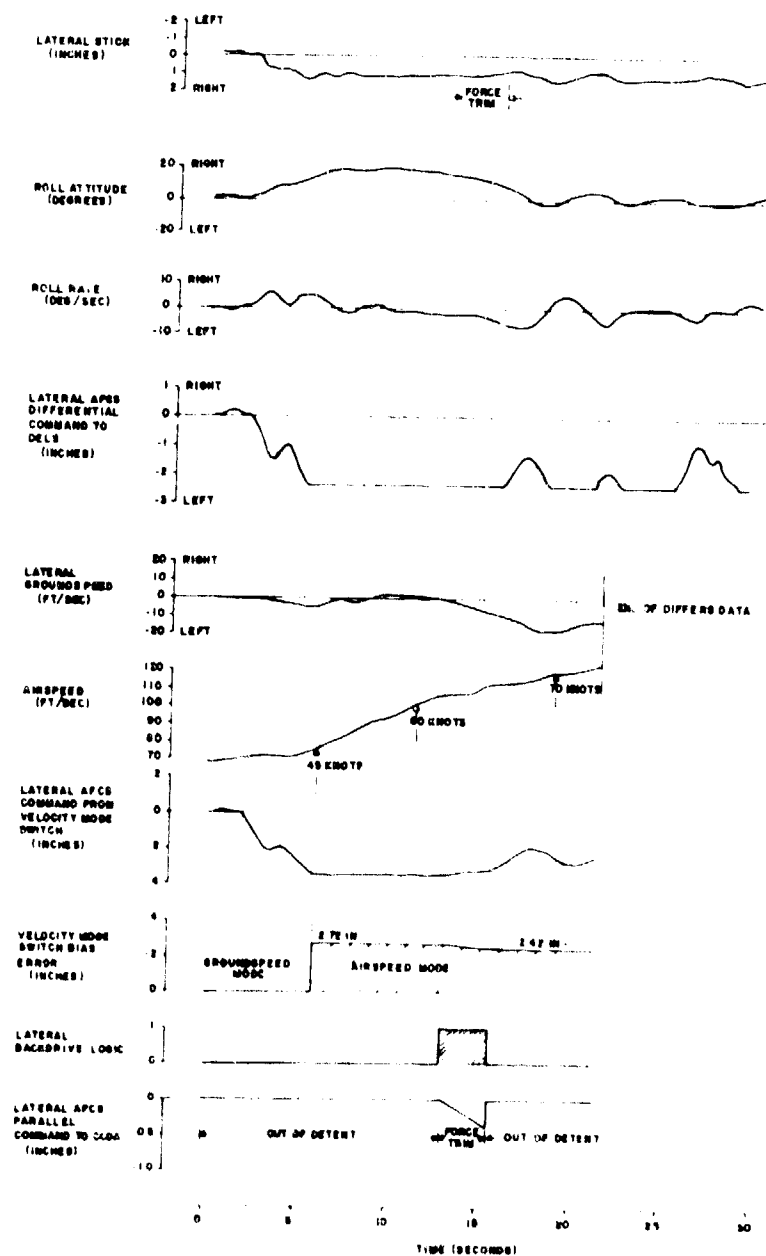
FIGURE 172.
VELOCITY MODE SWITCH DURING TURN MANEUVER - LATERAL AFCS SATURATION

492

RECOMMENDATION

Velocity Mode Transfer Switch - Incorporate a limit on the
output of the lateral velocity transfer switch to provide AFCS
control margin for damping. Revise logic to inhibit lateral
velocity mode transfer until bias magnitude is below a pre-
selected value.

5.3.1.5    Force Feel System

The 347 helicopter was equipped with a "fixed" control force-
feel system, consisting of breakout forces, linear gradients,
and viscous damping. Characteristics are plotted on Figure
173. In the ATC flight tests covering all areas of HLH flight
operations, there was no indication of any shortcoming in the
fixed force-feel system; nor did there appear to be much po-
tential for significant improvement in handling qualities
with a programmable force-feel system. The zero groundspeed
trimmability on Basic SCAS may benefit from force changes;
however, a much better capability will be provided through
the hover hold mode.

RECOMMENDATION

Force-Feel System - Eliminate programmable force feel from the
HLH requirements.

5.3.2    Altitude Hold

5.3.2.1    Barometric Reference

Reasonable altitude hold characteristics were realized on
barometric reference (A-2). During level flight, altitude
was held to within ±10 feet, as shown in a typical 60-knot
time history in Figure 174. Also evident in the figure are
small continuously varying collective changes to maintain
altitude in turbulent air. These, together with associated
power fluctuations, were very undesirable.

RECOMMENDATION

Provide barometric altitude hold in cruise through the longi-
tudinal AFCS by programming small attitude and airspeed
corrections, and retain collective pitch programming for
long-term trimming only.

493

FIGURE 173. 347/ATC DEMONSTRATOR FORCE-FEEL CHARACTERISTICS
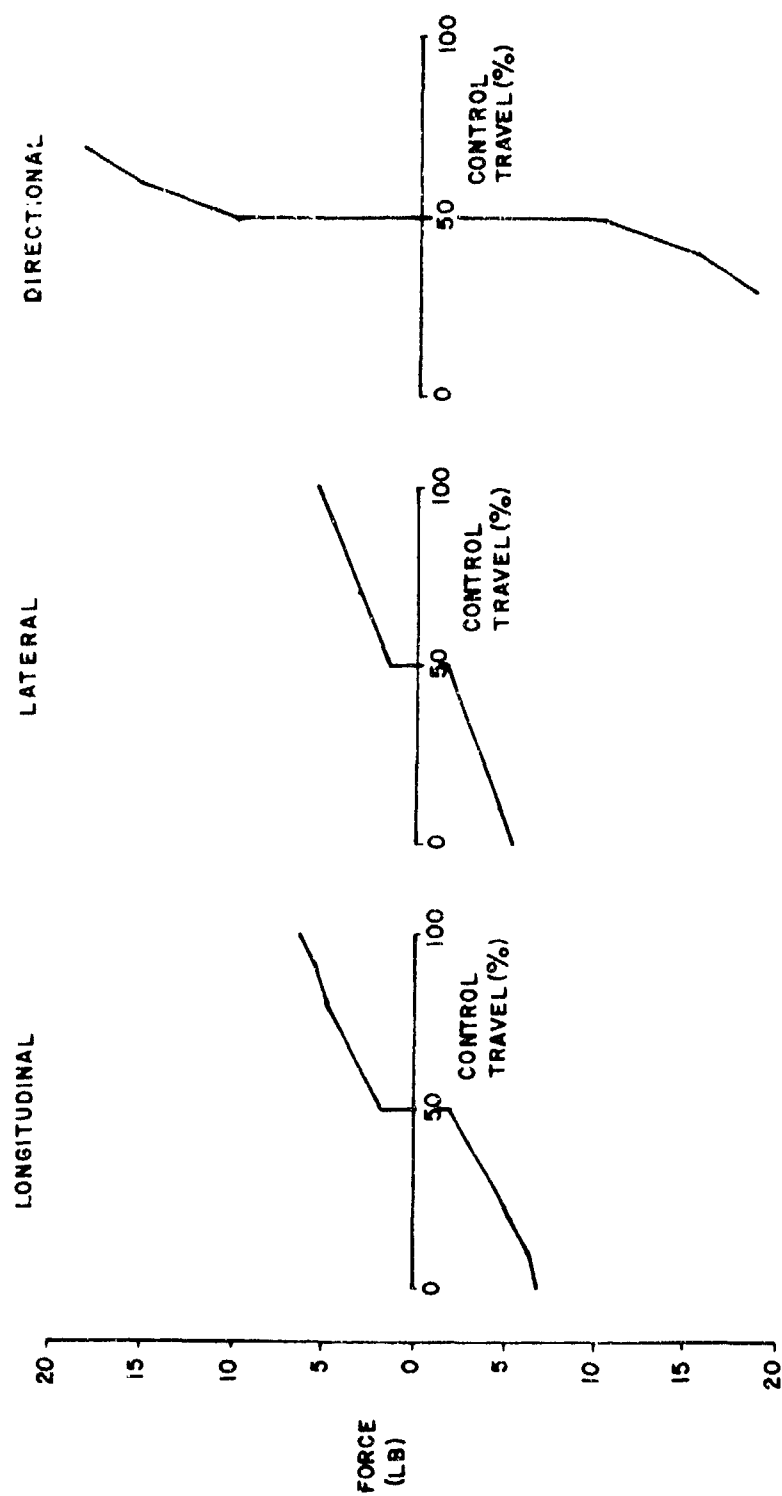
COLLECTIVE BREAKOUT (LB)

|  | MAG BRAKE RELEASE | LOCKED |
|---|---|---|
| UP | 6 | 1 |
| DOWN | 12 | 7.5 |

FLT 806 REC 4
IAS = 60 KNOTS
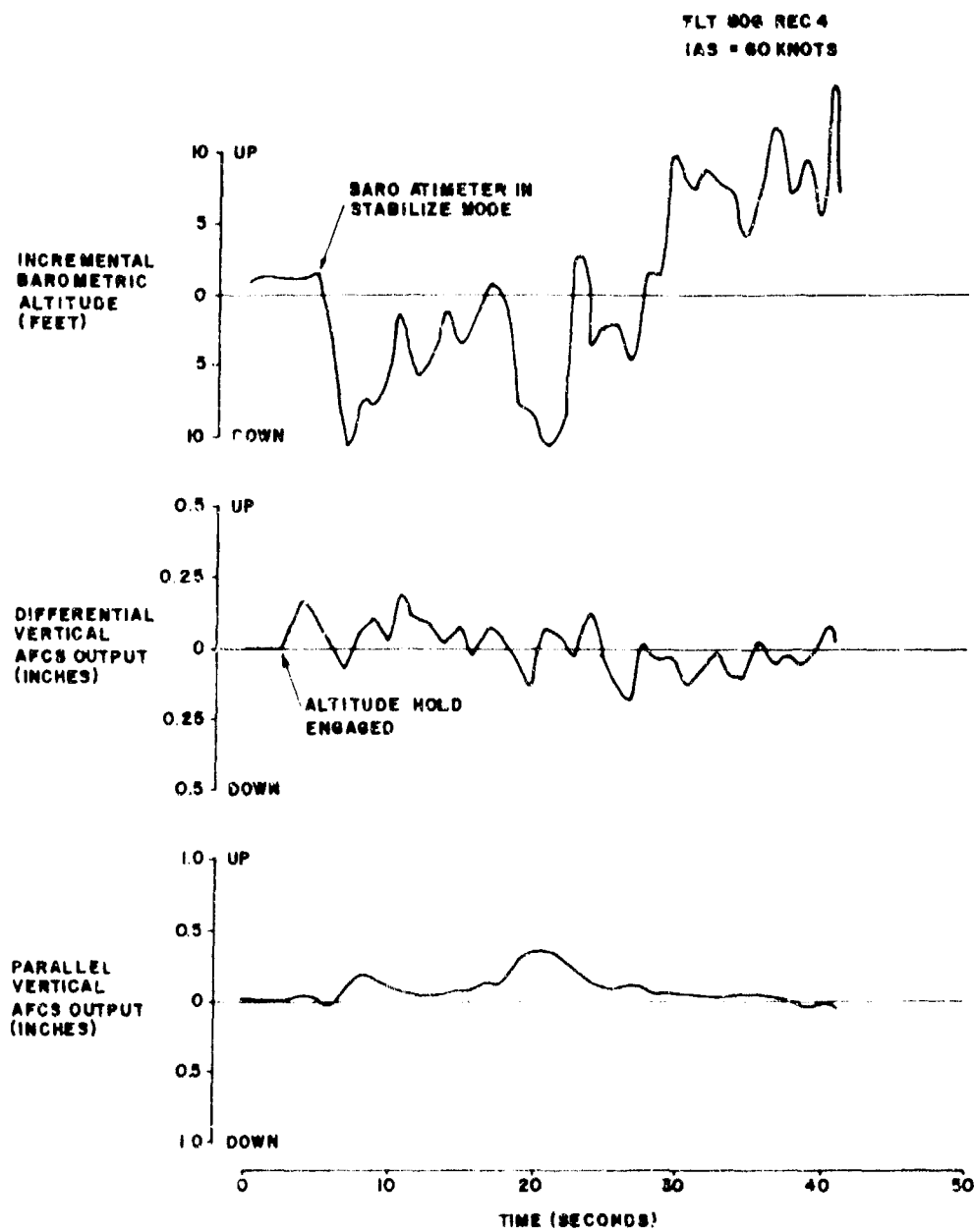
FIGURE 174,
BAROMETRIC ALTITUDE HOLD PERFORMANCE
STRAIGHT & LEVEL FLIGHT

495

Altitude hold engagements in climbs and descents are shown in Figures 175 to 178. Engagements are smooth with an altitude overshoot of approximately 1 foot for every 10-foot-per-minute climb or descent rate.

Altitude hold performance during turn entries and recoveries are presented in Figures 179 to 182 Approximately 60 feet were lost during 30-degree bank turns and required about 20 seconds to recover. Sixty feet were then gained during rollout. This was considered excessive. Altitude gain could not be increased without increasing the level flight torque fluctuations.

## RECOMMENDATION

Complement baro altitude with vertical acceleration, allowing higher low frequency baro gains. Consider using direct bank angle feed into collective to provide the bank turn requirement.

Altitude hold at the higher speeds was similar except that transmission overtorque by automatic collective pitch drive occurred when operating near torque limits (A-5). Test pilot monitor and collective override maintained acceptable limits in the ATC test program.

## RECOMMENDATION

Evaluate the requirement for and methods of limiting dynamic system overtorque in turn maneuvers and heavy load acquisition with altitude hold on.

5.3.2.2   Radar Reference

Altitude hold in the hover region on radar reference was acceptable when the sensor was performing satisfactorily (A1), but was substantially degraded during flight over grass due to frequent sensor noise spikes. A significant modification was required to the simulation-designed vertical axis due to this problem, as discussed in Section 2.1.3.4. A typical performance over concrete is seen in Figure 183, wherein radar rate and altitude signals show much higher frequency content than the precision hover altitude from the laser system. Hold performance is discussed in detail under Hover Hold.

496
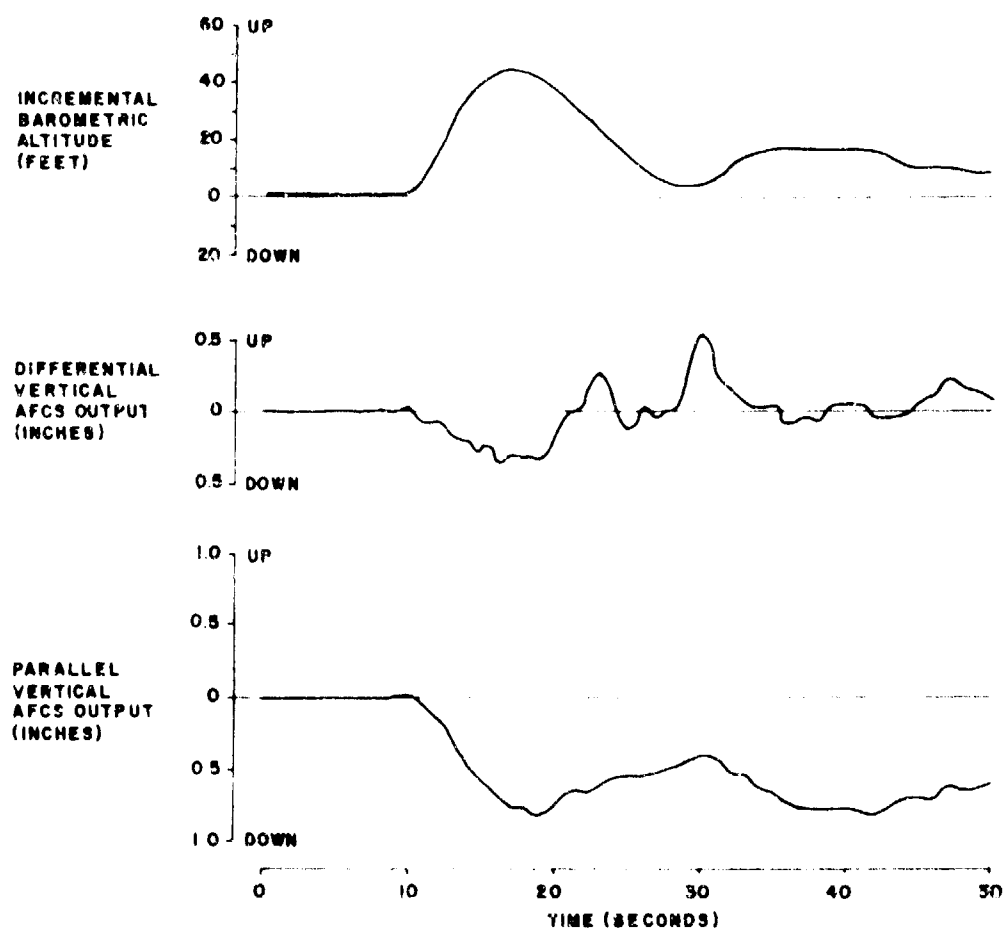
FIGURE 175.
BAROMETRIC ALTITUDE HOLD PERFORMANCE IN CLIMBS—
60 KNOTS

497

FLT 808 REC 10
IAS = 80 KN
RATE OF ACCENT = 1000 FPM
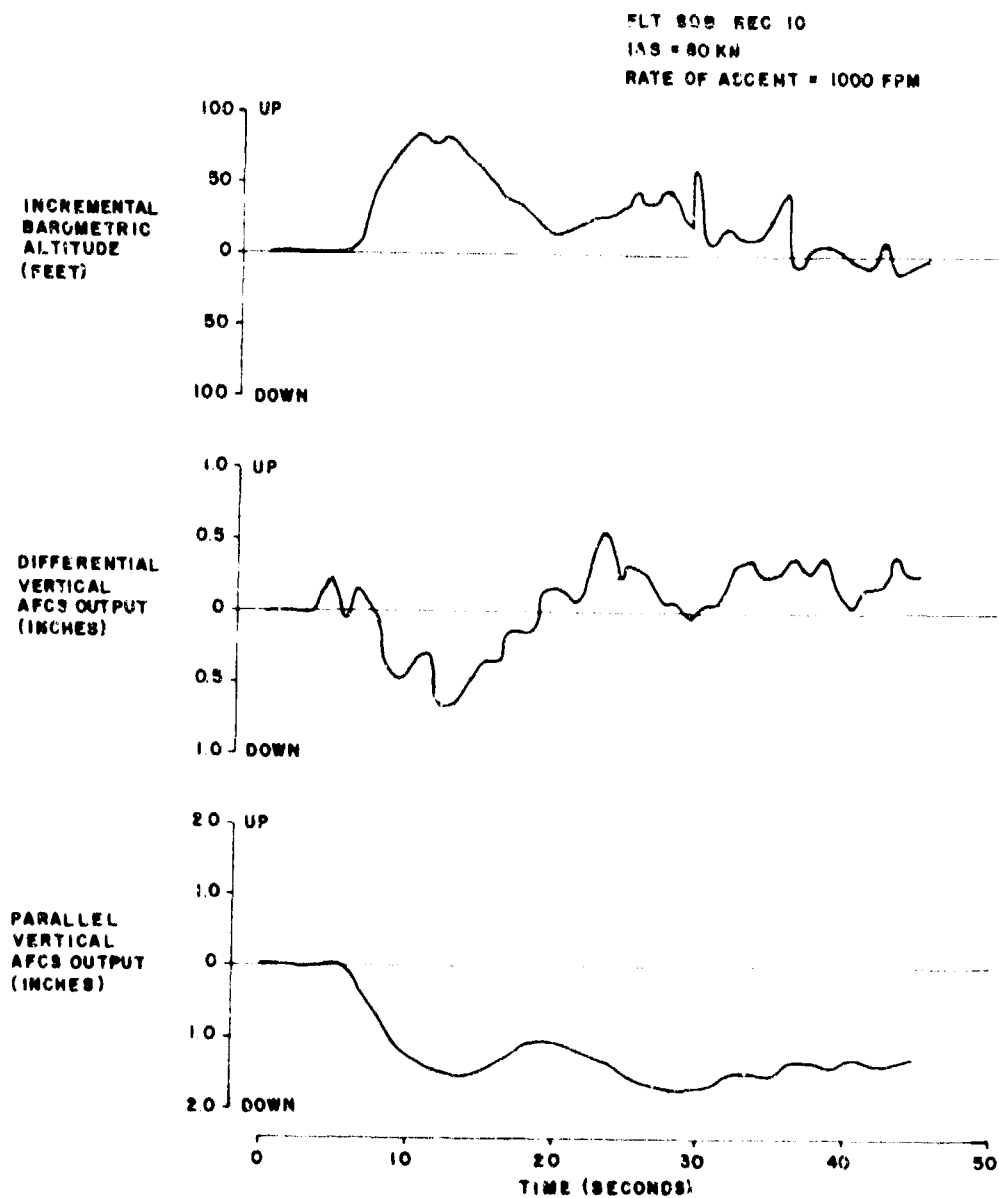
FIGURE 176.
BAROMETRIC ALTITUDE HOLD PERFORMANCE IN CLIMBS—
80 KNOTS

498
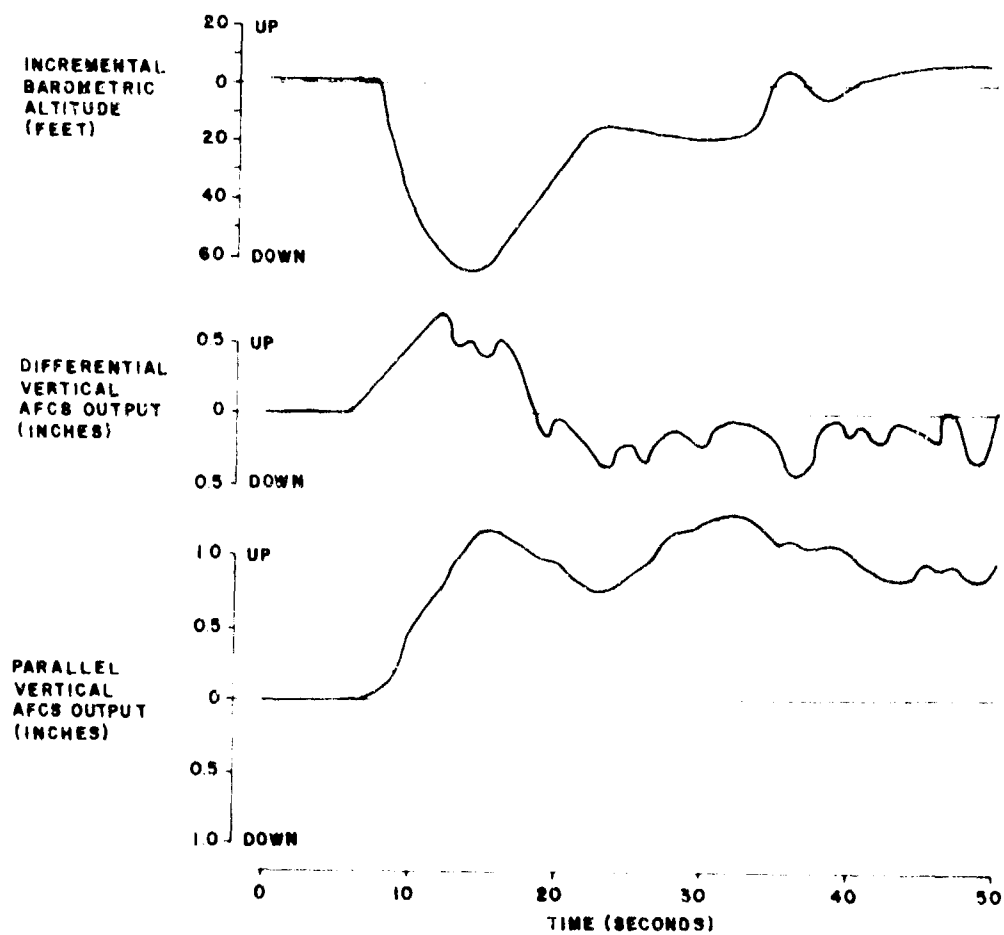
FIGURE 177.
BAROMETRIC ALTITUDE HOLD PERFORMANCE IN DESCENT —
60 KNOTS

FLT 808 REC 9
IAS = 80 KN
RATE OF DESCENT = 1000 FPM
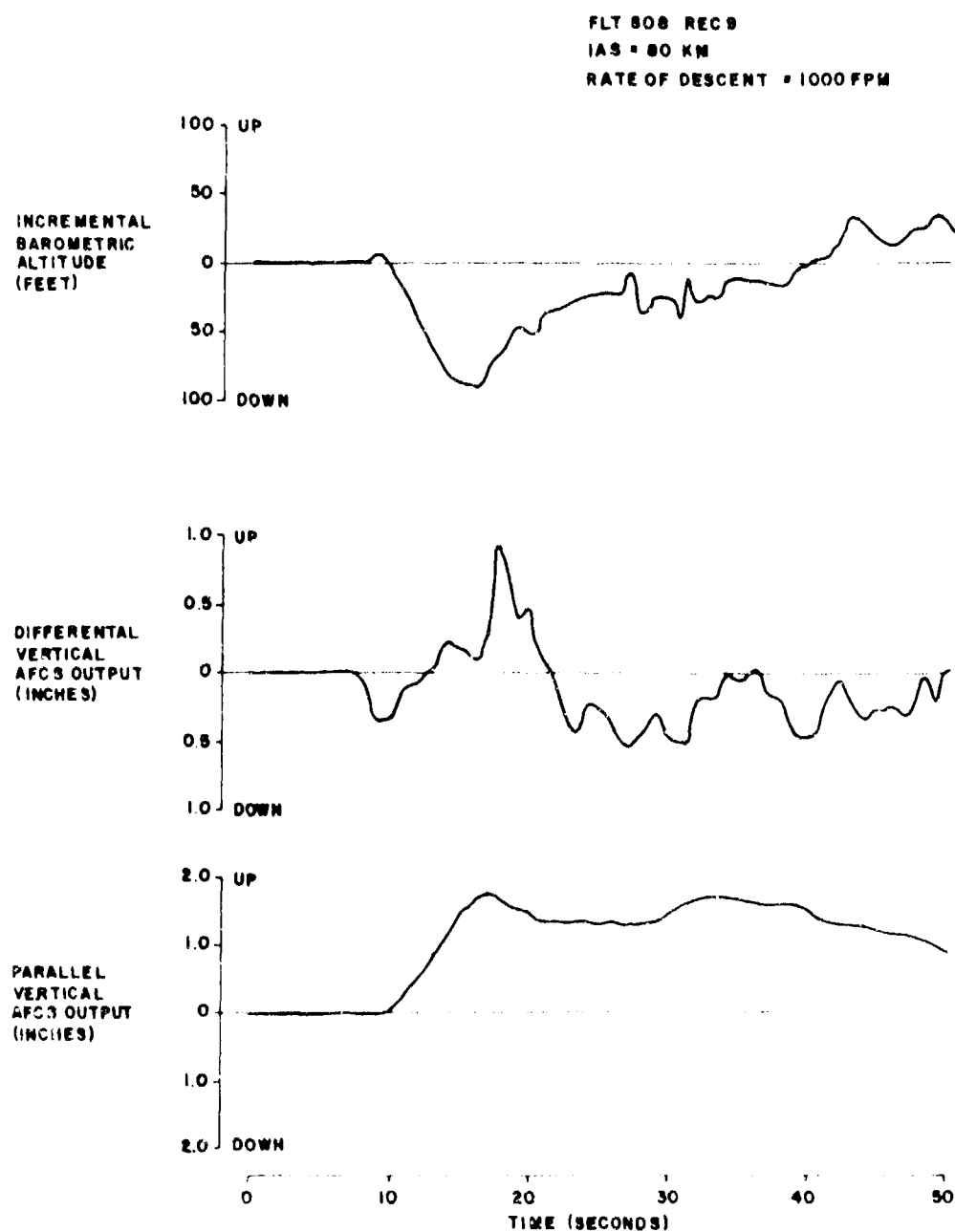
FIGURE 178.
BAROMETRIC ALTITUDE HOLD PERFORMANCE IN DESCENT —
80 KNOTS

500

**ROLL ATTITUDE (DEGREES)**

**INCREMENTAL BAROMETRIC ALTITUDE (FEET)**

**DIFFERENTIAL VERTICAL AFCS OUTPUT (INCHES)**

**PARALLEL VERTICAL AFCS OUTPUT (INCHES)**

TIME (SECONDS)
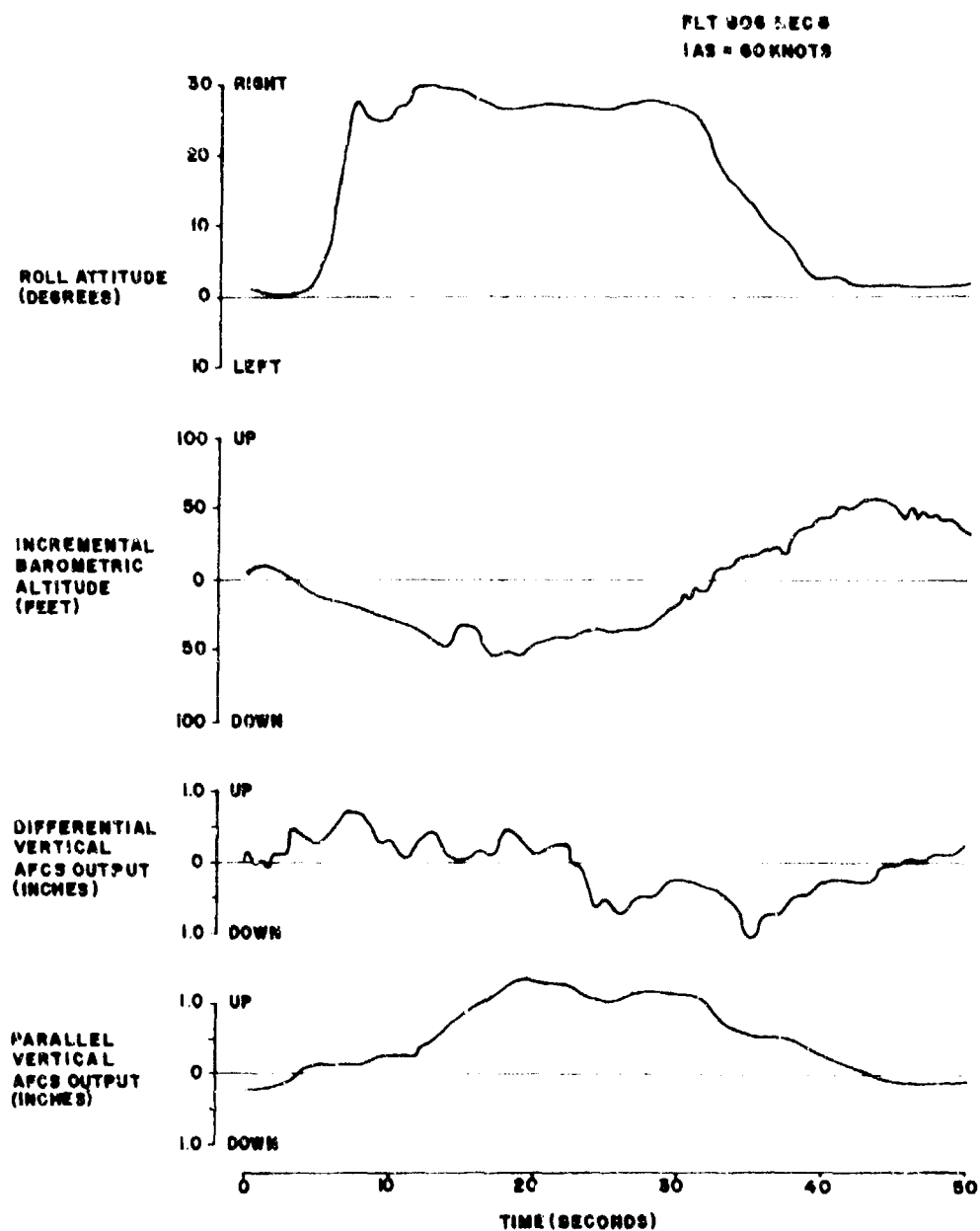
FIGURE 179.
BAROMETRIC ALTITUDE HOLD PERFORMANCE IN TURNS—
60 KNOTS

501
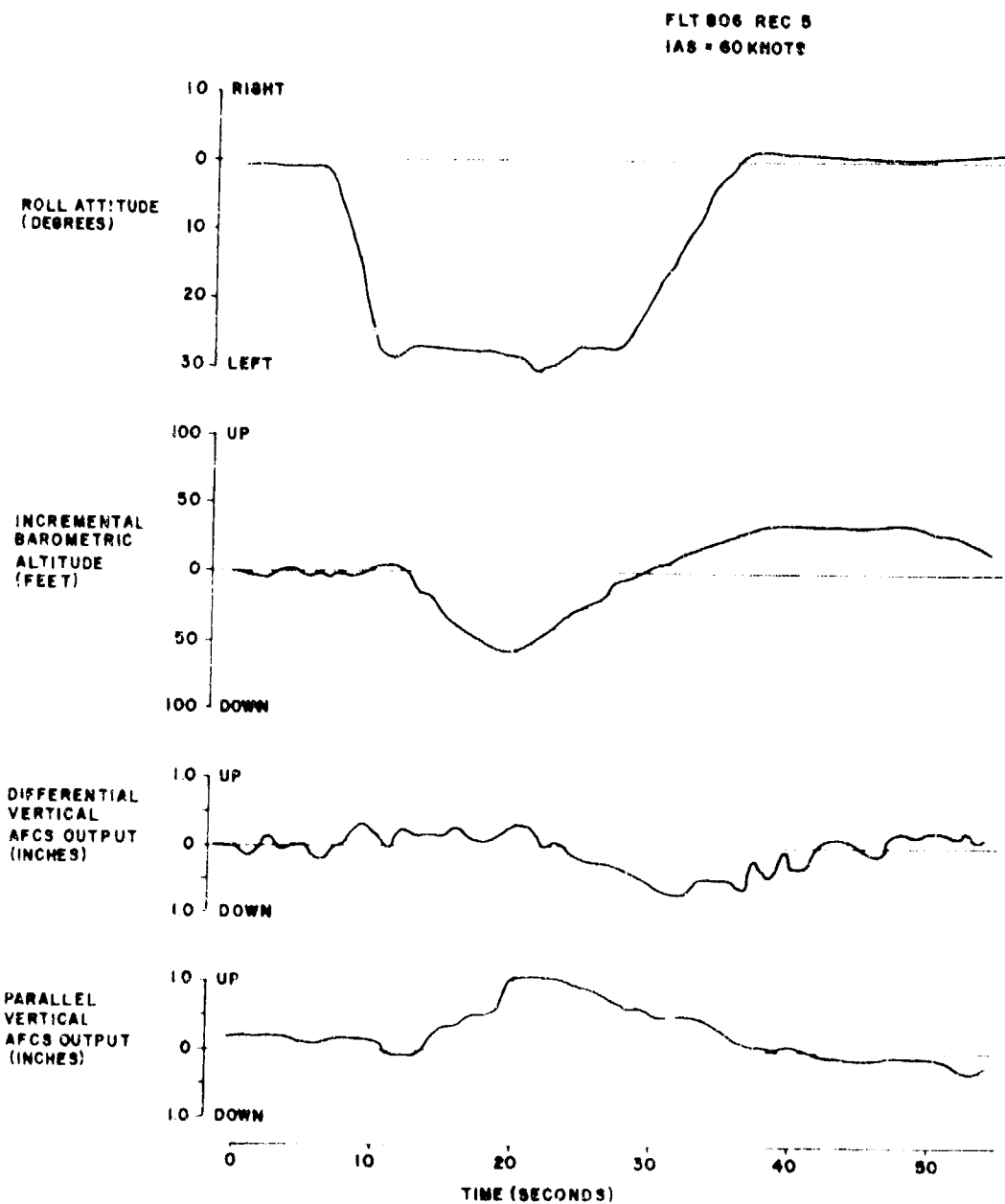
FIGURE 180.
BAROMETRIC ALTITUDE HOLD PERFORMANCE IN TURNS—
60 KNOTS
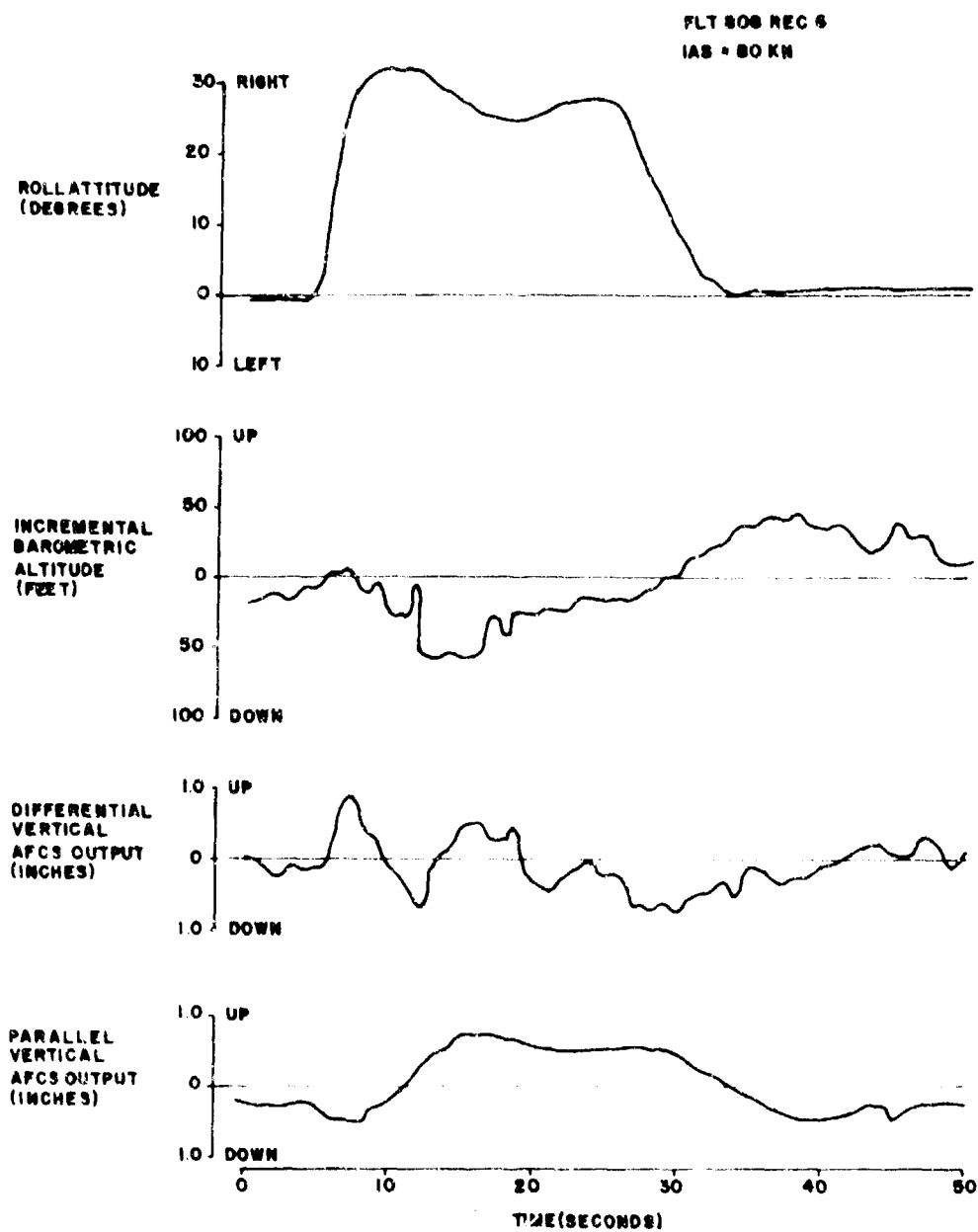
FIGURE 181.
BAROMETRIC ALTITUDE HOLD PERFORMANCE IN TURNS –
80 KNOTS

FLT 808 REC 5
IAS = 80 KN

ROLL ALTITUDE
(DEGREES)

INCREMENTAL
BAROMETRIC
ALTITUDE
(FEET)

DIFFERENTIAL
VERTICAL
AFCS OUTPUT
(INCHES)

PARALLEL
VERTICAL
AFCS OUTPUT
(INCHES)

TIME (SECONDS)
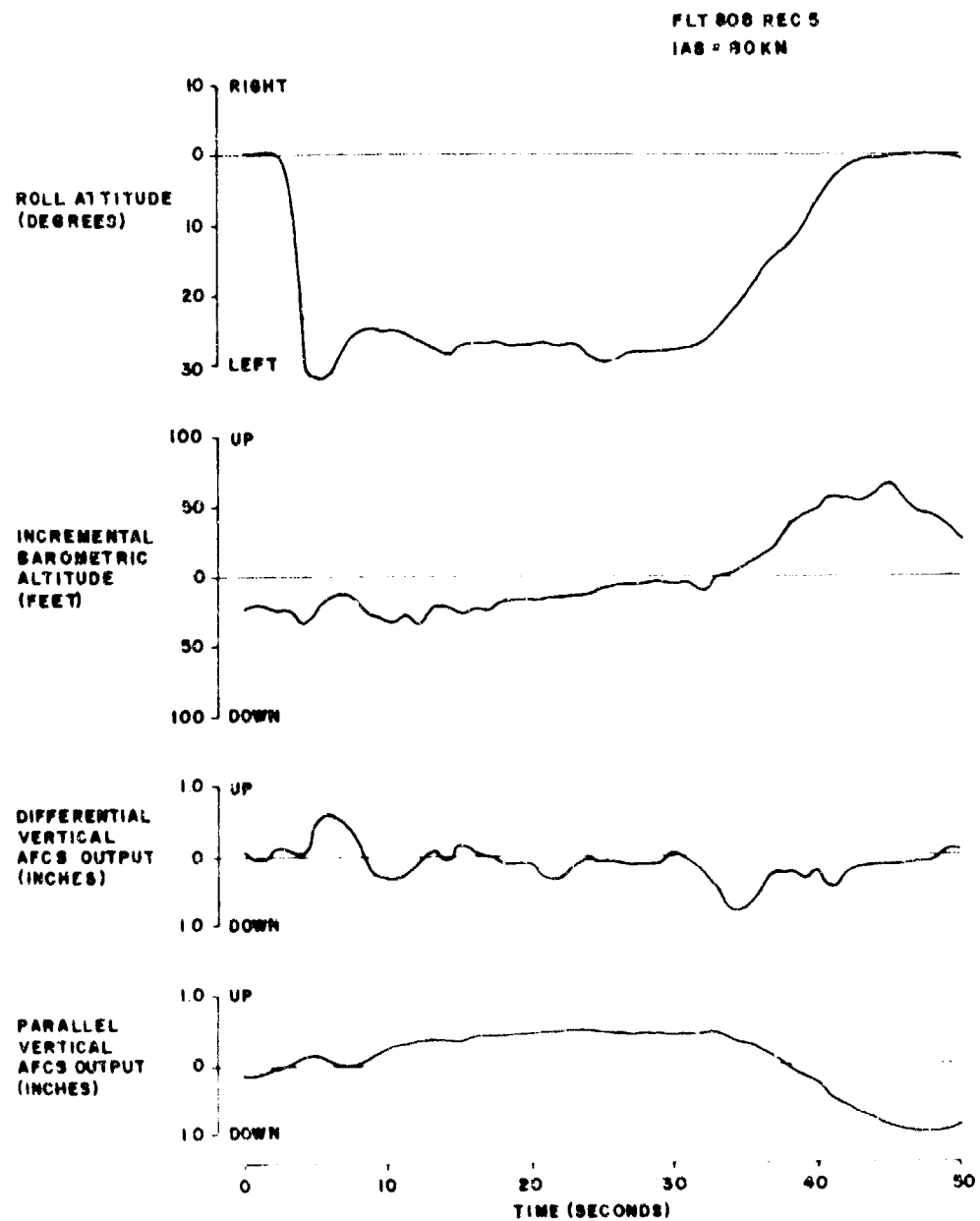
FIGURE 182.
BAROMETRIC ALTITUDE HOLD PERFORMANCE IN TURNS —
80 KNOTS

504
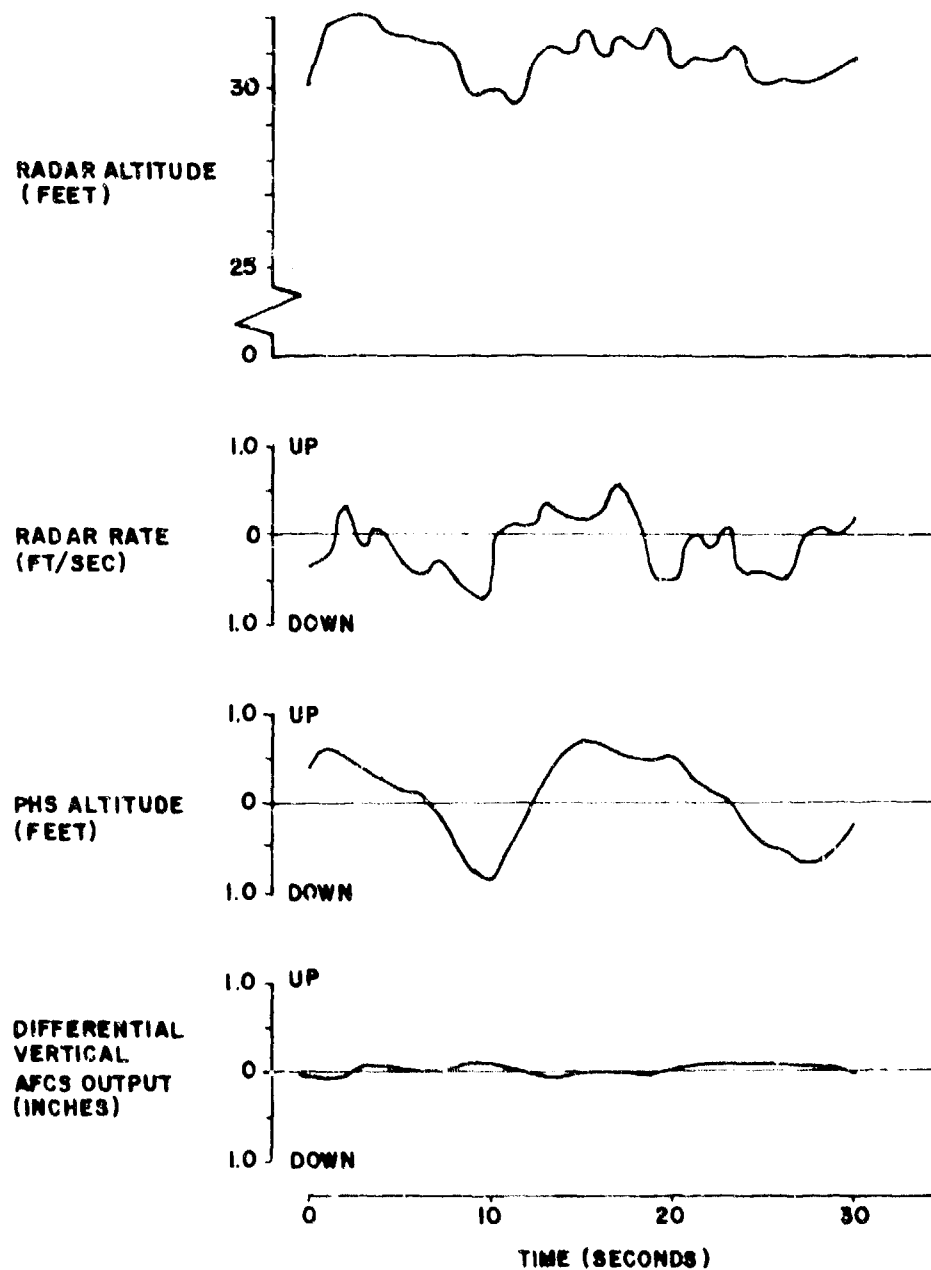
FIGURE 183.
RADAR ALTITUDE HOLD PERFORMANCE
STEADY HOVER

505

Figure 184 illustrates the type of radar altimeter signal generated over grass. It consists of almost continuous 1.33 Hz oscillation with an average amplitude of 1.5 feet. Also, there are random spikes of from 5 to 10 feet. The radar rate signal is obtained by differentiating the altitude signal, and therefore, it is also very noisy. For example, the large radar altitude spike, which occurs at approximately 11 seconds, generates a 6.5 ft/sec change in radar rate. This would require a vertical acceleration of approximately .41 g.

The problem was minimized by filtering the radar altitude signal with a 1-second lag ($T_{z12}$) and by generating a complementary vertical rate as discussed in Section 2.1.3.4.

RECOMMENDATION

Noise Spikes - Incorporate software modifications to compensate for signal deficiencies or improve existing sensor or replace with new sensor.

Since the radar altitude signal was generated by a single sensor, redundancy management could not be utilized to detect sensor failures. Therefore, any sensor failure transients are fed directly to the AFCS. This is extremely hazardous, especially for a hardover type failure near the ground or during load handling operations (U-8).

The effect of such a hardover failure was investigated by injecting a radar altimeter test signal into the system. The system response is shown on Figure 185. The test signal used consists of a 1-second, 100-foot radar altitude pulse. The radar altitude and radar rate signals consist of the test input and the actual aircraft response. The vertical AFCS output is driven hardover almost instantaneously. Since the AFCS is saturated, the vertical axis is operating open loop and the aircraft response is equivalent to the unaugmented aircraft. The aircraft response to such an input would cause the aircraft to descend 5 feet in approximately 1 second. This can be very dangerous, especially when the aircraft is in close proximity to the load and ground crewman.
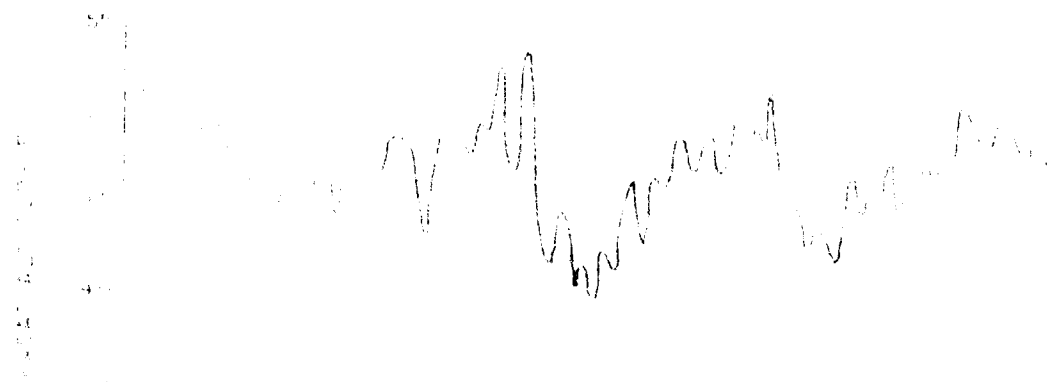
(TIME (SEC))
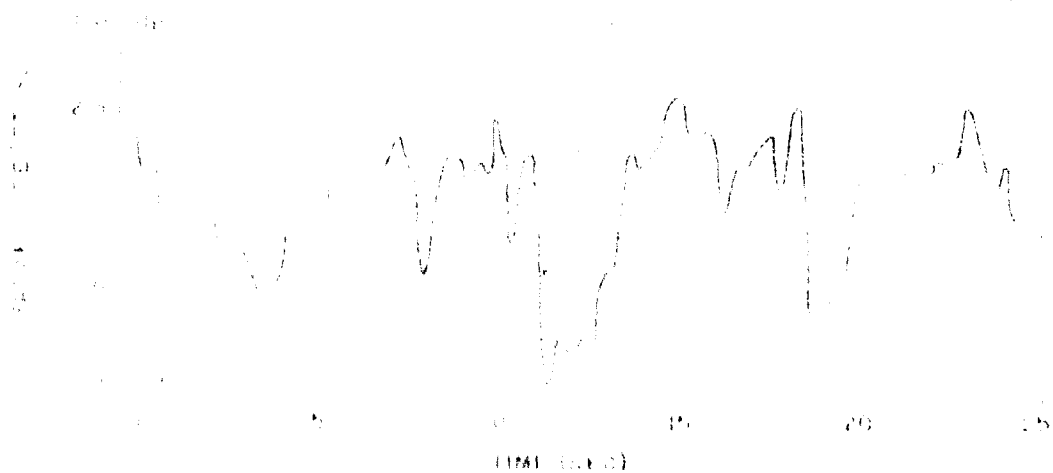
FIGURE 184.
PULSE RADAR ALTIMETER SPIKINS OVER GRASS
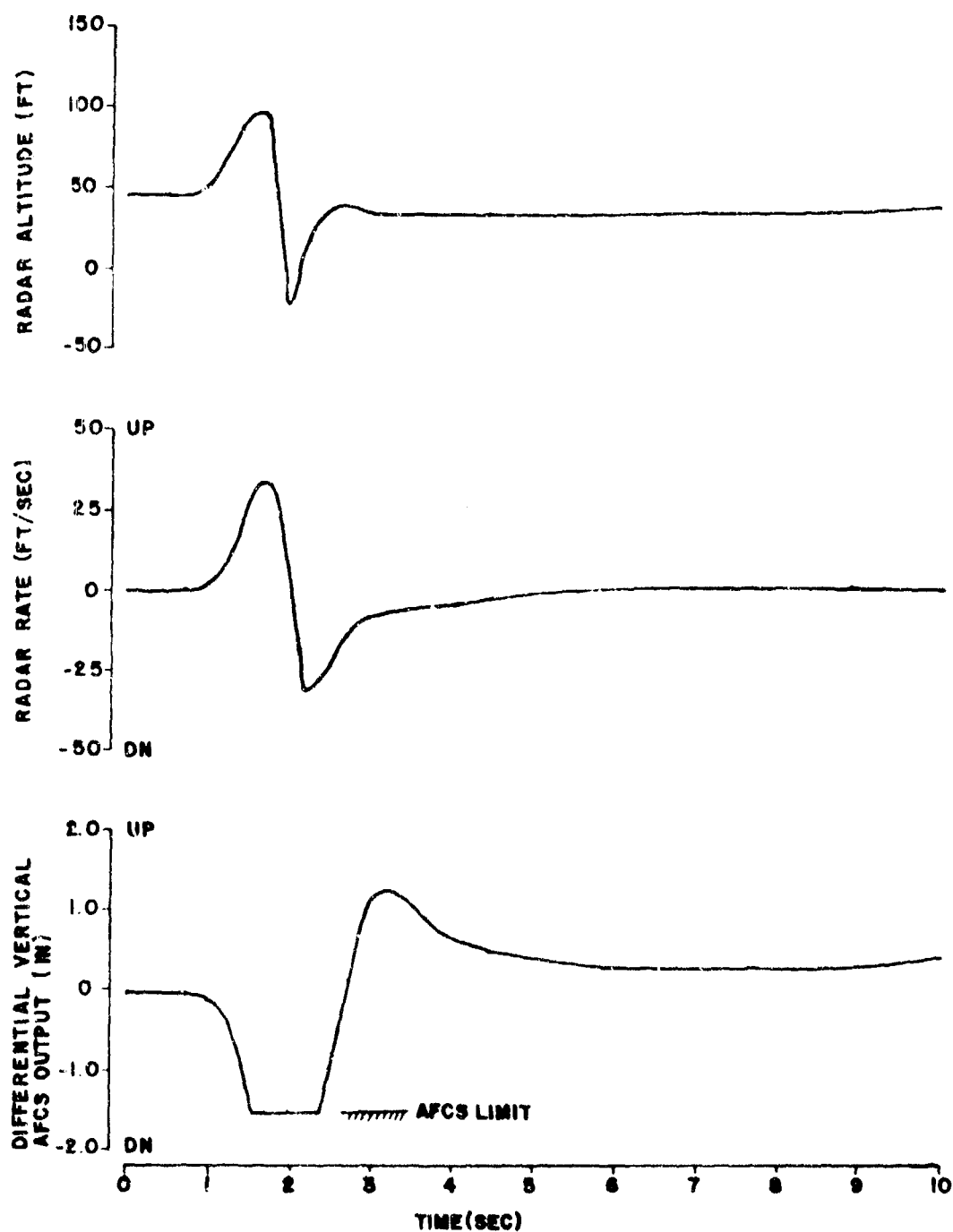
FIGURE 185.
RESPONSE TO SIMULATED RADAR ALTIMETER FAILURE

509

RECOMMENDATION

Radar Altimeter Failure - Incorporate vertical axis frequency splitter and complementary altitude filtering. Consider use of redundant sensor.

Radar altitude performance with an external load was unsatisfactory for cable lengths of approximately 50 feet or longer. Load interference with the radar beam during large amplitude longitudinal swings caused heavy vertical deviations (U-8). This was particularly objectionable on Hover Hold Mode as barometric reference could not be used.

RECOMMENDATION

External Load Interference - Incorporate barometric signal selection capability on hover hold or reconfigure hardware to solve problem; e.g., consider dual sensors, one forward and one aft,with appropriate software logic to determine signal validity.

In forward flight below 200 feet altitude, sharp movements of the collective were created in an attempt to follow the terrain contour.

RECOMMENDATION

Provide an airspeed interlock for the automatic altitude hold sensor logic to inhibit automatic selection of radar altitude above 50 knots.

5.3.2.3  Automatic Baro/Radar Reference Switching

Transitions through the 200-foot switch point were accomplished with no apparent transients (A-2).

5.3.3  Hover Trim

The Hover Trim mode, designed to automatically fly the aircraft to zero IMU groundspeed from any flight configuration, was evaluated under several initial conditions. A typical transition  from forward flight initiation at 130 knots showed that aircraft deceleration was mild; however, collective control input on barometric altitude hold was not quick enough to maintain zero rate of descent as helicopter airspeed was reduced below speed for

509

minimum power. This put the aircraft in an uncomfortable descent rate at low airspeed before altitude loss was arrested. The capability to initiate at high speed offered no significant mission enhancement.

Engagements at low groundspeeds (below 40 knots) were judged useful for trimming the aircraft to a hover when used in conjunction with radar altitude hold. System gains compromised for high-speed engagements were low and produced a very slow trim rate and, of course, any IMU drift was reflected in the final trim condition (A-5). No optimization was done on this mode. Manual trimming was relatively easy, however, and the mode does not appear warranted. One feature it does provide that was noticed by the pilot is a pseudo-position hold if engaged when IMU drift is zero. The integral velocity feedbacks not present on Basic SCAS are the reason. However, the Hover Hold mode provides a much tighter hold and can be drift cleared to absolute zero.

### 5.3.4    Hover Hold Mode and Load-Controlling Crewman

### 5.3.4.1    General

The load-controlling crewman uses the Hover Hold mode to precisely control or maintain helicopter velocity and/or position. Flight test results for two sub-modes of operation - Velocity Hold (IMU/Radar) and Position Hold (Precision Hover Sensor) are presented. Aircraft position hold data is included to compare position accuracy of different AFCS control modes. Comparisons between flight test results and simulation data are included.

The initial AFCS mechanization obtained through simulation was generally found to be acceptable except for the vertical axis. Poor vertical hold performance due to "noise" spiking of the radar rate/altitude signals necessitated a redesign of the vertical axis during the flight test program. (Note Section 2.1.3.1.3.)

A comparison of Hover Hold parameters defined by simulation and flight testing is presented in Table 25. Maximum LCC load shuttle velocity commands ranging from 13.5 to 15 ft/sec were satisfactory (A-2). In the lateral and longitudinal axes, however, an increase to 20 ft/sec, would be desirable. The maximum vertical velocity control was reduced from 8.0 to 6.0 ft/sec and directional yaw rate was increased from 5.0 to

510

## TABLE 25.
## AFCS HOVER HOLD PARAMETERS

| AXIS | COMPARISON OF SIMULATION AND FLIGHT TEST RESULTS | | | | | | | | | | | COMPARISON OF VELOCITY GAINS | |
|---|---|---|---|---|---|---|---|---|---|---|---|---|---|
| | MAXIMUM LCC COMMAND | | LCC COMMAND LAG -SECONDS | | LCC CONTROL SENSITIVITY RANGE -MIN/MAX- | | HOVER HOLD VELOCITY/YAW RATE GAIN | | HOVER HOLD POSITION HEADING GAIN | | | | HOVER HOLD MODE | BASIC SCAS MODE (LOW SPEED) |
| | SIM | FLT | SIM | FLT | SIM | FLT | SIM | FLT | SIM | FLT | | | FLT | FLT |
| LONGITUDINAL | FT/SEC | | 0.5 | 2.0 | FT/SEC/IN | | DEG LCP/FT/SEC | | DEG LCP/FT | | | | FT/SEC²/FT/SEC | FT/SEC |
| | 15.0 | 15.0 | | | 2.5-14.0 | 1.0-18.0 | 6.0 | 1.93 | 3.95 | 1.67 | | | 1.08 | 0.176 |
| LATERAL | FT/SEC | | 0.5 | 2.0 | FT/SEC/IN | | IN $\delta_S$/FT/SEC | | IN $\delta_S$/FT | | | | FT/SEC²/FT/SEC | FT/SEC |
| | 15.0 | 13.5 | | | 2.7-15.0 | 1.0-23.0 | 1.1 | 0.77 | 0.85 | 0.56 | | | 1.08 | 0.16 |
| VERTICAL | FT/SEC | | 0 | 0 | FT/SEC/IN | | IN $\delta_C$/FT/SEC | | IN $\delta_C$/FT (PHS) | | IN $\delta_C$/FT (RADAR) | | FT/SEC²/FT/SEC | FT/SEC |
| | 8.0 | 6.0 | | | 5.0-30.0 | 3.3-23.0 | 0.23 | 0.16 | 0.59 | 0.18 | 0.04 | 0.064 | 1.47 | 1.47 |
| DIRECTIONAL | DEG/SEC | | 0 | 0.5 | DEG/SEC/DEG | | IN $\delta_R$/DEG/SEC | | IN $\delta_R$/DEG | | | | | |
| | 5.0 | 8.0 | | | 0.17-0.67 | 0.3-1.2 | 0.08 | 0.2 | 0.1 | 0.2 | | | — | — |

SIM - SIMULATION
FLT - FLIGHT TEST

511

9.0 deg/sec. Increased LCC command lags in three axes were also found to be beneficial for the precision load placement task, since there was less tendency to overcontrol and excite the load. Without an external load, the small lag time constants defined during the simulation offered a more optimum aircraft longitudinal and lateral velocity response.

### 5.3.4.2  Velocity Hold (IMU/Radar)

Longitudinal and lateral hover hold velocity gains were reduced to improve aircraft ride qualities and soften response for load operations. Higher gains (longitudinal 3.0 degrees LCP/ft/sec, lateral 1.1 in. $\delta_s$/ft/sec) were evaluated and found to have acceptable stability. No degradation of hover hold performance with the lower velocity gain settings was evident to the pilot. Higher yaw rate and heading gains were desirable for a tighter heading hold when making maneuvers in other axes. Heading, velocity, and altitude hold were rated as A1.5 by pilot.

The nonlinear velocity command function relationships for all axes are shown on Figures 186 thru 189. Simulation and final flight test configurations are defined for comparison. The lateral nonlinear velocity command function (Figure 187) as well as the longitudinal was changed for precise load maneuvering to reduce velocity sensitivity for small controller inputs and to minimize load disturbances. The lateral velocity control sensitivity was reduced much more than the longitudinal in the small controller travel region (Figure 190). Blending from low sensitivity to the maximum shuttle velocity resulted in a rapid rate of change in sensitivity. This rate of change was particularly objectionable when large trim inputs to offset lateral IMU drifts were required. A larger lateral controller travel or capability to select either a high- or low-gain LCC velocity command function is required. The dual-gain method, one for shuttle maneuvers and one for load placement, is represented by the first and third flight test configurations in Figure 187. This method will be incorporated into the HLH prototype due to the cost of increasing LCC controller travels.

Start and completion of the drift-clear sequence required an on/off command by the LCC. Early release of the drift-clear button prior to zero velocity command from the controller would cause an aircraft transient and induce a small drift (rated A-4). A repeat of the drift-clear process was often

512
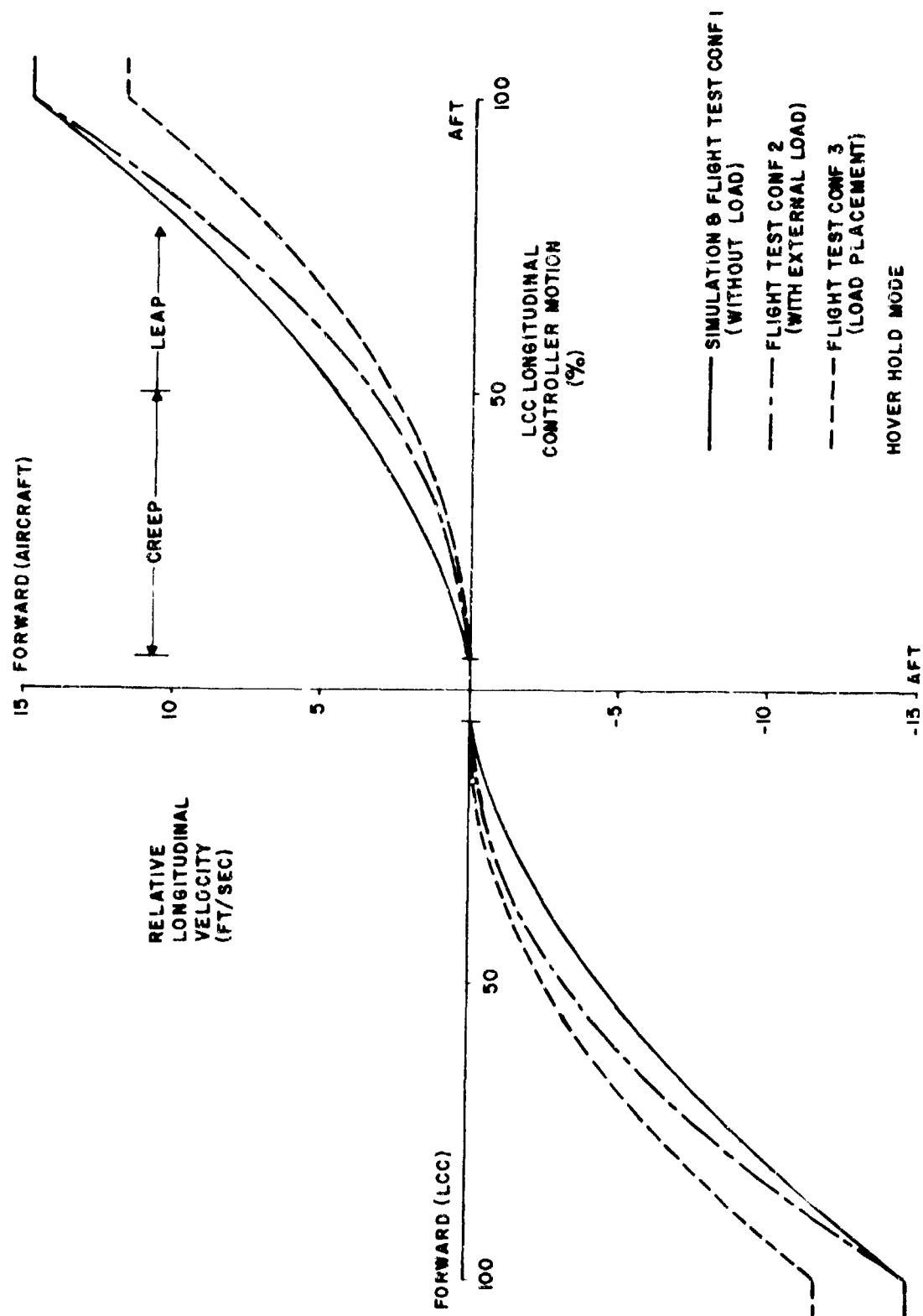
FIGURE 186. LCC LONGITUDINAL VELOCITY COMMAND RELATIONSHIP

513
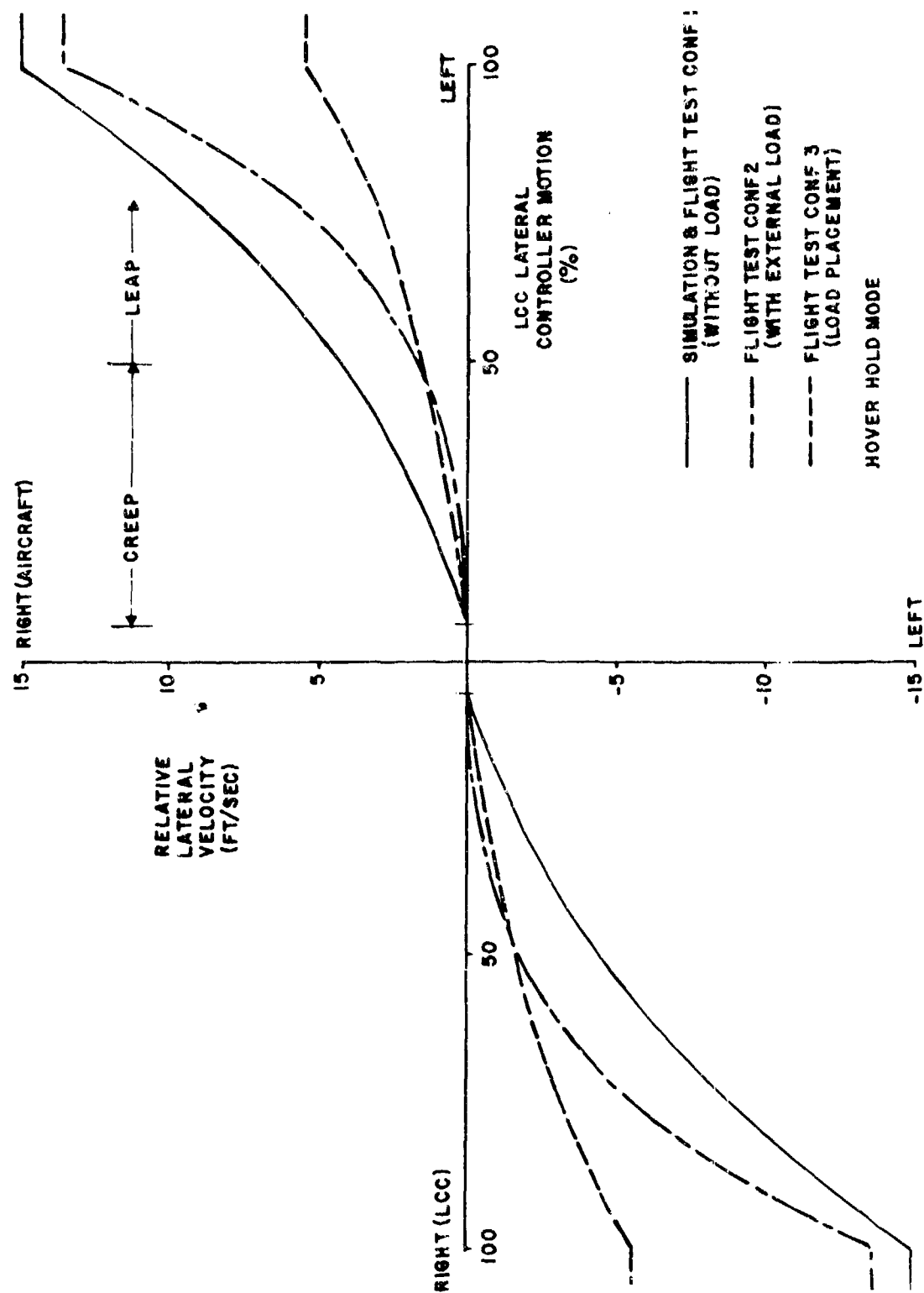
FIGURE 187. LCC LATERAL VELOCITY COMMAND RELATIONSHIP
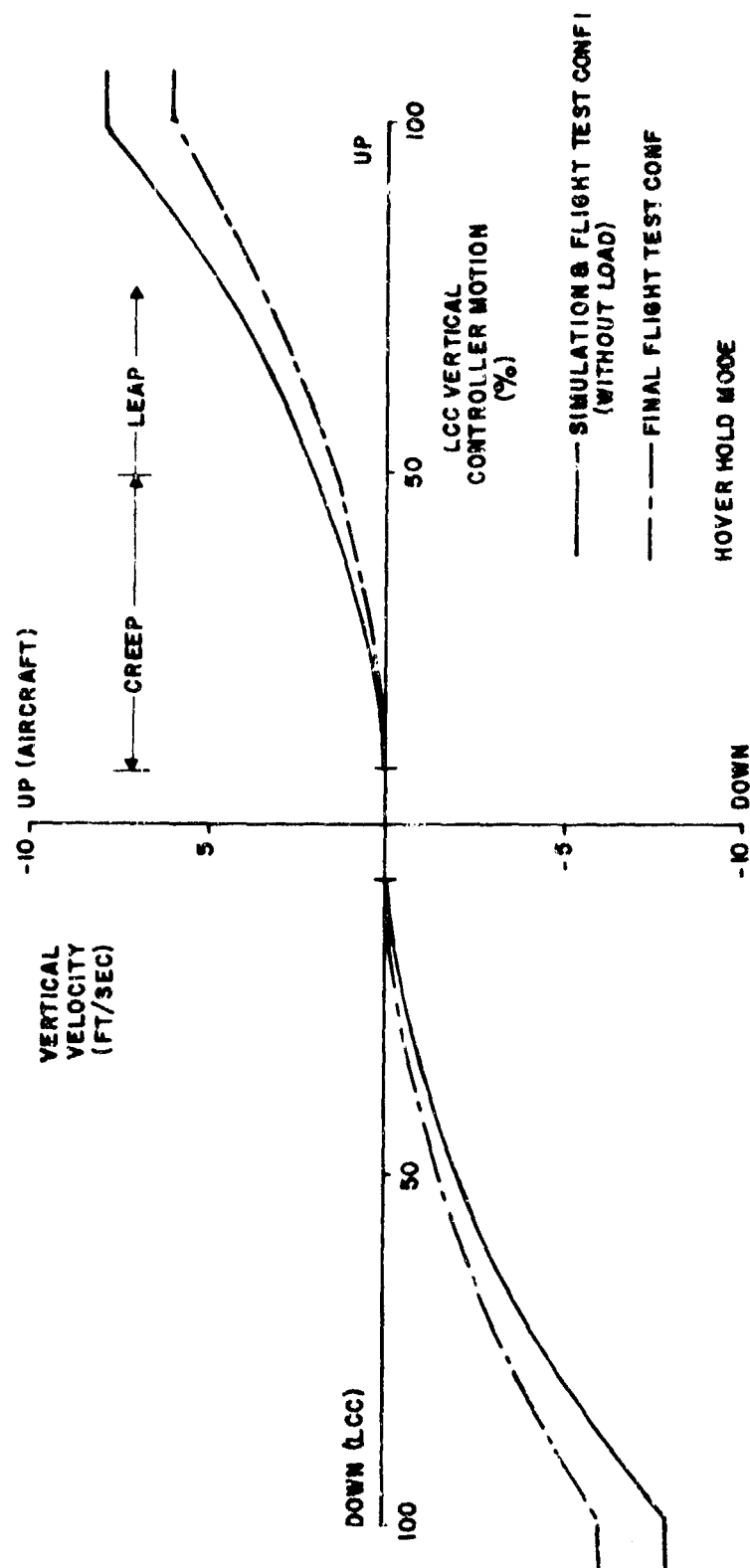
FIGURE 188. LCC VERTICAL VELOCITY COMMAND RELATIONSHIP
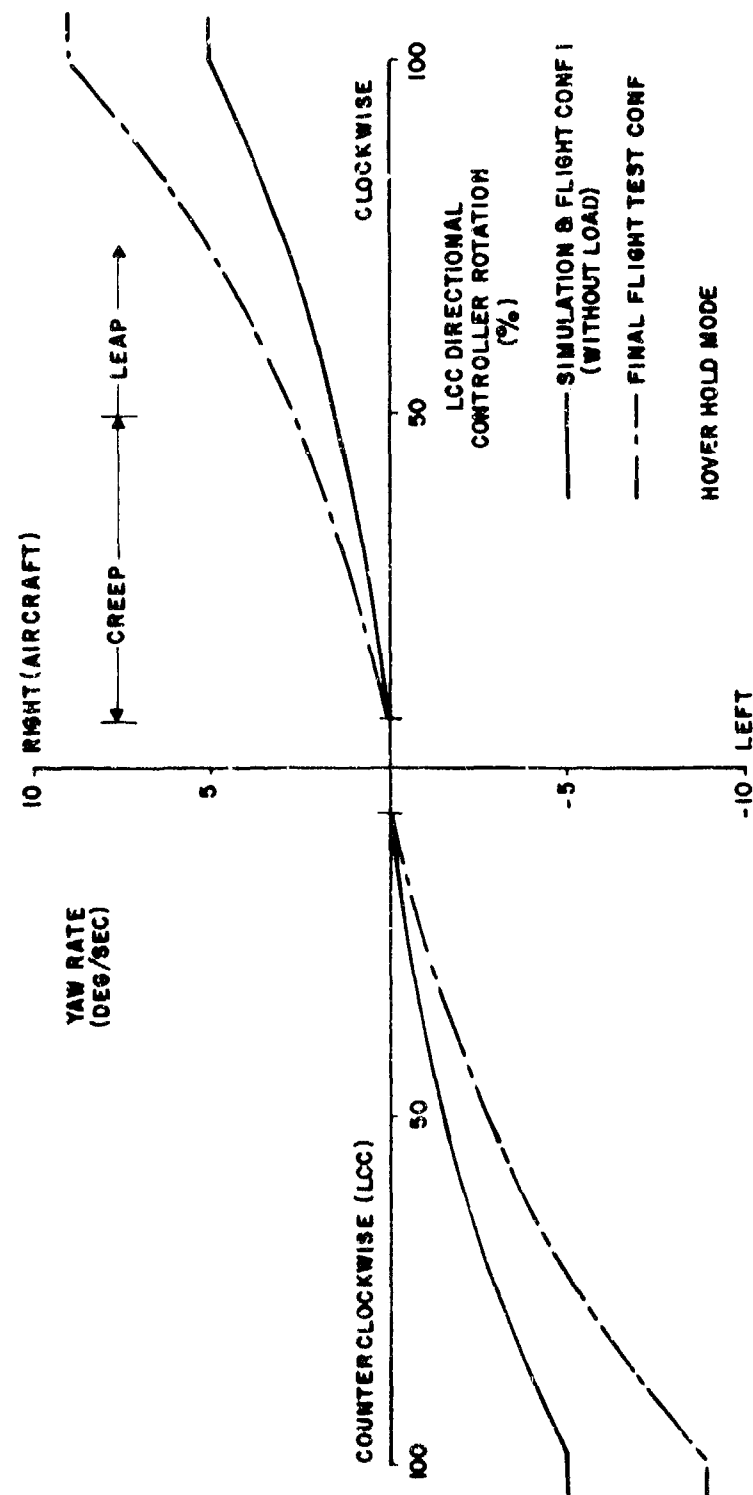
FIGURE 189. LCC DIRECTIONAL VELOCITY COMMAND RELATIONSHIP

516
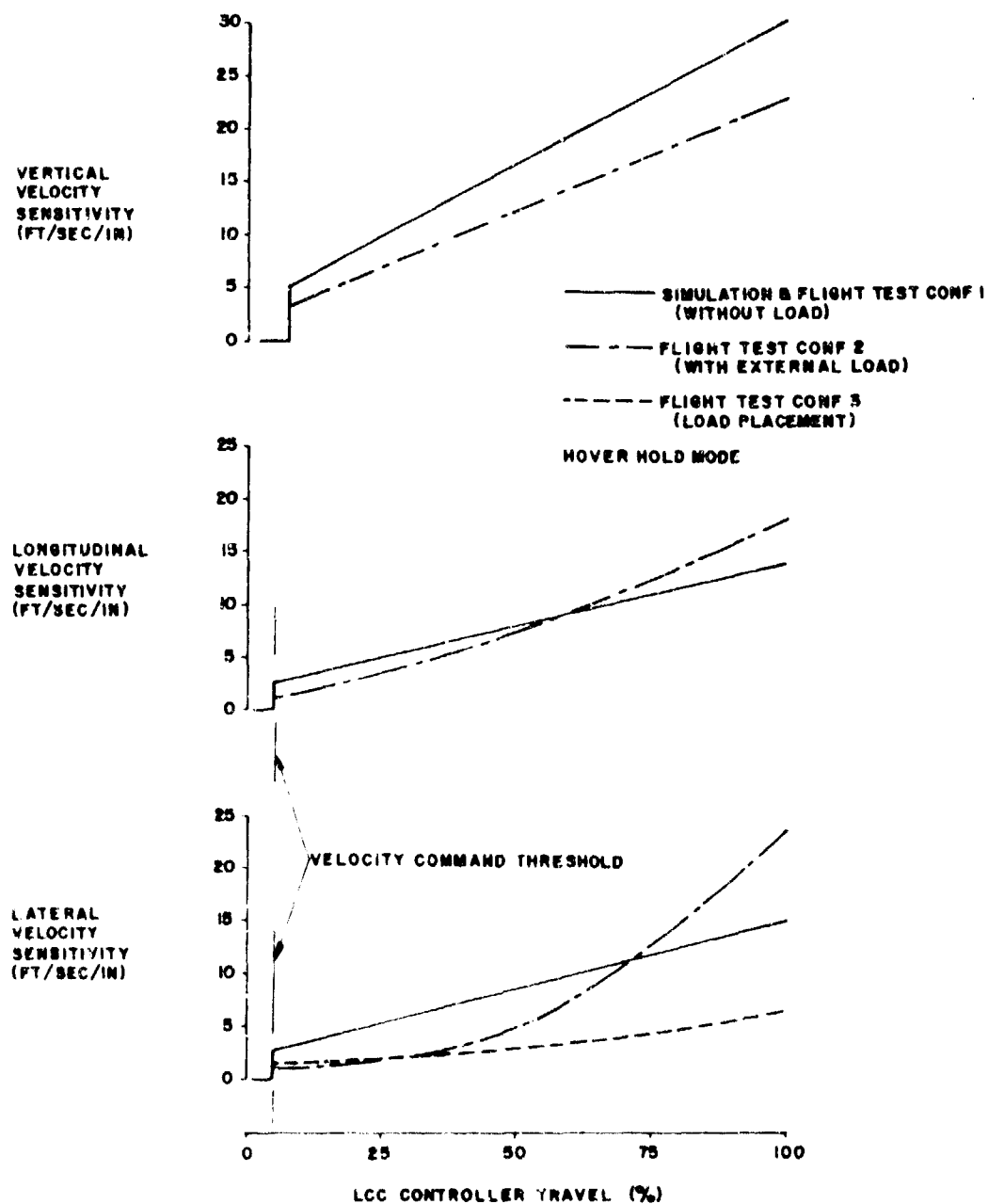
FIGURE 190. LCC VELOCITY CONTROL SENSITIVITY

517

required to obtain a good velocity trim, particularly in the lateral axis with its rapid rate of change of velocity sensitivity. The HLH procedure will be simplified to require only initiation by the LCC. Logic will control the remainder of the drift-clear sequence.

The velocity response to maximum LCC longitudinal and lateral controller inputs is presented in Figures 191 and 192. Both longitudinal and lateral responses show an initial linear acceleration of 1.7 $ft/sec^2$ and smooth deceleration to the commanded velocity. No interaxis coupling is evident from the data. With maximum longitudinal velocity command (15 ft/sec) the aircraft did not drift off its zero lateral velocity reference by more than 0.5 ft/sec. The lateral response time history shows the same trend with regard to longitudinal velocity. Longitudinal velocity response was attained with very small pitch attitude deviation (less than 0.5 degrees) from trim condition. However, the lateral velocity response required roll attitude change which creates a lateral load disturbance. Heading generally held to within 1.0 degree for velocity command inputs in other axes, while altitude hold was maintained to within 2.0 feet. Longitudinal control response and sensitivity was rated A1.5, and lateral was rated A-4, indicating further development is required to achieve precision load positioning objectives.

The LCC directional response is shown in Figure 193. A heading turn is executed through 180 degrees from a headwind to a tailwind condition. Wind conditions for this flight were reported to be steady at 12 knots, gusting to 20 knots. The aircraft performed the 9.0 deg/sec yaw rate turn with a maximum longitudinal drift of 2.0 ft/sec and lateral drift of 1.2 ft/sec. Both velocities returned to near zero trim when the turn was completed. Directional response and sensitivity was rated A1.5. The directional turn response data presented in Fig. 193 was obtained with higher than normal backdrive gains from the longitudinal and lateral velocity error signals. The velocity error integral commands backdrive the cockpit controls for trim compensation. Higher gains were beneficial during turns in winds, since long-term saturation of the velocity error limiters was prevented. Saturation of the velocity error limiters caused higher aircraft velocity drift and momentary loss of LCC control in that axis.

Fig. 194 shows another LCC directional turn with lower backdrive gains optimized for normal hover hold operation. A

518
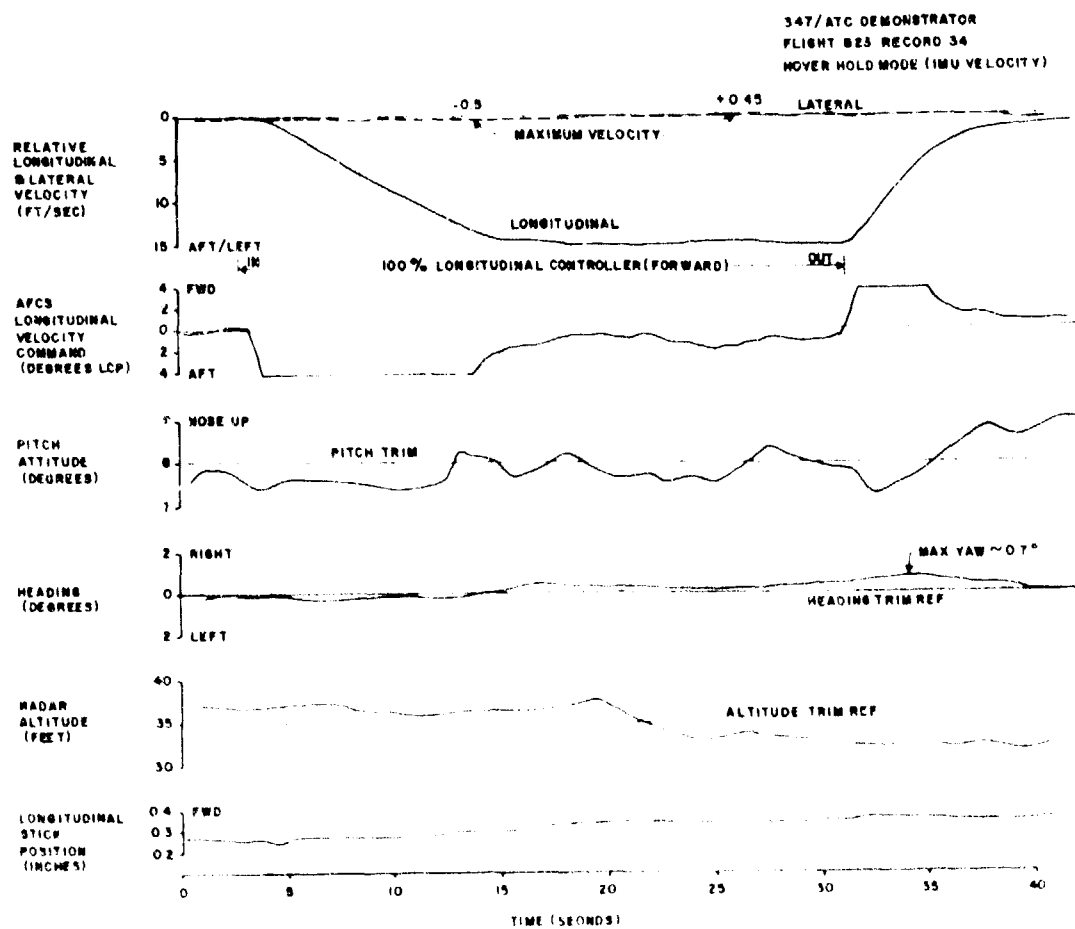
FIGURE 191. LCC LONGITUDINAL VELOCITY RESPONSE
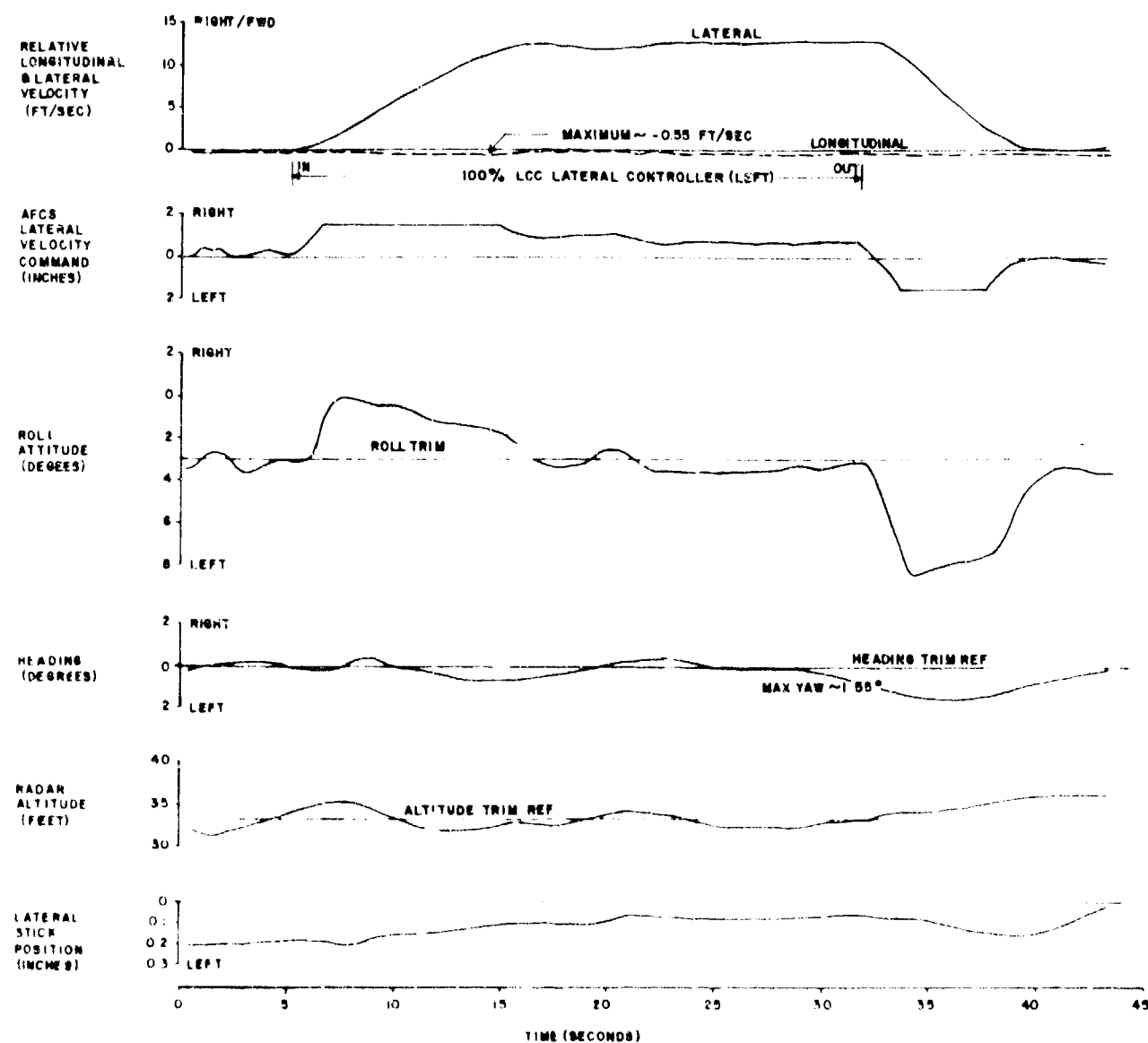
FIGURE 192.  LCC LATERAL VELOCITY RESPONSE

520
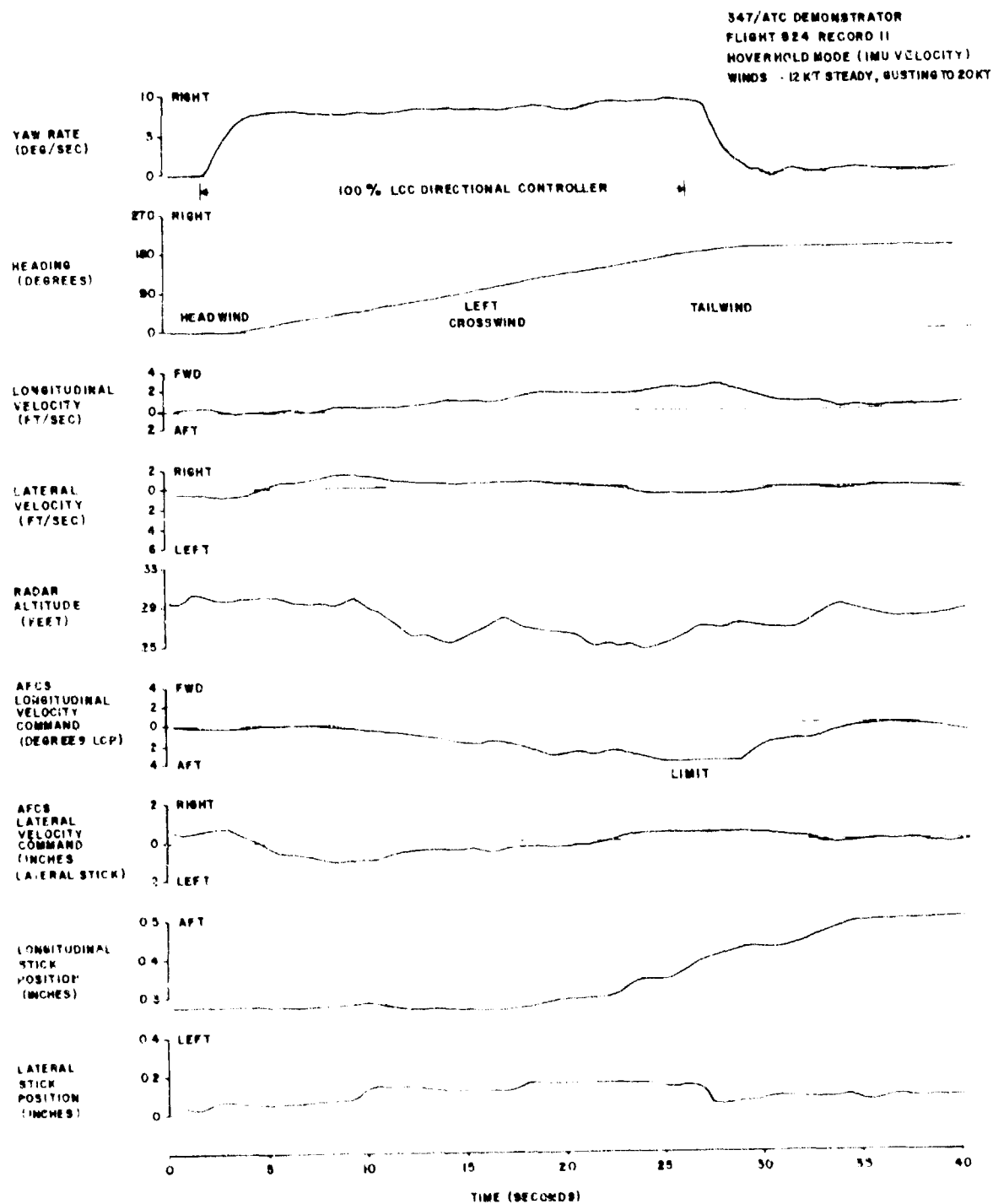
FIGURE 193. LCC DIRECTIONAL RESPONSE
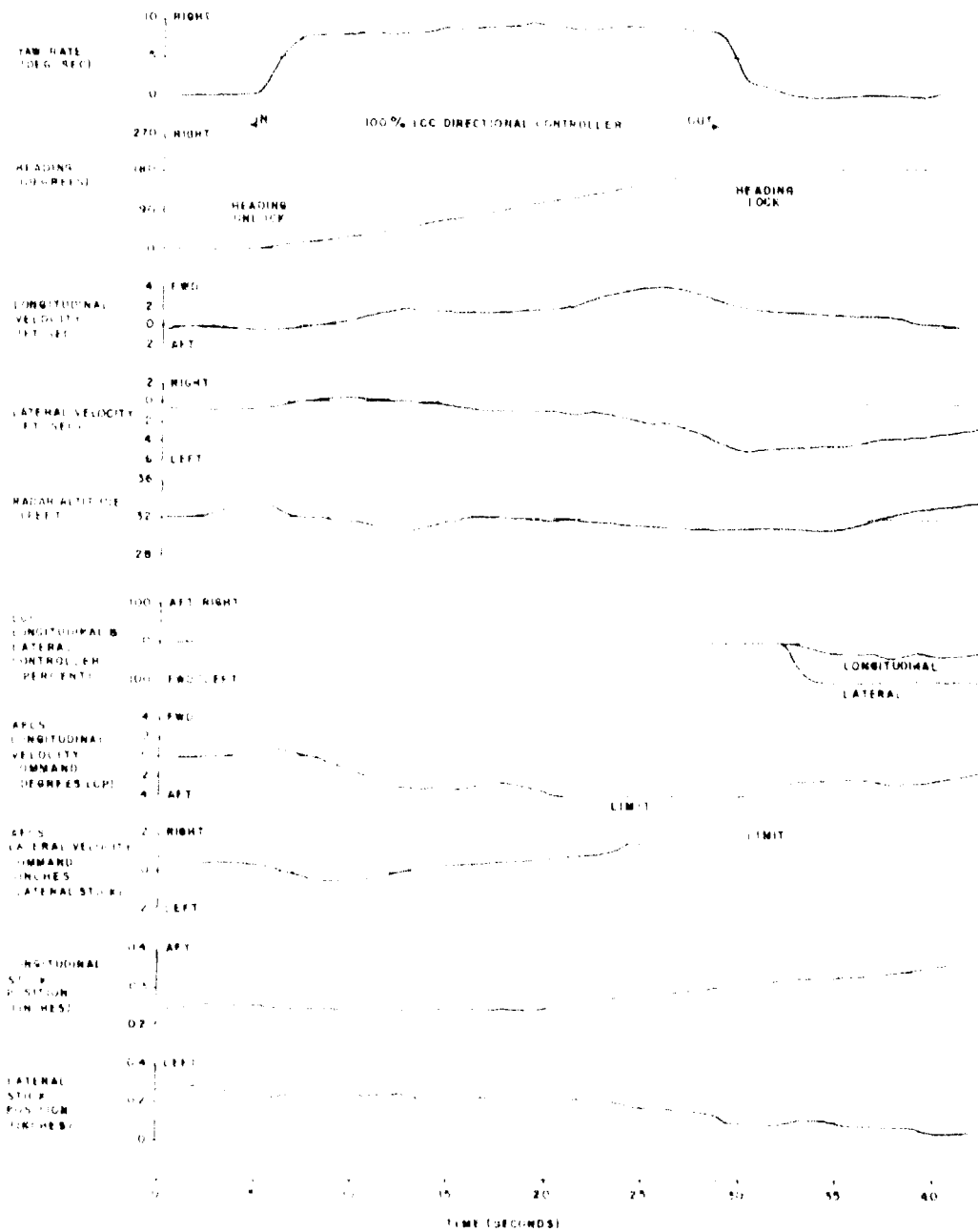
FIGURE 184 LCC DIRECTIONAL RESPONSE

180-degree heading turn, similar to that shown on Figure 193, resulted in considerably more longitudinal and lateral velocity drift and saturation of the velocity command limiters. The HLH directional AFCS will incorporate logic to increase the backdrive gains when a turn is commanded by the LCC, but otherwise the gains will be normally at a lower value.

A maximum vertical response commanded by the LCC is shown on Figure 195. A vertical velocity overshoot above the maximum 6.0 ft/sec steady state rate of climb is caused by the parallel backdriven cockpit control. If the LCC control were left in for a longer period of time, the aircraft would achieve a 6.0 ft/sec vertical rate of climb. The parallel backdrive gain from vertical velocity error was increased to overcome inherent aircraft vertical damping, particularly in the ground effect region, and to permit rapid load pickup. Logic was also added to switch on the backdrive command only when the LCC commands a vertical velocity. Figure 195 shows that longitudinal and lateral velocities were less than 0.75 ft/sec during the vertical climb, and the maximum heading deviation from trim was 0.5 degrees. Vertical control response and sensitivity was rated A1.5.

The final radar altitude hold configuration was acceptable with peak altitude excursions of around 2.5 feet in a hands-off hover. The LCC was able to effectively compensate for the vertical excursions due to radar spikes or gusts during load operations. The HLH Prototype will have radar altitude complemented with vertical acceleration to form a hybrid altitude reference. A low crossover frequency (0.1 rad/sec) will provide much more attenuation of radar altitude spikes, allowing an altitude gain increase to obtain performance similar to PHS operation on the 347 helicopter.

### 5.3.4.3 Position Hold (Precision Hover Sensor)

Position hold performance using PHS velocity and position signals was evaluated over a prepared target area to assure good position lock and assess feasibility. Position gains were reduced as shown on Table 25 for compatibility with the lower velocity (IMU/Radar) hold mode. Stability and position hold characteristics were evaluated by inserting AFCS single axis differential pulses or steps from a cockpit test function panel. Army Preliminary Evaluation (Flight No. 828) data records showing aircraft response to differential control inputs are summarized below.

347/ATC DEMONSTRATOR
FLIGHT 823 RECORD 40
HOVER HOLD MODE (RADAR)
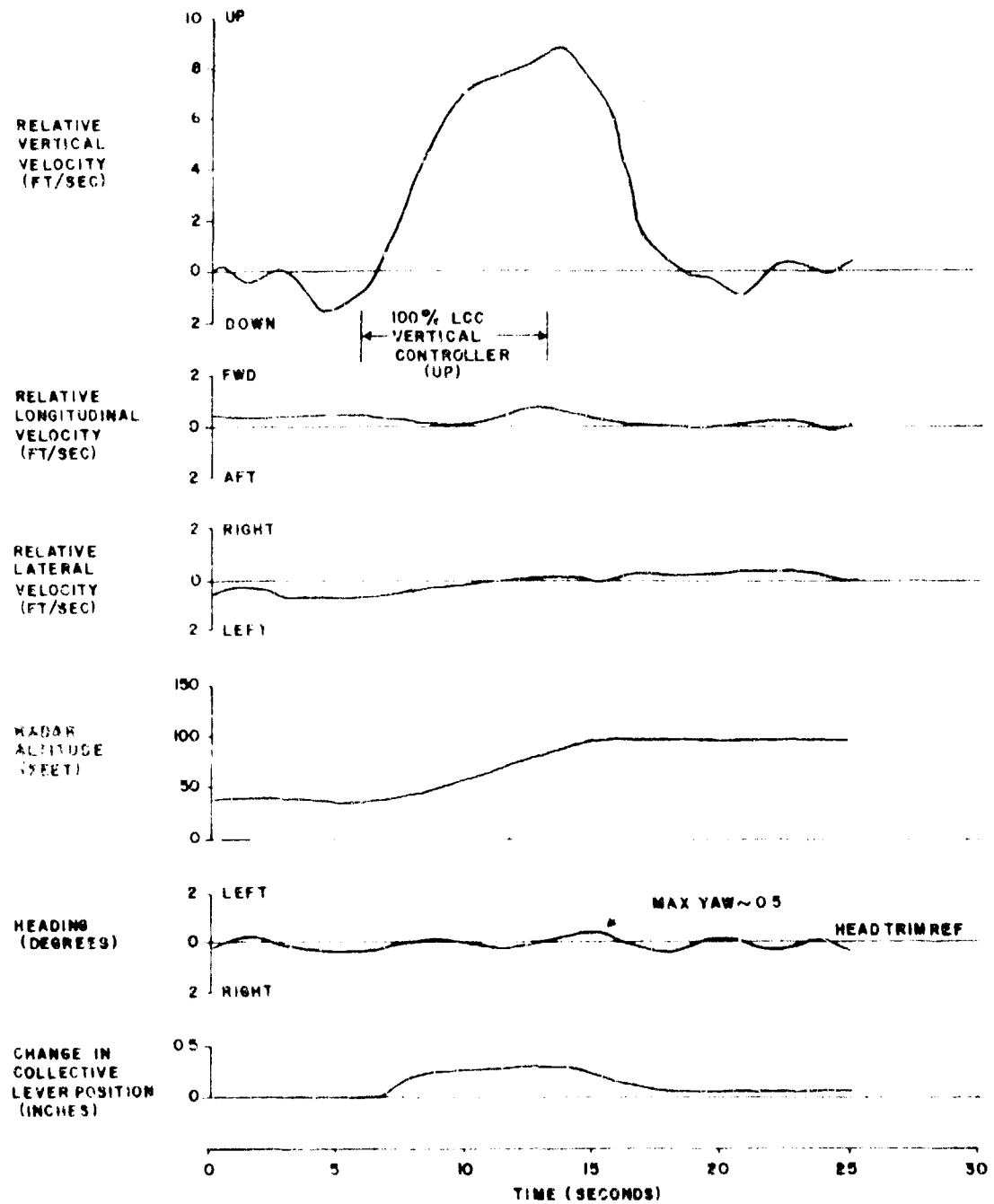
FIGURE 195. LCC VERTICAL VELOCITY RESPONSE

## TABLE 26.
### POSITION HOLD DATA SUMMARY

AFCS DIFFERENTIAL PULSE/STEP CONTROL INPUTS

| AXIS | CONTROL INPUT | TYPE | MAGNITUDE | FLIGHT # RECORD # | FIGURE |
|---|---|---|---|---|---|
| Longitudinal | Longitudinal Cyclic Pitch (Fwd & Aft) | 0.5-sec pulse | 1.5 deg | 31 | 196 |
| Longitudinal | Differential Collective Pitch (Nose Down & Up) | 0.5 sec | 1.5 in. | 32 | 197 |
| Lateral | Lateral Cyclic Pitch (Right & Left) | 0.5-sec pulse | 0.75 in. | 33 | 198 |
| Vertical | Collective Pitch (Up) | 0.5-sec pulse | 0.5 & 1.5 in. | 35 | 199 |
| Vertical | Collective Pitch (Down) | 0.5-sec pulse | 0.5 & 1.5 in. | 35 | 200 |
| Longitudinal | Longitudinal Cyclic Pitch (Fwd & Aft) | 5.0-6.0-sec step | 1.5 deg | 36 | 201 |
| Longitudinal | Differential Collective Pitch (Nose Down & Up) | 5.0-sec step | 1.5 in. | 36 | 202 |
| Vertical | Collective Pitch (Up) | 8.0-sec step | 0.5 in. | 38 | 203 |
| Lateral | Lateral Cyclic Pitch (Right) | 5.0-sec step | 0.75 in | 37 | 204 |
| Directional | Differential Lateral Cyclic Pitch (Left) | 6.0-sec step | 0.66 in. | 37 | 204 |

525

Aircraft position data shows the longitudinal and vertical position hold performance to be tighter than lateral. Lateral position deviations from the position zero reference were larger and more frequent, with peak excursions in some cases ranging from 1.0 to 2.0 feet. This can be seen on Figures 196 and 200 through 203. Longitudinal and lateral position changes resulting from relatively large longitudinal and lateral cyclic pitch control inputs (Figures 196, 198, 201, and 204) were not much larger than those obtained during normal position hold stabilization and were often difficult to detect by the LCC. Differential collective pitch pulses or steps (Figures 197 and 202) caused a 3.0-degree pitch attitude transient and resultant longitudinal position change that was corrected through longitudinal cyclic pitch (LCP). Vertical axis (collective pitch) differential test inputs resulted in larger vertical displacements from the trim reference, especially for the large magnitude input (1.5 inch equivalent cockpit control). The vertical motion was easier to detect by the LCC and often resulted in sensor unlock. Figure 199 shows a small and large magnitude "up pulse" time history response where the sensor unlocked in both cases and established a new vertical position reference. Aircraft vertical response to down pulses is presented in Figure 200. The first pulse (0.5 inch equivalent cockpit control) did not cause a sensor unlock. Vertical response to the second larger down pulse was well damped and returned quickly to its initial vertical trim position. A sensor unlock cycle occurred for an unknown reason, but could not be detected by the LCC since the unlock and relock happened when the aircraft position was near the initial reference condition. Aircraft response to a new vertical position resulted when a small magnitude vertical step (8.0 second duration) was commanded in the up direction (Figure 203). The response was well damped and the sensor did not unlock. Large magnitude step inputs (1.5 inch) could not be inserted without causing an unlock/relock PHS cycle due to vertical motion. The lateral AFCS differential command signals shown on Figures 198 and 204 exhibited a lightly damped 1.0 cycle/second oscillation not evident to the pilot. This lateral mode was more critical with an external load as discussed under load stabilization test results.

The ability of the LCC to maneuver the aircraft to a new position is shown on Figure 205. A single-axis longitudinal maneuver 17 feet forward and 32 feet aft is accomplished with a "creep" velocity of about 4.0 ft/sec. Time periods of transfer between either PHS or IMU/Radar velocities are

526

AUTOMATIC POSITION HOLD (PRECISION HOVER SENSOR)
347/ATC DEMONSTRATOR
FLT 828 REC 31
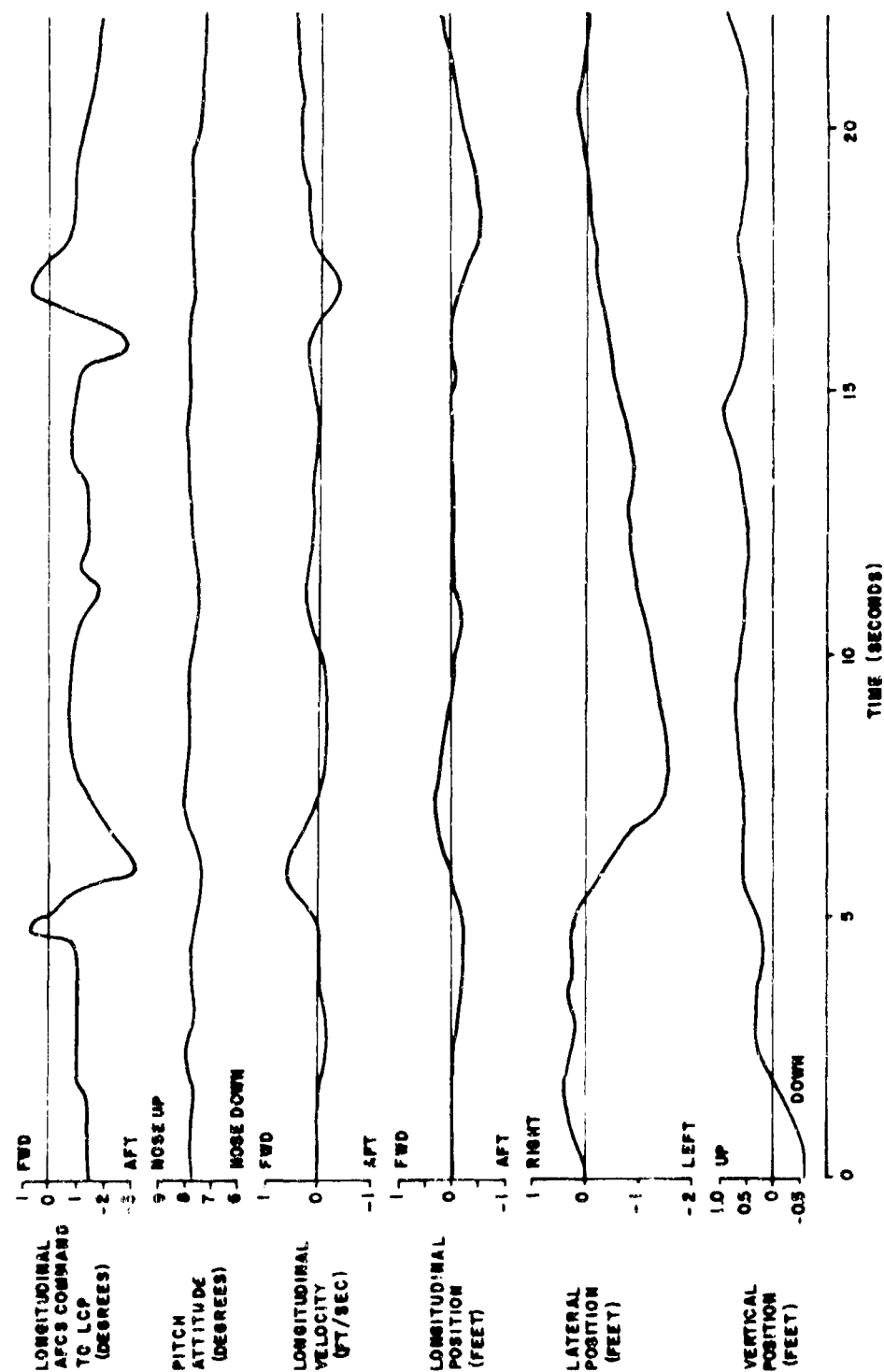
FIGURE 196.

AIRCRAFT RESPONSE TO AFCS LONGITUDINAL (LCP) DIFFERENTIAL PULSE

527

AUTOMATIC POSITION HOLD (PRECISION HOVER SENSOR)
347/ATC DEMONSTRATOR
FLT 928 REC 32
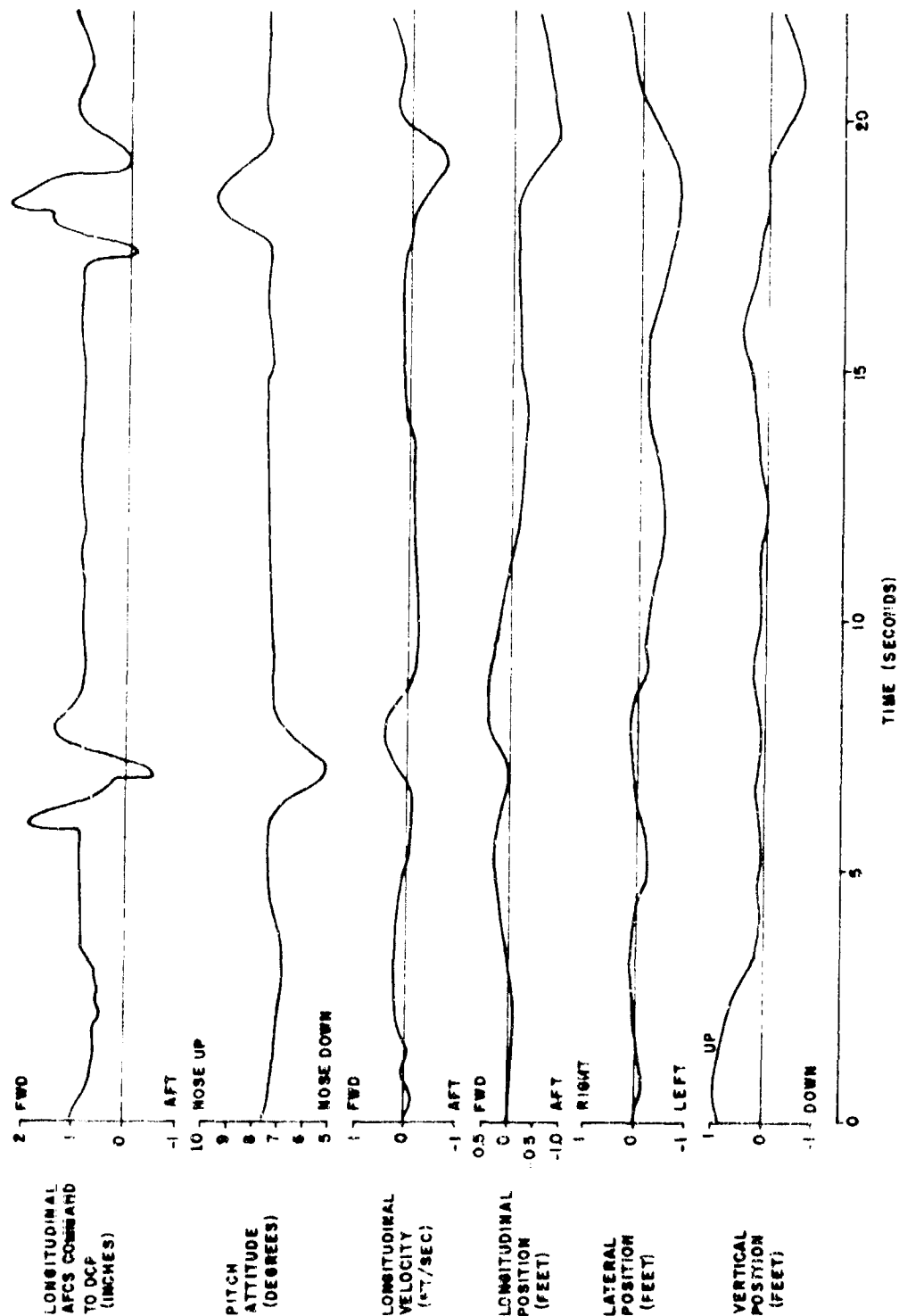
FIGURE 197.
AIRCRAFT RESPONSE TO AFCS LONGITUDINAL (DCP) DIFFERENTIAL PULSE

528

AUTOMATIC POSITION HOLD (PRECISION HOVER SENSOR)
347/ATC DEMONSTRATOR
FLT 873 REC 35
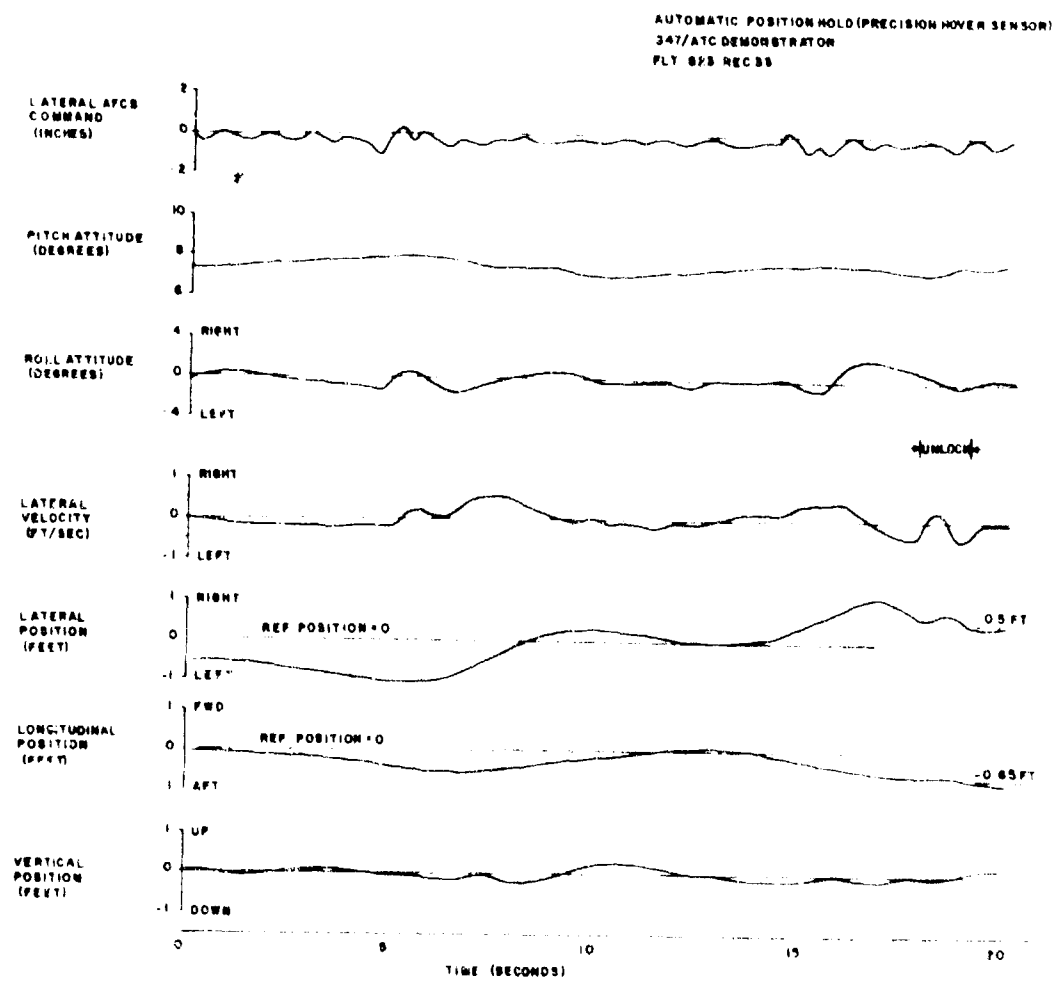
FIGURE 198.
AIRCRAFT RESPONSE TO AFCS LATERAL DIFFERENTIAL PULSE

529

FIGURE 199.

AIRCRAFT RESPONSE TO AFCS VERTICAL DIFFERENTIAL PULSE

530
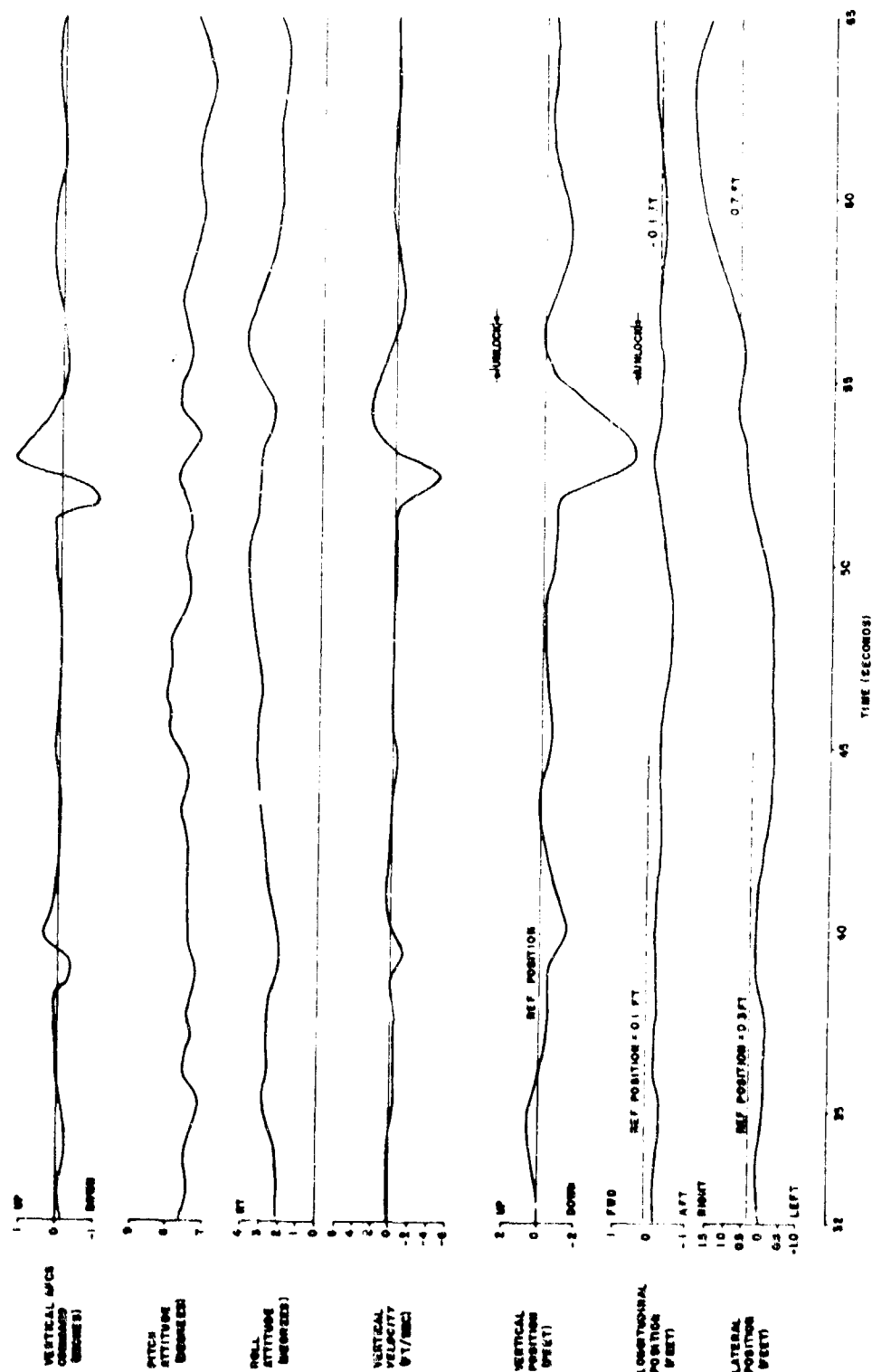
FIGURE 200.
AIRCRAFT RESPONSE TO AFCS VERTICAL DIFFERENTIAL PULSE

531
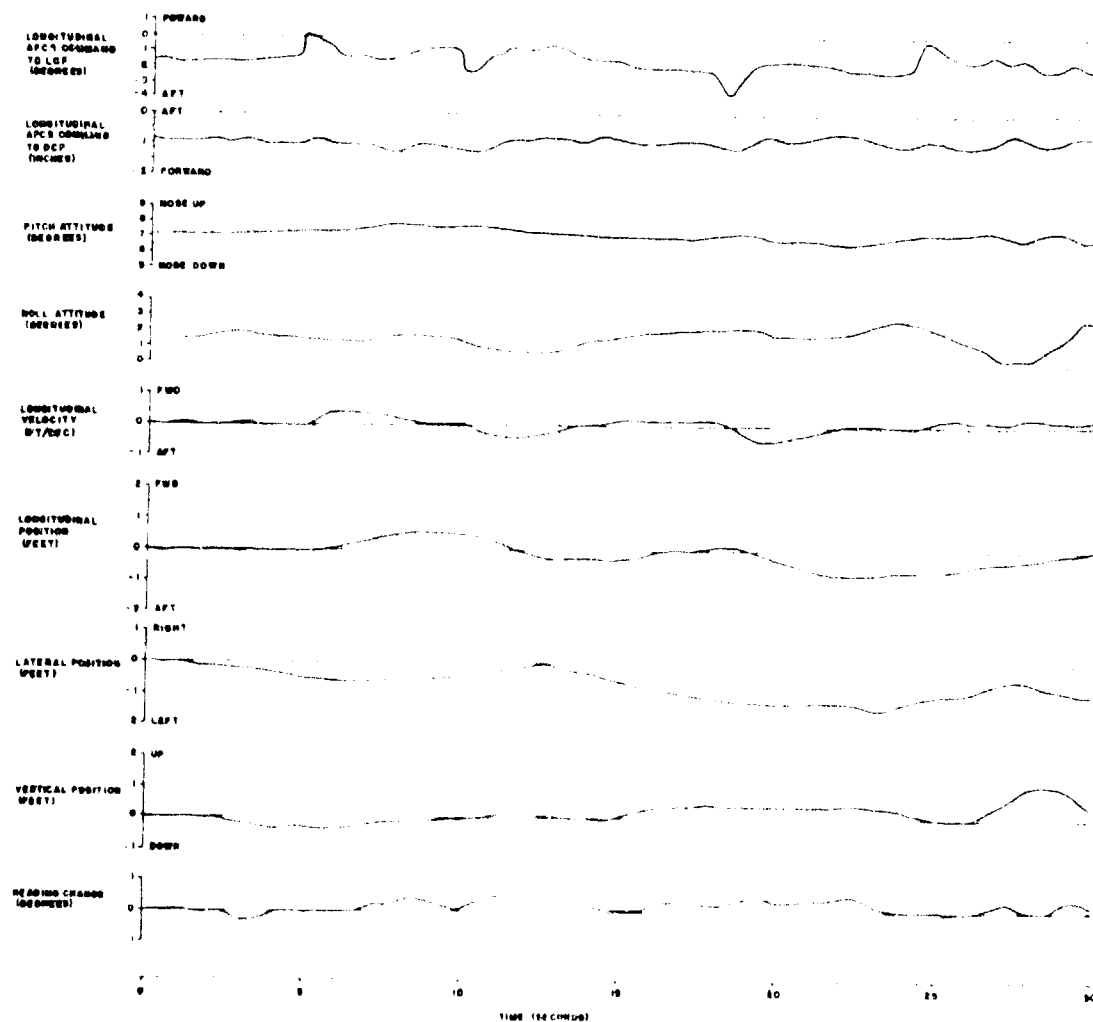
FIGURE 30H
AIRCRAFT RESPONSE TO AFCS LONGITUDINAL (LCP) DIFFERENTIAL STEP

532
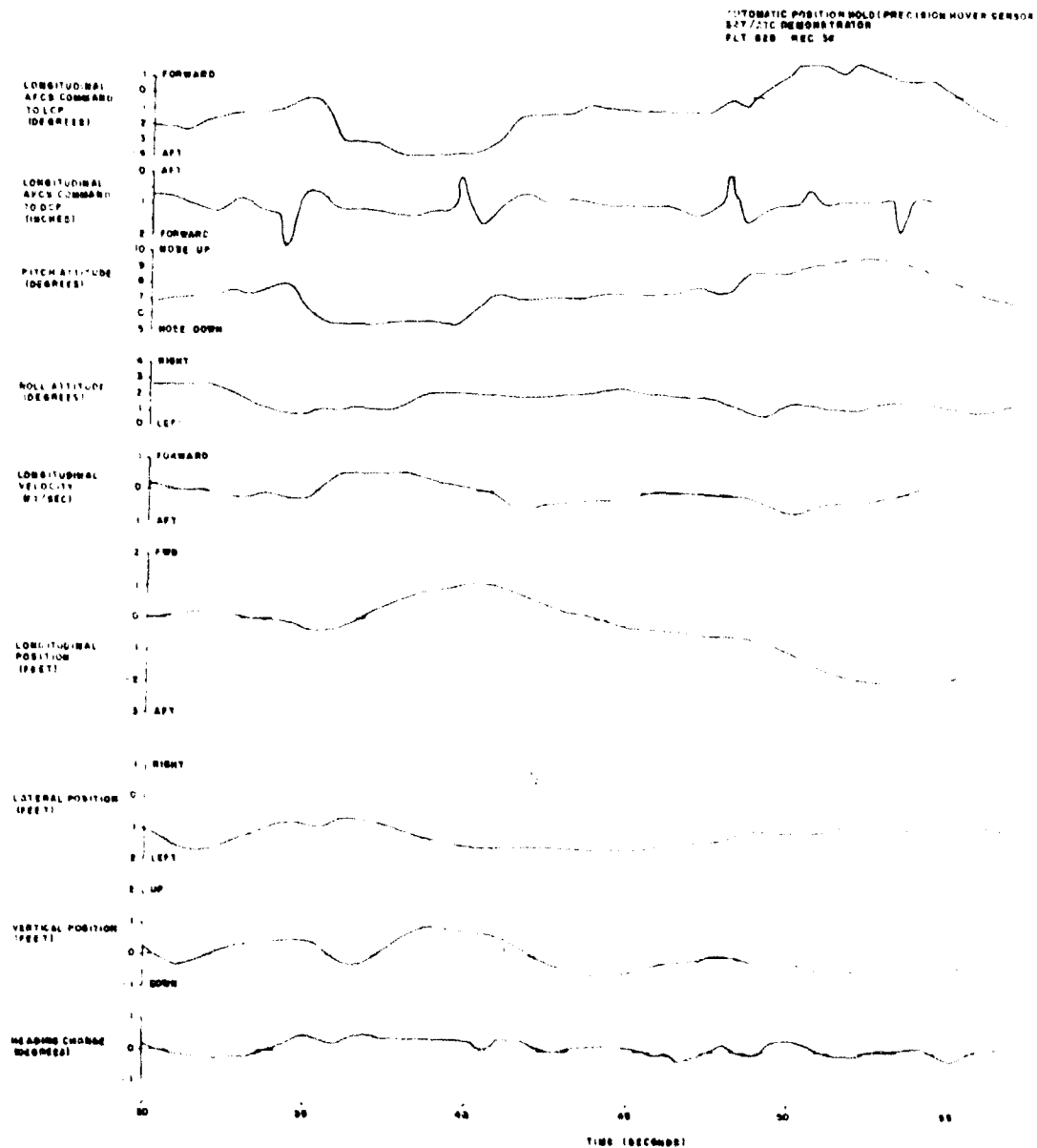
FIGURE 202
AIRCRAFT RESPONSE TO AFCS LONGITUDINAL (DCP) DIFFERENTIAL STEP
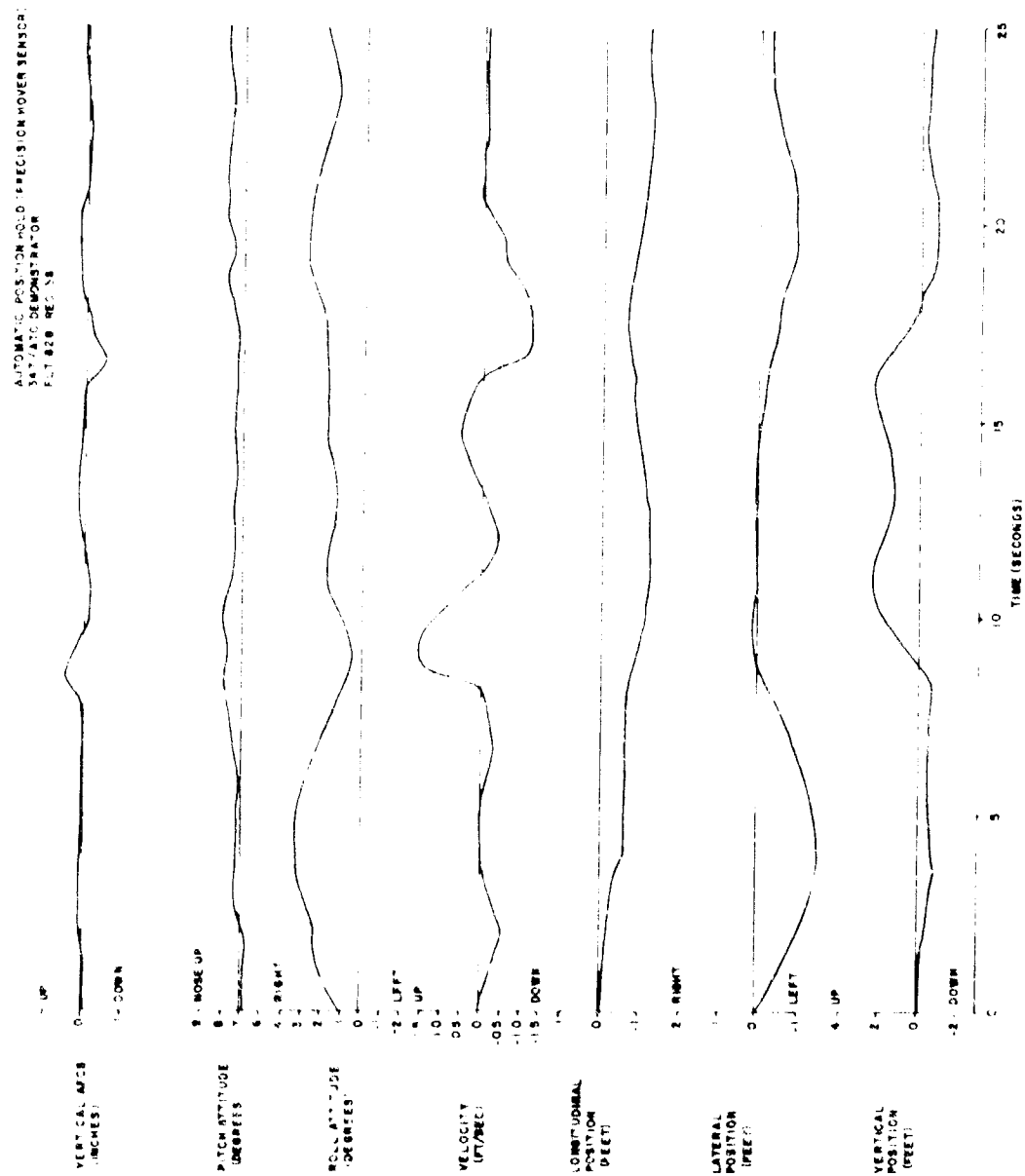
FIGURE 203
AIRCRAFT RESPONSE TO AFCS VERTICAL DIFFERENTIAL STEP

534
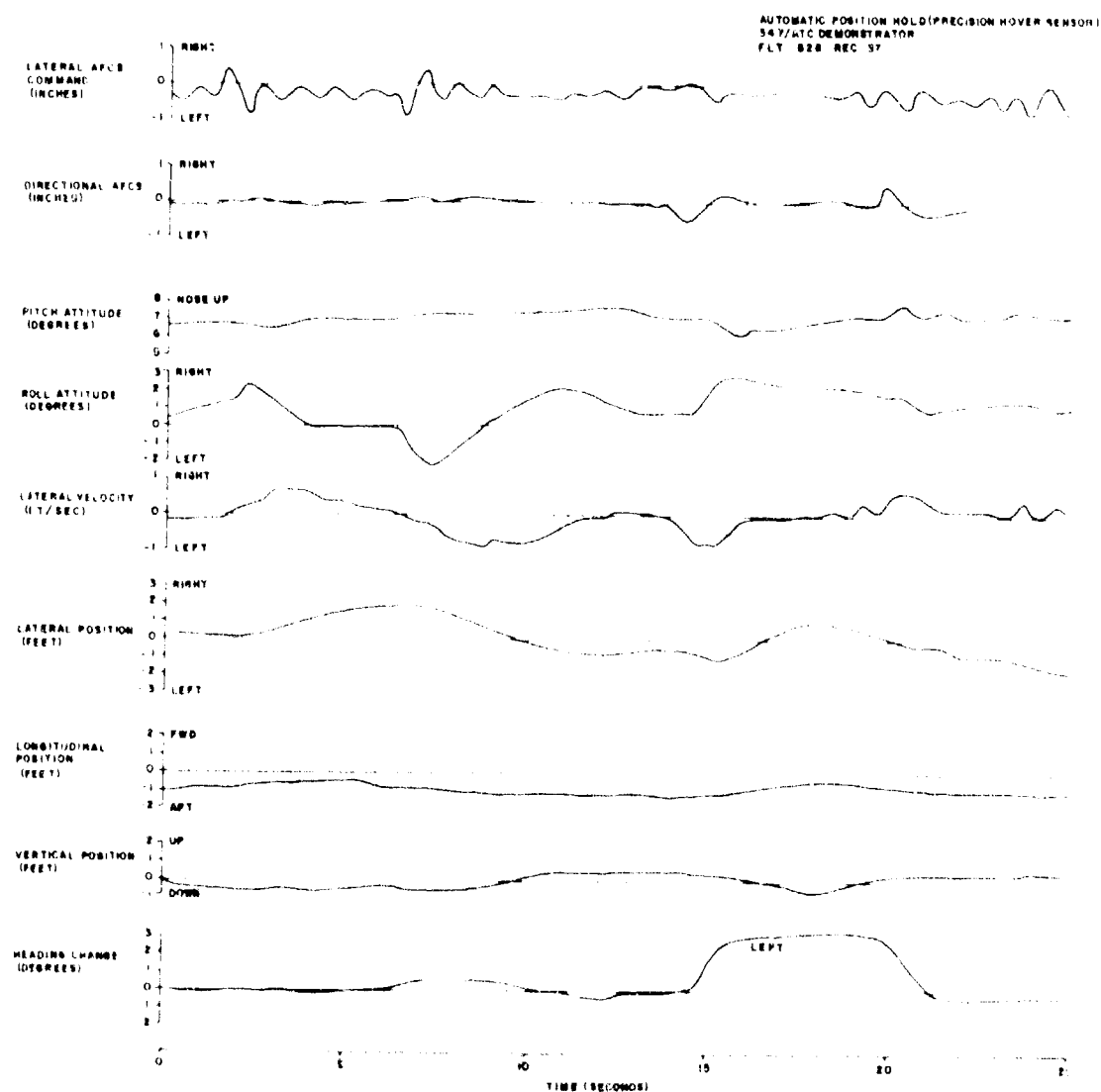
FIGURE 204.
AIRCRAFT RESPONSE TO AFCS LATERAL AND DIRECTIONAL DIFFERENTIAL STEP
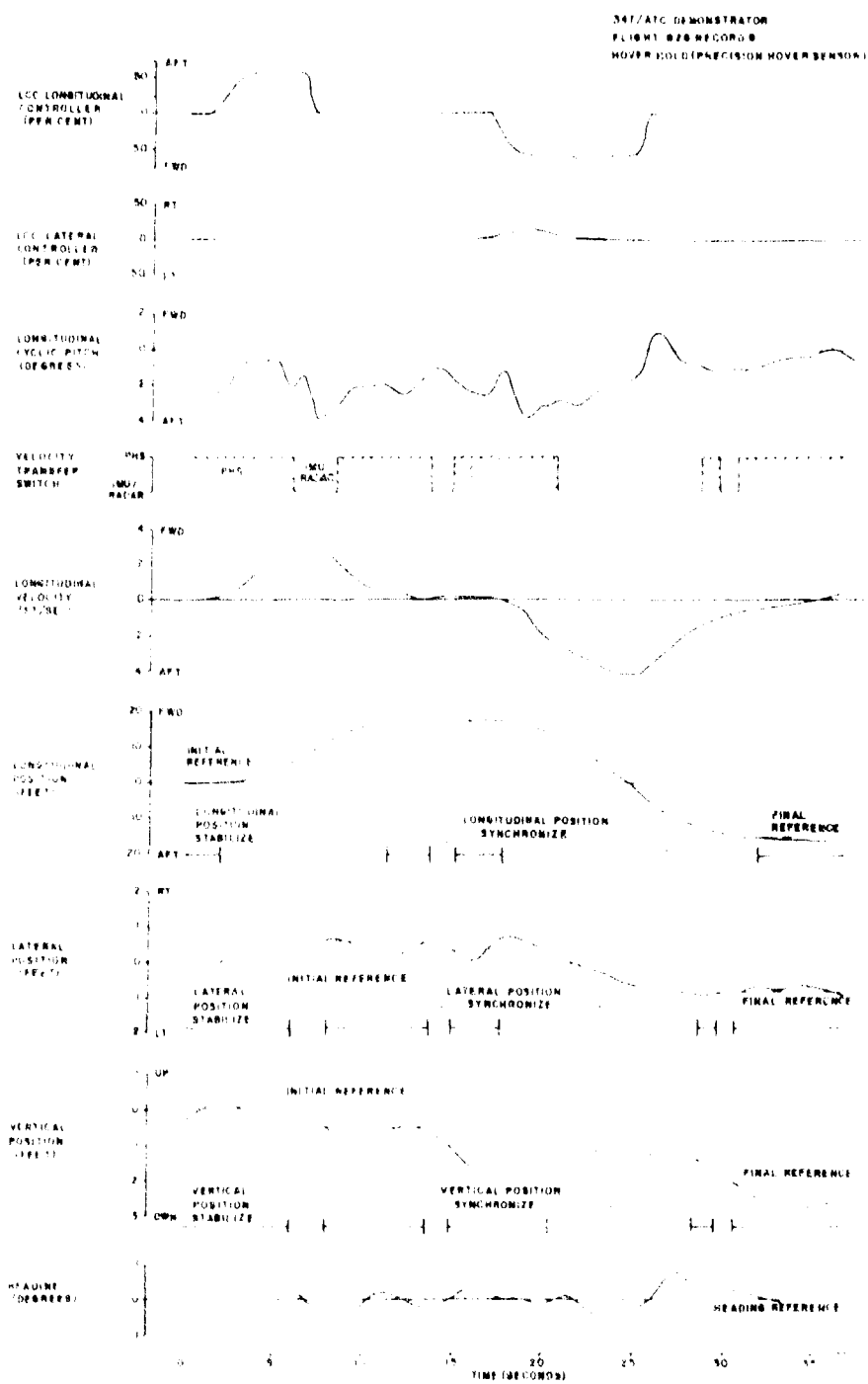
FIGURE 206. LCC LONGITUDINAL POSITION MANEUVER ON HOVER HOLD (PRECISION HOVER SENSOR)

5-36

indicated. Lateral and vertical PHS position references
shifted 0.8 feet left and 2.1 feet down, respectively, during
the maneuver. Position stability and synchronization cycles
due to PHS lock/unlock or LCC controller commands are shown
for each axis. While maneuvering aft, a small lateral con-
troller command caused lateral position synchronization and
drift to the left. Creep maneuvers on PHS exhibited occa-
sional small transients due to position loop synchronization.
Automatic drift clearing of the IMU during position stabili-
zation was a highly desirable feature.

5.3.4.4    Position Hold Comparisons

Aircraft positional hold accuracy was measured by photograph-
ing the bottom of the aircraft with a fixed focal length
70 mm camera fixed to the ground. Markings of known dimen-
sions were patterned on the bottom of the aircraft allowing
film data reduction for all motion variables. Photography
and data reduction were provided by personnel from the Naval
Air Development Center, Johnsville, Pa. Data from 2-minutete
runs were read at five times a second, RMS position data com-
puted, and horizontal plane data combined to form Circular
Error Probabilities (50-percent probability of being within
circle of radius = CEP).

Hands off position hold with PHS operating (Figure 206)
resulted in a CEP in the lateral and longitudinal axis of only
4.0 to 6.8 inches depending on turbulence level. Position
data is shown for a 3-second sample rate. The longitudinal axis
hold was approximately twice as good as lateral. Vertical
position varied from 2.5 to 4.3 inches RMS, and heading held
within 0.4 degree RMS. An aircraft altitude of 40 feet was
used for the test.

Similar data (Figure 207) was obtained without the PHS operat-
ing and the LCC in the loop to provide the positional correc-
tions required. CEP's in the lateral and longitudinal plane
vary from 14.9 to 17.3 inches for the same wind conditions.
Vertical and heading deviations of 16.2 inches and 0.32 degree
RMS resulted.

A comparison of helicopter position hold accuracy for the two
hover hold sub-modes of operation is given in Figure 208. The
position hold data, also shown in Figures 206 and 207, were
obtained from Flight 812 with the stronger wind turbulence
level. The position hold capability, as measured in terms of

537

347/ATC DEMONSTRATOR
VARIABLE WIND CONDITIONS AS NOTED
POSITION DATA SAMPLE 3 SECONDS
2-MINUTE RUN

WIND 10 TO 12 KN, GUSTING TO 24 KN

CEP (50%)

6.8 IN.

4.0 IN.

LONG (FT)

LAT (FT)

WIND 10 KN, MILD GUST

VERTICAL EXCURSION 4.3 IN. RMS
HEADING EXCURSION 0.36 DEG
FLIGHT 812 RECORD 11

VERTICAL EXCURSION 2.5 IN. RMS
HEADING EXCURSION 0.30 DEG
FLIGHT 795 RECORD 6
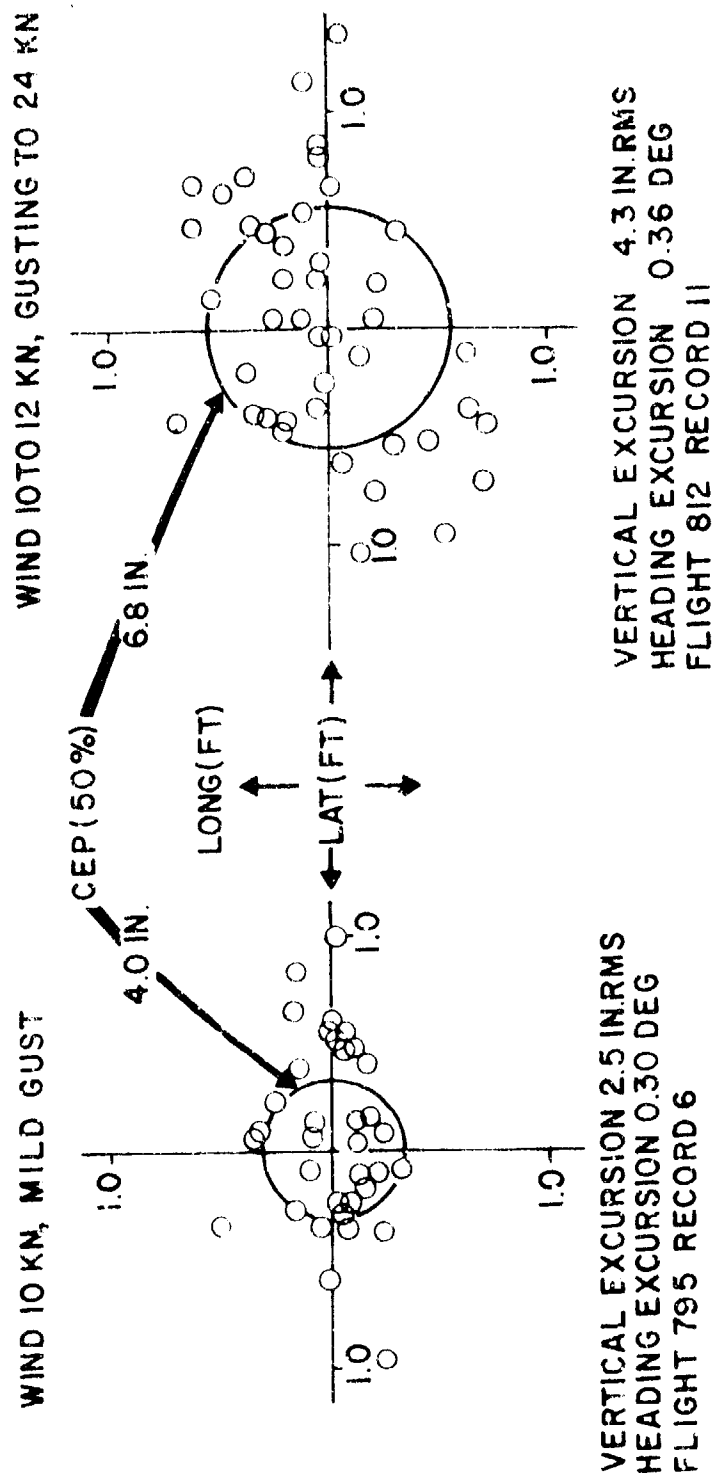
FIGURE 206.

HELICOPTER POSITION HOLD DATA WITH PRECISION HOVER SENSOR
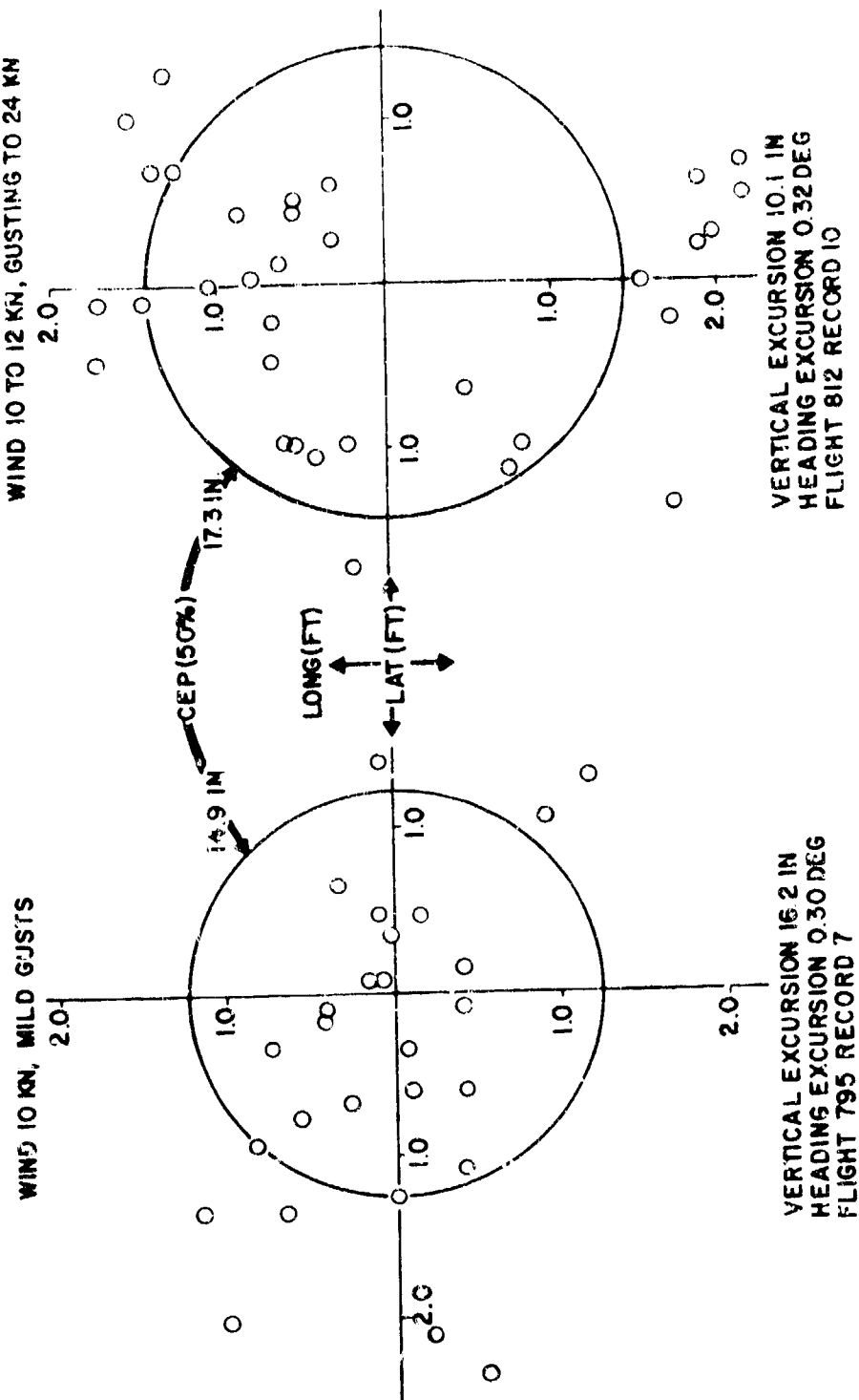
FIGURE 207.

HELICOPTER POSITION HOLD DATA WITH VELOCITY HOLD MODE 8 LCC CORRECTIONS

347/ATC DEMONSTRATOR
FLIGHT 812 RECORDS 10 & 11
WINDS 10 TO 12 KN, GUSTING TO 24 KN

POSITION HOLD-PHS
(HANDS OFF)

CEP (50%)

6.8 IN.

17 IN

LONG (FT)

LAT (FT)

VELOCITY HOLD- IMU/RADAR
(LCC CORRECTION)

1.0
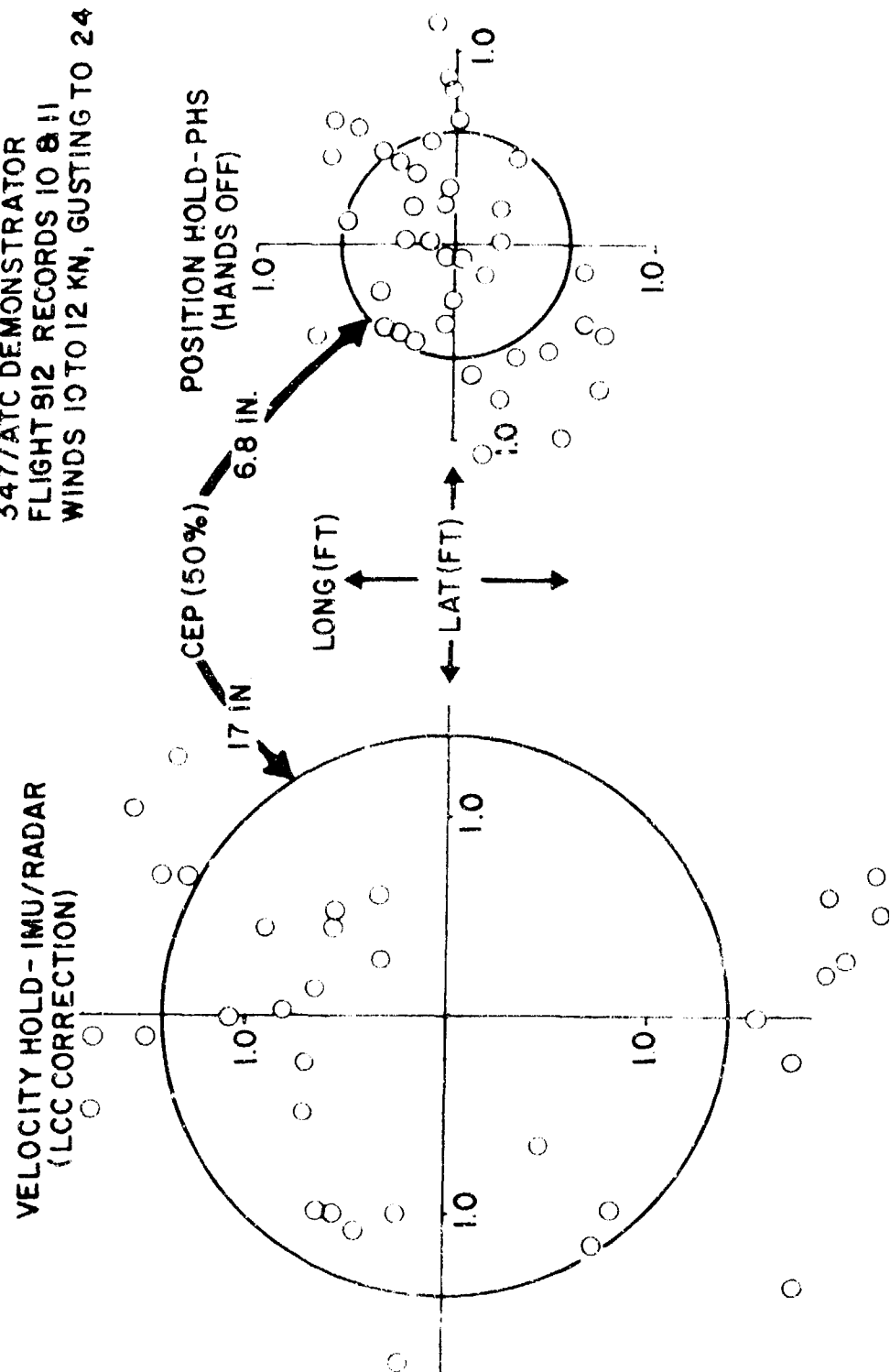
FIGURE 208. HELICOPTER POSITION HOLD COMPARISON
VELOCITY HOLD (IMU) VS POSITION HOLD (PHS)

540

CEP shows that the automatic position hold mode using the PHS was better than the velocity hold mode by a factor of 2.5. RMS position data was also computed for the longitudinal and lateral axes, as well as vertical and heading. A complete summary of the helicopter position data is given in Table 27.

Vertical hold performance with PHS was much better and is reflected by the higher position gain (factor of 3.0) shown in Table 25. Higher radar altitude gains on the velocity hold mode could not be used without increasing vertical excursions due to radar altitude spikes.

Data taken from Flight 812 with <u>pilot in control on basic SCAS</u> showed CEP's near 4 feet (Figure 209). The hold performance by the LCC on hover hold is significantly better than the pilot on SCAS due to improved visibility and velocity hold gains which are six times higher. Table 28 presents the comparison between basic SCAS and Hover Hold velocity gains normalized to linear acceleration per unit change in linear velocity.

Even though very good position hold capability could be attained with the LCC in the loop, the requirement for LCC corrections to hold position and to drift-clear the velocity reference to compensate for inherent IMU drift is shown by Figure 210. The data taken from Flight 795 was for a hands-off hover under mild turbulence after the LCC had trimmed the aircraft to zero velocity and performed a drift clear. During the next 75 seconds, the aircraft drifted as much as 1.4 feet in the longitudinal direction, and 4.0 feet laterally.

The validity of the position hold results obtained on the simulator is illustrated on Figure 211. Flight test position hold CEP data are superimposed on earlier simulation data for a position hold task using the automatic position hold, high gain velocity, and basic SCAS modes. Excellent trend correlation between flight and simulation data is evident with the simulation being somewhat optimistic. This is due in part to the higher simulation gains on position and velocity hold modes as noted previously (Table 25). The better simulator performance on Basic SCAS is due primarily to better visual information available (position tracking scope) than that in flight.

TABLE 27. HELICOPTER POSITION HOLD SUMMARY

| HOVER HOLD MODE | WINDS 10 KNOTS STEADY GUSTING TO 13 KNOTS FLIGHT 795 RECORDS 6 & 7 | | | | WINDS 10 TO 12 KNOTS STEADY GUSTING TO 20 TO 24 KNOTS FLIGHT 812 RECORDS 10 & 11 | | | |
|---|---|---|---|---|---|---|---|---|
| | $\sigma_X$ INCHES | $\sigma_Y$ INCHES | $\sigma_Z$ INCHES | $\sigma_\psi$ DEG | $\sigma_X$ INCHES | $\sigma_Y$ INCHES | $\sigma_Z$ INCHES | $\sigma_\psi$ DEG |
| AUTOMATIC POSITION HOLD (PHS) | 1.94 $CEP_{XY}=3.98$ | 4.94 | 2.46 | 0.30 | 4.09 $CEP_{XY}=6.76$ | 7.53 | 4.33 | 0.36 |
| VELOCITY HOLD (LCC CONTROL) | 7.24 $CEP_{XY}=14.86$ | 18.44 | 16.21 | 0.30 | 12.65 $CEP_{XY}=17.30$ | 16.86 | 10.07 | 0.32 |

347/ATC DEMONSTRATOR
FLIGHT 812
WIND: 10 TO 12 KN, GUSTING TO 24 KN
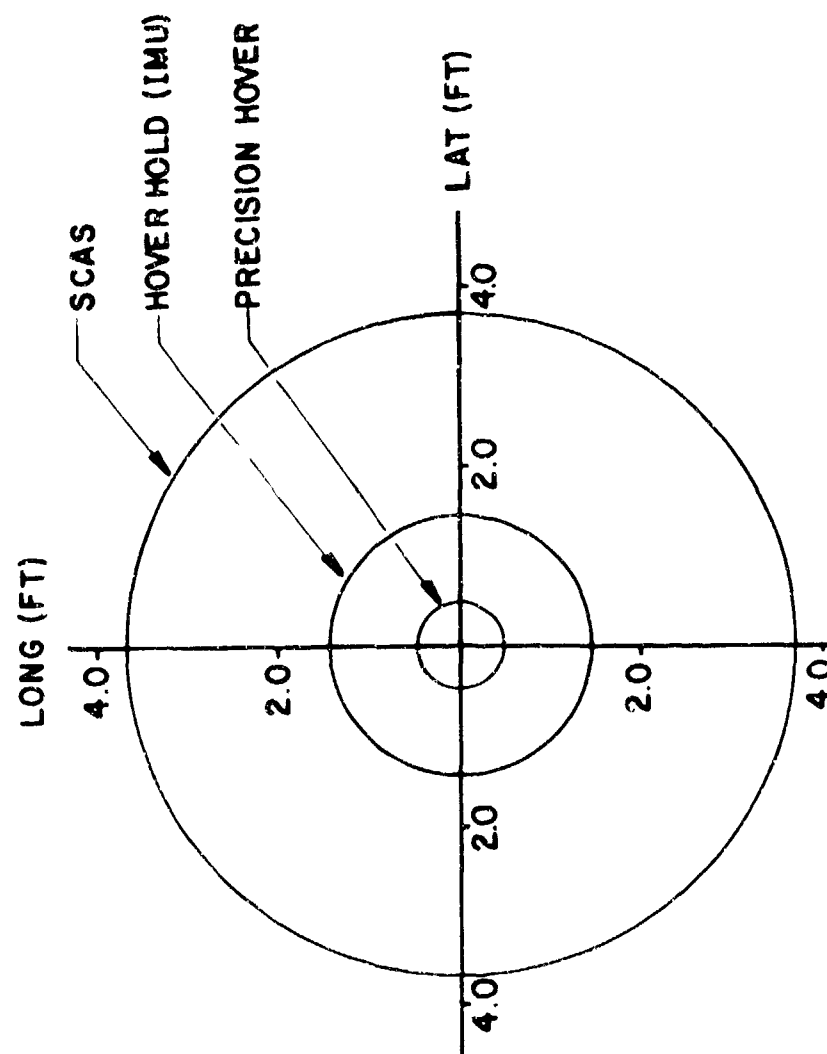
FIGURE 209.
HELICOPTER POSITION HOLD SUMMARY
CIRCULAR ERROR PROBABILITY

# TABLE 28.

## COMPARISION OF HOVER HOLD AND BASIC SCAS VELOCITY GAINS

| AXIS | VELOCITY GAINS | | | | BASIC AIRCRAFT/SCAS DATA |
|---|---|---|---|---|---|
| | HOVER HOLD MODE | | BASIC SCAS MODE (LOW SPEED) | | |
| | $\dfrac{\text{DEG LCP}}{\text{FT/SEC}}$ | $\dfrac{\text{FT/SEC}^2}{\text{FT/SEC}}$ | $\dfrac{\text{IN } \delta_B}{\text{FT/SEC}}$ | $\dfrac{\text{FT/SEC}^2}{\text{FT/SEC}}$ | |
| LONGITUDINAL | 1.93 | 1.08 | 0.1 | 0.176 | LONGITUDINAL CYCLIC CONTROL SENSITIVITY ($X_{BIC}$) 32.2 $\dfrac{\text{FT/SEC}^2}{\text{RAD LCP}}$<br><br>PITCH ATTITUDE GAIN ($K\theta$) BASIC SCAS 0.32 $\dfrac{\text{INCHES } \delta_B}{\text{DEG}}$ |
| | $\dfrac{\text{IN } \delta_s}{\text{FT/SEC}}$ | $\dfrac{\text{FT/SEC}^2}{\text{FT/SEC}}$ | $\dfrac{\text{IN } \delta_s}{\text{FT/SEC}}$ | $\dfrac{\text{FT/SEC}^2}{\text{FT/SEC}}$ | |
| LATERAL | 0.77 | 1.08 | 0.1 | 0.16 | ROLL ATTITUDE GAIN ($K\phi$) HOVER HOLD 0.4 $\dfrac{\text{INCHES } \delta_s}{\text{DEG } \phi}$<br><br>BASIC SCAS 0.35 $\dfrac{\text{INCHES } \delta_s}{\text{DEG } \phi}$ |
| | $\dfrac{\text{IN } \delta_c}{\text{FT/SEC}}$ | $\dfrac{\text{FT/SEC}^2}{\text{FT/SEC}}$ | $\dfrac{\text{IN } \delta_c}{\text{FT/SEC}}$ | $\dfrac{\text{FT/SEC}^2}{\text{FT/SEC}}$ | |
| VERTICAL | 0.18 | 1.47 | 0.18 | 1.47 | VERTICAL CONTROL SENSITIVITY ($Z\delta_c$) 8.18 $\dfrac{\text{FT/SEC}^2}{\text{INCHES } \delta_c}$ |
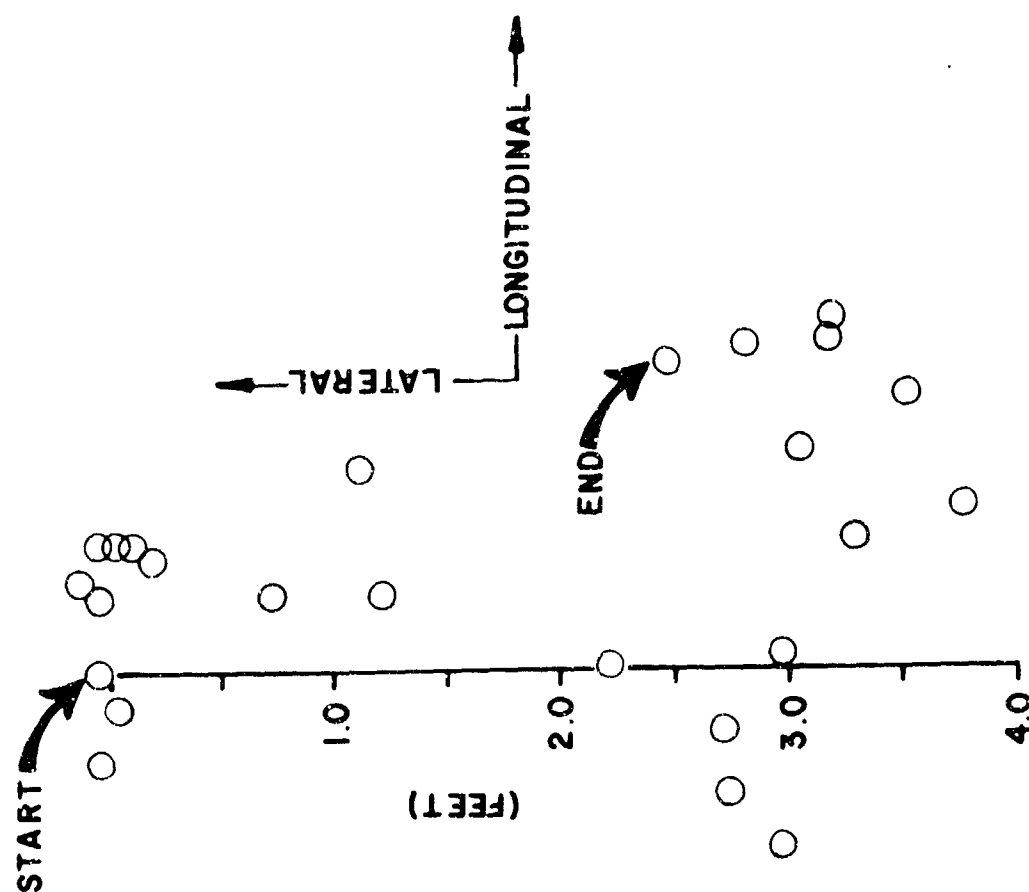
FIGURE 210.
VELOCITY HOLD MODE (IMU)

- 347/ATC DEMONSTRATOR
- FLIGHT 795
- HANDS OFF HOVER
- POSITION SAMPLE RATE: 3 SEC
- WIND: 10 KNOTS, MILD GUST

545

347/M-H ATC SIMULATION DATA (NOV '71-MAY '73)
347 FLIGHT TEST (DATA FROM PHOTOGRAPHIC MEASUREMENTS - OCT '74)

LONGITUDINAL

LATERAL

CEP = 3.98 IN
FLIGHT 795

SIMULATION
DATA

AUTOMATIC POSITION HOLD
PRECISION HOVER SENSOR

CEP = 14.86 IN
FLIGHT 793

SIMULATION
DATA

HIGH GAIN VELOCITY HOLD
(WITH PILOT CORRECTIONS)
IMU VELOCITY

SIMULATION DATA

CEP = 44 IN
FLIGHT 812

CONVENTIONAL ATTITUDE OR LOW GAIN
VELOCITY (WITH PILOT CORRECTIONS)
BASIC SCAS MODE

FIGURE 211

POSITION HOLD TASK - COMPARISON OF SIMULATION AND FLIGHT TEST DATA

### 5.3.5  Load Stabilization System

#### 5.3.5.1  Load/Cable Configurations and Test Conditions

##### 5.3.5.1.1  Confi;u.tions

Several cable lengths were used during the LSS flight testing
to obtain load handling information as a function of cable
length.  The cable lengths were:

- 10-foot inverted vee (11 feet forward and 9 feet aft)
- 20-foot inverted vee
- 3ɔ feet formed by 10-foɔ. vee with 20-foot riser
- 55 feet formed by 10-foot vee with 45-foot riser

Complete sling configuration details are contained in
Reference 11.  The evaluation with the 55-foot cables was very
brief since the load interfered with the radar altimeter when
it swung longitudinally on these long cables.  The 10-foot
cables were used for forward flight and were the primary con-
figuration for load positioning using the hover hold mode.
This is representative of the best HLH configuration for load
control.  Load positioning was also performed with the 30-foot
cables; however, this configuration was used primarily to
evaluate load position hold and aircraft/load centering.  The
30-foot cables are representative of the HLH requirement for
confined area maneuvering.  While the above cables were used
as a two-point suspension system, a 30-foot (total vertical
length) single point trolley suspension with a high density
load was evaluated in hover and forward flight.

An 8 x 8 x 20-foot MILVAN which weighs 4,600 pounds empty was
the primary load.  Because of the test aircraft's gross weight
limit, only a relatively small range of load weights were
evaluated; from the empty MILVAN without a top adapter (4,600
pounds) to high density Kirksite blocks (8,000 pounds).  The
load weight was 5,800 pounds (empty MILVAN with adapter) for
most of the flight evaluation.

##### 5.3.5.1.2  Test Conditions

A wide range of flight conditions and load handling tasks
were evaluated, including load acquisition, shuttling, posi-
tion hold, and positioning.  Turns, sideslips, climbs, and
descents were performed in forward flight and the load was
flown to the power-limited maximum airspeed.  Both VFR and

simulated IFR departures and approaches were performed. Load
damping and handling were evaluated for all AFCS modes of
operation including the three LSS sub-modes; damping, position
hold, and centering. The majority of testing was concentrated on
load operations with Hover Hold mode.

5.3.5.2  Load Damping Evaluations

5.3.5.2.1  Damping Measurements

Load damping and frequency were measured for all cable con-
figurations and modes by swinging the load axis by axis.  It
was found that AFCS pulses and LCC inputs were generally
inadequate for producing good load swings to measure damping
so the cockpit pilot provided the load excitation in most
cases.  In some cases, large amplitude swings were produced
by lifting the load off the ground with the aircraft offset
relative to the load.  Some representative time histories are
shown as noted below where LSS-off cases are superimposed on
the LSS-on cases.

| FIGURE | EXCITATION AXIS | AFCS MODE | CABLE LENGTH |
|--------|-----------------|-----------|--------------|
| 212 | Longitudinal | Hover Hold | 30 Feet |
| 213 | Lateral | Hover Hold | 30 Feet |
| 214 | Directional | Hover Hold | 30 Feet |
| 215 | Longitudinal | Basic SCAS - 60 kn | 10 Feet |
| 216 | Lateral | Basic SCAS - 60 kn | 10 Feet |

The increased damping, and decreased settling time, provided
automatically by the LSS, can be seen.  The associated air-
craft attitude response and AFCS differential input to the
aircraft are included in these time histories.  LSS damping
contributions were rated as good by pilot (A-3 to A-4).

The damping results are summarized by the following figures.

548

FIGURE 212. LONGITUDINAL LOAD STABILIZATION SYSTEM - HOVER HOLD

347/ATC DEMONSTRATOR (38,000 LB) • 30 FT CABLES • 5000-LB MILVAN
——————— LOAD STABILIZATION ON - FLIGHT 831 RECORD 3
— — — — LOAD STABILIZATION OFF - FLIGHT 834 RECORD 4

LOAD EXCITATION BY PILOT INPUT STOPPED AT TIME = 0

TIME (SECONDS)

LONGITUDINAL
ACCELERATION
AT COCKPIT
(FT/SEC2)

LONGITUDINAL
CABLE ANGLE
(DEGREES)

LONGITUDINAL
CYCLIC
(DEGREES)

LONGITUDINAL
AFCS OUTPUT
(INCHES)

550
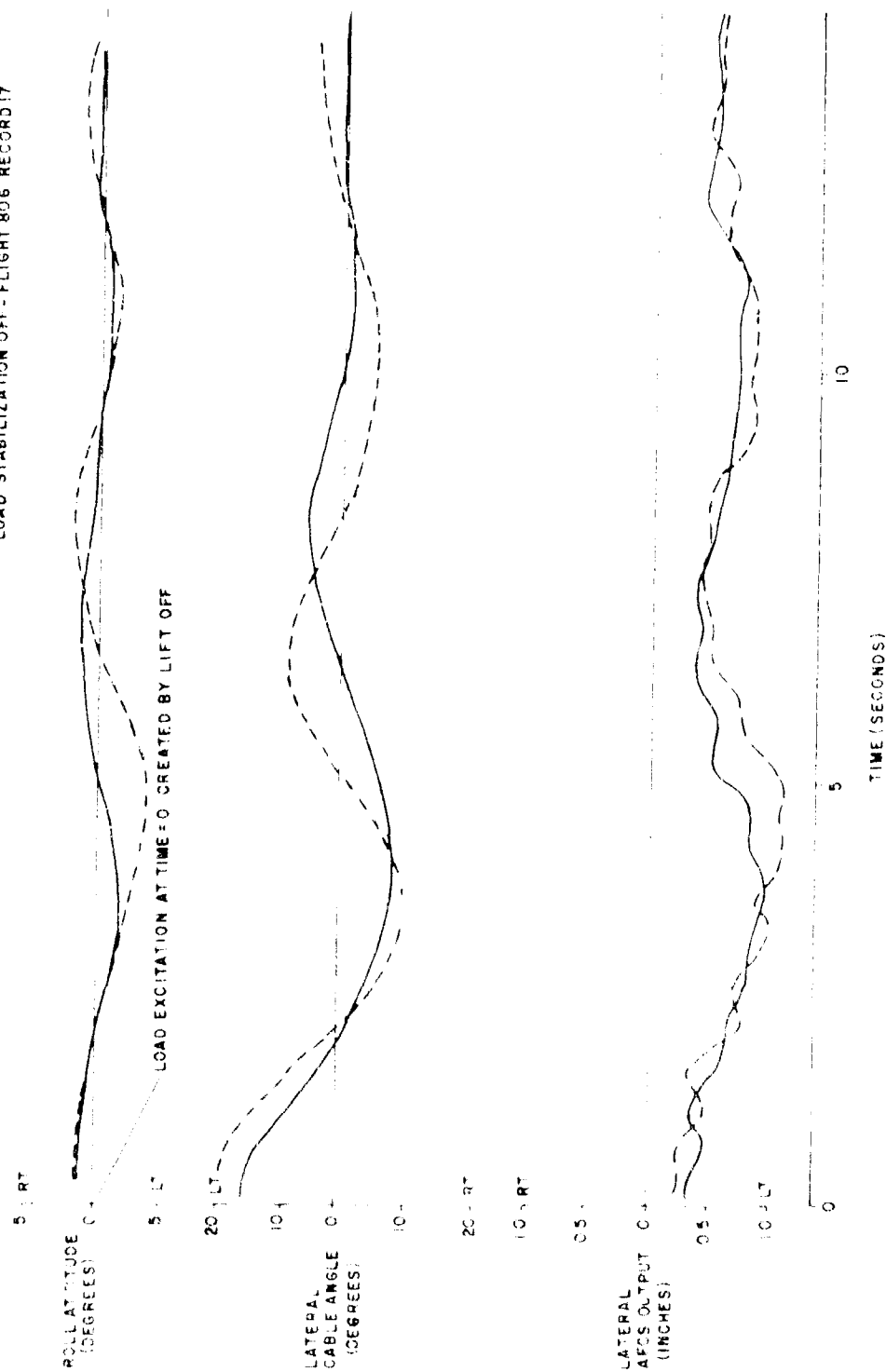
FIG 213 LATERAL LOAD STABILIZATION SYSTEM - HOVER HOLD
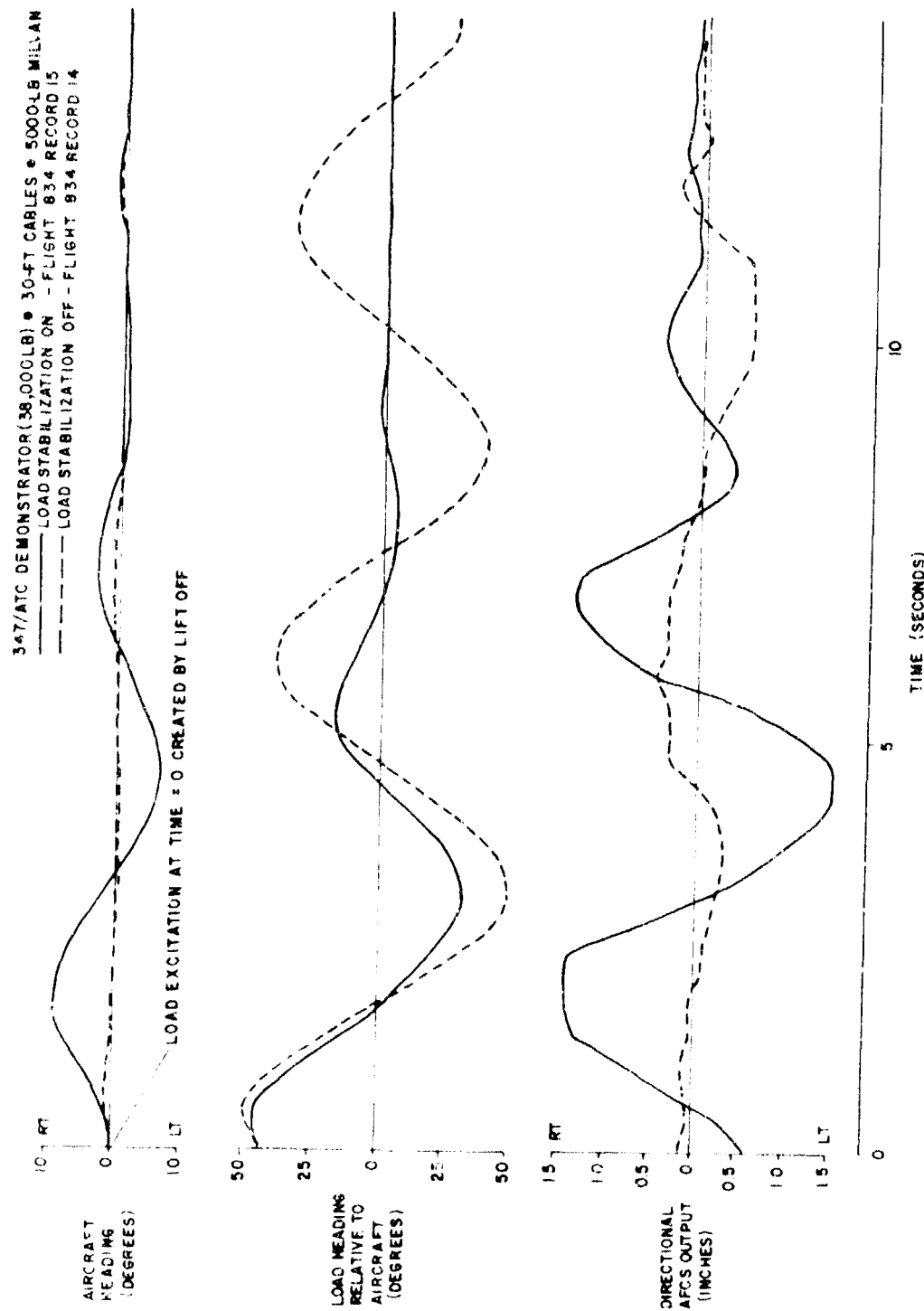
FIGURE 214. DIRECTIONAL LOAD STABILIZATION SYSTEM – HOVER HOLD
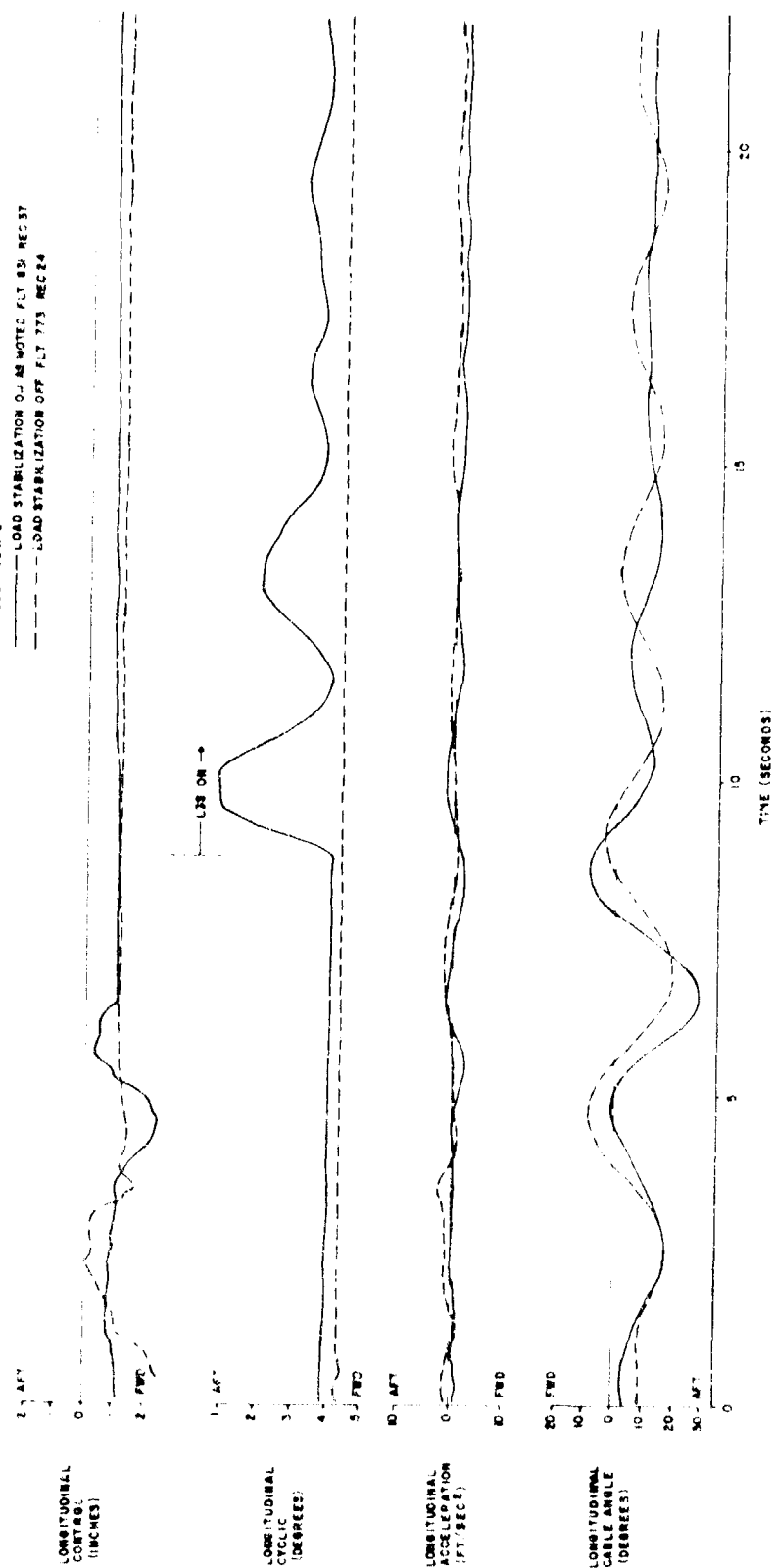
FIGURE 215.

LOAD STABILIZATION SYSTEM - LONGITUDINAL RESPONSE - FORWARD FLIGHT- BASIC SCAS

FIGURE 216. LOAD STABILIZATION SYSTEM - LATERAL RESPONSE - FORWARD FLIGHT- BASIC SCAS

553

| FIG. | A/S | MODE | LOAD | SUSPENSION | DATA |
|------|-----|------|------|------------|------|
| 217 | Hover | SCAS | MILVAN | Two Point<br>10 ft to 55 ft | Damping |
| 218 | Hover | SCAS | MILVAN | Two Point<br>10 ft to 55 ft | T 1/2 |
| 219 | Hover | SCAS | MILVAN | Two Point<br>10 ft to 55 ft | Frequency |
| 220 | Hover | Hover Hold | MILVAN | Two Point<br>10 ft to 55 ft | Damping |
| 221 | Hover | Hover Hold | MILVAN | Two Point<br>10 ft to 55 ft | T 1/2 |
| 222 | Hover | Hover Hold | MILVAN | Two Point 30 ft | Damping |
| 223 | Hover | Pos. Hold | MILVAN | Two Point 10 ft | T 1/2 |
| 224 | 60-90 kn | Basic SCAS | MILVAN | Two Point 10 ft | Frequency |
| 225 | 0 to 90 | SCAS/Hover Hold | High Density | Trolley 30 ft | |

The measured damping ratio spread shown reflects some uncer-
tainty in measurements and lack of precise repeatability
For several cases, the damping ratio is shown as being
greater than 25 percent critical because the exact damping
ratio becomes less certain and less important above the 25
percent level. The 20- and 55-foot cable configurations were
evaluated initially and very briefly so the LSS-on results
for these configurations do not benefit from the final system
improvements. It is anticipated that the LSS-on damping for
these cable lengths could be increased if some parameter varia-
tions were made.

The LSS significantly increases the load damping in almost all
cases, particularly when the basic damping is low. The load
is basically stable, i.e., at least neutrally damped, in all
cases and well damped in a few cases with the LSS off. The
dashed lines represent the MIL-H-8501A IFR minimum damping

554
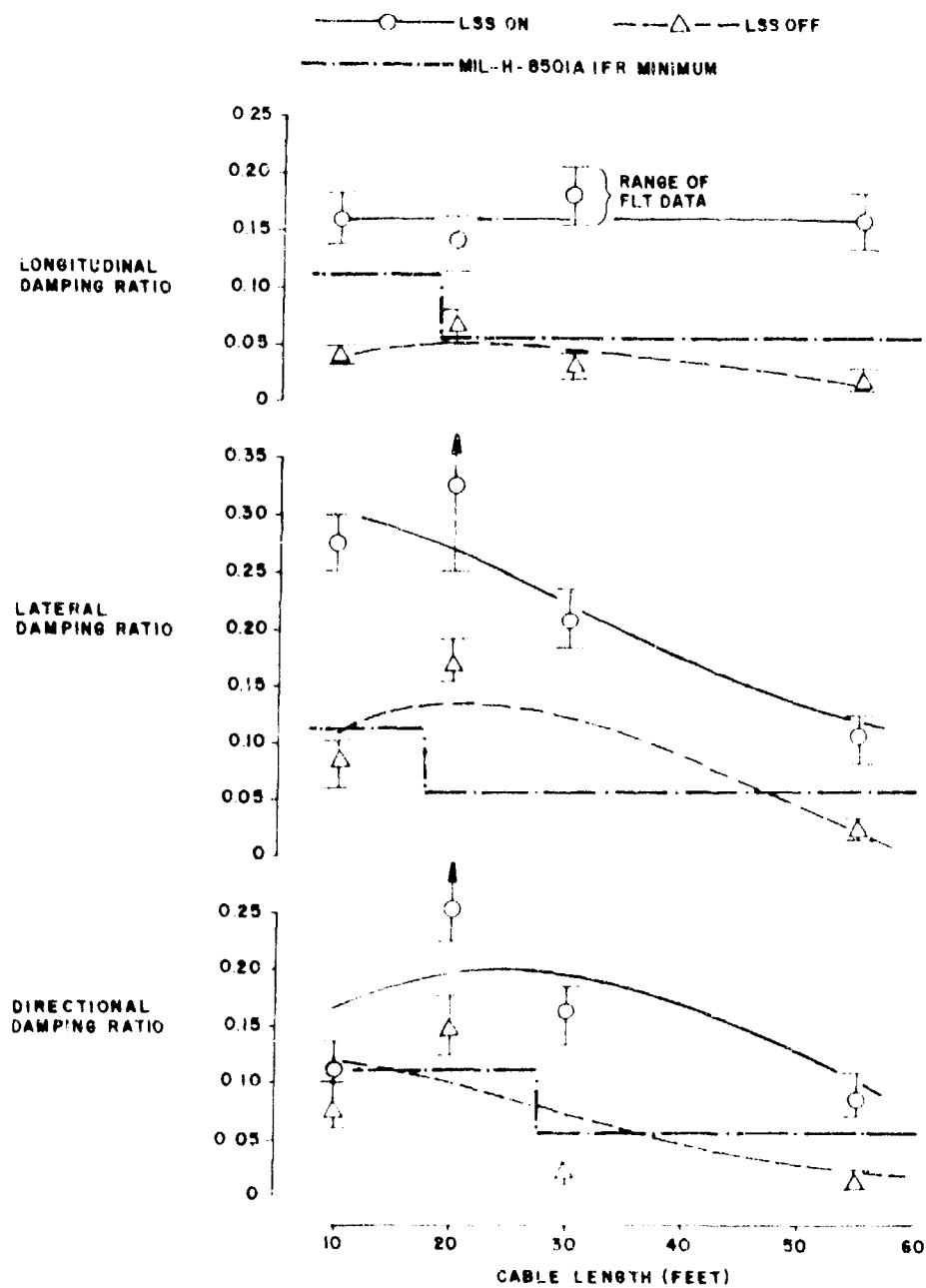
FIGURE 217.
LOAD DAMPING SUMMARY - SCAS - HOVER
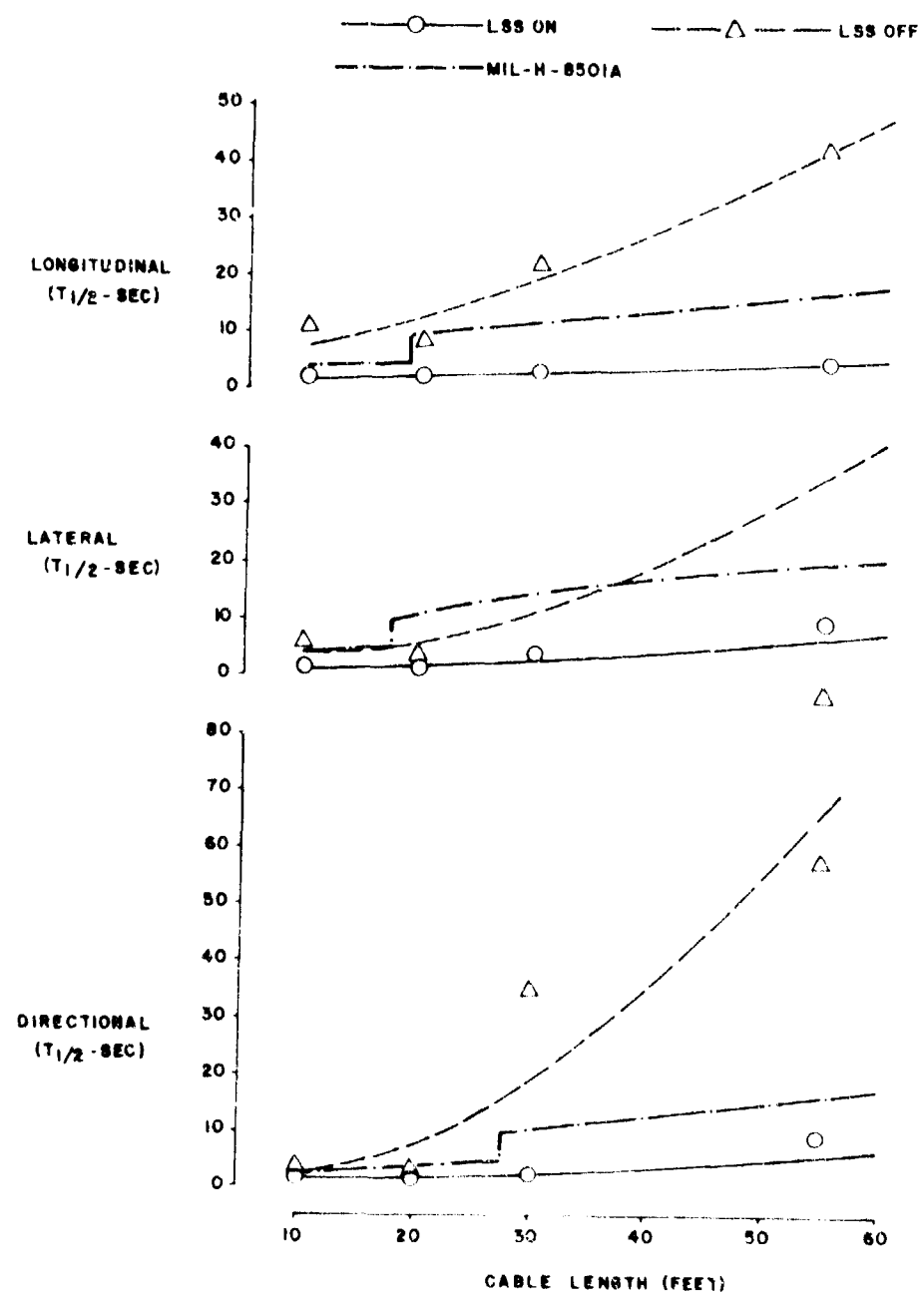
FIGURE 2i8.
LOAD TIME-TO-HALF  AMPLITUDE - SCAS

556
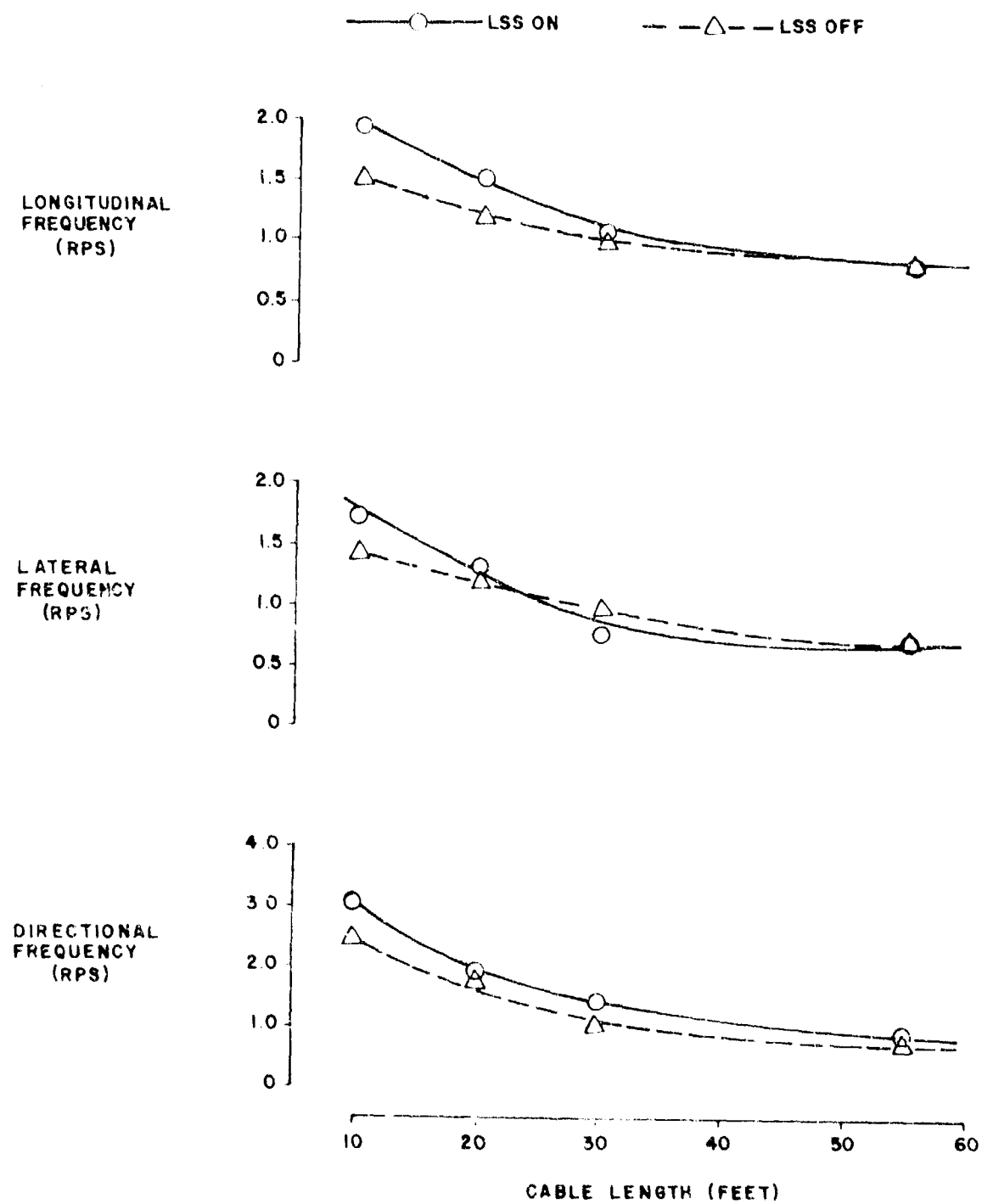
FIGURE 219.
LOAD PENDULUM FREQUENCY – SCAS
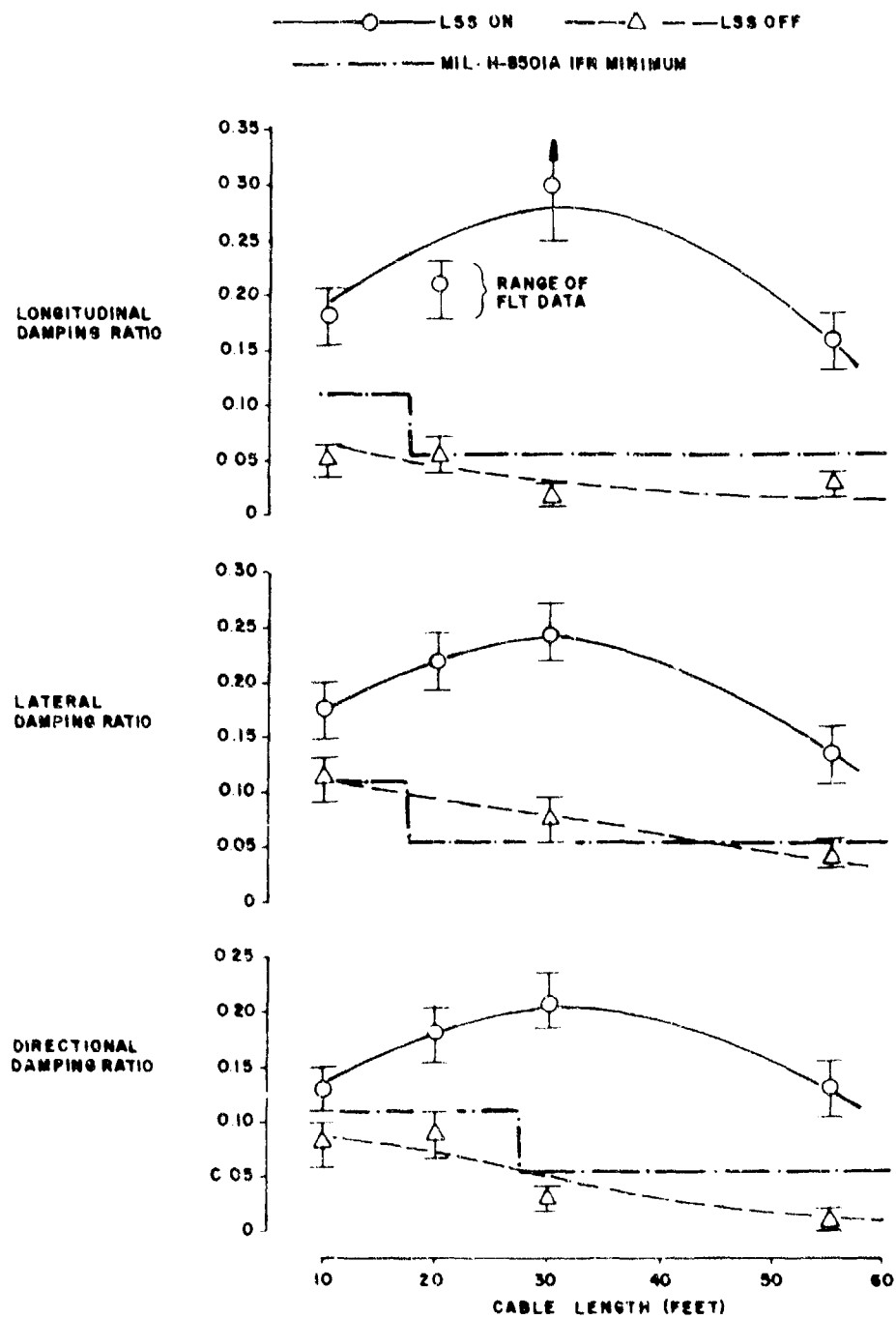
FIGURE 220
LOAD DAMPING SUMMARY - HOVER HOLD
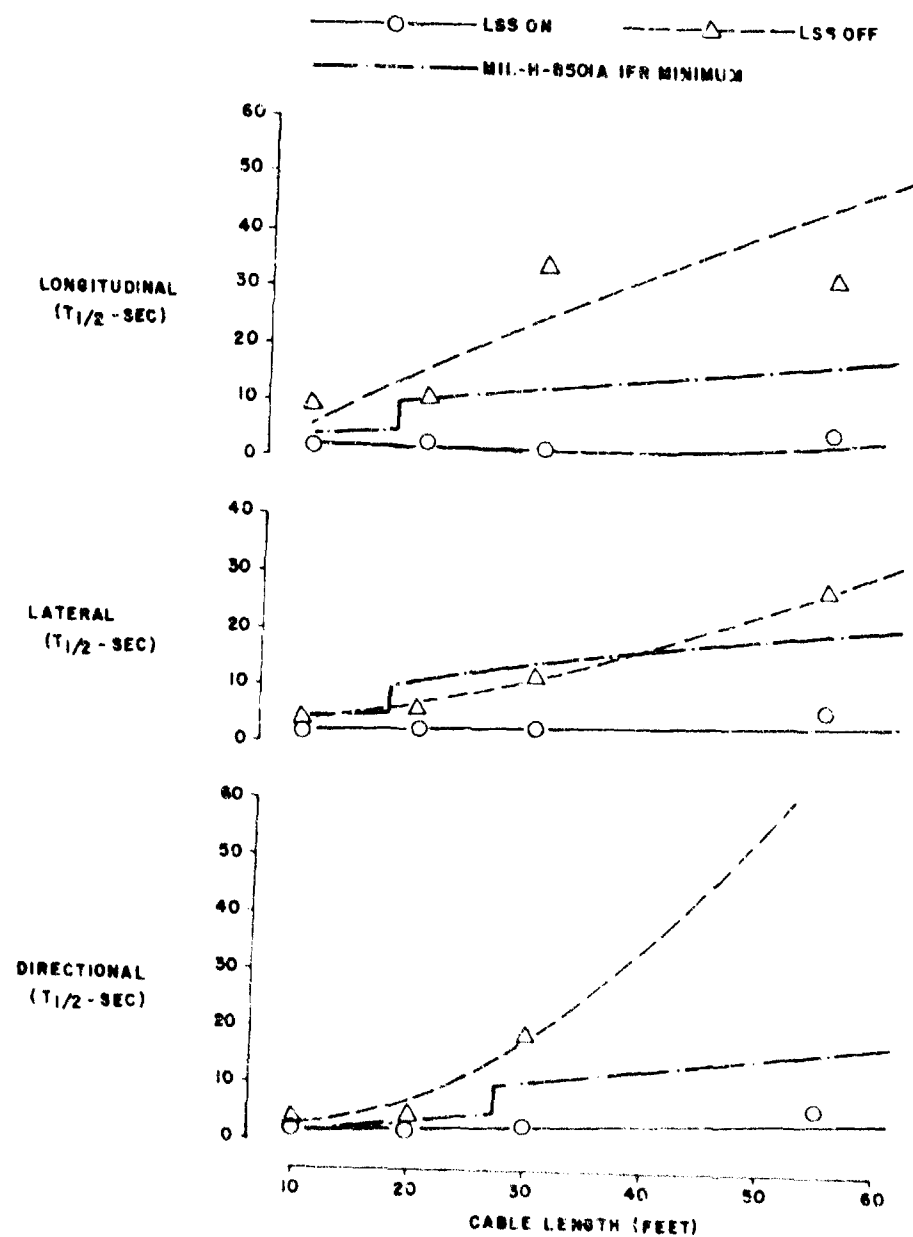
FIGURE 221.

LOAD TIME-TO-HALF AMPLITUDE-HOVER HOLD

559
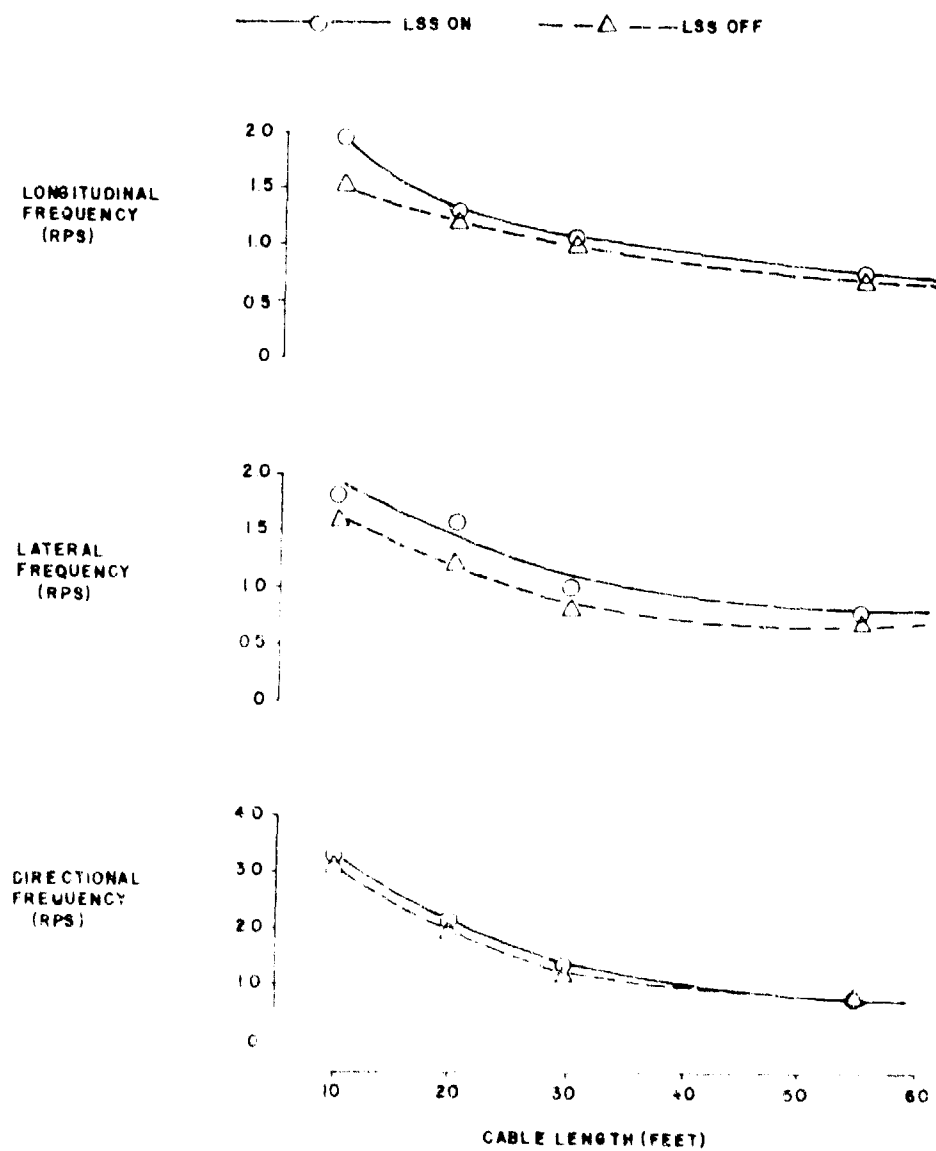
FIGURE 222.

LOAD PENDULUM FREQUENCY - HOVER HOLD
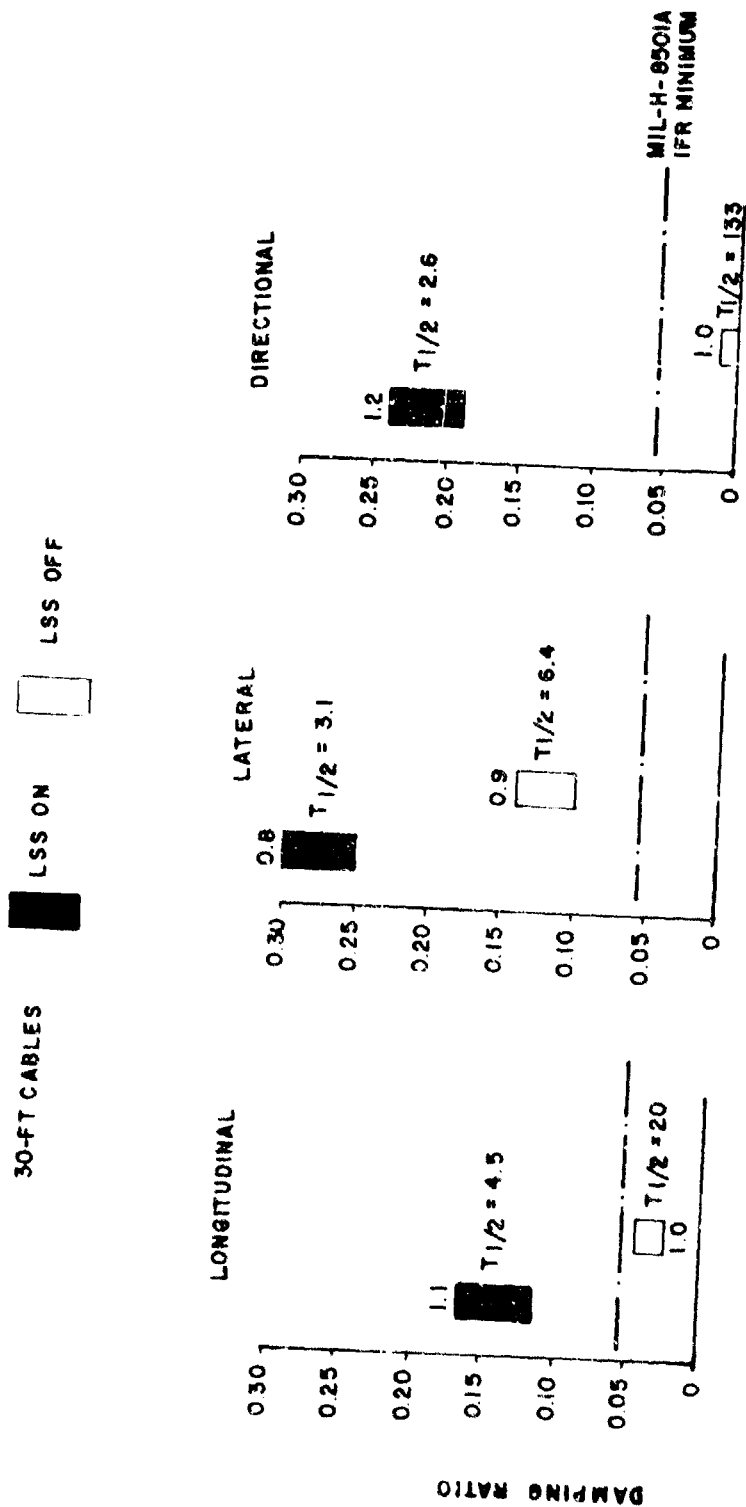
FIGURE 223.
LOAD DAMPING SUMMARY – PHS

561
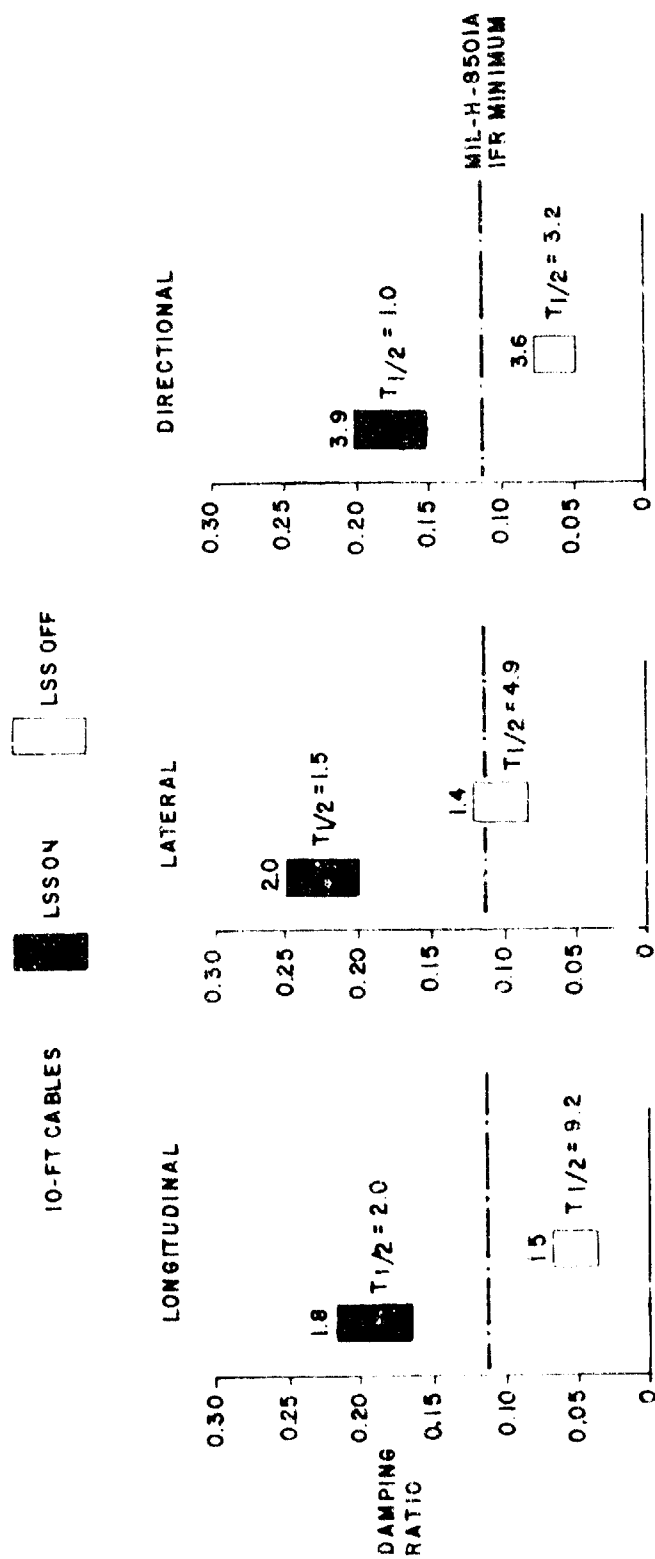
FIGURE 224.
LOAD DAMPING SUMMARY – FORWARD FLIGHT
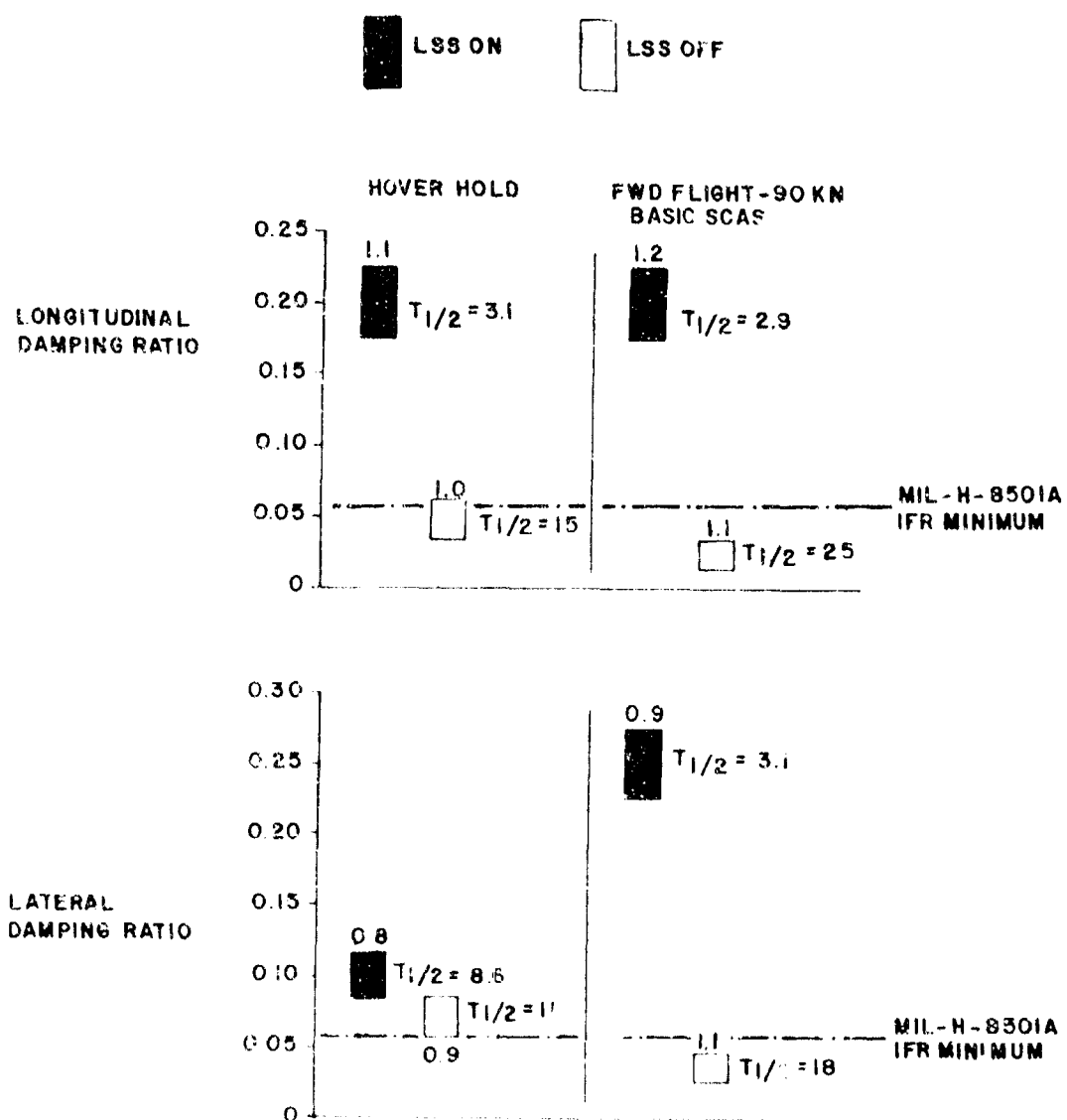
FIGURE 225.
LOAD DAMPING SUMMARY - HIGH DENSITY LOAD
TROLLEY SUSPENSION

requirements. While the basic load damping is substantially below the IFR minimum in most cases, the final LSS configuration increases the damping above this level in all cases. In fact, the damping is 20 percent critical or above in most cases with the LSS on. The damping improvement can be further appreciated by the time to one-half amplitude curves on Figures 218 and 221. The following trends are noted:

- Basic load damping (LSS off) is best laterally

- Basic load damping decreases with increased cable length

- LSS is least effective in damping directional load motion, particularly with the inverted vee configuration

- LSS damping (final configuration) remains fairly constant with changes in cable length

- LSS generally increases load frequency which yields a further reduction in load settling time

Increased LSS damping would be desirable for the longitudinal and lateral axes with PHS on to improve position hold and placement accuracy, and directionally with inverted vee cables in hover to eliminate the small residual directional load motions.

During some stability testing, the pilot had to use relatively large control inputs to excite the load, and then turn on the LSS to evaluate stability. If the lateral AFCS differential output limit was heavily exceeded, a large amplitude limit cycle occurred when the LSS was engaged. This problem did not occur during normal load handling or smaller intentional load swings. However, this indicates a potential deficiency ency requiring control law modification to prohibit its occurrence. This problem did not occur directionally or longitudinally with the final longitudinal LSS configuration. Similar experience with the longitudinal axis did occur when gain was too high.

5.5.5.2   Ride Qualities

Since the LSS uses the response the aircraft to damp the load, some reduction in ride qualities was anticipated. Pilot comments indicate that the aircraft motions produced by the LSS made the load feel like a heavier load (A-4). Degradation in

ride qualities was not significant, particularly when the load was not being purposely excited. In Table 29, the peak pilot-observed linear accelerations and aircraft attitude excursions are compared for load swings with the LSS on and off. As expected, the aircraft excursions, while the LSS is damping the load, are somewhat larger than those with the LSS off. After the LSS has damped the load, the excursions are substantially less than when the load is swinging with the LSS off. This can also be observed on the time histories shown previously (Figures 212 to 216).

5.3.5.2.3   In-Flight System Refinements

The final AFCS configuration block diagrams are shown in Section 4. While the LSS structure is almost identical to that developed analytically, several parameter values were changed to achieve improved damping levels for the test configurations. Since the analytical design was performed only for 20- and 50-foot cables, extrapolation of design parameter values was necessary for the 10- and 30-foot flight test configurations. This, in turn, required some small in-flight parameter adjustments. In addition, the final SCAS and Hover Hold parameters were somewhat different than those used during LSS analysis.

The test developed parameters are compared with analytical data in Table 30. The only significantly large load damping parameter change was KXCA1 - (longitudinal damping loop gain on Basic SCAS) which was reduced by 60 percent. There was more basic directional load motion in hover than anticipated with the 10-foot inverted-V suspension. The best damping of this mode was obtained using a lead-lag shaping (TN10/TN13) to provide some phase advance.

Excessive aircraft pitching occurred in response to all AFCS longitudinal cyclic inputs. Consequently, a term was added to the longitudinal AFCS differential collective input as a function of total cyclic input to compensate for the pitching hub moment generated by longitudinal cyclic ($M_{B1C}$ derivative). This provided a much better longitudinal response to LSS inputs, as well as to other AFCS cyclic inputs.

TABLE 29. COCKPIT ACCELERATION AND ATTITUDE EXCURSIONS DUE TO LOAD AND LSS

| | UNITS | 10-FT CABLES HOVER HOLD MODE ON | FWD FLIGHT AT 60 KN | 30-FT CABLES HOVER HOLD MODE ON |
|---|---|---|---|---|
| – Load Swinging – LSS Off | Ft/Sec² | <0.5 | 0.7 | 0.7 |
| – LSS Damping Load | | 2.9 | 1.6 | 2.1 |
| – After LSS has Damped Load | | <0.5 | <0.5 | <0.5 |
| – Load Swinging – LSS Off | Deg | 0.4 | <0.5 | 0.6 |
| – LSS Damping Load | | 1.0 | <0.5 | 0.7 |
| – After LSS has Damped Load | | <0.5 | <0.5 | <0.5 |
| – Load Swinging – LSS Off | Ft/Sec² | 1.5 | 1.5 | 2.0 |
| – LSS Damping Load | | 2.2 | 1.8 | 2.2 |
| – After LSS has Damped Load | | <0.5 | <0.5 | <0.5 |
| – Load Swinging – LSS Off | Deg | 2.3 | 1.1 | 3.5 |
| – LSS Damping Load | | 2.4 | 1.9 | 3.0 |
| – After LSS has Damped Load | | <0.5 | <0.5 | <0.5 |
| – Load Swinging – LSS Off | Deg | <0.5 | <0.5 | <0.5 |
| – LSS Damping Load | | <0.5 | 0.6 | 1.7 |
| – After LSS has Damped Load | | <0.5 | <0.5 | <0.5 |

NOTE: All excursion magnitudes are peak-to-peak and are normalized to cable angle excursions of 10 degrees peak-to-peak.

LOAD POSITION HOLD:

LSS ON

$\ddot{X}_{PO}$ = 0.9 ft/sec² (0.6)
  " = 0.3 deg (0.2)
$\ddot{Y}_{PO}$ = 1.7 ft/sec² (1.0)
  = 1.2° (1.2°)
  = 1.1° (0.9°)

LSS OFF

$\ddot{X}_{PO}$ = 0.8 ft/sec² (0.3)
  " = 0.2-0.3 deg (0.2)
$\ddot{Y}_{PO}$ = 1.3 ft/sec² (0.8)
  = 1.6° (1.1)
  = 0.2° (0.3)

## TABLE 30.
## LSS PARAMETERS - DAMPING

| | 10' CABLES | 20' CABLES | 20' CABLES ANALYSIS | 30' CABLES | 50' CABLES ANALYSIS | 55' CABLES |
|---|---|---|---|---|---|---|
| **LONGITUDINAL DAMPING** | | | | | | |
| *KXCA1 | 0.07 | 0.094 | 0.25 | 0.1 | 0.25 | 0.094 |
| TX5 | 2.0 | 2.0 | 2.0 | 2.0 | 2.0 | 2.0 |
| TX6 | 0.2 | 0.2 | 0.2 | 0.2 | 0.2 | 0.2 |
| KXC2 | 0.5 | 0.75 | 1.0 | 0.82 | 1.5 | 1.0 |
| TX4 | 0.1 | 0.1 | 0.1 | 0.1 | 0.1 | 0.1 |
| TX3 | 10.0 | 10.0 | 10.0 | 10.0 | 10.0 | 10.0 |
| TFS RATE | 3.0 | 3.0 | 3.0 | 3.0 | 3.0 | 3.0 |
| **LATERAL DAMPING** | | | | | | |
| KYCA1 | -0.13 | -0.13 | -0.13 | -0.13 | -0.13 | -0.13 |
| TY4 | 1.5 | 1.5 | 1.5 | 1.8 | 2.5 | 2.5 |
| KYCA2 | 0.01 | 0.04 | 0.04 | 0.08 | 0.175 | 0.175 |
| TY3 | 0.08 | 0.1 | 0.1 | 0.13 | 0.25 | 0.2 |
| KYCA3 | --- | --- | 0.031 | 0.047 | 0.13 | --- |
| TY2 | --- | --- | 0.25 | 0.4 | 0.75 | --- |
| TY1 | 10.0 | 10.0 | 10.0 | 10.0 | 10.0 | 10.0 |
| TFS RATE | 0.7 | 0.7 | 0.7 | 0.7 | 0.7 | 0.7 |
| **DIRECTIONAL DAMPING** | | | | | | |
| KNCA1 | 0.005 | 0.044 | --- | 0.069 | 0.35 | 0.087 |
| TN13 | 0.8 | 0.0 | --- | 0.0 | 0.0 | 0.0 |
| TN10 | 0.23 | 0.1 | --- | 0.37 | 0.4 | 0.3 |

567

Initially, the aircraft exhibited a high frequency (1 Hz) small amplitude roll limit cycle with the load and hover hold mode on. This limit cycle, which was perceptible to the pilot, appeared essentially independent of the LSS. The high lateral hover hold gains left a smaller than predicted gain margin for the roll mode even without a load. Aircraft lateral control power, and therefore AFCS loop gains, increases with an external load. It was reduced to an insignificant amplitude by reducing the roll stabilization gains (rate, attitude, lateral velocity) by 20 percent. However, this indicates that these gains (or at least one of these gains) will have to be further reduced with heavier loads. Gain scheduling with load weight is included on HLH.

A related limit cycle problem was found with the 30- and 55- foot inverted Y configurations in which the load would roll about its longitudinal axis at the same frequency as the residual aircraft roll limit cycle. This problem was amplified by a factor of 1.2 by the LSS since the load hooks were oscillating relative to the gravity vector. While time did not permit further investigation to reduce the limit cycle level, the following changes would most likely eliminate the problem.

- Sling load in a manner to eliminate load rolling tendency
- Further reduce roll stabilization gains
- Further reduce LSS gain at limit cycle frequency

5.3.5.3  Load Position Hold Evaluations

5.3.5.3.1  Load Position Hold

The accuracy with which the load's position can be held relative to the ground was measured using a precision photographic technique supplied by NADC. This was done for the following system mode build-up to measure the improvement afforded by each mode.

Hover hold without LCC corrections - LSS off
Hover hold without LCC corrections - LSS on
Hover hold with LCC corrections - LSS off
Hover hold with LCC corrections - LSS on
PHS - LSS off
PHS - LSS on
PHS - Load position hold on

A MILVAN loaded to 7600 pounds (total load weight) on 30-foot cables was used for all cases. Load altitude was 25 feet to bottom of box.

The load excursions for all the configurations are summarized in Table 31. The data is referenced to the MILVAN corner having the largest deviations. It must be pointed out that only a small sample for each configuration was measured, so the results may not be statistically accurate. From the Circular Error Probability data in Figure 226, it can be seen that the load position hold accuracy is dependent first on how well the aircraft is held with PHS results (approximately three times better than velocity-hold results). Deviations without load damping are approximately twice that of the helicopter without a load. Loading damping significantly reduced load excursions when PHS was engaged, but had a lesser effect with velocity hold only due to LCC input requirements. Load yaw excursions were reduced from 3 degrees to 1 degree RMS by the LSS.

The load position hold loops did not improve the load position hold capability for any axis in flight. It appeared that load excursions were produced primarily by aircraft attitude changes, rotor downwash, and any ground effect, rather than wind changes and gusts. Consequently, most of the load excursions were at or above the load pendulum frequency so that the net effect of the position hold loops was to reduce the damping. In addition, aircraft stability during operation with load position loops was described as loose, whereas with aircraft position loops only, the helicopter felt rock solid.

The best configuration was with the PHS and load damping which held the load within 8 inches CEP horizontally, 3 inches RMS vertically, and 1 degree RMS directionally in winds gusting to 24 knots. These impressive load excursions are only approximately 1.2 times larger than those of the aircraft without a load. Comparison with velocity hold indicates that substantial improvement in placement accuracy can be achieved with the position hold system. The load position hold accuracy did not appear to vary substantially as a function of turbulence. While precision measurements were not made under various wind conditions, pilot comments indicated that load excursions were not greatly affected by turbulence levels.

569

TABLE 31.

LOAD POSITION HOLD SUMMARY

| CONFIGURATION | WIND CONDITIONS | LOAD HORIZONTAL EXCURSIONS INCH CEP INCH RMS | LOAD VERTICAL EXCURSION INCH RMS | LOAD DIRECTIONAL EXCURSION DEGREE RMS | FLIGHT/RUN NO. |
|---|---|---|---|---|---|
| HOVER HOLD WITHOUT LOS DIRECTIONS - LSS OFF | 5 KNOTS STEADY, GUSTING TO 8 KNOTS | AIRCRAFT AND LOAD DRIFTED OFF TARGET AFTER APPROXIMATELY 1 MINUTE | | | 814/2 |
| HOVER HOLD WITHOUT LOS DIRECTIONS - LSS ON | 5 KNOTS STEADY, GUSTING TO 8 KNOTS | | | | 814/3 |
| HOVER HOLD WITH LOS DIRECTIONS - LSS OFF | 10 TO 12 KNOTS STEADY, GUSTING TO 24 KNOTS | $\sigma_X = 25.3$ $\sigma_Y = 27.7$ $CEP_{XY} = 31.2$ | 9.2 | 2.8 | 813/20 |
| HOVER HOLD WITH LOS DIRECTIONS - LSS ON | 10 TO 12 KNOTS STEADY, GUSTING TO 24 KNOTS | $\sigma_X = 20.6$ $\sigma_Y = 26.2$ $CEP_{XY} = 27.6$ | 7.2 | 1.02 | 813/21 |
| LHS - LSS OFF | 10 TO 12 KNOTS STEADY, GUSTING TO 24 KNOTS | $\sigma_X = 6.5$ $\sigma_Y = 11.8$ $CEP_{XY} = 12.3$ | 2.7 | 2.8 | 813/18 |
| LHS - LSS ON | 10 TO 12 KNOTS STEADY, GUSTING TO 24 KNOTS | $\sigma_X = 5.1$ $\sigma_Y = 7.9$ $CEP_{XY} = 7.5$ | 2.4 | 1.05 | 813/19 |
| LHS - LOAD POSITION HOLD | 5 KNOTS STEADY, GUSTING TO 8 KNOTS | $\sigma_X = 9.9$ $\sigma_Y = 16.7$ $CEP_{XY} = 15.2$ | 3.1 | 1.39 | 814/18 |

AUTOMATIC POSITION HOLD - PHS

HANDS OFF

VERTICAL EXCURSIONS 2.5 INCHES RMS

VELOCITY HOLD - IMU/RADAR

LCC CORRECTIONS

VERTICAL EXCURSION 10.0 INCHES RMS

WITHOUT LOAD STABILIZATION
CEP = 31.0 IN.    CEP = 12.3 IN

WITH LOAD STABILIZATION
CEP = 27.6 IN.    CEP = 7.6 IN

AIRCRAFT C G WITHOUT LOAD
CEP = 17.3 IN.    CEP = 6.8 IN

LSS LOAD POSITION HOLD
CEP = 15.2 IN

EMPTY MILVAN
30-FT CABLES
WIND 12 KN GUSTING TO 24 KN
LOAD HEIGHT = 25 FT
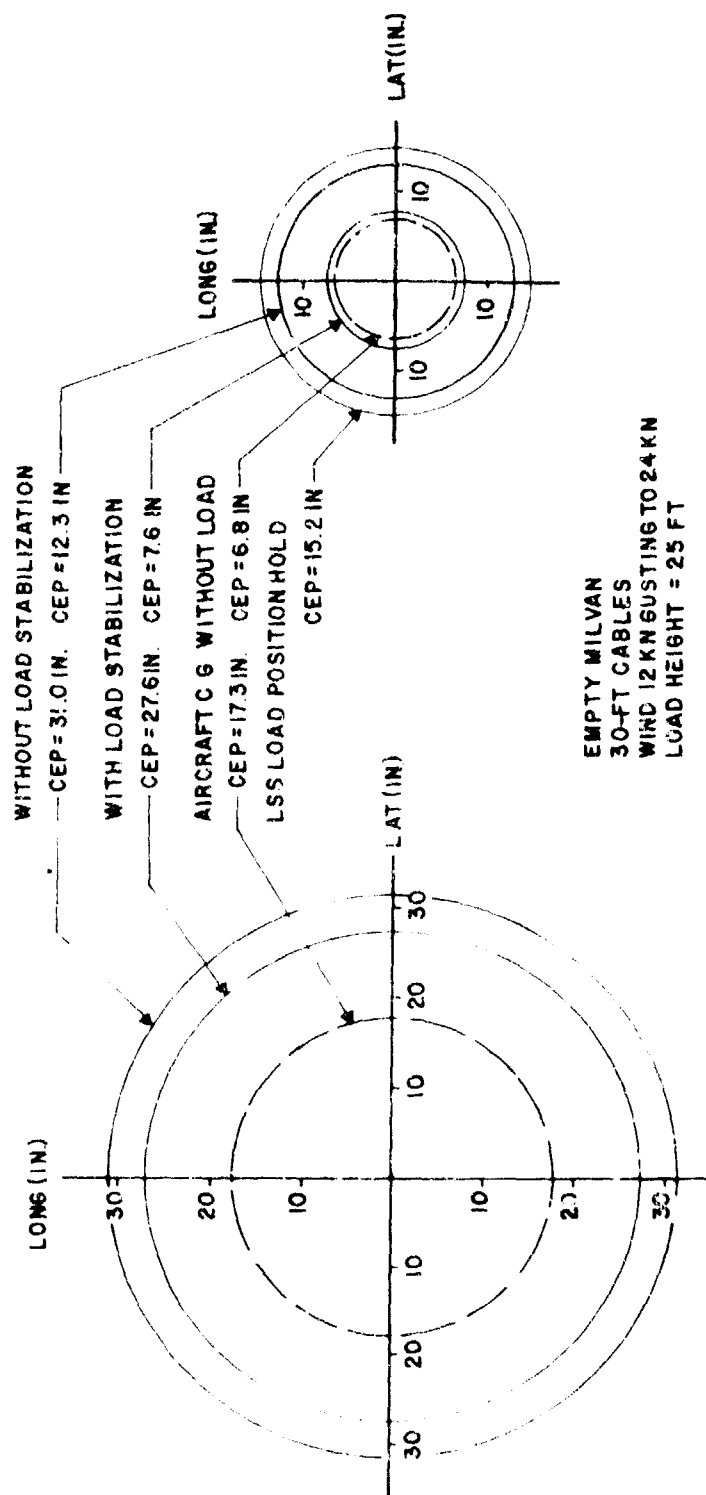
FIGURE 226. CIRCULAR ERROR PROBABILITIES OF LOAD POSITION EXCURSIONS ON HOVER HOLD MODE

571

5.3.5.3.2   In-Flight System Refinements - Load Position Hold
Mode

To achieve any apparent improvement of load position hold
with the position loops engaged, the position gains were
reduced substantially for all axes as shown in Table 32.  As
mentioned previously, no improvement in load hold was
achieved over that supplied by LSS damping.

TABLE 32.

LSS PARAMETERS - LOAD POSITION HOLD

|  | 20' CABLES ANALYSIS | 30' CABLES FLIGHT | 50' CABLES ANALYSIS |
|---|---|---|---|
| LONGIT. POSITION HOLD | | | |
| KXLL1 | 1.0 | 1.0 | 1.0 |
| KXLL1' | 0.2 | 0.15 | 0.4 |
| TXL1' | 0.5 | 0.25 | 0.5 |
| TXL2' | 1.0 | 0.5 | 1.0 |
| TXL3' | 3.33 | 5.0 | 3.33 |
| LAT. POSITION HOLD | | | |
| KYLL1 | 1.0 | 0.5 | 1.0 |
| KYLL1' | 0.1 | 0.05 | 0.4 |
| TYL1' | 0.2 | 0.2 | 0.2 |
| TYL2' | 0.0 | 0.0 | 0.0 |
| TYL3' | 10.0 | 10.0 | 10.0 |
| DIR. POSITION HOLD | | | |
| KNL1 | 1.0 | 0.25 | 1.0 |
| TN11 | 0.25 | 0.125 | 0.25 |
| TN12 | 8.0 | 16.0 | 8.0 |

### 5.3.5.4 Aircraft/Load Centering Mode

### 5.3.5.4.1 Aircraft/Load Centering

In Figure 227, the aircraft is automatically centered over the load longitudinally, laterally, and directionally. Tension is automatically drawn to approximately 1200 pounds in each cable when the LSS is switched on and then the aircraft is centered after the PHS is enabled. Occasional transients would occur during the centering maneuver due to the PHS relocking, but the centering operation was smooth otherwise. Load lift-off was accomplished without any noticeable load swing following centering.

A vertical pulse is applied with the tension control loops operating in Figure 228. It can be seen that the cable tensions quickly return to their desired value in a well-damped manner. It was found that the cables have to be very near the correct relative length for the trim pitch attitude. Otherwise, tension cannot be drawn on both cables. While the system would command the aircraft to climb to bring the cables taut, the aircraft motion was too abrupt. This confirmed the requirement for a reduced gain until one of the cables becomes taut. This feature was not included in the flight test configuration due to software capacity limitations.

The two cable tension sensors were prone to drift and had to be frequently re-nulled to provide an adequate signal for the centering mode.

Load centering works well for small (4 ft) aircraft offsets, but undesirable transients occur if a cable goes slack (rated U-7). It was difficult to draw tension on both cables without dragging the load if the aircraft was offset from the load a large amount with the load on the ground. Consequently, the tension control loops could not keep both cables straight during centering from large offsets. When a cable would go slack, the centering loops would receive incorrect cable angle information, resulting in undesirable aircraft transients and delays in centering. It appears that a better method of keeping both cables taut during centering from large offsets is required. The winch system of the HLH could provide this.

FIGURE 327. AIRCRAFT A INERTIAL N
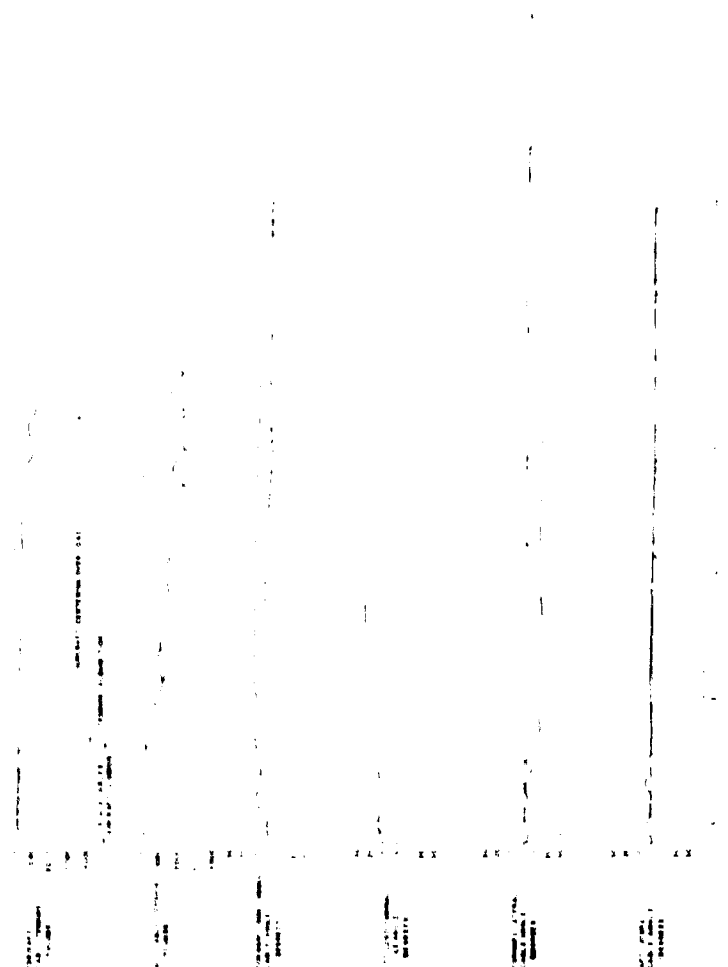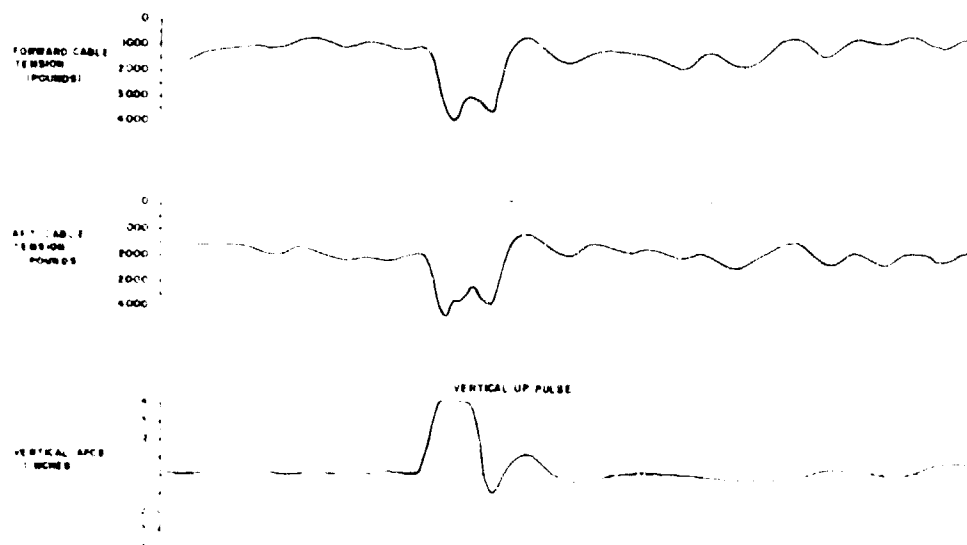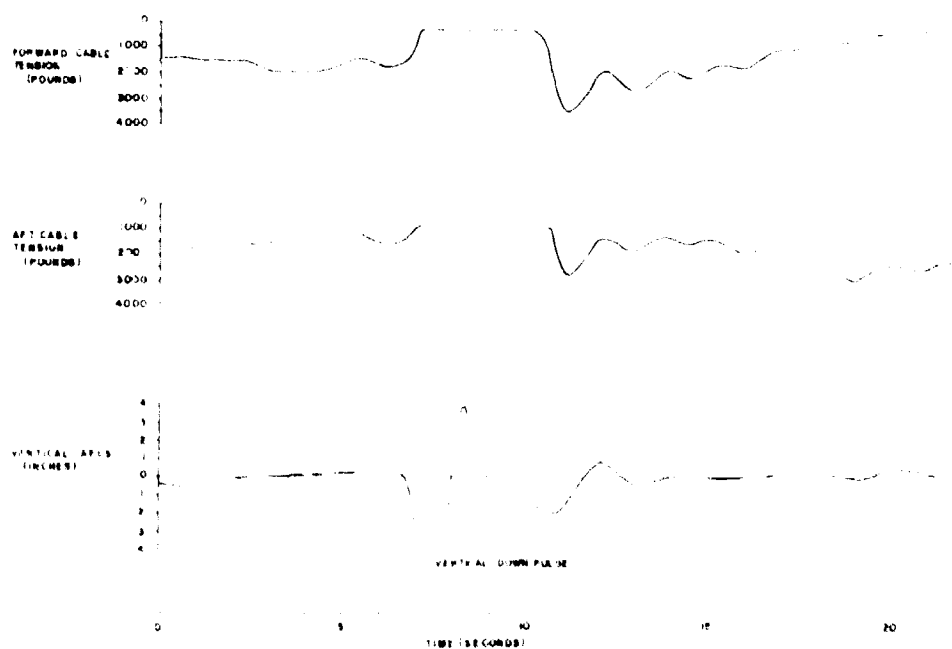
FIGURE 228. AIRCRAFT/LOAD CENTERING - VERTICAL TENSION CONTROL

While automatic centering proved feasible, its requirement is
very questionable. The pilots found manual centering to be an
easy task from the LCC station. However, automatic centering
may be more important when a high degree of centering accuracy
is required with longer cables or in low visibility
situations.

Although the centering mode was designed to operate with the
PHS, centering was also performed using the IMU velocities
instead of the PHS. A low-frequency (20-sec period) mild
lateral instability occurred in this case. This was due to
IMU drift in conjunction with the integral backdrive loops.
A destabilizing conflict occurred between the incorrect
velocity feedback (due to drift) and the position feedback
(derived from the cable angle measurements).

5.3.5.4.2   In-Flight System Refinements   Load/Aircraft
            Centering Mode

The major change in the centering loop configuration was the
elimination of the velocity compensation terms as these were
found unnecessary to avoid AFCS limiting. The longitudinal
and lateral centering rates were reduced by about 50 percent
by reducing the transient-free switch decay rates as shown in
Table 53. The tension stabilization loop gain was reduced by
50 percent to increase the attitudinal stability.

No logic changes were required; however, the smallest tension
discrete and its associated bias and hysteresis were removed
to allow software space for other changes. Consequently,
this piece of logic was not exercised.

Initially, the tension signals had a ±200-pound noise level
at 4 per rev which was reduced to an acceptable level by an
analog prefilter change to lower bandwidth near 1.7 Hz.

5.3.5.5   Load Handling Characteristics

5.3.5.5.1   LCC Operations

Load handling tasks including load hookup, shuttle, and place-
ment with longitudinal and lateral cables were performed. Execution of
these tasks was evaluated on board Hold IMU/Radar only, without
benefit of the PHS due to its operational problems; namely,
poor reliability and the requirement for a restricted target area.

## TABLE 33.

### LSS PARAMETERS – CENTERING MODE

|                   | 30' CABLES<br>FLIGHT DATA | 50' CABLES<br>ANALYSIS |
|-------------------|---------------------------|------------------------|
| LONGIT. CENTERING |                           |                        |
| KXLL4             | 0.4                       | 1.58                   |
| TFS RATE          | 0.2                       | 1.0                    |
| LAT. CENTERING    |                           |                        |
| KYLL4             | 0.5                       | 1.69                   |
| TY6               | 0.1                       | 1.67                   |
| TFS RATE          | 0.5                       | 1.0                    |
| DIR. CENTERING    |                           |                        |
| KNL2              | 0.5                       | 1.0                    |
| TFS RATE          | 2.0                       | 2.0                    |
| TENSION CONTROL   |                           |                        |
| KXTE              | $2 \times 10^{-4}$        | $5 \times 10^{-4}$     |
| KZTE2             | $5 \times 10^{-5}$        | $5 \times 10^{-5}$     |
| KCTE              | $3.0 \times 10^{-5}$      | $2.5 \times 10^{-5}$   |

Improved accuracy with the automatic position hold concept
would result, as indicated from position hold data shown
previously.

Rapid load cable hookup by a ground crewman was performed
easily since the LCC could precisely position the helicopter
and had excellent visibility.  MILVAN acquisition without
ground crewman assistance was accomplished by positioning a
top-lift adapter on the MILVAN.  Load maneuvering to maximum
shuttle groundspeeds could be performed routinely.

With the final hover hold configuration, the MILVAN on 10-foot
cables can be placed consistently within a one-foot accuracy
and on the transporter pins ($\pm$ 1-inch accuracy required)
occasionally.  The MILVAN was lowered onto the transporter
pins with relative ease using 15-inch guide vanes on the
transporter corners providing a funnel for the load.

Accurate placement requires patience on the part of the load
crewman.  Only smooth small inputs can be used to maneuver
the load the last few inches to avoid stirring up load oscil-
lations.  If load oscillations are created, it is best to go
hands off until all motion is damped and then proceed with
the placement task.  Time histories for typical load place-
ments by the LCC are shown in Figures 229, 230, 231, and 232
(LSS on).

LCC workload and time required for accurate MILVAN placement
was increased due to random abrupt lateral swaying of the
load, close to the ground, as shown in Figure 233.  As seen in
the cable tension trace, rotor downwash near the ground cre-
ates a buoyancy effect on the load, making the lateral compon-
ent of downwash more effective in creating lateral motion.
The 5800- to 7600-pound MILVAN on 10-foot cables has a peak
swing of about 3 feet to the aircraft's right with a steady
offset of 1 foot if the load is allowed to stabilize 1 to 2
feet off the ground.

Lateral load stabilization did not alleviate this problem,
and in fact made it worse.  To damp the load motion, the load
stabilization loop commands the aircraft to move in the direc-
tion of the load displacement, further increasing position
error.  LCC commands to return the load to its initial lateral
position are resisted by LSS, causing a tendency by the LCC to
overcontrol.  A lateral interrupt circuit designed to discon-
nect the lateral LSS when the LCC was out of detent was flight

578

FIGURE 276

LCC MILVAN PLACEMENT ON GROUND TRANSPORTER   —   LSS OFF

573
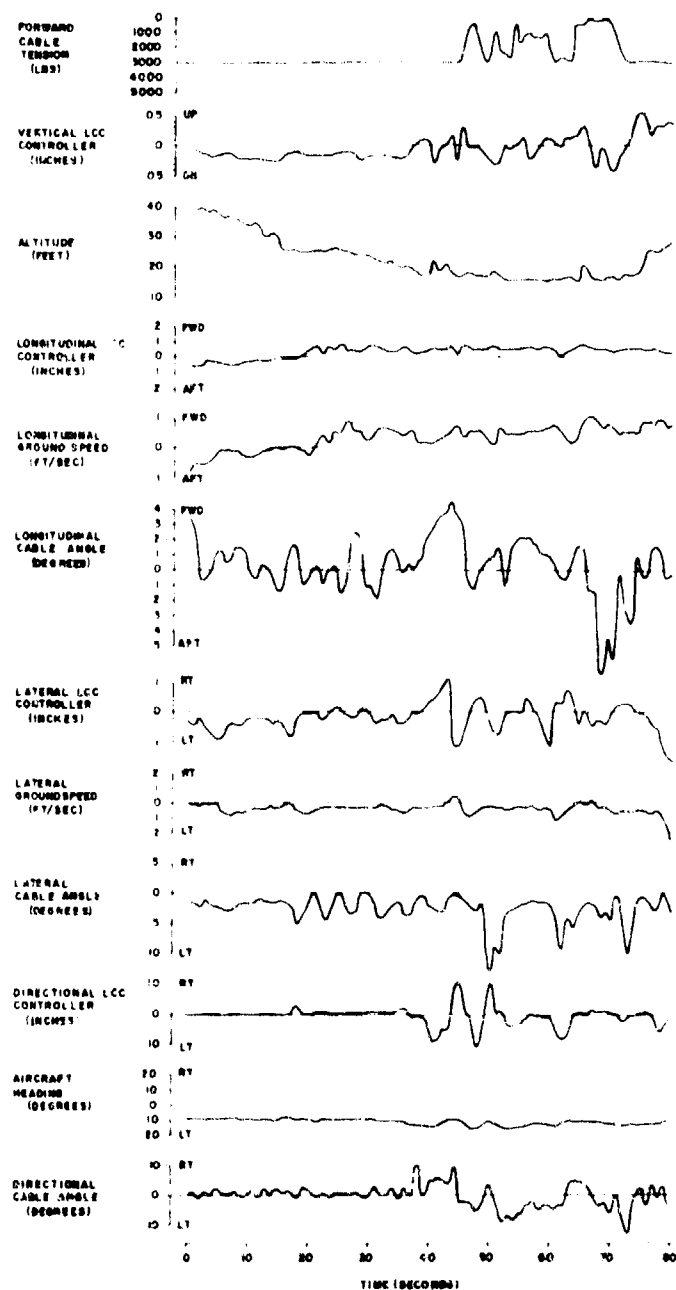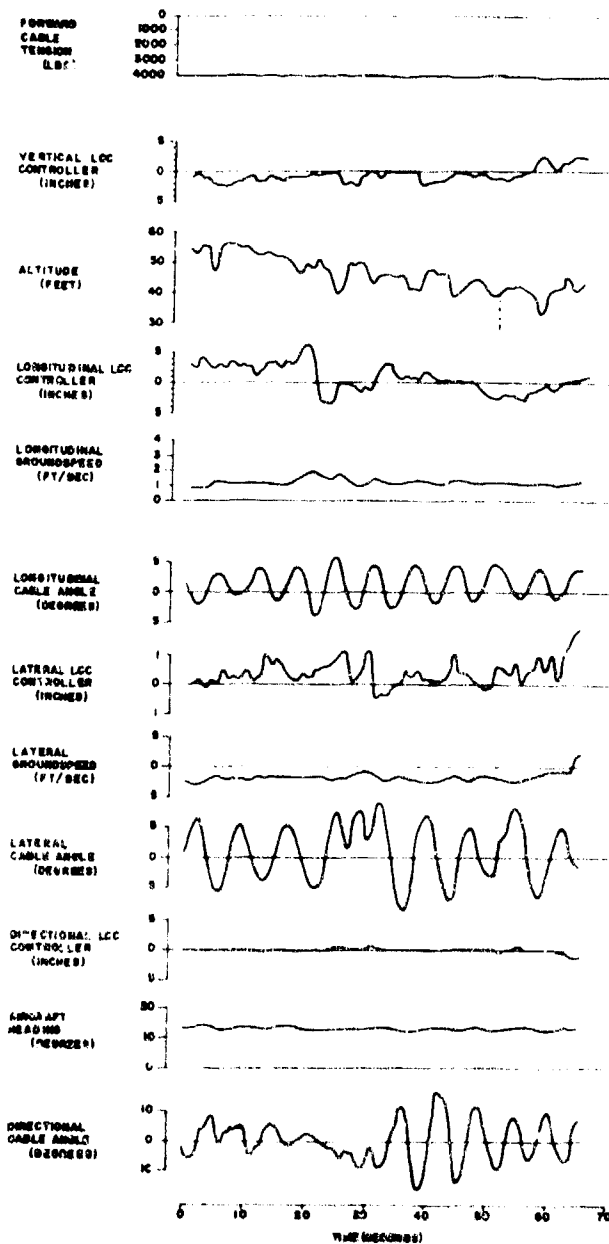
FIGURE 230
LCC MILVAN PLACEMENT ON GROUND TRANSPORTER
- LSS OFF

**FIGURE 251.**

LCC MILVAN PLACEMENT ON GROUND TRANSPORTER — LSS ON

581
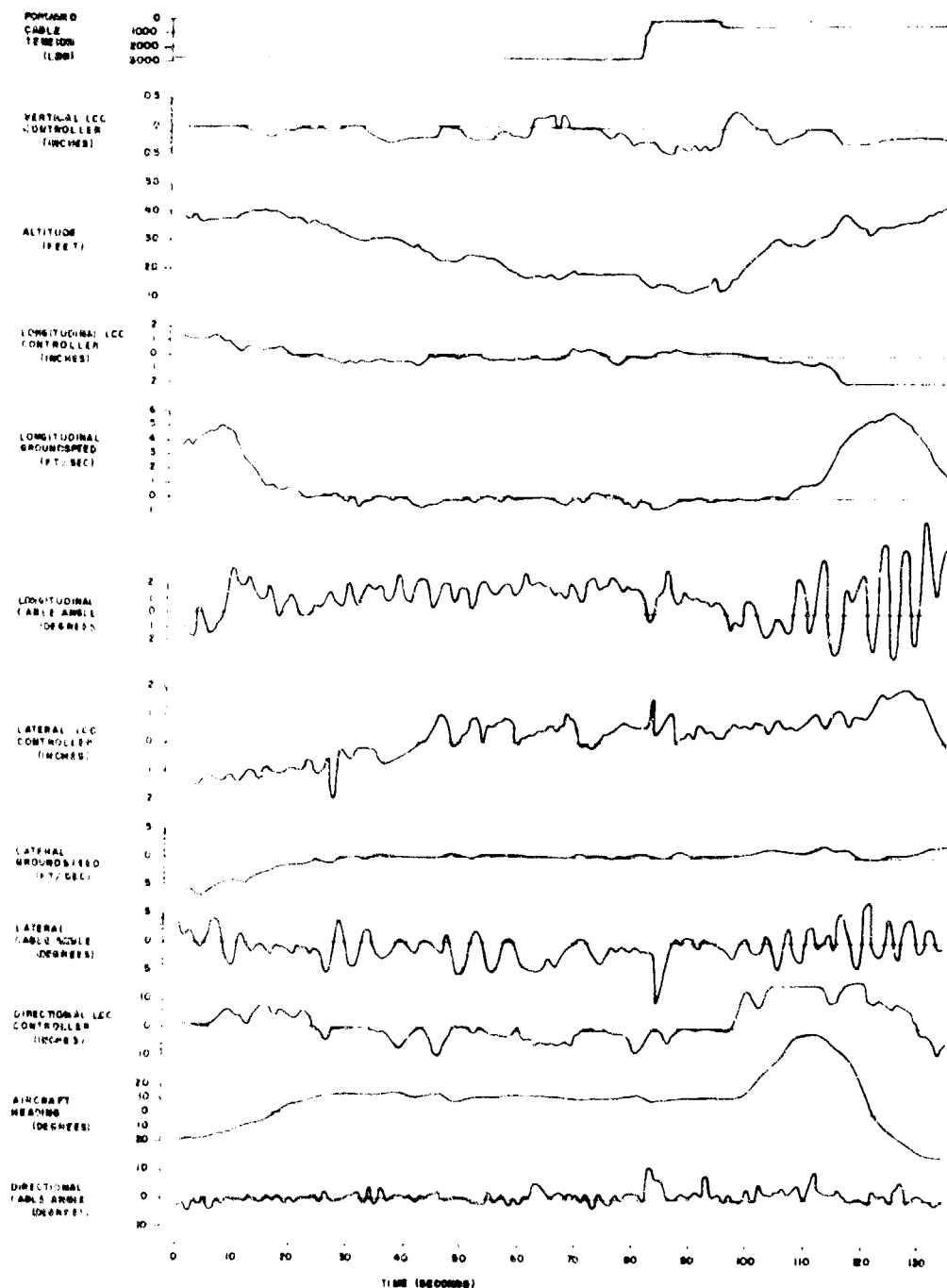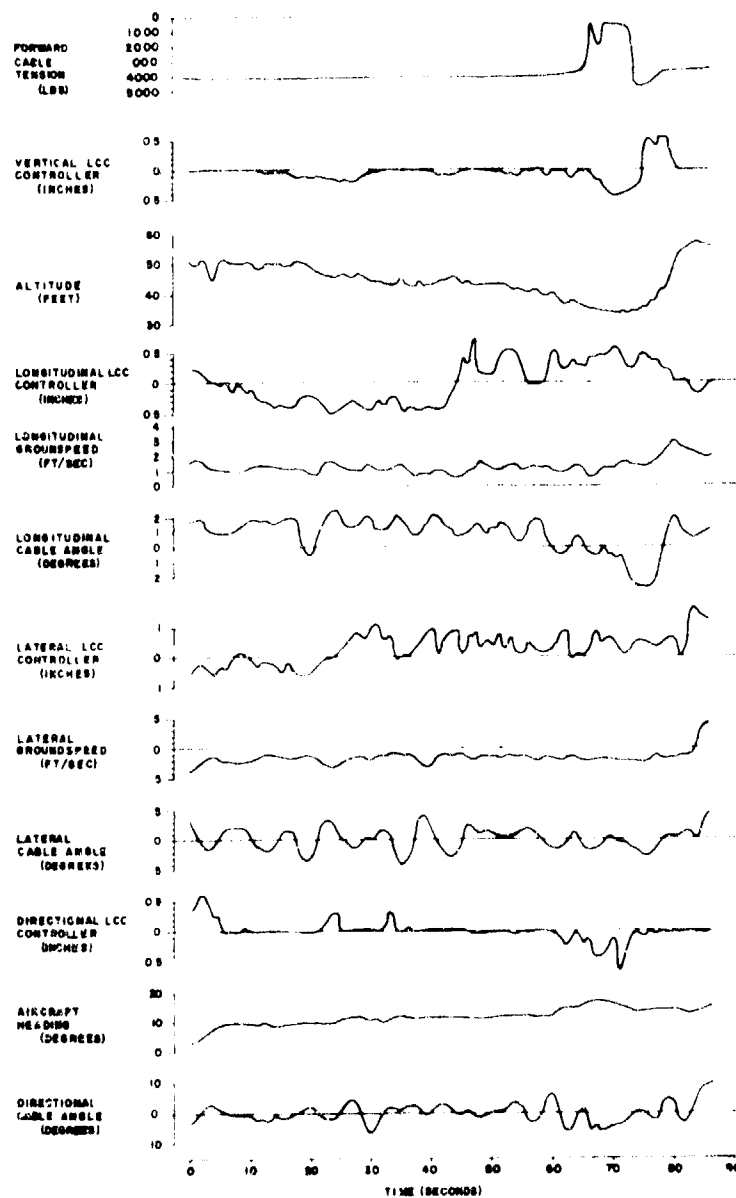
FIGURE 232

LCC MILVAN PLACEMENT ON GROUND TRANSPORTER

– LSS ON

582
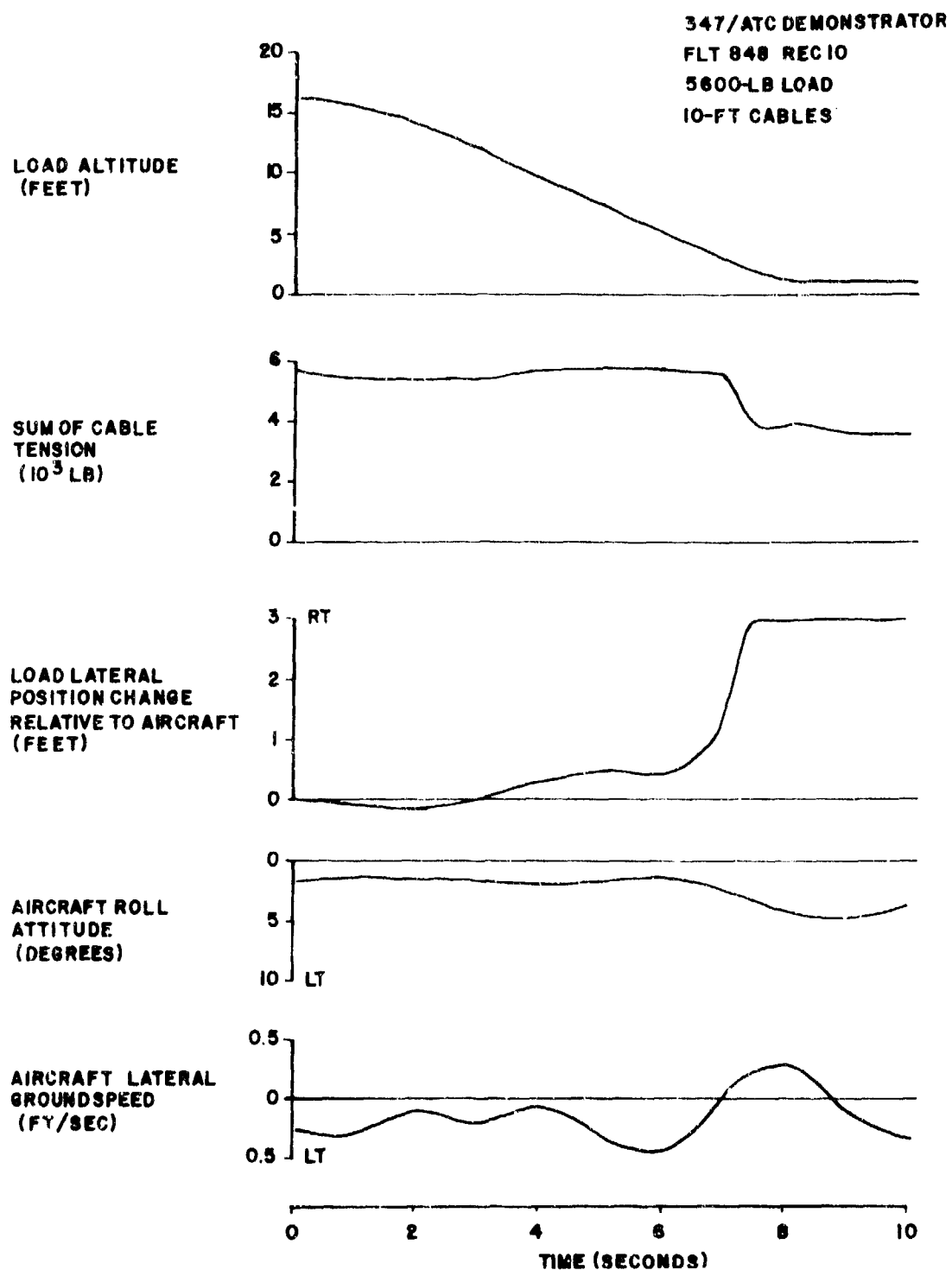
FIGURE 233. LOAD LATERAL SWAY DURING LOAD PLACEMENT

583

evaluated. Transients created by switching were unacceptable. The expedient solution was to set the lateral LSS gain to zero for short cable evaluations since this configuration exhibited reasonable load damping without stabilization (Figure 220). The problem was not apparent in the longitudinal or directional axes and load stabilization proved effective.

It is anticipated that the sway problem would be much less severe with heavier loads or longer cables. It should be less pronounced for all configurations with the HLH since its disc loading and downwash velocity are less than that of the 347 for the same load weight. However, studies should be performed to improve LSS effectiveness.

RECOMMENDATION

Reconfigure LCC/LSS interrupt to avoid transient problems noted in test and/or remechanize LSS to be compatible with load placement. An active arm load stabilization concept may afford an improvement here since the load can be controlled at a higher frequency without aircraft motion. However, it must be recognized that the load placement accuracy is attributed for the most part to the Hover Hold mode.

The load damping mode affords substantial help in all three axes during load placements with 30-foot cables since the basic load damping is much lower and the load sway is less. It is particularly beneficial in stopping large amplitude directional limit cycling. With load damping, the load could be placed on a transporter with guides, although the task is more difficult than with short cables. Limited testing with a 55-foot cable length indicated that load stabilization was definitely required as load oscillations could not be stopped with LCC or pilot corrections.

5.3.5.5.2  Pilot Operations

The load was well behaved and could be handled easily in forward flight. This is true for all forward flight maneuvering including turns, sideslips, climbs, and descents. The load was also well behaved at the power-limited maximum airspeed. The load presented no problems during departures and approaches regardless of whether they were VFR, simulated IFR, or automatic approaches. For the relatively light load used (5800 lb), the load was basically well behaved in forward flight so there was no real LSS requirement.

5.3.5.6   Simulation Test Comparison

While several design changes were made during the flight test
development of the LSS, most of the analytical design produced
generally the anticipated results.  Flight test and analytical
load damping ratios and frequencies are compared on Figures
234 - 238. Correlation is quite good when considering that
only limited testing was accomplished with 20- and 55-foot
configurations.  The poorest was the longitudinal damping
ratio with PHS engaged as only one-third of the analytical result
was achieved.  Although parameter variations were not made in
flight to check trends, the lateral load damping did not
appear to be as sensitive to LSS and non-LSS parameter varia-
tions as the analysis predicted.

The following are significant known deficiencies or omissions
in the analytical models:

- Rotor downwash and ground effects on the load were not
  modeled.  Consequently, the lateral load sway problem
  did not appear in the analysis.  This was the only
  serious shortcoming.

- Basic load damping (LSS off) was generally better than
  the analytical models predicted.

- Inverted-V analytical representation appears
  inadequate.  There were larger directional load
  excursions at a lower frequency than the model predicted.

These deficiencies should be corrected before further load
handling analysis is performed.
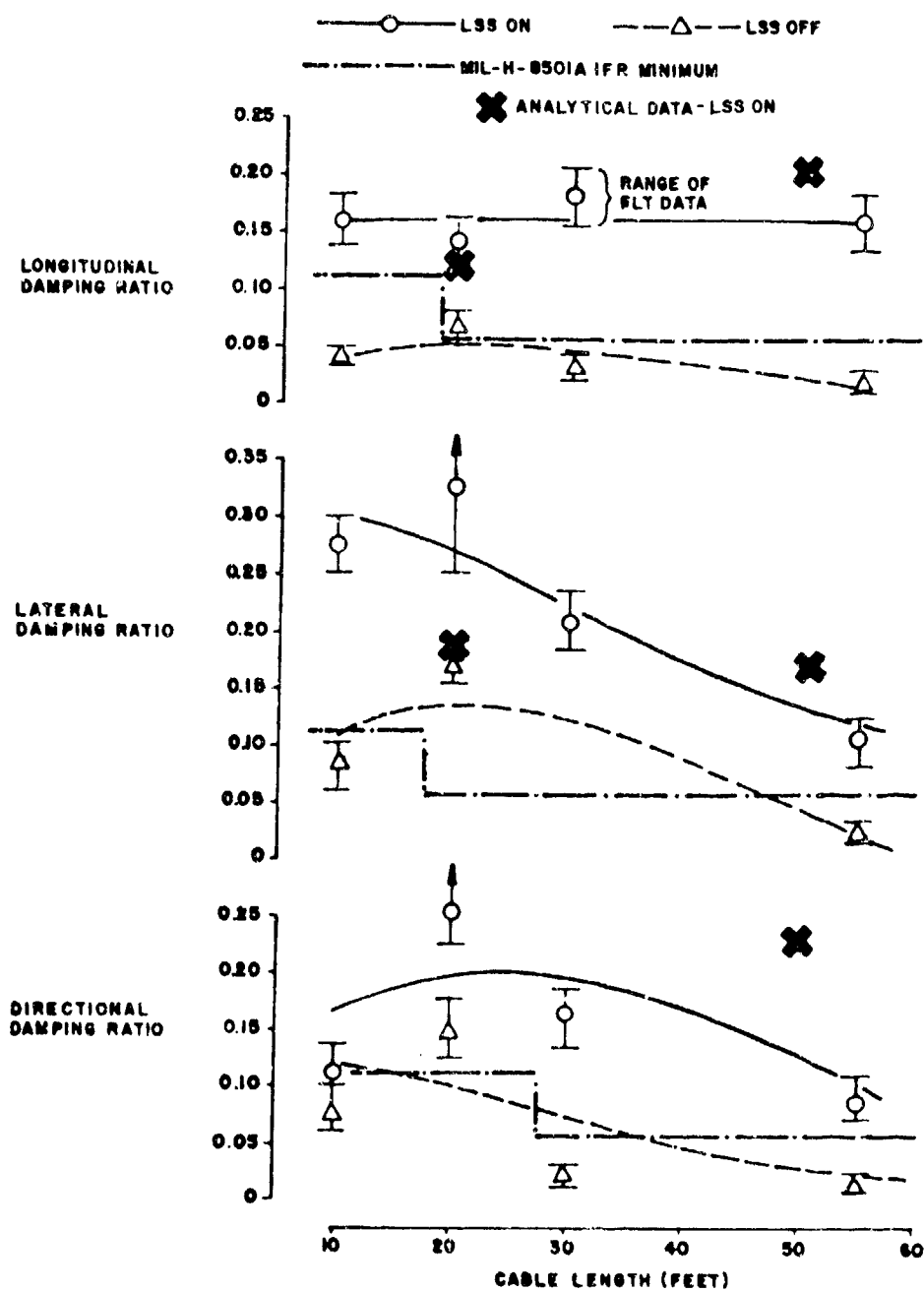
FIGURE 234.
SIMULATION-FLIGHT TEST DATA COMPARISON
LOAD DAMPING SUMMARY - SCAS - HOVER
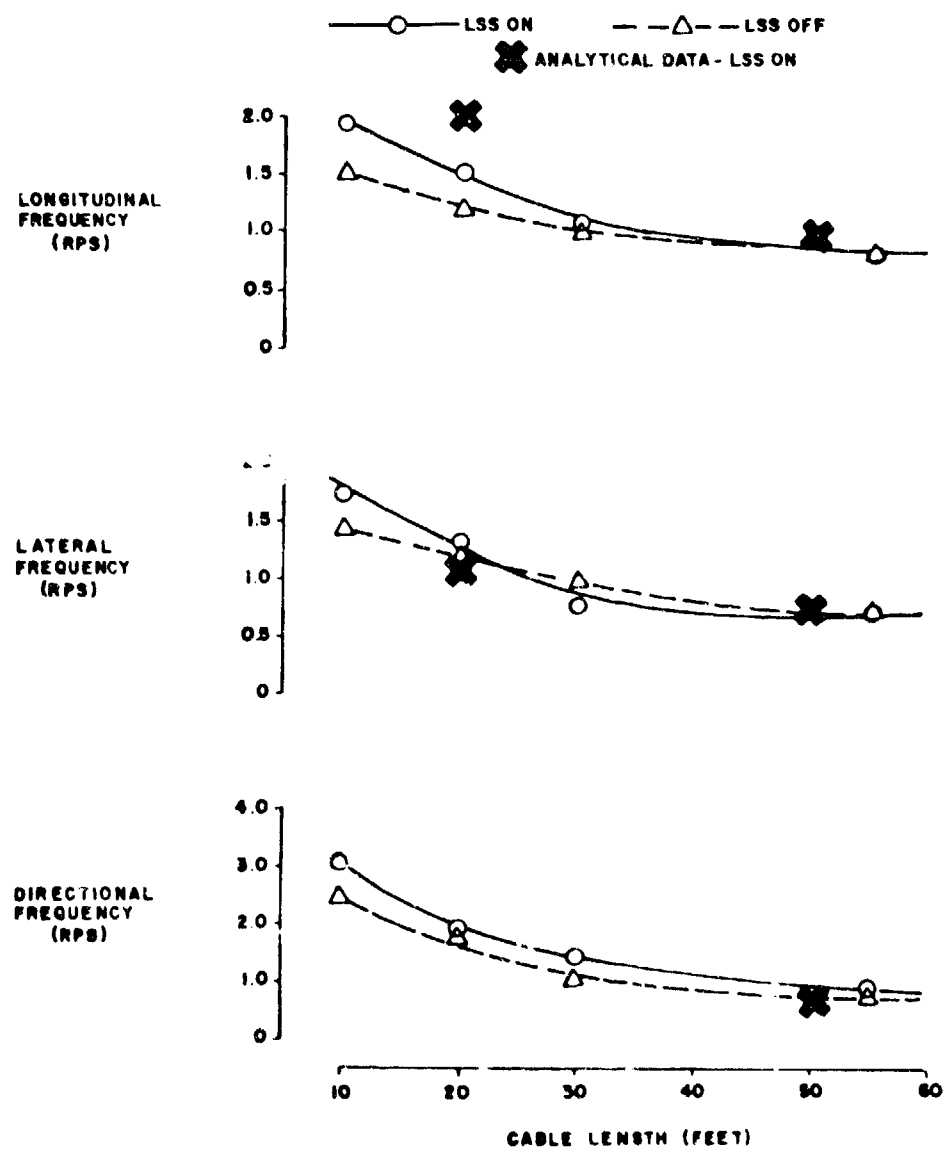
FIGURE 235.
SIMULATION- FLIGHT TEST DATA COMPARISON
LOAD PENDULUM FREQUENCY - SCAS

587
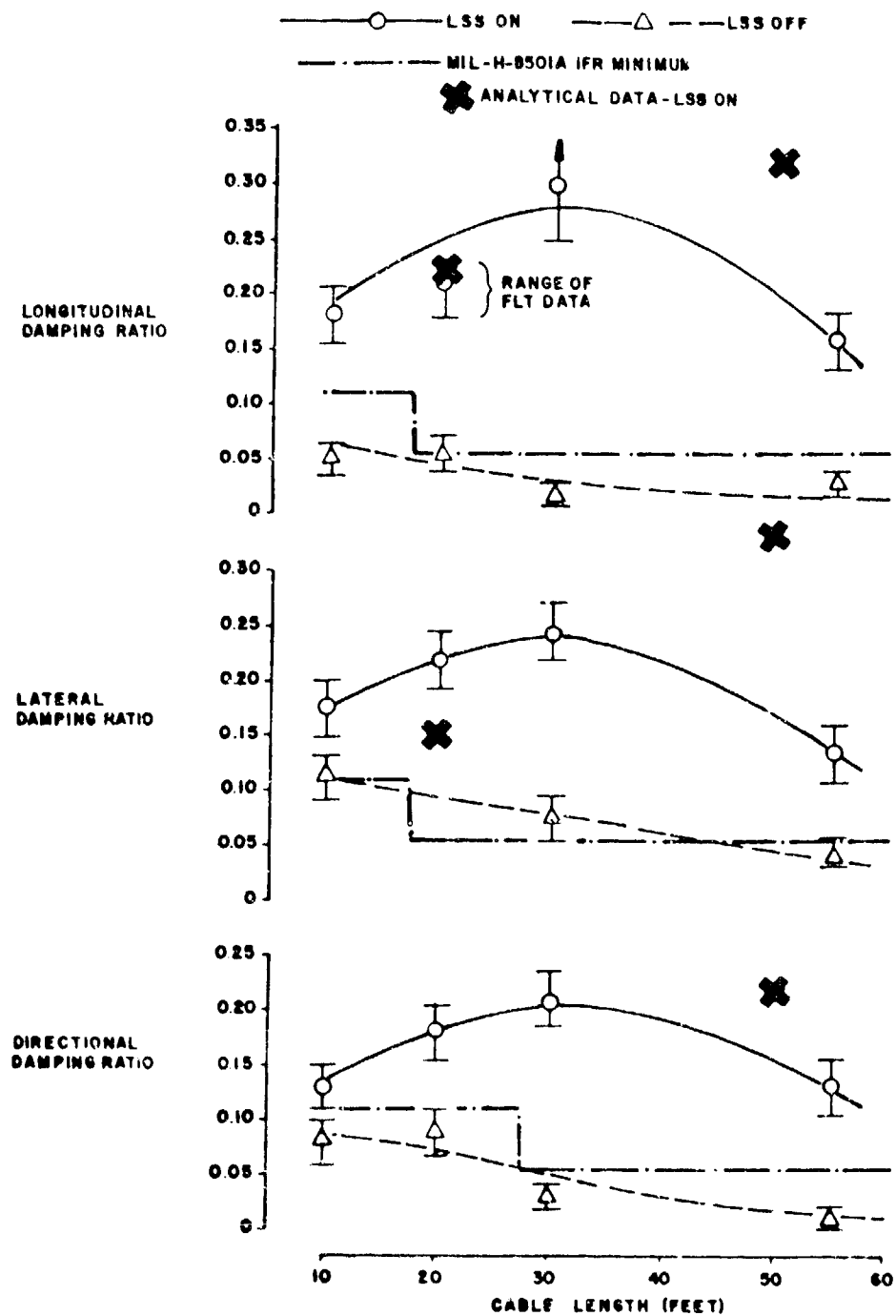
FIGURE 236.
SIMULATION- FLIGHT TEST DATA COMPARISON
LOAD DAMPING SUMMARY - HOVER HOLD
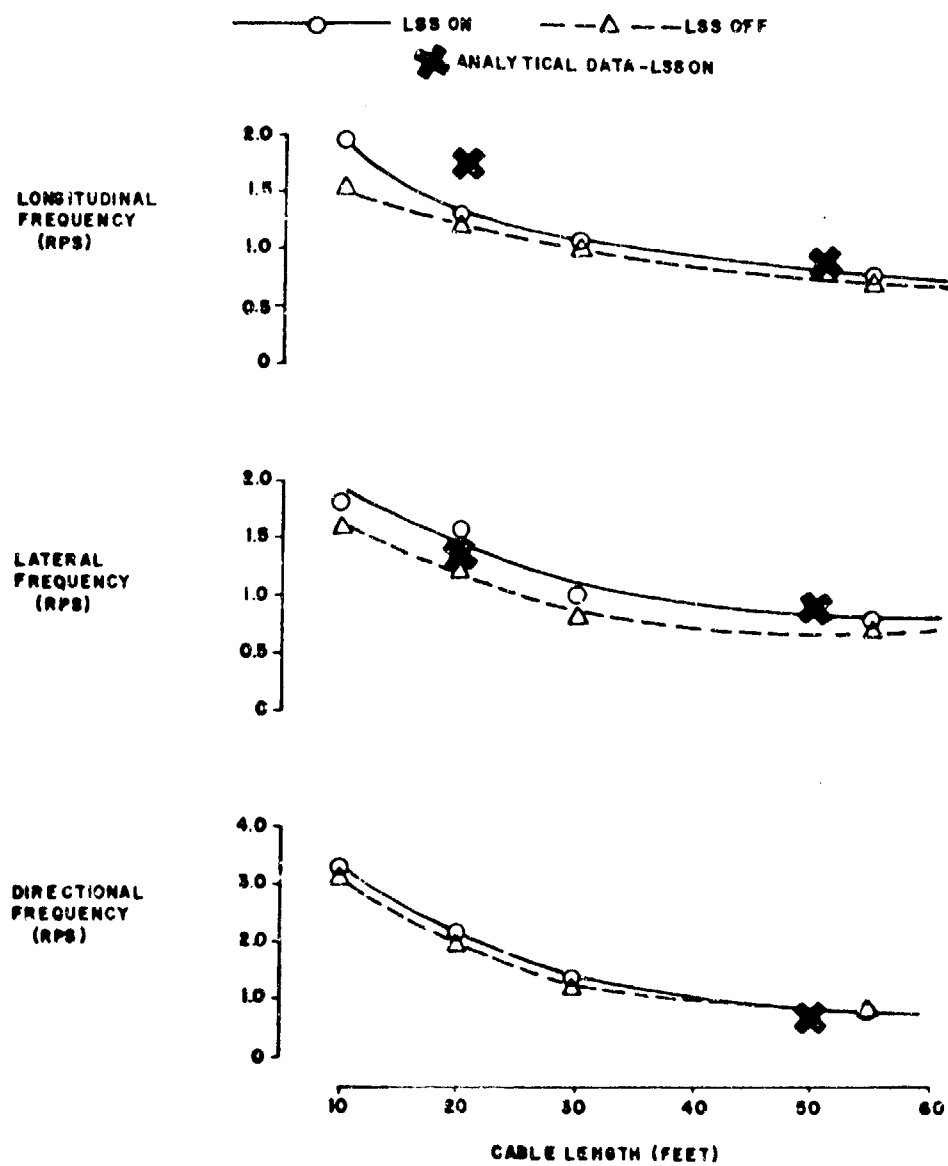
FIGURE 237.
SIMULATION - FLIGHT TEST DATA COMPARISON
LOAD PENDULUM FREQUENCY - HOVER HOLD

589
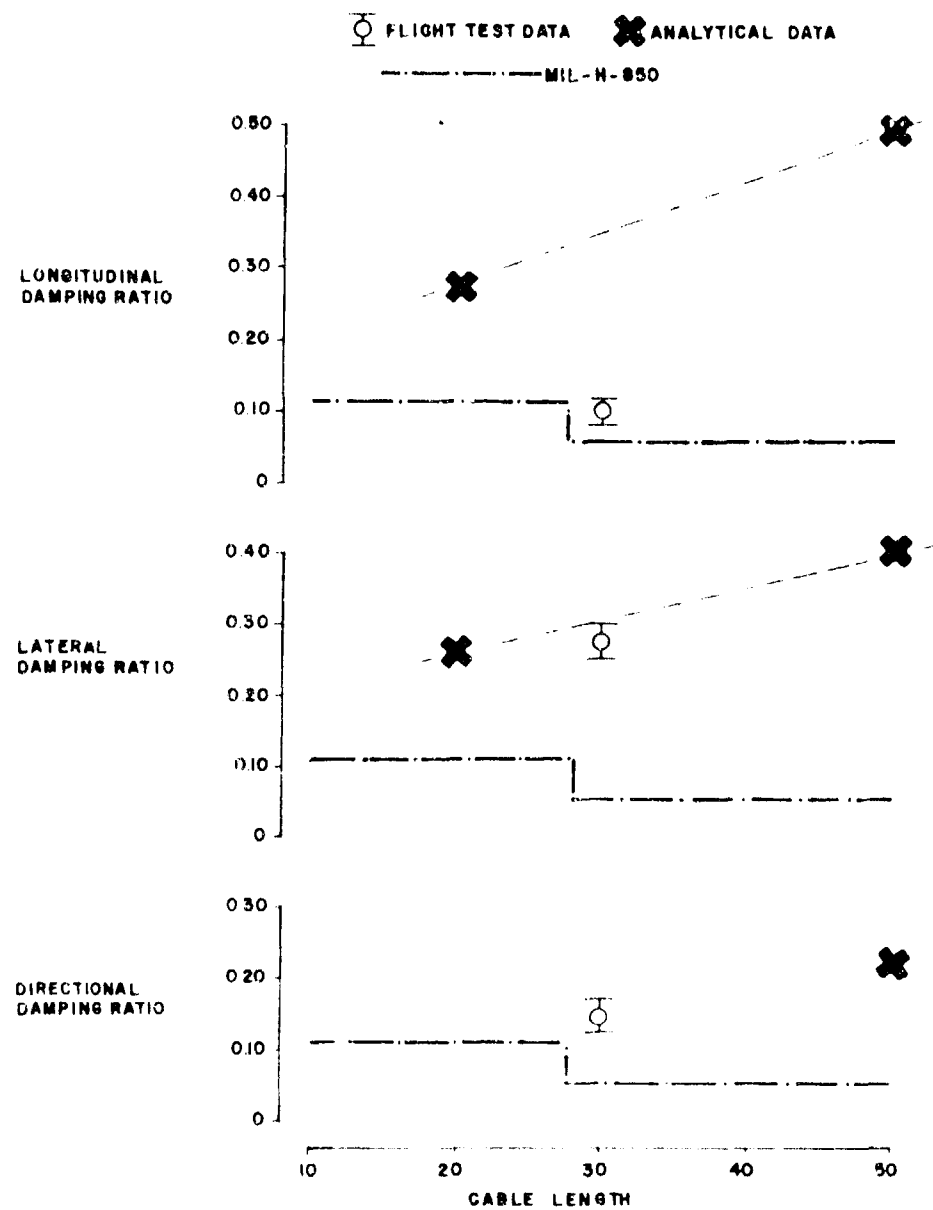
FIGURE 238.
SIMULATION-FLIGHT TEST DATA COMPARISON
LOAD DAMPING-PHS-LSS ON

### 5.3.6  Automatic Approach to Hover

### 5.3.6.1  Description and Test Results

The automatic approach to hover mode was configured for demon-
strating the feasibility to manually (following flight directo.
commands) or automatically fly the aircraft down an approach
path terminating in a stabilized hover.  A "preset" approach
profile was used, starting at 1,000 feet above the terrain and
about 2-1/2 miles from the intended hover point and descending
to a 100-foot hover following a flaring maneuver initiated .le
1/2 mile out at 295 feet.

Because of the fixed profile used, the point of termination
depended upon where the pilot engaged the approach.  Precise
maneuvering was required to reach an initial approach gate
which ensured terminal hover over the desired area.  The con-
cept mechanized for the test program was intended for demon-
stration of control processing only and requires additional
functional capability for operational implementation.

Manually controlled approaches using the flight director ref-
erence were easily accomplished under VFR and simulated IFR
conditions (under the hood) both with and without external
loads.  The approach profile flown by the aircraft was very
close to the planned path (A-3).

Automatic coupled approaches were also performed very satis-
factorily (A-2.5), again with and without loads.

### 5.3.6.2  Approach to Hover Performance

Data for several automatic approaches, completely hands off,
are shown in Fig.239 to 242 for the conditions listed below.

| Figure | No Load | Load | Load Stabilization |
|--------|---------|------|--------------------|
| 239 |  | MILVAN | Off |
| 240 |  | MILVAN | On |
| 241 |  | Hi Density | Off |
| 242 | X |  |  |

591
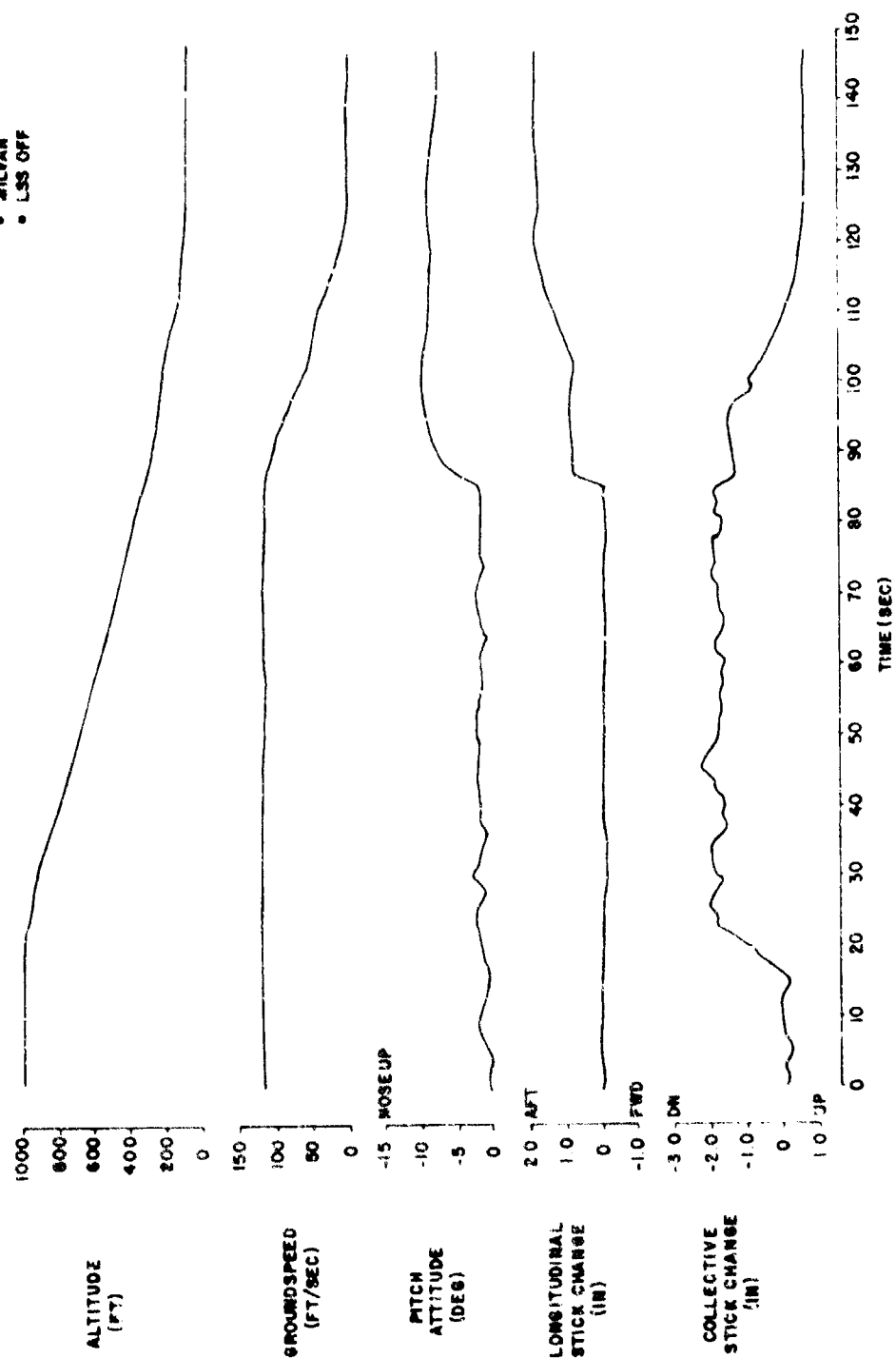
FIGURE 239. COUPLED AUTOMATIC APPROACH TO HOVER

592
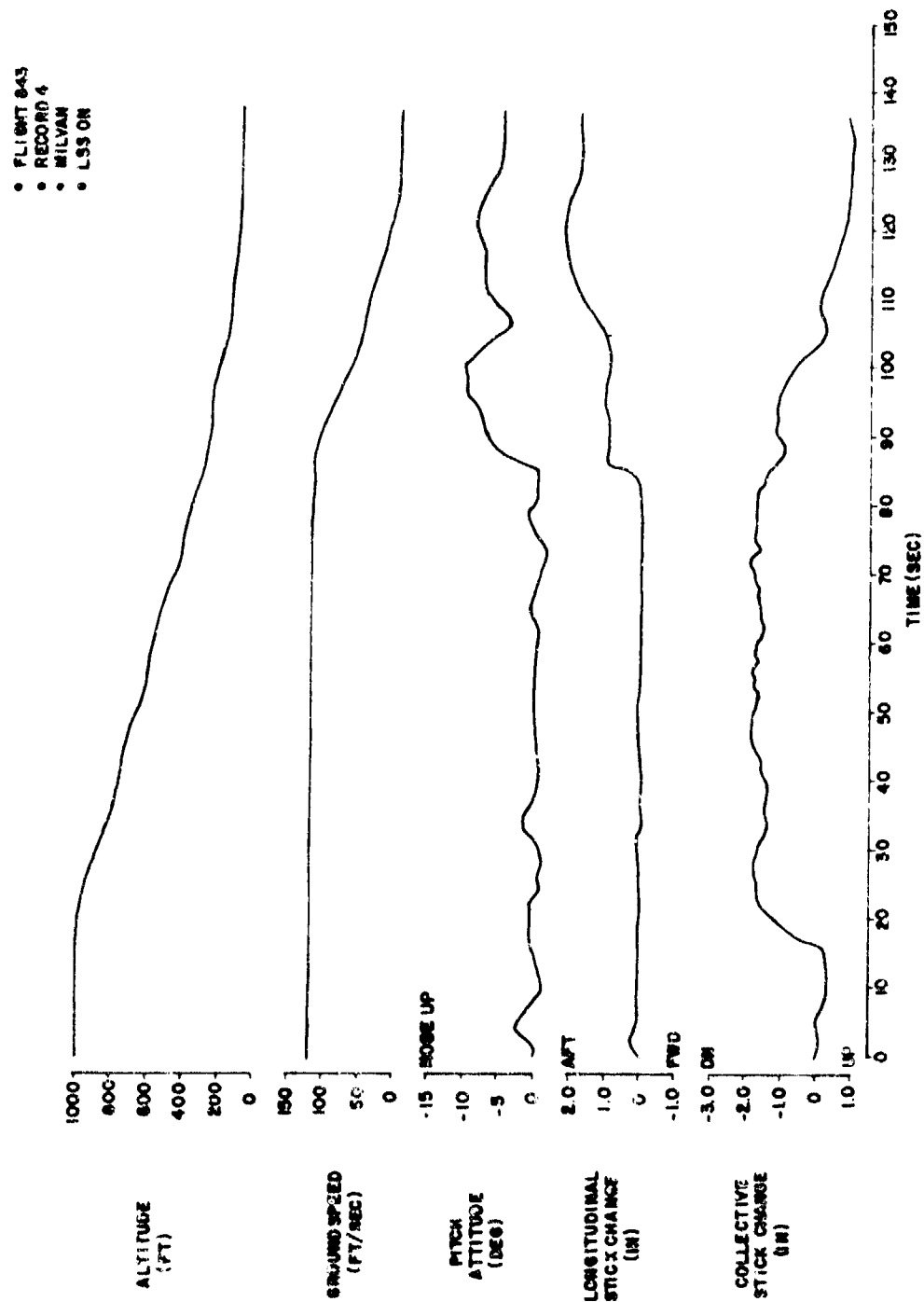
FIGURE 240. COUPLED AUTOMATIC APPROACH TO HOVER

593

FIGURE 241. COUPLED AUTOMATIC APPROACH TO HOVER

* FLIGHT 843
* RECORD 11
* HIGH DENSITY LOAD
* LSS OFF

ALTITUDE (FT)

GROUNDSPEED (FT/SEC)

PITCH ATTITUDE (DEG)

LONGITUDINAL STICK CHANGE (IN)

COLLECTIVE STICK CHANGE (IN)

TIME (SEC)

594
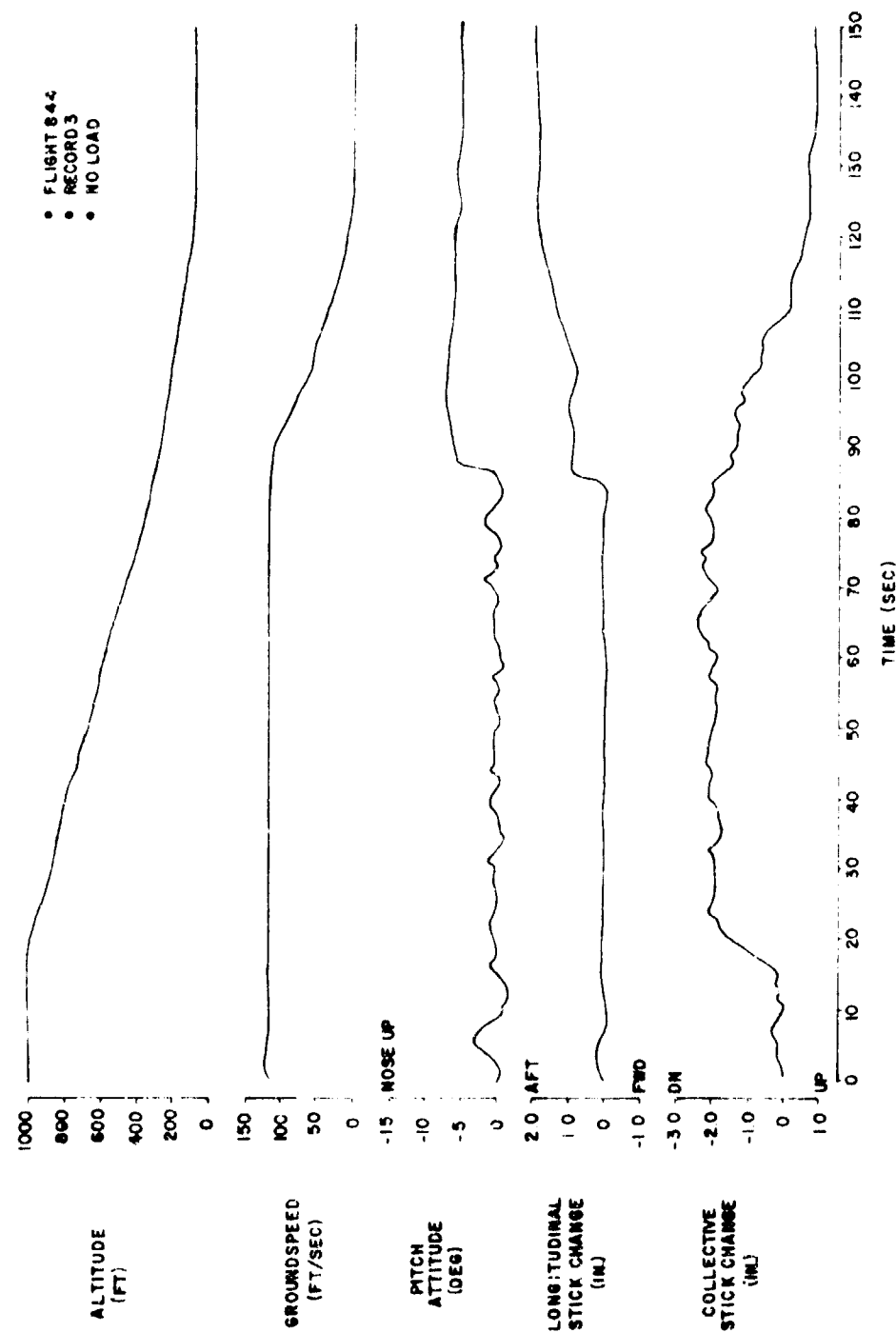
FIGURE 24.2. COUPLED AUTOMATIC APPROACH TO HOVER

595

These show that the system maintains the desired profile without excessive control or attitude deviations. Also, the system performance is essentially independent of aircraft configuration (i.e., external load or load stabilization). The exact profile errors for the automatic approach with a MILVAN and no LSS are shown on Figure 243. The groundspeed error is minimal down to the flare point where it increases to 7.5 fps which is slightly higher than the specified value of 4 knots (6.7 fps). However, the altitude error is much more significant. At the initial descent point (distance to go = 10370 feet), the altitude error jumps quickly to 60 feet, and is being slowly reduced to approximately 35 feet at the flare point where it jumps back to 60 feet. After the flare, the error is finally reduced to zero. At first glance, this error appears extreme; however, the desired altitude profile was generated assuming instantaneous changes in descent rate at the initial descent and flare points. Obviously, this is not realistic, and results in large altitude errors. A more realistic approach would have been to generate a vertical rate profile which corresponded more closely to actual aircraft capabilities, and then derive an altitude profile from this rate profile.

Fig. 244 illustrates a manual approach. As expected, this shows that a manual approach is not as precise as an automatic approach. This can be attributed to pilot lag and the necessity to continually scan four separated flight director command bars. Furthermore, this particular manual approach was performed after only three previous manual approaches. A comparison of flight director commands for a manual and automatic approach, Fig. 245, further emphasizes the automatic system ability to track the desired commands. This shows that the automatic systems track the flight director commands almost instantaneously while the pilot has a significant time delay.

Although the auto approach system was evaluated as being acceptable, occasionally the auto approach system would cause excessive pitch attitude excursion which the pilot felt was objectionable. Fig. 246 illustrates such an approach. This pitch problem was caused primarily by the fact that no attitude limits were incorporated in the approach control laws. Attitude was commanded by longitudinal control to follow groundspeed profile. If helicopter got behind groundspeed (too fast) increased attitude was commanded. This in turn caused longitudinal AFCS attitude authority limit to be

596
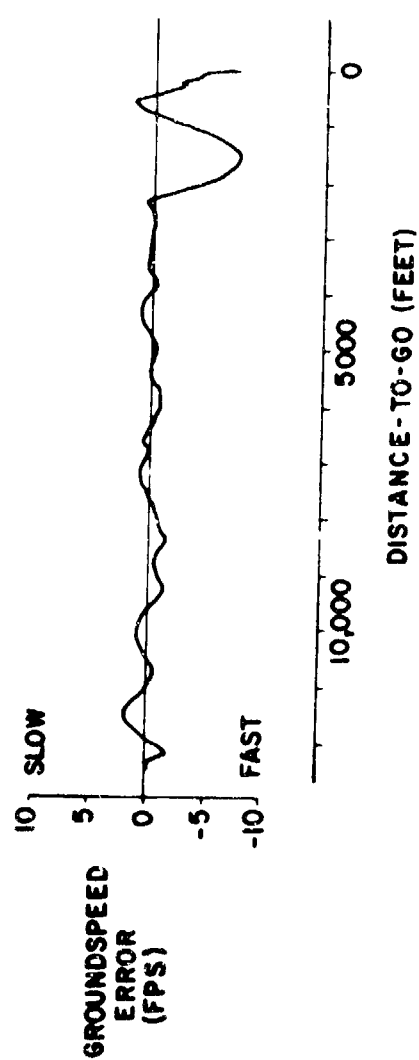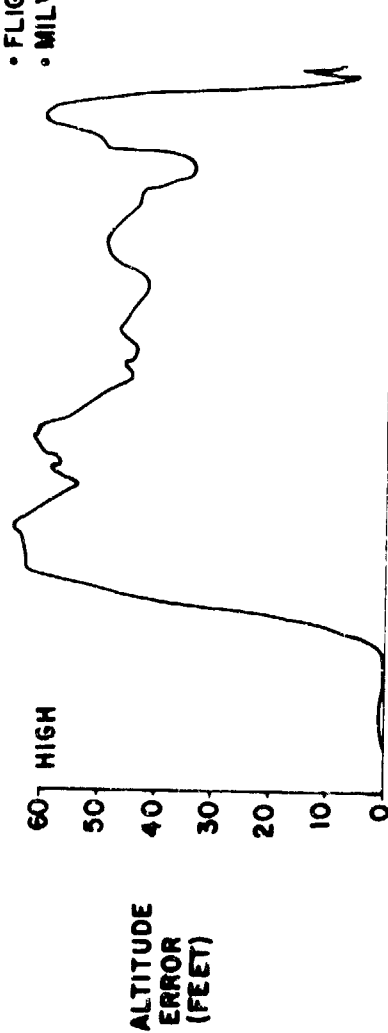
FIGURE 243. AUTOMATIC APPROACH TO HOVER - PROFILE ERROR
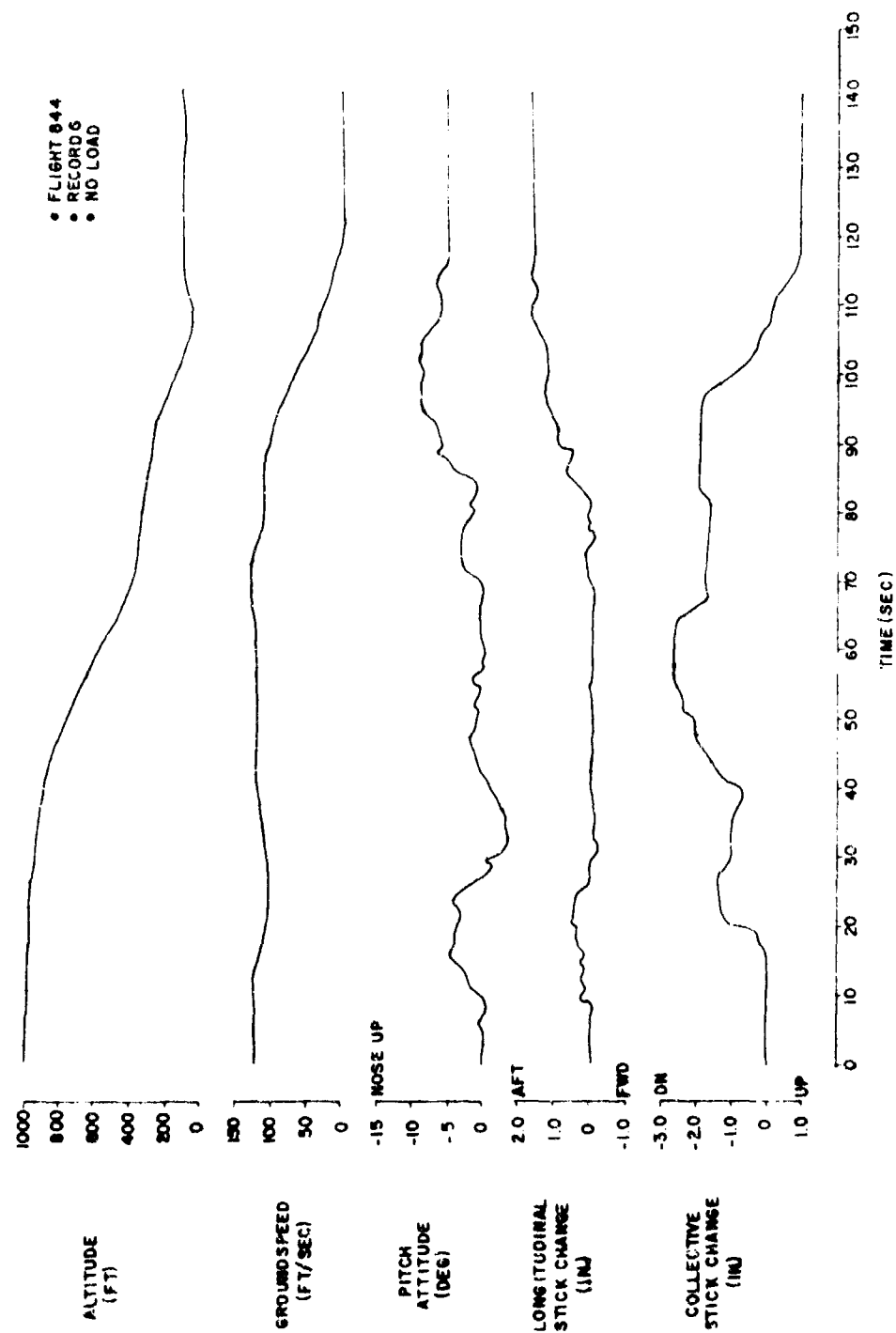
FIGURE 244. MANUAL APPROACH TO HOVER
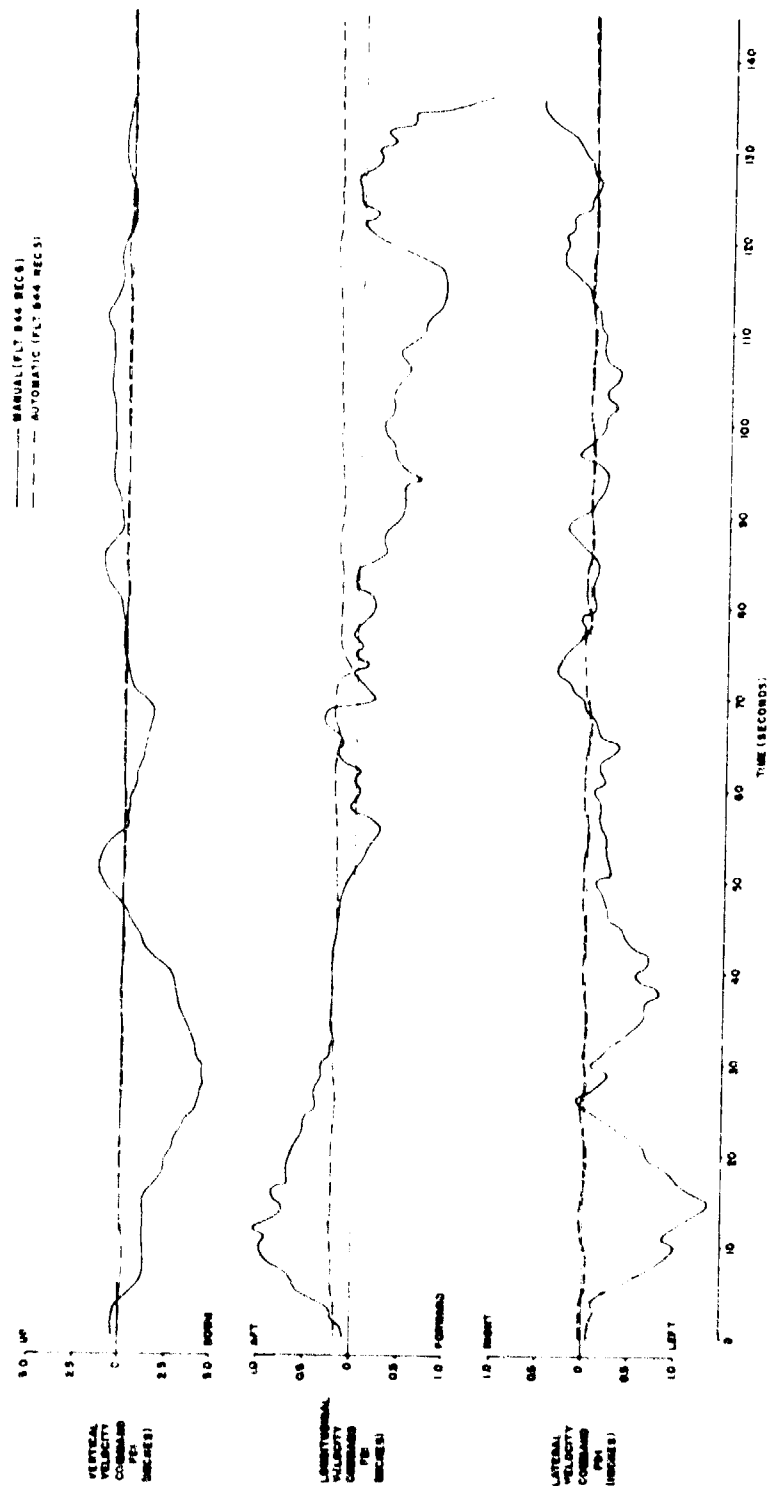
FIGURE 245. TYPICAL FLIGHT DIRECTOR ERROR SIGNALS

599
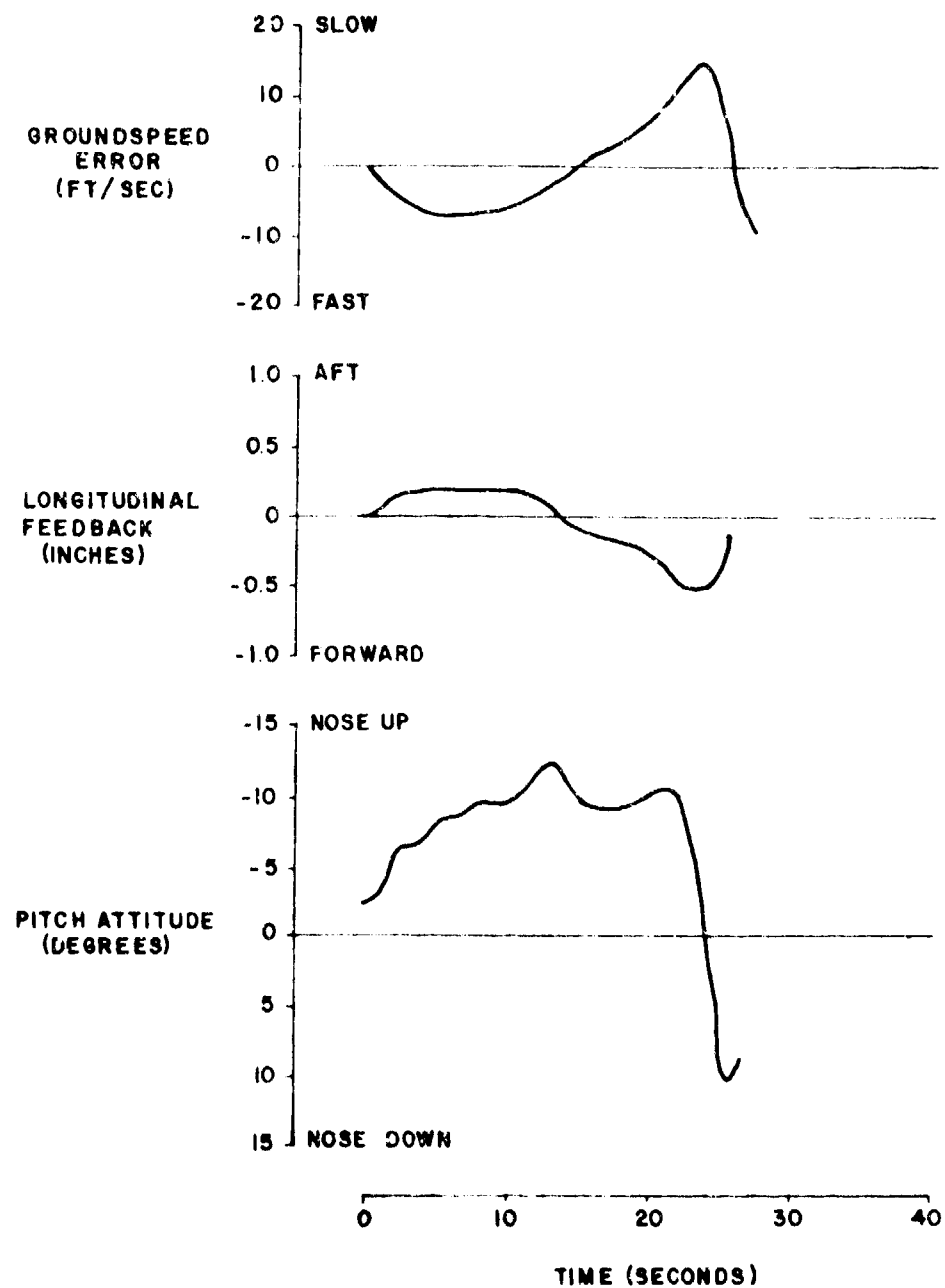
FIGURE 246.

AAH PITCH DOWN PROBLEM

exceeded which resulted in gradual pitch-up and stick moving forward in cockpit. This is similar to the problem noted under the Basic SCAS write-up in Section **5.3.1.**3. The maneuver was either terminated by the pilot or ridden out; fairly sharp pitch-down occurred as lower airspeeds were reached.

One possible method for correcting this problem would be to provide tighter groundspeed control by optimizing the open loop longitudinal stick function $F_{BDB}$. This would permit tighter limits on the feedback loop. Also, since the problem was one of pitching down, the limit could be asymmetrical to further constrain the forward stick motion. Pitch limiting would need to be incorporated along with steep flare controllability recommendations of 5.3.1.3.

An alternative solution would be to reconfigure the longitudinal control loops for pitch attitude control. For this concept, the longitudinal SCAS would be configured in the attitude hold mode, and the open loop stick functions $F_{BDB}$ would correspond to the desired pitch attitude response. The desired groundspeed function would be modified to correspond to the groundspeed profile generated by the desired attitude profile. The necessary gains and functions would be developed through further simulation and flight test evaluation.

5.3.6.3  In-Flight System Refinements

As the flight evaluation was being performed, it became necessary to introduce control law and parameter refinements in order to solve in-flight problems. The following is a list of the system modifications.

5.3.6.3.1  Complementary Vertical Rate Signal

The original auto approach system used radar rate for rate of descent reference. However, uneven terrain features (trees, houses, river banks, etc.) caused large radar rate spikes which in turn caused excessive collective activity. Figure 247 illustrates a typical radar rate signal during an approach. Filtering and gain reduction of the rate feedback reduced the effect of the spikes, but degraded system performance. A similar problem encountered on the vertical hover hold system was solved by using a complementary vertical rate signal which utilizes heavily filtered radar rate for low-frequency information and vertical acceleration for high-frequency rate data.
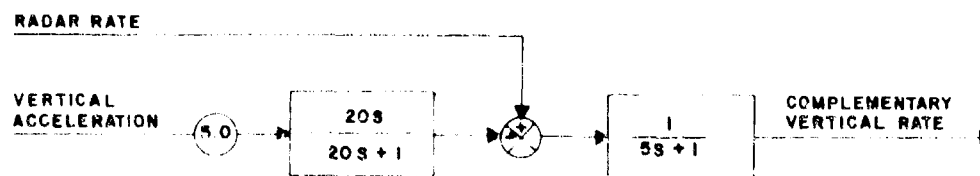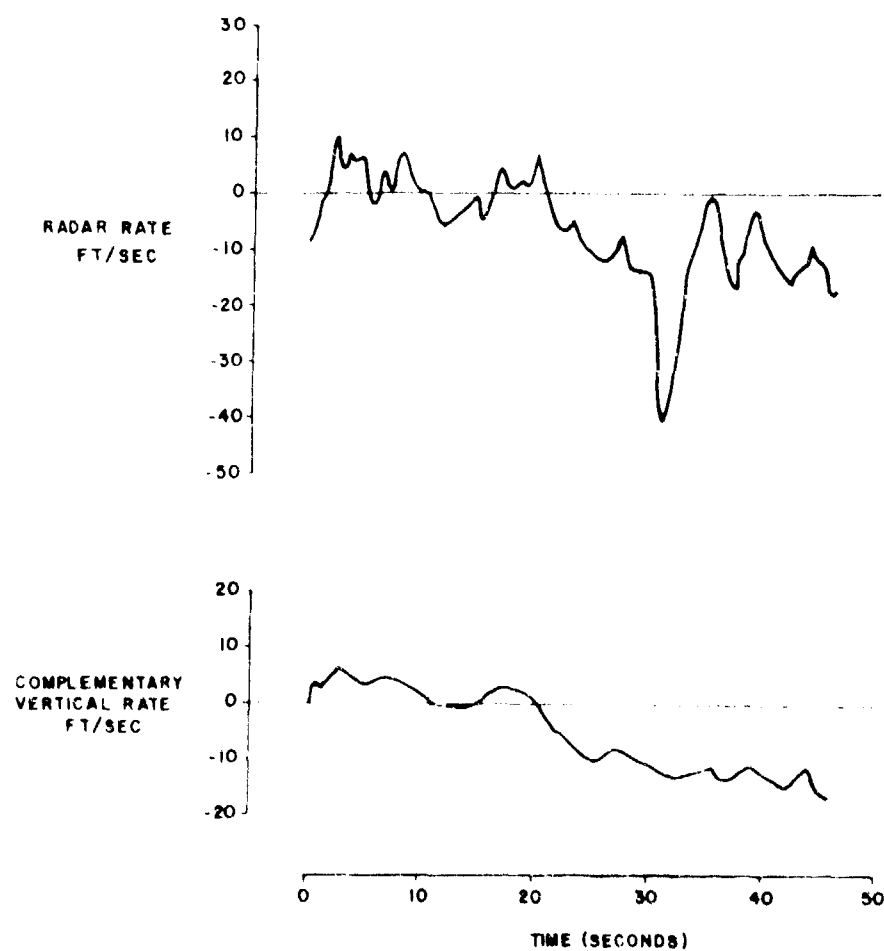
FIGURE 247.

RADAR RATE VS COMPLEMENTARY VERTICAL RATE

This was implemented on the auto approach system and proved to be very effective as illustrated in Figure 247.

## 5.3.6.3.2 Altitude Transient-Free Switch

Originally, the transfer from barometric to radar altitude reference was accomplished by a linear phasing from baro to radar as a function of distance from the hover point. This eliminates any step transient during transfer by ramping in the difference between baro and radar. However, it was found that rather large differences between baro and radar could occur, causing high ramp rates and producing objectionable transients (Figure 248). In order to overcome this problem, the switch from baro to radar was accomplished using a transient-free switch This switch permitted transition from baro to radar and ramped in the difference between baro and radar with a controlled rate of 4 fps.

Figure 249 illustrates the transient-free switch operation. When the distance-to-go, Dx, is greater than 1000 feet, the radar altitude is synchronized and the output of the transient-free switch is barometric altitude. For Dx less than 1000 feet, the TFS ouput equals the summation of

- Baro altitude at Dx = 1000 feet

- Difference between radar altitude and the radar altitude at Dx = 1000 feet, $h_R$

Several combinations of switching point and ramp rate were tried, and switching at 1000 feet with a ramp rate of 4 fps as found to give acceptable response.

## 5.3.6.3.3 Low Airspeed Collective Bias Loop

At low airspeeds near hover, it was found that additional up collective was required to compensate for collective trim shift, particularly in tailwinds. This was provided through the low airspeed collective bias loop. This loop operates by generating an approximately airspeed signal for airspeeds
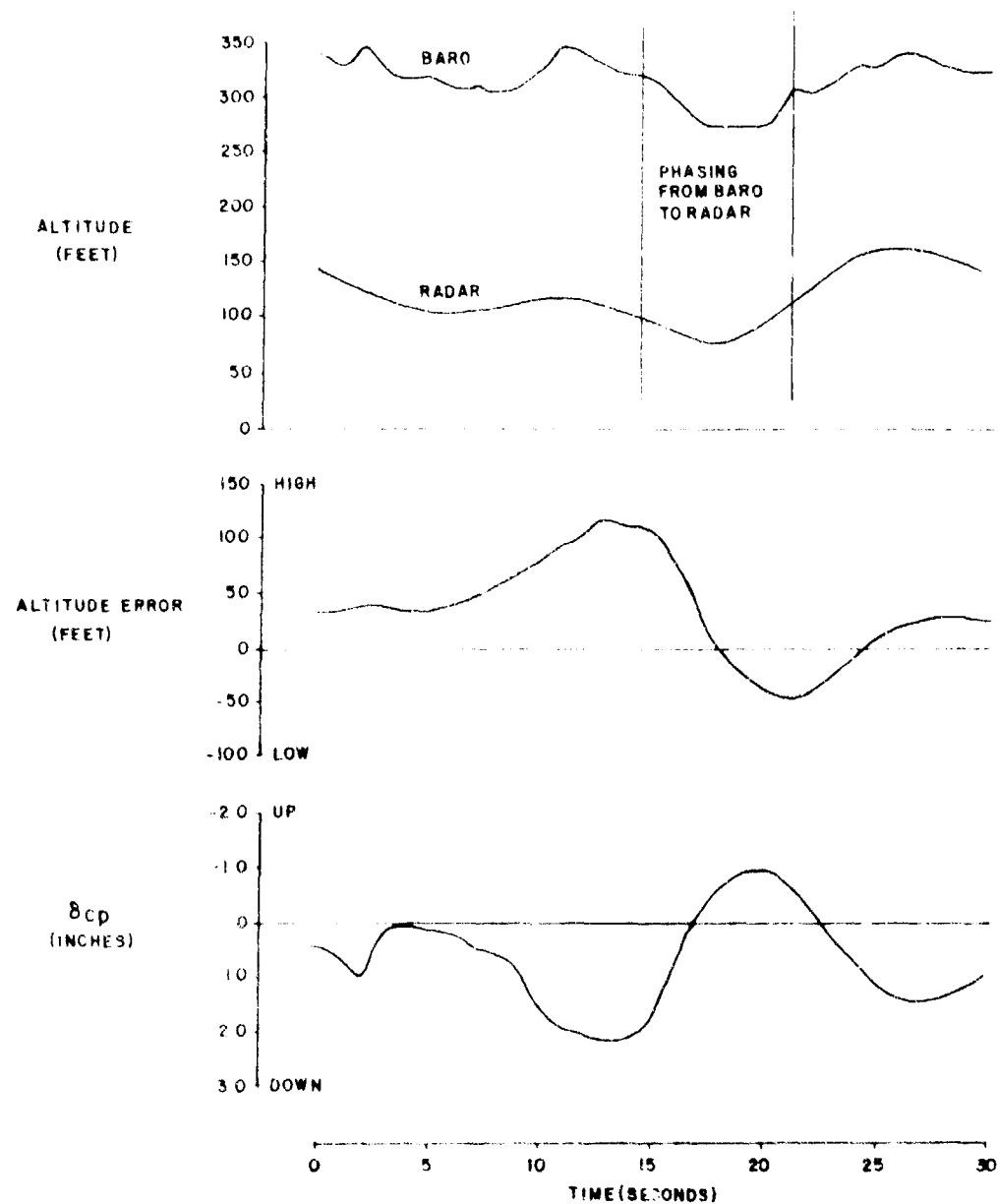
FIGURE 248.
BARO TO RADAR PHASING TRANSIENT

604
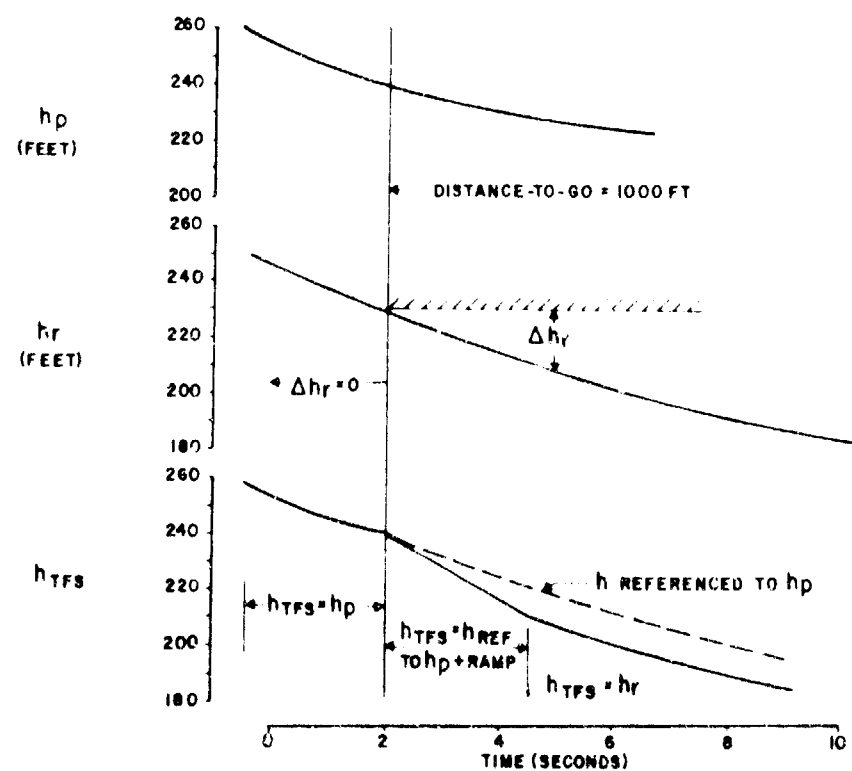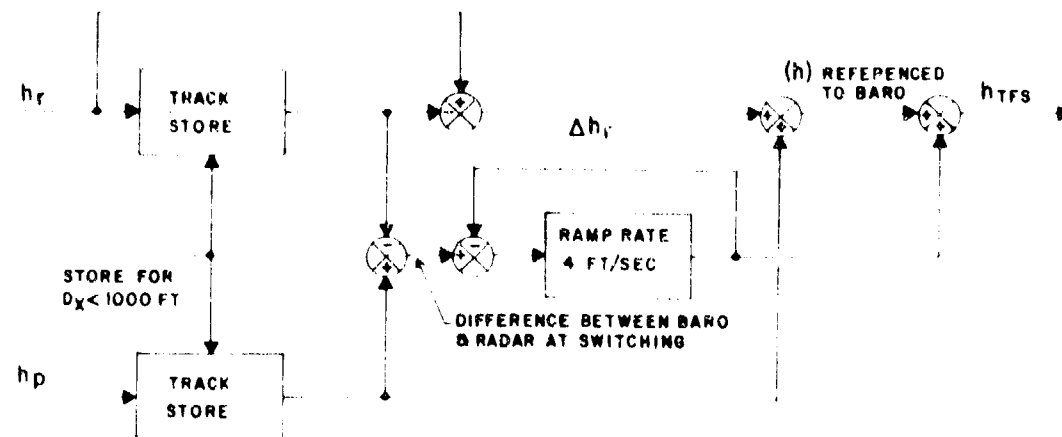
FIGURE 249.
ALTITUDE TRANSIENT-FREE SWITCH

605

less than 40 knots. This airspeed drives a function genera-
tor which provides an up collective step when the airspeed is
less than 25 knots. This step function is fed to the total
collective command through a lag, $T_{Z17}$, which softens the step
input. The airspeed approximation is generated by determining
the difference between airspeed and longitudinal groundspeed.
This difference is held when the distance-to-go is less than
2290 feet. The approximate airspeed is equal to

Approx. A/S = Long.Groundspeed + (A/S - Long.Groundspeed)
DX = 2290'

A 1/2-inch step at 25 knots airspeed through a 1-second lag
was found to give acceptable response.

5.3.6.3.4  Gains, Time Constants and Limiters

The following gain and time constant changes significantly
improved the system response characteristics:

|  | ANALYSIS | FLIGHT |
|---|---|---|
| $K_{SYD}$ | .005 in./ft | .0038 in./ft |
| $K_{SYV}$ | .05 in./fps | .0625 in./fps |
| $K_{BXV}$ | .015 in./fps | .036 in./fps |
| $K_{CZV}$ | .70 in./fps | .135 in./fps |
| $F_{CZH}$ | .01 in./ft | .0185 in./ft |
| $T_{Z8}$ | 10.0 sec | 50.0 sec |
| $T_{ZFD2}$ | .75 sec | 1.5 sec |

The rate limits on $L_{Z6}$ and $L_{Z7}$ and on $F_{CZV}$ and $F_{CDC}$ were re-
quired to reduce the excessive collective activity at the
beginning of the descent and flare phases. The limiters $L_{M9}$
and $L_{M10}$ on the longitudinal groundspeed loop were implement-
ed to limit longitudinal overcontrol.

5.3.6.3.5  Collective Flare Compensation

The pitch attitude/rate of descent coupling was not as strong
as anticipated; therefore, the collective flare compensation
loop was eliminated.

## 6.0   AFCS EQUIPMENT PERFORMANCE EVALUATION

### 6.1   FLIGHT CONTROL COMPUTER SUBSYSTEM

A large portion of this section is devoted to the problems
encountered and resolutions made during the develo ment of the
HLH-ATC AFCS.   Few of the problems discussed have a major impact
upon the design for the HLH Prototype AFCS.   The general per-
formance of the AFCS throughout the ATC program has been con-
sidered very satisfactory in meeting the system requirements
and due credit must be given to the General Electric Company
for a thorough design and test support effort.

Problems discussed are classed with each individual item of
equipment:

#### Computer

- Read-only-memory integrated circuit reliability
- Clock pulse distortion
- System shutdown following individual cross-channel LRU
  failure.

#### IOP

- Input discrete failures
- Analog-to-digital converter reliability
- Analog ac demodulator reliability
- Digital-to-analog converter reliability
- Sensor signal conditioning circuit leakage
- Power supply low temperature operation
- Mode logic board reliability
- Input data voter failure identification
- BITE modification for unused IOP outputs channel to
  channel

### 6.1.1  Flight Control Computers

#### 6.1.1.1  ROM Integrated Circuit Reliability

Prior to the acceptance tests, several ROM devices had failed
to consistently program to the zero state after being erased
to the one state.  Devices that failed to properly program in
the ROM programmer unit also failed in the same bit locations
when programmed on the Spectrum Dynamics Memory Programmer.

Modifications were made to the ROM programmer unit to improve
the programming capability and to reduce the power dissipated
on the ROM boards during programming.  This appeared to reduce
the frequency of failures, but did not eliminate the problem.

Several ROM device failures occurred during the humidity qual-
ification tests, which are reported in Section 4.1.2.  In an
attempt to appraise the degrading effects of humidity on the
ROMs a random sample of three brand new devices were subjected
to the same humidity profile test as those on the computer
boards, but no failures were found.  This focused attention
on the circuit board conformal coating process with probability
of line-to-line (pin-to-pin) conduction paths forming with the
moisture after being exposed to the humidity cycle; however,
no conclusion was made.

Continued failures have been experienced throughout the flight
program with no identification of the problem.  It appears
that the frequency of failures increases with the number of
times the board is programmed with no specific pattern of events.
It is, however, clear that this remains a major problem for the
prototype AFCS operation and can only be combatted at this time
by providing spare boards to permit a smooth flight test program
to proceed.  Each time a ROM failure is experienced, the device
is replaced.  No resolution is forthcoming from the device
manufacturer and there is no substitute device.  Other equiv-
alent devices would necessitate redesign work.

#### 6.1.1.2  Clock Pulse Distortion

Triplex testing prior to acceptance tests uncovered a problem
in computer clock pulse distortion which impacted the cross
channel timing synchronization and clock monitoring.  This
problem was resolved by additional ground grids  on the computer
timing and synchronization printed circuit boards.

608

### 6.1.2  Input/Output Processors

#### 6.1.2.1  Input Discrete Failures

Throughout the flight program, unexplained IOP input discrete failures occurred in flight, which for the most part resulted in system first level failures and in a few instances, system shutdown when the first occurrence had not been reset. In all cases experienced, the failure was resetable and could not be duplicated by trial and error on the ground. No pattern of events could be established from the inflight information nor from any recorded data to identify the discrete or combination thereof causing the problem. It was not clearly established that the problem was due to discretes delaying or malfunctioning; the cause could have been noise on the monitor itself. The problem remains unsolved and can only be further pursued for the prototype program.

Three factors make this problem difficult to trace; one, the inherent design problem of combining all discrete information into 16-bit serial data words and therefore losing identity of individually failed discretes. Two, the inability of the data recording system to register raw discrete information in the entirety required to troubleshoot the problem, as well as the inability to record the event as it occurs randomly. Three, the inability to duplicate the problem on the ground or in the laboratory, in an environment which offers detail scrutiny.

An attempt was made to change the discrete failure monitoring technique from eight accumulated samples from every eighth iteration to 15 consecutive samples, but without apparent success. At least this would have proven a deterrent for one discrete to have delayed for a period of more than 150 ms before being declared failed. It appears unreasonable to expect such a delay from any single system discrete, therefore placing more emphasis on the problem being due to more than one discrete delay and possibly noise.

#### 6.1.2.2  A/D Converter Reliability

Analog-to-digital converter failures have been manifested in several ways, none of which have led to a complete interruption of data transmission from IOP to computers:

A pitch axis disturbance with a racheting characteristic was traced to the fact that the median value of the pitch rate gyro signal was following a square wave pattern, also noted on roll rate, though less frequent. Pitch attitude data also followed the same trend, but

not coincident with pitch rate information.  These
deviations were not large enough to cause failure
indications.

A rash of simultaneous single channel sensor failures
would be indicated, which most often were resetable
indicating transient malfunction of the device.  More
often, the problem would be evidenced by erratic high
static offset readings - the same device in similar
location at a later time would appear normal.

The accumulation of these problems occurred during the
flight program and were always solved by the replacement
of the A/D module device.  It became apparent that the
module device was sustaining high junction temperatures
when operating in the aircraft during the summer months.
The installation of cooling fans in the IOP lids over the
A/D card location apparently succeeded in reducing the
junction temperatures to a satisfactory level to increase
device life expectancy/reliability.

The vendor has reported to have had problems with these
devices on other programs and is investigating the use of
more expensive upgraded temperature range pin compatible
devices as a solution for the prototype AFCS.  Should this
solution not succeed, a substitute device will require
board design to be compatible.

6.1.2.3  Analog AC Demodulator

A number of failures of the HIC demodulator flatpack devices
has occurred throughout the program.  The AC reference has
been observed on the output of some of the sensor demodulator
networks (which appears as a static null offset at the PCDU)
and no reason for the failures has been forthcoming, as no set
of circumstances has been gathered to pinpoint a reason for
the failures.  A proposed solution to this problem is to
screen these devices upon equipment return to the vendor and
replace those units which have degraded performance.

6.1.2.4  Digital/Analog Converter Reliability

Two problems were encountered with the DAC and Sample/Hold
amplifier card, one of which resulted in DELS shutdown of AFCS
and the other in a malfunction of longitudinal CCDA drive.
Replacing the D/A module apparently solved the problem and this
practice will continue for the prototype AFCS upon the occur-
rence of a malfunction.

610

6.1.2.5  Input Data Voter Failure Identification

This problem was associated with identification of an input
data voter failure in one of the three computers which is
induced by a simulated triplex sensor failure and the conse-
quent sensor select switchover from median select to averaging.
This failure occurred relatively infrequently in a non-
repeatable manner since it was an induced failure that followed
a sensor failure.  It was immediately resettable by Error Re-
set.  The bit time synchronization circuitry of the median
select outputs was modified to insure triplex signal corre-
spondence at the inputs to the computer input data voters.


6.2  SENSORS

6.2.1  Airspeed Sensor

Two types of problems associated with the sensing and genera-
tion of linear airspeed were encountered during flight test-
ing:

- Dynamic tracking accuracy between the triplex sensors,and
- Airspeed fluctuations during forward flight acceleration.


Subsequent to the resolution of these problems, the performance
of the airspeed sensors was satisfactory for AFCS operation.

6.2.1.1  Dynamic Tracking

The Precision Airspeed Trim (PAST) sensors were originally
designed for the Model 347 Flight Demonstration Program in
the 1968-1970 time frame.  In that application, the PAST units
were employed in a dual configuration,driving two independently
operating channels of signal processing and actuation with no
requirement for close cross-channel tracking.  However, in the
utilization of those units in the HLH/ATC program, problems
associated with cross-channel mistrack resulted in a number of
airspeed first-failure indications.  Analysis of flight data
and subsequent laboratory testing identified differing dynamic
response characteristics between the several PAST units.  This
situation was satisfactorily resolved by adjustment of servo
loop phase compensation in the less sensitive units to match
the response of the more sensitive units.  These adjustments
did not degrade AFCS performance in any way.

611

This type of problem cannot occur in the air data modules developed for the HLH prototype aircraft as these units utilize completely electronic processing of the dynamic-pressure-to-linear-airspeed shaping in contrast to the electro-mechanical servos utilized in the PAST units.

### 6.2.1.2 Airspeed Fluctuations During Acceleration

During longitudinal accelerations into forward flight, a pitch-up problem was encountered at about 40 knots, followed by an excessive pitch-down between 50 to 60 knots. This condition did not become evident until after the triplex Precision Airspeed Trim (PAST) unit servo loop gains had been tightened up to eliminate airspeed failure trips resulting from dynamic mismatch. With the tight servo loops, the airspeed was responding to the effect of rotor tip vortex effects, causing a fictitiously excessive speed increase between 40 and 45 knots. This spurious effect was compensated for by slowing down the PAST response. The 50- to 60-knot pitch-down problem was compensated for by replacing the wide angle Pitot heads with narrow-angle heads. This effectively compensated for the undesirable rotor downwash effects.

### 6.2.2 Reference Barometric Altitude

The design of the reference barometric altitude unit used for the 347 HLH flight control system demonstrator aircraft was essentially the altitude hold feature of the Canadian CH-147 ATS box. The collective A and B cards from that box were modified to meet the requirements of the altitude hold and automatic approach to hover modes of the HLH/ATC AFCS. The barometric transducer and these two modified cards were interconnected and repackaged to form the reference barometric altitude units.

Since the CH-147 and the 347 has concurrent flight test programs, some of the developmental problems experienced on the CH-147 AFCS altitude sensor were also experienced with the 347 altitude sensor. As the problems were resolved for the CH-147, and if applicable for the 347, the modifications were made to the altitude synchronizers at the Engineering Laboratory and returned to the aircraft for test and evaluation.

Problems encountered with the altitude synchronizer are listed below with a brief description of the problems as experienced on the 347 aircraft:

- Large engage errors
- Drift
- Data spiking
- Hardovers
- Excessive time lag from synchronize to stabilize

612

### 6.2.2.1  Large Engage Errors

During the functional testing of the altitude synchronizer
on the aircraft, numerous BARO ALT sensor failure indications
were experienced seconds after the BARO ALT HOLD mode was
selected.  Investigations revealed that the HI GAIN output was
randomly jumping from approximately -5 MUs (.024 Vdc) in SYNC
mode to -200 to -400 MUs (1 Vdc to 2 Vdc) in the STAB mode.
In engineering units, this is about .6 ft. to 50 ft.  These
jumps exceeded the failure detection threshold levels, thereby
causing a sensor fail condition.  This problem was attributed
to the short time constant of the analog synchronizer loop.
Another suspect area was the second-stage amplifier which had
a relatively low gain because of the dual tracking requirement
of 250 ft and 500 ft, thereby making it more susceptible
to noise.  The resolution of this problem is discussed in
section 6.2.2.6.

### 6.2.2.2  Drift

Drifting of the HI GAIN output was observed with the altitude
synchronizer in the STABILIZE mode.  This drift was random in
polarity, rate, and magnitude.  Occasionally, this drift caused
the absolute difference between the channel A sensor and the
channel C sensor to exceed the failure detection threshold
levels, thereby causing a sensor fail condition.  This problem
was attributed to improper handling of the FET in the synchro-
nizer loop during equipment fabrication causing the relay
module (FET, relay and holding capacitor) to be excessively
heat sensitive.  This relay module was subjected to temperature
changes up to 20°F between the SYNC and STAB modes.  The
resolution of this problem is discussed in section 6.2.2.6.

### 6.2.2.3  Hardovers

Hardovers were experienced with the serial number 1 unit on
both the HI gain and LO gain outputs.  Both were traced to
defective components.  In the former, the HI gain output
amplifier AR4 was replaced and in the latter, a relay in the
relay module was defective.

6.2.2.4 Excessive Time Lag

During the BARO altitude hold evaluation, the pilot complained
of excessive overshoots or undershoots of the aircraft if the
mode was selected in a rate of climb or descent. A time lag
of 2-3 seconds was measured from the synchronize to the
stabilize mode. This time lag was consistent with the reported
overshoots/undershoots of 25 ft at 500 ft/min and 50 ft at
1000 ft/min rates of climb or descent. Since this operating
condition was not envisaged at the time the altitude units
were designed, the time lag was not considered excessive.
The time lag is adjustable; however, it was not altered during
the ATC flight test program.

6.2.2.5 Problem Work Arounds

Because of the numerous developmental problems experienced with
the reference altitude units, work around methods were employed
in the aircraft installation of this sensor, e.g.:

1.  The redundancy level of the baro was specified as duplex,
    but because of the aforementioned problems, especially
    the engage errors and drift, a single sensor was wired
    into a duplex configuration. This effectively prevented
    the failure detection system from disabling the BARO
    altitude hold mode.

2.  The BARO sensor was vented to the cabin towards the
    end of the flight test program. It was theorized that
    external static pressure disturbances and the pneumatic
    filters installed in the static ports could have contri-
    buted to the unexplained altitude deviations in the BARO
    hold mode and large tracking errors ($\geq$ 100 ft) between
    BARO and RADAR in the AAH mode.

These changes were employed for flight test expediency and
will not be resorted to for the HLH prototype program, for which
a sensing device of new design is being developed.

6.2.3 Inertial Measurement Unit

The Carousel IV Inertial Navigation System (INS) used as a
velocity attitude and vertical acceleration sensor was con-
sidered satisfactory for the 347/HLH ATC flight control system.
Two minor problem areas were encountered throughout the flight
test program with little or no impact on the scheduled flights.

● Random Drifting in Hover

Early evaluation of hovering over a spot with basic SCAS and IMU-referenced groundspeed feedback revealed some difficulty in trimming the controls precisely for zero velocity. This problem was attributed to three main reasons:

(1) Ineffective beep trim during parallel back drive (bias elimination)

(2) high lateral and longitudinal control sensitivities

(3) HMU drift

The first two were addressed by control law changes and the third was believed to be caused by the sensor. Since the sensor performance was within specification, the vendor - DELCO Electronics - was consulted. They reviewed our alignment procedure and made change recommendations. Essentially their recommendation was to allow the system to remain in the coarse azimuth submode of alignment for approximately 10 minutes before entering the fine align mode. They also suggested that we should not allow the Performance Index (PI) of alignment to go below 5 if there were aircraft disturbances during the time of alignment. They said it was possible that a large Z-gyro bias term could be entered into the alignment equations while going down to a $PI = 0$.

The flight test program revealed that the best procedure was to leave the system in a PI of 7 for approximately 10 minutes and to perform a double alignment. This of course did not completely eliminate the IMU drift but it seemed to reduce some of the excessive groundspeed drift that was experienced early in the flight test program.

● Inflight IMU Groundspeed Failures

On two occasions during flights X725 and X838, IMU ground speed failures were reported on the AFCS sensor failure status panel. This sensor failure caused the lateral and longitudinal axis to be shut down, thereby aborting the flights. Inflight analysis and ground testing indicated that groundspeed difference between the no. 1 and no. 2 IMUs was exceeding the failure monitoring threshold levels of 16 fps. In both cases, the suspect IMU was replaced with a spare and returned to the vendor for further investigation. The large groundspeed buildup was confirmed by the vendor and repaired by replacing a $1.2KH_z$

inverter in one case and replacing a lateral gyro in the
other. Both failures occurred with the same IMU.
Throughout the integration and functional and flight test-
ing, seven hardware malfunctions were experienced with the
Carousel IV INS. Six were with the navigation units
(one as a result of human error) and one with a control
display unit. In all cases, a spare unit was used on
the aircraft and the defective unit was sent back to
the vendor. The vendor confirmed all failures and re-
paired and returned them.

### 6.2.4  Attitude/Heading Reference System (AHRS)

The performance of the AHRS as an attitude sensor was judged
satisfactory. However, the attempt to convert the magnetic
heading output into true heading was considered unsatisfactory.

During the first months of the flight test program, numerous
channel B (ASN-76) heading failures were observed on the AFCS
sensor failure panel. These failures were random and in most
cases were resettable after the failure had occurred.

Ground tests revealed nothing since the failure could not be
duplicated. However, it was observed that on occasions the
channel B heading signal was not tracking the two INS heading
signals for that particular heading of the aircraft.

Further observations of this problem, both on the ground and
in flight, showed that the heading difference between the
ASN-76 magnetic heading output and the INS heading output
varied from approximately 2.5 degrees to 14.5 degrees west.
(The local variation in the test area was published to be
9.7 degrees west - the value to which the magnetic heading
adapter differential synchro was set.) This variance was
not predictable, i.e., not heading-sensitive, but was affected
by engines running, aircraft located inside or outside of the
hangar, and the proximity of large metallic objects. Since
the magnetic variation anomalies did not affect the performance
of the AFCS, other than nuisance AFCS first-fail indications,
it was decided to live with this situation for the ATC program
and re-evaluate the use of this signal for the prototype
program.

### Hardware Failures

Two displacement gyroscopes were rejected from the aircraft -
one for causing erroneous malfunction indication on the
compass controller, and the other for excessive drift of the
directional gyro. Both gyros were replaced with no impact
on the flight program.

## 6.2.5  Radar Altimeter

The APN-194 radar altimeter was originally designed to provide flight crews of fixed and rotary wing aircraft with an indication of absolute height above terrain.  The application of this system to the automatic control of a helicopter in hover flight is a radical departure from the original design intent. The recognition of this situation early in the design phase of the ATC program dictated the need for certain modifications to the basic altimeter system.  These changes included:

- Development of a rate adapter unit to provide a high sensitivity vertical rate output of + 50 fps with accuracy of ± 0.1 fps + 0.5 percent of actual rate. This is in contrast to the standard rate output from the R/T unit with a ceiling of ± 500 fps and accuracy of ± 5 fps + 5 percent of actual rate.

- Reduction of the receiver tracking rate from ± 2000 fps to ± 150 fps.  This capability was designed into the original system for helicopter applications.

- Increase in the sensitivity range control gain by 4 dB for low-altitude operation (0 to 20 feet).

### 6.2.5.1  Operating Problems and Resolution

During the initial evaluations of the radar altitude hold mode, considerable spiking (± 10-12 feet over grass and ± 3-5 ft over hard surfaced runways) was observed on the pilot's indicator and was also reflected in the aircraft closed-loop response.  This condition was the result of RF fading, a condition which is evident with almost any RF receiving device when there is little or no relative motion between the aircraft and the ground, as in hover flight.

Attempts to minimize this problem included a succession of equipment changes including:

- Installation of a blanker unit to reduce the rate of outbound sweep of the track gate upon loss of video.

- Further adjustment of the sensitivity range control gain.

- Adjustment of the post-detect integrator to position the track gate lower on the leading edge of the video.

- Further reduction of the tracking rate to ± 30 fps.

617

- Installation of hardware filters on the altitude output (time constant = 0.1 sec) and on the altitude rate output (0.9 sec second order break frequency).

- Changed antenna transmission lines from RG 223 to RG 214 coax cables.

These changes, along with the incorporation of software complementary filtering of the radar rate signal with vertical acceleration in the FCCs, reduced the effects of spiking to a level at which the altitude and hover hold modes could be acceptably evaluated. It was, however, necessary for vendor field service to perform recalibrations and readjustments of the equipment on three additional occasions throughout the flight testing.

While operating with external loads on long slings (30 ft to 50 ft ) both during the terminal phase of rapid decelerating flares and during radical longitudinal maneuvers by the LCC, there were occurrences when the load swung forward into the antenna beam. This introduced large "up" step commands into the vertical axis response of the aircraft. As the load swung back aft, the reverse situation occurred, with a large downward command.

The transmitter and receiver antenna mounts were modified to cant the antennas further forward from the original 5 degrees to 10 degrees. This tended to decrease the frequency and duration of the problem but did not eliminate it completely for the larger amplitude load swings.

6.2.5.2 Proposed Changes

For the HLH prototype AFCS, the following system changes will be incorporated to further improve radar altitude and hover hold mode vertical response:

- Radar altimeter antennas will be canted forward the maximum amount possible without deteriorating signal quality during flare maneuvers.

- Radar altitude and rate IOP signal conditioning filter breakpoints will be reduced in frequency to help attenuate noise.

- Computer software will be modified to:

  (1) Rate limit the radar altitude and rate inputs.

  (2) Decrease the complementary filter breakpoint frequency in the rate path.

  (3) Incorporate complementary filtering into the altitude path.

For the production aircraft, several hardware alternatives exist:

- Dual radar altimeter installation - one in the nose and the other in the aft fuselage. This would provide the means to discriminate between ground and external load signal return.

- Development of a new radar altimeter utilizing an electronically scanned phased array antenna to eliminate spiking effects.

- Development of a new type of absolute altimeter using laser, ultrasonic, or superhigh-frequency radio transmission techniques.

6.2.6   Precision Hover Sensor

The precision hover sensor, as developed for the HLH/ATC program, was intended to provide a performance capability satisfactory to support evaluation of the precision hover features of the AFCS. To attain this goal at minimal cost and within an acceptable development time, the PHS was designed for the most part using off-the-shelf components.

6.2.6.1   Operating Problems and Resolution

During the early flight evaluation of the PHS, several types of developmental problems were experienced:

- Excessive noise on the three-axis velocity signals - Resolved by isolation of the gimbal torque motor excitation from the PHS electronic power supply and by incorporation of additional shielding around the electronic components.

619

- Erratic performance of the longitudinal incremental position and velocity outputs - The platform gimbal system was rebalanced and mechanical limiting of the gimbal freedom in the nose-up direction was corrected by shimming up the gimbal reference from 5 degrees to 8 degrees.

- Erratic performance of the lateral incremental position and velocity outputs - The platform lateral axis roll stabilization gyro was not gimballing properly. This led to roll disturbances, overcorrections, and oscillations in aircraft response. Replacement of the lateral gyro corrected this situation.

- Vertical spiking - Differences in reflectivity of the laser return from the high contrast ground scene resulted in spiking on the PHS vertical velocity output. This condition was corrected by a series of adjustments to the rangefinder electronics filter networks.

- Zoom lens hangups - During vertical translations of the aircraft, the intensifier zoom lens exhibited a tendancy to hang up in a random manner. This resulted in erroneous sensitivity changes in the x and y axis position and velocity signals. An improved gear design satisfactorily resolved this problem.

The most significant problem in the operation of the PHS was the inability of the sensor in flight to lock on to any but a very high contrast ground scene. This also was the only PHS problem not satisfactorily resolved during the test program. The basic problem was associated with providing satisfactory gain through the optical chain from the intensifier zoom lens to the correlation, so that the correlation could retain a lock-on for low intensity - low contrast ground scenes.

A number of changes were made in an attempt to extend the range of lock-on performance. These included:

- Decreasing the correlation bandwidth to improve the signal-to-noise ratio.

- Increasing the gain of the intensifier up to the safe operating limit of the correlation; i.e., without burning spots on the tube.

- Correlation storage time was reduced, the function notation was modified, and the threshold criteria for the lock-on logic was changed.

620

All of the above resulted in minor improvement only. This necessitated the limitation of precision hover testing to operation over a high-contrast checkerboard ground scene painted on an unused taxi strip. Emphasis was limited to development of AFCS signal processing to control the aircraft to valid PHS signals rather than on optimization of the sensor performance as well.

6.2.6.2 Proposed Changes

The design of a PHS for a production installation would first be preceded by an investigation of state-of-the-art developments, particularly in the areas of correlations, intensifiers, and fiber optic transmission techniques.

The correlation optical chain would be simplified by eliminating the vidicon direct viewing scene. This would allow direct fiber optics coupling between the intensifier chain and the correlation, thus eliminating the need for relay optics. This would also lower the gain and output requirements on the intensifier.

Optical stabilization would be used rather than a mechanically stabilized platform, to prevent aircraft pitch and roll from introducing errors in position and velocity measurements. Light weight mirrors would be servo controlled to stabilize the optical signals for the correlation optical chain. They would have to be of the same quality as that in the current PHS, while the rangefinder would require less accuracy, and the illuminator would only have to be accurate to within a degree or two.

The rangefinders could be simplified by improving the coarse ranging measurement and by eliminating the fine range portion of the system.

The above changes should result in a considerably more compact design with a total weight of less than 125 pounds.

6.2.7 Cable Tension Sensor

The performance of the cable tension sensor required as an input for the LSS mode of AFCS operation was considered satisfactory. Minor nuisance problems were encountered which required changing a trimming resistor on the strain gage balance bridge network,

621

After laboratory calibration of the strain-gaged cargo hook bolts, they were installed on the aircraft. A snug fit of the bolts was encountered, especially on the aft cargo hook, requiring the application of some force during the installation. The forward and aft cable tension signals inputs to the AFCS were monitored in a static unloaded condition. These signals indicated a large negative bias for the aft hook (-600 to 700 lb) and a positive bias for the forward hook +300 lb). It was theorized that the static loading on the bolts changed as a result of the snug installation.

During the flight program, it was observed that the large negative bias on the aft cable tension sensor reappeared. Investigation of this problem revealed that this signal was sensitive to electrical loads. Turning on the No. 2 INS blower caused this signal to change from a null condition to approximately -600 to -700 pounds. Apparently all aircraft electrical loads were not on when the cable tension sensor was calibrated on the aircraft.

In both of the above cases, a simple resistor change in the cable tension electronic assembly was made with no impact on the flight program.

## 6.3    GENERAL COMMENTS AND RECOMMENDATIONS

### 6.3.1    Flight Control Computer Subsystem

The ICP 733 incremental computer system has demonstrated excellent performance throughout the HLH-ATC program. Some 1400 hours of system operation have been accrued during the program and no major line-replaceable unit failure has accrued. Although a number of component malfunctions within the combined hardware sets have been experienced, these have not compromised flight safety at any time nor significantly degraded system flight performance. Resolution of many of the previously discussed hardware problems and expected resolutions on pending problems should make   _ increased reliability of the prototype AFCS hardware.

The excellent system hardware flight performance can be considered to be due to an initially solid design backed by extensive laboratory debug and bench testing, followed by integration tests. Some 20 percent of the average accumulated unit hours were spent at the vendor's facility, followed by a further 12 percent during integration tests at the contractor's facility. The triplex hardware configuration utilized a further 21 percent of the total time in support of software checkout.

Integration of the AFCS sensors with the computer complex on the aircraft was time consuming and must be avoided in the future if time on the aircraft is of prime importance. Too many interface problems were encountered which could have been rectified sooner, had provisions been incorporated in the integration test laboratory for coupling of sensors "open loop" to the flight control system.

The choice of erasable ROM devices was perhaps premature considering the developmental nature of the program. The procurement of this device from sole source, which at the time was leading the market, gave rise to an excepted development risk. The use of this device demanded a change in the existing computer memory accessing scheme. Developmental problems arose which were finally overcome; however, the problem of ROM device failures remains unsolved. This problem in itself has caused considerable reprogramming effort coupled with device replacements. Insufficient spare ROM board provisions also contributed to program delays. Core memory units supplanting the ROM boards could have reduced the development risks and might have facilitated a more rapid software program checkout in the early AFCS control law development stages, at perhaps an initial cost increase and some risk associated with passing qualification tests and susceptibility to memory wipeout from power transients. It is not clear at this stage whether the loss of memory due to power transients would have proven a flight safety hazard, considering the nature of the AFCS-DELS interface.

Performance of the hardwired mode logic is satisfactory once the integrity of the wiring has been established, but again, the developmental nature of the AFCS logic in requiring numerous changes has made it very difficult to provide reliable boards. Rewiring efforts resulted in continual resoldering and rerouting of existing wires to the integrated circuit components, which caused many errors necessitating troubleshooting and fixing.

The ICP computer system was developed at a period where the advantage of processing speed was of importance in the application of digital processors in the flight controls field. State-of-the-art whole word machines lacked memory capacity and speed to accomplish the tasks demanded of a complex AFCS. However, in recent years, there has been a rapid development of the whole word machine in memory capacity and speed, making it a much more viable proposition for the flight controls field where its capabilities as a general purpose machine can be explored for computation of many more tasks than solely flight control functions.

In review of the computer characteristics relative to the HLH-AFCS application, several points are evident:

- There has been no evidence of control bandwidth limitations for the aircraft short period modes caused by machine slew rate limiting.

- Accuracy of control performance has not been limited by computer-IOP limitations, but rather by the fidelity of long-term control input motions.

- Computer program memory sizing was barely marginal to handle all modes except the approach to hover. A separate tape was programmed to handle the approach to hover mode with removal of load stabilization modes. The memory was initially sized to have approximately 80 percent growth with all modes considered. Program development with more detailed definition of modes and functions led to the absorption of the program memory to virtually its full capacity. It must be realized, however, that algorithm usage developed with the program requirements and no concerted effort was made to condense the software for economic reasons. Herein lies one of the disadvantages of the ICP computer architecture: It is presently not possible to automatically condense the program memory instructions for maximum economy as can be bone with the whole word machine. The flexibility of software with the whole word machine permits reassembly of instructions on a ground-based host computer to effectively pack all core space. Doing this job by hand on the ICP system is time consuming and requires the skill of a highly qualified programmer.

- The algorithm process is definitely versatile and efficient for the solution of linear differential equations, but is not economical for solution of nonlinear functions and processing of all kinds of decision-making networks, that which is typically found in VTOL aircraft involving a great variety of flight modes. The computer therefore only fulfills a proportion of the total AFCS task.

- Redundancy management of physically dispersed flight control sensors appeared satisfactory where like sensors were involved, however, this was not satisfactory where different sensor types were involved. An example is the incompatibility of the ASN76 attitude/heading reference set with the similar information derived from the Inertial Navigation System, specifically for heading angle.

624

Considerable caution must be exercised when integrating different sensor types into a triplex system to insure channel-to-channel compatibility of signal characteristics, specifically where median selection is used.

● The input/output processor units lack the capability to remove the effects of power supply variations on sensor inputs. These effects were most notable in the synchro-to-dual-ac signal conversions of the attitude/heading reference signals. Fluctuation of ac supply reference causes significant change in the peak outputs of the converted signals; this, however, was muted somewhat later due to rescaling of pitch and roll attitudes, but the problem remains with heading.

● Maintenance of the ICP system has been relatively good. Most of the unit repairs/modifications were accomplished at the vendor's facility where the necessary skill and support equipment was based. Troubleshooting and minor repairs/mods were made at the integration test stand utilizing field support engineering skill. Modifications to AFCS equipment at the aircraft were avoided whenever possible in keeping with the adopted policy on vendor maintained equipment. Only three occasions were noted where vendor field support was called to troubleshoot the equipment internally on the aircraft, and it was not clear whether this activity could or could not have been done at the laboratory. Many system problems were reduced to the circuit card level; cards were either dispatched to the test stand for further diagnosis or returned to vendor for repair. Card swapping between redundant channels was a recognized problem diagnosis "tool" made relatively easy by having enough access room above the unit covers, therefore not requiring the units to be disconnected. Handling of the equipment high-density bayonet connectors was first anticipated to be a problem; however, this was not the case, perhaps due to the few times the cables had to be disconnected and perhaps due to the care with which they were handled by knowledgeable personnel. The proto-type AFCS, however, may present a different maintenance problem from the 347 ATC aircraft in that there is no space allocated for access to cards within each unit, thus frequency of disconnects may be increased.

## 6.3.2   Sensing Equipment

The principal objective of the Model 347 HLH Fly-By-Wire Demonstrator aircraft program was to evaluate and demonstrate the control concepts developed for the HLH, utilizing an equipment complement with the functional capability necessary to support this objective.   Program cost effectiveness dictated the utilization, whenever possible, of hardware developed for and available from previous flight test programs.   To this end, the sideslip electronic units and Precision Airspeed Trim (PAST) units from the original Model 347 test program were used.

The sideslip units provided satisfactory performance throughout the Task III flight testing with no modifications required.

The PAST linear airspeed and longitudinal cyclic pitch cams were changed to provide outputs compatible with the AFCS processing requirements.   As described in Section 6.2.1, it was necessary to adjust servo loop sensitivities to correct for inadequate cross channel dynamic tracking.

Tracking problems were also experienced with the reference barometric altitude unit, as described in Section 6.2.2. These units were based on a design for a nonredundant installation in the Canadian CH-147.

The above problems emphasize the fact that sensors to be utilized in cross channel monitored/signal select configuration must be designed and tested to satisfy the system level requirements.

Problems with sensor redundancy management were experienced where different types of equipment were used to provide a particular sensed parameter.   An example is the incompatibility of the ASN76 attitude/heading reference set with the similar information derived from the Inertial Navigation Systems, specifically for heading angle (refer to Section 6.2.4). Considerable caution must be exercised when integrating different sensor types into a triplex system to insure channel-to-channel compatibility of signal characteristics, specifically where median selection is used and relatively tight failure-monitor tolerances are required.

626

For the prototype HLH, a single ASN-76 will be used in conjunction with two Carousel IV INSs to provide triplex pitch and roll attitude information similar to the ATC system; however, the redundancy management in the IOPs will be modified to accept only the dual heading signals from the INS.

The kinematic sensing configuration for the Production HLH will be completely changed, in that either a pentad or hexad skewed redundant arrangement of strapdown angular rate and linear acceleration sensing elements is recommended. This type of sensing arrangement provides three-axis angular rate outputs in addition to the attitude, heading, velocity, and acceleration signals available from a gimbaled system. Also, the cost of a strapdown system is considerably less, while offering savings in weight and power as well.

Initial integration of the majority of the AFCS sensors with the computer complex was performed on the aircraft during systems functional test. This activity consumed considerably more time than had been anticipated, as a result of interface problems which could have been rectified in the integration test laboratory. The necessary laboratory facilities and tests will be planned for in the prototype and production HLH programs to avoid the recurrence of this situation.

# APPENDIX A
## HLH/ATC 347 DEMONSTRATOR AIRCRAFT AUTOMATIC
### FLIGHT CONTROL SYSTEM DATA PACKAGE

The complete definition of the AFCS software and logic for the demonstration aircraft is contained in this appendix. It represents the final system definition including all modifications identified during flight test. The data is presented in the following order.

1. AFCS Functional Block Diagrams
   Longitudinal Axis
   Lateral Axis
   Directional Axis
   Vertical Axis
   Auto Approach to Hover
   Sensor Preprocessing

2. AFCS Mode Logic Definition

3. AFCS Parameter Design Values

4. AFCS Function Definition

FIGURE A-1. AFCS FUNCTIONAL BLOCK DIAGRAM - LONGITUDINAL AXIS

AXIS

FIGURE A-2. AFCS FUNCTIONAL BLOCK DIAGRAM - VERTICAL AXIS

631

DIRECT ELECTRICAL LINKAGE SYSTEM

SENSORS

ROTOR, AIRFRAME AND LOAD DYNAMICS
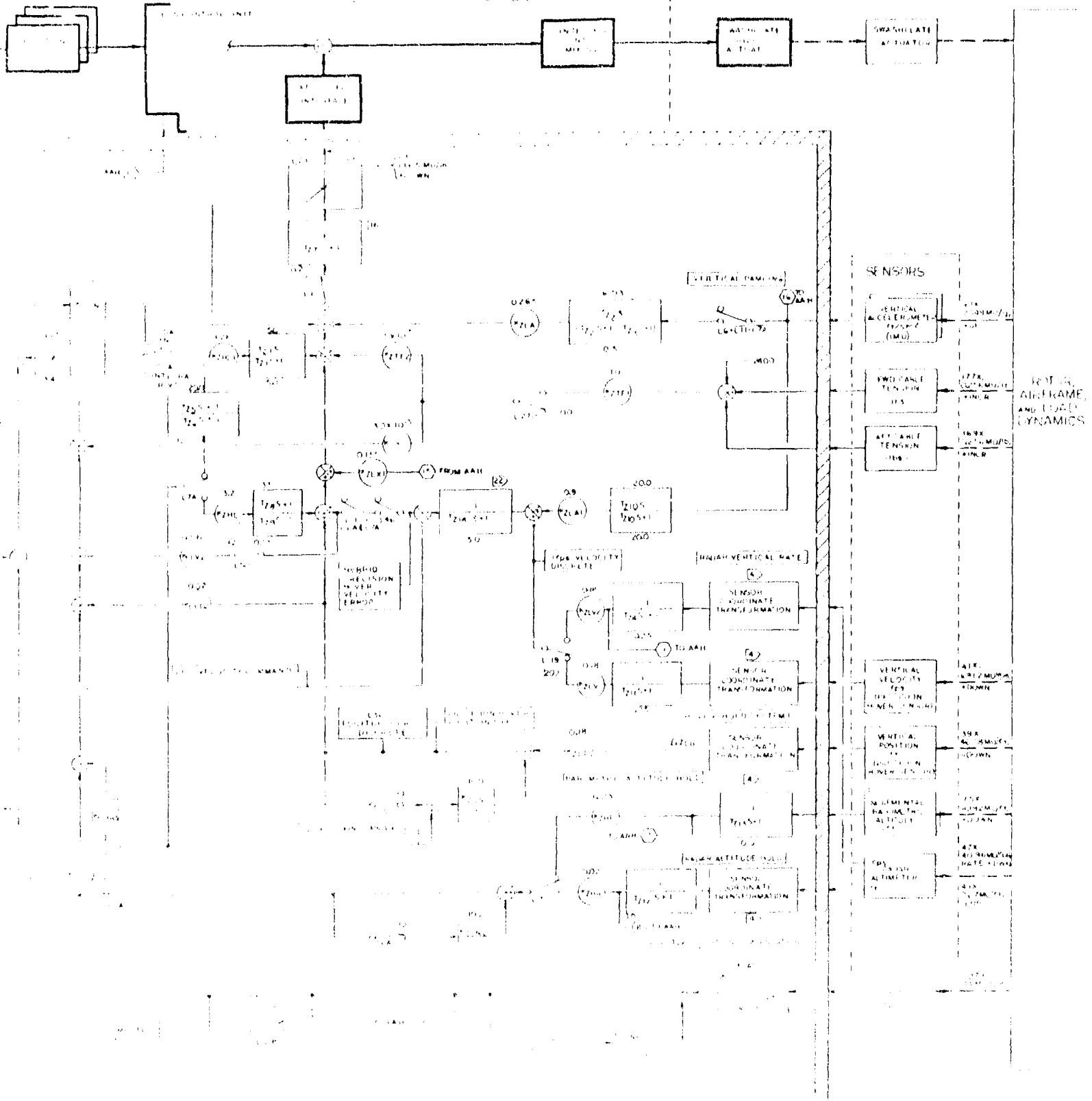
TICAL AXIS

BEST AVAILABLE COPY

FIGURE A-3. AFCS FUNCTIONAL BLOCK DIAGRAM - LATERAL AXIS

FIGURE A-4. AFCS FUNCTIONAL BLOCK DIAGRAM - DIRECTIONAL AXIS

NOTES

SENSORS

ROTOR,
AIRFRAME,
AND LOAD
DYNAMICS

ECTIONAL AXIS

FIGURE A-5. AFCS FUNCTIONAL BLOCK DIAGRAM - SENSOR PREPROCESSING

637

## NOTES



SENSORS

IOP

LSS FUNCTIONS

PITCH
ATTITUDE GYRO
$\theta$ (deg)

FWD LONG
CABLE ANGLE
$P_F$ (deg)

AFT LONG
CABLE ANGLE
$P_R$ (deg)

FWD CABLE
TENSION
$T_F$ (lb)

AFT CABLE
TENSION
$T_R$ (lb)

ROLL
ATTITUDE
$\phi$ (deg)

FWD LATERAL
CABLE ANGLE
$X_F$ (deg)

AFT LATERAL
CABLE ANGLE
$X_R$ (deg)

$$T_{KLPH} = \frac{(H+L)\,\theta + LP_F}{57.3}$$

$$F_{RLC} = \frac{L}{57.3}\left(\theta + \frac{T_F P_F + T_R P_R}{T_F + T_R}\right)$$

$$F_{YLPH} = \frac{(H+L)\phi}{57.3} + \frac{L(X_F + X_R)}{2(57.3)}$$

$$F_{YLC} = \frac{L}{57.3}\left(\phi + \frac{X_F + X_R}{2}\right)$$

$$T_{NLPH} = \frac{L(X_F - X_R)}{LLX}$$

FIGURE A-6. AFCS FUNCTIONAL BLOCK DIAGRAM -
AUTO APPROACH TO HOVER
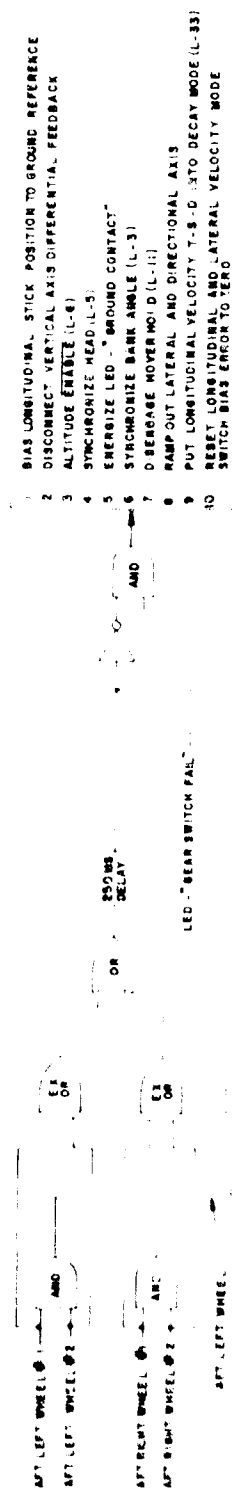
FIGURE A-7. AFCS MODE LOGIC DEFINITION (SHEET 1)

L-3 BANK ANGLE SYNCHRONIZATION

GROUND CONTACT (L-1)
GROUND VELOCITY MODE(G)-MAX LATERAL
LATERAL AFCS ENGAGE (L-3C)
LATERAL SYSTEM TEST PARALLEL EXCITATION
LATERAL STICK OUT-OF-DETENT

L-24 LOGIC

LATERAL BEEP TRIM (POSITIVE)
LATERAL BEEP TRIM (NEGATIVE)
CYCLIC BAR BRAKE

LATERAL STICK BEEP TRIM
TO L-5, L-45

ENERGIZE LED - "ROLL STAR"

SYNC

LATERAL BEEP TRIM (L-30)
VELOCITY MODE CHANGE (GL-33C)
ROLL RATE | > 5 DEG/SEC
ROLL ATTITUDE ERROR (RE)>0 8)

LED-"ROLL RATE"

LED -"ROLL ATT ERROR"

L-4 DIRECTIONAL AND LONGITUDINAL CONTROL RESPONSE

1  HEADING SYNC CONTROL (L-5)
2  ADD LONGITUDINAL AUTO HOVER TRIM INTEGRAL GAIN PATH
3  ADD LATERAL AUTO HOVER TRIM INTEGRAL GAIN PATH
4  SWITCH DIRECTIONAL BEEP TRIM TO PARALLEL DRIVE INTEGRAL PATH
5  DIFFERENTIAL ROLL ATTITUDE BEEP TRIM (L-24)

(L-4A)

1  REMOVE PEDAL CONTROL RESPONSE QUICKENING AND SWITCH TRANSIENT FREE TO YAW RATE GAIN AND SIGNAL SHAPING FOR HIGH SPEED FLIGHT (TPS, 5 SEC RAMP OUT)
2  REMOVE PEDAL POSITIONING INPUT TO LATERAL AXIS (TPS, 5 SEC RAMP OUT)

(L-4B)

AIRSPEED > 45 KNOTS (HYSTERESIS 40-45 KNOTS)
LED - "DIFF PRESS"
DIFFERENTIAL PRESSURE | > 0.5 PSI

FIGURE A-7.  AFCS MODE LOGIC DEFINITION (SHEET 2)

642

FIGURE A-7. AFCS MODE LOGIC DEFINITION (SHEET 3)

FIGURE A-7  AFCS MODE LOGIC DEFINITION (SHEET 4)

A-7 ALTITUDE HOLD REFERENCE

RADAR ALTITUDE < 200 FT

RADAR ALTITUDE < 220 FT

PILOT MANUAL SELECT BARO

PILOT MANUAL SELECT RADAR

RADAR RATE OPERATIVE (L-46)

RADAR ALTITUDE < 240/220 FT (20 FT HYSTERESIS)

ALTITUDE ENABLE (L-64)

CONVERT TO RADAR REFERENCE

RADAR ALTITUDE HOLD
MODE SELECT PANEL - RADAR ALTITUDE HOLD
MODE LIGHT

BARO ALTITUDE HOLD
MODE SELECT PANEL - BARO ALTITUDE HOLD
MODE LIGHT

FIGURE A-7. AFCS MODE LOGIC DEFINITION (SHEET 5)

L-8 PRECISION HOVER POSITION

LONGITUDINAL SYSTEM TEST PARALLEL EXCITATION
LATERAL SYSTEM TEST PARALLEL EXCITATION
LONGITUDINAL STICK OUT-OF-DETENT
LATERAL STICK OUT-OF-DETENT
ENGAGE HOVER HOLD (L-11)

L-19
L-27C

L-8A LONGITUDINAL PHS POSITION STABILIZE

(LONGITUDINAL PHS VELOCITY) < 0.5 FPS
L-8 LOGIC
LCC LONGITUDINAL CONTROLLER) > 0.1 IN

0.2 SEC DELAY

LED "LCC LONG THRES HOLD"

LCC ENABLE (L-20)

LONGITUDINAL PHS POSITION STABILIZE
LED "LONG POSN STAB"
L-34, L-15, L-27

L-8B LATERAL PHS POSITION STABILIZE

(LATERAL PHS VELOCITY) < 0.5 FPS
L-8 LOGIC
(LCC LATERAL CONTROLLER) > 0.1 IN

0.5 SEC DELAY

LED "LCC LAT THRES HOLD"

LCC ENABLE (L-20)

LATERAL PHS POSITION STABILIZE
LED "LAT POSN STAB"
L-34, L-15, L-27
CHANGE IN LATERAL LOAD DAMPING SHAPING

L-8C VERTICAL PHS POSITION STABILIZE

(VERTICAL PHS VELOCITY) < 1.0 FPS
RADAR RATE OPERATIVE (L-44)
VERTICAL SYSTEM TEST PARALLEL EXCITATION
COLLECTIVE BIAS ERASE
L-27D
L-8 LOGIC
(LCC VERTICAL CONTROLLER) > 0.4 IN

0.5 SEC DELAY

LED "LCC VERT THRES HOLD"

LCC ENABLE (L-20)

VERTICAL PHS POSITION STABILIZE
LED "VERT POSN STAB"
L-8, L-14, L-27

L-8A, L-8B, L-8C

646

FIGURE A-7. AFCS MODE LOGIC DEFINITION (SHEET 6)

FIGURE A-7. AFCS MODE LOGIC DEFINITION (SHEET 7)

L-14 VERTICAL POSITION COMMAND PULSE
L-14A VERTICAL POSITION COMMAND PULSE - NEGATIVE

PRECISION HOVER POSITION IN STABILIZE (L-8C)
PILOT ENABLE LCC CONTROLLER(L-20)
LCC VERTICAL CONTROLLER>POSITION BEEP DETENT(-0.05IN)
AND → ACTIVATE NEGATIVE VERTICAL POSITION COMMAND PULSE

L-14B VERTICAL POSITION COMMAND PULSE - POSITIVE

PRECISION HOVER POSITION IN STABILIZE (L-8C)
PILOT ENABLE LCC CONTROLLER (L-20)
LCC VERTICAL CONTROLLER>POSITION BEEP DETENT (+0.05IN)
AND → ACTIVATE POSITIVE VERTICAL POSITION COMMAND PULSE

L-15 LONGITUDINAL POSITION COMMAND PULSE
L-15A LONGITUDINAL POSITION COMMAND PULSE - NEGAT.VE

PRECISION HOVER POSITION IN STABILIZE (L-8A)
PILOT ENABLE LCC CONTROLLER(L-20)
LCC LONGITUDINAL CONTROLLER>POSITION BEEP DETENT(-0.05IN)
AND → ACTIVATE NEGATIVE LONGITUDINAL POSITION COMMAND PULSE

L-15B LONGITUDINAL POSITION COMMAND PULSE - POSITIVE

PRECISION HOVER POSITION IN STABILIZE(L-8A)
PILOT ENABLE LCC CONTROLLER (L-20)
LCC LONGITUDINAL CONTROLLER>POSITION BEEP DETENT(+0.05IN)
AND → ACTIVATE POSITIVE LONGITUDINAL POSITION COMMAND PULSE

L-16 LATERAL POSITION COMMAND PULSE
L-16A LATERAL POSITION COMMAND PULSE - NEGATIVE

LATERAL PRECISION HOVER HOLD IN STABILIZE (L-8B)
PILOT ENABLE LCC CONTROLLER (L-20)
LCC LATERAL CONTROLLER POSITION BEEP DETENT(-0.05IN)
AND → ACTIVATE NEGATIVE LATERAL POSITION COMMAND PULSE

L-16B LATERAL POSITION COMMAND PULSE - POSITIVE

LATERAL PRECISION HOVER HOLD IN STABILIZE (L-8B)
PILOT ENABLE LCC CONTROLLER (L-20)
LCC LATERAL CONTROLLER>POSITION BEEP DETENT(+0.05IN)
AND → ACTIVATE POSITIVE LATERAL POSITION COMMAND PULSE

FIGURE A-7. AFCS MODE LOGIC DEFINITION (SHEET 8)

FIGURE A-7. AFCS MODE LOGIC DEFINITION (SHEET 9)

649

L-24 DIFFERENTIAL ROLL ATTITUDE BEEP TRIM

AIRSPEED > 45 KNOTS (L-4A)

(ROLL ATTITUDE) > 0.073, +0.4 (LL5)

— LED - "ROLL LIMIT DETECT"

AND

TRANSFER FROM PARALLEL TO DIFFERENTIAL ROLL ATTITUDE BEEP TRIM
L-3 LOGIC

L-25 - DELETED

L-26 COLLECTIVE POSITION COMPENSATION

ANN ENGAGE (L-2A)

ALTITUDE HOLD (L-6A)

OR

AIRSPEED SCHEDULED COLLECTIVE POSITION STABILIZED
L-30.0

FIGURE A-7. AFCS MODE LOGIC DEFINITION (SHEET 10)

650

FIGURE A-7. AFCS MODE LOGIC DEFINITION (SHEET 11)

651

L-28 STICK BEEP TRIM DISCONNECT

A/FC BEEP STICK TRIM (L-22)
COUPLED AUTO APPROACH/RAV GUIDANCE MODE (L-28)
HOVER HOLD ENGAGE (L-11)

L-29 - DELETED

DISCONNECT LONGITUDINAL AND LATERAL BEEP TRIM
L-35 INPUT
LED - "BEEP DISCONNECT"

FIGURE A-7. AFCS MODE LOGIC DEFINITION (SHEET 12)

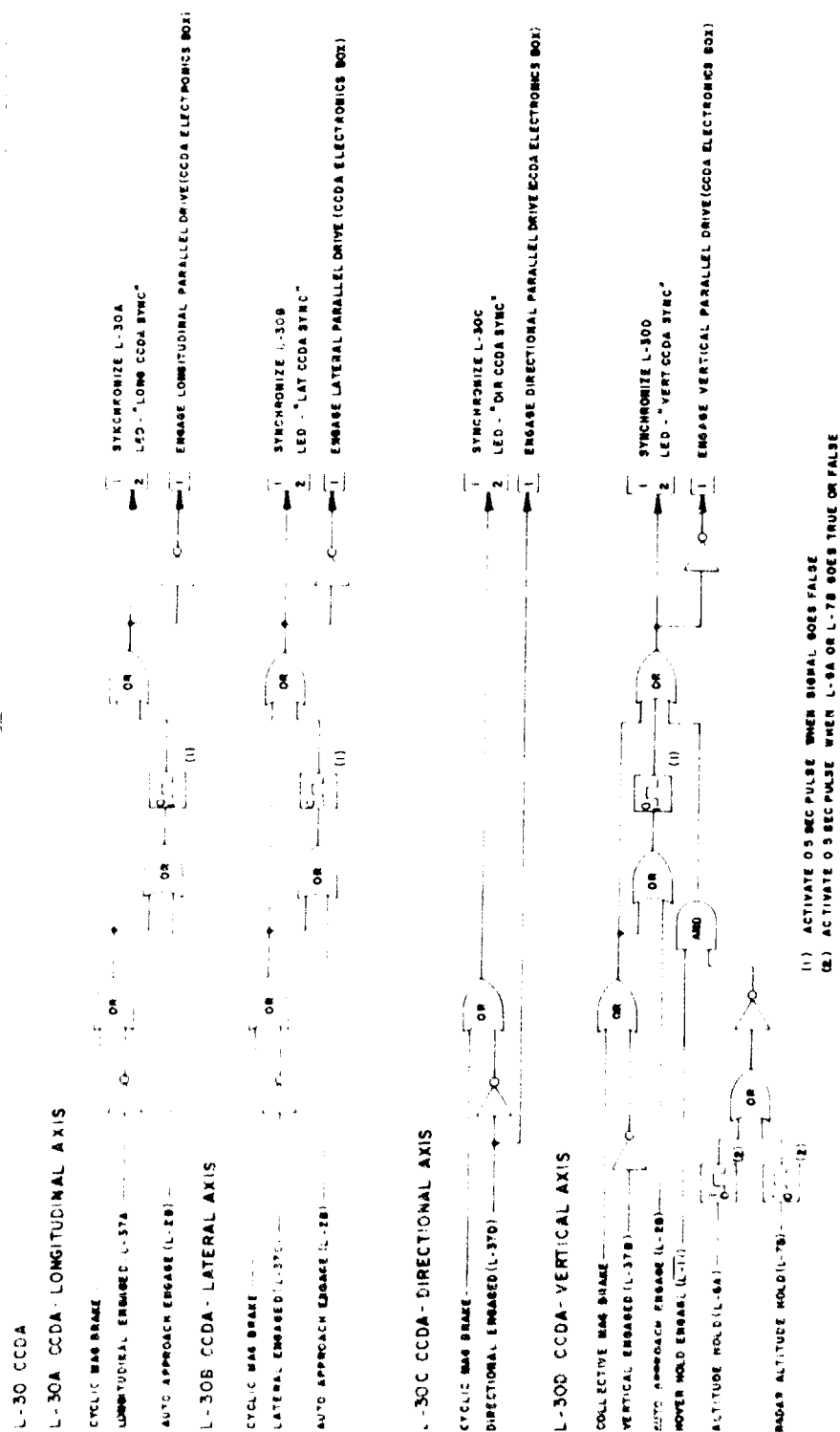FIGURE A-7. AFCS MODE LOGIC DEFINITION (SHEET 13)

653

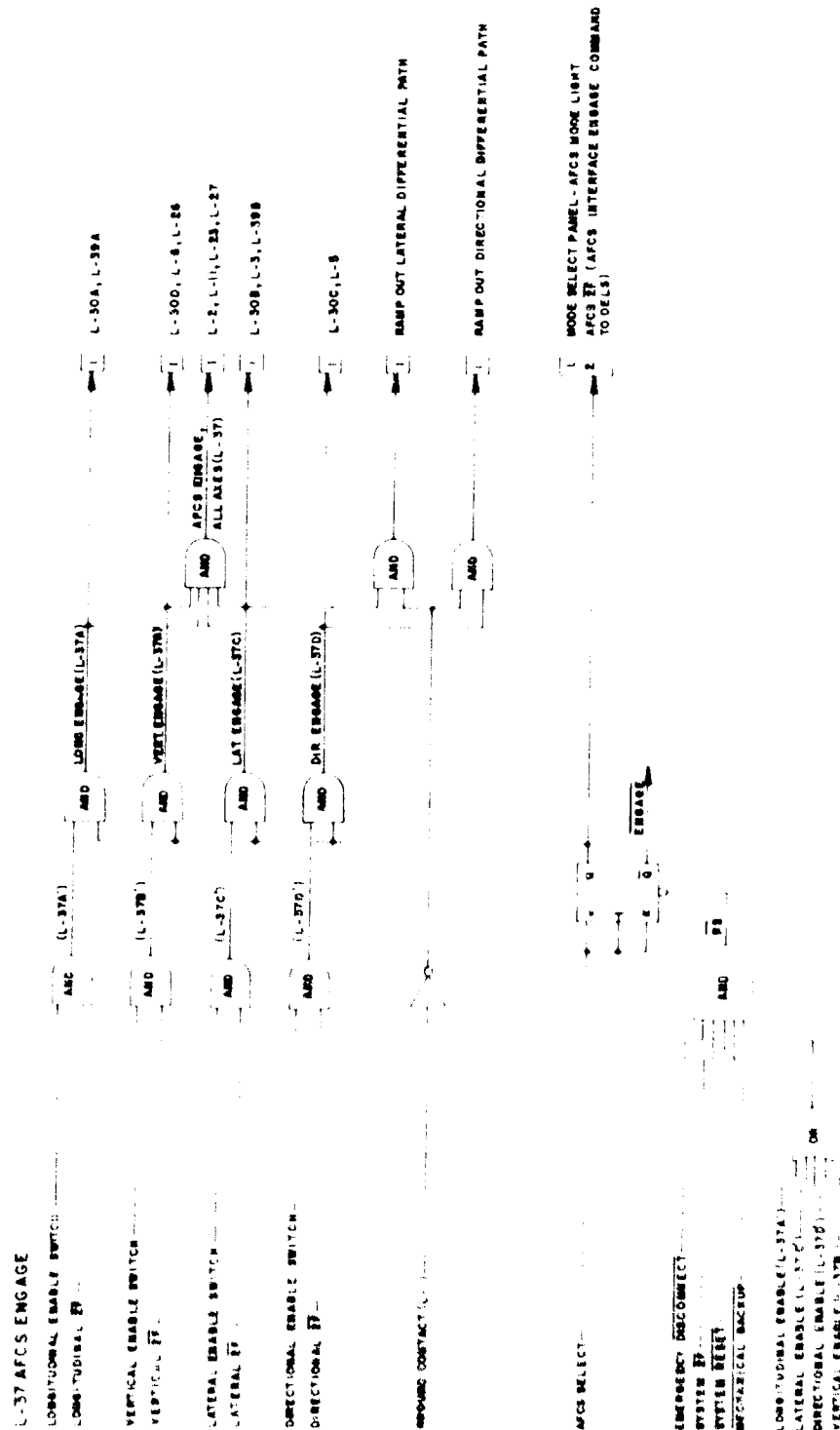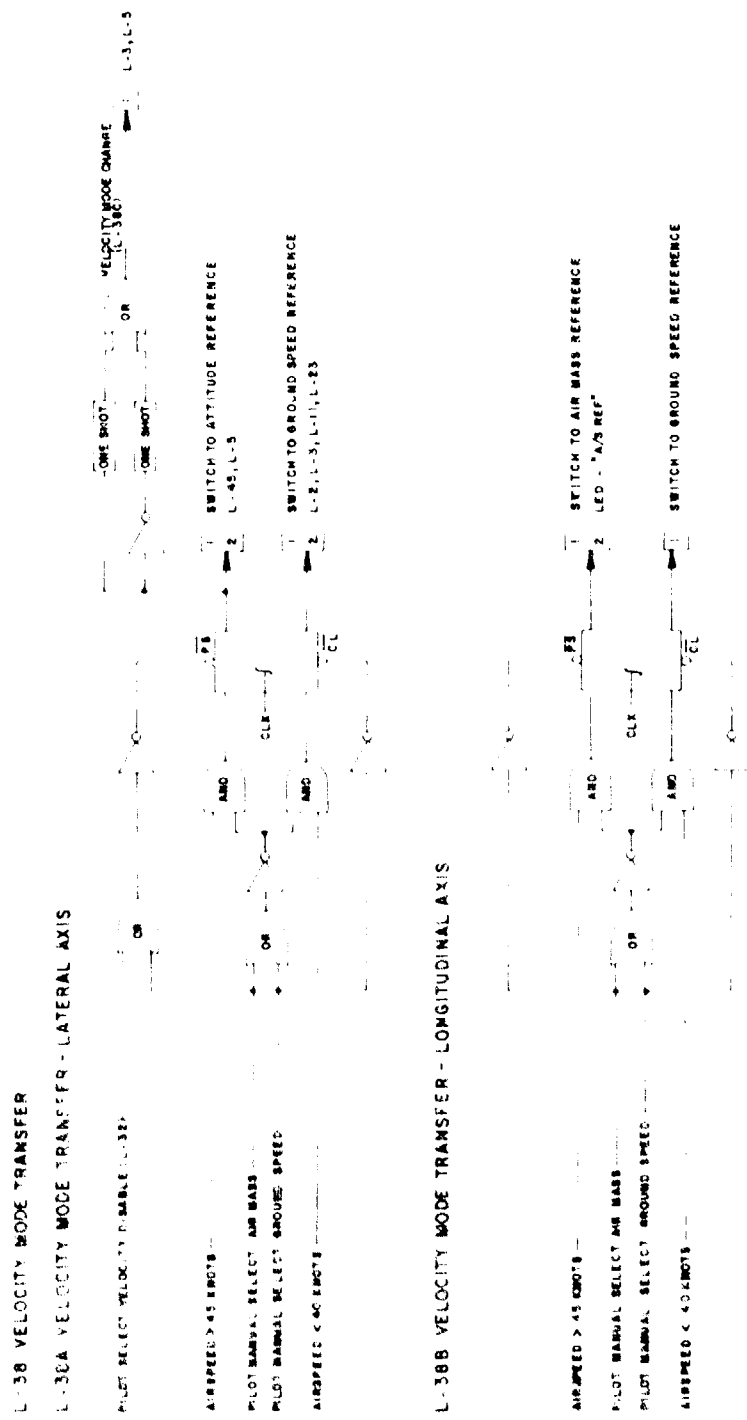L-31 - DELETED

L-32 VELOCITY MODE DISABLE

HOVER HOLD ENGAGE

VELOCITY MODE DISABLE

OR (L-32A) → 1  TRANSFER LONGITUDINAL VELOCITY CONTROL SIGNALS FROM TRACK TO STORE

(L-32) → 2  TRANSFER LATERAL TFS TO ATTITUDE REFERENCE (L-30A)  L-2

L-33 VELOCITY DEL... SELECT SWITCH

VELOCITY DECAY SELECT

GROUND CONTACT

OR (L-33A) → 1  TRANSFER LONGITUDINAL TRACK-STORE - DECAY TO DECAY MODE (0.65 IN/SEC)

→ 2  L-2

L-34 IMU DRIFT CLEAR

AND (L-34A) → 1  IMU SYNC

→ 2  MODE SELECT PANEL - DRIFT CLEAR LIGHT

(L-34B) →  RESET OUTPUT OF $K_{18H4}$ AND $K_{18L4}$ INTEGRATORS TO ZERO

L-35 - DELETED

L-36 PRECISION HOVER SENSOR RELOCK

LONGITUDINAL PRECISION HOVER POSITION ERROR < 0.2 FT

LATERAL PRECISION HOVER POSITION ERROR < 0.2 FT

VERTICAL PRECISION HOVER POSITION ERROR < 0.2 FT

PPS INTERNAL RELOCK THRESHOLD (RELOCK DISBAND)

AND → 1  PHS RELOCK COMMAND (TO PHS)

→ 2  L-19

→ 3  LED - "PHS RELOCK COM"

LED - "PHS INT THRESHOLD"

FIGURE A-7.  AFCS MODE LOGIC DEFINITION (SHEET 14)

654

FIGURE A-7. AFCS MODE LOGIC DEFINITION (SHEET 15)
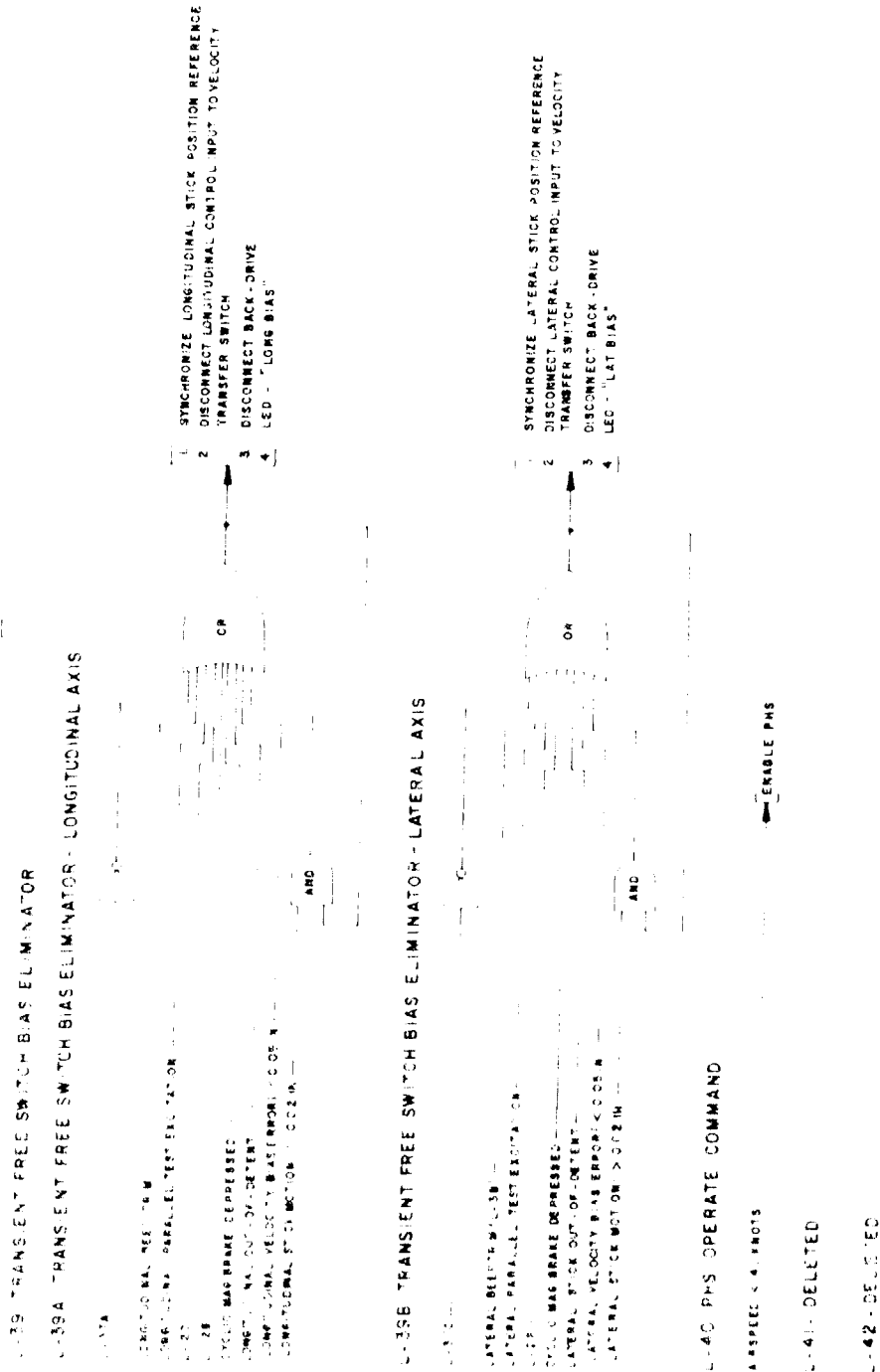
FIGURE A-7. AFCS MODE LOGIC DEFINITION (SHEET 16)

-39 TRANSIENT FREE SWITCH BIAS ELIMINATOR

-39A TRANSIENT FREE SWITCH BIAS ELIMINATOR - LONGITUDINAL AXIS

1. SYNCHRONIZE LONGITUDINAL STICK POSITION REFERENCE
2. DISCONNECT LONGITUDINAL CONTROL INPUT TO VELOCITY
   TRANSFER SWITCH
3. DISCONNECT BACK-DRIVE
4. LED - "LONG BIAS"

-39B TRANSIENT FREE SWITCH BIAS ELIMINATOR - LATERAL AXIS

1. SYNCHRONIZE LATERAL STICK POSITION REFERENCE
2. DISCONNECT LATERAL CONTROL INPUT TO VELOCITY
   TRANSFER SWITCH
3. DISCONNECT BACK-DRIVE
4. LEC - "LAT BIAS"

-40 PHS OPERATE COMMAND

-41 DELETED

-42 DELETED

FIGURE A-1. AFCS MODE LOGIC DEFINITION (SHEET 17)

FIGURE A-7. AFCS MODE LOGIC DEFINITION (SHEET 18)

L-43 LATERAL STICK BANK ANGLE REFERENCE

SYNCHRONIZE LATERAL STICK/BANK ANGLE ERROR SIGNAL

L-44 COCKPIT GROUND SPEED DISPLAY

SWITCH TO HIGH SENSITIVITY GROUND SPEED SIGNAL
28 VDC LAMP (GROUND SPEED INDICATOR SCALE LIGHT)

L-45 BIAS ELIMINATOR DYNAMICS

L-45 DISCONNECT FEED FORWARD DYNAMICS TO BIAS ELIMINATOR (LATERAL AXIS)

L-46 RADAR RATE OPERATIVE

CLOSE L-46
L-7, L-BC

L-47 INVALID APPROACH NAV SIGNALS

FLIGHT DIRECTOR WARNING FLAG

L-48 6MM FLARE MODE INITIATION

STABILIZE PITCH ATTITUDE IN AFH COMPUTATIONS
ADD FLARE MODE COMPENSATION LOOP

658

L-49 - DELETED

L-50 VERTICAL VELOCITY ERROR INTEGRAL BACKDRIVE SWITCH

SWITCH IN INTEGRAL BACKDRIVE GAIN KCLV2

L-51 VERTICAL HYBRID HOVER HOLD

ENGAGE COMPLEMENTARY RATE DAMPING LOOP

L-52 VERTICAL ACCELERATION

ENGAGE VERTICAL ACCELERATION DAMPING LOOP

FIGURE A-7. AFCS MODE LOGIC DEFINITION (SHEET 19)

TABLE A-1   AFCS PARAMETER DESIGN VALUES (SHEET 1)

- LONGITUDINAL AXIS -

| SYMBOL | UNITS | DESCRIPTION | VALUE |
|---|---|---|---|
| | deg/sec | Pitch Rate | |
| | deg/sec | Pitch Rate Increase for Hover Hold | |
| | deg | Pitch Attitude | |
| | deg/sec | Pitch Attitude Increase on Hover Hold | |
| | | Airspeed | |
| | | Longitudinal Groundspeed | |
| | | Longitudinal Stick Position Gradient (Low Gain) | |
| | | Longitudinal Stick Gradient - Attitude Control Path | |
| | | Longitudinal Stick Position Gradient (High Gain) | |
| | /sec | Longitudinal Stick Reference Synchronizer (2) | |
| | sec | Pitch Attitude Reference Synchronization (Hover Hold) (2) | |
| | sec | Pitch Rate Reference Synchronization (Hover Hold)(2) | |
| | deg | Up Trim Top Gain | |
| | deg | Longitudinal LCC Velocity Command | |
| | deg | Longitudinal Position - Precision Hover | |
| | deg/sec | Longitudinal Velocity - Precision Hover | |
| | deg/sec | Longitudinal Groundspeed - IMC | |
| | volts/kt | Relative Longitudinal Groundspeed Display - Low Sensitivity | |
| KX354 | volts/deg | Relative Longitudinal Groundspeed Display - High Sensitivity | 0.10 |
| KXCA | deg/deg | Longitudinal Load Damping (Hover Hold On) | 0.205 |
| KXCA | deg/deg | Longitudinal Load Damping (Hover Hold Off) | 0.82 |
| KXLL | ft/ft | Load Longitudinal Position | 0.1 |
| KXLL4 | ft/ft | Longitudinal Load Centering | 1.0 |
| KXTE | deg/in | Longitudinal Cable Tension Equalization | 0.4 |
| KXLCF | deg/deg | Forward Rotor Longitudinal Cyclic Pitch | 0.002 |
| KXLCA | deg/deg | Aft Rotor Longitudinal Cyclic Pitch | 1.0 |
| KXSN1 | 1/sec | Longitudinal Position Synchronization (2) | 1.0 |
| KXSN2 | 1/sec | Longitudinal Load Position Synchronization (2) | 100.0 |
| KXSN3 | 1/sec | Longitudinal Load Centering Synchronization (2) | 100.0 |
| KXSN4 | 1/sec | Velocity Reference Synchronization (2) | 100.0 |

663

# TABLE A-1 AFCS PARAMETER DESIGN VALUES (SHEET 2)

## - LONGITUDINAL AXIS -

| PARAMETER | | DESCRIPTION | VALUE |
|---|---|---|---|
| SYMBOL | UNITS | | |
| K-BTR1 | in/sec | Longitudinal Stick Beep Trim | 0.0625 |
| K-BTR2 | in s-g/ft sec | Longitudinal Auto Hover Trim | 0.002 |
| K-BTR3 | in sec inch | Longitudinal Stick Backdrive (Velocity Bias Elimination) | 0.0125 |
| K-BTR4 | in sec ft/sec | Longitudinal Auto Hover Trim (High Speed) | 0.00013 |
| K-BTR5 | in sec deg | Longitudinal Velocity Error- Precision Hover | .00125 |
| K-BTR6 | in/sec-deg | Longitudinal Position Error - Precision Hover | .0025 |
| K-BSN | 1 sec | CCDA Synchronization (2) | -100.0 |
| TM3 | sec | Longitudinal Lag (Differential Path) | 0.10 |
| TM4 | sec | Longitudinal Stick Gradient Lag | 0.75 |
| TX1 | sec | Longitudinal Cyclic Pitch Lead (Low Speed/Hover Hold) | 1.0 |
| TX2 | sec | Longitudinal Cyclic Pitch Lag (Low Speed/Hover Hold) | 0.5 |
| TX3 | sec | Longitudinal Load Damping Washout | 10.0 |
| TX4 | sec | Longitudinal Load Damping Lag (Hover Hold On) | 0.1 |
| TX5 | sec | Longitudinal Load Damping Lead Hover Hold Off | 2.0 |
| TX6 | s | Longitudinal Load Damping Lag | 0.2 |
| TX8 | sec | Longitudinal Cyclic Pitch Lag (Low Speed/Hover Hold) | 0.1 |
| TX9 | sec | Longitudinal LCC Comand Lag | 2.0 |
| TXL1 | sec² | Longitudinal Load Position Hold Shaping 2nd Order | 0.36 |
| TXL2 | sec | Longitudinal Load Position Hold Shaping Lead | 0.80 |
| TXL3 | sec² | Longitudinal Load Position Hold Shaping 2nd Order | 1.25 |
| TXL4 | sec | Longitudinal Load Position Hold Shaping Lag | 5.25 |
| -- | deg | LCC Longitudinal Position "Beep" Command | 0.28 |

TABLE A-1. AFCS PARAMETER DESIGN VALUES (SHEET 3)

| PARAMETER | | DESCRIPTION | VALUE |
|---|---|---|---|
| SYMBOL | UNITS | | |
| | inch | Total DCP Differential Control (1) | +4.0 |
| | inch/sec | Longitudinal Stick Gradient Rate Limit | +0.5 |
| | in/sec | Longitudinal Auto Hover Trim | +10.0 |
| | inch | Longitudinal Parallel Proportional Control Limit (1) | +4.0 |
| | inch | Longitudinal Parallel Integral Control Limit | +4.0 |
| | in/sec | Longitudinal Differential Asymmetrical Limit | 4 in.Aft<br>1.5 in.Fwd |
| | deg | Precision Hover Velocity Command | +1.0 |
| | deg | Precision Hover Position Command | +3.0 |
| | deg | Aft Rotor LCP Control Limit (1) | +4.0 |
| | deg | Forward Rotor LCP Control Limit (1) | +4.0 |
| | deg | LCP into DCP Limit | +4.0 |

# TABLE A-2. AFCS PARAMETER DESIGN VALUES (SHEET 1)

## - VERTICAL AXIS -

| PARAMETER Symbol | Units | DESCRIPTION | VALUE |
|---|---|---|---|
| | ft | Altitude (Radar) | 0.02 |
| | ft | Altitude (Pressure) | 0.013 |
| | in | Altitude Hold (Differential Command - Radar) | 3.2 |
| | in | Altitude Hold - Baro (Differential Command) | 1.26 |
| | in | Vertical Position (Precision Hover) | 0.18 |
| | in/ft sec | Vertical Velocity (Precision Hover) | 0.18 |
| | in/ft/s | Vertical Rate - Auto Approach | 0.135 |
| | in/ft/sec | Radar Vertical Velocity | 0.18 |
| | in/ft/sec | Vertical Acceleration (Pressure) | 0.265 |
| | in/ft sec | Vertical Acceleration - Radar | 0.7 |
| | sec | Collective Compensation Schedule Synchronization (2) | 100.0 |
| | sec | Altitude Synchronization (2) | 100.0 |
| | sec | Vertical Position Synchronization (2) | 100.0 |
| | in | Cable Tension Hold | 1.0 |
| | in | Cable Tension Hold Differential Command | .00005 |
| | in sec | CCDA Synchronization (2) | -100.0 |
| | in/sec/in | Vertical Hover Position Integral Command | 0.02 |
| | in/sec/in | Vertical Hover Velocity Integral Command | 0.192 |
| | in/in | Altitude Hold Proportional Command (Pressure) | 1.0 |
| | in/sec/in | Altitude Hold Integral Command (Pressure) | 0.20 |
| | in/sec/in | Altitude Hold Integral Command (Radar) | 0.10 |
| | in/sec/in | Cable Tension Hold Integral Command | 0.00003 |
| | sec | Vertical/Position Error Washout (Differential Command) | 5.0 |
| | sec | Vertical Acceleration Washout (Pressure) | 6.03 |
| | sec | Vertical Acceleration Lag (Pressure) | 0.5 |
| | sec | Radar Vertical Velocity Lag | 0.25 |
| | sec | Altitude Error Lead (Differential Command Path-Pressure) | 20.0 |
| | sec | Altitude Error Lag (Differential Command Path-Pressure) | 10.0 |
| | sec | Vertical Lag (Differential Path) | 0.2 |
| | sec | Altitude Error Lead - Radar (Differential Command Path) | 1.33 |
| | sec | Altitude Error Lag - Radar (Differential Command Path) | 0.33 |
| | sec | Vertical Acceleration Washout for Complementary Rate | 20.0 |

663

TABLE A-2.   AFCS PARAMETER DESIGN VALUES (SHEET 2)

– VERTICAL AXIS –

| PARAMETER | | DESCRIPTION | VALUE |
|---|---|---|---|
| SYMBOL | UNITS | | |
| τ.1.1 | sec | PHS Vertical Rate Lag | 0.25 |
| τ.1.2 | sec | Radar Altitude Lag | 1.0 |
| τ.1.3 | sec | Baro Altitude Lag | 0.5 |
| τ.1.4 | sec | Complementary Vertical Rate Lag | 5.0 |
| | | | |
| τ.2.1 | inch | Vertical Differential AFCS Command (1) | ±1.5 |
| τ.2.2 | inch | Vertical Parallel Proportional Control Limit (1) | ±4.0 |
| τ.2.3 | inch | Vertical Parallel Integral Control Limit | ±3.4 |

TABLE A-3    AFCS PARAMETER DESIGN VALUES (SHEET 1)

- LATERAL AXIS -

| SYMBOL | UNITS | DESCRIPTION | VALUE |
|---|---|---|---|
| KLAR | in deg/sec | Roll Rate | 0.154 |
| KLAR1 | in deg/sec | Roll Rate Increase (Hover Hold) | 0.022 |
| KLAD1 | in deg | Roll Attitude (High Speed Stabilization) | 0.30 |
| KLAD2 | in deg | Roll Attitude (Low Speed Stabilization) | 0.35 |
| KLAD3 | in/in | Limited Roll Attitude Stick Gradient at High Speed | 0.10 |
| KLAD4 | in deg | Roll Attitude Increase (Hover Hold) | 0.05 |
| KLCF1 | in/in | Lateral Control Response Quickening | 1.5 |
| KLCP4 | in/in | Lateral Control Gradient | 0.25 |
| KDTR | in/in/sec | Roll Attitude Beep Trim (Differential) | 0.0095 |
| KLSK1 | 1/sec | Roll Attitude Synchronization (2) | 100.0 |
| KLSK2 | 1 sec | Lateral Stick Reference Synchronization (Backdrive Dynamics)(2) | |
| KLSN3 | 1 sec | Lateral Stick Reference Synchronization (Security) | 100.0 |
| | | Blanket (2) | |
| KLSN4 | 1 sec | Lateral Stick Reference Synchronization at High Speed (Backdrive Dynamics)(2) | 100.0 |
| KLSN5 | 1 sec | Roll Attitude Reference Synchronization (Hover Hold)(2) | 100.0 |
| | | | 100.0 |
| KLCC | in ft | Lateral LCO Vel Feedforward | 0.5 |
| KLPD | in ft | Lateral Position - Precision Hover | 0.56 |
| KLPV | in ft/sec | Lateral Velocity - Precision Hover | 0.77 |
| KLSD1 | in ft sec | Lateral Groundspeed - IMC | 0.77 |
| KLSD2 | in ft sec | Lateral Groundspeed (Low Speed Stabilization) | 0.1 |
| KLSD3 | in ft sec | Relative Lateral Groundspeed Display - Low Sensitivity | 0.154 |
| KLSD4 | in ft sec | Relative Lateral Groundspeed Display - High Sensitivity | 0.512 |
| KLDA1 | in deg | Lateral Load Damping (Hover Hold Off) | -0.13 |
| KYDA2 | in deg | Lateral Load Damping (Hover Hold On) | 0.01 |
| KYDA3 | deg deg | Lateral Load Damping (Lateral Position Hold Stabilized) | 0.047 |
| KYP1 | ft ft | Lateral Load Damping (Roll Attitude Compensation) | 2.0 |
| KLL1 | ft ft | Load Lateral Position | 0.5 |
| KLL4 | 1/sec | Lateral Load Centering | 0.5 |
| KLSN1 | 1 sec | Lateral Position Synchronization (2) | 100.0 |
| KLSN2 | 1 sec | Lateral Load Position Synchronization (2) | 100.0 |
| KLLS | 1 sec | Lateral Load Centering Synchronization (2) | 100.0 |
| KLLV | 1 sec | Velocity Reference Synchronization (2) | 100.0 |

TABLE A-3. AFCS PARAMETER DESIGN VALUES (SHEET 2)

LATERAL AXIS

| PARAMETER | DESCRIPTION | VALUE |
|---|---|---|
| | Roll Attitude Parallel Trim Command | 0.0625 |
| | Lateral Position Error - Precision Hover | 0.0070 |
| | Lateral Velocity Error - Precision Hover | 0.095 |
| | Lateral Stick Error Trim Parallel | |
| | | |
| | Lateral Velocity Washout Position Bias Elimination | |
| | Lateral Velocity Washout Hover Speed | -100.0 |
| | | |
| | | |
| | Lateral Acceleration Lag | |
| | | |
| | Attitude Response Washout | |
| | | |
| | Roll Attitude Washout | |
| | Lead Washout Lateral Position Hover Hold | |
| | Lead Washout Lag Hover Hold On | |
| | Lead Washout Lag Hover Hold Off | |
| | Lateral Forward Loop | |
| | Lateral Position Hold Shaping 2nd Order Lead | 0.138 |
| | Lateral Position Hold Shaping | 0.214 |
| | Lateral Position Hold Shaping 2nd Order Lag | |
| | Lateral Position Hold Shaping | 10.2 |
| | | |
| | FPC Lateral Position "Beep" Command | 0.093 |

TABLE A-3   AFCS PARAMETER DESIGN VALUES (SHEET 3)

- LATERAL AXIS -

| PARAMETER | | DESCRIPTION | VALUE |
|---|---|---|---|
| 114 | inch | Roll Attitude (High Speed)/Lateral Precision Velocity Control | ±1.5 |
| 115 | inch | Limited Roll Attitude Stick Gradient | ±0.5, −0.675 |
| 116 | ft/sec | Lateral Auto Hover Trim | +5.0 |
| 117 | inch/sec | Lateral Stick Gradient Rate Limit | ±0.5 |
| 118 | inch | Lateral Parallel Proportional Control Limit (1) | ±1.0 |
| 119 | inch | Lateral Parallel Integral Control Limit | ±0.8 |
| 1111 | inch | Lateral Differential AFCS Command (1) | ±2.5 |
| 1112 | in/sec | Lateral Precision Hover Velocity   Error Rate Limit | 1.4 |

TABLE A-4. AFCS PARAMETER DESIGN VALUES

- DIRECTIONAL AXIS

| PARAMETER | | DESCRIPTION |
|---|---|---|
| SYMBOL | UNITS | |
| KYS | in | Directional LCC Yaw Rate Command |
| KYAD1 | in deg/sec | Yaw Rate/Airspeed > 45 kn ts |
| KYAD2 | in deg/sec | Yaw Rate/Airspeed < 45 kn ts |
| KYP1 | in | Pedal Control Response - washout |
| KYP2 | in | Yaw Roll Compensation |
| KYH | in deg | Heading Hold |
| KYHI | in deg | Heading Hold Gain Increment |
| KYBTR | in sec | Heading Beep Trim Differentiator |
| KYDCA1 | in deg | Directional Load Damping |
| KYH1 | deg/deg | Load Heading Hold |
| KYH2 | deg/deg | Directional Load Center |
| KYHSN1 | sec | Heading Synchronization |
| KYSN4 | sec | Load Heading Synchronization |
| KYHSN5 | sec | Directional Load Synchronization |
| KYRTR | inch sec | Directional Pedal Beep Trim |
| KYRHD | in/in | Heading Sideslip Integrator |
| KYRSN | 1 sec | CCDA Synchronization |
| KYN1 | sec | Roll Rate Lag |
| KYN2 | sec | Sideslip Lag |
| KYN3 | sec | Directional Control Quickening |
| KYN4 | sec | Yaw Rate Washout - Airspeed |
| KYN10 | sec | Directional Load Damping Lag |
| KYN11 | sec | Load Heading Lead |
| KYN12 | sec | Load Heading Lag |
| KYN13 | sec | Directional Load Damping Lag |
| KYN16 | sec | Directional Lag Differentiator |
| KYN17 | sec | Directional Yaw Rate Lag |
| LYN2 | inch | Yaw Rate Turn Entry Rate Limit |
| LYN6 | inch | Directional Parallel |
| LYN9 | inch | Directional Parallel |
| LYN10 | inch | Directional Differentiator |
| LYN11 | inch | Heading Rate Synchronization Rate |

TABLE A-5    AFCS PARAMETER DESIGN VALUES

- SENSOR PARAMETERS -

| PARAMETER | | DESCRIPTION | VALUE |
|---|---|---|---|
| SYMBOL | UNITS | | |
| TISN1 | 1 sec | IMC Velocity Drift Clear Synchronizer - $V_N$ (2) | 100.0 |
| TISN2 | 1 sec | IMC Velocity Drift Clear Synchronizer - $V_E$ (2) | 100.0 |
| THSN | 1 sec | Heading Synchronizer (2) | 100.0 |

669

## TABLE A-6. AFCS PARAMETER DESIGN VALUES
### - AUTOMATIC APPROACH TO HOVER -

| PARAMETER SYMBOL | UNITS | DESCRIPTION | VALUE |
|---|---|---|---|
| KBX1 | in/ft/sec | Longitudinal Groundspeed | 0.036 |
| KBXD | in/ft | Longitudinal Displacement | 0.003 |
| KBSG2 | in/in | Longitudinal CCDA Proportional Command | 1.0 |
| KCLC | in | Collective Lever | 2.0 |
| KCZV | in/ft/sec | Vertical Velocity | 0.135 |
| KCZD | in/ft | Vertical Displacement | 0.01 |
| KCZDI | in/ft-sec | Vertical Displacement Error Integral Command | 0.0004 |
| KCSG2 | in/in | Vertical CCDA Proportional Command | 1.0 |
| KSYV | in/ft/sec | Lateral Groundspeed | 0.0625 |
| KSYD | in/ft | Lateral Displacement | 0.0038 |
| KSG4 | in/in | Lateral CCDA Proportional Commands | 1.0 |
| LM9 | in | Longitudinal Track Velocity Error Integral Limit | 1.0 |
| LM10 | in | Longitudinal Track Velocity Error Limit | 1.0 |
| L26 | fps/sec | Commanded Vertical Velocity Rate Limit | 1.5 |
| L27 | in/sec | Collective Lever Rate Limit | 0.3 |
| T215 | sec | Complementary Rate Lag | 5.0 |
| T216 | sec | Vertical Acceleration Lag | 20.0 |
| T55 | sec | Low Airspeed Collective Bias Lag | 1.0 |
| T51 | sec | Collective Command Washout (Flare Mode) | 50.0 |
| KCZA2 | fps/fps | Vertical Acceleration | 5.0 |
| TFD0 | sec | Vertical Velocity Command Lag | 1.5 |
| TFD4 | sec | Vertical Error Lag | .75 |
| TFD6 | sec | Longitudinal Velocity Command Lag     Flight Director | .75 |
| TFD1 | sec | Lateral Displacement Error Lag     Command Shaping | .75 |
| TFD5 | sec | Lateral Velocity Command Lag | .75 |

# TABLE A-7. AFCS PARAMETER DESIGN VALUES
## -NOTES-

| PARAMETER | | DESCRIPTION | VALUE |
|---|---|---|---|
| SYMBOL | UNITS | | |
| | | NOTES: | |
| | | (1) Limit will be provided by Flight Control Computer output scaling. | |
| | | (2) All synchronizer gains provide a time constant of 1/K sec. Actual synchronization times implemented in GE computer could be instantaneous or a function of computer slew rate limit and variable scaling. | |

671
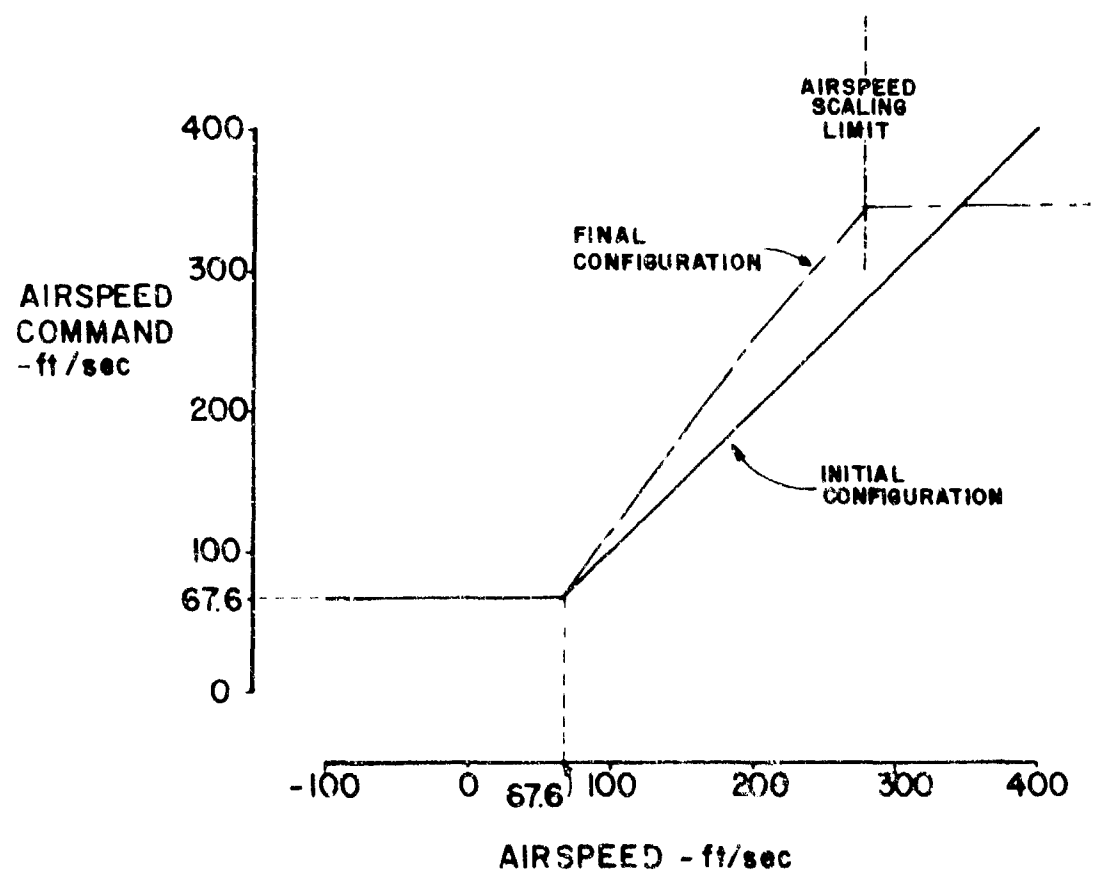
FIGURE A-8. AIRSPEED COMMAND FUNCTION

672
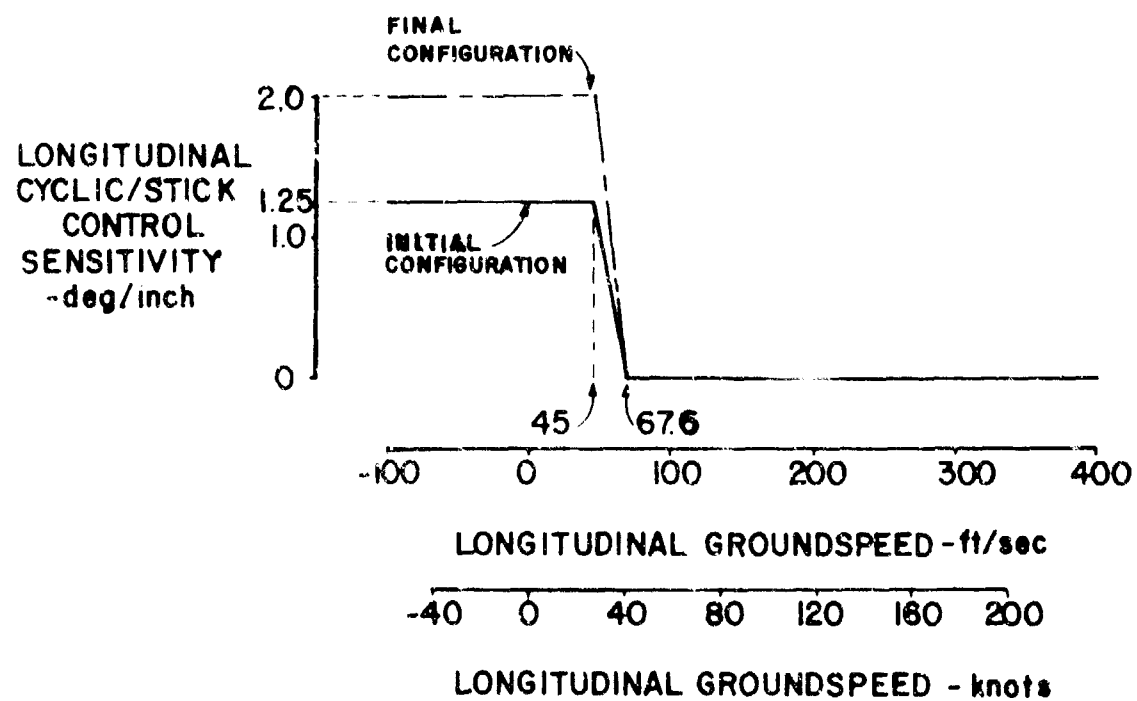
FIGURE A-9. LONGITUDINAL CYCLIC CONTROL SENSITIVITY SCHEDULE

673
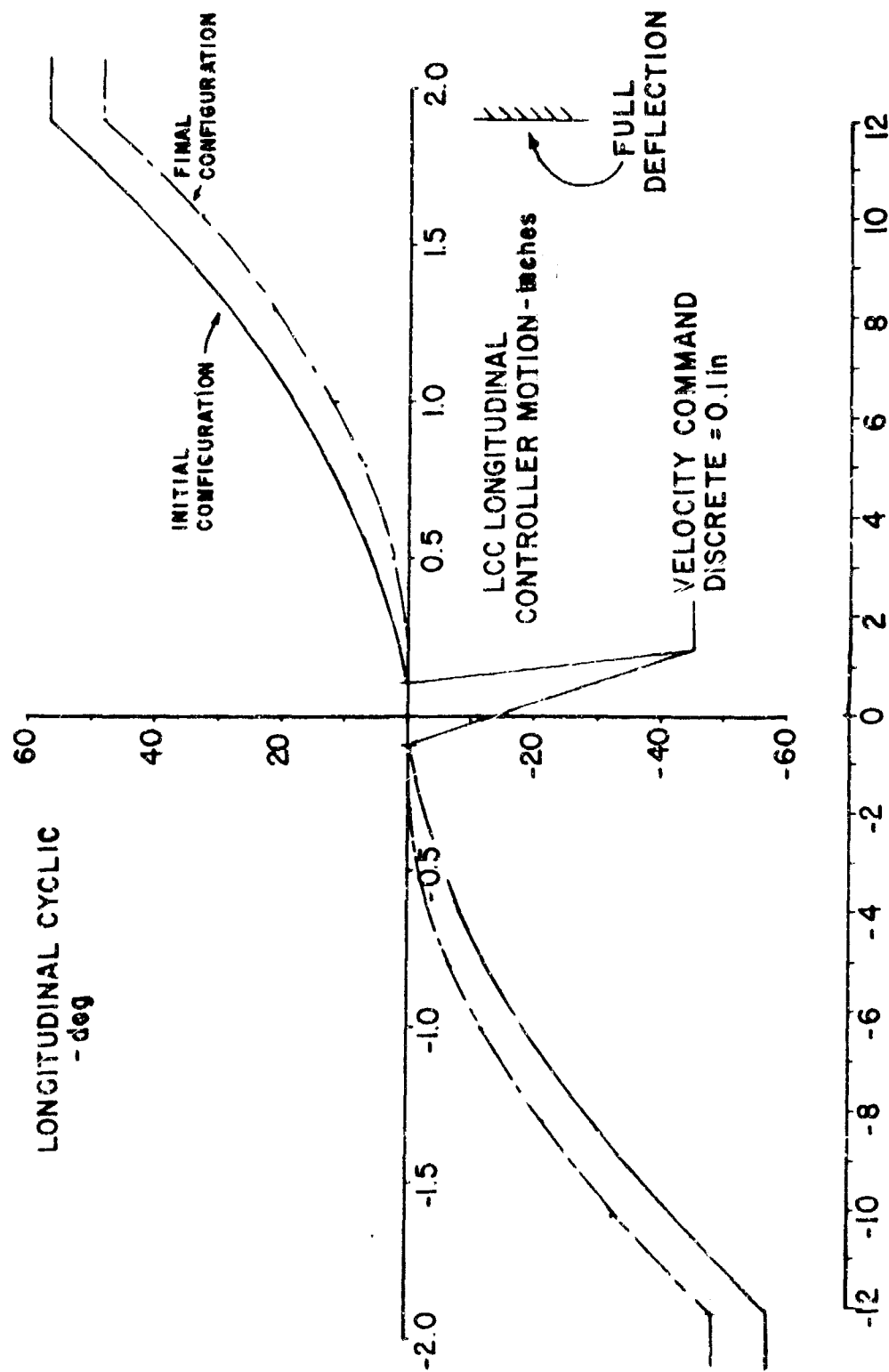
FIGURE A-10. LCC LONGITUDINAL VELOCITY COMMAND FUNCTION
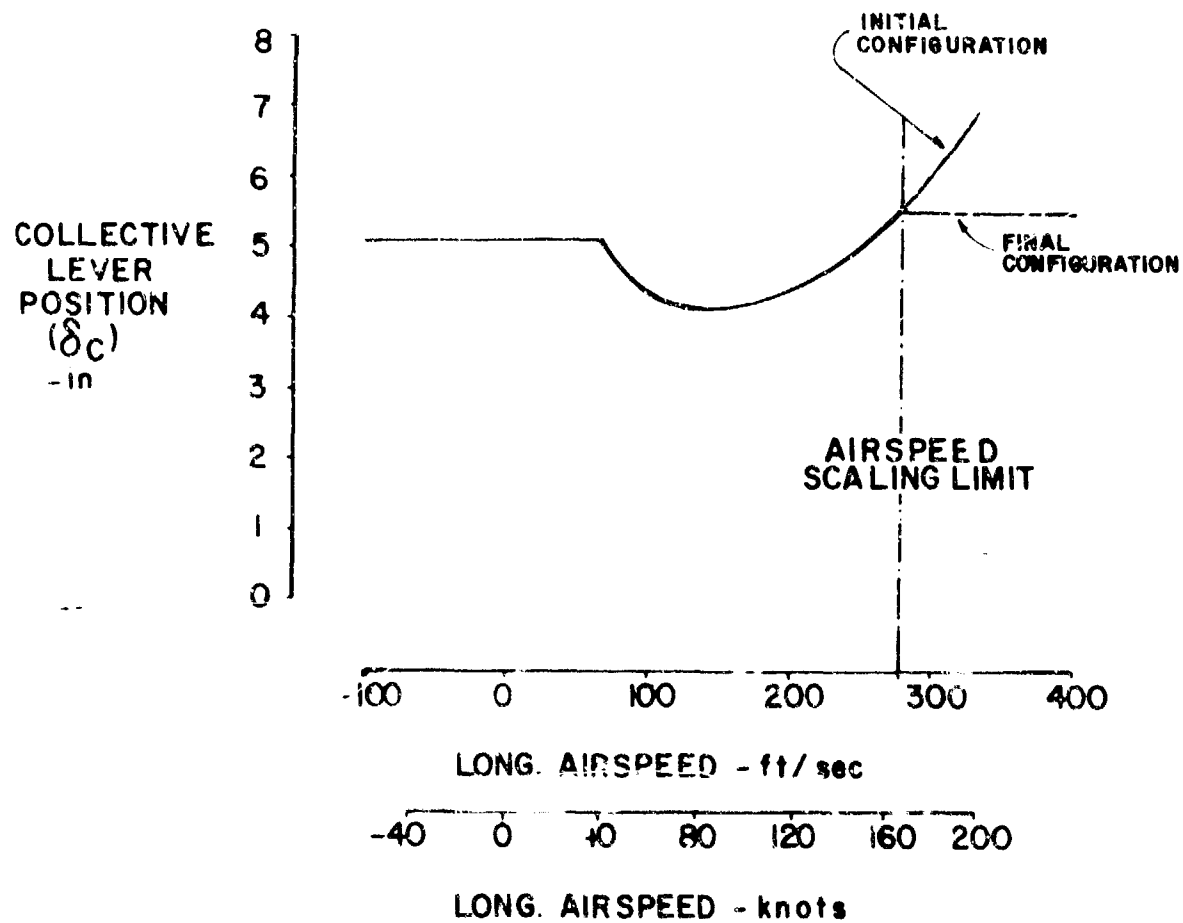
FIGURE A-11   COLLECTIVE POSITION COMPENSATION
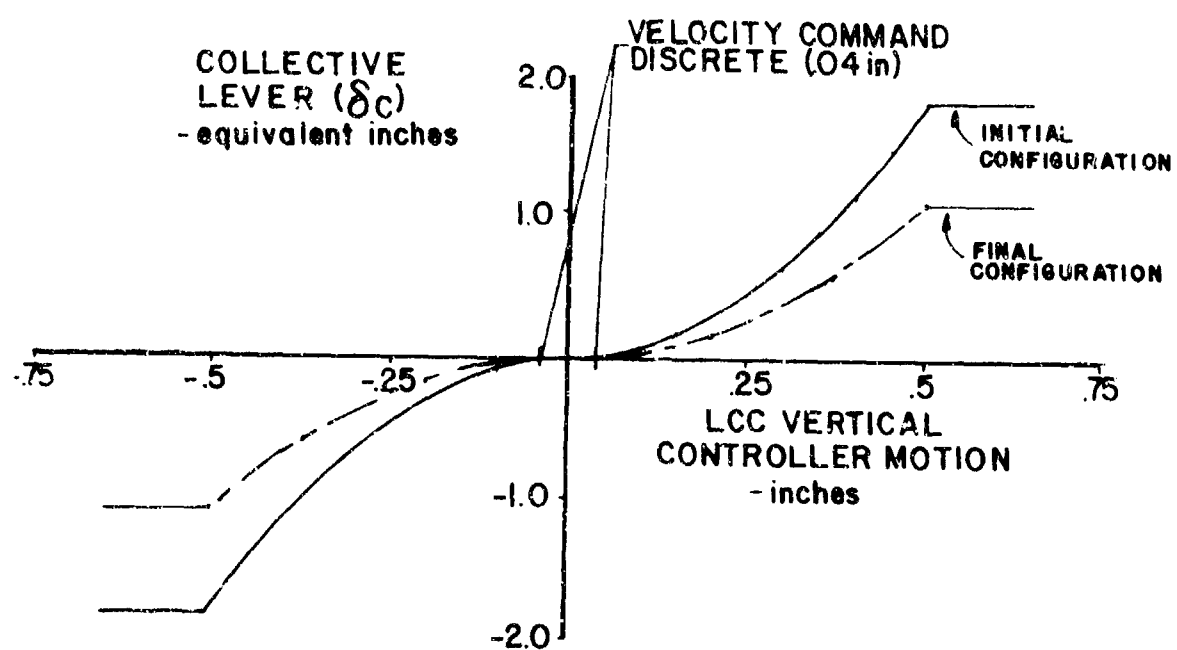
FIGURE A-12. LCC VERTICAL VELOCITY COMMAND FUNCTION
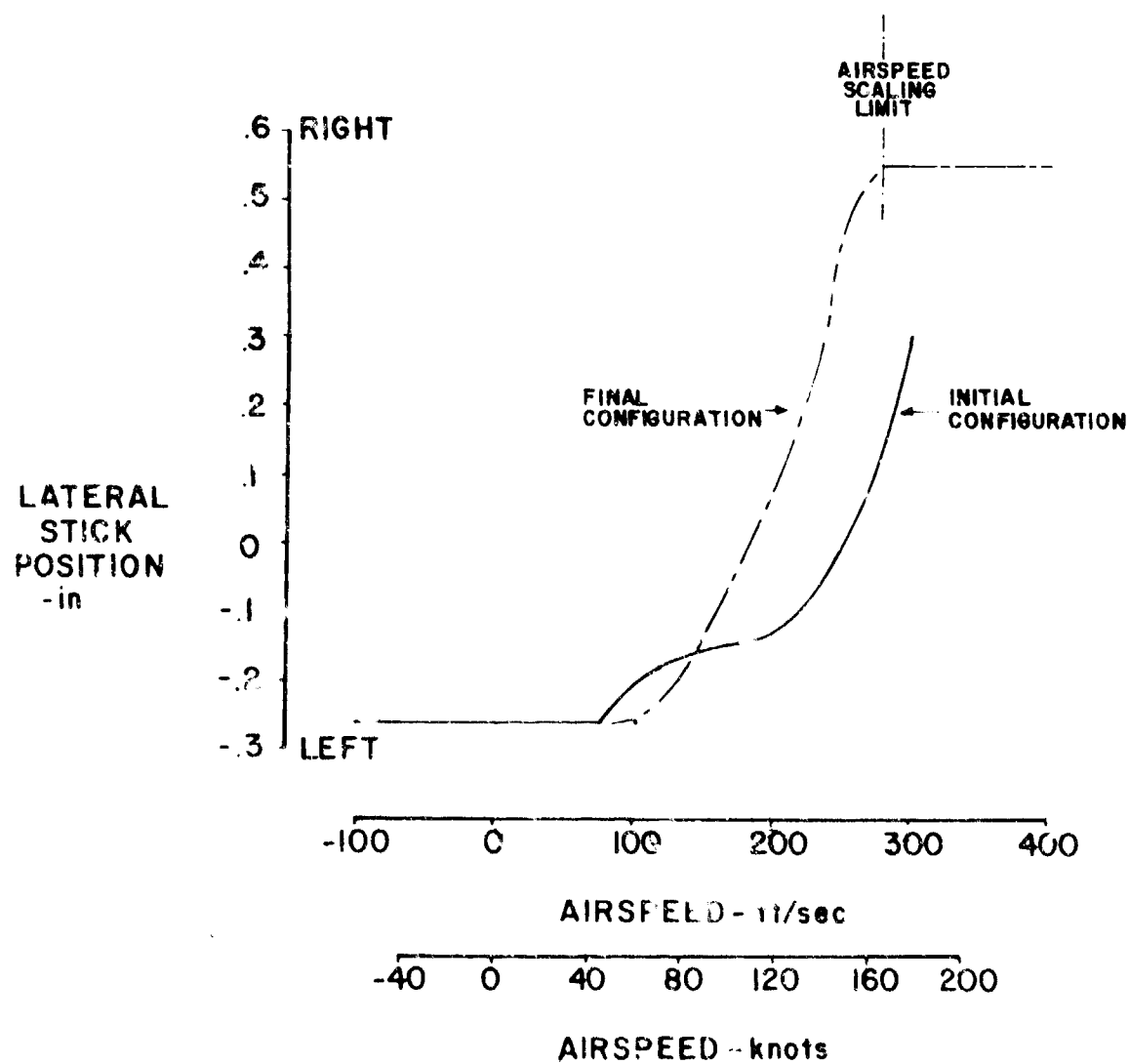
FIGURE A-13   LATERAL STICK TRIM COMPENSATION SCHEDULE

67
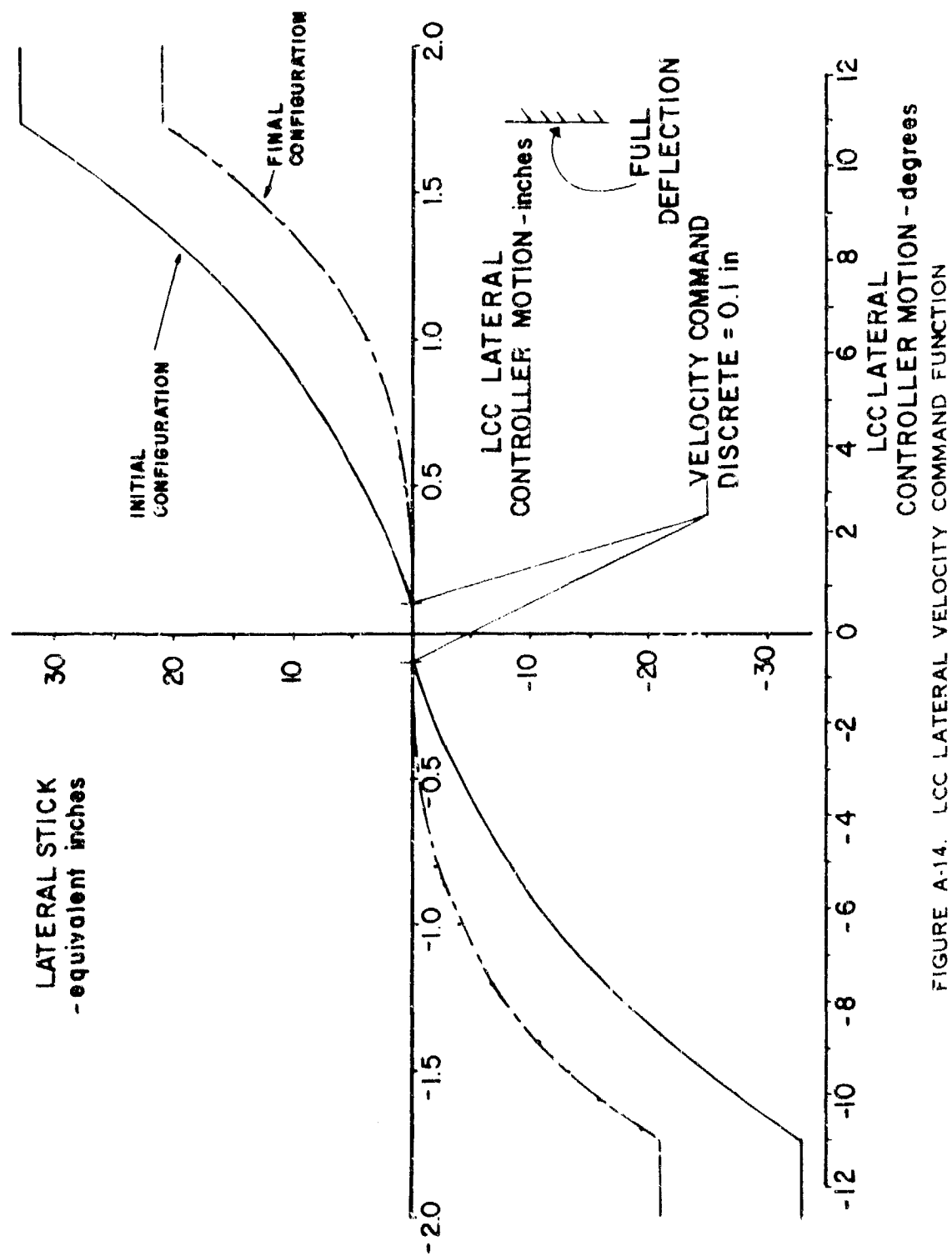
FIGURE A-14. LCC LATERAL VELOCITY COMMAND FUNCTION
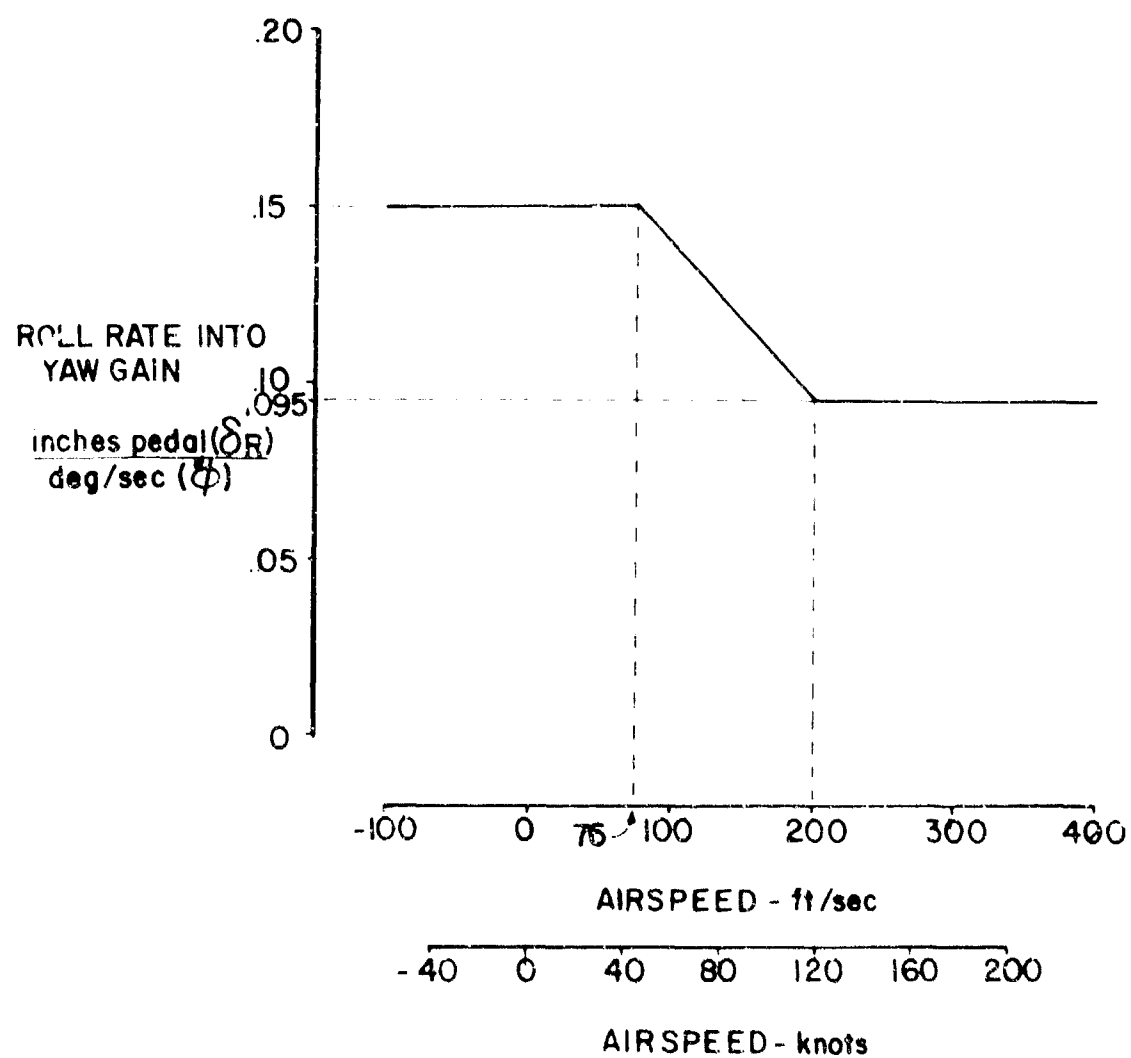
FIGURE A-15   TURN COORDINATION GAIN SCHEDULE
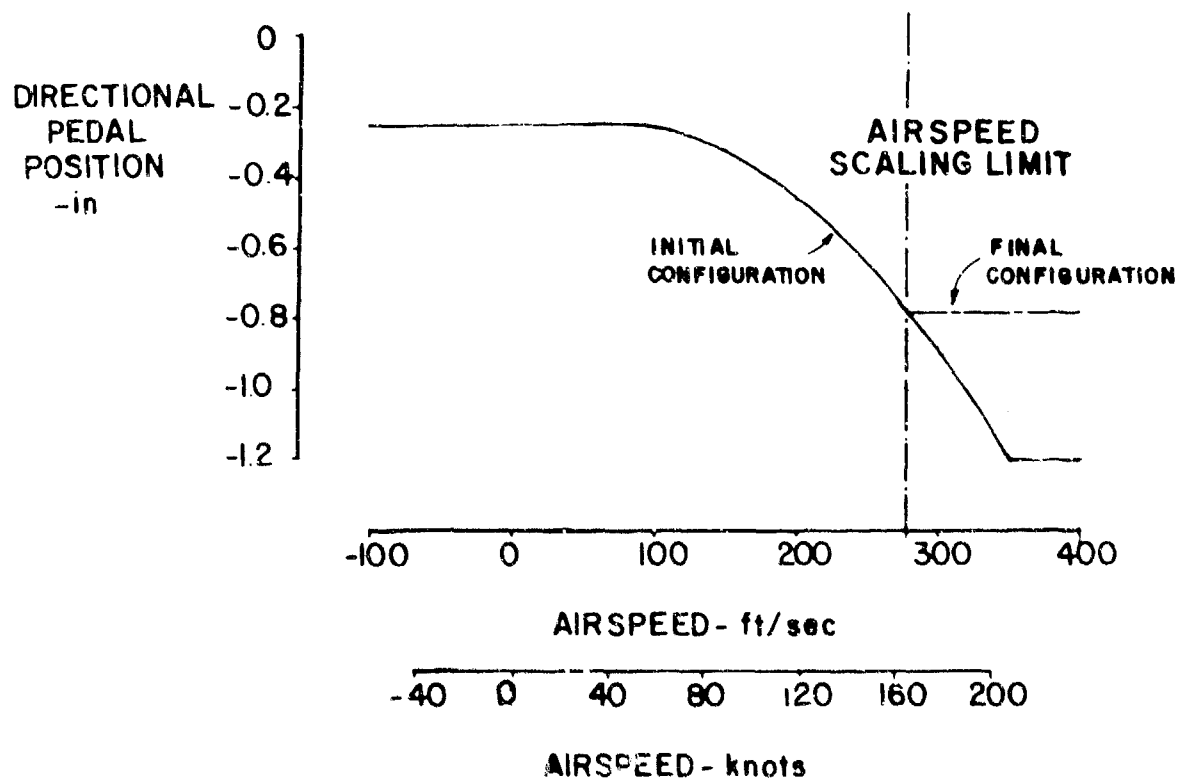
FIGURE A-16  PEDAL TRIM OFFSET SCHEDULE

680
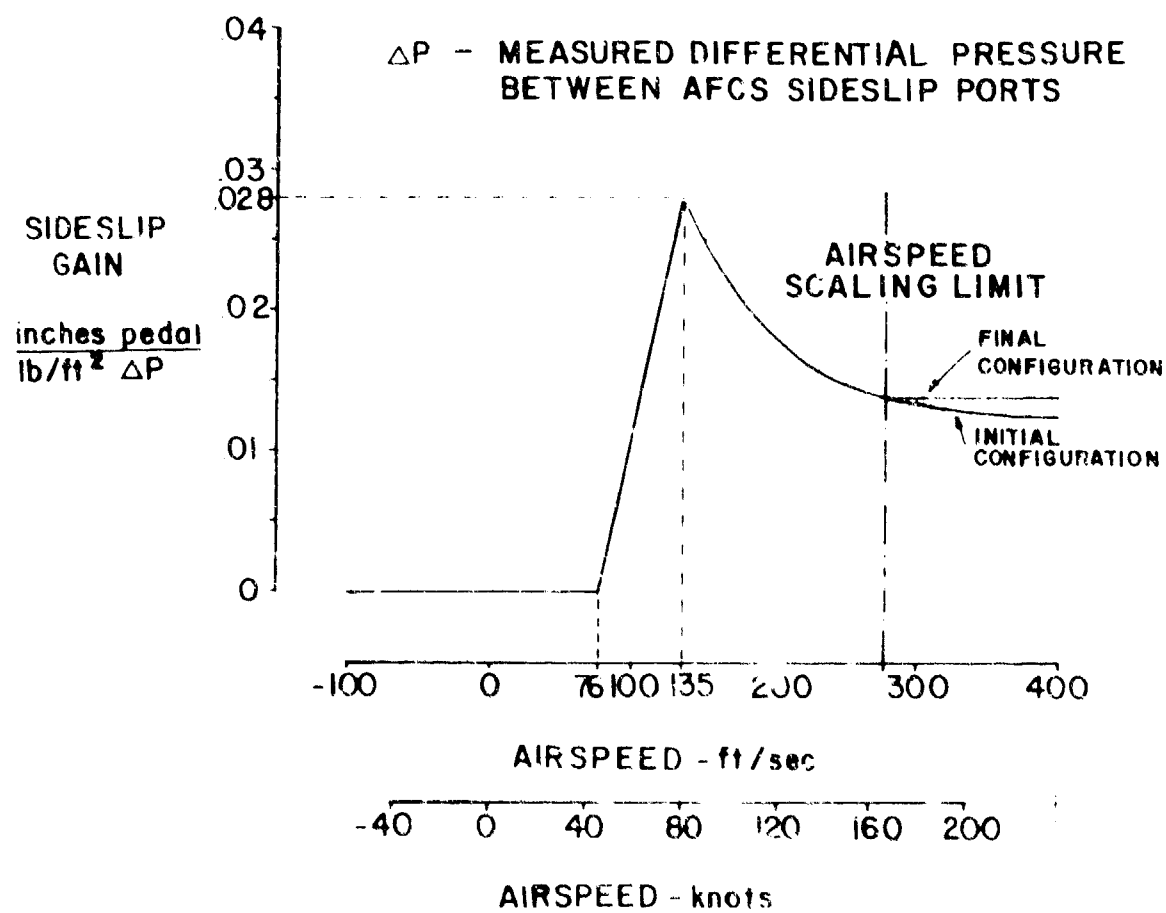
FIGURE A-17   SIDESLIP GAIN SCHEDULE
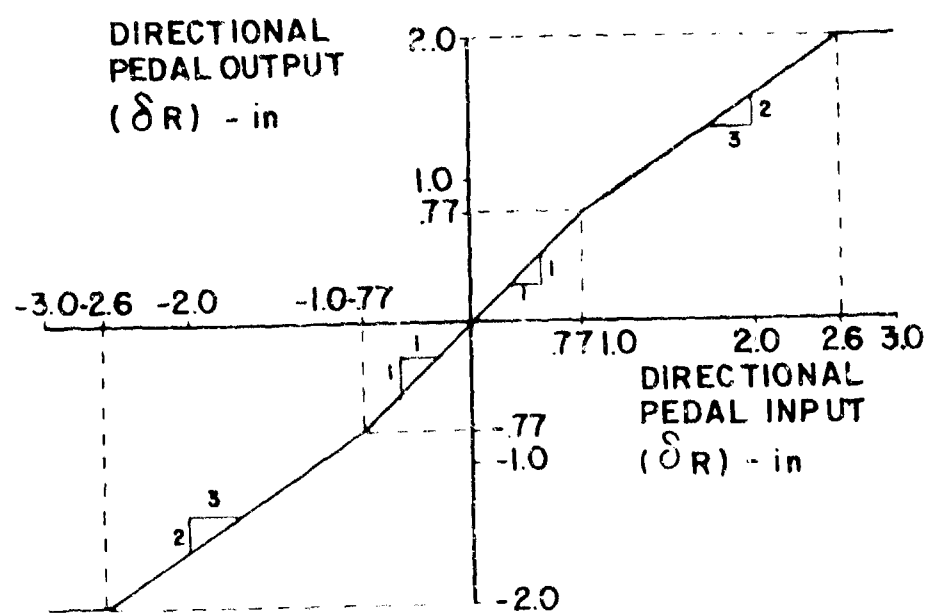
FIGURE A-18. SIDESLIP GAIN REDUCTION

682
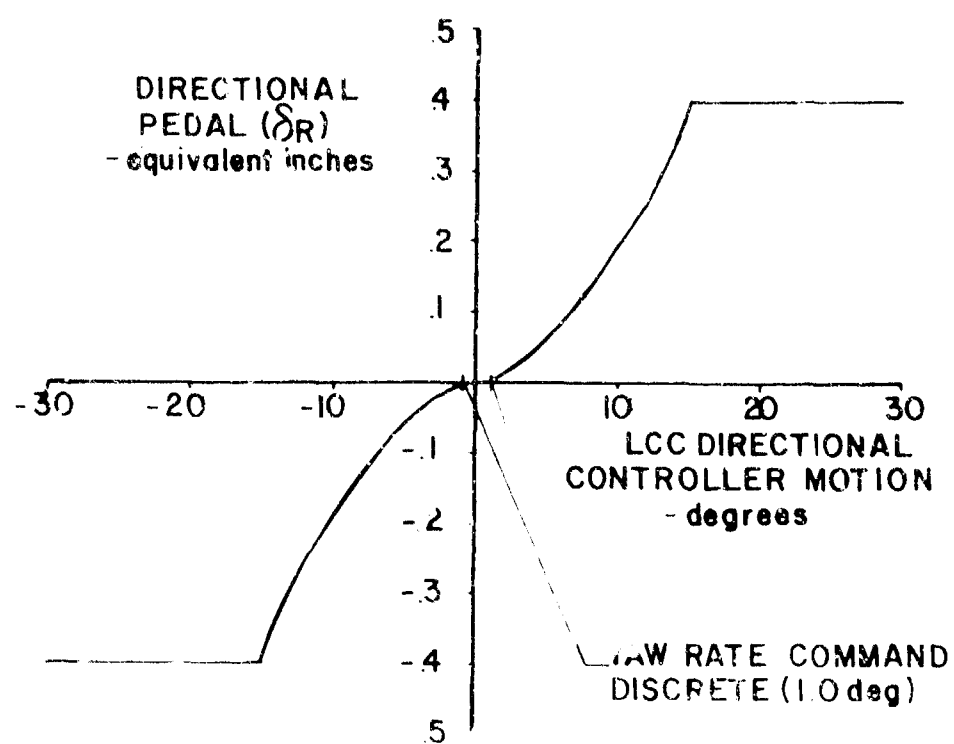
FIGURE A-1.  LCC TURN RATE COMMAND FUNCTION
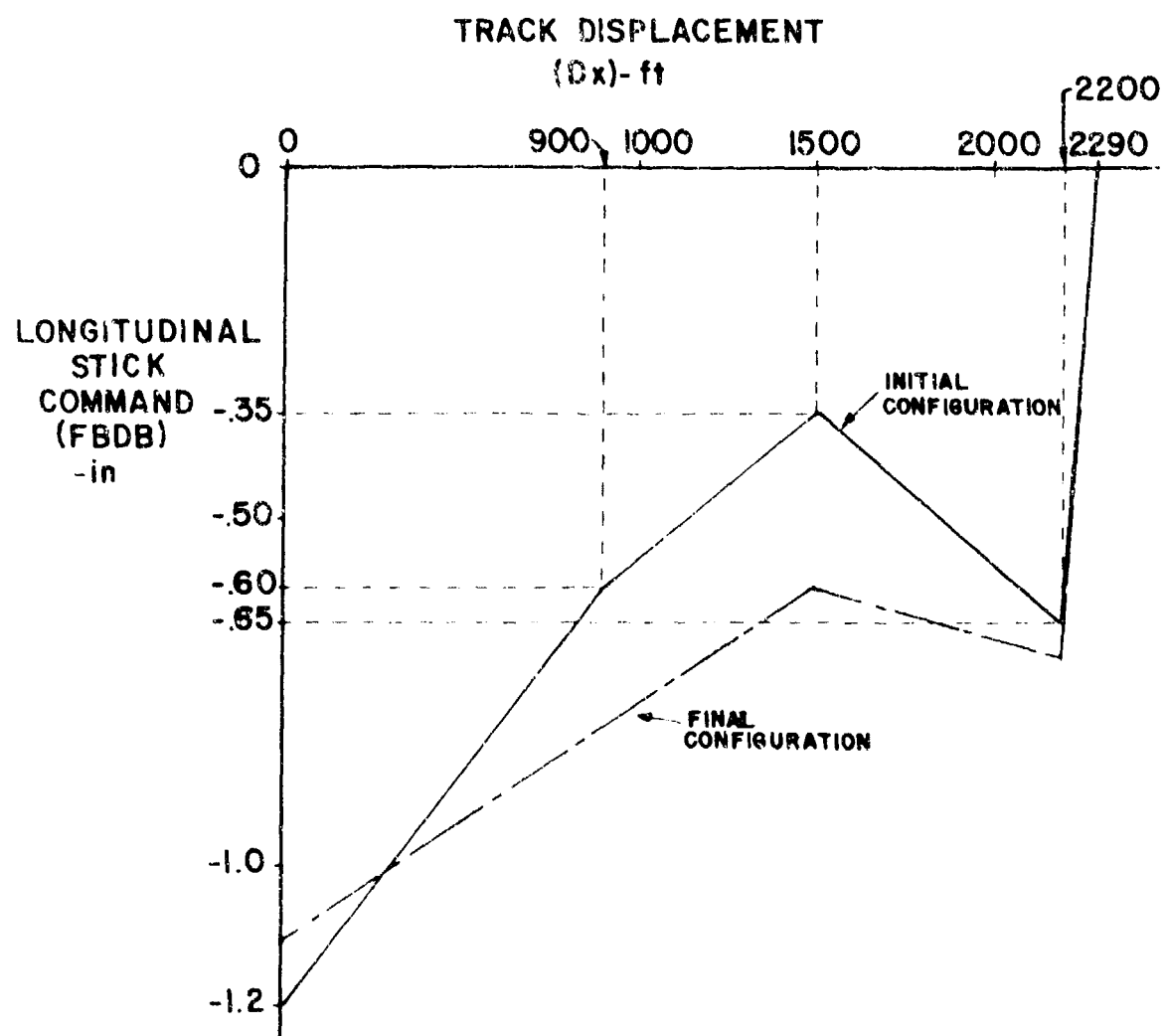
FIGURE A-20. LONGITUDINAL STICK COMMAND FUNCTION
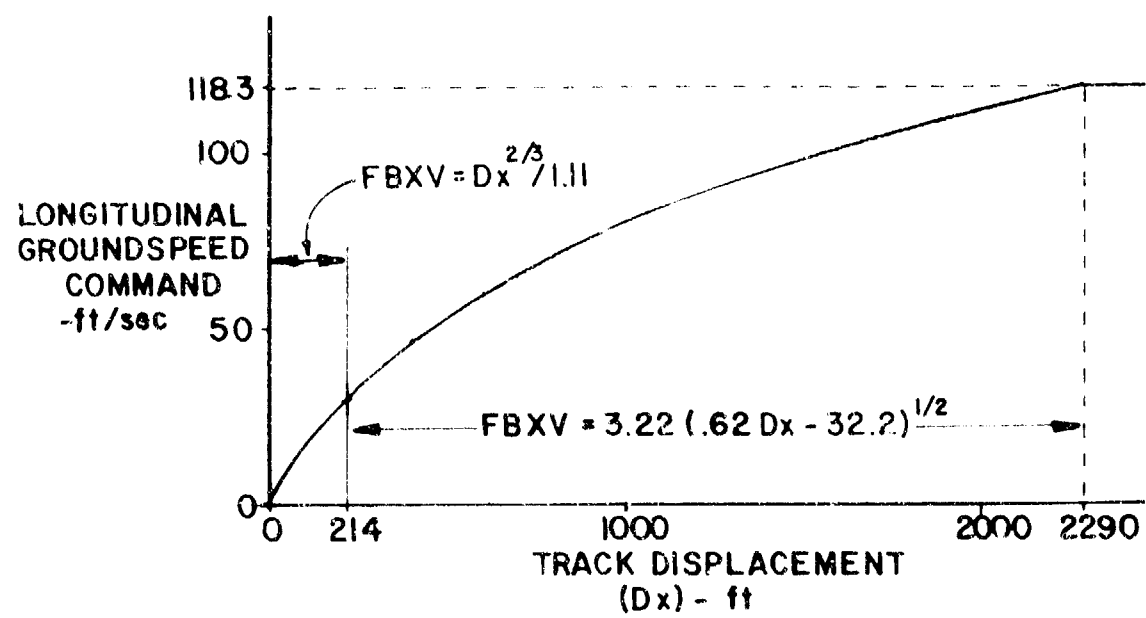
FIGURE 4-21. LONGITUDINAL GROUNDSPEED COMMAND FUNCTION
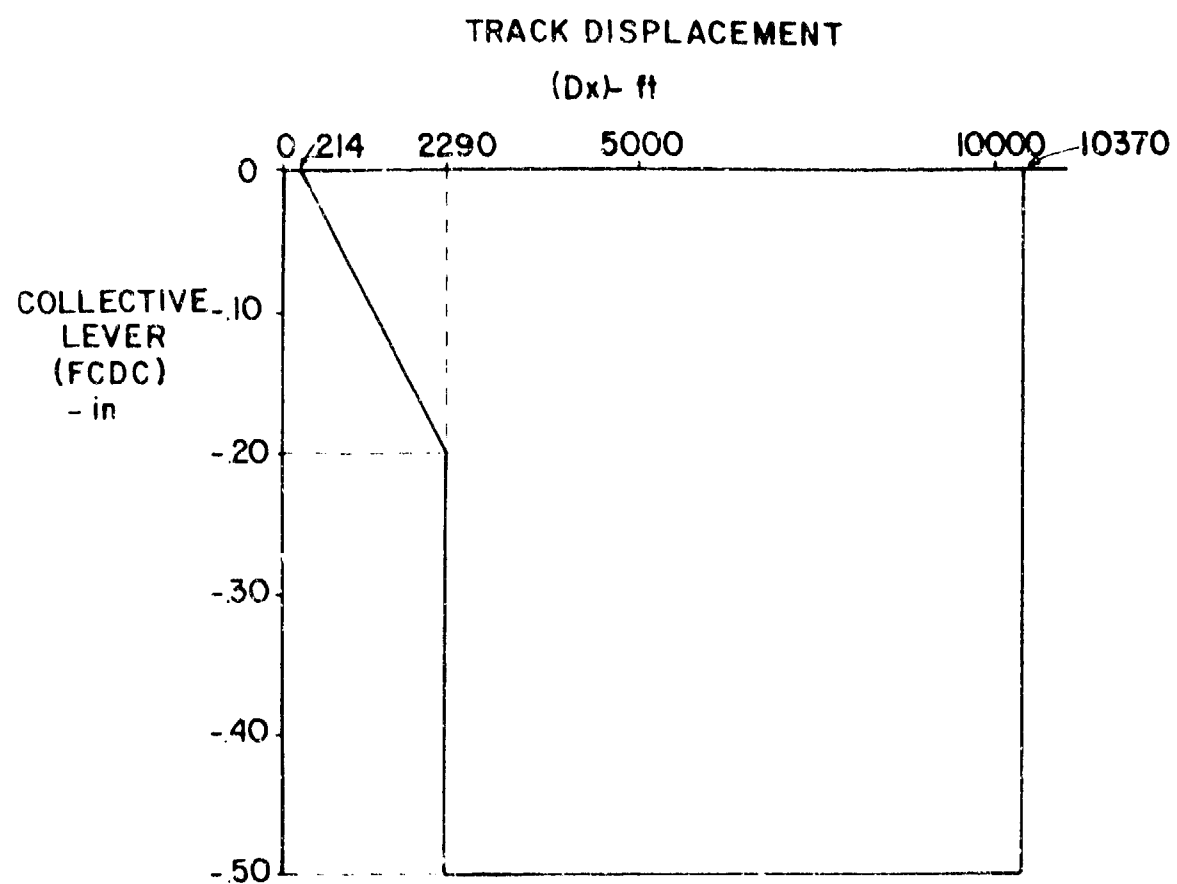
FIGURE A-22. COLLECTIVE LEVER COMMAND FUNCTION

686
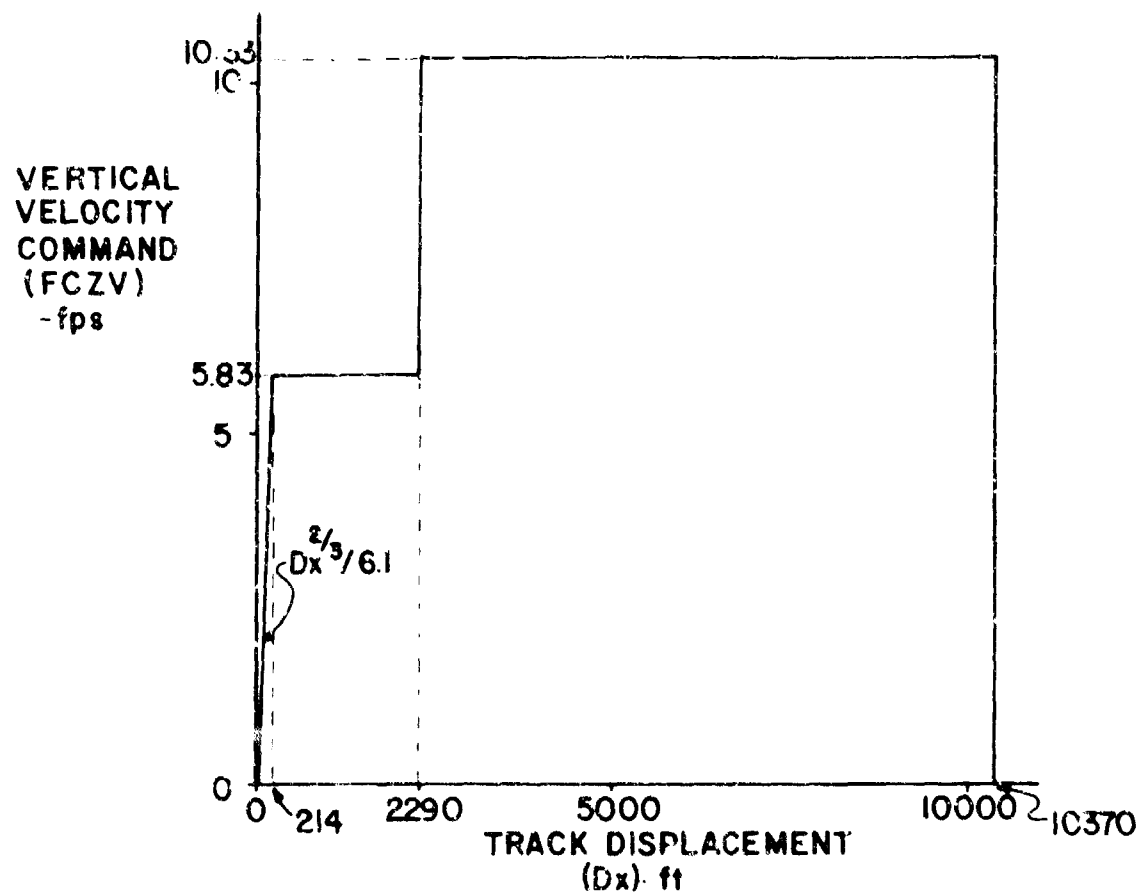
FIGURE A-23. VERTICAL VELOCITY COMMAND FUNCTION

687
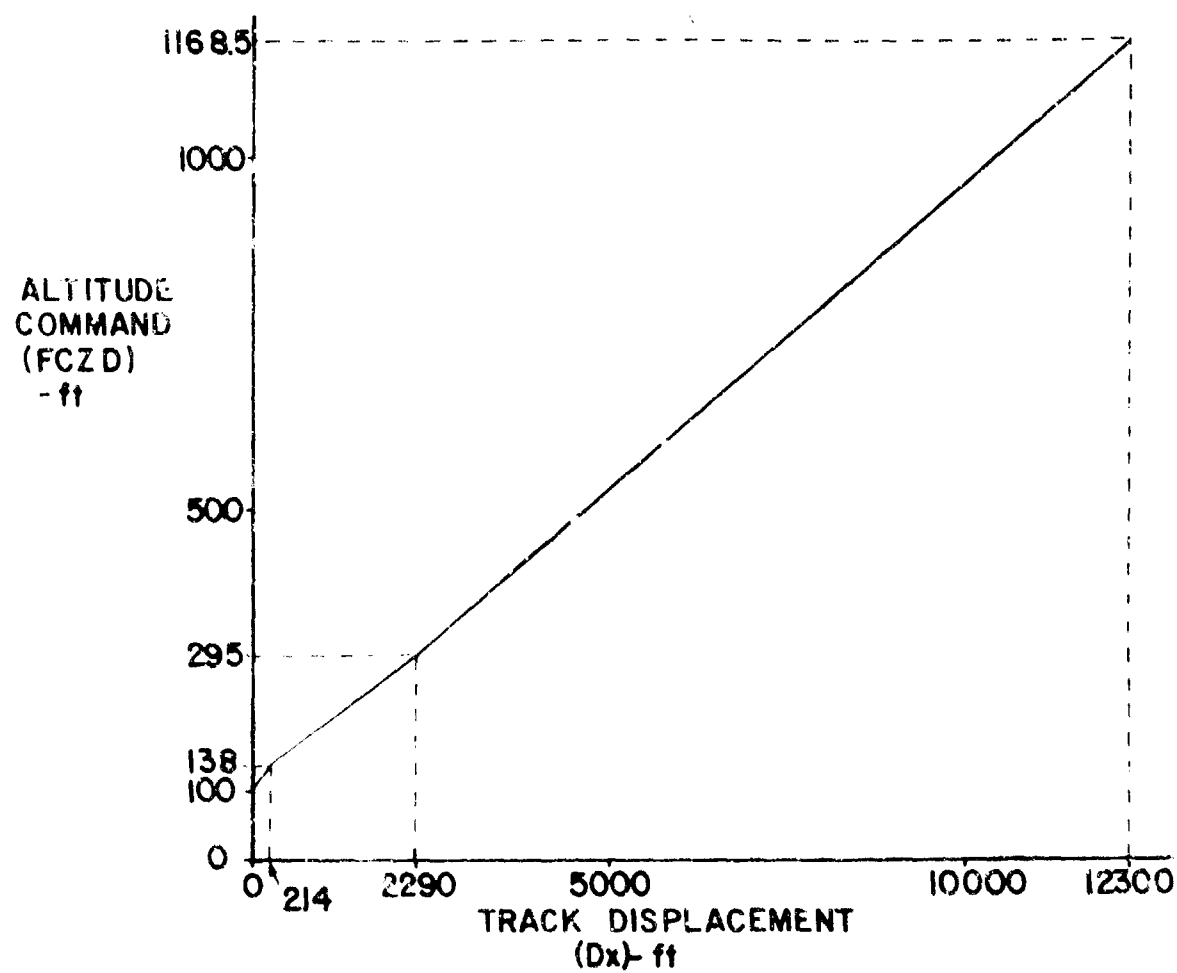
FIGURE A-24. ALTITUDE COMMAND FUNCTION

688
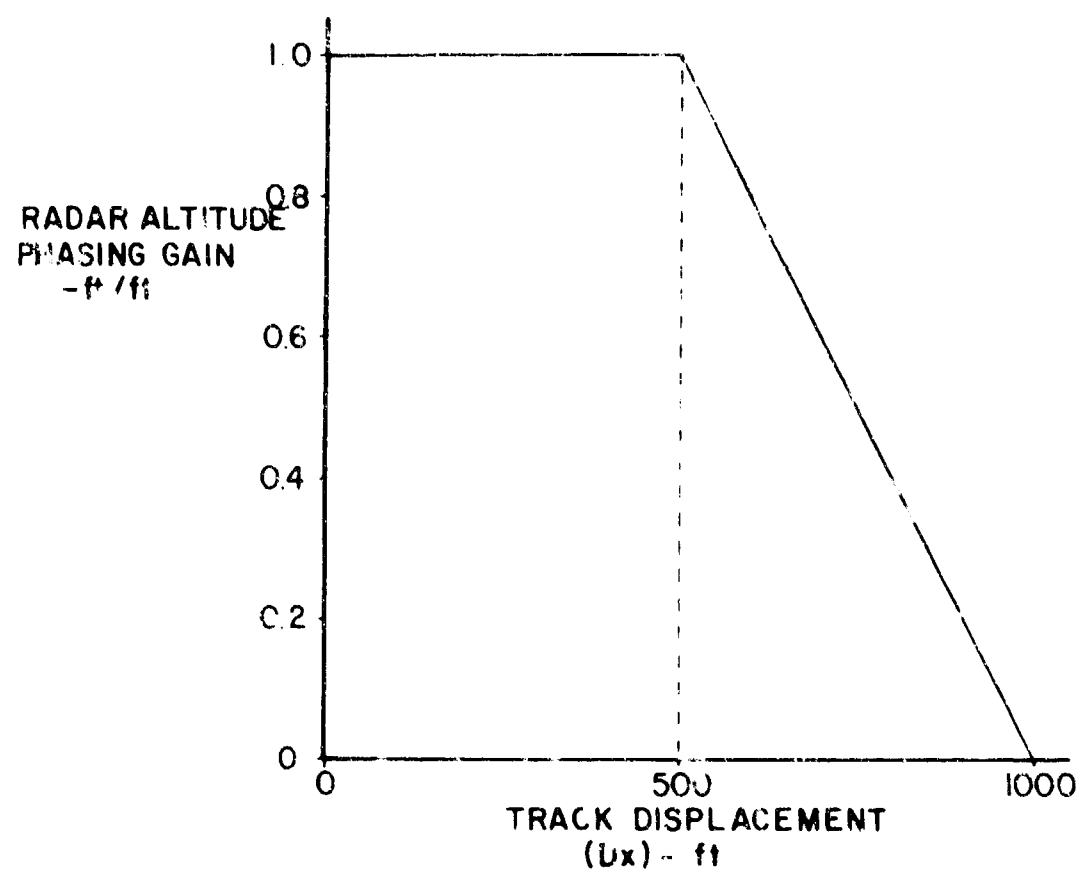
FIGURE A-25. RADAR ALTITUDE GAIN SCHEDULE

DELETED FOR FINAL CONFIGURATION
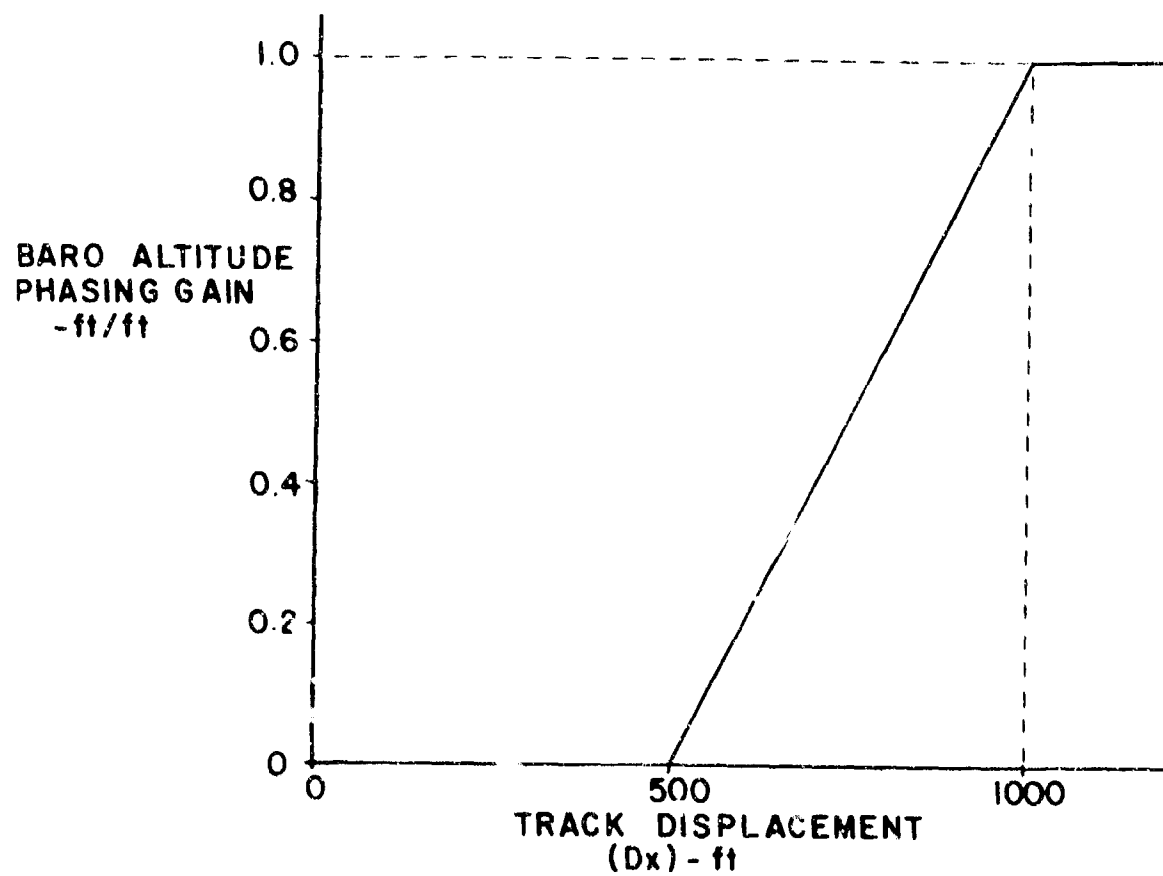


FIGURE A-26. BAROMETRIC ALTITUDE GAIN SCHEDULE

690
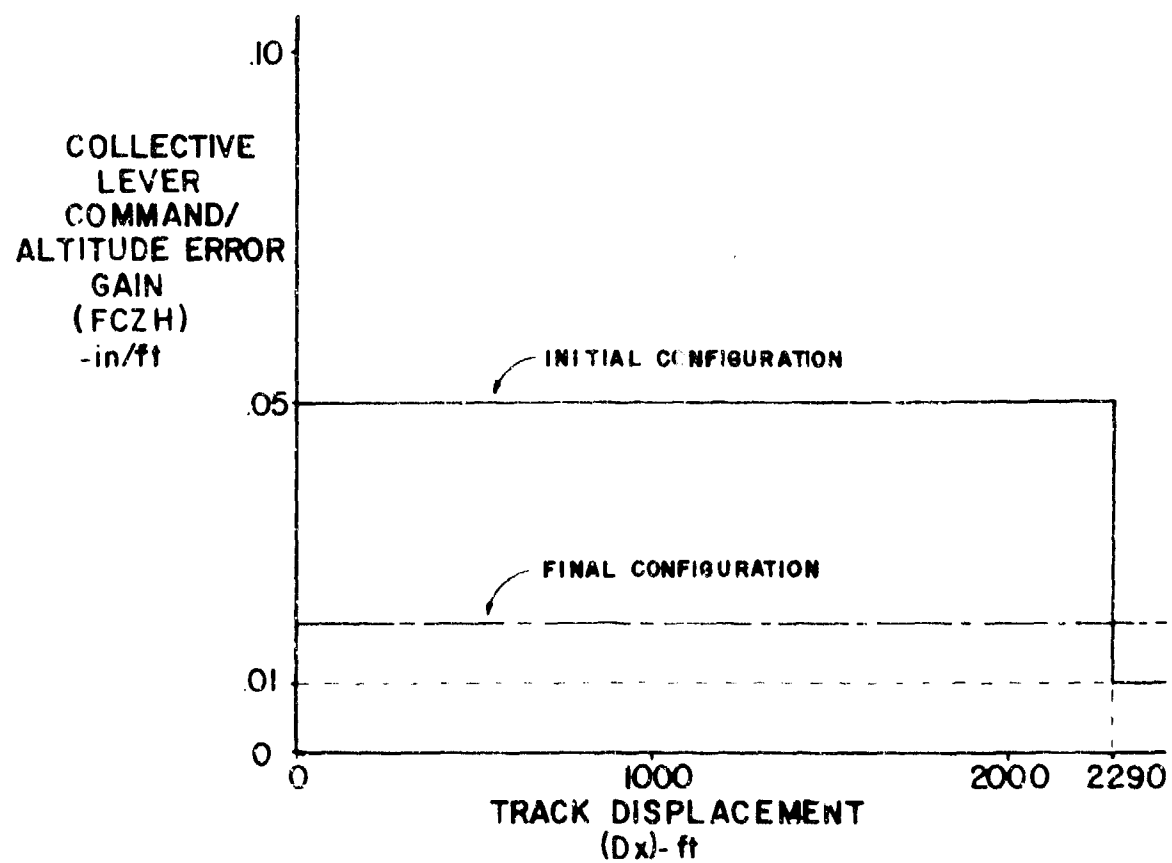
FIGURE A-27. VERTICAL DISPLACEMENT ERROR GAIN SCHEDULE
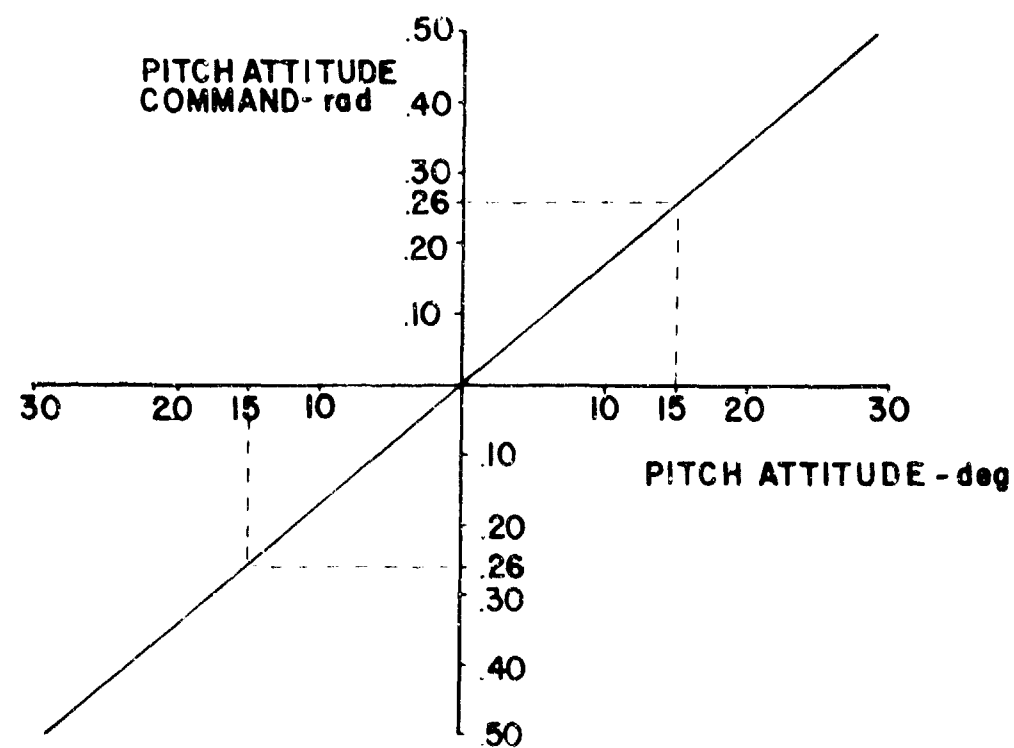
FIGURE A-28. PITCH ATTITUDE COMMAND FUNCTION

692
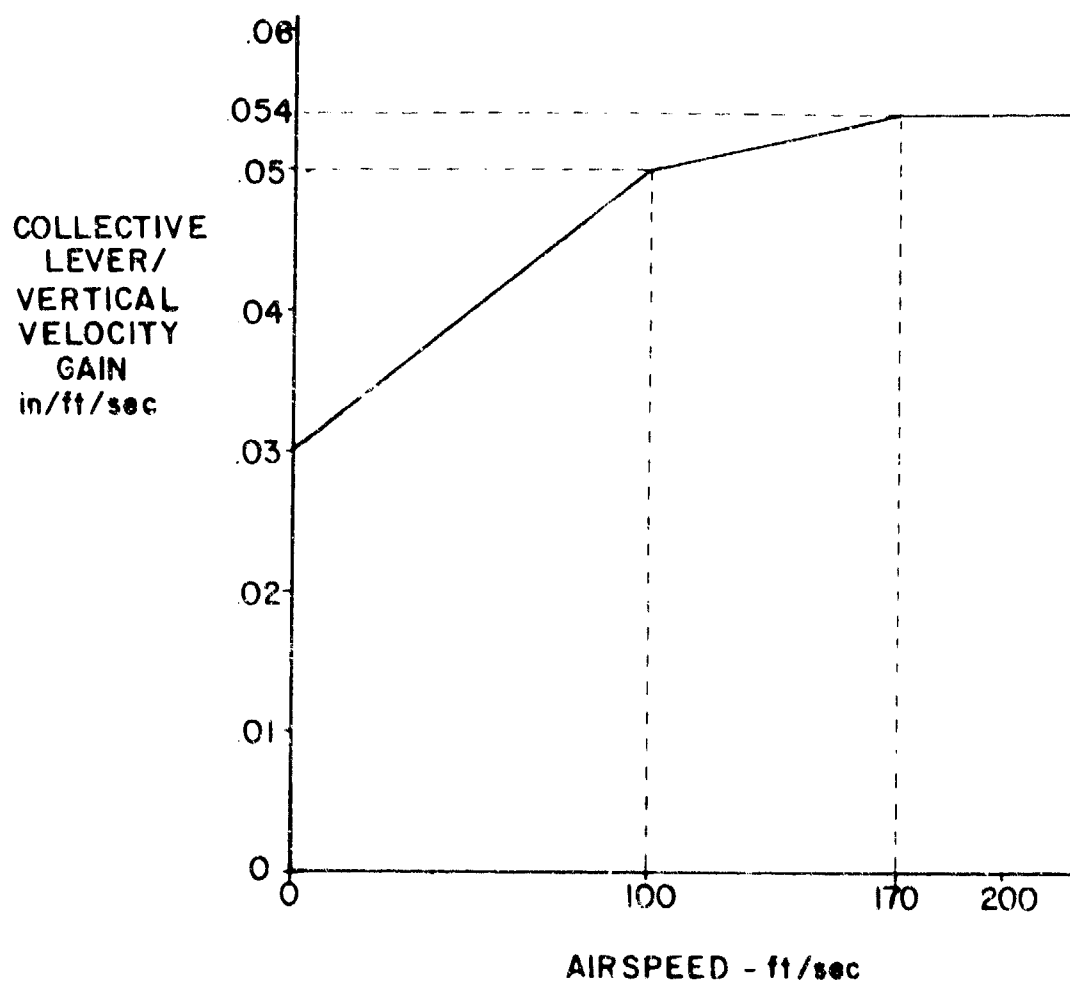
FIGURE A-29  COLLECTIVE FLARE SCHEDULE

693

FGU✳

✳GAIN SCHEDULE USED IN LSS
COMPUTATION (FNLS1 AND
FNLS2) AND PHASES IN HIGH
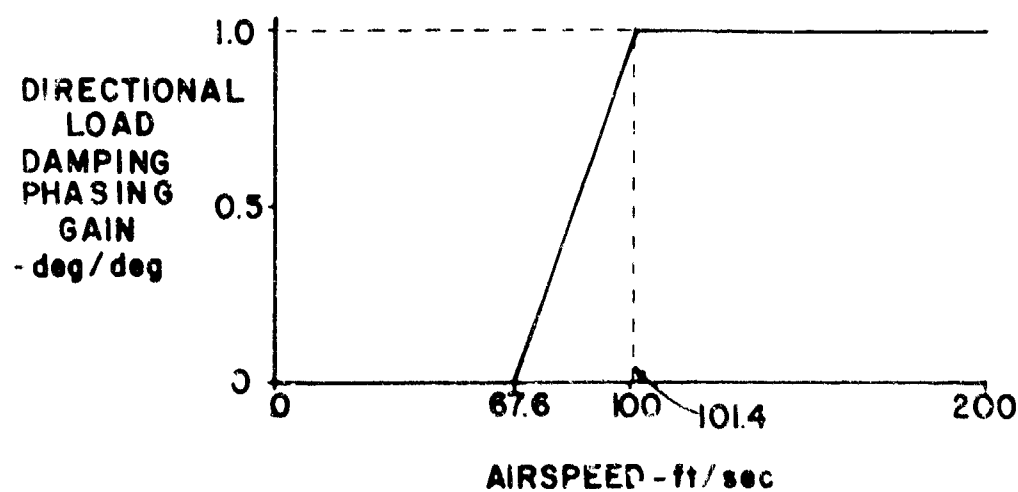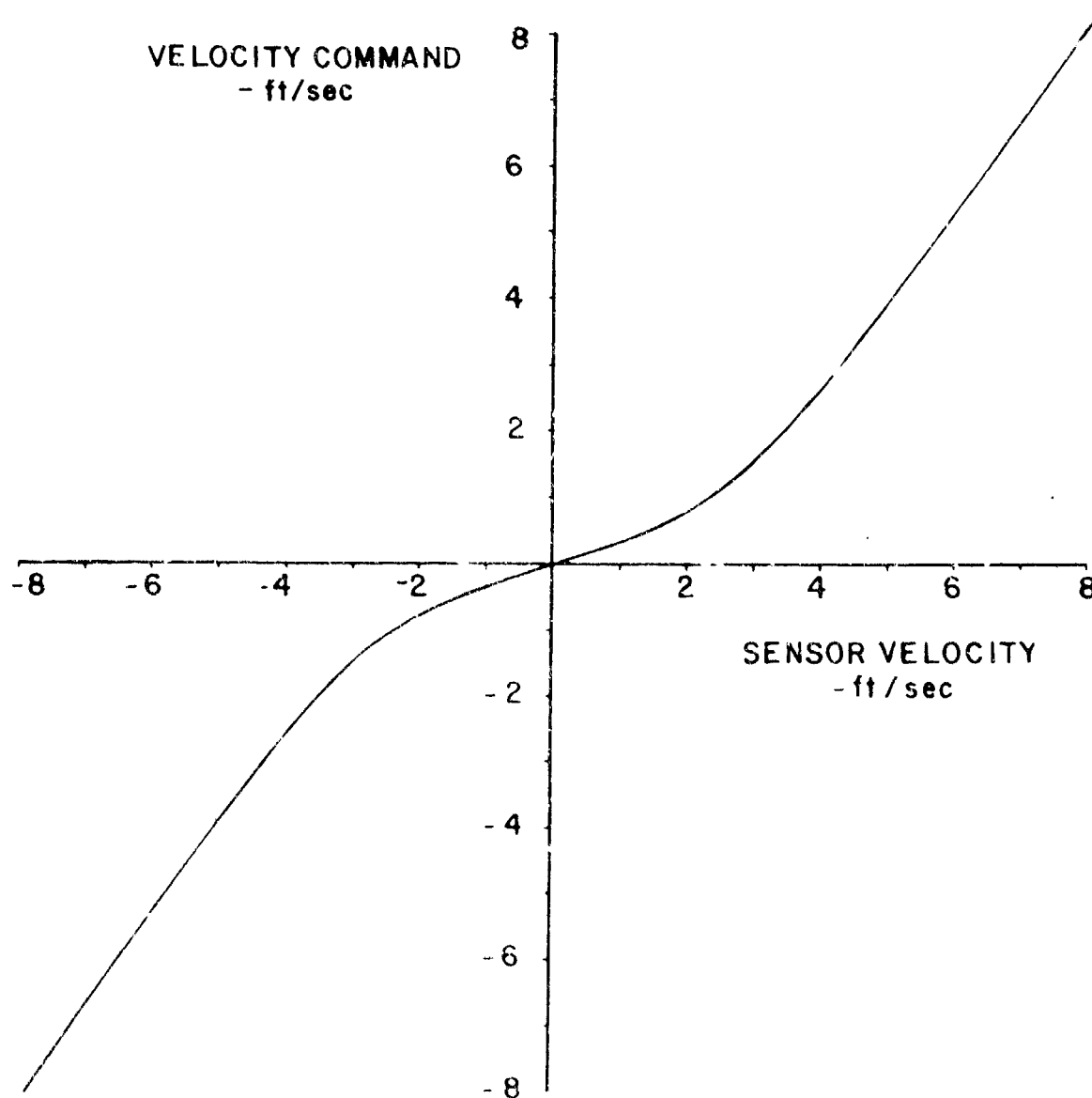SPEED DIRECTIONAL LOAD
DAMPING LOOPS



FIGURE A-30. DIRECTIONAL LOAD DAMPING GAIN SCHEDULE

694

# FXPHS, FYPHS, FZPHS

**DELETED FOR FINAL CONFIGURATION**

## BASED ON INPUT SCALING OF 5 volts/7.67 ft/sec



NOTE: PHS VELOCITY SHAPING FUNCTIONS (FXPHS, FYPHS AND FZPHS) ARE REQUIRED IN EACH AXIS TO ACCOUNT FOR MEASURED NON-LINEAR SENSOR OUTPUT DATA

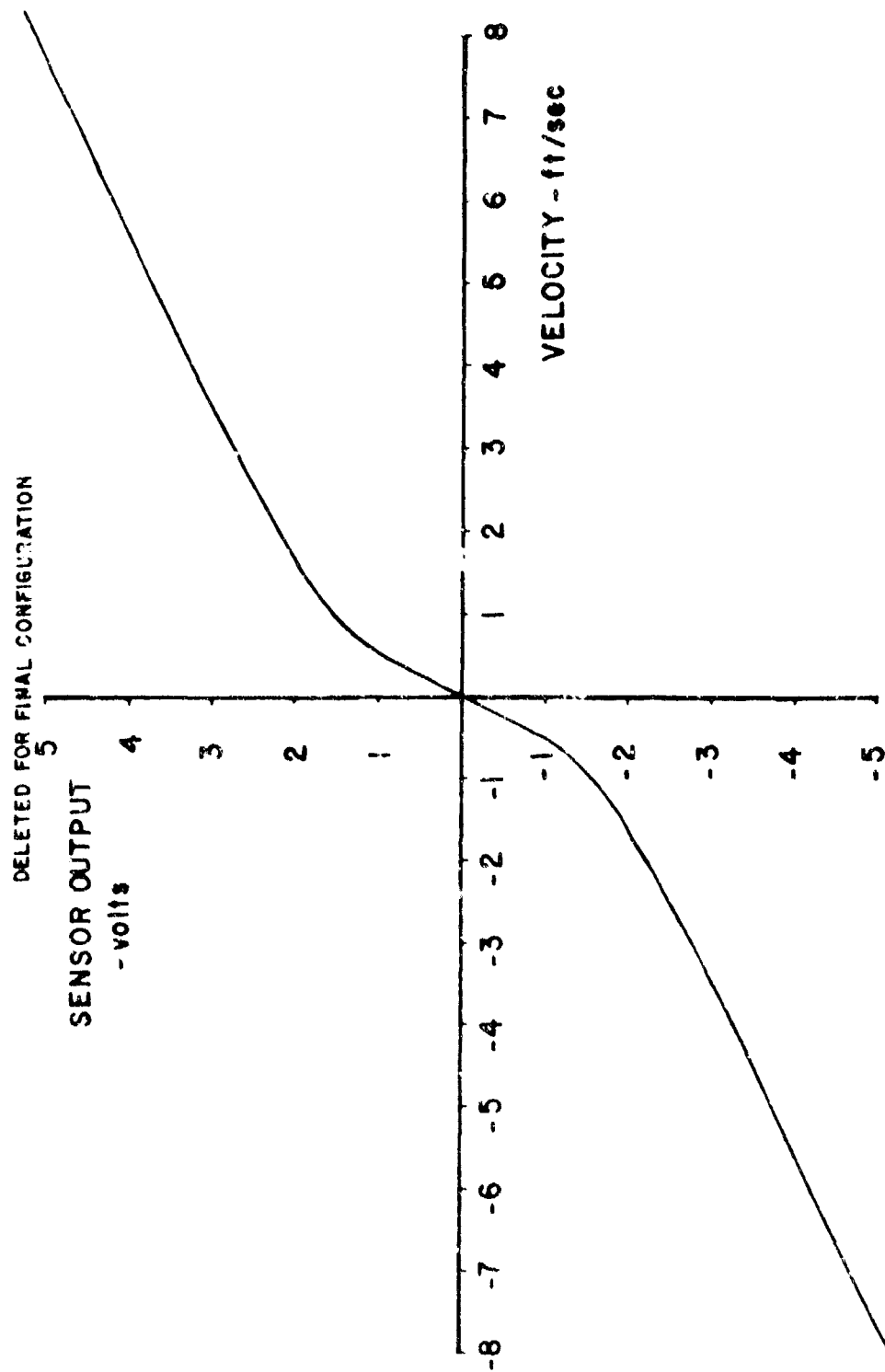FIGURE A-31 PRECISION HOVER SENSOR VELOCITY COMPENSATION

FIGURE A-32. PRECISION HOVER SENSOR CALIBRATION - LONGITUDINAL AXIS
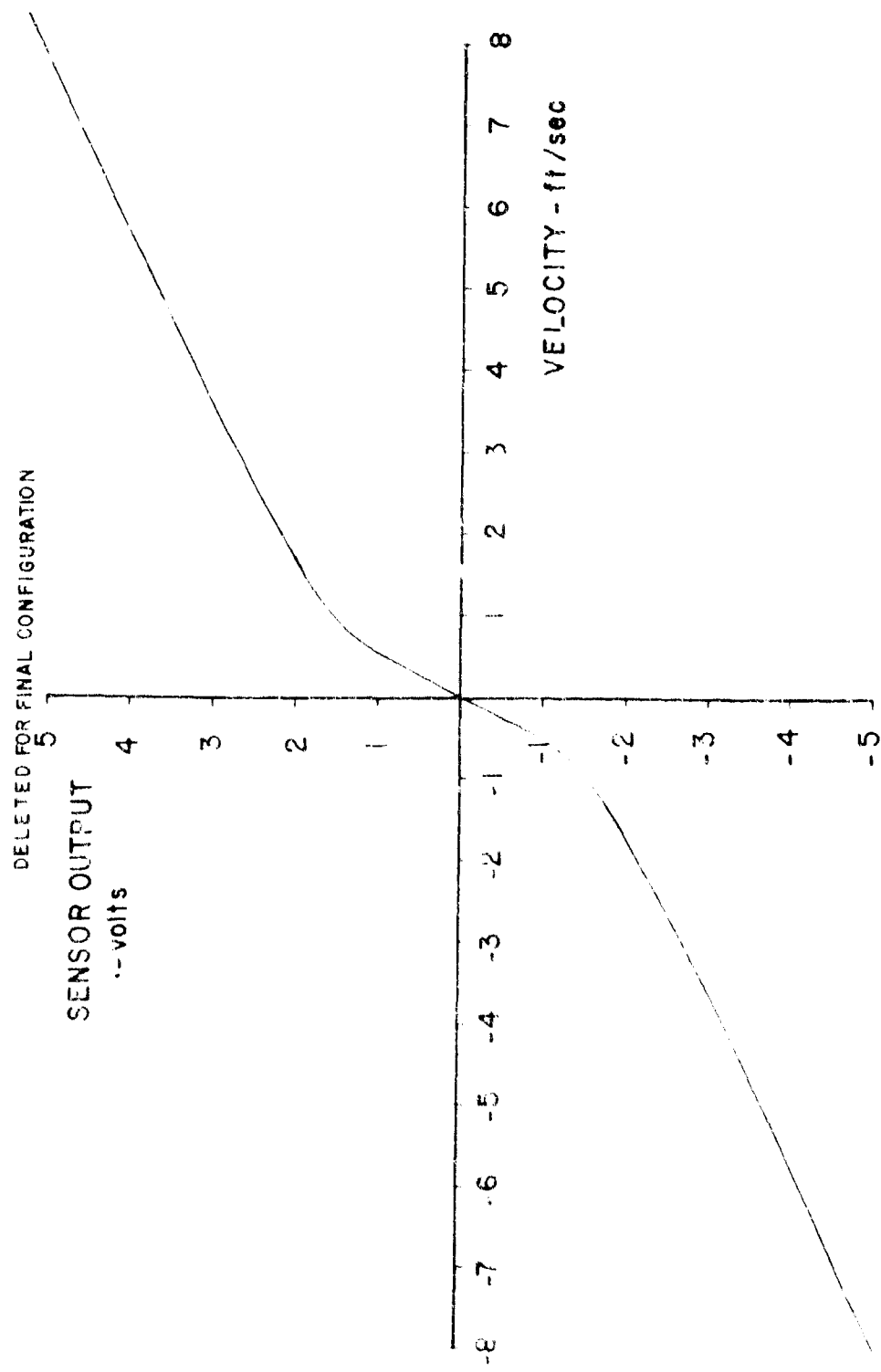
696

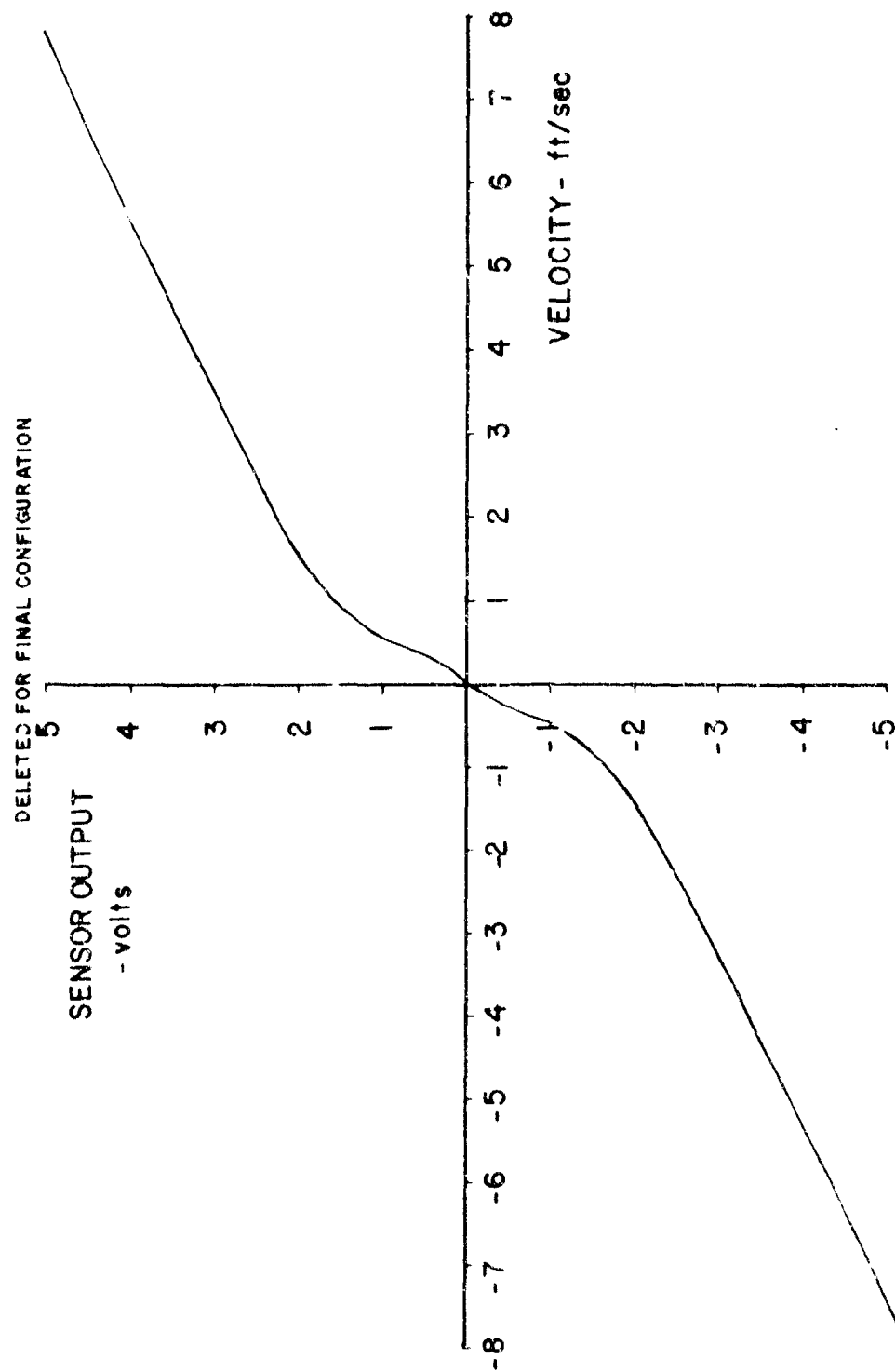FIGURE A-33  PRECISION HOVER SENSOR CALIBRATION - LATERAL AXIS

FIGURE A-34. PRECISION HOVER SENSOR CALIBRATION - VERTICAL AXIS
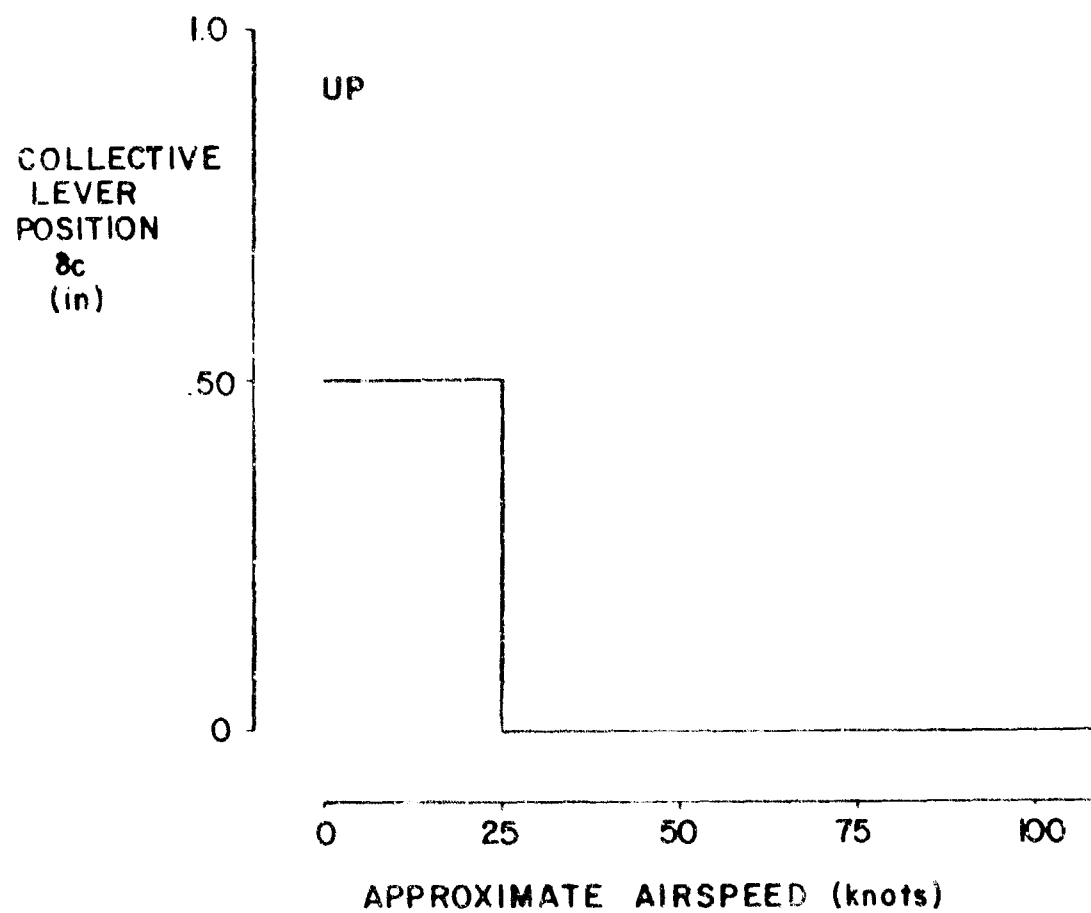
FDCB ADDED FOR FINAL CONFIGURATION



FIGURE A-35   LOW AIRSPEED COLLECTIVE BIAS

699

# REFERENCES

1. Sanders, Thomas, ADVANCED TECHNOLOGY COMPONENT PROGRAM – FLIGHT CONTROL SYSTEM – TASK 1, PART 1, SUMMARY REPORT, Report No. D01-10095-1, Boeing Vertol Company, Philadelphia, PA 19142, 30 December 1971.

2. HLH ADVANCED TECHNOLOGY COMPONENT PROGRAM STATEMENT OF WORK, Contract DAAJ01-71-C-0840(P6A), U. S. Army Aviation Systems Command, St. Louis, MO 63166.

3. McKercher, Donald, PRIME ITEM DESCRIPTION DOCUMENT FOR THE HEAVY LIFT HELICOPTER, VOLUMES I AND II, Report No. S301-10000, Boeing Vertol Company, Philadelphia, PA 19142, 20 January 1972.

4. MIL-H-8501A, MILITARY SPECIFICATION – HELICOPTER FLYING AND GROUND HANDLING QUALITIES; GENERAL REQUIREMENTS FOR, Department of Defense, Washington, D. C., 7 September 1961.

5. Harper, R. P., and Cooper, G. E., A REVISED PILOT RATING SCALE FOR THE EVALUATION OF HANDLING QUALITIES, Report No. 153, Cornell Aeronautical Laboratory, September 1966.

6. Mouat, Darryl B., A THEORETICAL DISCUSSION OF THE PRECISION HOVER SYSTEM FOR THE HEAVY LIFT HELICOPTER, Document No. D301-10128-1, Boeing Vertol Company, Philadelphia, PA 19142, 7 August 1972.

7. Garnett, Theodore S., FULL FLIGHT ENVELOPE MATH MODEL FOR 347/HLH CONTROL SYSTEM ANALYSIS – CONTROL DOCUMENT, Document No. D301-10148-1, Boeing Vertol Company, Philadelphia, PA 19142, 12 June 1972.

8. Sinacori, John B., A PRACTICAL APPROACH TO MOTION SIMULATION, AIAA paper presented at the Annual Flight Simulation Conference, San Francisco, CA, September 1973.

9. Sinacori, John B., APPLICATION OF THE NORTHROP ROTATIONAL SIMULATOR TO HELICOPTERS AND V/STOL AIRCRAFT (USER'S GUIDE), Northrop Corporation; USAAVLABS Technical Report 70-26, U. S. Army Aviation Materiel Laboratories, Fort Eustis, Virginia 23604, May 1970, AD 873037.

10. Garnett, Theodore S., EVALUATION OF LOAD CONTROLLING CREWMAN CONTROLLER – FINAL REPORT, DOA Delivery Order 0012, Contract DAAJ01-73-A-0017, Boeing Vertol Company, Philadelphia, PA 19142, January 1974.

## REFERENCES (CONCLUDED)

11.  HLH/ATC FLIGHT CONTROLS - GROUND AND FLIGHT TEST REPORT - TASK
     III, Report No. D301-10208-2, Boeing Vertol Company, Philadelphia,
     PA  19142, 13 March 1975.

## LIST OF ACRONYMS

| Acronym | Definition |
|---------|------------|
| AAH | Automatic Approach to Hover |
| AFCS | Automatic Flight Control System |
| AHRS | Attitude/Heading Reference System |
| AHT | Automatic Hover Trim |
| ATC | Advanced Technology Component |
| BITE | Built-In Test Equipment |
| BOA | Basic Ordering Agreement |
| CEP | Circular Error Probability |
| CG | Aircraft Center of Gravity |
| C/H | Cooper-Harris Pilot Rating |
| DAC | Digital/Analog Converter |
| DCP | Differential Collective Pitch Control |
| DELS | Direct Electrical Linkage System - 347 |
| FCS | Flight Control System |
| HLH | Heavy Lift Helicopter |
| IAS | Indicated Airspeed |
| IMU | Inertial Measuring Unit |
| INS | Inertial Navigation System |
| IOP | Input-Output Processor |
| LAS/WAVS | Large Amplitude Simulator With Wide Angle Visual System |
| LCC | Load-Controlling Crewman |
| LCCC | Load-Controlling Crewman's Controller |
| LCP | Longitudinal Cyclic Pitch Control |

| Acronym | Definition |
|---------|------------|
| LSS | Load Stabilization System |
| PAST | Precision Airspeed Trim |
| PECS | Primary Electrical Control System - HLH |
| PFCS | Primary Flight Control System |
| PFFU | Programmable Force-Feel Unit - HLH |
| PHS | Precision Hover Sensor |
| PIDD | Prime Item Description Document |
| ROM | Read-Only-Memory |
| SCAS | Stability and Control Augmentation System |
| SOW | Statement of Work |
| 347 | Model 347 Flight Research Vehicle |